

**APPLICATION OF CHAMELEON CATALYST AND VAPOL/VANOL  
IMIDODIPHOSPHORIMIDATE CATALYSTS IN ASYMMETRIC CATALYSIS**

**By**

**Aliakbar Mohammadlou**

**A DISSERTATION**

**Submitted to  
Michigan State University  
in partial fulfillment of the requirements  
for the degree of**

**Chemistry—Doctor of Philosophy**

**2020**

## ABSTRACT

### APPLICATION OF CHAMELEON CATALYST AND VAPOL/VANOL IMIDODIPHOSPHORIMIDATE CATALYSTS IN ASYMMETRIC CATALYSIS

By

Aliakbar Mohammadlou

In chapter 1 the discovery of chameleon catalysts was discussed. The chameleon catalyst was defined as an agent that can catalyze different reactions with different mechanisms. We have found that a chiral biaryl borate ester with two VANOL ligands and one boron complex is an extremely active catalyst for the epoxidation of aldehydes and the aziridination of imines. Mechanistic investigation revealed that this catalyst can catalyze epoxidation aziridination reactions with a different mechanism. We have shown that the aforementioned catalyst acts as a Lewis acid in the epoxidation of aldehydes and Brønsted acid in the aziridination of imines. X-ray structural analysis, Hammett study, and  $^{11}\text{B}$ -NMR study support our hypothesis.

In chapter two the discovery and utility of the aluminum VAPOL catalyst and aluminum VANOL catalyst were explored. We have found that a chiral biaryl aluminum with two VAPOL ligands and one aluminum complex is an extremely active catalyst for the epoxidation of aldehydes with diazo acetamide. The excellent performance of aluminum VAPOL catalyst has also shown in the total synthesis of (–)-tedanalactam which was accomplished in only 5 steps with excellent enantioinduction in 37% overall yield. The aluminum catalyst also performed well in the aziridination reaction transforming the imine into the aziridine with good yield and excellent ee. We believe the aluminum catalyst also acts as a chameleon; however, more experiments are required to show the chameleon behavior of these complexes.

In chapter three, inspired by Benjamin List's imidodiphosphorimidate catalysts, VANOL imidodiphosphorimidate (VIP) and VAPOL imidodiphosphorimidate (VAPIP) catalysts were

synthesized. X-ray structural analysis aided us to perform crystal engineering on VIP derivatives and design a highly efficient VIP catalyst for the asymmetric halonium-ion induced spiroketalization. VIP catalysts were also explored in the asymmetric intramolecular Schmidt reaction; however, no asymmetric induction was observed after exploring the reaction with a library of these catalysts.

I dedicate my dissertation to my dearest parents and also my brother, Hassan, for all of  
their support and love



## ACKNOWLEDGMENT

### **Professor Wulff**

I would like to express my deepest thanks and sincere gratitude to my Ph.D. advisor Prof. Wulff. Words cannot express how grateful I am for letting me be a member of your research group. For me, you are the one who changed my life entirely. Thanks a billion for showing me how to be a good synthetic chemist and also how to think and communicate like a scientist. You are my chemistry hero and it is my dream to be a chemist like you. Being in your lab and working under your supervision was the most exciting time of my life. I have enjoyed every single day of my graduate school under your guidance. I will miss our scientific discussion in our group meeting and post-group meeting the most. Finally, all I can say is thanks.

### **Prof. Borhan**

I also would like to thanks my second adviser Prof. Borhan. My gratitude to you knows no bounds because of all of the supports that I gain from you in my graduate school. I am proud that I was a part of your research team and also deeply appreciate your support and also your guidance in my graduate school. Again, thanks a billion for being there for me in which I am always in debt to you.

### **Prof. Maleczka and Prof. Jones**

I also would like to thanks my committee members Prof. Maleczka and Prof. Jones for their time and their effort in leading me through graduate school. I took CEM 852 with Prof. Maleczka which help me to build up my knowledge in organic synthesis and I am deeply thankful for that.

### **Dr. Vasileiou**

My deepest thanks and appreciation also goes to Chrysoula who supported me a lot in graduate school. Chrysoula, you are a very nice and supportive person, hopefully, one day I can pay back your kindness.

### **My Lab Mates in Wulff's group**

Undoubtedly, I had the best lab mates ever. Yubai, you were the nicest, knowledgeable, and quite lab mate that I had. I appreciate your passion for training me in the lab. Xiaopeng, thank you very much for teaching and also leading me in the chameleon project. I enjoyed our time doing research together a lot. Your smartness and also diligent in chemistry will make you a great chemist in the future. Li, thank you very much for being there for me, I gain your enormous support and also your invaluable friendship. You are smart and you will be a great chemist in near future. Yijing thanks a lot for all of your support, looking forward to seeing you in great places.

### **My lab Mates in Babak's Lab**

Babak's research group is a collection of nice, smart, knowledgeable, and diligent people. First of all, I should thank Ankush for collaborating on spiroketal project. Ankush, you are nice, industrious and a sharp person. I enjoyed my time in collaborating with you and also learned a lot from you. Debarshi and Soham, thanks a lot for being there for me, you are like my brothers and I wish you all the best in your future carrier. I should also thank my other lab member including Aritra, Dan, Emily, Mitch, Mehdi, Rahele, Aria, Jiao Jiao, Behrad, Homa, and Ishita for making Babak's lab a fantastic place to explore the chemistry.

### **My Undergraduate Students**

One of the privileges of being in the Wulff's lab is to get a chance to work with the best and talented undergraduate students at MSU. I should thanks to my undergraduate students, Emily,

Brendyne, Brian, and Virginia for their hard work and also their talent that they brought to our projects. Undoubtedly, all of them will be great scientists in the future.

### **My Classmates and Friends Outside of the Lab**

I would like to thanks my classmates including Johnathan, James, Gracelou, Ben, Evert, Ahinsa, and Nick for being there for me. I have already missed most of them since they graduated. A million thanks for my beloved friends, Mehdi, Nariman, Alireza, Reza, Rasoul, Kiana, Ali, Mehraban, Zahra, and many others who made my graduate school journey full of joys and excitements.

### **Saeedeh**

Saeedeh, I am blessed and thankful for being with you. You are my happiness and I would not be able to end my graduate school journey without your support. Thanks a lot for being there for me and I am very excited about what future has in the store for us.

## TABLE OF CONTENTS

LIST OF TABLES.....	xi
LIST OF FIGURES.....	xiii
LIST OF SCHEMES.....	xiv
Chapter 1	
Chameleon Catalyst.....	1
1.1. Introduction.....	2
1.1.1. Bronsted acid-assisted chiral Lewis acid (BLA) catalyst acts as a Lewis acid in Presence of aldehyde .....	3
1.1.2. Does the BLA catalyst act as a Lewis acid in Presence of imine or nitron? .....	6
1.2. Chameleon catalyst catalyzed asymmetric catalytic epoxidation of aldehyde with diazo compound .....	9
1.2.1. Introduction .....	9
1.2.2. Asymmetric catalytic epoxidation of aldehydes with diazo acetamides catalyzed by chiral polyborate organocatalysts .....	11
1.2.3. BLA catalyst derived from VANOL ligand as an extremely active catalyst in the epoxidation of aldehyde with diazo compound.....	15
1.2.4. Study of the Effect of DMSO in the Epoxidation Reaction .....	16
1.3. Asymmetric catalytic aziridination catalyzed by VANOL spiroborate anion .....	19
1.3.1. Introduction .....	19
1.3.2. VANOL spiroborate catalyze aziridination reaction.....	21
1.4. Experimental evidence for the chameleon behavior of catalyst I-3 .....	29
1.4.1. Crystal structure .....	29
1.4.2. Hammett study .....	33
1.4.2.1. Rational for the experiment .....	33
1.4.2.2. Hammett study for the aziridination reaction .....	36
1.4.2.3. Hammett study for epoxidation reaction .....	39
1.4.3. <sup>11</sup> B-NMR study .....	41
1.4.3.1. Rational for the experiment .....	41
1.4.3.2. <sup>11</sup> B-NMR of the catalyst I-3 and catalyst I-83 in presence of aldehyde and imine ..	42
1.4.3.3. Unfavorable binding of benzaldehyde to the catalyst I-3 .....	44
1.4.3.4. The use of as surrogates for benzaldehyde .....	45
1.4.3.5. Hammett study of catalyst I-3 in presence of amide .....	46
1.4.3.6. Hammett study of catalyst I-83 in presence of imine .....	48
1.5. Conclusion .....	50
1.6. Experimental .....	51
REFERENCES.....	76

## Chapter 2

Chameleon catalyst: Aluminum-VANOL Aluminum-VAPOL Catalysts as Efficient Catalysts in the Epoxidation of Aldehydes and Aziridination of Imines, Total Synthesis of (–) Tedanalactam.....81

2.1. Introduction: A brief history of aluminum catalysts in catalytic asymmetric synthesis.....	82
2.1.1. Aluminum catalyzed asymmetric catalytic reduction of ketone .....	82
2.1.1.1. Meerwein–Ponndorf–Verley reduction .....	82
2.1.1.2. Asymmetric hydroboration of ketone.....	84
2.1.2. Asymmetric catalytic Pudovik reaction .....	87
2.1.3. Asymmetric catalytic Strecker reaction of aldimines and ketimines .....	89
2.1.4. Claisen rearrangement.....	90
2.1.5. Diels-Alder reaction .....	92
2.1.6. Heteroatom Diels-Alder reaction .....	96
2.1.7. Catalytic asymmetric Michael addition reactions .....	98
2.1.8. Asymmetric Michael addition of Horner-Wadsworth-Emmons reagents and enones .....	105
2.2. Evaluating the Aluminum VANOL/VAPOL complexes as efficient catalysts in asymmetric catalytic epoxidation of aldehydes. ....	108
2.2.1. Optimization of epoxidation reaction.....	108
2.2.2. Epoxidation of aromatic aldehydes catalyzed by aluminum-VAPOL catalyst. ....	113
2.2.3. Epoxidation of aliphatic aldehydes and the total synthesis of (–)-tedanalactam .....	116
2.2.3.1. Introduction: A summary of all previous synthesis of (–)-tedanalactam .....	116
2.2.3.2. Aluminum catalyzed epoxidation of aliphatic aldehydes.....	122
2.2.3.3. Total synthesis of (–)-tedanalactam .....	130
2.3. Aluminum VANOL/VAPOL complexes as efficient catalysts in asymmetric catalytic aziridination of imine .....	131
2.4. Aluminum VANOL/VAPOL complexes as chameleon catalysts .....	134
2.5. Conclusion.....	135
2.6. Experimental.....	136
REFERENCES.....	161

## Chapter 3

Rational Design of VANOL/VAPOL Imidodiphosphorimidate Catalysts And Their Application in Asymmetric Halonium-Ion Induced Spiroketalization And Asymmetric Intramolecular Schmidt Reaction.....165

3.1. Introduction.....	166
3.1.1. The discovery of chiral biaryl phosphoric acid catalyst.....	166
3.1.2. VAPOL and VANOL phosphoric acid catalysts.....	173
3.1.3. Discovery and development of <i>N</i> -Triflyl-BINOL phosphoramidate .....	176
3.1.4. Synthesis of <i>N</i> -Triflyl-VANOL/VAPOL phosphoramidate .....	180
3.1.5. Rational design and synthesis of imidodiphosphoric acid catalysts .....	181
3.1.6. Synthesis and catalytic investigation of VAPOL imidodiphosphoric acid catalyst .....	185
3.1.7. Further attempts to improve the acidity of confined Brønsted acid catalyst.....	186

3.1.8. Extremely active imidodiphosphorimidate (IDPi) organocatalysts; a breakthrough in Brønsted acid catalysis .....	187
3.2. Extremely active imidodiphosphorimidate catalysts for asymmetric halonium-ion induced spiroketalization .....	193
3.2.1. Brønsted acid catalyzed halofunctionalization of alkenes .....	193
3.2.2. Chemical synthesis of spiroketals .....	197
3.2.3. Mechanistically inspired halonium ion-induced spiroketalization.....	203
3.2.4. Asymmetric catalytic halonium ion-induced spiroketalization.....	209
3.3. Asymmetric catalytic intramolecular Schmidt reaction.....	225
3.3.1. Introduction .....	225
3.3.2. VIP catalyst catalyzed intramolecular Schmidt reaction.....	229
3.4. Summary .....	232
3.5. Experimental .....	233
REFERENCES .....	271

## LIST OF TABLES

<b>Table I-1.</b> Epoxidation of aldehyde in presence of different sulfoxides .....	18
<b>Table I-2.</b> Epoxidation of benzaldehyde in the presence of chiral sulfoxides .....	19
<b>Table I-3.</b> Optimization of aziridination reaction .....	22
<b>Table I-4.</b> Further optimization of aziridination reaction .....	23
<b>Table I-5.</b> Different methods in catalyst preparation .....	24
<b>Table I-6.</b> Substrate scope of aziridination reaction .....	26
<b>Table I-7.</b> Substrate scope of aziridination reaction .....	28
<b>Table I-8.</b> Aziridination reaction catalyzed by spiroborate catalyst derived from 5,5'- disubstituted VANOL.....	37
<b>Table I-9.</b> Hammett plot of aziridination reaction .....	38
<b>Table I-10.</b> Hammett study in epoxidation reaction .....	39
<b>Table II-1.</b> Temperature optimization in aluminum catalyzed epoxidation reaction .....	109
<b>Table II-2.</b> Solvent and ligand optimization in aluminum VANOL/VAPOL catalyzed epoxidation reaction .....	110
<b>Table II-3.</b> Study of catalyst loading and diazo compound .....	111
<b>Table II-4.</b> Scope of aromatic substrate .....	115
<b>Table II-5.</b> Epoxidation of aldehyde II-166 to II-69 .....	124
<b>Table II-6.</b> Epoxidation of aldehyde II-171 catalyzed by chiral aluminum complexes .....	126
<b>Table II-7.</b> Substrate scope of aliphatic aldehydes .....	129
<b>Table II-8.</b> Aziridination reaction catalyzed by spiro-aluminate catalyst II-189.....	132
<b>Table III-1.</b> Catalyst optimization in a Mannich-type reaction .....	167
<b>Table III-2.</b> The effect of hydroxy group on reactivity in Mannich reaction .....	169

<b>Table III-3.</b> Catalyst optimization in Mannich-type reaction of N-Boc-imine III-18a .....	171
<b>Table III-4.</b> Catalyst optimization in the asymmetric reduction of imine .....	175
<b>Table III-5.</b> <i>N</i> -triflyl BINOL phosphoramidate catalyzed Diels-Alder reaction.....	177
<b>Table III-6.</b> <i>N</i> -triflyl BINOL phosphoramidate catalyzed enantioselective protonation of silyl enol ether .....	179
<b>Table III-7.</b> BINOL, VANOL and VAPOL Brønsted acid catalyst catalyzed symmetric spiroketalization .....	209
<b>Table III-8.</b> Asymmetric catalytic Schmidt reaction .....	229
<b>Table III-9.</b> Imidodiphosphorimidate catalysts catalyzed Schmidt reaction .....	230



## LIST OF FIGURES

<b>Figure I-1.</b> Cocrystal of spiroborate anion I-83b and imine I-84b.....	30
<b>Figure I-2.</b> Cocrystal of spiroborate anion I-83b and imine I-84b.....	30
<b>Figure I-3.a.</b> Cocrystal of spiroborate anion I-83b and imine I-84b.....	32
<b>Figure I-3.b.</b> Cocrystal of spiroborate anion I-83b and imine I-84b .....	32
<b>Figure I-4.</b> Cocrystal of spiroborate anion I-83c and imine I-84b.....	33
<b>Figure I-5.</b> Expected Hammett plot for the aziridination reaction.....	35
<b>Figure I-6.</b> Expected Hammett plot for the epoxidation reaction .....	35
<b>Figure I-7a.</b> <sup>11</sup> B-NMR of catalyst I-3 .....	43
<b>Figure I-7b.</b> <sup>11</sup> B-NMR of catalyst I-3 in presence of aldehyde (1.0 equiv).....	43
<b>Figure I-7c.</b> <sup>11</sup> B-NMR of catalyst I-83a in presence of imine, R = H, PG = Bzh, Ar = Ph.....	43
<b>Figure I-7d.</b> <sup>11</sup> B-NMR of co-crystal of catalyst I-83b in presence of imine, R = tBu, PG = MEDAM, Ar = Me <sub>2</sub> N-C <sub>6</sub> H <sub>4</sub> .....	43
<b>Figure I-7e.</b> <sup>11</sup> B-NMR of co-crystal of catalyst I-83c in presence of imine, R = Ad, PG = MEDAM, Ar = Me <sub>2</sub> N-C <sub>6</sub> H <sub>4</sub> .....	43
<b>Figure I-8.</b> <sup>11</sup> B-NMR of catalyst I-3 in presence of different equivof aldehyde .....	44
<b>Figure I-9a.</b> <sup>11</sup> B-NMR of catalyst I-3 in presence of 200 equiv aldehyde.....	45
<b>Figure I-9b.</b> <sup>11</sup> B-NMR of catalyst I-3 in presence of 1.0 equiv DMF .....	45
<b>Figure I-9c.</b> <sup>11</sup> B-NMR of catalyst I-3 in presence of 1.0 equiv N,N-dimethyl benzamide.....	45
<b>Figure I-10.</b> Hammett study of catalyst I-3 in presence of amide .....	47
<b>Figure I-11.</b> Hammett study of catalyst I-83 in presence of imine .....	49

## LIST OF SCHEMES

<b>Scheme I-1.</b> Concept of chameleon catalyst .....	2
<b>Scheme I-2.</b> Brønsted acid-assisted chiral Lewis acid .....	3
<b>Scheme I-3.</b> 2 <sup>nd</sup> generation of BLA catalyst .....	5
<b>Scheme I-4.</b> Diels-Alder reaction catalyzed by catalyst I-19 .....	5
<b>Scheme I-5.</b> Aldol type and aza Diles-Alder reaction of imine I-20.....	6
<b>Scheme I-6.</b> Dynamic ligand exchange between catalysts I-27 and I-25.....	6
<b>Scheme I-7.</b> Pickett-Spengler reaction promoted by I-25 complex .....	8
<b>Scheme I-8.</b> Diazo addition to aldehyde .....	9
<b>Scheme I-9.</b> Catalytic asymmetric aldol addition of diazo to aldehydes .....	10
<b>Scheme I-10.</b> Asymmetric catalytic Roskamp reaction .....	11
<b>Scheme I-11.</b> Asymmetric catalytic epoxidation of aldehyde with diazo acetamide.....	12
<b>Scheme I-12.</b> Asymmetric catalytic cis- and trans-aziridination .....	13
<b>Scheme I-13.</b> Catalyst I-48 catalyzed asymmetric epoxidation .....	14
<b>Scheme I-14.</b> Asymmetric catalytic epoxidation catalyzed by catalyst catalyst I-3 .....	16
<b>Scheme I-15.</b> Epoxidation reaction .....	17
<b>Scheme I-16.</b> Aziridination catalyzed by spiroborate anion-copper complex .....	20
<b>Scheme I-17.</b> Spiroborate anion induced enantioselectivity in asymmetric hydrogenation .....	20
<b>Scheme I-18.</b> Aziridination reaction .....	27
<b>Scheme I-19.</b> Different mechanism.....	29
<b>Scheme I-20.</b> Synthesis of 5,5'-disubstituted VANOL ligand.....	34
<b>Scheme I-21.</b> Aziridination and epoxidation reaction.....	36

<b>Scheme I-22a.</b> cis- and trans-aziridination.....	41
<b>Scheme I-22b.</b> Proposed mechanism for the epoxidation.....	41
<b>Scheme II-1.</b> MPV reduction .....	82
<b>Scheme II-2.</b> Catalytic MPV reduction.....	83
<b>Scheme II-3.</b> Asymmetric catalytic MPV reduction.....	83
<b>Scheme II-4.</b> Proposed catalytic cycle .....	84
<b>Scheme II-5.</b> Ketone hydroboration.....	85
<b>Scheme II-6.</b> Proposed mechanism.....	86
<b>Scheme II-7.</b> Asymmetric catalytic Pudvik reaction .....	87
<b>Scheme II-8.</b> Asymmetric catalytic Pudvik reaction .....	88
<b>Scheme II-9.</b> Asymmetric catalytic Strecker reaction .....	89
<b>Scheme II-10.</b> Asymmetric Claisen reaction .....	90
<b>Scheme II-11a.</b> Asymmetric Claisen reaction .....	91
<b>Scheme II-11b.</b> Synthesis of ligand II-60 .....	91
<b>Scheme II-12.</b> Asymmetric catalytic Diels-Alder reaction.....	92
<b>Scheme II-13.</b> Asymmetric catalytic Diels-Alder reaction.....	94
<b>Scheme II-14.</b> Asymmetric catalytic Diels-Alder reaction.....	95
<b>Scheme II-15.</b> Additives in the Diels-Alder reaction.....	96
<b>Scheme II-16.</b> Proposed catalytic cycle .....	97
<b>Scheme II-17.</b> Asymmetric catalytic hetero atom Diles-Alder reaction.....	98
<b>Scheme II-18.</b> Catalytic asymmetric Michael addition reactions .....	99
<b>Scheme II-19.</b> Proposed mechanism.....	100
<b>Scheme II-20.</b> Asymmetric tandem Michael addition enolate reaction.....	102

<b>Scheme II-21.</b> Proposed mechanism .....	103
<b>Scheme II-22.</b> Conjugate addition of nitroso to enone .....	104
<b>Scheme II-23.</b> Asymmetric Michael addition of Horner-Wadsworth-Emmons reagent .....	105
<b>Scheme II-24.</b> Proposed mechanism .....	106
<b>Scheme II-25.</b> Michael addition .....	107
<b>Scheme II-26.</b> Epoxidation reaction .....	108
<b>Scheme II-27.</b> Epoxidation reaction catalyzed by Aluminum-VANOL-DMSO-complex .....	112
<b>Scheme II-28.</b> Structure of II-14, aluminum-VANOL catalyst .....	113
<b>Scheme II-29.</b> Enantioinduction reversal in epoxidation reaction catalyzed with boron and aluminum catalysts .....	114
<b>Scheme II-30.</b> Piperidine alkaloids in kava shrubs .....	116
<b>Scheme II-31.</b> Retrosynthesis analysis of (–)-tedanalactam II-123 by Tilve <sup>22</sup> .....	117
<b>Scheme II-32.</b> Total synthesis of (–)-tedanalactam <sup>22</sup> .....	118
<b>Scheme II-33.</b> Retrosynthesis of (–)-tedanalactam by Nagarapu <sup>23</sup> .....	119
<b>Scheme II-34.</b> Total synthesis of (–)-tedanalactam by Nagarapu <sup>23</sup> .....	120
<b>Scheme II-35.</b> Total synthesis of (–)-tedanalactam presented by Sartillo-Piscil <sup>24</sup> .....	121
<b>Scheme II-36.</b> Total synthesis of natural product II-165 presented by Sartillo-Piscil .....	123
<b>Scheme II-37.</b> Enantioinduction reversal in epoxidation reaction catalyzed with boron and aluminum catalysts .....	127
<b>Scheme II-38.</b> Total synthesis of (–)-tedanalactam .....	130
<b>Scheme II-39.</b> Enantioinduction reversal in epoxidation reaction catalyzed with boron and aluminum catalysts .....	133
<b>Scheme II-40.</b> Aluminum-VANOL catalyst possess chameleon behavior .....	134
<b>Scheme III-1.</b> Proline catalyzed asymmetric C-C formation .....	166
<b>Scheme III-2.</b> Asymmetric catalytic Mannich type reaction .....	168

<b>Scheme III-3.</b> Basicity of imine vs amine.....	169
<b>Scheme III-4.</b> Proposed mechanism .....	170
<b>Scheme III-5.</b> Catalyst optimization in Mannich type reaction of N-Boc-imine III-18 .....	172
<b>Scheme III-6.</b> Direct alkylation of diazo compound.....	173
<b>Scheme III-7.</b> Direct alkylation of diazo compound.....	174
<b>Scheme III-8.</b> Asymmetric reduction of imine III-28 catalyst by chiral phosphoric acid catalyst .....	176
<b>Scheme III-9.</b> N-triflyl BINOL phosphoramidate catalyzed Diles-Alder reaction .....	178
<b>Scheme III-10.</b> Proposed mechanism for enantioselective protonation of silyl enol ether .....	180
<b>Scheme III-11.</b> Synthesis of VANOL/VAPOL phosphoramidate.....	182
<b>Scheme III-12.</b> BINOL phosphoric acid catalyzed asymmetric spiroketalization .....	183
<b>Scheme III-13.</b> Dual functionality of BINOL phosphoric acid .....	183
<b>Scheme III-14.</b> Confined BINOL Brønsted acid catalyzed asymmetric spiroketalization.....	184
<b>Scheme III-15.</b> Enantioselective Freidel-Crafts reaction.....	185
<b>Scheme III-16.</b> Asymmetric vinylogous Mannich reaction.....	186
<b>Scheme III-17.</b> Asymmetric Prins cyclzation .....	187
<b>Scheme III-18.</b> Synthesis and catalytic utility of imidodiphosphoramidate IDP <sub>i</sub> in heteroatom Diels-Alder reaction .....	188
<b>Scheme III-19a.</b> Enantioselective olefin protonation .....	189
<b>Scheme III-19b.</b> Hammett study.....	189
<b>Scheme III-20.</b> Proposed mechanism for enantioselective protonation of olefin.....	190
<b>Scheme III-21a.</b> Classical carbocation vs non-classical carbocation .....	191
<b>Scheme III-21b.</b> Enantioselective S <sub>N</sub> 1 reaction reported by Jacobsen .....	191
<b>Scheme III-21c.</b> Stereoselective reaction onto non-classical carbocation.....	191
<b>Scheme III-21d.</b> Anchimeric effect in exo vs endo isomer .....	112

<b>Scheme III-22.</b> Generation of non-classical carbocation with various substrates .....	192
<b>Scheme III-23.</b> Enantioselective bromocyclization catalyzed by BINOL phosphoric acid catalyst .....	194
<b>Scheme III-24a.</b> Enantioselective bromocyclization catalyzed by BINOL phosphoric acid catalyst.....	195
<b>Scheme III-24b.</b> Proposed mechanism for the bromocyclization with III-40 .....	195
<b>Scheme III-24c.</b> Enantioselective polyene cyclization .....	196
<b>Scheme III-25.</b> Natural products containing spiroketal component .....	198
<b>Scheme III-26a.</b> Anomerich effect in spiroketal .....	199
<b>Scheme III-26b.</b> Anomerich effect in [6,6]-spiroketal .....	199
<b>Scheme III-26c.</b> Anomerich effect in [6,5] and [5,5] spiroketals .....	199
<b>Scheme III-27a.</b> General approach in synthesis of spiroketal .....	200
<b>Scheme III-27b.</b> Dynamic stereoselective spiroketalization .....	200
<b>Scheme III-28.</b> Confined BINOL Brønsted acid catalyzed asymmetric spiroketalization.....	201
<b>Scheme III-29.</b> BINOL Brønsted acid catalyzed asymmetric spiroketalization.....	202
<b>Scheme III-30.</b> Vinyl substituted spiroketal synthesis catalyzed by Ir-(P, olefin) complex .....	203
<b>Scheme III-31a.</b> Commonly depicted electrophilic addition of halide to olefin .....	204
<b>Scheme III-31b.</b> The effect of the nucleophile in the halofunctionalization of olefin .....	204
<b>Scheme III-31c.</b> Nucleophile-assisted alkene activation (NAAA) .....	204
<b>Scheme III-32.</b> Bromo spiroketalization with unprotected pendant alcohol .....	206
<b>Scheme III-33.</b> Stereoselective halonium ion induced spiroketalization.....	207
<b>Scheme III-34.</b> Dibromo spiroketalization in the absence of EtOH .....	208
<b>Scheme III-35a.</b> Asymmetric catalytic spiroketalization catalyzed by VAPIP III-163a.....	211
<b>Scheme III-35b.</b> Asymmetric catalytic spiroketalization catalyzed by VAPIP III-163b .....	212

<b>Scheme III-36.</b> Synthesis of 6,6'-Naph <sub>4</sub> VIP catalyst .....	213
<b>Scheme III-37.</b> Asymmetric catalytic spiroketalization catalyzed by 7,7'-Ar <sub>4</sub> VIP catalyst .....	214
<b>Scheme III-38.</b> Asymmetric catalytic spiroketalization catalyzed by 7,7'-Naph <sub>4</sub> VIP catalyst .....	215
<b>Scheme III-39.</b> Asymmetric catalytic spiroketalization catalyzed by catalyst III-165j .....	216
<b>Scheme III-40.</b> Asymmetric catalytic spiroketalization catalyzed by catalyst III-165j .....	217
<b>Scheme III-41.</b> Dihedral angle effect in spiroketalization .....	218
<b>Scheme III-42.</b> Asymmetric catalytic spiroketalization catalyzed by catalyst III-169f .....	220
<b>Scheme III-43.</b> Asymmetric catalytic spiroketalization catalyzed by 7,7'-R <sub>4</sub> VIP catalysts .....	221
<b>Scheme III-44.</b> Asymmetric catalytic spiroketalization catalyzed by 7,7'-tBu <sub>4</sub> VIP catalysts ...	222
<b>Scheme III-45.</b> Asymmetric catalytic spiroketalization catalyzed by catalyst III-169k .....	223
<b>Scheme III-46.</b> Asymmetric catalytic spiroketalization catalyzed by 7,7'-R <sub>4</sub> VIP catalyst .....	225
<b>Scheme III-47.</b> Intramolecular Schmidt reaction .....	225
<b>Scheme III-48.</b> Product inhibition in Schmidt reaction .....	226
<b>Scheme III-49.</b> Asymmetric intramolecular Schmidt reaction with chiral auxiliaries .....	227
<b>Scheme III-50.</b> Asymmetric Schmidt reaction mediated by chiral Brønsted acid .....	227
<b>Scheme III-51.</b> Overcoming product inhibition in Schmidt reaction .....	228
<b>Scheme III-52.</b> Protonated HFIP is the actual catalyst in Schmidt reaction .....	231

## **Chapter 1**

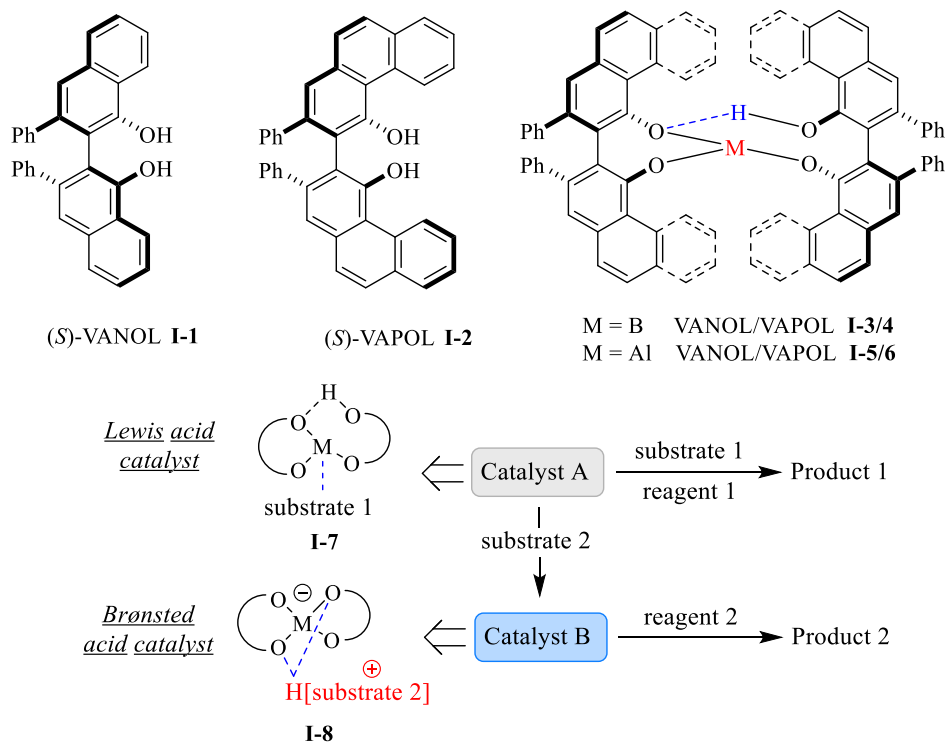
### **Chameleon Catalyst**



## 1.1. Introduction

We define chameleon catalyst as an agent that can catalyze different reactions with different mechanisms (Scheme I-1). In other words, catalyst A can catalyze the reaction of substrate 1 and reagent 1 to give product 1. In the presence of substrate 2 the same catalyst forms a complex that is distinctly different from catalyst A (catalyst B) both in function and structure. Catalyst B will promote the formation of product 2 by a mechanism that is different from the mechanism by which catalyst A operates. Recently, we have discovered that VANOL/VAPOL catalysts type **I-3 - I-6** are extremely efficient in activating aldehydes via a Lewis acid-Lewis base interaction and imine via protonation.<sup>25</sup> In other words, an aldehyde will coordinate to the catalyst **A** and form a Lewis acid/Lewis base complex **I-7** whereas, the same catalyst will protonate an imine and form a spiroborate/aluminate anion **I-8** which hydrogen bonds to a protonate imine; therefore, the catalyst acts as a chiral Brønsted acid catalyst.

**Scheme I-1.** Concept of Chameleon Catalyst

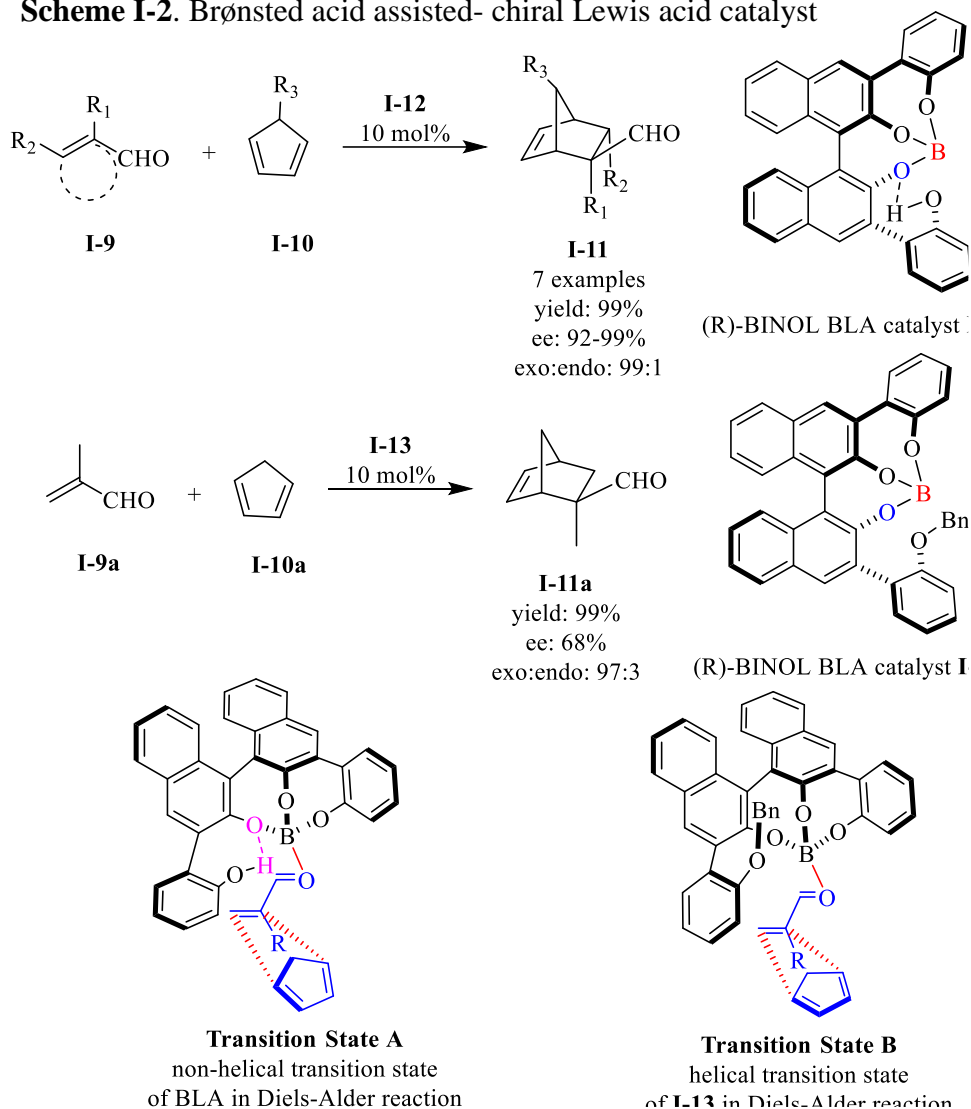


### 1.1.1. Brønsted acid-assisted chiral Lewis acid (BLA) catalyst acts as a Lewis acid in

#### Presence of aldehyde

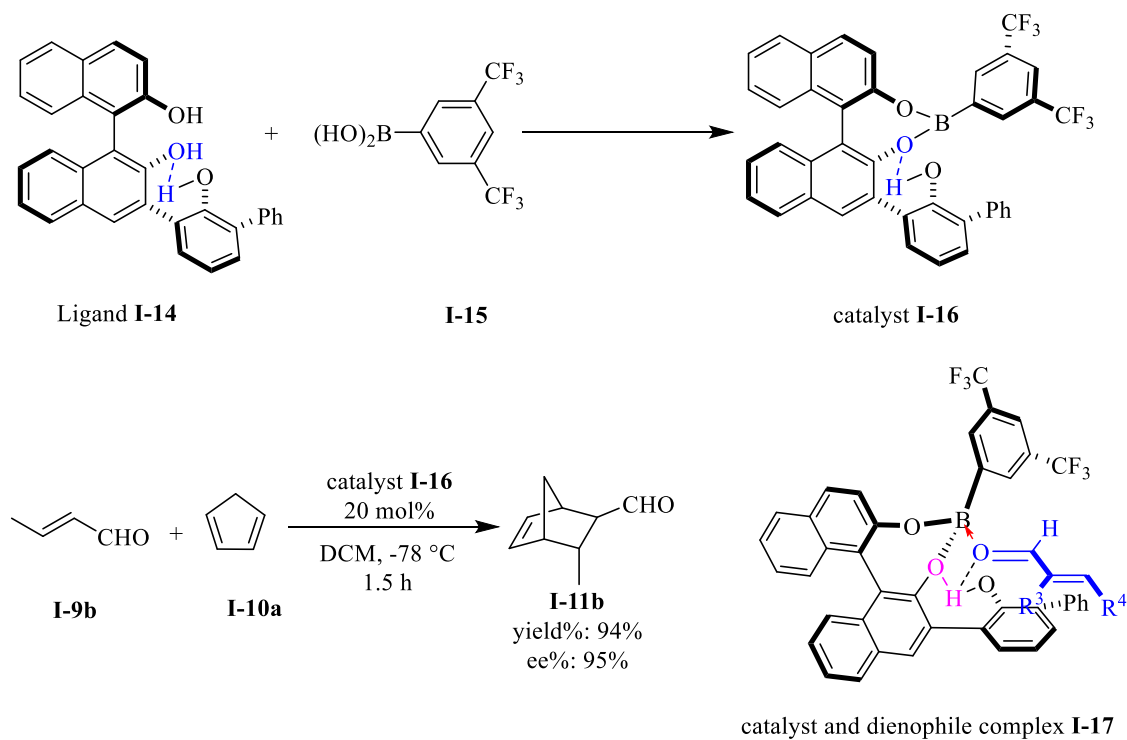
Yamamoto was the first to report the asymmetric catalytic Diels-Alder reaction of  $\alpha$ -substituted  $\alpha$ ,  $\beta$ - enals **I-9** with dienes in presence of boron-BINOL catalyst **I-12**.<sup>2</sup> The structure of the catalyst (structure **I-12**, scheme I-2) was proposed to be a three coordinated boron species with an intramolecular hydrogen bond between the hydroxyl of a phenoxy moiety and the oxygen of naphthol. The aforementioned hydrogen bonding was crucial in this catalytic system since it was proposed to lead to an increase in Lewis acidity of the boron and  $\pi$ -basicity of the phenoxy moiety.

**Scheme I-2.** Brønsted acid assisted- chiral Lewis acid catalyst



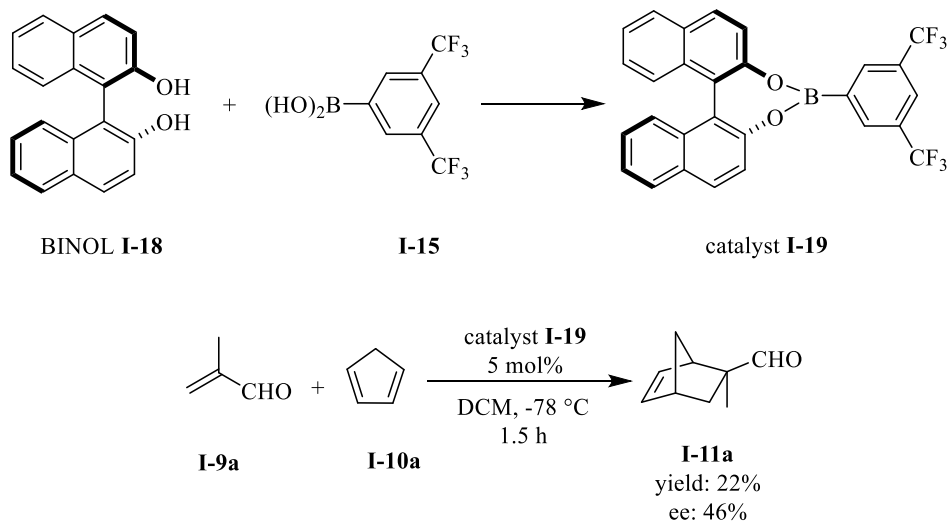
The dienophile activated via a Lewis acid-Lewis base interaction (complex **I-7**, scheme I-1) and the phenoxy moiety blocks the *si*-face of the dienophile via  $\pi$ - $\pi$  interaction between the  $\pi$ -acidic dienophile and the  $\pi$ -basic phenoxy moiety. As a result, the *Re* face of the dienophile remains open to the diene's approach (transition state A, scheme I-2). As a proof of concept, a control experiment was conducted to shed light on the necessity of the aforementioned intramolecular hydrogen bond in the asymmetric catalytic Diels-Alder reaction. Therefore, a boron catalyst **I-13** was synthesized but the same catalyst yielded the Diels-Alder adduct with only 68% *ee* (scheme I-2, eq. 2). These results enabled Yamamoto to propose a fixed non-helical transition state Brønsted acid assisted-chiral Lewis acid (BLA) catalyst with tetrol BINOL ligand (transition state A, scheme I-2) and a helical transition state with triol BINOL ligand (transition state B, scheme I-2). However, the BLA catalyst **I-12** had limited scope, the presence of an  $\alpha$ -substitution on the  $\alpha$ ,  $\beta$ -unsaturated enals was required for good enantioselectivity. Later, in 1996, Yamamoto reported the 2<sup>nd</sup> generation BLA catalyst which was highly reactive for  $\alpha$ -unsubstituted and  $\beta$ -substituted  $\alpha$ ,  $\beta$ -enals substrates **I-9b** (scheme I-3).<sup>3,4</sup> BLA catalyst **I-16** was prepared in situ by treating boronic acid **I-15** and chiral triol ligand **I-14**. The structure of this catalyst was proposed to be a three coordinate boron species with an intramolecular hydrogen bond between the hydroxy of the phenol substituent and the naphthol oxygen of the BINOL. The enantioselectivity and diastereoselectivity were rationalized based on the catalyst and aldehyde complex **I-17** which was analogous to the proposed transition state for BLA catalyst **I-12** (transition state A in scheme I-2). The higher reactivity of BLA 2<sup>nd</sup> generation catalyst (catalyst **I-16**) was due to the strong electron withdrawing effect of the trifluoromethyl groups as well as the intramolecular hydrogen bond in the catalyst. These two effects concomitantly increased the Lewis acidity of BINOL-BLA catalyst **I-16** and made it a highly reactive catalyst for a wide substrate of dienophiles.

**Scheme I-3.** 2<sup>nd</sup> generation of BLA catalyst



Catalyst **I-19** was also investigated in the Diels-Alder reaction; however, the desired product was produced in only 22% yield and 46% *ee* (scheme I-4).

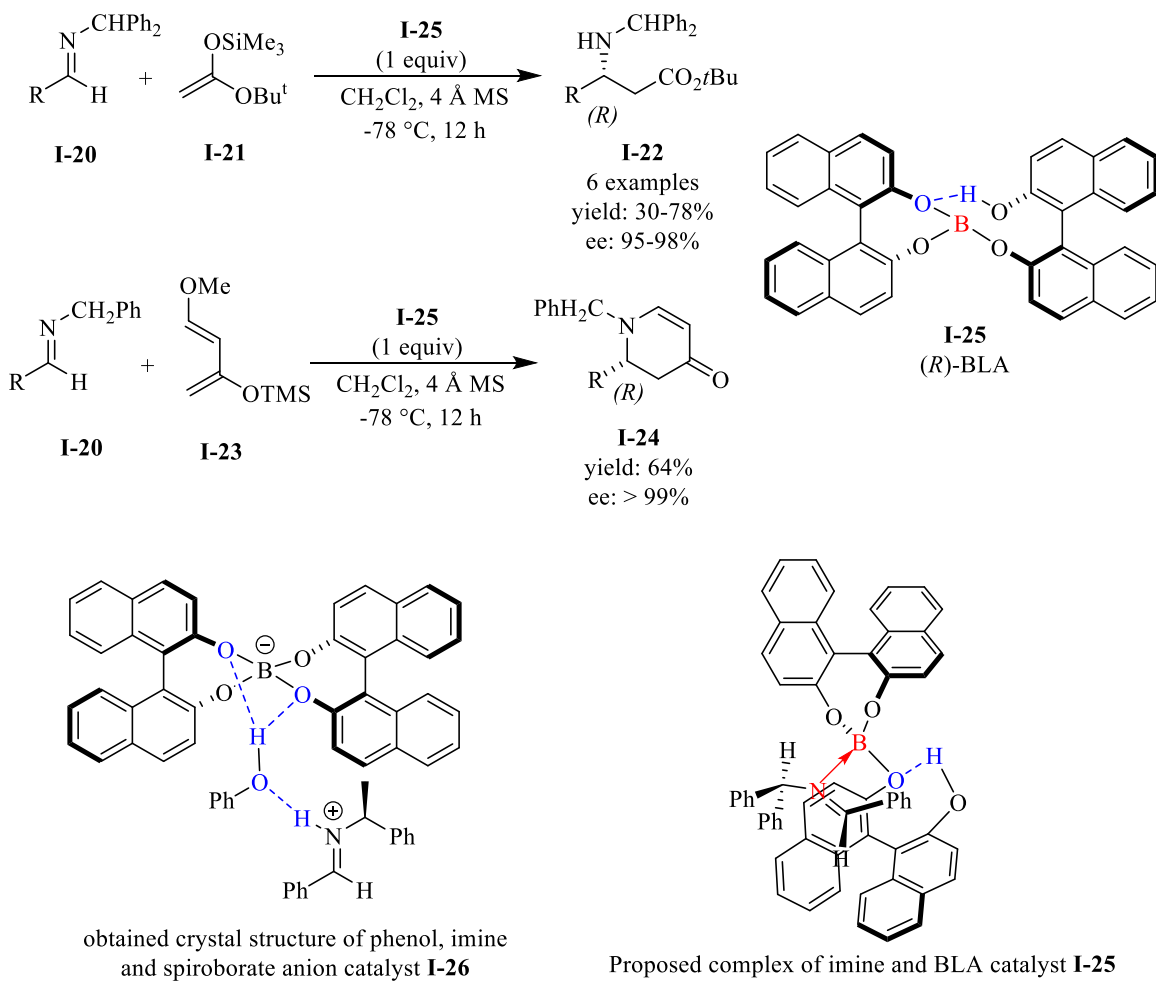
**Scheme I-4.** Diels-Alder reaction catalyzed by catalyst **I-19**



### 1.1.2. Does the BLA catalyst act as a Lewis acid in Presence of imine or nitrone?

In 1994, Yamamoto also reported a biaryl-boron BLA catalyst **I-25** as an efficient promoter for the asymmetric aza Diels-Alder and adol-type reaction of imine **I-20** (scheme I-5).<sup>5</sup> The catalyst was prepared from a 2:1 ratio of BINOL ligand and a borate ester. Structurally, as depicted in scheme 5 the biaryl-boron catalyst **I-25** demonstrated a three coordinated boron species with an intramolecular hydrogen bond between the hydroxy of one BINOL ligand and an oxygen of the other ligand and thus has a proposed structure similar to that of catalyst **I-12** (scheme I-2).

**Scheme I-5.** Aldol-type and aza-Diels-Alder reaction of imine I-20

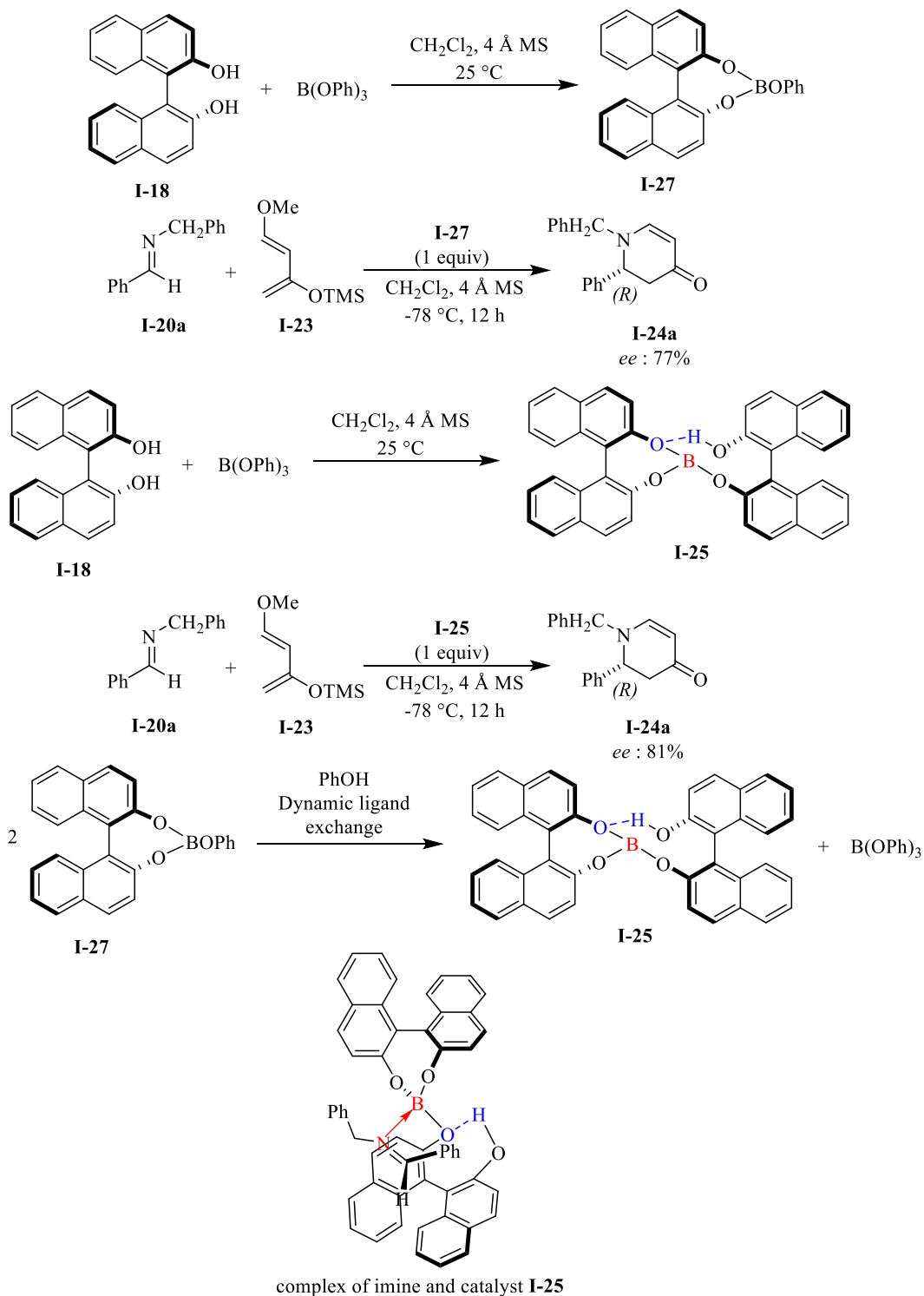


Due to the higher basicity of products in the aza Diels-Alder and aldol-type reactions, a stoichiometric amount of the catalyst was used in order to avoid product inhibition. Crystal structure analysis of a co-crystal of BLA catalyst **I-25**, chiral imine and phenol, revealed the presence of spiroborate anion **I-26** species, hydrogen bonded to phenol which in turn was H-bonded to a protonated imine.<sup>6</sup> This structure clearly indicated that there was not a bonding interaction between the nitrogen of the imine and the boron of the catalyst. This paper was the first report of the chiral spiro-borate anion **I-26** derived from the BLA catalyst **I-25**. However, in this report, it was proposed that the BLA catalyst **I-25** functions as a Lewis acid catalyst and that the imine was activated via Lewis acid-Lewis base interaction as indicated in complex of imine and catalyst **I-25**, this mechanism for imine activation was proposed for both the aldol type reaction with silyl ketene acetal **I-12** and Diels-Alder reaction with diene **I-23** (unified mechanism) (scheme I-5).

The aza-Diels-Alder reaction was further explored by Bull and James.<sup>7</sup> In order to gain more information about the structure of the enantioinducing catalyst species, a non-linear study was pursued. Two sets of experiments were conducted by using scalemic BINOL species. In the first experiment, the catalyst was prepared with 1.0 equiv of BINOL ligand **I-18** and 1.0 equiv of B(OPh)<sub>3</sub> (scheme I-6, catalyst **I-27**). In the second experiment, the catalyst was prepared with 2.0 equiv of BINOL ligand **I-18** and 1.0 equiv of B(OPh)<sub>3</sub> (catalyst **I-25**). Both of the catalysts **I-27** and **I-25** demonstrated a significant positive non-linear effect which clearly showed the involvement of two BINOL ligands in the active catalyst species. As a result, it was proposed that the active catalyst in both reactions is catalyst **I-25** and that catalyst **I-27** could be converted to catalyst **I-25** via dynamic ligand exchange with phenol. In terms of mechanism, it was proposed that the catalyst **I-25** was acting as Lewis acid catalyst in presence of imine, the same mechanism

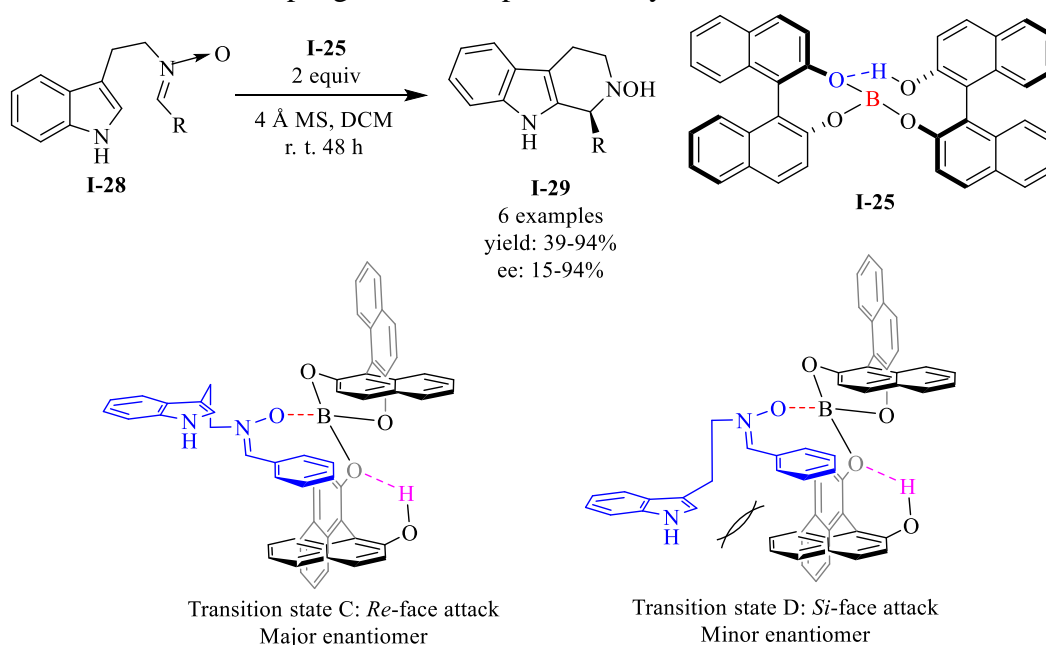
which was proposed by Yamamoto for the same reaction (scheme I-6, complex of imine and catalyst **I-25**).

**Scheme I-6.** Dynamic ligand exchange between catalysts **I-27** and **I-25**



In 1998, Nakagawa reported catalyst **I-25** mediates the Pictet-Spengler reaction of nitron **I-28**.<sup>8</sup> He also proposed that the catalyst acts as a Lewis acid mediator and activates the nitron **I-28** via Lewis acid-Lewis base interaction (scheme I-7). These reports have led people to assume that catalyst **I-25** (activation of imine or nitron via Lewis acid-Lewis base interaction with catalyst **I-25**) activates imines and nitrones via a transition state involving Lewis acid activation by boron even though there was no evidence for this.

**Scheme I-7.** Pictet-Spengler reaction promoted by **I-25**



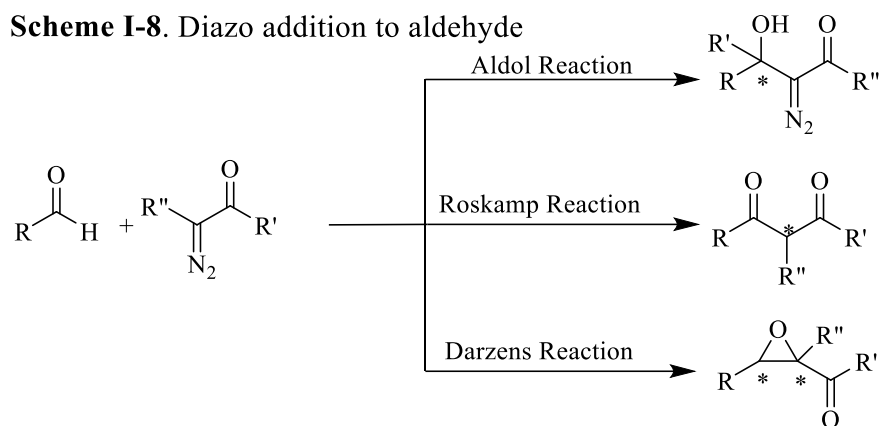
## 1.2. Chameleon catalyst catalyzed asymmetric catalytic epoxidation of aldehyde with diazo compound

### 1.2.1. Introduction

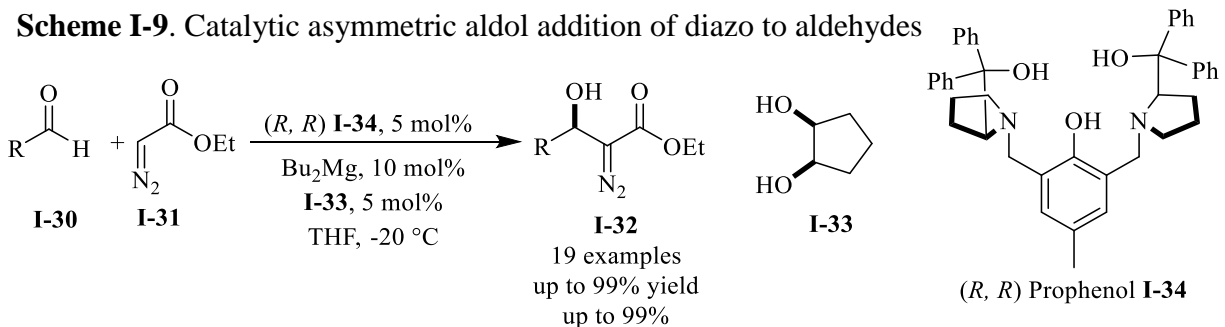
Chiral epoxides are important structural motifs in organic synthesis because of their facile transformation to a wide variety of target molecules.<sup>9</sup> Therefore, synthesis of chiral epoxides has drawn great attention in asymmetric catalysis. The most common approach to the synthesis of enantioenriched epoxide is the oxidation of alkenes in presence of a proper catalyst. Sharpless was the one who first presented an elegant strategy in the epoxidation of primary and secondary allylic



alcohols by using  $\text{Ti}(\text{O}^i\text{Pr})_4$  and diethyl tartarate as a chiral ligand in presence of *tert*-butyl hydroperoxide (THP) as an oxidant.<sup>10</sup> An uncommon approach to the synthesis of chiral epoxides relies on the asymmetric addition of diazo compounds to readily available aldehydes. In the desired addition of a diazo to an aldehyde in a Darzens type reaction, which yields the epoxide, there can be competing reactions. These include, the Roskamp reaction and the aldol reaction (scheme I-8).<sup>11,12</sup>

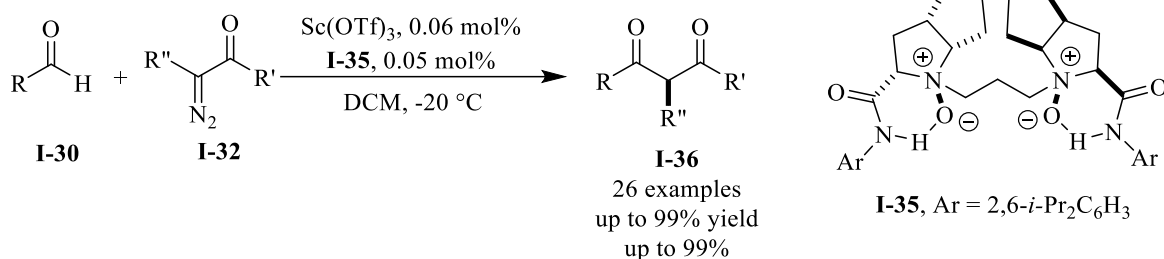


The first well developed reaction involving the addition of the diazo compound to an aldehyde, is the aldol addition. The asymmetric version of this reaction was reported by Trost, which involved the asymmetric addition of ethyl diazoacetate **I-31** to an aldehyde **I-30** catalyzed by a chiral dinuclear magnesium-Propenol complex (scheme I-9).<sup>13,14</sup>



The second competing reaction with the Darzens type reaction is known as the Roskamp reaction, along with its asymmetric version documented by Feng (scheme 10).<sup>15</sup>

### Scheme I-10. Asymmetric catalytic Roskamp reaction

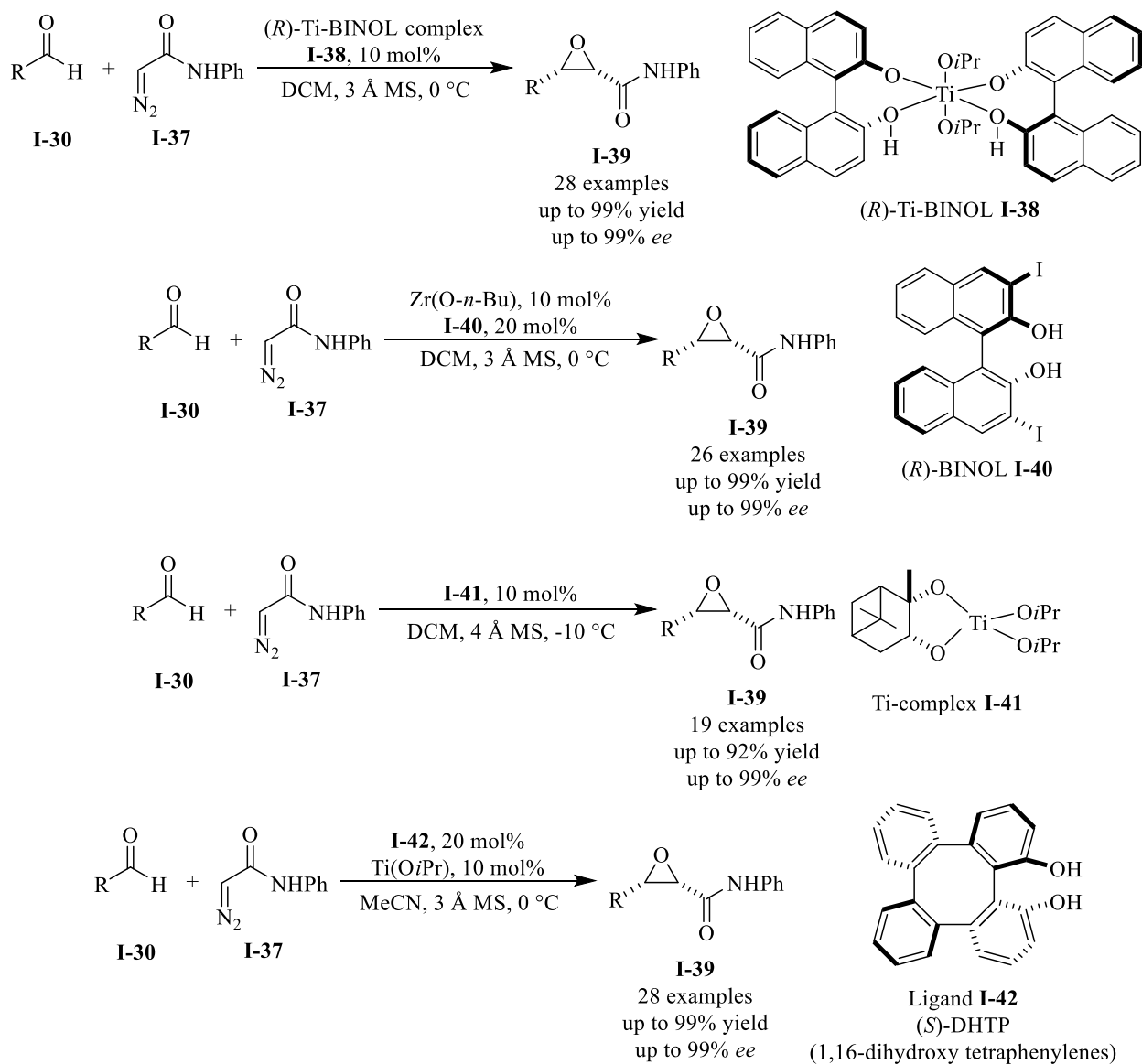


In 2009, Gong was able to overcome these challenges and reported the first efficient asymmetric catalytic diazo Darzens reaction of aldehyde **I-30** with secondary  $\alpha$ -diazo acetamide **I-37** (scheme I-11).<sup>16</sup> Chiral titanium-BINOL complex **I-38** enabled him to achieve excellent yield and enantioselectivity in the epoxidation of aldehyde **I-30**. In 2011, he also reported an air-stable zirconium complex with 3,3'-diiodo-BINOL **I-40** as an efficient catalyst in the asymmetric diazo Darzens reaction.<sup>17</sup> However, the structure of the active catalyst is not known to date.<sup>18</sup> Wide substrate scope was tolerated and epoxides **I-39** were produced with excellent yield and *ee* but *no explanation was given about the nature of the diastereoselectivity (cis vs. trans-selectivity)*. Sun and Wong also reported the asymmetric catalytic diazo Darzens reaction catalyzed by a (+)-pinanediol **I-41**- $\text{Ti}(\text{O}^i\text{Pr})_4$  and 1, 16-dihydroxytetraphenylene **I-42**- $\text{Ti}(\text{O}^i\text{Pr})_4$  complexes (scheme I-11).<sup>19,20</sup> To the best of our knowledge, to date, there was no reported non-transition metal catalyst catalyzed asymmetric diazo Darzens of aldehyde with diazo compound.

#### 1.2.2. Asymmetric catalytic epoxidation of aldehydes with diazo acetamides catalyzed by chiral polyborate organocatalysts

Our lab has discovered that a VANOL/VAPOL derived-BOROX catalyst **I-46/I-47** is an efficient catalyst for the synthesis of both *cis* and *trans*-aziridines (scheme 12).<sup>21,22,23</sup> The reaction between imine **I-43** and ethyl diazoacetate **I-31** yielded *cis*-aziridines **I-44** with excellent yield and *ee*. Inspired by the asymmetric catalytic aziridination reported by Mauroka,<sup>24</sup> we have found that simply changing the ethyl diazoacetate **I-31** to the secondary diazo acetamide **I-39**, the

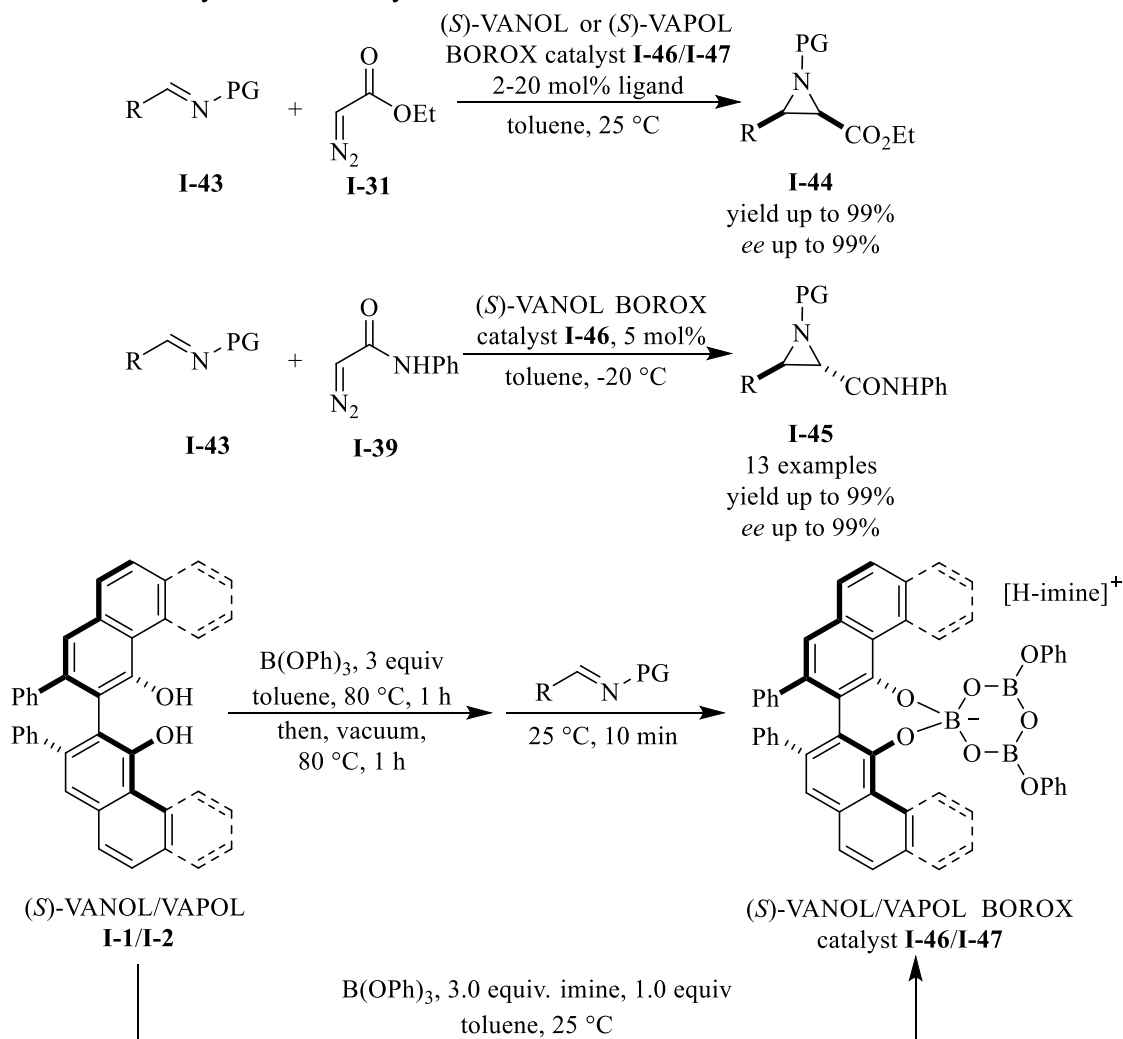
**Scheme 11.** Asymmetric catalytic epoxidation of aldehyde with diazo acetamide



VANOL/VAPOL-BOROX catalyst **I-46/I-47** can catalyze the asymmetric *trans*-aziridination of imine **I-43**. The nature of this switch in diastereoselectivity from *cis* to *trans*-aziridination was found to be because of an extra-hydrogen bond that the secondary diazo acetamide **I-39** can form with the BOROX catalyst.<sup>25</sup> We have also discovered that the VANOL/VAPOL-BOROX catalysts **I-46/I-47** can be assembled by mixing either the VANOL ligand **I-46** or VAPOL ligand

**I-47**, B(OPh)<sub>3</sub> and an imine or amine since imines or amines are basic enough to assemble the catalyst **I-46/I-47**.<sup>26</sup>

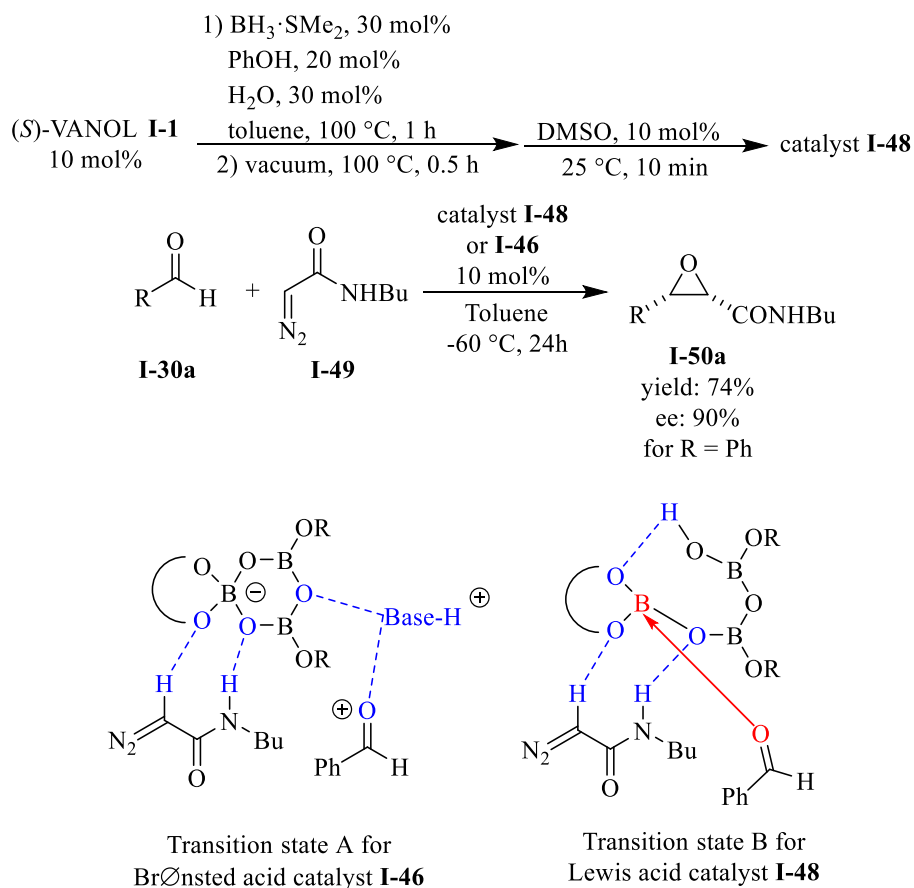
**Scheme 12.** Asymmetric catalytic *cis*- and *trans*-aziridination



Next we turned our attention toward asymmetric catalytic epoxidation reactions catalyzed by BOROX catalyst **I-46/I-47**. Neither diazoacetamide **I-49** nor aldehyde **I-30a** are basic enough to assemble the BOROX catalyst. Therefore, it was envisioned that a non-reacting base might help to assemble the BOROX catalyst but not intervene in the reaction. After extensive screening, it was found that DMSO was the optimum base in assembling the active catalyst. This finding led us to develop a highly efficient catalytic system for the epoxidation of aldehydes **I-30** with diazo

acetamide **I-49** (scheme I-13).<sup>1</sup> The catalyst was prepared by mixing 10 mol% of VANOL ligand, 30 mol% of  $\text{BH}_3\cdot\text{SMe}_2$ , 20 mol% of  $\text{PhOH}$  and 30 mol% of  $\text{H}_2\text{O}$  followed by heating the mixture at 100 °C for 1 hour, and then applying high vacuum at 100 °C in order to remove the volatiles. This was followed by addition of 10 mol% of DMSO and stirring the obtained mixture for another hour. This catalyst was highly reactive in the asymmetric epoxidation of aldehyde **I-30** with secondary diazo acetamide **I-49**. A wide range of aromatic and aliphatic aldehydes were tolerated and yielded epoxides **I-50** in good yields and excellent enantioselectivities.

**Scheme I-13.** Catalyst I-48 catalyzed asymmetric epoxidation



Next, we investigated whether the BOROX catalyst **I-46/I-47** is the active catalyst in this reaction. The study of the reaction showed a linear relationship between the *ee* of the epoxide **I-50** and the *ee* of the VANOL ligand **I-1**. This result clearly indicated that the active catalyst contains only

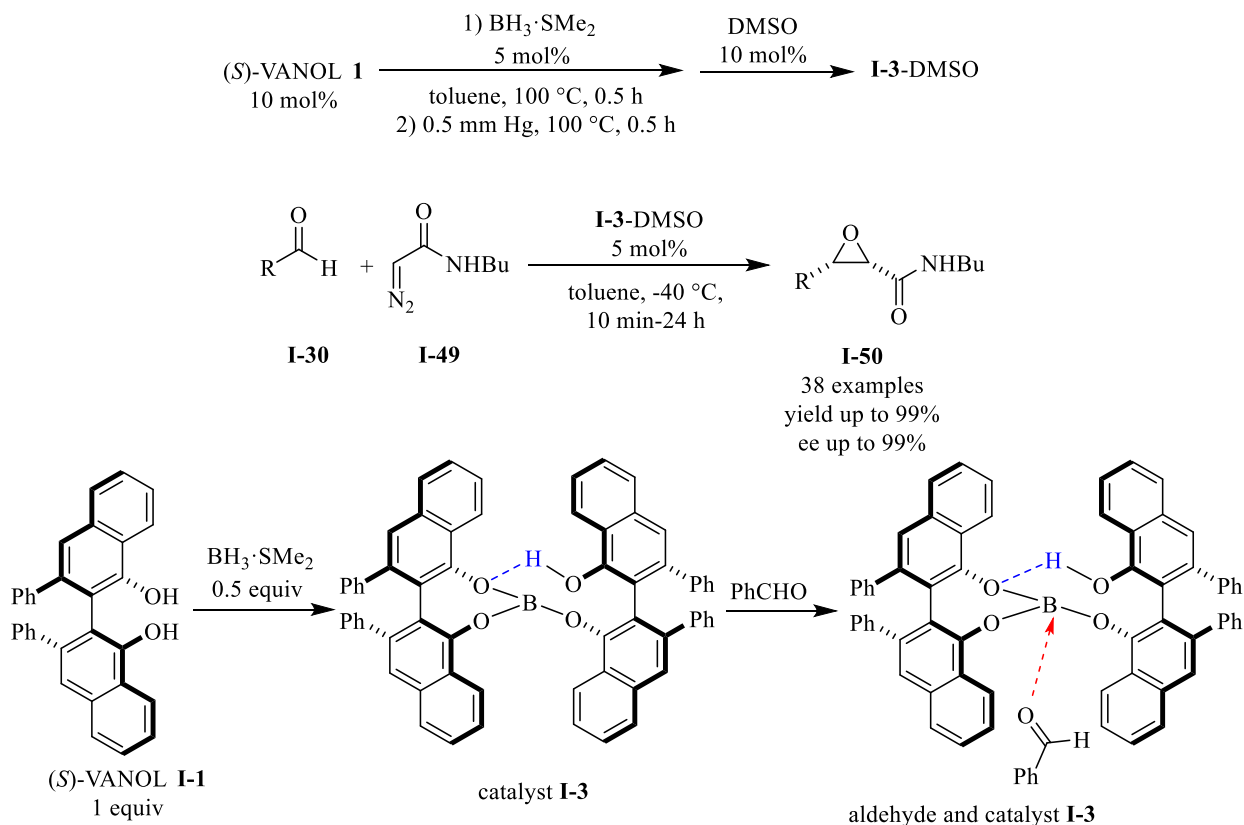
one chiral VANOL ligand **I-1**. Unfortunately, the exact nature of this catalyst is not known yet; however, we propose that the aldehyde **I-30** could undergo activation through either of two transition states as depicted in scheme 13. Either the boroxinate catalyst acts as the Brønsted acid catalyst **I-46** and activates the aldehyde via hydrogen bonding, or the boroxinate core of the catalyst is protonated yielding neutral pyro-borate catalyst **I-48**, which can activate the aldehyde **I-30** via Lewis acid-Lewis base interaction (scheme I-13, transition state A and B).

### **1.2.3. BLA catalyst derived from VANOL ligand as an extremely active catalyst in the epoxidation of aldehyde with diazo compound**

After extensive screening, a new catalyst with two VANOL ligands and one boron species was realized (scheme I-14 catalyst **I-3**). In the presence of a catalytic amount of DMSO (10 mol%), catalyst **I-3** performed exceptionally in the epoxidation of aldehyde **I-30** with diazo acetamide **I-49**.<sup>1</sup> A wide range of substrates were converted to *cis*-epoxides **I-50** with high yield and excellent enantio-induction. Perfect diastereoselectivity was also observed during the course of epoxidation reaction (>100: 1 *cis* : *trans*); however, the origin of this diastereoselectivity is not presently clear. It is assumed that the ability of the diazo acetamide **I-49** to hydrogen bond with the catalyst **I-3** might be responsible for the observed diastereoselectivity. The structure of catalyst **I-3** was proposed to be a three coordinated boron species with an intramolecular hydrogen bond between the hydroxy group of one ligand and an oxygen atom of the other one. Presumably, the 2 to 1 VANOL-boron catalyst acts as a Brønsted acid assisted chiral Lewis acid (BLA) catalyst which was reported by Yamamoto for BINOL and BINOL's derivatives, activating the aldehyde via Lewis acid-Lewis base interaction.<sup>2,5</sup> BLA catalyst derived from VANOL and VAPOL ligands had not been reported before. In addition, BLA catalysts have not been useful in any reaction other than the Diels-Alder reaction. In order to gain a more in-depth understanding of the structure of

the VANOL BLA catalyst **I-3**, a non-linear study was conducted. The observed strong positive non-linear effect is consistent with the proposed structure for the catalyst **I-3** in the epoxidation reaction.<sup>1</sup>

**Scheme I-14.** Asymmetric catalytic epoxidation catalyzed by catalyst **I-3**

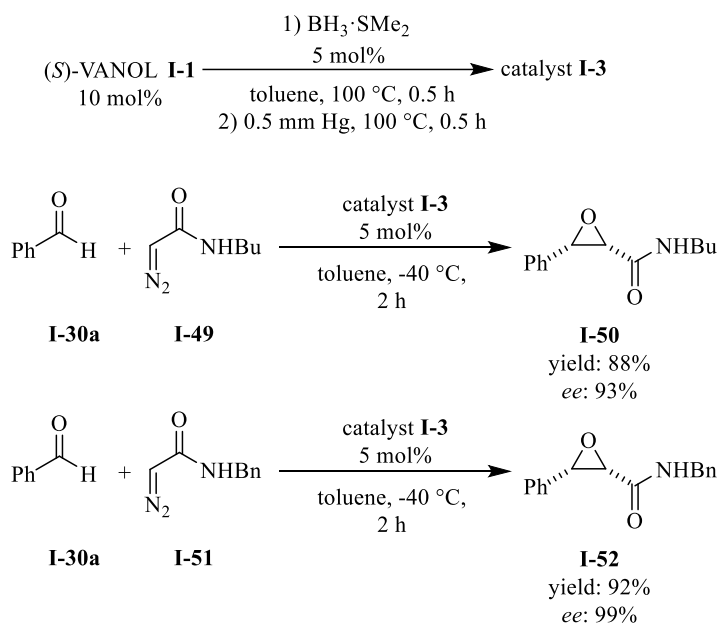


#### 1.2.4. Study of the Effect of DMSO in the Epoxidation Reaction

The VANOL BLA catalyst **I-3** was prepared by reacting 2.0 equiv of VANOL ligand **I-1** with 1.0 equiv  $\text{BH}_3 \cdot \text{SMe}_2$  and heating the mixture at 100 °C for 1 hour followed by applying a high vacuum for 0.5 hour at 100 °C in order to remove the volatiles. Finally, the active catalyst was obtained by adding 2.0 equiv of DMSO (scheme I-14). Catalyst **I-3-DMSO** complex performed excellent in the epoxidation reaction; specifically, it catalyzed the asymmetric addition of diazo acetamide **I-49** to benzaldehyde **I-30a** to yield epoxide **I-50a** with 99% yield and 99% *ee*. It was also found that by leaving out the DMSO, the catalyst could catalyze the same reaction; however, with slight

deterioration of the yield (88%), *ee* (93%) and also with slower rate (10 min vs 2 h, scheme 15). After screening a number of secondary diazo acetamide, we found that by using N-benzyl diazo acetamide **I-51** in place of N-butyl diazo acetamide **I-49**, excellent yield (99%) and excellent *ee* (99%) could be obtained with catalyst **I-3** in the absence of DMSO.

**Scheme I-15.** Epoxidation reaction



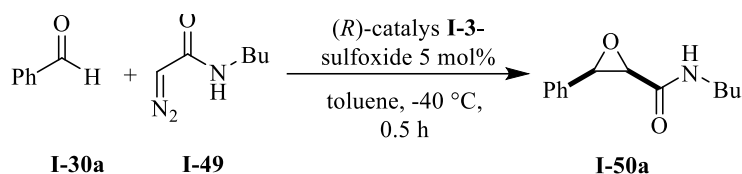
Next, the effect of the nature of the sulfoxide was explored in the epoxidation reaction (table 1). In the absence of any sulfoxide, catalyst **I-3** converted benzaldehyde smoothly to the desired epoxide **I-54** in 96% yield and 85% *ee* (table 1, entry 1). DMSO boosted both the yield and the asymmetric induction as expected and yielded the epoxide **I-54** in 99% yield and 94% *ee* (table 1, entry 2). Dibenzyl sulfoxide as well as diphenyl sulfoxide also performed well in the epoxidation reaction and yielded the epoxide with slightly diminished *ee*, compared with DMSO. In general, sulfoxide addition concomitantly increased the *ee* and the yield of the reaction.



**Table I-1.** Epoxidation of aldehyde in presence of different sulfoxides

$  \begin{array}{c}  \text{(S)-VANOL } \mathbf{1} \xrightarrow[\text{toluene, } 100^\circ\text{C, } 0.5\text{ h}]{\begin{array}{c} 1) \text{ BH}_3\cdot\text{SMe}_2 \\ 5\text{ mol\%} \end{array}} \xrightarrow[\text{2) } 0.5\text{ mm Hg, } 100^\circ\text{C, } 0.5\text{ h}]{\begin{array}{c} \text{sulfoxide} \\ 10\text{ mol\%} \end{array}} \text{catalyst } \mathbf{I-3}\text{-sulfoxide} \\  10\text{ mol\%}  \end{array}  $			
entry	sulfoxide	%yield of <b>I-54</b>	% <i>ee</i> of <b>I-54</b>
1	none	96	85
2	DMSO	99	94
3	diphenyl sulfoxide	93	91
4	dibenzyl sulfoxide	94	90

Next question that arose was, whether or not the sulfoxide is involved in the enantiodetermining step. In order to evaluate this possibility, the epoxidation reaction was conducted in the presence of a chiral sulfoxide (table 2). Since the chiral sulfoxide can form a matched or mismatched complex with the catalyst, it is to be expected that the chirality of the sulfoxide should affect the *ee* of the product **I-50a** if it is involved in the enantiodetermining step. The epoxidation reaction was conducted by using (*R*)-benzyl methyl sulfoxide and also its enantiomer, but no change in *ee* of the epoxide **I-50** was observed in either case (table 2, entry 2 and 3). Similar results were obtained with (*R*)-methyl phenyl sulfoxide and its enantiomer which clearly shows that the sulfoxide is not likely participating in enantiodetermining step (table 2 entry 4 and 5). So far, the exact rule of DMSO in the epoxidation reaction remains obscure and more experiments need to be done in order to elucidate it.

**Table I-2.** Epoxidation of benzaldehyde in the presence of chiral sulfoxides

entry	sulfoxide	Epoxide	ee
1	none	86	91
2	( <i>R</i> )-benzyl methyl sulfoxide	91	97
3	( <i>S</i> )-benzyl methyl sulfoxide	91	97
4	( <i>R</i> )-phenyl methyl sulfoxide	85	96
5	( <i>S</i> )-phenyl methyl sulfoxide	86	96

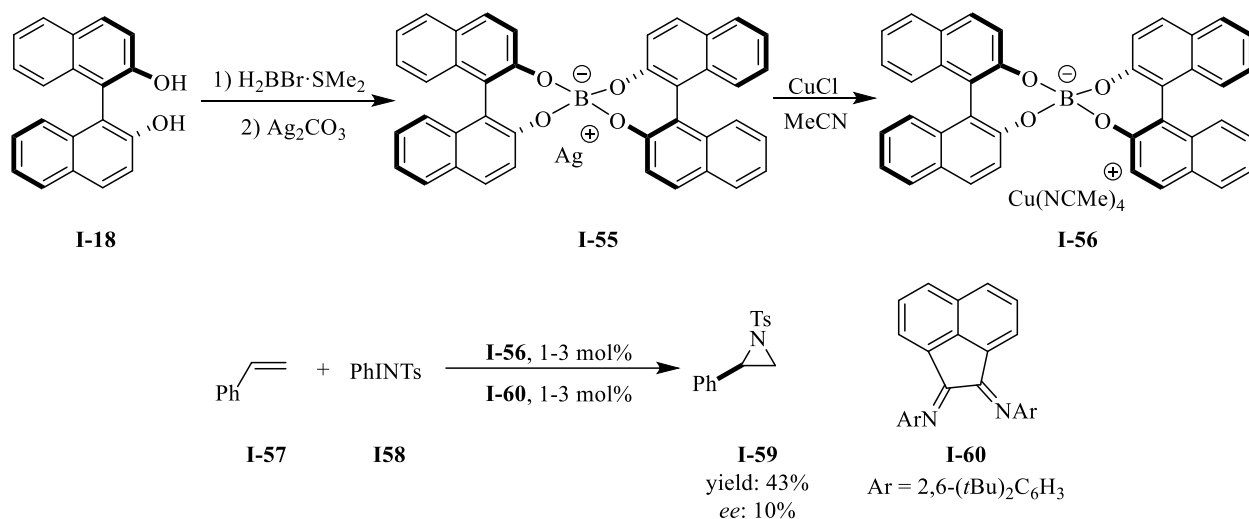
### 1.3. Asymmetric catalytic aziridination catalyzed by VANOL spiroborate anion

#### 1.3.1. Introduction

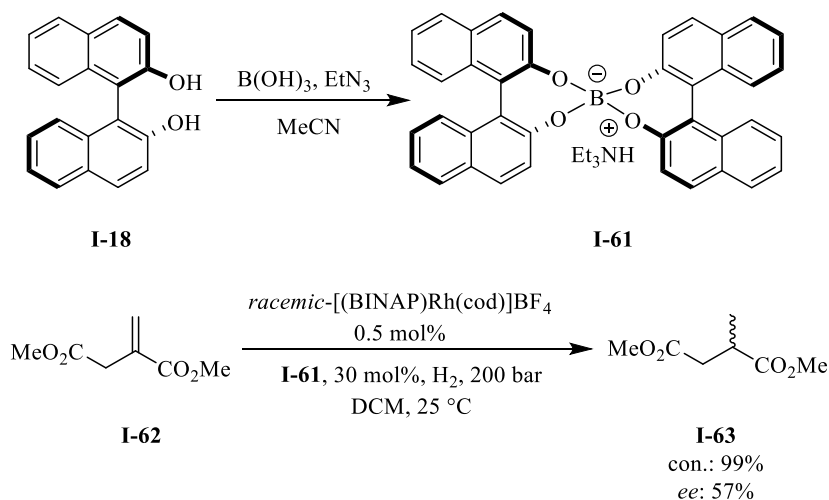
Chiral spiroborate anion of BINOL have been the subject of many studies over the last two decades. In 2003, Arndtsen reported that the BINOL spiroborate anion as a counterion in **I-56** induced enantioselectivity in copper-catalyzed asymmetric aziridination (scheme 16).<sup>27</sup> Unfortunately, the BINOL spiroborate copper complex **I-56** yielded the desired aziridine **I-59** with only 10% *ee*. Presumably, the poor performance of the catalyst was due to weak interactions between the spiroborate anion and the copper.

Leitner reported that the asymmetric hydrogenation of dimethyl itaconate **I-62** catalyzed by a *racemic* BINAP rhodium complex in the presence of the BINOL spiroborate anion **I-61** (scheme 17).<sup>28</sup> In this report, the spiroboarte anion **I-61** induced the enantioselectivity in hydrogenation of dimethyl itaconate **I-62** with only 57% *ee*.

**Scheme I-16.** Aziridination catalyzed by spiroborate anion-copper complex



**Scheme I-17.** Spiroborate anion induced enantioselectivity in asymmetric hydrogenation



Chiral spiroborate anions have also been used in the resolution of BINOL,<sup>29</sup> as a chiral shift reagent,<sup>29</sup> Friedel-Crafts reactions<sup>30</sup> and the ring opening of meso aziridiniums.<sup>31</sup> To the best of our knowledge, chiral spiroborate anions have not been useful in producing useful asymmetric induction in any asymmetric catalytic reaction (the highest achieved *ee* with spiroborate anion was only 57%, scheme I-17).<sup>28</sup>

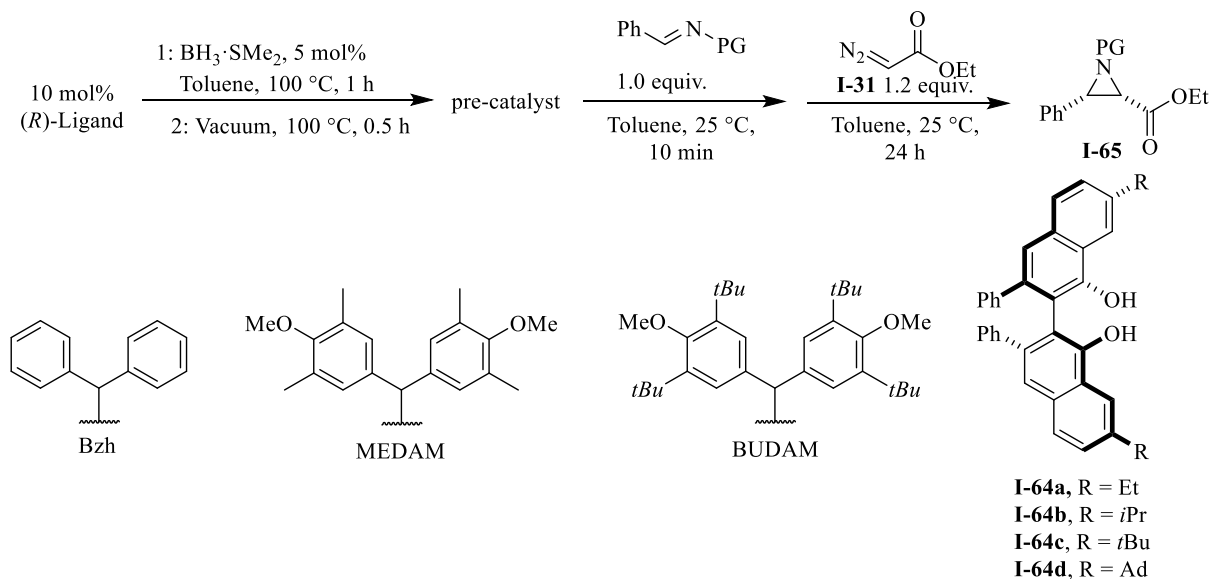
### 1.3.2. VANOL spiroborate catalyze aziridination reaction

After successful epoxidation with the meso-boron catalyst **I-3** (scheme I-1), we turned our attention toward the aziridination reaction catalyzed with catalyst **I-3**. The catalyst was prepared under the condition which is indicated in table 3. We were delighted to observe that catalyst **I-3** was able to catalyze the aziridination reaction with imine **I-20a** and ethyl diazo acetate **I-31**, which yielded aziridine **I-65a** with 85% yield but with only 41% *ee* (table I-3, entry 1). It was observed that the MEDAM and BUDAM groups on the imine gave superior results in comparison to the Bzh imine as the protecting group (Table I-3, entry 2 and 3). Performing the aziridination reaction with (*S*)-7,7'-Et<sub>2</sub>VANOL ligand **I-64a** yielded the desired product in 94% and 81% *ee* (table 3, entry 4). (*S*)-7,7'-*i*Pr<sub>2</sub>VANOL **I-64b** was also investigated and aziridine **I-65a** was afforded in 86% yield and 88% *ee* (table I-3, entry 5). After investigating ligands **I-64a** and **I-64b**, we noticed that increasing the size of substituents in 7,7'-positions leads to a higher induction of the enantioselectivity. Ligand **I-64c** bearing adamantyl as a bulky substituents in 7,7'-positions furnished aziridine **I-65a** in 85% yield and 89% *ee* (table I-3, entry 6). To our delight, ligand (*S*)-7,7'-*t*Bu<sub>2</sub>VANOL, **I-64** performed well and produced aziridine **I-65a** with high yield and excellent enantioselectivity (Table I-3, entries 7-9). It is worth noting that neither VAPOL **I-4** nor BINOL **I-18** were effective ligands in this reaction (table I-3, entries 10-13).

Further optimizations were conducted where temperature and catalyst loading were evaluated for their effect on the course of aziridination. A substantial increase in the *ee* was observed by decreasing the temperature to -45 °C (41% *ee* vs 75% *ee*, table I-4 entries 1-4); however, a significant decrease in the rate of reaction was observed and only 35% of the desired product **I-65a** was produced after 3.5 days (table I-4 entry 4). Conducting the reaction with 5 mol% catalyst loading derived from 7,7'-*t*Bu<sub>2</sub>VANOL ligand yielded the aziridine in 85% yield and 93% *ee*.

Decreasing the catalyst loading to 2.5 mol% produced aziridine with a slight decrease in the yield

**Table I-3.** Optimization of aziridination reaction



entry	Ligand	PG	imine	aziridine	yield%	ee%
1	( <i>S</i> )-VANOL, <b>I-3</b>	Bzh	<b>I-20a</b>	<b>I-65a</b>	85	-41
2	( <i>S</i> )-VANOL, <b>I-3</b>	MEDAM	<b>I-20b</b>	<b>I-65b</b>	92	-86
3	( <i>S</i> )-VANOL, <b>I-3</b>	BUDAM	<b>I-20c</b>	<b>I-65c</b>	79	-80
4	( <i>R</i> )-7,7'-Et <sub>2</sub> VANOL, <b>I-64a</b>	Bzh	<b>I-20a</b>	<b>I-65a</b>	94	81
5	( <i>S</i> )-7,7'- <i>i</i> Pr <sub>2</sub> VANOL, <b>I-64b</b>	Bzh	<b>I-20a</b>	<b>I-65a</b>	86	-88
6	( <i>S</i> )-7,7'-Ad <sub>2</sub> VANOL, <b>I-64c</b>	Bzh	<b>I-20a</b>	<b>I-65a</b>	85	-89
7	( <i>R</i> )-7,7'- <i>t</i> Bu <sub>2</sub> VANOL, <b>I-64d</b>	Bzh	<b>I-20a</b>	<b>I-65a</b>	85	94
8	( <i>R</i> )-7,7'- <i>t</i> Bu <sub>2</sub> VANOL, <b>I-64d</b>	MEDAM	<b>I-20b</b>	<b>I-65b</b>	78	97
9	( <i>R</i> )-7,7'- <i>t</i> Bu <sub>2</sub> VANOL, <b>I-64d</b>	BUDAM	<b>I-20c</b>	<b>I-65c</b>	95	96
10	( <i>S</i> )-VAPOL, <b>I-4</b>	Bzh	<b>I-20a</b>	<b>I-65a</b>	35	-34
11	( <i>S</i> )-VAPOL, <b>I-4</b>	MEDAM	<b>I-20b</b>	<b>I-65b</b>	<10 <sup>1</sup>	<i>N.D.</i> <sup>2</sup>
12	( <i>S</i> )-BINOL, <b>I-18</b>	Bzh	<b>I-20a</b>	<b>I-65a</b>	53	5
13	( <i>S</i> )-BINOL, <b>I-18</b>	MEDAM	<b>I-20b</b>	<b>I-65b</b>	<10	<i>N.D.</i> <sup>2</sup>

1. NMR yield, 2. N. D.: Not Determined

but same induction (table I-4, entry 6). With 1 mol% catalyst loading, the reaction was too slow and only 15% yield (NMR) of the aziridine **I-65b** was observed after 24 hours (table I-4, entry 7). As a control experiment the reaction was done in the absence of catalyst and no product was detected after 24 hours in the NMR spectrum (table I-4, entry 8).

**Table I-4.** Further optimization of aziridination reaction

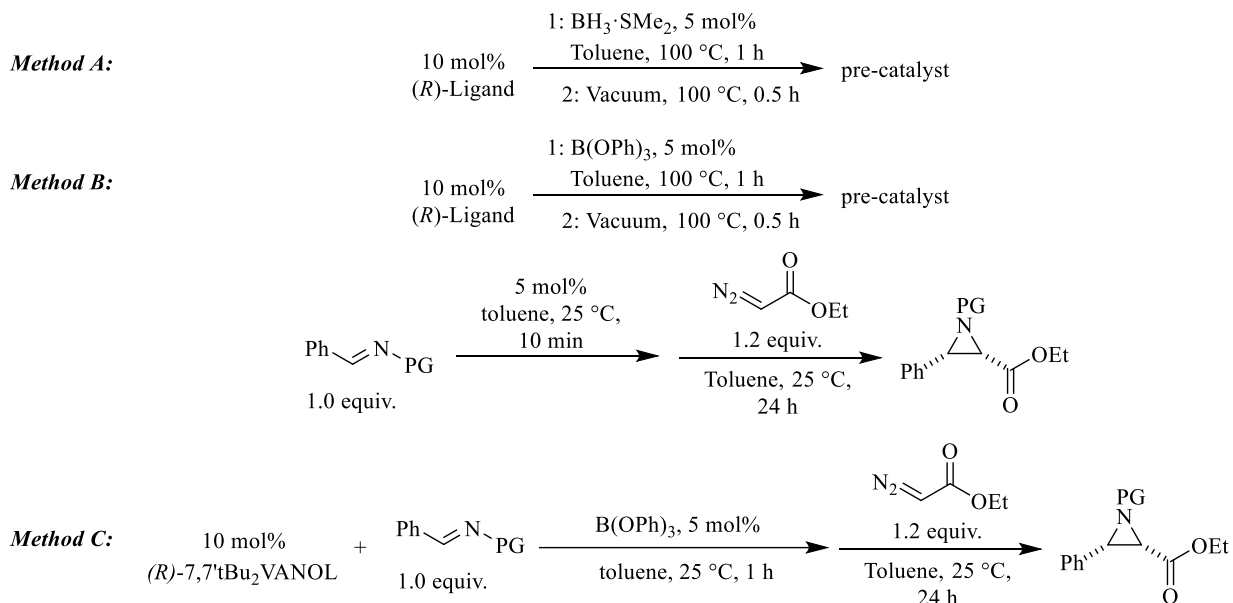
entry	Ligand	PG	imine	cat. loading X mol%	T/°C	time/h	yield%	ee%
1	(S)-VANOL, <b>I-3</b>	Bzh	<b>I-20a</b>	5	25	24	85	-41
2	(S)-VANOL, <b>I-3</b>	Bzh	<b>I-20a</b>	5	0	24	84	-44
3	(S)-VANOL, <b>I-3</b>	Bzh	<b>I-20a</b>	5	-20	36	55	-53
4	(S)-VANOL, <b>I-3</b>	Bzh	<b>I-20a</b>	5	-45	84	35	-75
5	(R)-7,7'tBu <sub>2</sub> VANOL, <b>I-64d</b>	MEDAM	<b>I-20b</b>	5	25	24	85	93
6	(R)-7,7'tBu <sub>2</sub> VANOL, <b>I-64d</b>	MEDAM	<b>I-20b</b>	2.5	25	24	66	93
7	(R)-7,7'tBu <sub>2</sub> VANOL, <b>I-64d</b>	MEDAM	<b>I-20b</b>	1	25	24	15 <sup>1</sup>	N. D. <sup>2</sup>
8	—	MEDAM	<b>I-20b</b>	0	25	24	N. R. <sup>3</sup>	N. D. <sup>2</sup>

1. NMR yield, 2. N. D.: Not Determined, 3. N. R.: No Reaction

Finally, different methods of preparing the catalyst were evaluated (table I-5). In method B, B(OPh)<sub>3</sub> was used as the boron source in place of BH<sub>3</sub>·SMe<sub>2</sub>. It was revealed that both methods were equally effective and both catalysts yielded aziridine **I-65a** with comparable results. We have discovered the self-assembly of the BOROX catalyst **I-46/I-47** simply by mixing VANOL/VAPOL **I-3/I-4** ligands, B(OPh)<sub>3</sub> and imine (scheme I-12).<sup>26</sup> Inspired by our previously

reported aziridination catalyzed by self-assembled BOROX catalyst **I-47** (scheme I-12), 10 mol% of (*R*)-7,7'-*t*Bu<sub>2</sub>-VANOL **I-64d** and 5 mol% B(OPh)<sub>3</sub> were reacted in presence of 1.0 equiv. of

**Table I-5.** Different method in catalyst preparation



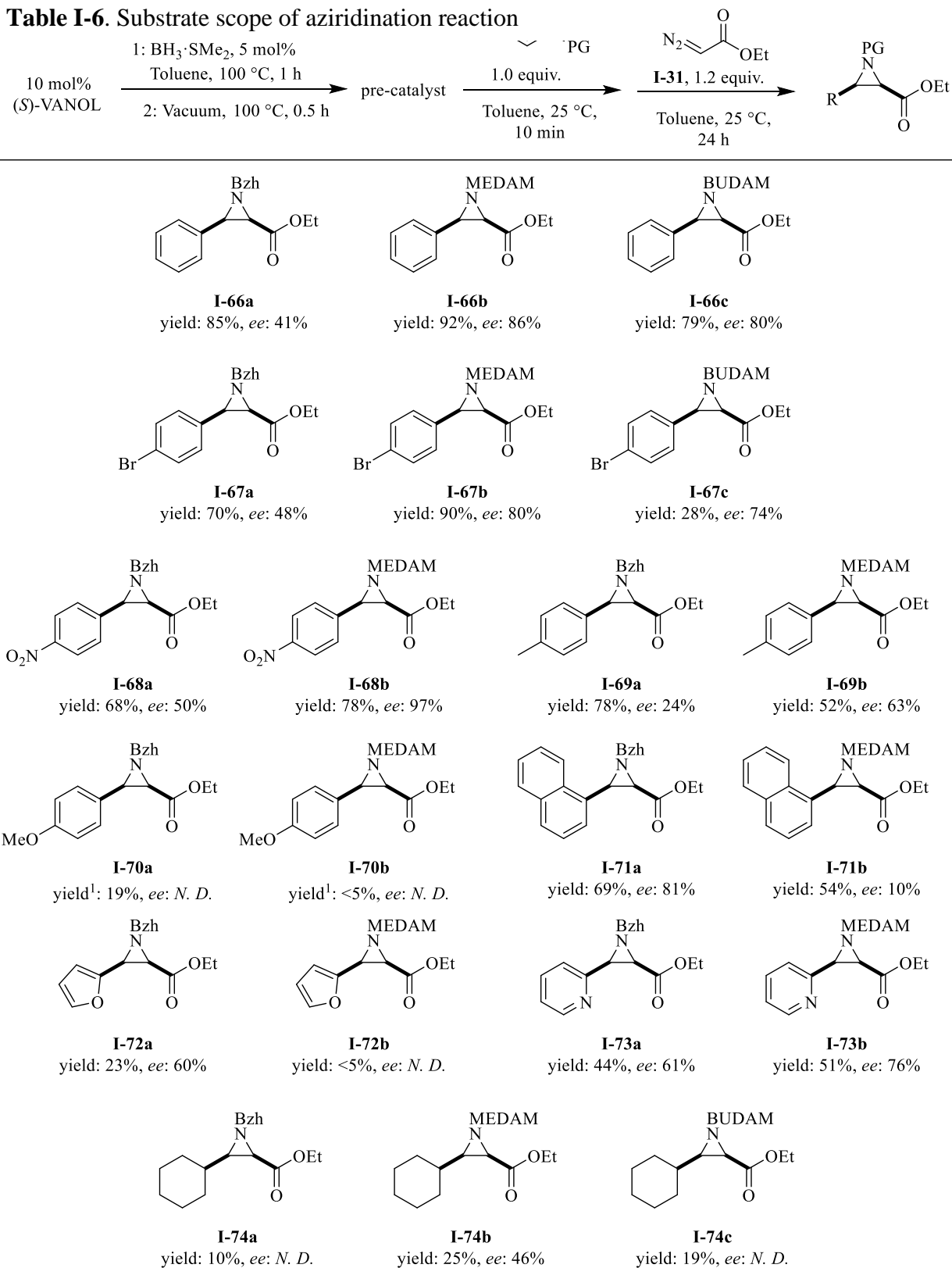
entry	method	Ligand	PG	Aziridine	time/h	yield%	ee% <sup>3</sup>
1	A	( <i>S</i> )-VANOL	Bzh	<b>I-65a</b>	24	84	-41
2	A	( <i>S</i> )-VANOL	MEDAM	<b>I-65b</b>	24	92	-86
3	A	( <i>R</i> )-7,7' <i>t</i> Bu <sub>2</sub> VANOL	Bzh	<b>I-65a</b>	36	85	-93 <sup>3</sup>
4	A	( <i>R</i> )-7,7' <i>t</i> Bu <sub>2</sub> VANOL	MEDAM	<b>I-65b</b>	84	78	-97 <sup>3</sup>
5	B	( <i>S</i> )-VANOL	Bzh	<b>I-65a</b>	12	80	-46
6	B	( <i>S</i> )-VANOL	MEDAM	<b>I-65b</b>	25	83	-84
7	B	( <i>R</i> )-7,7' <i>t</i> Bu <sub>2</sub> VANOL	Bzh	<b>I-65a</b>	12	86	-96 <sup>3</sup>
8	B	( <i>R</i> )-7,7' <i>t</i> Bu <sub>2</sub> VANOL	MEDAM	<b>I-65b</b>	24	99	-98 <sup>3</sup>
9	C	( <i>R</i> )-7,7' <i>t</i> Bu <sub>2</sub> VANOL	MEDAM	<b>I-65b</b>	22	20 <sup>1</sup>	N. D. <sup>2</sup>

1. NMR yield, 2. N. D.: Not Determined, 3. enantiomer of **I-65** was produced

imine, in order to investigate the self-assembly of the catalyst, but only 20% yield (NMR) of the desired product was observed (table I-5, method c).

After identification of the optimum reaction condition, the efficiency of the catalyst with regards to substrate scope were examined. The screening of the substrate scope was pursued with the catalyst prepared by *method A* derived from the VANOL ligand. Substrates bearing a bromine as an electron withdrawing group in the para position with Bzh as the protecting group worked well under these reaction conditions and yielded aziridine **I-67a** with a 70% yield; however, with only 48% *ee*. By changing the protecting group to MEDAM, the yield was increased to 90% and *ee* was increased to 80%. With BUDAM as the protecting group produced aziridine **I-67c** with lower yield (28%) and *ee* (74%) compared to the MEDAM protecting group. Imines bearing NO<sub>2</sub> as the electron withdrawing yielded aziridine **I-68a** with good yield (68%) and moderate enantioselectivity (50%). As expected, with MEDAM as the protecting group, aziridine **I-68b** was obtained with increased yield of 78% yield and an increased *ee* of 97%. Electron donating groups such methyl, methoxy and dimethylamine in the *para* position did not perform well under the optimum reaction conditions. The imine derived from cyclohexane carboxaldehyde as the aliphatic substrate also did not work well providing product in 46% *ee* with MEDAM as the protecting group. Imines derived from trimethyl acetaldehyde as a bulky substrate produced only 22% yield with Bzh and <10% yield with MEDAM as protecting groups (not shown in the table I-6). Other aromatic substrates such as 1-naphthalene were also evaluated, which produced aziridine **I-71a** with 69% yield and good enantioselectivity (81%). However, with MEDAM as the protecting group, moderate yield and low enantioselectivity was unexpectedly obtained. 4-Pyridine carboxaldehyde produced <10% yield of the aziridine (not shown in the table I-6); presumably, due to the basicity of pyridine. Presumably pyridine coordinates with the catalyst and completely

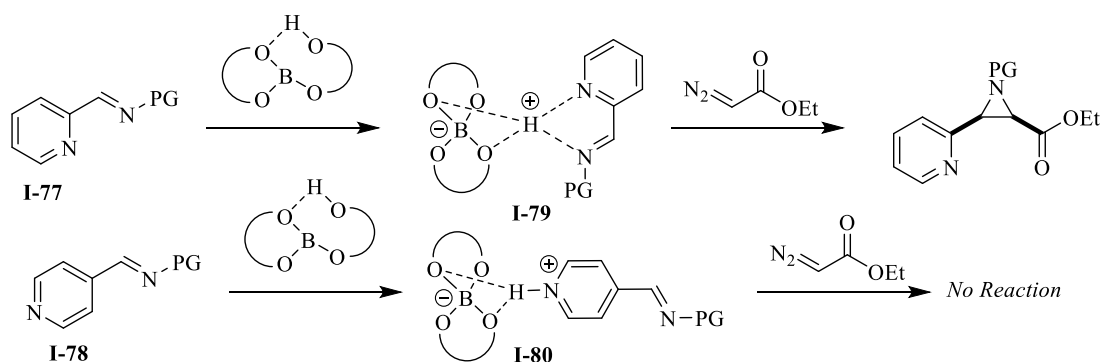


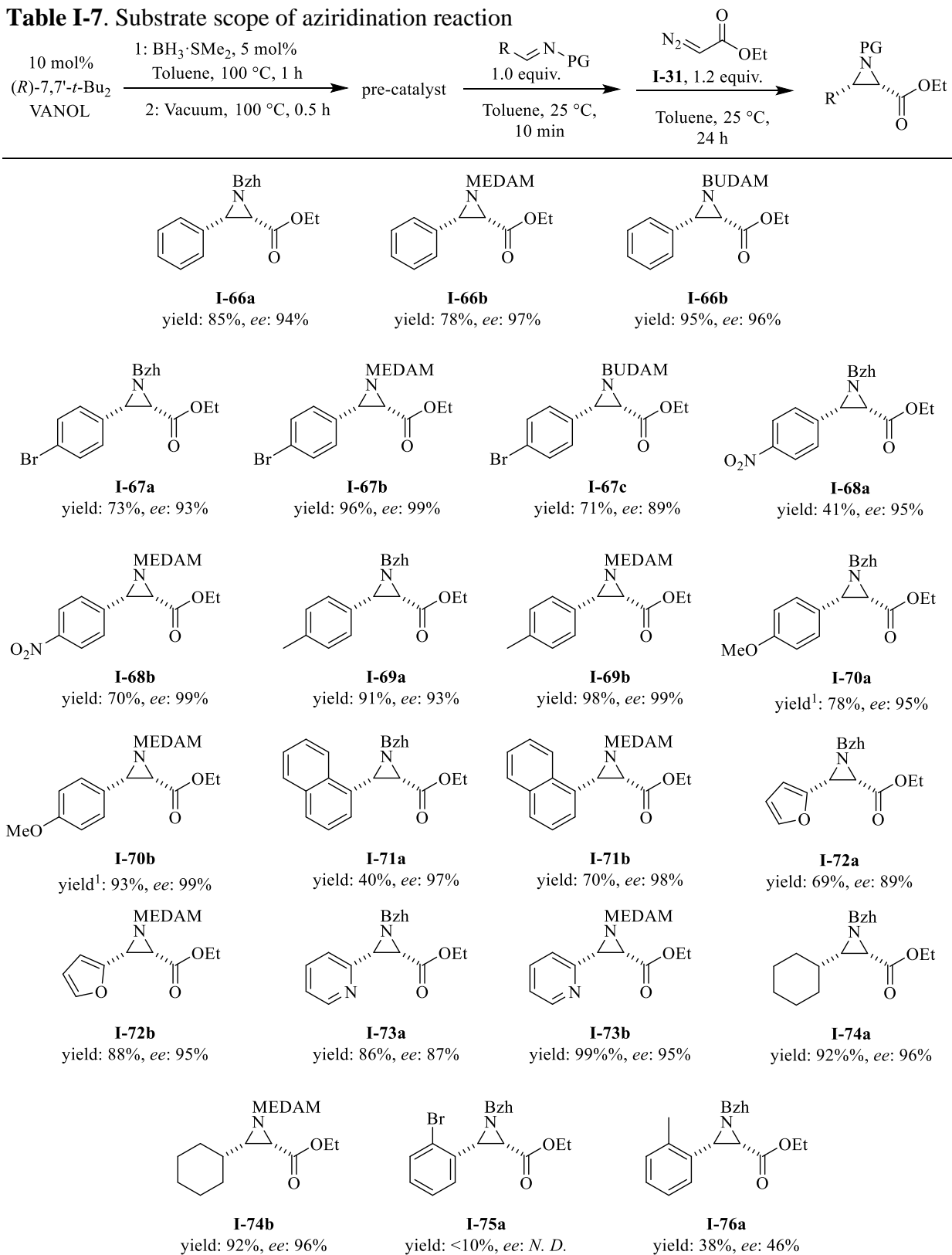
**Table I-6.** Substrate scope of aziridination reaction

1. NMR yield

shuts down the reaction. Interestingly, 2-pyridine carboxaldehyde performed excellently and yielded aziridine **I-73b** with moderate yield and excellent *ee* with MEDAM as the protecting group. A significant difference in reactivity profile of imine **I-77** and imine **I-78** could be because of the following reason (scheme I-18). In imine **I-78**, the nitrogen of pyridine is far from the nitrogen of the imine; therefore, due to less steric crowding around the nitrogen of the pyridine, it interacts first with the catalyst and deactivates the catalyst (scheme I-18). In contrast, since in imine **I-77**, the nitrogen of the pyridine is closer to the nitrogen of the imine, it could undergo activation through the proposed complex **I-79** as depicted in scheme 18 and yield the desired product. Next, we turned our attention toward substrate scope screening with catalyst derived from 7,7'-*t*Bu<sub>2</sub>-VANOL ligand **I-64d**. We were delighted to observe this catalyst could catalyze the reaction of a broad scope of substrates bearing different electron donating and electron withdrawing groups in the para-position of the phenyl substituent in imine **I-20** and yields aziridines with excellent yield and *ees*. With regards to the aliphatic substrate, imine derived from cyclohexane carboxaldehyde worked well and yielded aziridines with excellent yield and *ee*. It is also worth noting that imines bearing benzhydryl as the protecting group were converted to the aziridines in excellent *ee* with 7,7'-*t*Bu<sub>2</sub>VANOL **I-64d** as the optimum ligand. These results were appealing since the benzhydryl amine is commercially available. However, *ortho*-substituted substrates did not work well;

**Scheme I-18.** Aziridination reaction



**Table I-7.** Substrate scope of aziridination reaction

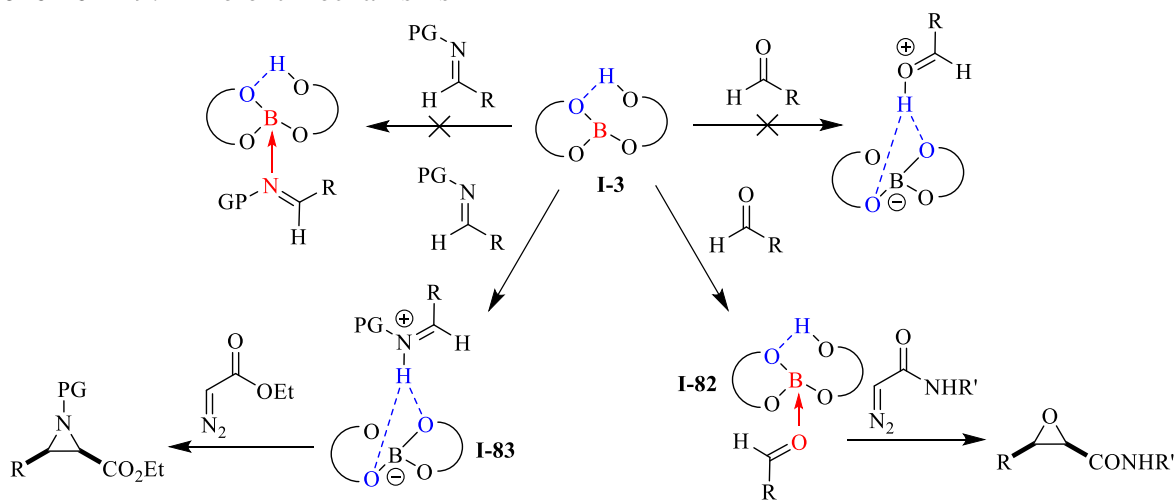
1. NMR yield

presumably, because of steric hindrance. Excellent results were also obtained with imine derived from 1-naphthaldehyde and heteroatom aromatic substrates.

#### 1.4. Experimental evidence for the chameleon behavior of catalyst **I-3**

The mechanistic scenario which is envisioned for the epoxidation and aziridination reactions are summarized in scheme 19. We believed that the catalyst **I-3** is acting as a Brønsted acid assisted chiral Lewis acid catalyst in the epoxidation reaction where the aldehyde is activated via a Lewis acid Lewis base interaction (scheme I-19, complex **I-82**). The activated aldehyde then undergoes reaction with the diazoacetamide to give the desired epoxide. The path to the aziridines on the other hand begins with the deprotonation of the catalyst **I-3** to give the ion pair **I-83** consisting of a spiroborate anion H-bonded to the protonated iminium ion. Then, the activated imine undergoes reaction with ethyl diazo acetate to give aziridine as the product.

**Scheme I-19.** Different mechanisms

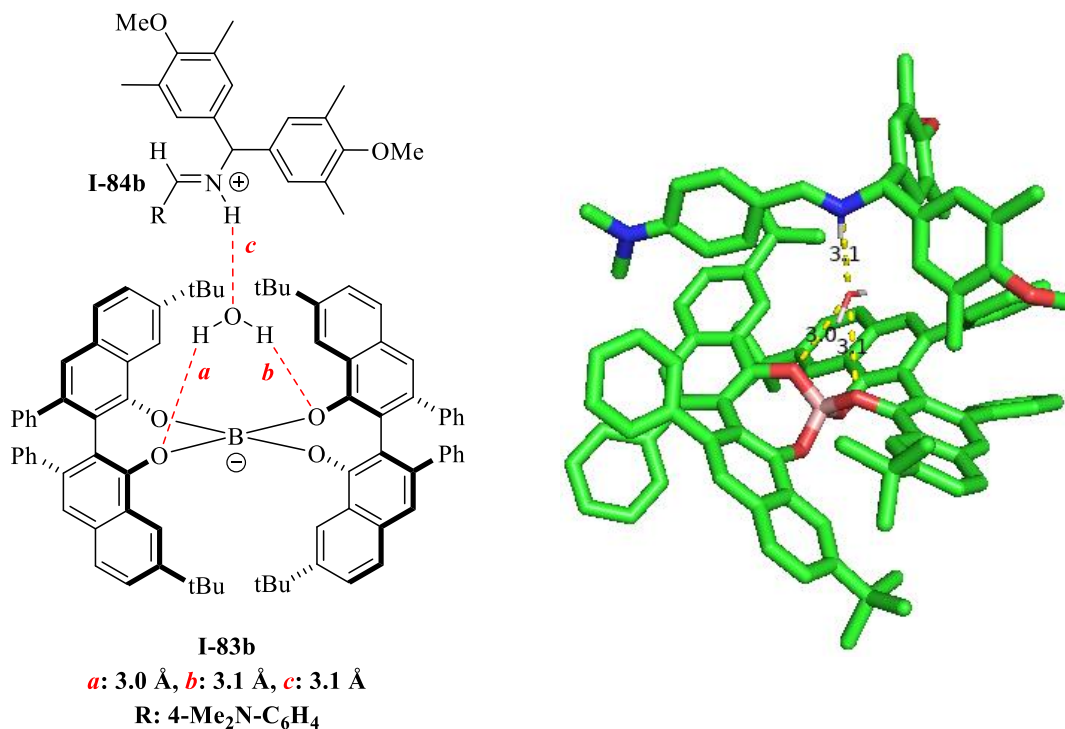


##### 1.4.1. Crystal structure

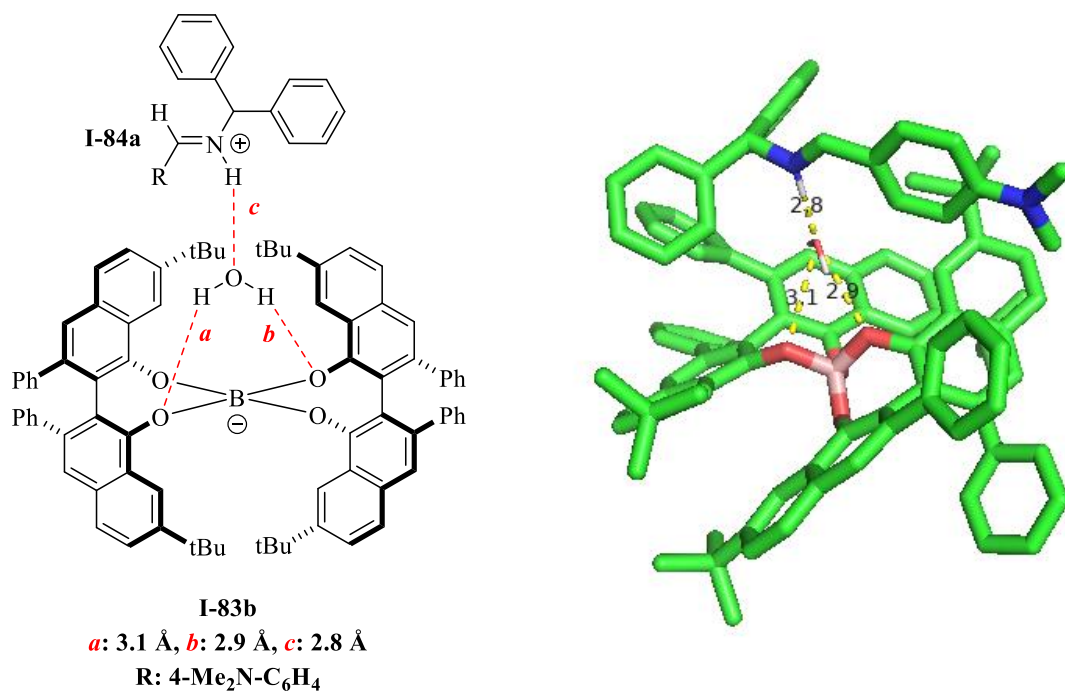
We began to consider the possibility of chameleon behavior of catalyst **I-3** when we were investigating the co-crystal of catalyst **I-3** in presence of an imine. Our attempt to grow the co-crystal of catalyst **I-3** and imine **I-84b** was successful and they crystalized with one molecule of

water. The crystal structure of this catalyst showed a protonated imine H-bonded to a water molecule which in turn was H-bonded to the spiroborate anion **I-83b** (figure I-1).

**Figure I-1.** Co-crystal of spiroborate anion I-83b and imine I-84b

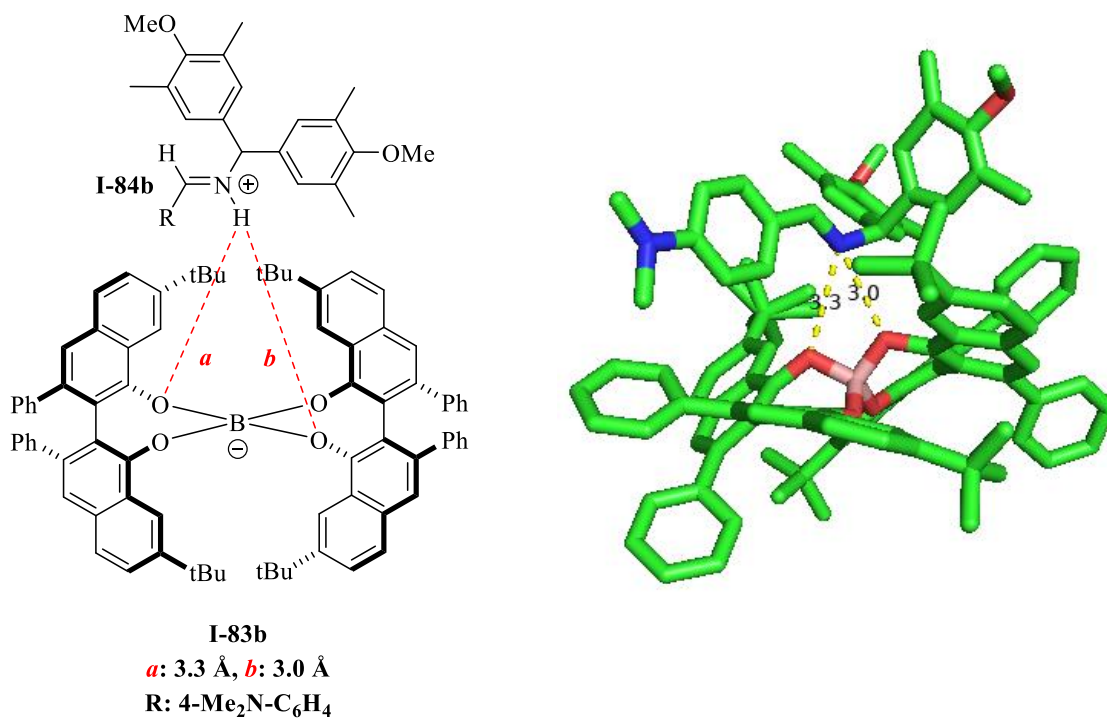


**Figure I-2.** Co-crystal of spiroborate anion I-83b and imine I-84a

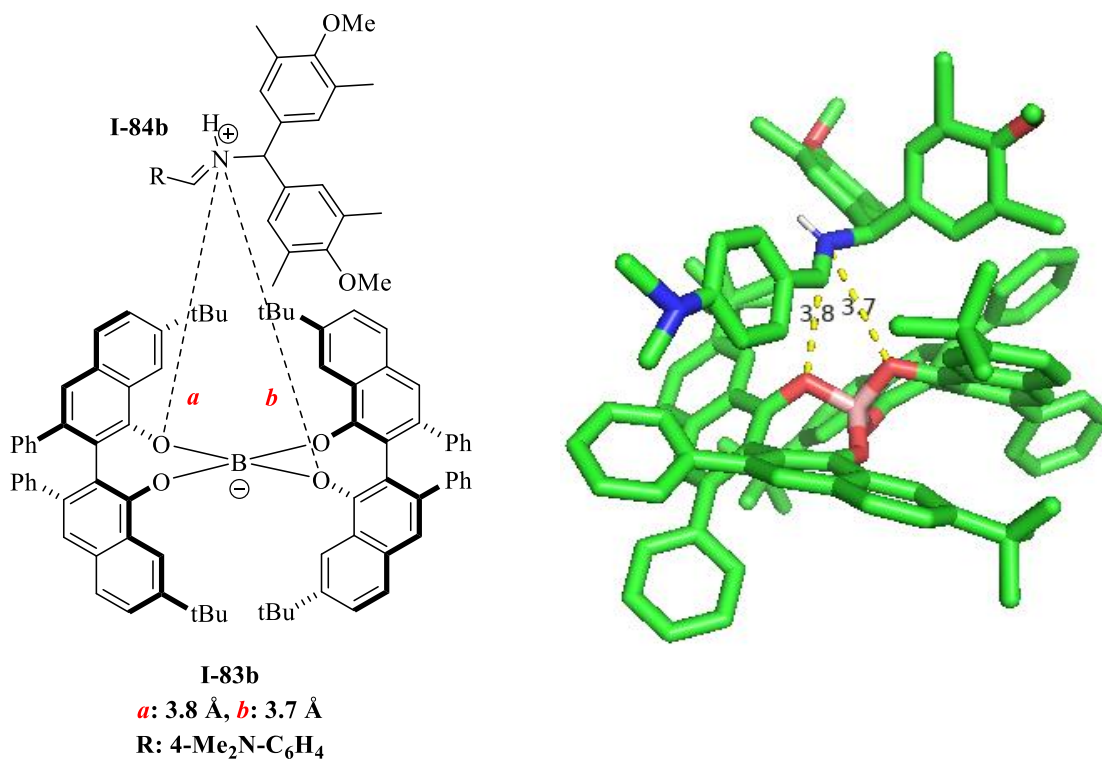


A similar crystal structure was obtained with catalyst **I-83b**, imine **I-84a** and a molecule of water (figure I-2). Eventually, we were able to grow a water-free crystal of the catalyst **I-83b** and imine **I-84b**. Interesting results were obtained by analyzing the co-crystal. First of all, two different conformers of imine **I-84b** were crystalized in crystal lattice. The first conformer revealed a bi-furcated hydrogen bond (N-H-O<sub>1</sub>:3.0Å, N-H-O<sub>2</sub>:3.3Å) with the catalyst and the second conformer was bonded to the catalyst via electrostatic interaction (N-O<sub>1</sub>:3.7Å, N-O<sub>2</sub>:3.8Å).<sup>32</sup> The ratio of these conformers were 66 to 34 (figure I-3a and I-3b). Moreover, the crystal structure did not show any bonding interaction between the nitrogen of the imine **I-84b** and boron of the catalyst **I-83b**. Another crystal structure was obtained with catalyst **I-83c** and imine **I-84b** (figure I-4). This crystal structure revealed only one conformation of the imine in the crystal lattice which has a protonated imine forming a bi-furcated hydrogen bond with the spiroborate anion **I-83c** (N-H-O<sub>1</sub>:3.0Å, N-H-O<sub>2</sub>:3.2Å). These crystal structures suggested the existence of spiroborate anion **I-83** as the catalyst in the aziridination reaction since no bonding interaction was observed between the nitrogen of imine **I-84** and boron of the catalyst **I-83**. These structures were in sharp contrast with Yamamoto's proposed unified mechanism (scheme I-5). Therefore, we began to speculate that the catalyst **I-3/I-83** might follow a different mechanism (Brønsted acid) in presence of amine. Since no mechanistic information could be obtained from the crystal structure analysis, we decided to conduct more experiments to show the dual nature of the catalyst **I-3/I-83**.

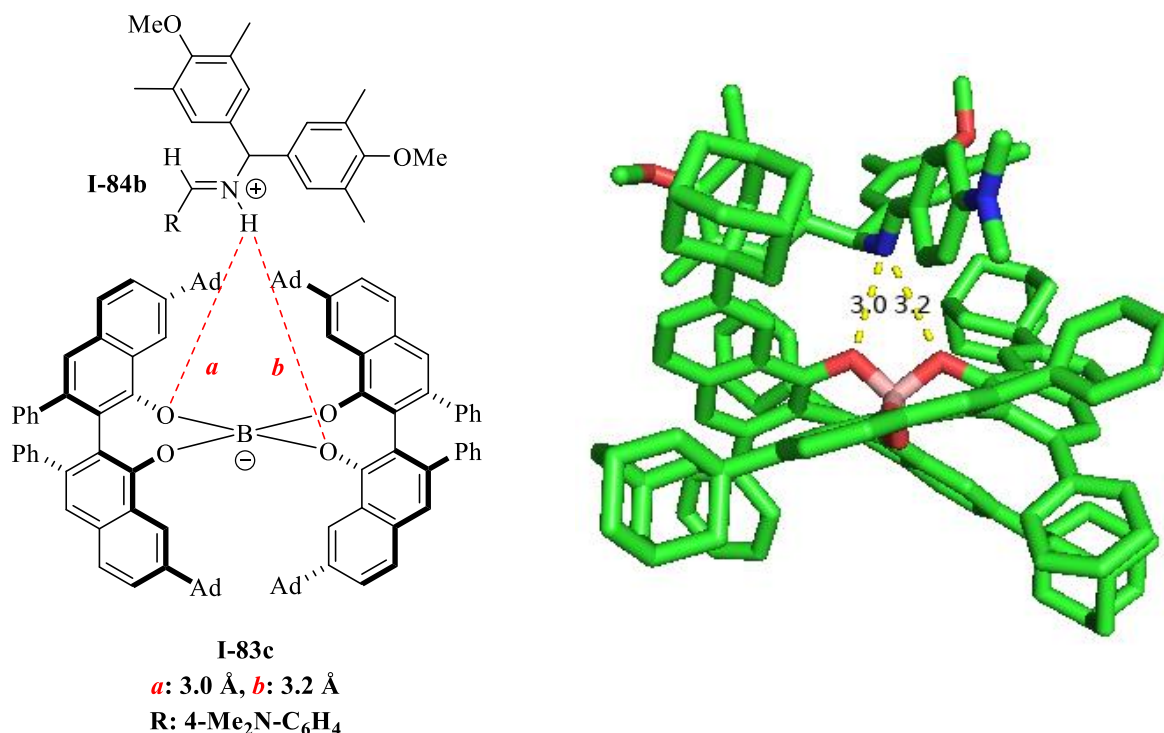
**Figure I-3.a.** Co-crystal of spiroborate anion I-83b and imine I-84b



**Figure I-3.b.** Co-crystal of spiroborate anion I-83b and imine I-84b



**Figure I-4.** Co-crystal of spiroborate anion **I-83c** and imine **I-84b**



## 1.4.2. Hammett study

### 1.4.2.1. Rational for the experiment

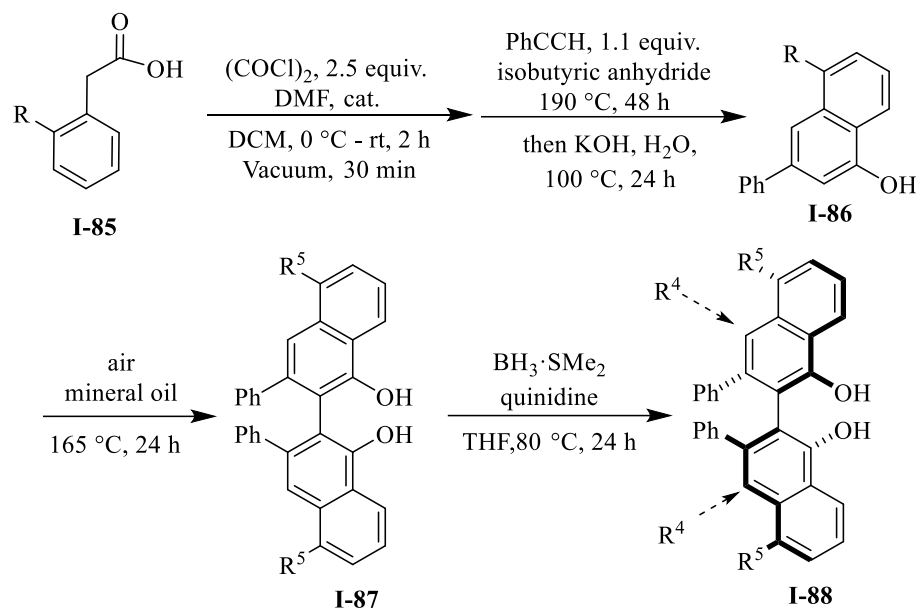
In order to differentiate between the two different mechanisms (Brønsted acid and Lewis acid) of the catalyst **I-3** in aziridination and epoxidation reactions, a Hammett study carried out which involved looking at the correlation of the electronic nature of the substituent R<sup>5</sup> in VANOL ligand **I-88** with the enantiomeric ratio of the product from the aziridination reaction and also from the epoxidation reaction (scheme I-20).

We hypothesized that if the catalyst acts as a Brønsted acid in the aziridination reaction, an electron donating group in positions 5 and 5' should increase the electron density of the spiroborate anion **I-83**. As a result, the hydrogen bond between the protonated imine and the spiroborate anion should become stronger which will allow the iminium ion to have a stronger hydrogen bond to the catalyst which would be expected to lead to a higher rates and higher asymmetric induction. In



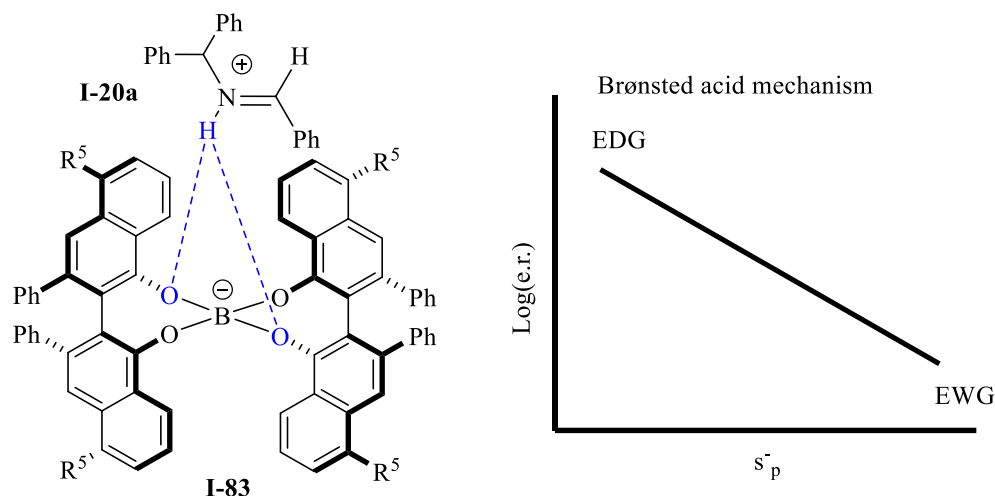
contrast, spiroborate anion catalysts derived from the corresponding VANOL ligands with electron withdrawing groups will form weaker hydrogen bonds with the imminium ion which would be expected to result in a slower rate and lower asymmetric induction. Therefore, a Hammett plot with negative slope would be expected in aziridination reaction (figure I-5).

**Scheme I- 20.** Synthesis of 5,5'-disubstituted VANOL ligand



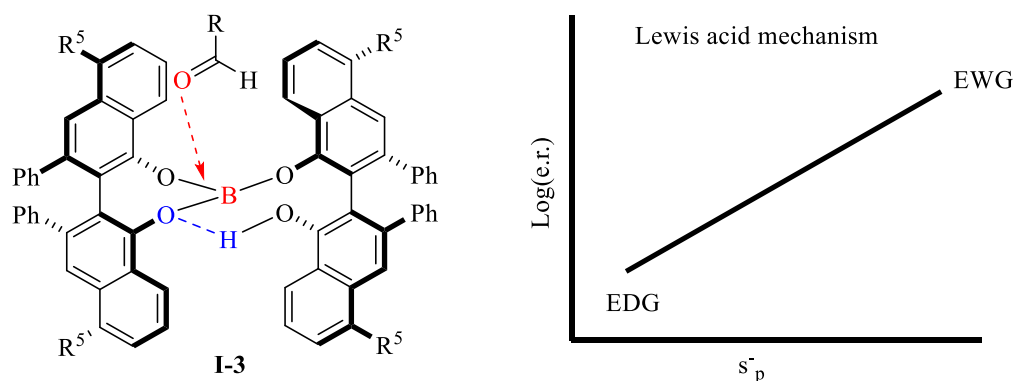
The 5,5'-disubstituted-VANOL ligands were synthesized from compound **I-85** as depicted in scheme 20.<sup>32</sup> We placed substituents at position 5 to: 1) minimize the steric effect during the course of the reaction since the subject of Hammett study is to investigate electronic effects 2) Position 5 had conjugation with the naphthol oxygen of the VANOL ligand. Position 4 is also in conjugation with naphthol oxygen of the VANOL. However, we have previously reported that introducing any substituents at position 4 negatively effects the outcome of the aziridination reaction presumably by altering the dihedral angle of the phenyl groups in the backbone of the VANOL ligand and thus the conformation of the naphthalenes.<sup>34</sup>

**Figure I-5.** Expected Hammett plot for the aziridination reaction



Exactly the opposite would be expected for the epoxidation reaction. Electron withdrawing groups at  $R^5$  would increase the Lewis acidity of the boron in catalyst **I-3** leading to a tighter binding of the aldehyde to the catalyst and thus to a greater rate and higher asymmetric induction. On the other hand, the opposite effect would be expected by incorporating electron donating groups in positions 5, 5' in catalyst **I-3**. As a result, a Hammett plot with positive slope would be expected in epoxidation reaction.

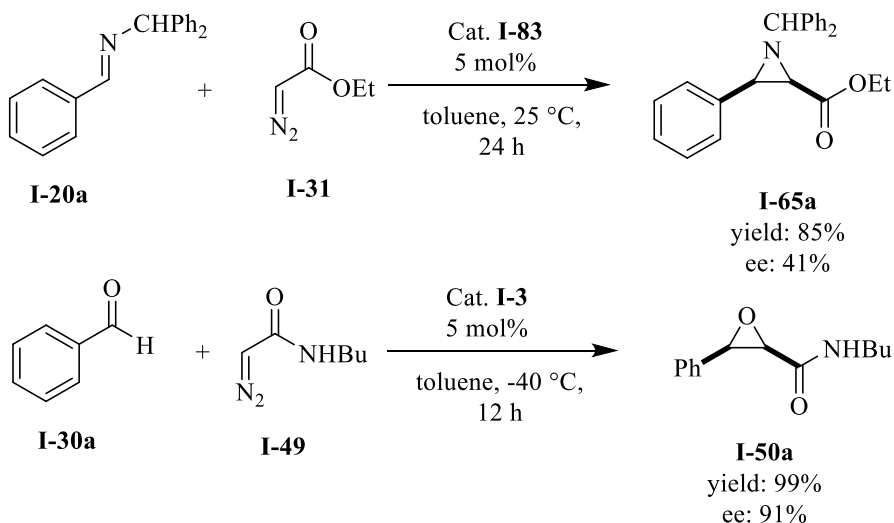
**Figure I-6.** Expected Hammett plot for the epoxidation reaction



In order to establish the dual nature of the chameleon catalyst, it was crucial to run aziridination and epoxidation reactions with exactly the same catalyst and under exactly the same conditions.

For aziridination reactions, benzhydryl imine of benzaldehyde **I-20a** was chosen since it gave aziridine **I-65a** with moderate *ee*; therefore, we were able to measure changes in the asymmetric induction in either direction. Because of the same reason, benzaldehyde was chosen for the epoxidation reaction which produced the product in 91% *ee*. The *ee* of this reaction was not moderate but it was the lowest observed *ee* for the epoxidation reaction (scheme I-21).

**Scheme I-21.** Aziridination and epoxidation reaction

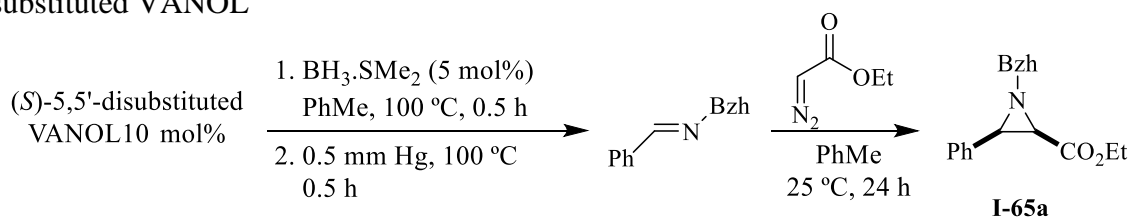


#### 1.4.2.2. Hammett study for the aziridination reaction

The hypothesis for the chameleon catalyst first was tested in the aziridination reaction. In order to ensure reproducible results, each reaction was repeated at least three times (table 8). The aziridination reaction with the spiroborate anion catalyst derived from VANOL ligand **I-88a** bearing a methoxy gave as the electron donating group in positions 5 and 5' gave the product in a range of 77-80% yield and 64-67% *ee* (table I-8, entry 1-3). Next, ligand **I-88b** with a methyl group in positions 5, 5' was used, yielding aziridine **I-65a** in a range of 75-77% yield and 54-56% *ee* (table I-8, entry 4-6). The catalyst derived from the unsubstituted VANOL ligand **I-1**, yielded aziridine **I-65a** with a range of 72-75% yield and 49-54% *ee* (table I-8, entry 7-9). The aziridination

reaction was conducted by using VANOL ligands with electron withdrawing groups in 5, 5'-position. To our delight, a decreasing trend in *ee* of the aziridine **I-65a** was observed by moving

**Table I-8.** Aziridination reaction catalyzed by spiroborate catalyst derived from 5,5'-disubstituted VANOL

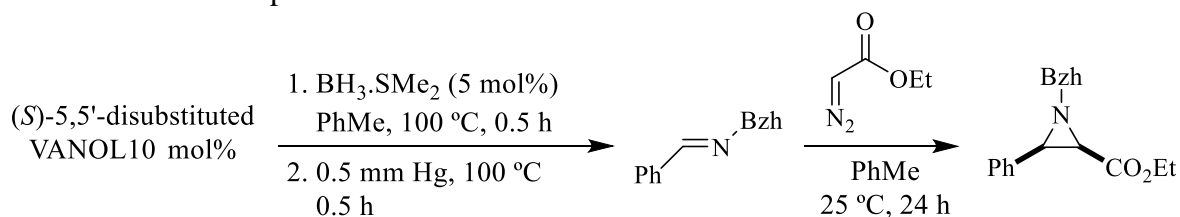


entry	Ligand		Yield%	e. r.
1	5,5'-MeO <sub>2</sub> VANOL	<b>I-88a</b>	80	82:18
2	5,5'-MeO <sub>2</sub> VANOL	<b>I-88a</b>	78	83.5:16.5
3	5,5'-MeO <sub>2</sub> VANOL	<b>I-88a</b>	77	83.5:16.5
4	5,5'-Me <sub>2</sub> VANOL	<b>I-88b</b>	75	78:22
5	5,5'-Me <sub>2</sub> VANOL	<b>I-88b</b>	75	78:22
6	5,5'-Me <sub>2</sub> VANOL	<b>I-88b</b>	77	77:23
7	VANOL	<b>I-1</b>	78	76:24
8	VANOL	<b>I-1</b>	75	77:23
9	VANOL	<b>I-1</b>	72	74.5:25.5
10	5,5'-Br <sub>2</sub> VANOL	<b>I-88d</b>	77	70:40
11	5,5'-Br <sub>2</sub> VANOL	<b>I-88d</b>	75	69:31
12	5,5'-Br <sub>2</sub> VANOL	<b>I-88d</b>	72	69.5:30.5
13	5,5'-Cl <sub>2</sub> VANOL	<b>I-88e</b>	78	82.5:17.5
14	5,5'-Cl <sub>2</sub> VANOL	<b>I-88e</b>	76	77.6:22.4
15	5,5'-Cl <sub>2</sub> VANOL	<b>I-88e</b>	75	75.8:24.2
16	5,5'-(CF <sub>3</sub> ) <sub>2</sub> VANOL	<b>I-88f</b>	73	57.5:42.5
17	5,5'-(CF <sub>3</sub> ) <sub>2</sub> VANOL	<b>I-88f</b>	75	57:43
18	5,5'-(CF <sub>3</sub> ) <sub>2</sub> VANOL	<b>I-88f</b>	77	55.5:44.5

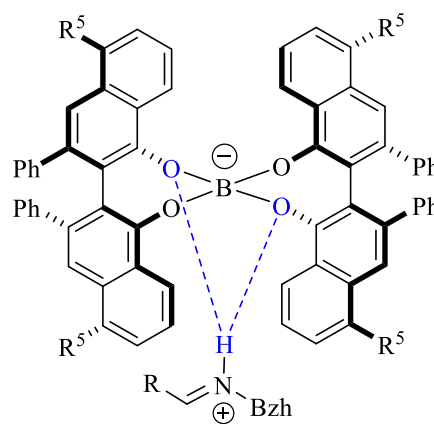
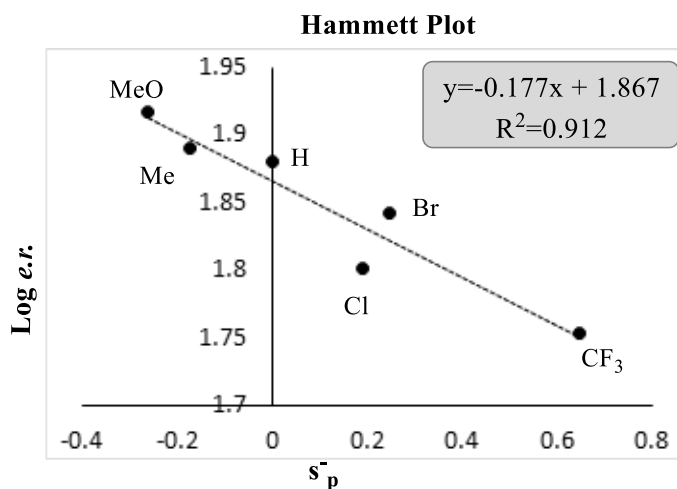
from bromo as a mild electron withdrawing substituent to the trifluoromethyl group as a stronger electron withdrawing one (table I-8, entry 10-18). The average of the enantiomeric ratios for each ligand in the aziridination reaction was plotted against the  $\sigma^-_p$  constant since these  $\sigma$  values were developed for phenols and anilines.<sup>35</sup> The Hammett plot revealed a negative slope of 0.177 and  $R^2$

value of 0.912. These results were in good agreement with the mechanistic interpretation outlined in scheme 19 where a spiroborate anion type **I-83** is the catalyst. Therefore, this Hammett study supports the mechanism in which the catalyst acts as a Brønsted acid.

**Table I-9.** Hammett plot of aziridination reaction



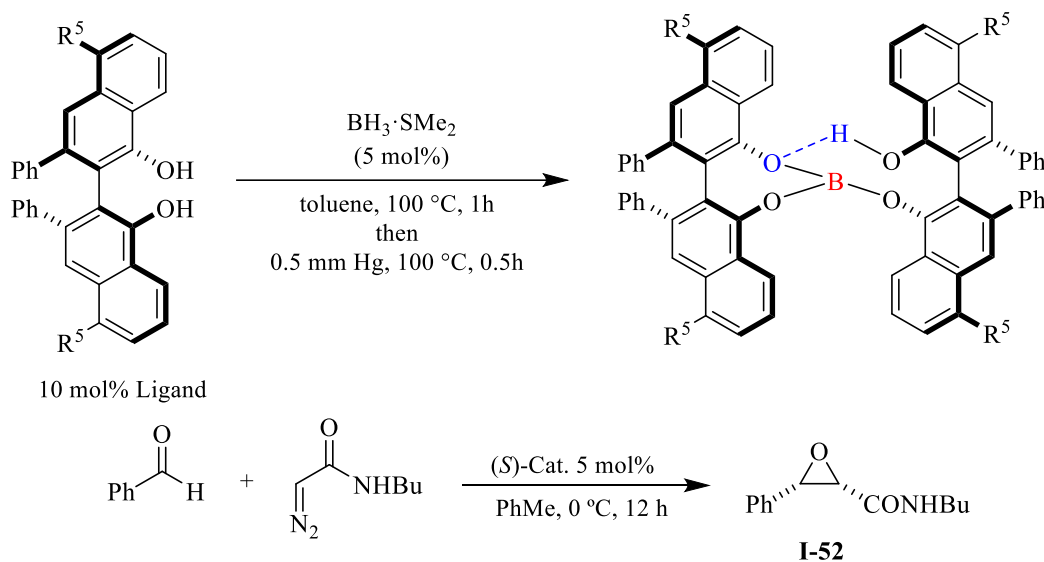
entry	Ligand	Yield%	e. r.	log(er)	$s_p^-$
1	5,5'-MeO <sub>2</sub> VANOL	78	82.5:17.5	1.91645	-0.26
2	5,5'-Me <sub>2</sub> VANOL	76	77.6:22.4	1.89014	-0.17
3	VANOL	75	75.8:24.2	1.87995	0
4	5,5'-Br <sub>2</sub> VANOL	74	69.5:30.5	1.84198	0.25
5	5,5'-Cl <sub>2</sub> VANOL	69	63.2:36.8	1.80106	0.19
6	5,5'-(CF <sub>3</sub> ) <sub>2</sub> VANOL	75	56.6:43.4	1.75320	0.65



### 1.4.2.3. Hammett study for epoxidation reaction

After successful completion of the Hammett study for the aziridination reaction next we turned our attention toward conducting the same study for the epoxidation reaction. However, unexpected results were obtained (table I-10).

**Table I-10.** Hammett study in epoxidation reaction



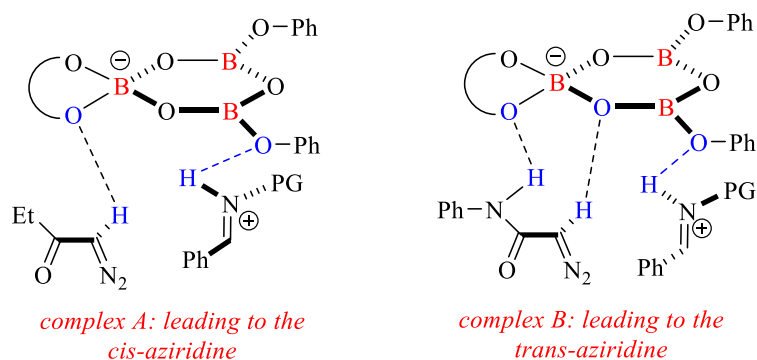
entry	ligand	isolated yield%	e. r.
1	5,5'-MeO <sub>2</sub> VANOL	92	96:4
2	VANOL	85	95:5
3	5,5'-Br <sub>2</sub> VANOL	88	95:5
4	5,5'-Cl <sub>2</sub> VANOL	72	95:5
5	5,5'-(CF <sub>3</sub> ) <sub>2</sub> VANOL	13	N. D.

First of all, there was no correlation between the electronic nature of R<sup>5</sup> and the asymmetric induction in the epoxidation reaction. In fact, no change was observed in the *ee* of the epoxide product with electron donating as well as electron withdrawing groups. This is presumably because of the long distance between Lewis acid component of the catalyst and R<sup>5</sup> groups on the ligand (table I-10, entry 1-4). In addition, we were surprised to observe an extremely slow rate for the

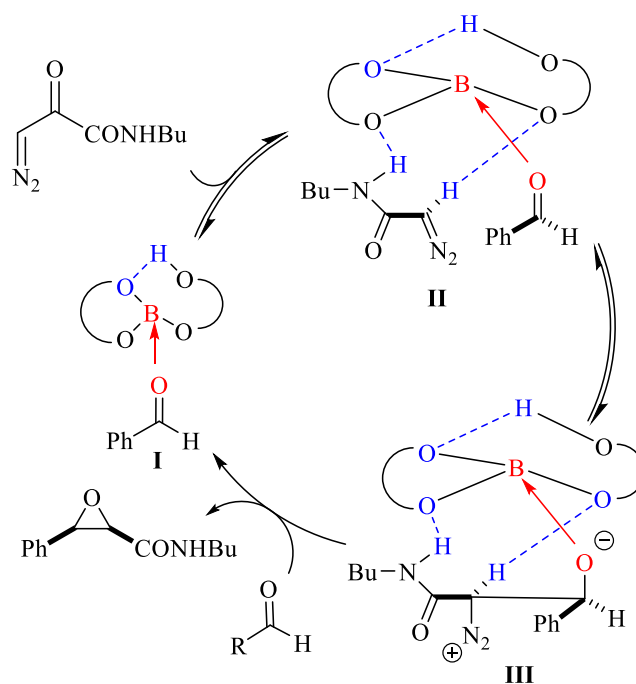
epoxidation reaction carried out with catalyst **I-3** derived from ligand **I-88f** bearing CF<sub>3</sub> as a strong electron withdrawing group.

We have previously reported that the BOROX catalyst can catalyze *cis*-aziridination of imine **I-20a** with ethyl diazo acetate.<sup>27</sup> Extensive isotope effect and mechanistic studies revealed that in the transition state, both ethyl diazoacetate and protonated imine are H-bonded to the BOROX catalyst (scheme I-22a, complex A). The aforementioned H-bond brings activated imine and ethyl diazoacetate in close proximity which leads to the formation of the desired *cis*-aziridine. Interestingly, conducting same reaction with diazo acetamide in place of ethyl diazoacetate, yielded *trans*-aziridine as the major diastereomer.<sup>23,25</sup> After performing a computational study, it was shown that of the formation an extra hydrogen bond between diazo acetamide **I-37** and the BOROX catalyst is the reason of this switch in diastereoselectivity (scheme I-22b, complex B). An explanation for the lack of an electronegative effect on the epoxidation reaction might be that a hydrogen bond is present in the epoxidation reaction between the catalyst and secondary diazo acetamide **I-49**. It is true that by incorporating a strong electron withdrawing group in position R<sup>5</sup> in the ligand **I-88f** the Lewis acidity of the catalyst will increase but simultaneously, the diazo acetamide **I-49** will form a weaker hydrogen bond with the catalyst **I-3** which result a significant decrease in rate of the reaction. This observation enabled us to propose the mechanism depicted in scheme I-22b for the epoxidation reaction of aldehydes with diazo acetamide. The aldehyde undergoes activation through coordinating to the catalyst **I-3** followed by H-bond formation between complex **I** and diazo compound to give complex **II**. Nucleophilic attack of the diazo compound on the activated aldehyde followed by subsequent ring closure and nitrogen gas extrusion completes the mechanistic cycle.

**Scheme I-22a.** *cis*- and *trans*-aziridination



**Scheme I-22b.** Proposed mechanism for the epoxidation



### 1.4.3. $^{11}\text{B}$ -NMR study

#### 1.4.3.1. Rational for the experiment

Since the charge distribution around the boron nucleus is not symmetrical, it is classified as a *quadrupolar* nucleus. Therefore, if substituents around the quadrupolar boron nucleus possess a cubic symmetry such as  $T_d$ , a sharp absorption would be expected for the  $^{11}\text{B}$ -NMR. In contrast, lack of symmetry around the boron atom, would result in broadening the  $^{11}\text{B}$ -NMR spectrum.<sup>36</sup>



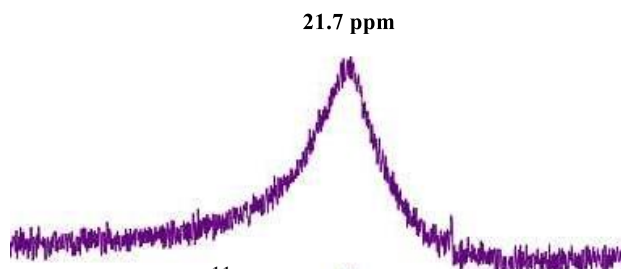
It was envisioned that the  $^{11}\text{B}$ -NMR would enable us to distinguish between coordination of the carbonyl to the catalyst and deprotonation of the catalyst with imine. Our hypothesis was, if the benzaldehyde coordinates to the boron of the catalyst, electronic modulation of the benzaldehyde should effect this coordination. In other words, an electron rich benzaldehyde should have a strong tendency to coordinate to the catalyst which results in a more  $T_d$  boron species and lead to an upfield shift and a sharpening of  $^{11}\text{B}$ -NMR absorption. On the other hand, an electron poor benzaldehydes would be expected to weakly coordinate to the catalyst; as a result, the boron of the catalyst will be more like a three coordinated species. Therefore, a downfield shift and broadening of the  $^{11}\text{B}$ -NMR absorption would be expected for the boron of the catalyst. In contrast, if the imine deprotonates the catalyst, any change in the electronic nature of the imine should not have any impact on the  $^{11}\text{B}$ -NMR spectrum since electron rich and electron poor imines will both change the strength of the H-bond but not chemical environment around the boron species of the catalyst.

#### **1.4.3.2. $^{11}\text{B}$ -NMR of the catalyst **I-3** and catalyst **I-83** in presence of aldehyde and imine**

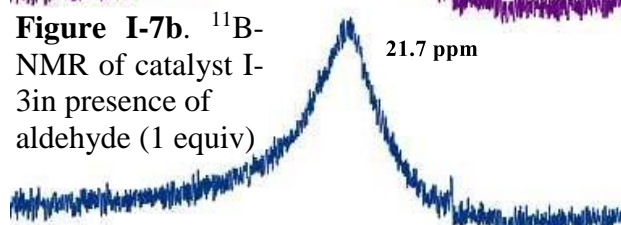
In order to pursue the  $^{11}\text{B}$ -NMR study, first the catalyst was prepared under optimum condition and then subjected to the  $^{11}\text{B}$ -NMR study. The NMR spectrum of the catalyst **I-3** showed a broad absorption at  $\delta = 21.7$  ppm which is typical for a three coordinated borate ester (figure I-7a). The  $^{11}\text{B}$ -NMR spectrum of the catalyst did not change in the presence of 1.0 equiv of the benzaldehyde perhaps due to unfavorable equilibrium for binding (figure I-7b). In contrast, upon the addition of benzhydryl imine of benzaldehyde **I-20a**, the broad peak at 21.7 ppm of catalyst **I-3** is replaced by a sharp absorption at  $\delta = 9.92$  ppm (figure I-7c). This is also the type of  $^{11}\text{B}$ -NMR spectrum seen for the crystal of spiroborate anions **I-83b** and **I-83c** in presence of imine (scheme I-7d and I-7e). An uncharacterized borate ester peak at  $\delta = 6.39$  ppm was also observed for the co-crystal of

catalyst **I-83c** and imine. It should be noted that peak was not present in the solution of **I-83c** + imine but only appear after this catalyst was crystalized.

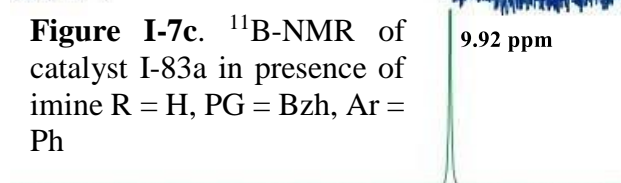
**Figure I-7a.**  $^{11}\text{B}$ -NMR of catalyst I-3



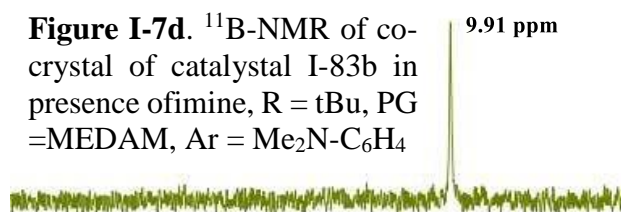
**Figure I-7b.**  $^{11}\text{B}$ -NMR of catalyst I-3 in presence of aldehyde (1 equiv)



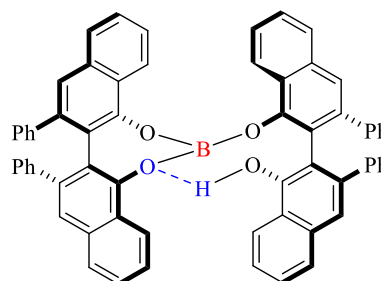
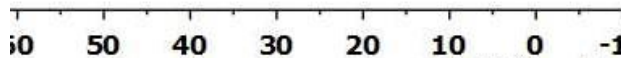
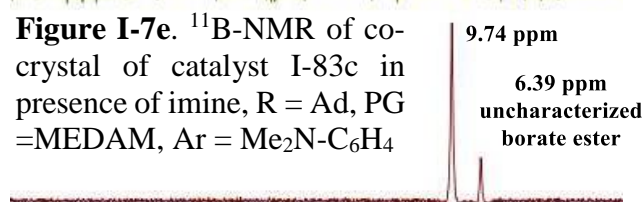
**Figure I-7c.**  $^{11}\text{B}$ -NMR of catalyst I-83a in presence of imine R = H, PG = Bzh, Ar = Ph



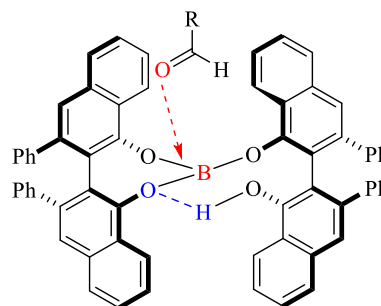
**Figure I-7d.**  $^{11}\text{B}$ -NMR of co-crystal of catalyst I-83b in presence of imine, R = tBu, PG = MEDAM, Ar = Me<sub>2</sub>N-C<sub>6</sub>H<sub>4</sub>



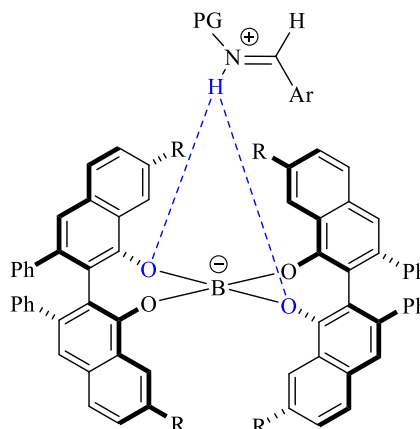
**Figure I-7e.**  $^{11}\text{B}$ -NMR of co-crystal of catalyst I-83c in presence of imine, R = Ad, PG = MEDAM, Ar = Me<sub>2</sub>N-C<sub>6</sub>H<sub>4</sub>



**I-3**



**I-3 + aldehyde (1.0 equiv)**



**I-83a + imine (1.0 equiv):** R = H, PG = Bzh, Ar = Ph

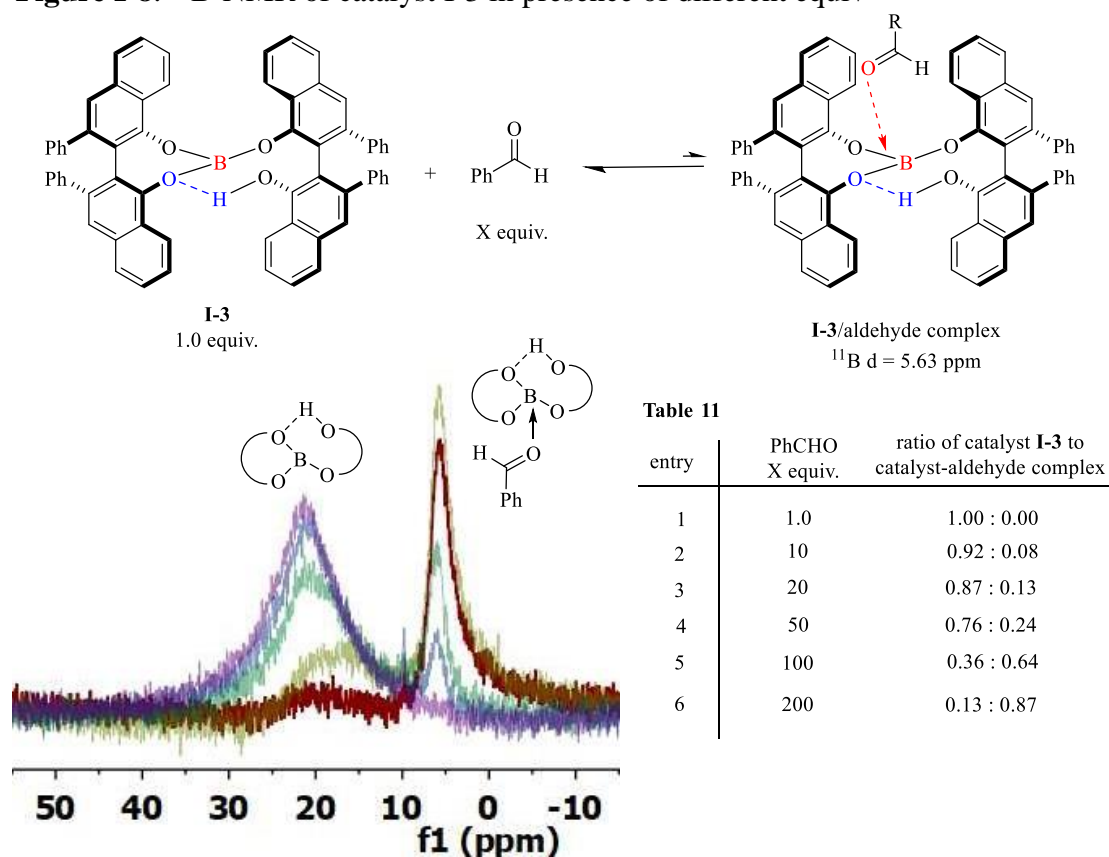
**I-83b + imine:** R = tBu, PG = MEDAM, Ar = Me<sub>2</sub>N-C<sub>6</sub>H<sub>4</sub>

**I-83c + imine:** R = Ad, PG = MEDAM, Ar = Me<sub>2</sub>N-C<sub>6</sub>H<sub>4</sub>

### 1.4.3.3. Unfavorable binding of benzaldehyde to the catalyst I-3

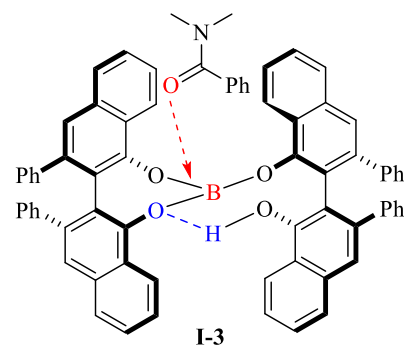
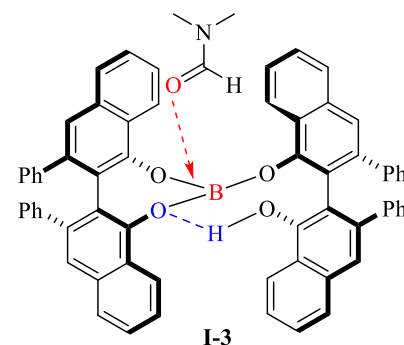
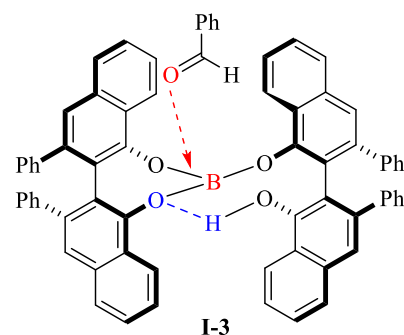
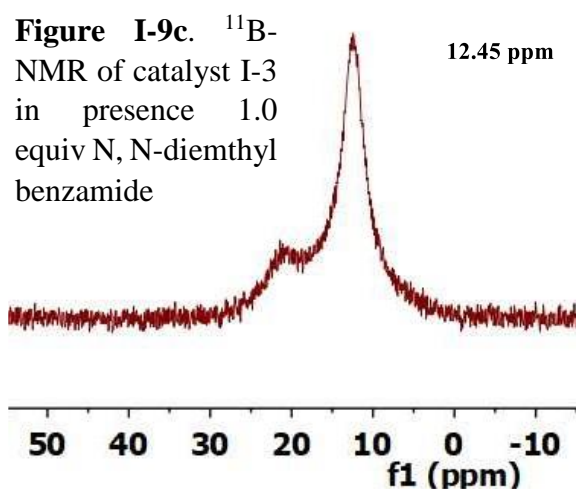
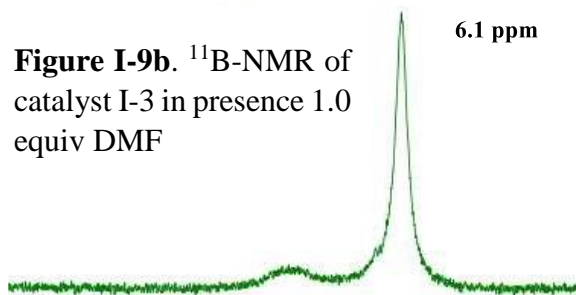
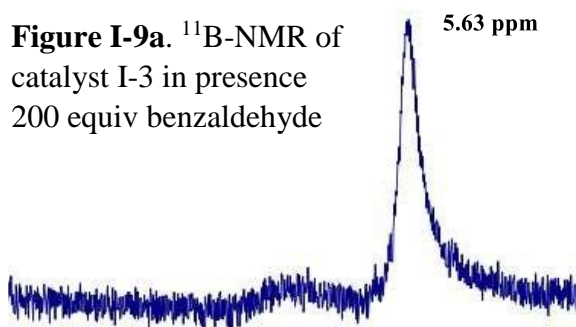
Addition of 1.0 equiv of benzaldehyde did not cause any change in the  $^{11}\text{B}$ -NMR spectrum of the catalyst **I-3** (scheme I-7b). It was thought that the coordination of the aldehyde to the catalyst is not favorable. Based on Le Chatelier's principle, it was decided to increase the concentration of benzaldehyde in order to see if a shift in the equilibrium of the catalyst **I-3** and aldehyde mixture toward the complex of catalyst **I-3** and benzaldehyde could be realized. Increasing the equivalents of benzaldehyde from 1 equiv to 200 equiv caused a significant decrease in the absorption of the three coordinated boron species in catalyst **I-3** which resonated around 20 ppm (figure I-8). Concurrently, a new peak at  $\delta = 5.63$  ppm started to resonate with an increasing intensity relative to the equivalents of benzaldehyde, which presumably belonged to the complex of catalyst **I-3** and benzaldehyde (figure I-8, table 11).

**Figure I-8.**  $^{11}\text{B}$ -NMR of catalyst I-3 in presence of different equiv



#### 1.4.3.4. The use of amides as surrogates for benzaldehyde

In order to avoid super stoichiometric addition of benzaldehyde (figure 9a), it was decided to use an amide as a surrogate for benzaldehyde due to its higher nucleophilicity. We were thrilled to observe a significant change in the  $^{11}\text{B}$ -NMR spectrum upon addition of 1.0 equiv of dimethyl formamide (DMF) (figure 9b vs 9c).

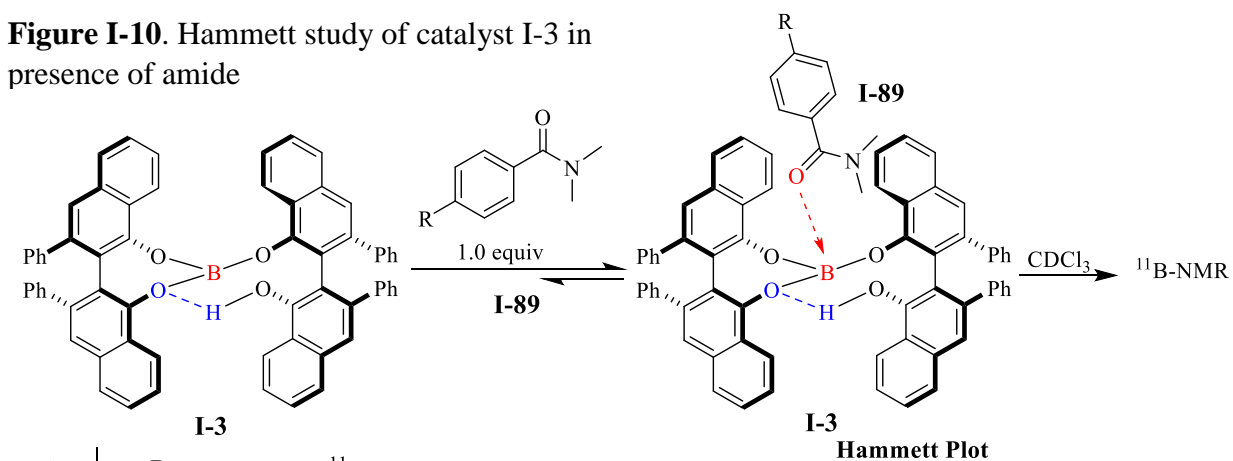


The absorption at ~20 ppm was largely replaced by a sharp peak, which resonated at  $\delta = 6.1$  ppm presumably belonging to the complex of catalyst **I-3** and DMF. Addition of 1.0 equiv. of N,N-dimethyl benzamide **I-89a** also caused a significant change in  $^{11}\text{B}$ -NMR but this time the corresponding peak for complex of catalyst **I-3** and dimethylbenzamide **I-89a** appeared at  $\delta = 12.45$  ppm which was deshielded compared with complex of catalyst **I-3** and DMF (figure 9c). This deshielding could be explained because of steric hindrance; in other words, the carbonyl in dimethyl benzamide **I-89a** cannot coordinate to the catalyst **I-3** as strong as DMF, which leads to a less negative charge accumulation on boron; therefore, the  $^{11}\text{B}$ -NMR of catalyst **I-3** and dimethyl benzamide **I-89a** complex appears at a higher chemical shift.

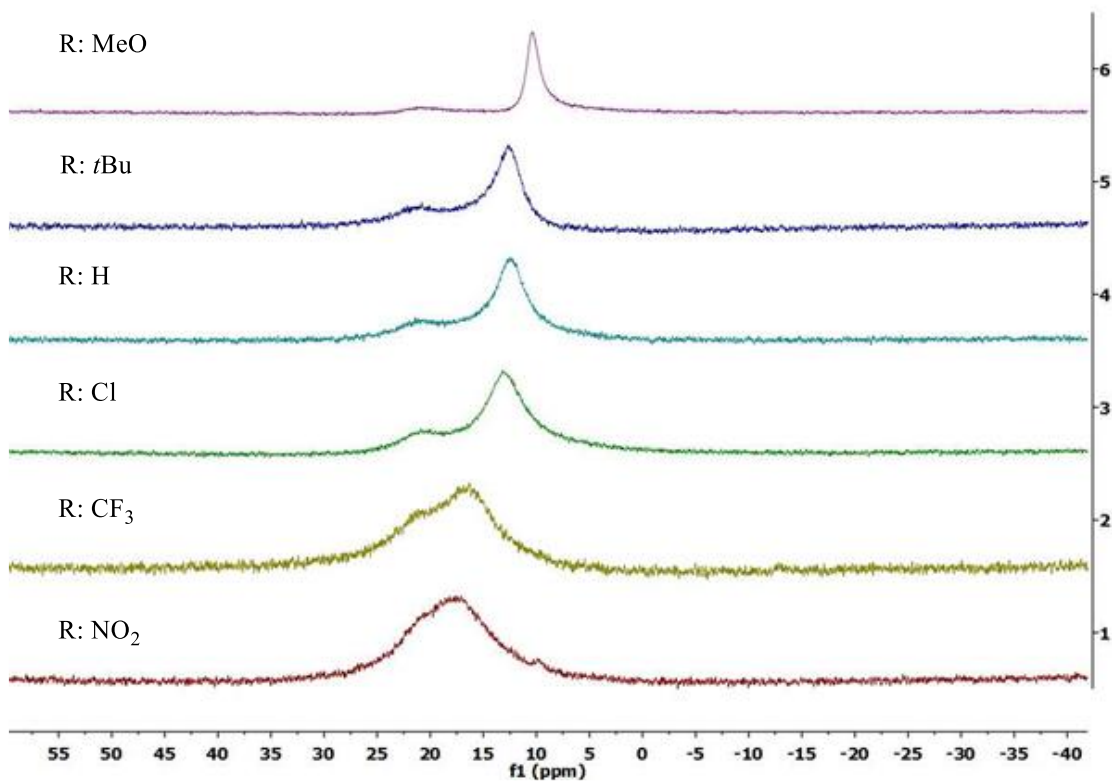
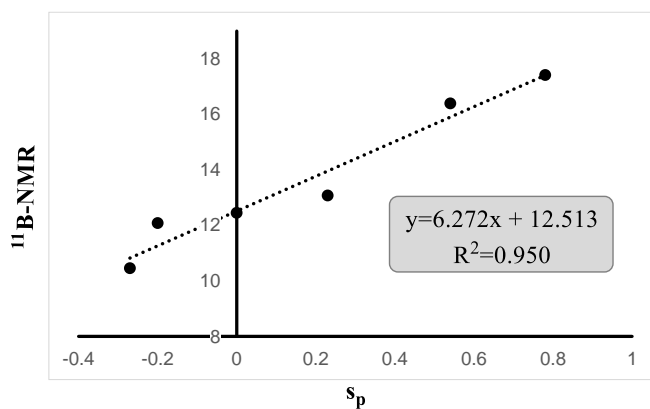
#### 1.4.3.5. Hammett study of catalyst **I-3** in presence of amide

A Hammett study was conducted which involved looking at the correlation between the electronic nature of substituents in *para*-position ( $\text{R}^4$ ) of dimethyl benzamide **I-89** and the chemical shift of boron in the catalyst **I-3** (figure 10). If the carbonyl coordinates to the catalyst, electron donating groups in position  $\text{R}^4$  of the dimethyl benzamide **I-89** would make it a stronger nucleophile leading to a more sturdy coordination to the catalyst **I-3**. As a result, the corresponding  $^{11}\text{B}$  absorption will become sharper and also resonate at lower chemical shift. Exactly the opposite effect would be expected with an electron withdrawing group in  $\text{R}^4$  of the dimethyl benzamide **I-89**. These groups would decrease the nucleophilicity of the dimethyl benzamide and this in turn should result in a more loosely coordinated amide to the catalyst **I-3** which would be expected to lead to a deshielded and broad  $^{11}\text{B}$ -NMR peak. The NMR study was pursued with the synthesis of dimethyl benzamide **I-89** bearing different electron donating and electron withdrawing groups in the *para*-position of the phenyl ring (figure 10). Interestingly, electron donating groups resulted in shielded and sharper  $^{11}\text{B}$ -NMR absorptions; in contrast, electron withdrawing groups generated deshielded and broader

**Figure I-10.** Hammett study of catalyst I-3 in presence of amide



entry	R	amide	$^{11}\text{B-NMR}$	$s_p$
1	MeO	<b>I-89b</b>	10.45	-0.27
2	<i>t</i> -Bu	<b>I-89c</b>	12.08	-0.2
3	H	<b>I-89a</b>	12.45	0
4	Cl	<b>I-89d</b>	13.07	0.23
5	CF <sub>3</sub>	<b>I-89e</b>	16.39	0.54
6	NO <sub>2</sub>	<b>I-89f</b>	17.41	0.78

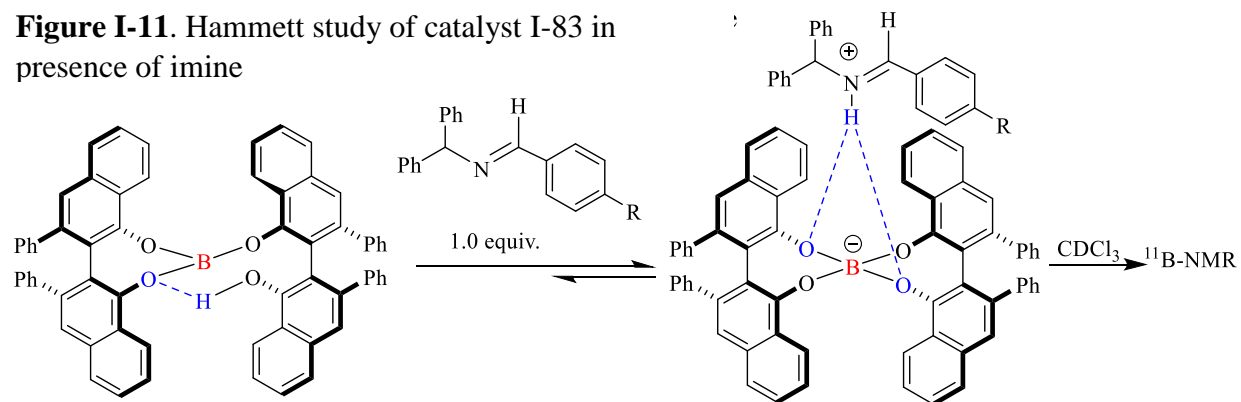


$^{11}\text{B}$ -NMR peaks. The chemical shift of the  $^{11}\text{B}$  in catalyst **I-3** was plotted against the  $\sigma_p$  constant since these  $\sigma$  values were developed for the benzoic acid. We were pleased to observe good correlation between the electronic nature of the  $\text{R}^4$  substituents in dimethyl benzamide **I-89** and the chemical shift of the catalyst **I-3** with a 0.95  $\text{R}^2$  value and a large positive slope (+6.272). This plot clearly indicates a Lewis acid-Lewis base interaction between amide **I-89** and catalyst **I-3**. It is also worth noting that the binding equilibrium for the electron rich amides (**I-89b**, **I-89c**) is favorable toward the complex of catalyst **I-3** and amide **I-89** so that the absorption at  $\delta$  21.7 ppm is largely replaced by the corresponding catalyst/amide peak. However, introducing electron poor substituents at  $\text{R}^4$  position makes this binding less favorable; as a result, only partial conversion of catalyst **I-3** to catalyst **I-3** amide **I-89** complex is observed in the  $^{11}\text{B}$ -NMR spectrum.

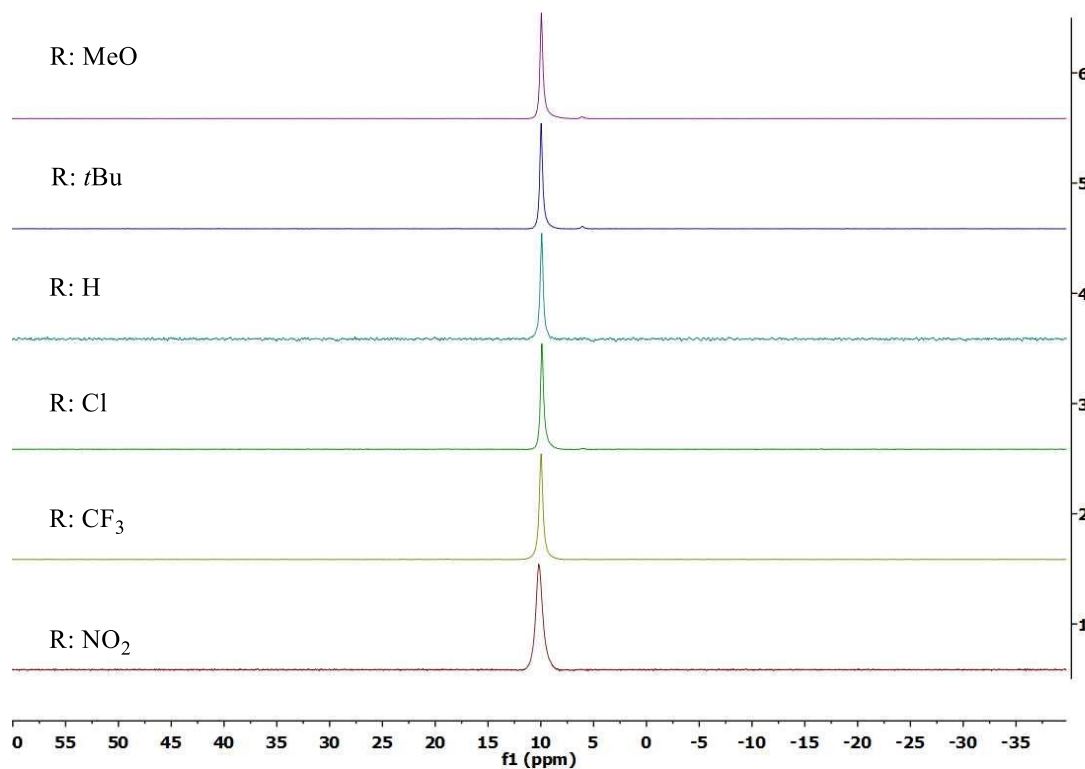
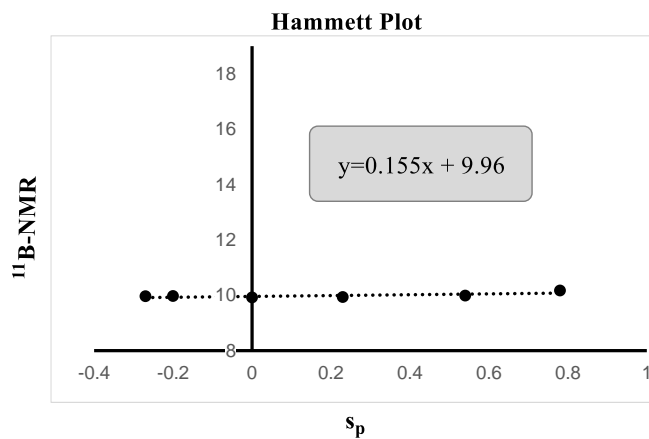
#### 1.4.3.6. Hammett study of catalyst **I-83** in presence of imine

Next, we looked at the correlation between the electronic nature of substituents  $\text{R}^4$  in benzhydryl imine with the chemical shift of  $^{11}\text{B}$ -NMR of catalyst **I-83** (figure 11). It was expected to observe no change in the  $^{11}\text{B}$ -NMR chemical shift of spiroborate anion **I-83** in presence of a number of benzhydryl imines bearing different electron donating and electron withdrawing substituents at the  $\text{R}^4$  position of the phenyl ring. In fact, electron rich or electron poor imines would make the H-bond between iminium ion and spiroborate anion **I-83** stronger or weaker, respectively. As it was expected, with electron rich and electron poor imines, no change in chemical shift of the spiroborate anion **I-83** was observed. This result was in good agreement with the proposed structure of the spiroborate anion **I-83** H-bonded to iminium ion.

**Figure I-11.** Hammett study of catalyst I-83 in presence of imine



entry	R	amide	$^{11}\text{B}$ -NMR	$s_p$
1	MeO	<b>I-90a</b>	9.96	-0.27
2	<i>t</i> -Bu	<b>I-91a</b>	9.97	-0.2
3	H	<b>I-20a</b>	9.92	0
4	Cl	<b>I-92a</b>	9.93	0.23
5	$\text{CF}_3$	<b>I-93a</b>	9.98	0.54
6	$\text{NO}_2$	<b>I-94a</b>	10.17	0.78





## 1.5. Conclusion

In summary, we have developed an extremely active catalyst for the epoxidation reaction. Epoxides were produced with high yields and *ees*. The same catalyst was also highly reactive in the aziridination reaction and yielded aziridines with excellent yields and *ees*. In terms of mechanism, our findings were in sharp contrast with Yamamoto's proposed unified mechanism. We have shown that the catalyst derived from 2 VANOL ligands and 1 boron species follows two different mechanisms in the epoxidation and aziridination reactions. After conducting mechanistic studies, it was observed that VANOL meso-borate catalyst acts as a Brønsted acid catalyst in the presence of an imine and as a Lewis acid catalyst in the presence of an aldehyde. Therefore, this catalyst was named as the chameleon catalyst since its function depends on the substrate. To the best of our knowledge, there are no other examples of catalysts which their mechanism of action depend on the substrates. We believe, our discovery will add a new class of catalyst (chameleon catalyst) to the asymmetric catalysis.

## 1.6. Experimental

### General method for the preparation of catalyst:

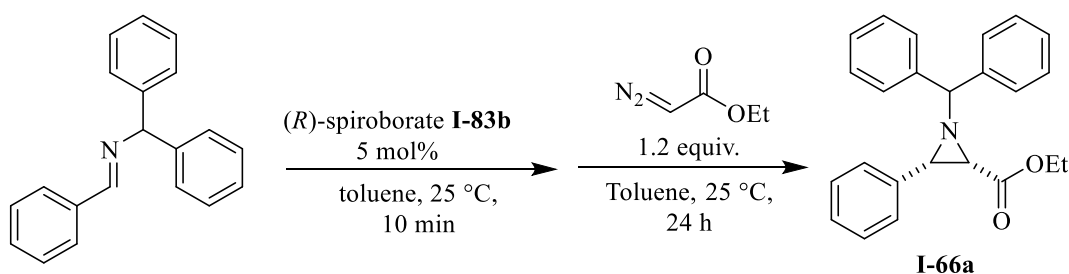
**Method A:** The catalyst was prepared in 25 mL pear-shaped flask in which its 14/20 joint was replaced with a high vacuum threaded T-shaped Teflon vacuum. To this Schlenk flask, which was flame dried and cooled under the continuous flow of the nitrogen from its side arm, was added (*R*)-7,7'-*t*Bu<sub>2</sub>VANOL (0.049 mmol, 28 mg) followed by the addition of 2 mL of freshly distilled toluene. The obtained mixture was stirred at room temperature for 5 min until the ligand was fully dissolved. Next, the Schlenk flask was charged with BH<sub>3</sub>•SMe<sub>2</sub> (0.019 mmol, 13  $\mu$ L, 2 M in toluene). The Teflon valve was closed and the obtained solution was heated at 100 °C for 1 hour followed by removing the volatile by opening the Teflon valve that was connected to vacuum of the Schlenk flask carefully in order to apply the vacuum gradually. After evaporation of the volatiles, the resulting white solid was heat at 100 °C for 0.5 hour under vacuum. The Schlenk flask then was taken out of the oil bath, filled with nitrogen gas and was allowed to cool to room temperature.

**Method B:** The catalyst was prepared in 25 mL pear-shaped flask in which its 14/20 joint was replaced with a high vacuum threaded T-shaped Teflon vacuum. To this Schlenk flask, which was flame dried and cooled under the continuous flow of the nitrogen from its side arm, was added (*R*)-7,7'-*t*Bu<sub>2</sub>VANOL (0.05 mmol, 28 mg) followed by the addition of 2 mL of freshly distilled toluene. The obtained mixture was stirred at room temperature for 5 min until the ligand was fully dissolved. Next, the Schlenk flask was charged with B(OPh)<sub>3</sub> (0.02 mmol, 7.1 mg). The Teflon valve was closed and the obtained solution was heated at 100 °C for 1 hour followed by removing the volatile by opening the Teflon valve that was connected to vacuum of the Schlenk flask carefully in order to apply the vacuum gradually. After evaporation of the volatiles, the resulting

white solid was heat at 100 °C for 0.5 hour under vacuum. The Schlenk flask then was taken out of the oil bath, filled with nitrogen gas and was allowed to cool to room temperature.

**Method C:** A flamed dried round bottom flask under nitrogen gas was charged with (*R*)-7,7'-*t*Bu<sub>2</sub>VANOL (0.049 mmol, 28 mg), triphenyl borate (0.019 mmol, 7.1 mg), imine **I-20b** (0.499 mmol, 135 mg) and 2 mL of toluene. The resulting mixture was stirred for 1 hour at room temperature.

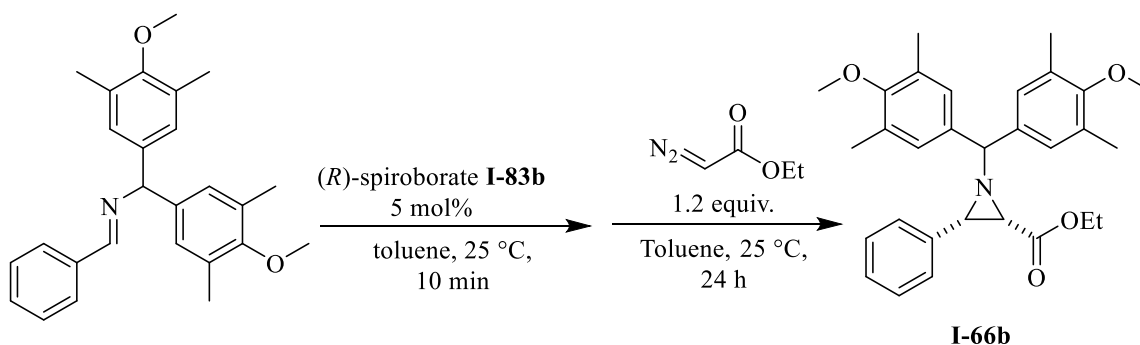
**General method for the asymmetric catalytic aziridination (table 7):**



**(2*S*,3*S*)-ethyl-1-benzhydryl-3-phenylaziridine-2-carboxylate **I-66a**:** To the white solid catalyst a Schlenk flask under nitrogen flow was added imine (0.499 mmol, 135 mg) followed by the addition of 2 mL of toluene and the mixture was stirred at room temperature for 10 minutes. To the resulting solution, ethyl diazo acetate (0.59 mmol, 74  $\mu$ L) was added and the reaction mixture was stirred at room temperature for 24 hours. Crude reaction mixture was transferred to a 50 mL round bottom flask and the solvent was removed under reduced pressure which afford an off-white solid as the crude mixture. At this point, conversion, NMR yield and *cis/trans* ratio was determined by using triphenylmethane as the internal standard (conversion: 95%, NMR yield: 92%, *cis/trans*: >100:1). The crude product was purified via gravity column chromatography using 19:1 hexane: ethyl acetate as the eluent which afforded the desired product **I-66a** as an off-white solid with 85% isolated yield (0.425 mmol, 152 mg). The enantiomeric excess of the product was determined to be 94% by HPLC (CHIRALCEL OD-H column, 90:10 hexane: *i*PrOH as eluents at 222 nm, 0.7

mL/min flow rate).  $R_t$ : 4.75 minute (major enantiomer),  $R_t$ : 10.15 minute (minor enantiomer) (table 7). When this reaction was repeated with a catalyst prepared from the VANOL ligand, the aziridine **I-66a** was obtained in 85% yield (0.425 mmol, 152 mg) with 41% *ee* (table 6).

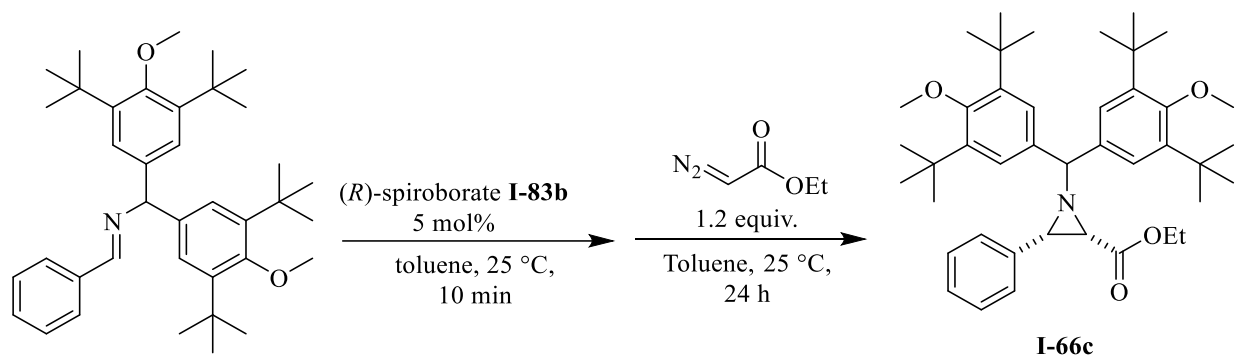
Spectral data for **I-66a**:  $^1\text{H}$  NMR (500 MHz, Chloroform-*d*)  $\delta$  0.99 (t,  $J$  = 7.1 Hz, 3H), 2.69 (d,  $J$  = 6.8 Hz, 1H), 3.23 (d,  $J$  = 6.8 Hz, 1H), 3.89 – 4.02 (m, 3H), 7.16 – 7.26 (m, 2H), 7.22 – 7.31 (m, 5H), 7.31 – 7.39 (m, 2H), 7.38 – 7.47 (m, 2H), 7.48 – 7.54 (m, 2H), 7.59 – 7.65 (m, 2H).  $^{13}\text{C}$  NMR (126 MHz, a Chloroform-*d*)  $\delta$  13.97, 46.39, 48.05, 60.60, 76.79, 127.21, 127.22, 127.34, 127.43, 127.54, 127.78, 127.80, 128.51, 135.02, 142.39, 142.52, 167.76. These data are in agreement with literature values.<sup>21,34</sup>



**(2*S*,3*S*)-ethyl-1-(bis(4-methoxy-3,5-dimethylphenyl)methyl)-3-phenylaziridine-2-**

**carboxylate I-66b (table 7):** The aziridine was prepared by the procedure detailed in *method A* starting with the corresponding imine (0.499 mmol, 194 mg) and the crude product was purified via column chromatography using hexane: ethylacetate 9:1 as the eluent. The desired *cis*-aziridine **I-66b** was obtained as a white solid in 78% isolated yield (0.390 mmol, 185 mg) and 97% *ee* by the HPLC analysis (CHIRALCEL OD-H column, 99:1 hexane: *i*PrOH as eluents at 226 nm, 0.7 mL/min flow rate).  $R_t$ : 9.6 minute (major enantiomer),  $R_t$ : 12.6 minute (minor enantiomer). When this reaction was repeated with a catalyst prepared from the VANOL ligand, the aziridine **I-66b** was obtained in 92% isolated yield (0.460 mmol, 218 mg) with 86% *ee* (table 6).

Spectral data for **I-66b**:  $^1\text{H}$  NMR (500 MHz, Chloroform-*d*)  $\delta$  1.01 (t,  $J = 7.1$  Hz, 3H), 2.21 (s, 6H), 2.23 – 2.29 (m, 6H), 2.59 (dd,  $J = 6.8, 0.5$  Hz, 1H), 3.14 (d,  $J = 6.8$  Hz, 1H), 3.65 (s, 3H), 3.70 (d,  $J = 6.5$  Hz, 4H), 3.88 – 4.02 (m, 2H), 7.11 – 7.15 (m, 2H), 7.16 – 7.29 (m, 5H), 7.36 – 7.42 (m, 2H).  $^{13}\text{C}$  NMR (126 MHz, Chloroform-*d*)  $\delta$  14.03, 16.19, 16.26, 46.25, 48.20, 59.55, 59.61, 60.52, 127.22, 127.37, 127.72, 127.78, 127.84, 130.61, 130.63, 135.28, 137.79, 137.95, 155.89, 156.05, 168.03. These data are in agreement with the literature values.<sup>38</sup>

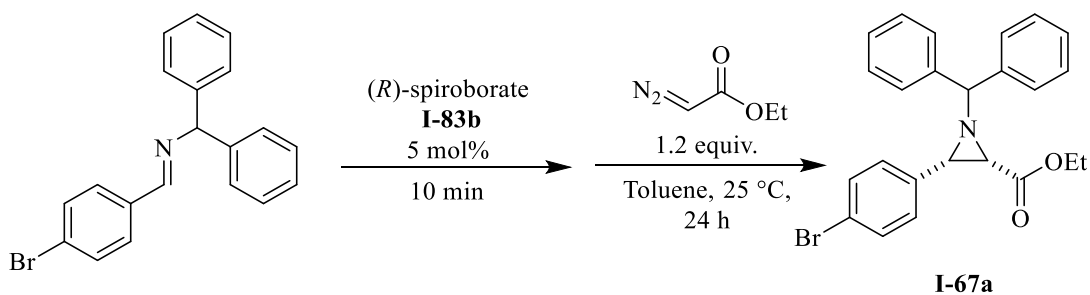


**(2*S*,3*S*)-ethyl-1-(bis(4-methoxy-3,5-di-tert-butylphenyl)methyl)-3-phenylaziridine-2-carboxylate **I-66c** (table 7):**

The aziridine was prepared by the procedure detailed in *method A* starting with the corresponding imine (0.498 mmol, 278 mg) and the crude product was purified via column chromatography using hexane: ethylacetate 20:1 as the eluent. The desired *cis*-aziridine **I-66c** was obtained as a white solid in 95% isolated yield (0.475 mmol, 305 mg) and 96% *ee* by the HPLC analysis (CHIRALCEL OD-H column, 99:1 hexane: *i*PrOH as eluents at 225 nm, 1 mL/min flow rate).  $R_t$ : 5.2 minute (minor enantiomer),  $R_t$ : 9.4 minute (major enantiomer). When this reaction was repeated with a catalyst prepared from the VANOL ligand, the aziridine **I-66c** was obtained in 79% isolated yield (0.395 mmol, 254 mg) with 80% *ee* (table 6).

Spectral data for **I-66c**:  $^1\text{H}$  NMR (500 MHz, Chloroform-*d*)  $\delta$  1.01 (td,  $J = 7.1, 2.0$  Hz, 3H), 1.35 (dd,  $J = 2.9, 1.1$  Hz, 18H), 1.43 (dd,  $J = 3.1, 1.2$  Hz, 18H), 2.65 – 2.71 (m, 1H), 3.20 (dd,  $J = 6.8,$

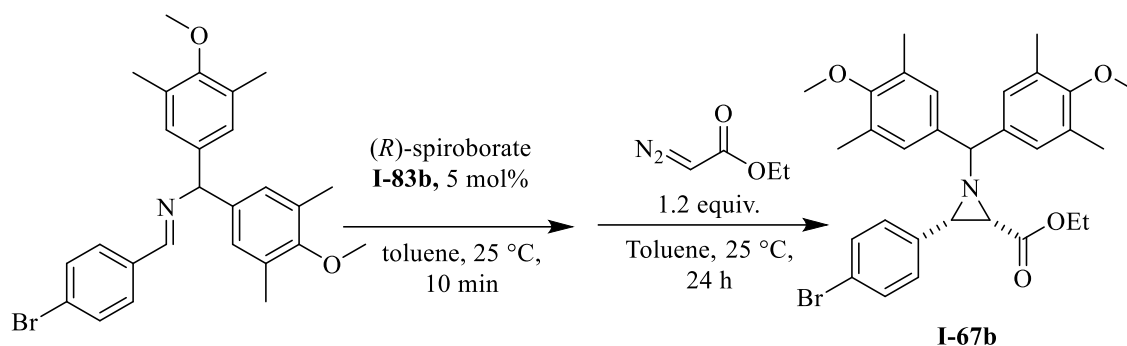
2.7 Hz, 1H), 3.63 (d,  $J = 2.3$  Hz, 3H), 3.69 (d,  $J = 2.6$  Hz, 3H), 3.86 (d,  $J = 3.2$  Hz, 1H), 3.87 – 4.01 (m, 2H), 7.18 – 7.25 (m, 1H), 7.27 (td,  $J = 7.9, 7.5, 1.9$  Hz, 2H), 7.36 (d,  $J = 3.0$  Hz, 2H), 7.43 – 7.50 (m, 2H), 7.48 – 7.54 (m, 2H).  $^{13}\text{C}$  NMR (126 MHz, Chloroform- $d$ )  $\delta$  13.99, 32.06, 32.15, 35.73, 35.80, 46.37, 48.82, 60.55, 63.95, 64.04, 76.78, 125.36, 125.47, 127.26, 127.60, 128.16, 135.32, 136.71, 136.86, 143.00, 143.07, 158.22, 158.23, 168.30. These spectral data match with the literature values.<sup>39</sup>



**(2S,3S)-ethyl-1-benzhydryl-3-(4-bromophenyl)aziridine-2-carboxylate I-67a (table 7):** The aziridine was prepared by the procedure detailed in *method A* starting with the corresponding imine (0.498 mmol, 175 mg) and the crude product was purified via column chromatography using hexane: ethylacetate 9:1 as the eluent. The desired *cis*-aziridine **I-67a** was obtained as a white solid in 73% isolated yield (0.365 mmol, 159 mg) and 93% *ee* by the HPLC analysis (CHIRALCEL OD-H column, 98:2 hexane: *i*PrOH as eluents at 222 nm, 1 mL/min flow rate).  $R_t$ : 3.37 minute (minor enantiomer),  $R_t$ : 13.48 minute (major enantiomer). When this reaction was repeated with a catalyst prepared from the VANOL ligand, the aziridine **I-67a** was obtained in 70% isolated yield (0.395 mmol, 254 mg) with 48% *ee* (table 6).

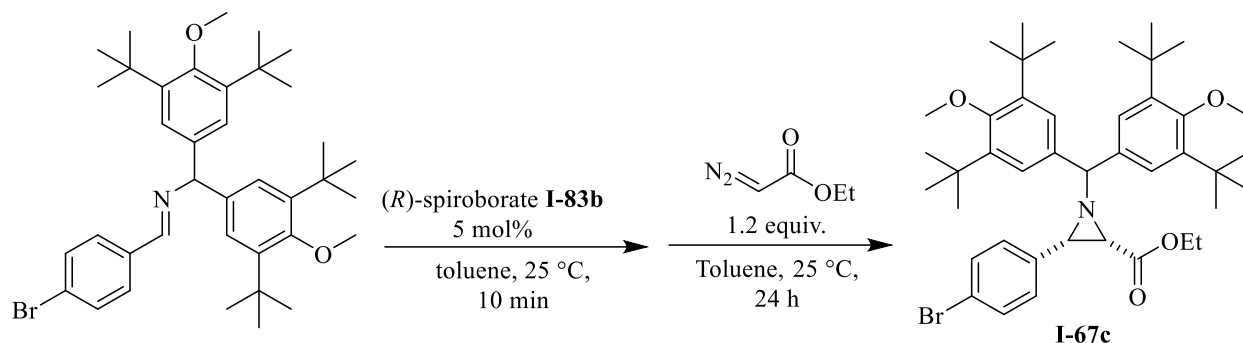
Spectral data for **I-67a**:  $^1\text{H}$  NMR (500 MHz, Chloroform- $d$ ) 1.04 (t,  $J = 7.1$  Hz, 3H), 2.70 (d,  $J = 6.8$  Hz, 1H), 3.15 (d,  $J = 6.8$  Hz, 1H), 3.93 – 4.01 (m, 3H), 7.21 – 7.30 (m, 3H), 7.26 – 7.38 (m, 5H), 7.36 – 7.42 (m, 2H), 7.43 – 7.50 (m, 2H), 7.56 – 7.62 (m, 2H).  $^{13}\text{C}$  NMR (126 MHz, Chloroform- $d$ )  $\delta$  14.04, 46.48, 47.37, 60.77, 77.60, 121.36, 127.14, 127.30, 127.43, 127.52,

128.54, 129.56, 130.91, 134.05, 142.15, 142.32, 167.45. One  $sp^2$  carbon is not located. These spectral data match with the literature values.<sup>21,34</sup>



**(2*S*,3*S*)-ethyl-1-(bis(4-methoxy-3,5-dimethylphenyl)methyl)-3-(4-bromophenyl)aziridine-2-carboxylate **I-67b** (table 7):** The aziridine was prepared by the procedure detailed in *method A* starting with the corresponding imine (0.499 mmol, 233 mg) and the crude product was purified via column chromatography using hexane: ethylacetate 5:1 as the eluent. The desired *cis*-aziridine **I-67b** was obtained as a white solid in 96% isolated yield (0.485 mmol, 265 mg) and 99% *ee* by the HPLC analysis (CHIRALCEL OD-H column, 99:1 hexane: *i*PrOH as eluents at 226 nm, 0.7 mL/min flow rate).  $R_t$ : 8.5 minute (minor enantiomer),  $R_t$ : 12.0 minute (major enantiomer). When this reaction was repeated with a catalyst prepared from the VANOL ligand, the aziridine **I-67a** was obtained in 90% isolated yield (0.455 mmol, 248 mg) with 80% *ee* (table 6).

Spectral data for **I-67b**:  $^1\text{H}$  NMR (500 MHz, Chloroform-*d*)  $\delta$  1.05 (t,  $J$  = 7.1 Hz, 3H), 2.21 (s, 6H), 2.27 (s, 6H), 2.60 (d,  $J$  = 6.8 Hz, 1H), 3.06 (d,  $J$  = 6.8 Hz, 1H), 3.62–3.67 (s, 7H), 3.96 (qt,  $J$  = 7.3, 3.7 Hz, 2H), 7.09 (s, 2H), 7.19 (s, 2H), 7.25 – 7.32 (m, 2H), 7.34 – 7.41 (m, 2H).  $^{13}\text{C}$  NMR (126 MHz, Chloroform-*d*)  $\delta$  14.10, 16.22, 16.27, 46.34, 47.55, 59.57, 59.61, 60.68, 121.23, 127.32, 127.66, 129.61, 130.70, 130.83, 134.32, 137.58, 137.76, 155.96, 156.11, 167.72. One  $sp^2$  and one  $sp^3$  are not located. These data are in agreement with the literature values.<sup>40</sup>

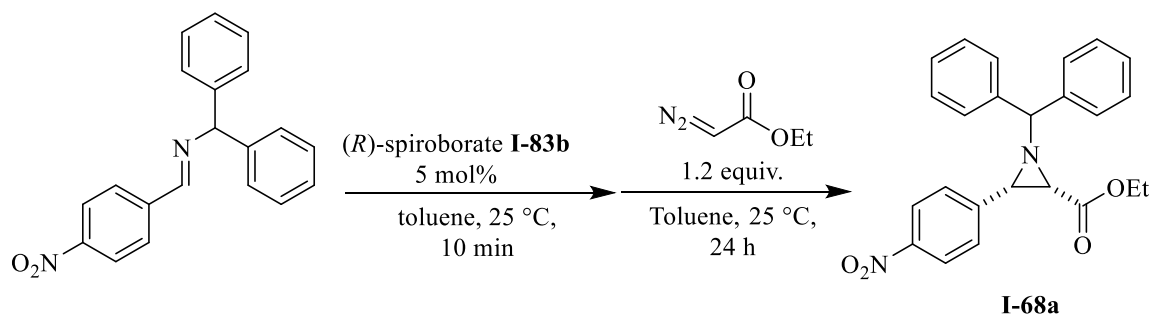


**(2*S*,3*S*)-ethyl-1-(bis(4-methoxy-3,5-di-*tert*-butylphenyl)methyl)-3-(4-**

**bromophenyl)aziridine-2-carboxylate **I-67c** (table 7):** The aziridine was prepared by the procedure detailed in *method A* starting with the corresponding imine (0.499 mmol, 317 mg) and the crude product was purified via column chromatography using hexane: ethylacetate 20:1 as the eluent. The desired *cis*-aziridine **I-67c** was obtained as a white solid in 71% isolated yield (0.355 mmol, 256 mg) and 89% *ee* by the HPLC analysis (Pirkle covalent (R, R) Whelk-O1 column, 99:1 hexane: *i*PrOH as eluents at 225 nm, 1 mL/min flow rate). *R*<sub>t</sub>: 5.4 minute (minor enantiomer), *R*<sub>t</sub>: 9.2 minute (major enantiomer). When this reaction was repeated with a catalyst prepared from the VANOL ligand, the aziridine **I-67c** was obtained in 28% isolated yield (0.141 mmol, 101 mg) with 74% *ee* (table 6).

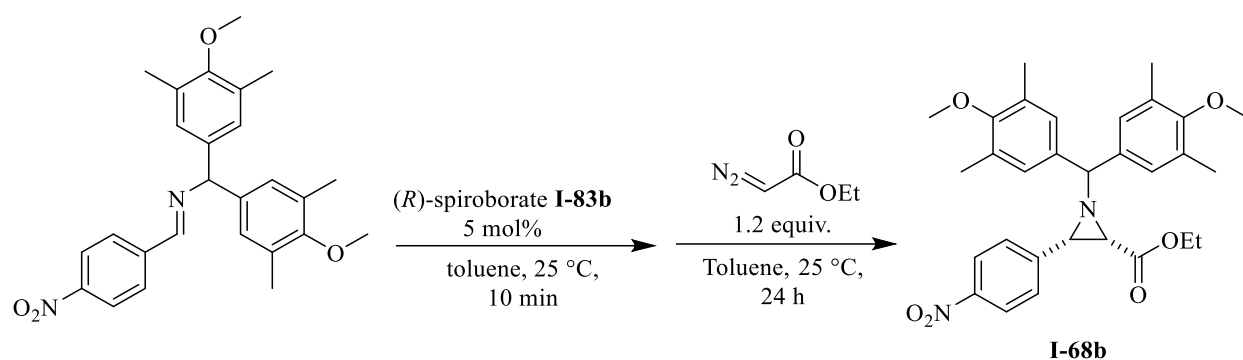
Spectral data for **I-67c**: <sup>1</sup>H NMR (500 MHz, Chloroform-*d*) δ 1.03 (t, *J* = 7.1 Hz, 3H), 1.30-1.37 (s, 36H), 2.67 (s, 1H), 3.13 (s, 1H), 3.61 (s, 3H), 3.67 (s, 3H), 3.86 – 4.03 (m, 3H), 7.30 (s, 2H), 7.32 – 7.42 (m, 6H). <sup>13</sup>C NMR (126 MHz, Chloroform-*d*) δ 14.04, 31.60, 32.04, 32.11, 35.72, 35.79, 46.35, 48.10, 60.71, 63.98, 64.04, 77.15, 125.27, 125.36, 129.89, 130.69, 134.40, 136.43, 136.61, 143.10, 143.13, 167.97. Two *sp*<sup>2</sup> carbon are not located. These spectral data match with the literature values.<sup>39</sup>





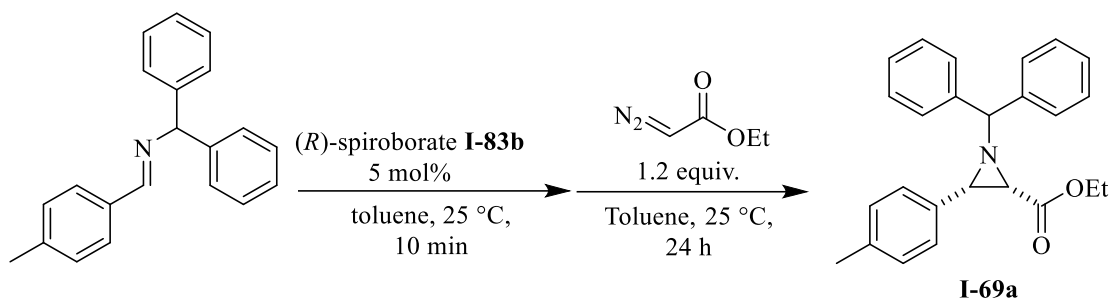
**(2S,3S)-ethyl-1-benzhydryl-3-(4-nitrophenyl)aziridine-2-carboxylate I-68a** (table 7): The aziridine was prepared by the procedure detailed in *method A* starting with the corresponding imine (0.499 mmol, 158 mg) and the crude product was purified via column chromatography using hexane: ethylacetate 5:1 as the eluent. The desired *cis*-aziridine **I-68a** was obtained as a white solid in 41% isolated yield (0.205 mmol, 82.5 mg) and 95% *ee* by the HPLC analysis (CHIRALCEL OD-H column, 90:10 hexane: *i*PrOH as eluents at 222 nm, 0.7 mL/min flow rate).  $R_t$ : 8.8 minute (minor enantiomer),  $R_t$ : 11.4 minute (major enantiomer). When this reaction was repeated with a catalyst prepared from the VANOL ligand, the aziridine **I-68a** was obtained in 68% isolated yield (0.341 mmol, 137 mg) with 50% *ee* (table 6).

Spectral data for **I-68a**:  $^1\text{H}$  NMR (500 MHz, Chloroform-*d*)  $\delta$  1.03 (t,  $J = 7.2$  Hz, 3H), 2.80 (d,  $J = 6.9$  Hz, 1H), 3.26 (d,  $J = 6.8$  Hz, 1H), 3.92 – 4.02 (m, 3H), 7.17 – 7.27 (m, 1H), 7.28 (ddt,  $J = 9.1, 7.4, 1.9$  Hz, 3H), 7.31 – 7.40 (m, 2H), 7.43 – 7.50 (m, 2H), 7.55 – 7.64 (m, 4H), 8.09 – 8.16 (m, 2H).  $^{13}\text{C}$  NMR (126 MHz, Chloroform-*d*)  $\delta$  14.03, 46.91, 47.07, 60.97, 76.76, 123.07, 127.03, 127.35, 127.44, 127.69, 128.62, 128.66, 128.77, 141.81, 142.03, 142.48, 147.38, 166.97. These data are in agreement with the literature values.<sup>21,34</sup>



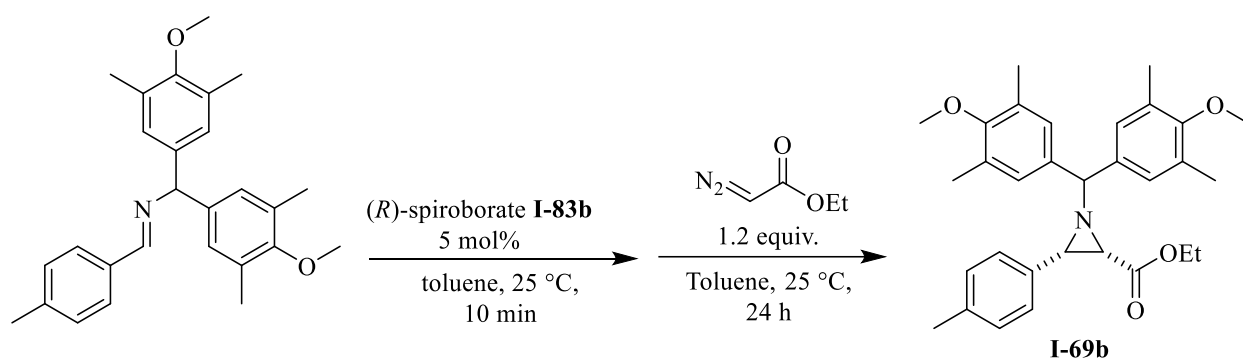
**(2*S*,3*S*)-ethyl-1-(bis(4-methoxy-3,5-dimethylphenyl)methyl)-3-(4-nitrophenyl)aziridine-2-carboxylate **I-68b** (table 7):** The aziridine was prepared by the procedure detailed in *method A* starting with the corresponding imine (0.499 mmol, 216 mg) and the crude product was purified via column chromatography using hexane: ethylacetate 9:1 as the eluent. The desired *cis*-aziridine **I-68b** was obtained as a white solid in 70% isolated yield (0.351 mmol, 181 mg) and 99% *ee* by the HPLC analysis (CHIRALCEL OD-H column, 99:1 hexane: *i*PrOH as eluents at 226 nm, 0.7 mL/min flow rate).  $R_t$ : 17.2 minute (minor enantiomer),  $R_t$ : 28.0 minute (major enantiomer). When this reaction was repeated with a catalyst prepared from the VANOL ligand, the aziridine **I-68b** was obtained in 78% isolated yield (0.391 mmol, 202 mg) with 97% *ee* (table 6).

Spectral data for **I-68b**:  $^1\text{H}$  NMR (500 MHz, Chloroform-*d*)  $\delta$  1.04 (t,  $J$  = 7.1 Hz, 3H), 2.21 (s, 6H), 2.27 (s, 6H), 2.71 (d,  $J$  = 6.8 Hz, 1H), 3.18 (d,  $J$  = 6.7 Hz, 1H), 3.64 (s, 3H), 3.72 (s, 3H), 3.75 (s, 1H), 3.95 (qd,  $J$  = 7.1, 1.7 Hz, 2H), 7.09 (s, 2H), 7.18 (s, 2H), 7.56 – 7.63 (m, 2H), 8.09 – 8.16 (m, 2H).  $^{13}\text{C}$  NMR (126 MHz, Chloroform-*d*)  $\delta$  14.10, 16.24, 16.28, 46.81, 47.27, 59.57, 59.63, 60.90, 77.03, 123.00, 127.23, 127.57, 128.82, 130.84, 130.88, 137.27, 137.49, 142.80, 147.22, 156.07, 156.23, 167.23. These data are in agreement with the literature values.<sup>38</sup>



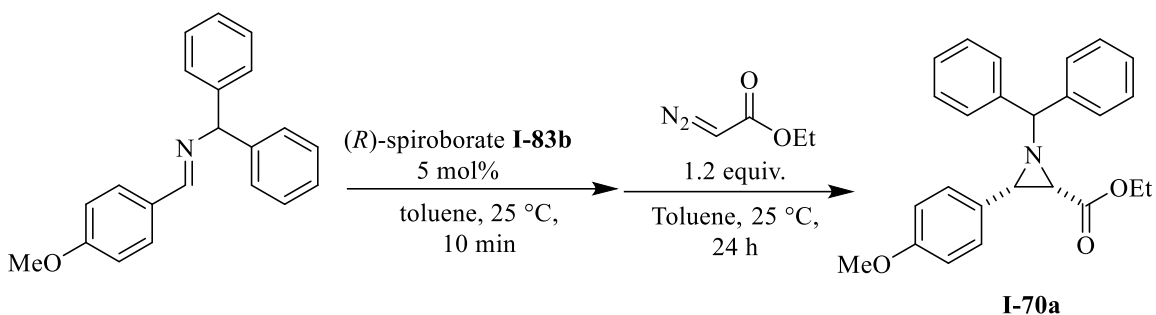
**(2*S*,3*S*)-ethyl-1-benzhydryl-3-(4-methylphenyl)aziridine-2-carboxylate I-69a (table 7):** The aziridine was prepared by the procedure detailed in *method A* starting with corresponding imine (0.499 mmol, 143 mg) and the crude product was purified via column chromatography using hexane: ethylacetate 9:1 as the eluent. The desired *cis*-aziridine **I-69a** was obtained as a white solid in 91% isolated yield (0.455 mmol, 169 mg) and 93% *ee* by the HPLC analysis (CHIRALCEL OD-H column, 90:10 hexane: *i*PrOH as eluents at 222 nm, 0.7 mL/min flow rate).  $R_t$ : 4.2 minute (minor enantiomer),  $R_t$ : 7.65 minute (major enantiomer). When this reaction was repeated with a catalyst prepared from the VANOL ligand, the aziridine **I-69a** was obtained in 78% isolated yield (0.391 mmol, 145 mg) with 24% *ee* (table 6).

Spectral data for **I-69a**:  $^1\text{H}$  NMR (500 MHz, Chloroform-*d*)  $\delta$  1.02 (t,  $J$  = 7.1 Hz, 3H), 2.30 (s, 3H), 2.65 (d,  $J$  = 6.8 Hz, 1H), 3.19 (d,  $J$  = 6.8 Hz, 1H), 3.92 – 4.00 (m, 3H), 7.04 – 7.09 (m, 2H), 7.14 – 7.25 (m, 1H), 7.21 – 7.32 (m, 5H), 7.34 (dd,  $J$  = 8.4, 6.9 Hz, 2H), 7.46 – 7.52 (m, 2H), 7.57 – 7.64 (m, 2H).  $^{13}\text{C}$  NMR (126 MHz, Chloroform-*d*)  $\delta$  14.01, 21.16, 46.35, 48.04, 60.56, 77.75, 127.18, 127.22, 127.37, 127.53, 127.66, 128.47, 131.96, 136.91, 142.45, 142.55, 167.84. These spectral data are in agreement with the literature values.<sup>37</sup>



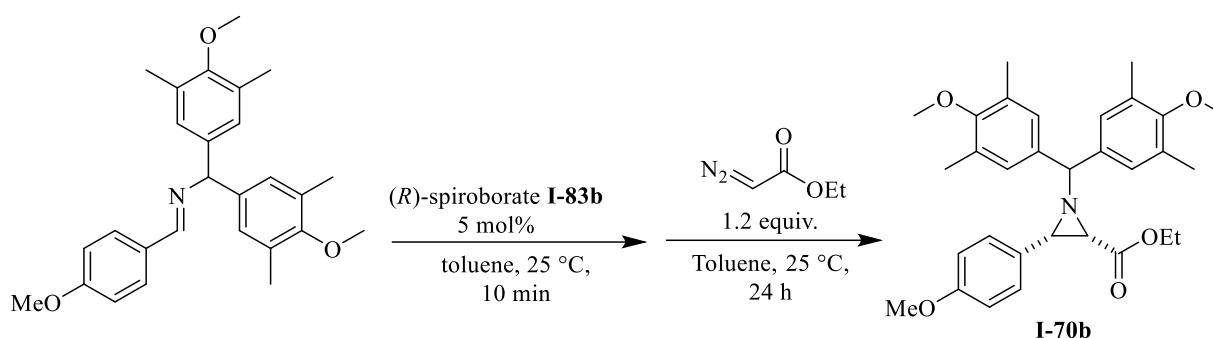
**(2S,3S)-ethyl-1-(bis(4-methoxy-3,5-dimethylphenyl)methyl)-3-(4-methylphenyl)aziridine-2-carboxylate I-69b (table 7):** The aziridine was prepared by the procedure detailed in *method A* starting with the corresponding imine (0.499 mmol, 201 mg) and the crude product was purified via column chromatography using hexane: ethylacetate 9:1 as the eluent. The desired *cis*-aziridine **I-69b** was obtained as a white solid in 98% isolated yield (0.491 mmol, 239 mg) and 99% *ee* by the HPLC analysis (CHIRALCEL OD-H column, 99:1 hexane: *i*PrOH as eluents at 226 nm, 0.7 mL/min flow rate).  $R_t$ : 9.4 minute (minor enantiomer),  $R_t$ : 11.8 minute (major enantiomer). When this reaction was repeated with a catalyst prepared from the VANOL ligand, the aziridine **I-69b** was obtained in 52% isolated yield (0.261 mmol, 127 mg) with 63% *ee* (table 6).

Spectral data for **I-69b**:  $^1\text{H}$  NMR (500 MHz, Chloroform-*d*)  $\delta$  1.05 (t,  $J = 7.1$  Hz, 3H), 2.22 (s, 6H), 2.29 (d,  $J = 11.1$  Hz, 6H), 2.30 (s, 3H), 2.56 (d,  $J = 6.8$  Hz, 1H), 3.11 (d,  $J = 6.8$  Hz, 1H), 3.65–3.68 (m, 7H), 3.97 (qd,  $J = 7.1, 2.5$  Hz, 2H), 7.07 (d,  $J = 7.8$  Hz, 2H), 7.13 (s, 2H), 7.21 (s, 2H), 7.26 – 7.31 (m, 2H).  $^{13}\text{C}$  NMR (126 MHz, Chloroform-*d*)  $\delta$  14.08, 16.19, 16.25, 21.15, 46.19, 48.21, 59.54, 59.60, 60.49, 77.09, 127.39, 127.71, 127.79, 128.42, 130.56, 130.60, 132.22, 136.79, 137.86, 137.99, 155.87, 156.02, 168.12. These spectral data are in agreement with the literature values.<sup>38</sup>



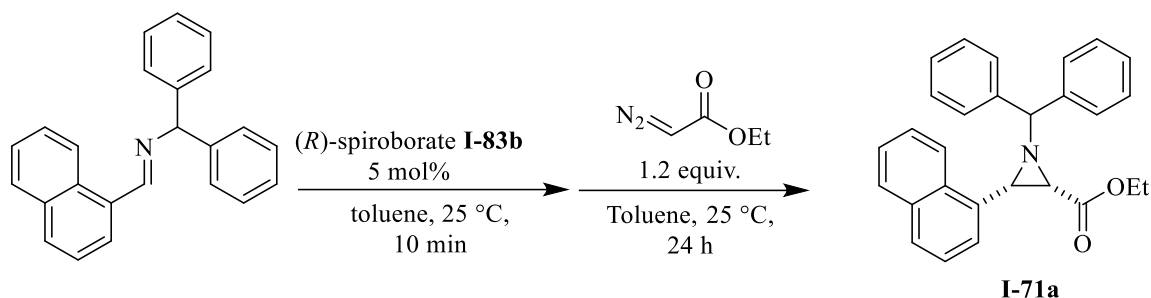
**(2*S*,3*S*)-ethyl-1-benzhydryl-3-(4-methoxyphenyl)aziridine-2-carboxylate **I-70a** (table 7):** The aziridine was prepared by the procedure detailed in *method A* starting with the corresponding imine (0.499 mmol, 151 mg) and the crude product was purified via column chromatography using hexane: ethylacetate 9:1 and 1% Et<sub>3</sub>N as the eluent. The desired *cis*-aziridine **I-70a** was obtained as a white solid in 78% isolated yield (0.391 mmol, 151 mg) and 95% *ee* by the HPLC analysis (CHIRALCEL OD-H column, 95:5 hexane: *i*PrOH as eluents at 222 nm, 0.7 mL/min flow rate). *R*<sub>t</sub>: 6.4 minute (minor enantiomer), *R*<sub>t</sub>: 14.8 minute (major enantiomer). When this reaction was repeated with a catalyst prepared from the VANOL ligand, the aziridine **I-70a** was obtained in 19% NMR yield (table 6).

Spectral data for **I-70a**: <sup>1</sup>H NMR (500 MHz, Chloroform-*d*) δ 1.02 (t, *J* = 7.1 Hz, 3H), 2.62 (d, *J* = 6.8 Hz, 1H), 3.16 (d, *J* = 6.8 Hz, 1H), 3.75 (s, 3H), 3.91 – 4.01 (m, 3H), 6.75 – 6.84 (m, 2H), 7.13 – 7.21 (m, 1H), 7.20 – 7.31 (m, 5H), 7.33 (d, *J* = 15.3 Hz, 2H), 7.44 – 7.52 (m, 2H), 7.52 – 7.65 (m, 2H). <sup>13</sup>C NMR (126 MHz, Chloroform-*d*) δ 14.02, 46.33, 47.74, 55.16, 60.53, 77.71, 113.22, 127.11, 127.16, 127.21, 127.35, 127.51, 128.45, 128.87, 142.41, 142.56, 158.89, 167.86. One *sp*<sup>2</sup> carbon is not located. These data are in agreement with the literature values.<sup>34</sup>



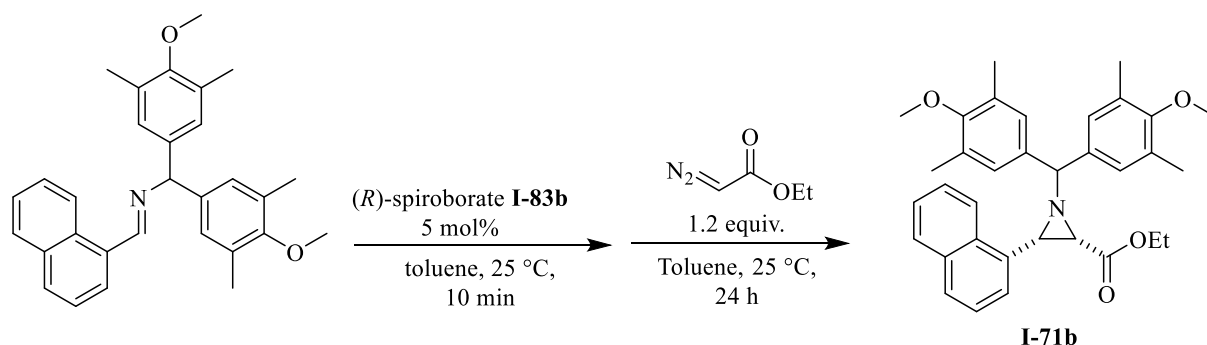
**(2*S*,3*S*)-ethyl-1-(bis(4-methoxy-3,5-dimethylphenyl)methyl)-3-(4-methoxyphenyl)aziridine-2-carboxylate **I-70b** (table 7):** The aziridine was prepared by the procedure detailed in *method A* starting with the corresponding imine (0.499 mmol, 209 mg) and the crude product was purified via column chromatography using hexane: ethylacetate 9:1 and 1% Et<sub>3</sub>N as the eluent. The desired *cis*-aziridine **I-70b** was obtained as a white solid in 93% isolated yield (0.465 mmol, 234 mg) and 99% *ee* by the HPLC analysis (CHIRALCEL OD-H column, 99:1 hexane: *i*PrOH as eluents at 226 nm, 0.7 mL/min flow rate). *R*<sub>t</sub>: 12.2 minute (minor enantiomer), *R*<sub>t</sub>: 19.4 minute (major enantiomer). When this reaction was repeated with a catalyst prepared from the VANOL ligand, the aziridine **I-70b** was obtained in 5% NMR yield (table 6).

Spectral data for **I-70b**: <sup>1</sup>H NMR (500 MHz, Chloroform-*d*) δ 1.04 (t, *J* = 7.1 Hz, 3H), 2.20 (s, 6H), 2.26 (s, 6H), 2.53 (d, *J* = 6.7 Hz, 1H), 3.08 (d, *J* = 6.8 Hz, 1H), 3.65 (s, 3H), 3.66 (s, 1H), 3.70 (s, 3H), 3.76 (s, 3H), 3.96 (dtd, *J* = 10.4, 7.9, 7.3, 4.5 Hz, 2H), 6.78 (dd, *J* = 8.7, 2.0 Hz, 2H), 7.10 (s, 2H), 7.19 (s, 2H), 7.24 – 7.33 (dd, *J* = 8.7, 2.0 Hz, 2H). <sup>13</sup>C NMR (126 MHz, Chloroform-*d*) δ 14.10, 16.20, 16.24, 46.18, 47.89, 55.19, 59.54, 59.60, 60.49, 113.14, 127.37, 127.38, 127.75, 128.92, 130.57, 130.59, 137.82, 137.99, 155.86, 156.01, 158.78, 168.15. One *sp*<sup>2</sup> carbon is not located. These spectral data are in agreement with the literature values.<sup>38</sup>



**(2*S*,3*S*)-ethyl-1-benzhydryl-3-(naphthalen-1-yl)aziridine-2-carboxylate I-71a (table 7):** The aziridine was prepared by the procedure detailed in *method A* starting with the corresponding imine (0.499 mmol, 161 mg) and the crude product was purified via column chromatography using hexane: ethylacetate 9:1 as the eluent. The desired *cis*-aziridine **I-71a** was obtained as a white solid in 40% isolated yield (0.205 mmol, 81.5 mg) and 97% *ee* by the HPLC analysis (CHIRALCEL OD-H column, 99:1 hexane: *i*PrOH as eluents at 222 nm, 0.7 mL/min flow rate).  $R_t$ : 27.1 minute (minor enantiomer),  $R_t$ : 33.2 minute (major enantiomer). When this reaction was repeated with a catalyst prepared from the VANOL ligand, the aziridine **I-71a** was obtained in 69% isolated yield (0.345 mmol, 141 mg) with 81% *ee* (table 6).

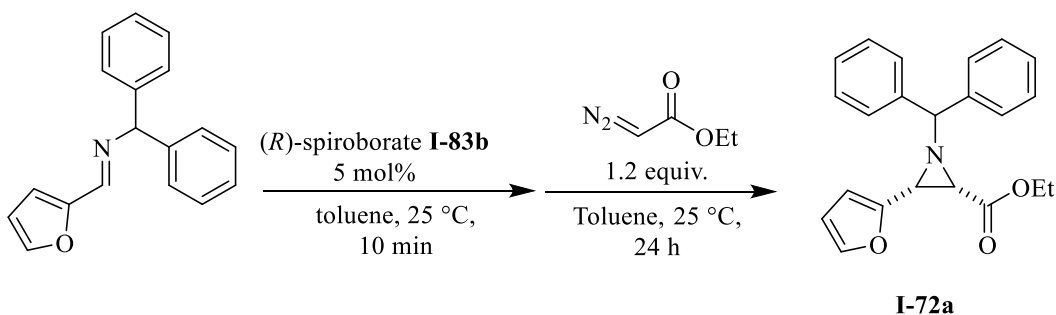
Spectral data for **I-71a**:  $^1\text{H}$  NMR (500 MHz, Chloroform-*d*)  $\delta$  0.65 (t,  $J = 7.1$  Hz, 3H), 2.93 (d,  $J = 6.9$  Hz, 1H), 3.68 – 3.83 (m, 3H), 4.10 (s, 1H), 7.19 – 7.52 (m, 9H), 7.53 – 7.59 (m, 2H), 7.62 – 7.74 (m, 4H), 7.78 – 7.86 (m, 1H), 8.08 – 8.14 (m, 1H).  $^{13}\text{C}$  NMR (126 MHz, Chloroform-*d*)  $\delta$  13.61, 46.05, 46.42, 60.42, 78.01, 122.97, 125.34, 125.44, 125.87, 126.56, 127.15, 127.20, 127.64, 127.91, 128.53, 128.59, 130.51, 131.43, 133.06, 142.26, 142.50, 167.81. Two  $sp^2$  carbons are not located. These spectral data are in agreement with the literature values.<sup>34</sup>



**(2*S*,3*S*)-ethyl-1-(bis(4-methoxy-3,5-dimethylphenyl)methyl)-3-(naphthalen-1-yl)aziridine-2-carboxylate **I-71b** (table 7):** The aziridine was prepared by the procedure detailed in *method A* starting with the corresponding imine (0.499 mmol, 219 mg) and the crude product was purified via column chromatography using hexane: ethylacetate 9:1 as the eluent. The desired *cis*-aziridine **I-71b** was obtained as a white solid in 70% isolated yield (0.351 mmol, 183 mg) and 98% *ee* by the HPLC analysis (CHIRALCEL OD-H column, 99:1 hexane: *i*PrOH as eluents at 226 nm, 0.7 mL/min flow rate).  $R_t$ : 8.1 minute (minor enantiomer),  $R_t$ : 16.3 minute (major enantiomer). When this reaction was repeated with a catalyst prepared from the VANOL ligand, the aziridine **I-71b** was obtained in 54% isolated yield (0.271 mmol, 131 mg) with 10% *ee* (table 6).

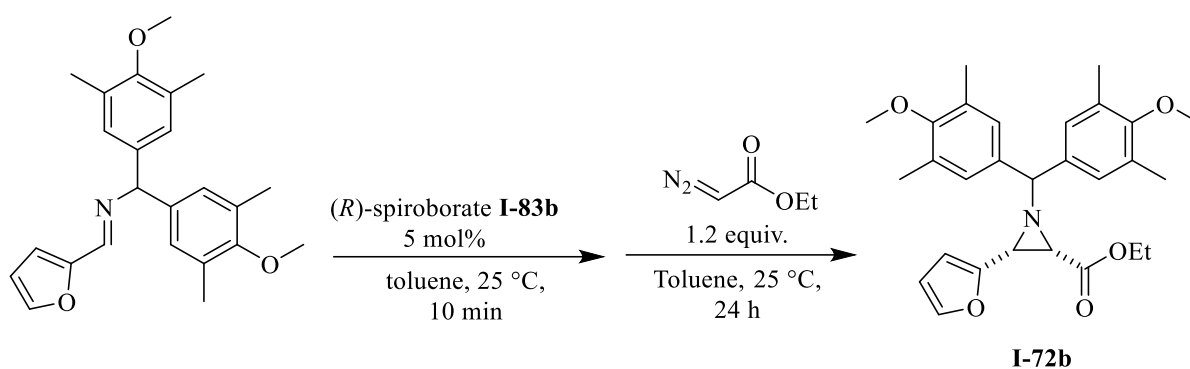
**Spectral data for **I-71b**:**  $^1\text{H}$  NMR (500 MHz, Chloroform-*d*)  $\delta$  0.68 (t,  $J$  = 7.1 Hz, 3H), 2.25 (s, 6H), 2.30 (s, 6H), 2.86 (d,  $J$  = 6.8 Hz, 1H), 3.64 (d,  $J$  = 20.8 Hz, 4H), 3.73 (s, 3H), 3.72 – 3.83 (m, 2H), 3.84 (s, 1H), 7.21 (s, 2H), 7.26 (s, 2H), 7.37 – 7.51 (m, 3H), 7.71 (d,  $J$  = 7.6 Hz, 2H), 7.81 (dd,  $J$  = 7.8, 1.6 Hz, 1H), 8.10 (d,  $J$  = 8.2 Hz, 1H).  $^{13}\text{C}$  NMR (126 MHz, Chloroform-*d*)  $\delta$  13.70, 16.22, 16.28, 45.98, 46.66, 59.57, 59.64, 60.37, 77.46, 123.07, 125.33, 125.44, 125.85, 126.61, 127.34, 127.55, 128.13, 128.51, 130.71, 130.73, 130.83, 131.46, 133.07, 137.71, 137.97, 155.92, 156.24, 168.05. These spectral data are in agreement with the literature values.<sup>38</sup>





**(2*S*,3*S*)-ethyl-1-benzhydryl-3-(furan-2-yl)aziridine-2-carboxylate I-72a (table 7):** The aziridine was prepared by the procedure detailed in *method A* starting with the corresponding imine (0.499 mmol, 131 mg) and the crude product was purified via column chromatography using hexane: ethylacetate 9:1 as the eluent. The desired *cis*-aziridine **I-72a** was obtained as a white solid in 69% isolated yield (0.345 mmol, 119 mg) and 89% *ee* by the HPLC analysis (CHIRALCEL OD-H column, 90:10 hexane: *i*PrOH as eluents at 222 nm, 1 mL/min flow rate).  $R_t$ : 4.3 minute (minor enantiomer),  $R_t$ : 8.8 minute (major enantiomer). When this reaction was repeated with a catalyst prepared from the VANOL ligand, the aziridine **I-72a** was obtained in 23% isolated yield (0.115 mmol, 39.9 mg) with 60% *ee* (table 6).

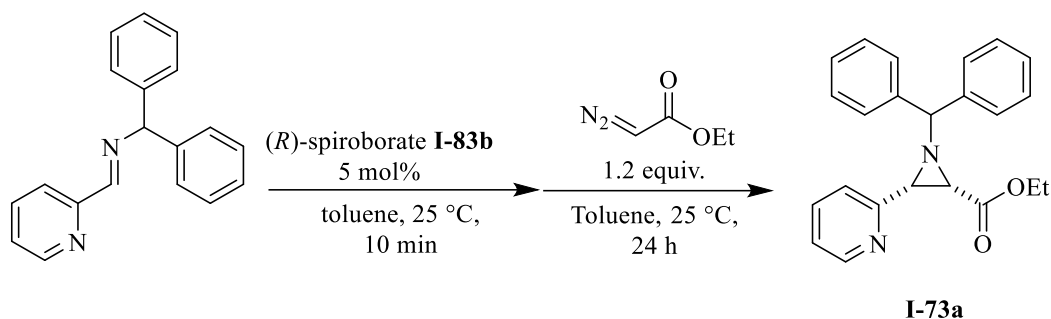
Spectral data for **I-72a**:  $^1\text{H}$  NMR (500 MHz, Chloroform-*d*)  $\delta$  1.14 (t,  $J = 7.1$  Hz, 3H), 2.70 (d,  $J = 6.5$  Hz, 1H), 3.14 (d,  $J = 6.5$  Hz, 1H), 3.94 (s, 1H), 4.02 – 4.16 (m, 2H), 6.27 – 6.36 (m, 2H), 7.18 – 7.38 (m, 7H), 7.44 – 7.52 (m, 2H), 7.50 – 7.58 (m, 2H).  $^{13}\text{C}$  NMR (126 MHz, Chloroform-*d*)  $\delta$  14.06, 41.68, 45.43, 60.90, 77.52, 108.03, 110.42, 127.34, 127.38, 127.42, 127.43, 128.46, 128.55, 141.95, 141.99, 142.08, 149.57, 167.48. These spectral data are in agreement with the literature values.<sup>21</sup>



**(2*S*,3*S*)-ethyl-1-(bis(4-methoxy-3,5-dimethylphenyl)methyl)-3-(furan-2-yl)aziridine-2-**

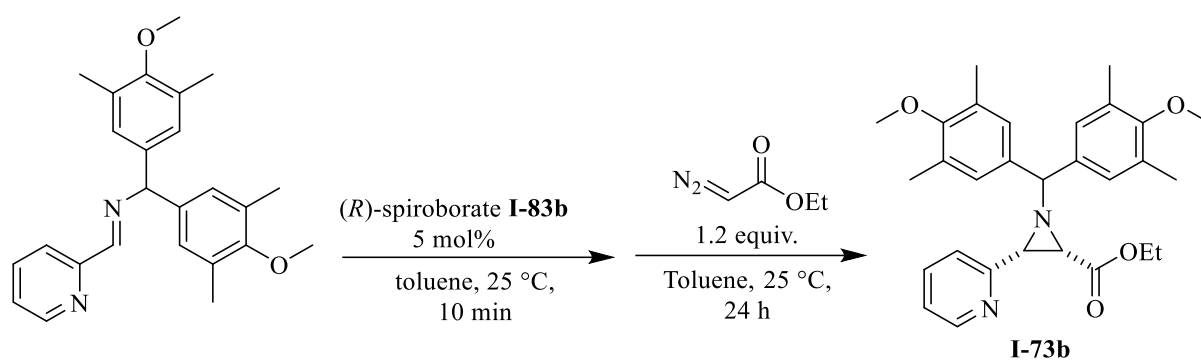
**carboxylate I-72b (table 7):** The aziridine was prepared by the procedure detailed in *method A* starting with the corresponding imine (0.499 mmol, 189 mg) and the crude product was purified via column chromatography using hexane: ethylacetate 15:1 and 1% Et<sub>3</sub>N as the eluent. The desired *cis*-aziridine **I-72b** was obtained as a white solid in 88% isolated yield (0.441 mmol, 204 mg) and 95% *ee* by the HPLC analysis (CHIRALCEL OD-H column, 99.5:0.5 hexane: *i*PrOH as eluents at 226 nm, 0.7 mL/min flow rate). *R*<sub>t</sub>: 23.8 minute (minor enantiomer), *R*<sub>t</sub>: 39.15 minute (major enantiomer). When this reaction was repeated with a catalyst prepared from the VANOL ligand, the aziridine **I-72b** was obtained in 5% NMR yield (table 6).

Spectral data for **I-72b**: <sup>1</sup>H NMR (500 MHz, Chloroform-*d*) δ 1.15 (td, *J* = 7.1, 2.1 Hz, 3H), 2.24 (m, 12H), 2.61 (dd, *J* = 6.5, 2.2 Hz, 1H), 3.04 (dd, *J* = 6.5, 2.1 Hz, 1H), 3.65-3.71 (m, 7H), 4.09 (m, 2H), 6.26 – 6.33 (m, 2H), 7.05-7.14 (m, 4H), 7.24 – 7.30 (m, 1H). <sup>13</sup>C NMR (126 MHz, Chloroform-*d*) δ 14.10, 16.17, 16.21, 41.77, 45.30, 59.57, 59.59, 60.83, 76.88, 108.02, 110.36, 127.50, 127.65, 130.58, 130.66, 137.36, 137.46, 141.84, 149.76, 156.01, 156.04, 167.74. These data are in agreement with the literature values.<sup>38</sup>



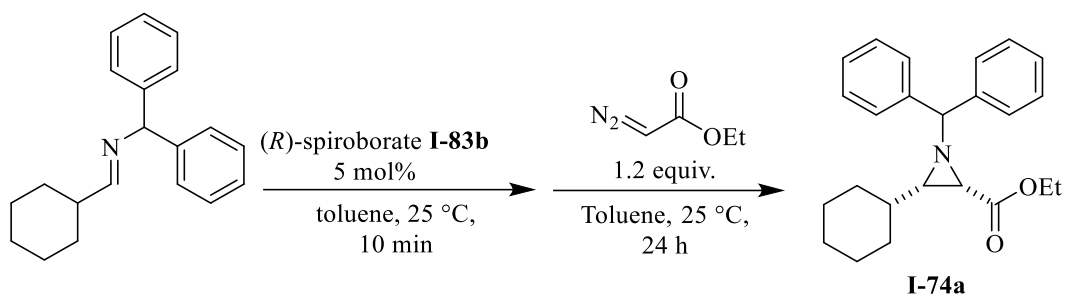
**(2S,3S)-ethyl-1-benzhydryl-3-(pyridin-2-yl)aziridine-2-carboxylate I-73a (table 7):** The aziridine was prepared by the procedure detailed in *method A* starting with the corresponding imine (0.499 mmol, 136 mg) and the crude product was purified via column chromatography using hexane: ethylacetate 9:1 as the eluent. The desired *cis*-aziridine **I-73a** was obtained as a white solid in 86% isolated yield (0.441 mmol, 204 mg) and 87% *ee* by the HPLC analysis (CHIRALCEL OD-H column, 90:10 hexane: *i*PrOH as eluents at 222 nm, 1 mL/min flow rate).  $R_t$ : 5.3 minute (minor enantiomer),  $R_t$ : 9.7 minute (major enantiomer). When this reaction was repeated with a catalyst prepared from the VANOL ligand, the aziridine **I-73a** was obtained in 44% isolated yield (0.22 mmol, 79 mg) with 61% *ee* (table 6).

Spectral data for **I-73a**:  $^1\text{H}$  NMR (500 MHz, Chloroform-*d*)  $\delta$  1.02 (t,  $J = 7.1$  Hz, 3H), 2.79 (d,  $J = 6.9$  Hz, 1H), 3.41 (d,  $J = 6.9$  Hz, 1H), 3.96 (qd,  $J = 7.1, 1.0$  Hz, 2H), 4.02 (s, 1H), 7.11 (ddd,  $J = 6.9, 4.8, 2.1$  Hz, 1H), 7.15 – 7.22 (m, 1H), 7.22 – 7.30 (m, 3H), 7.31 – 7.39 (m, 2H), 7.46 – 7.52 (m, 2H), 7.57 – 7.67 (m, 4H), 8.42 – 8.47 (m, 1H).  $^{13}\text{C}$  NMR (126 MHz, Chloroform-*d*)  $\delta$  13.97, 46.05, 49.29, 60.73, 77.46, 122.39, 122.73, 127.11, 127.28, 127.50, 127.55, 128.35, 128.54, 136.00, 142.16, 142.36, 148.62, 155.18, 167.51. These spectral data are in agreement with the literature values.<sup>41</sup>



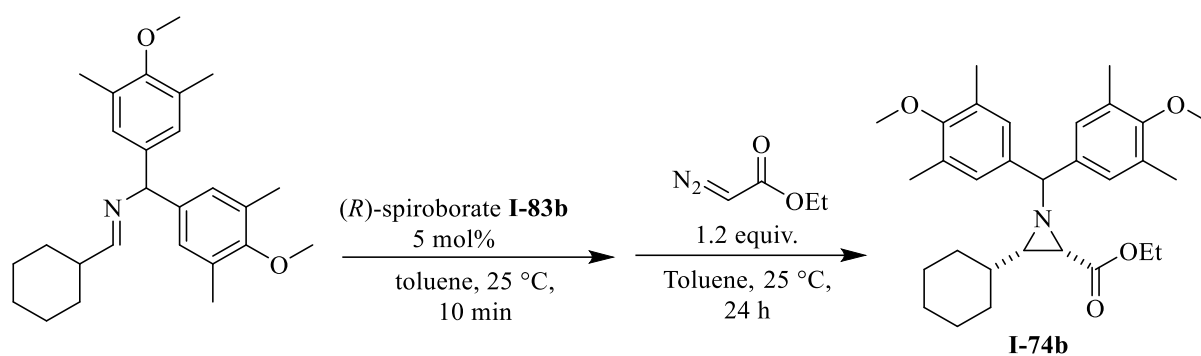
**(2S,3S)-ethyl-1-(bis(4-methoxy-3,5-dimethylphenyl)methyl)-3-(pyridin-2-yl)aziridine-2-carboxylate **I-73b**:** The aziridine was prepared by the procedure detailed in *method A* starting with corresponding imine (0.499 mmol, 237 mg) and the crude product was purified via column chromatography using hexane: ethylacetate 4:1 and 1% Et<sub>3</sub>N as the eluent. The desired *cis*-aziridine **I-73b** was obtained as a white solid in 99% isolated yield (0.495 mmol, 235 mg) and 95% *ee* by the HPLC analysis (CHIRALCEL OD-H column, 99:1 hexane: *i*PrOH as eluents at 226 nm, 0.7 mL/min flow rate). R<sub>t</sub>: 16.95 minute (minor enantiomer), R<sub>t</sub>: 31.95 minute (major enantiomer). When this reaction was repeated with a catalyst prepared from the VANOL ligand, the aziridine **I-73b** was obtained in 51% isolated yield (0.255 mmol, 121 mg) with 76% *ee* (table 6).

Spectral data for **I-73b**: <sup>1</sup>H NMR (500 MHz, Chloroform-*d*) δ 0.67 (t, *J* = 7.1 Hz, 3H), 2.25 (s, 6H), 2.29 (s, 6H), 2.85 (d, *J* = 6.8 Hz, 1H), 3.63–3.67 (m, 4H), 3.72 (s, 3H), 3.68 – 3.83 (m, 2H), 3.83 (s, 1H), 7.20 (s, 2H), 7.36 – 7.51 (m, 3H), 7.67 – 7.74 (m, 2H), 8.09 (dt, *J* = 8.9, 1.0 Hz, 1H). <sup>13</sup>C NMR (126 MHz, Chloroform-*d*) δ 14.01, 16.18, 16.24, 45.89, 49.43, 59.54, 59.61, 60.65, 122.30, 122.82, 127.32, 127.76, 130.65, 130.68, 135.88, 137.55, 137.76, 148.56, 155.42, 155.94, 156.07, 167.74. One *sp*<sup>3</sup> carbon was not located. These spectral data match with the literature values.<sup>38</sup>



**(2*S*,3*S*)-ethyl-1-benzhydryl-3-cyclohexylaziridine-2-carboxylate I-74a (table 7):** The aziridine was prepared by the procedure detailed in *method A* starting with the corresponding imine (0.499 mmol, 139 mg) and the crude product was purified via column chromatography using benzene: dichloromethane 200:1 as the eluent. The desired *cis*-aziridine **I-74a** was obtained as a white solid in 92% isolated yield (0.461 mmol, 167 mg) and 96% *ee* by the HPLC analysis (CHIRALCEL OD-H column, 99:1 hexane: *i*PrOH as eluents at 226 nm, 1 mL/min flow rate).  $R_t$ : 3.5 minute (minor enantiomer),  $R_t$ : 7.0 minute (major enantiomer). When this reaction was repeated with a catalyst prepared from the VANOL ligand, the aziridine **I-74a** was obtained in 10% NMR yield (table 6).

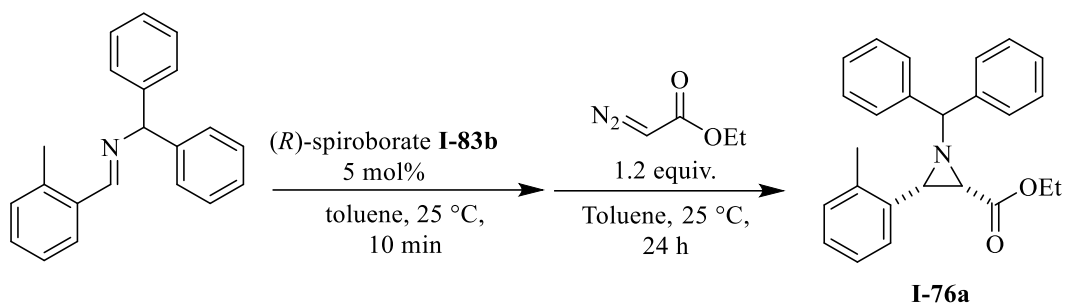
Spectral data for **I-74a**:  $^1\text{H}$  NMR (500 MHz, Chloroform-*d*)  $\delta$  0.45 – 0.57 (m, 1H), 0.90 – 1.20 (m, 4H), 1.17 – 1.24 (m, 1H), 1.26 (t,  $J = 7.1$  Hz, 3H), 1.28 – 1.36 (m, 1H), 1.41 – 1.50 (m, 2H), 1.51 – 1.58 (m, 1H), 1.62 (dt,  $J = 8.8, 5.5$  Hz, 1H), 1.81 (dd,  $J = 9.4, 6.9$  Hz, 1H), 2.27 (d,  $J = 6.9$  Hz, 1H), 3.62 (s, 1H), 4.14 – 4.30 (m, 2H), 7.18 – 7.27 (m, 2H), 7.24 – 7.36 (m, 4H), 7.32 – 7.38 (m, 2H), 7.47 – 7.53 (m, 2H).  $^{13}\text{C}$  NMR (126 MHz, Chloroform-*d*)  $\delta$  14.31, 25.37, 25.56, 30.13, 30.73, 36.29, 43.43, 52.15, 60.73, 78.19, 126.90, 127.07, 127.52, 128.29, 128.33, 128.37, 142.32, 142.72, 169.66. One  $sp^3$  carbon is not located. These spectral data are in agreement with the literature values.<sup>34</sup>



**(2*S*,3*S*)-ethyl-1-(bis(4-methoxy-3,5-dimethylphenyl)methyl)-3-cyclohexylaziridine-2-**

**carboxylate I-74b (table 7):** The aziridine was prepared by the procedure detailed in *method A* starting with the corresponding imine (0.499 mmol, 197 mg) and the crude product was purified via column chromatography using hexane: DCM: Et<sub>2</sub>O 4:2:0.1 as the eluent. The desired *cis*-aziridine **I-74b** was obtained as a white solid in 92% isolated yield (0.461 mmol, 221 mg) and 96% *ee* by the HPLC analysis (CHIRALCEL OD-H column, 99:1 hexane: *i*PrOH as eluents at 223 nm, 0.7 mL/min flow rate). *R*<sub>t</sub>: 10.2 minute (minor enantiomer), *R*<sub>t</sub>: 12.5 minute (major enantiomer). When this reaction was repeated with a catalyst prepared from the VANOL ligand, the aziridine **I-74b** was obtained in 25% isolated yield (0.125 mmol, 59.9 mg) with 46% *ee* (table 6).

Spectral data for **I-74b**: <sup>1</sup>H NMR (500 MHz, Chloroform-*d*) δ 0.46 – 0.58 (m, 1H), 0.89 – 1.04 (m, 1H), 1.02 – 1.09 (m, 1H), 1.10 (ddt, *J* = 12.7, 8.9, 4.4 Hz, 1H), 1.18 – 1.32 (m, 5H), 1.39 – 1.47 (m, 2H), 1.48 – 1.55 (m, 1H), 1.60 (dt, *J* = 13.6, 3.2 Hz, 1H), 1.73 (dd, *J* = 9.3, 6.9 Hz, 1H), 2.13 – 2.27 (m, 13H), 3.36 (s, 1H), 3.63-3.69 (m, 6H), 4.12 – 4.21 (m, 1H), 4.19 – 4.30 (m, 1H), 6.95 (s, 2H), 7.11 (s, 2H). <sup>13</sup>C NMR (126 MHz, Chloroform-*d*) δ 14.32, 16.04, 16.15, 25.34, 25.52, 26.16, 30.09, 30.82, 36.33, 43.45, 52.24, 59.56, 59.61, 60.62, 77.48, 127.33, 128.52, 130.30, 130.42, 137.55, 138.09, 155.72, 156.24, 169.77. These data are in agreement with the literature values.<sup>38</sup>

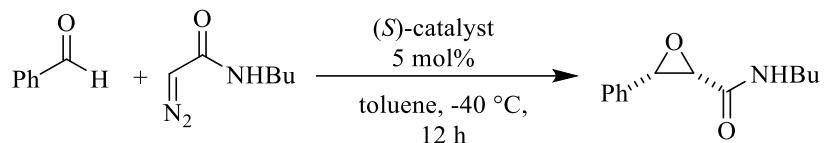


**(2*S*,3*S*)-ethyl-1-benzhydryl-3-(2-methyl-phenyl)-aziridine-2-carboxylate **I-76a** (table 6):** The aziridine was prepared by the procedure detailed in *method A* with VANOL ligand and the corresponding imine (0.499 mmol, 143 mg) and the crude product was purified via column chromatography using hexane: ethylacetate 9:1 as the eluent. The desired *cis*-aziridine **I-76a** was obtained as a white solid in 38% isolated yield (0.19 mmol, 71 mg) and 46% *ee* by the HPLC analysis (CHIRALCEL OD-H column, 99:1 hexane: *i*PrOH as eluents at 222 nm, 1 mL/min flow rate).  $R_t$ : 6.1 minute (minor enantiomer),  $R_t$ : 7.5 minute (major enantiomer).

Spectral data for **I-76a**:  $^1\text{H}$  NMR (500 MHz, Chloroform-*d*)  $\delta$  0.91 (t,  $J$  = 7.1 Hz, 3H), 2.31 (s, 3H), 2.74 (d,  $J$  = 6.8 Hz, 1H), 3.22 (d,  $J$  = 6.8 Hz, 1H), 3.91 (q,  $J$  = 7.1 Hz, 2H), 3.97 (s, 1H), 7.01 – 7.11 (m, 1H), 7.12 (hd,  $J$  = 5.5, 5.0, 3.2 Hz, 2H), 7.17 – 7.39 (m, 7H), 7.47 – 7.58 (m, 2H), 7.58 – 7.65 (m, 2H).  $^{13}\text{C}$  NMR (126 MHz, Chloroform-*d*)  $\delta$  13.86, 18.82, 45.62, 46.93, 60.49, 77.92, 125.36, 127.13, 127.16, 127.54, 127.74, 128.50, 128.51, 129.11, 133.12, 136.01, 142.41, 142.56, 167.97. These spectral data are in agreement with the literature values.<sup>21,34</sup>

### General method for the asymmetric catalytic epoxidation

*Preparing the stock solution of the catalyst illustrated for VANOL:* Method A was used to prepare the catalyst from (*S*)-VANOL (0.075 mmol, 33 mg), 3 mL of toluene and  $\text{BH}_3\cdot\text{SMe}_2$  (0.037 mmol, 19  $\mu\text{L}$ ). To the obtained white solid was added 3 mL of anhydrous toluene and the resulting solution was stirred at room temperature for 10 minutes.



*General method for preparing epoxide **I-52** (scheme 15):* A flamed dried 25 mL round bottom flask was charged with N-butyl diazo acetamide (0.49 mmol, 74 mg), 3 mL toluene and benzaldehyde (0.61 mmol, 64  $\mu$ L). The resulting cloudy mixture and the stock solution of the catalyst were cooled down at -40 °C for 15 minutes in a cold bath. Then, 2 mL of the stock solution of the catalyst made from the appropriate ligand was transferred to the round bottom flask containing the mixture of starting materials and the resulting solution in the round bottom flask was stirred at -40 °C for 12 hours. The reaction was quenched by adding 1 mL of methanol and the solvent was removed under reduced pressure. At this point, the NMR yield was determined by using Ph<sub>3</sub>CH as the internal standard (conv. 99%). The crude epoxide was purified via column chromatography (flash column, hexane: ethyl acetate, 3:1 to 1:1) and the epoxide **I-52** was obtained as a white solid with 88% isolated yield (0.44 mmol, 96 mg) and 93% *ee* by HPLC analysis (Pirkle covalent (R, R) Whelk-O1 column, 93:7 hexane: *i*PrOH as eluents at 228 nm, 1 mL/min flow rate). *R*<sub>t</sub>: 13.8 min (major enantiomer), *R*<sub>t</sub>: 24.6 min (minor enantiomer). The epoxidations with the catalysts prepared from the ligands **I-88a-I-88f** in table 10 were also performed with the above procedure.

Spectral data for **I-52**: <sup>1</sup>H NMR (500 MHz, Chloroform-d)  $\delta$  0.72 (t, *J* = 7.2 Hz, 3H), 0.89-1.04 (m, 4H), 2.82-2.88 (m, 1H), 3.08 (dq, *J* = 13.6, 6.9 Hz, 1H), 3.77 (d, *J* = 4.8 Hz, 1H), 4.31 (d, *J* = 4.8 Hz, 1H), 5.84 (s, 1H), 7.35–7.28 (m, 5H); <sup>13</sup>C NMR (126 MHz, Chloroform-d)  $\delta$  13.53, 19.62, 31.17, 38.21, 56.27, 58.08, 126.49, 128.31, 128.38, 133.19, 165.95. These spectral data are in agreement with the literature values.<sup>1</sup>



## General method for the synthesis of imines

All imines were synthesized via standard procedure developed in our lab and the spectral data of these imines were in good agreement with the reported data in the literature.<sup>34,37,39</sup>

## General method for the crystal growth of water free spiroborate anion-iminium cation cocrystal

*Procedure A: Growing the co-crystal of catalyst I-83c and imine I-84b (figure 4):* Method A was used to prepare the catalyst from (*S*)-7,7'-Ad<sub>2</sub>VANOL (0.199 mmol, 142 mg), 2 mL toluene and BH<sub>3</sub>•SMe<sub>2</sub> (0.11 mmol, 13  $\mu$ L). Then, imine **I-84b** (0.11 mmol, 43 mg) was added and the mixture was dissolved in 2 mL of anhydrous CH<sub>2</sub>Cl<sub>2</sub>. 1 mL of the resulting solution was transferred into a flamed dried 4 mL vial followed by slow addition of 3 mL freshly distilled hexane (the layer between CH<sub>2</sub>Cl<sub>2</sub> and hexane should not be disturb). Next, the 4 mL vial was placed into another 20 mL vial, capped and wrapped with parafilm. Crystals were formed after 24 hours and they were collected after 48 hours. Unfortunately these crystals were not stable at room temperature in open air. Since the crystal lattice contains two molecules of CH<sub>2</sub>Cl<sub>2</sub>, removing the mother liquor caused the evaporation the CH<sub>2</sub>Cl<sub>2</sub> in the crystal lattice, which led to the subsequent collapse of the lattice. As a result, melting points for the crystals could not be obtained.

Spectral data for crystal of catalyst **I-83c** and imine **I-84b**: <sup>1</sup>H NMR (500 MHz, Chloroform-*d*)  $\delta$  1.11 (dd, *J* = 11.8, 2.8 Hz, 5H), 1.18 – 1.30 (m, 7H), 1.39 (d, *J* = 12.0 Hz, 5H), 1.46 (d, *J* = 12.2 Hz, 5H), 1.62 – 1.68 (m, 5H), 1.72 (d, *J* = 12.0 Hz, 1H), 1.79 (d, *J* = 12.4 Hz, 1H), 1.85 (d, *J* = 3.3 Hz, 6H), 2.02 (d, *J* = 2.8 Hz, 1H), 2.06 – 2.14 (m, 15H), 2.16 – 2.29 (m, 4H), 2.95 (s, 4H), 3.44 – 3.55 (m, 2H), 3.66 (s, 4H), 5.30 (s, 1H), 5.68 (s, 1H), 5.84 (s, 1H), 6.54 (s, 3H), 6.56 – 6.66 (m, 7H), 6.79 (t, *J* = 7.6 Hz, 3H), 6.96 (td, *J* = 7.6, 5.7 Hz, 4H), 7.03 – 7.10 (m, 3H), 7.24 (dd, *J* = 8.6, 2.0 Hz, 2H), 7.29 (s, 1H), 7.51 (d, *J* = 8.5 Hz, 1H), 7.63 – 7.72 (m, 3H), 7.76 (d, *J* = 8.7 Hz, 1H),

8.26 (d,  $J = 1.8$  Hz, 1H).  $^{11}\text{B}$  NMR (160 MHz, Chloroform- $d$ )  $\delta$  9.74, 6.39. CCDC number: 1820122

*Co-crystal of catalyst **I-83b** and imine **I-84b** (figure 3):* Procedure A was used in order to grow the co-crystal of catalyst **I-83b** and imine **I-84b**.

Spectral data for crystal of catalyst **I-83b** and imine **I-84b**:  $^1\text{H}$  NMR (500 MHz, Chloroform- $d$ )  $\delta$  0.07 (s, 3H), 0.55 (s, 18H), 1.21 (t,  $J = 7.0$  Hz, 2H), 1.49 (s, 10H), 1.56 (s, 8H), 1.81 (s, 1H), 2.73 (s, 1H), 3.48 (q,  $J = 7.0$  Hz, 1H), 3.63 (s, 3H), 3.68 (s, 2H), 5.30 (s, 2H), 5.84 (s, 1H), 6.61 (td,  $J = 5.1, 2.3$  Hz, 6H), 6.71 (t,  $J = 7.7$  Hz, 4H), 6.90 – 7.00 (m, 4H), 7.00 – 7.10 (m, 1H), 7.18 (s, 2H), 7.22 – 7.31 (m, 4H), 7.55 (d,  $J = 8.6$  Hz, 2H), 7.60 (d,  $J = 1.9$  Hz, 2H), 7.68 (dd,  $J = 8.6, 2.0$  Hz, 1H), 7.75 (d,  $J = 8.7$  Hz, 1H), 8.30 (d,  $J = 1.9$  Hz, 1H).  $^{11}\text{B}$  NMR (160 MHz, Chloroform- $d$ )  $\delta$  9.90. CCDC number: The data for this crystal has not been deposited in the CCDC as of yet.

*Co-crystal of catalyst **I-83b** and imine **I-84b** (figure 1):* Procedure A was used in order to grow the co-crystal of catalyst **I-83b** and imine **I-84b**. It should be noted that the undistilled solvents ( $\text{CH}_2\text{Cl}_2$  and hexanes) were used in growing the crystal of the catalyst **I-83b** and the imine **I-84b** (figure 1), therefore, the catalyst and the imine were crystalized with a molecule of water in the crystal lattice.

*Co-crystal of catalyst **I-83b** and imine **I-84a** (figure 2):* Procedure A was used in order to grow the co-crystal of catalyst **I-83b** and imine **I-84a**. It should be noted that the undistilled solvents ( $\text{CH}_2\text{Cl}_2$  and hexanes) were used in growing the crystal of the catalyst **I-83b** and the imine **I-84a** (figure 2), therefore, the catalyst and the imine were crystalized with a molecule of water in the crystal lattice.

## **REFERENCES**

## REFERENCES

- 1) Gupta, A. K.; Yin, X.; Mukherjee, M.; Desai, A.; Mohammadlou, A.; Jurewicz, K.; Wulff, W. D., "Catalytic Asymmetric Epoxidation of Aldehydes with Two VANOL-derived Chiral Borate Catalysts." *Angew. Chem. Int. Ed.* **2019**, 58, 3361–3367.
- 2) Kazuaki, I.; Yamamoto, H., "Brønsted Acid Assisted Chiral Lewis Acid (BLA) Catalyst for Asymmetric Diels-Alder Reaction" *J. Am. Chem. Soc.*, **1994**, 116, 1561–1562.
- 3) Ishihara, K.; Kurihara, H.; Yamamoto, H., "A new powerful and practical BLA catalyst for highly enantioselective Diels- Alder reaction: an extreme acceleration of reaction rate by Brønsted acid" *J. Am. Chem. Soc.*, **1994**, 118, 3049–3050.
- 4) Ishihara, K.; Kurihara, H.; Matsumoto, M.; Yamamoto, H., "Design of Brønsted acid-assisted chiral Lewis acid (BLA) catalysts for highly enantioselective Diels- Alder reactions" *J. Am. Chem. Soc.* **1998**, 120, 6920–6930.
- 5) Ishihara, K.; Miyata, M.; Hattori, K.; Tada, T.; Yamamoto, H., "A New Chiral BLA Promoter for Asymmetric Aza Diels-Alder and Aldol-Type Reactions of Imines" *J. Am. Chem. Soc.*, **1994**, 116, 10520–10524.
- 6) Green, S.; Nelson, A.; Warriner, S.; Whittaker, B., "Synthesis and investigation of the configurational stability of some dimethylammonium borate salts" *J. Chem. Soc. Perkin transactions I*, **2000**, 4403–4408.
- 7) Cros, J. P.; Pérez-Fuertes, Y.; Thatcher, M. J.; Arimori, S.; Bull, S. D.; James, T. D., "Non-Linear Effects Operate and Dynamic Ligand Exchange Occurs When Chiral BINOL–boron Lewis Acids Are Used for Asymmetric Catalysis." *Tetrahedron, Asymmetry* **2003**, 14, 1965–68.
- 8) Yamada, H.; Kawate, T.; Matsumizu, M.; Nishida, A.; Yamaguchi, K.; Nakagawa, M., "Chiral Lewis Acid-Mediated Enantioselective Pictet–Spengler Reaction of N b -Hydroxytryptamine with Aldehydes" *J. Org. Chem.* **1998**, 63, 6348–6354.
- 9) Pirkle, W. H.; Rinaldi, P. L., "General method for the synthesis of high enantiomeric purity chiral epoxides" *J. Org. Chem.* **1978**, 43, 3803–3807.
- 10) Katsuki, T.; Sharpless, K. B., "The first practical method for asymmetric epoxidation" *J. Am. Chem. Soc.* **1980**, 102, 5974–5976.
- 11) Weinreb, S. M.; Trost, B. M., Comprehensive organic synthesis. *Fleming, I. (eds. 5)*, **1991**.
- 12) Liu, Y.; Provencher, B. A.; Bartleson, K. J.; Deng, L., "Highly Enantioselective Asymmetric Darzens Reactions with a Phase Transfer Catalyst" *Chem. Sci.* **2011**, 2, 1301–1304.

- 13) Trost, B. M.; Malhotra, S.; Fried, B. A., "Magnesium-Catalyzed Asymmetric Direct Aldol Addition of Ethyl Diazoacetate to Aromatic, Aliphatic, and  $\alpha,\beta$ -Unsaturated Aldehydes" *J. Am. Chem. Soc.*, **2009**, *131*, 1674–1675.
- 14) Trost, B. M.; Malhotra, S.; Koschker, P.; Ellerbrock, P., "Development of the Enantioselective Addition of Ethyl Diazoacetate to Aldehydes: Asymmetric Synthesis of 1,2-Diols" *J. Am. Chem. Soc.* **2012**, *134*, 2075–2084.
- 15) Li, W.; Wang, J.; Hu, X.; Shen, K.; Wang, W.; Chu, Y.; Lin, L.; Liu, X.; Feng, X., "Catalytic Asymmetric Roskamp Reaction of  $\alpha$ -Alkyl- $\alpha$ -diazoesters with Aromatic Aldehydes: Highly Enantioselective Synthesis of  $\alpha$ -Alkyl- $\beta$ -keto Esters" *J. Am. Chem. Soc.*, **2010**, *132*, 8532–8533.
- 16) Liu, W.-J.; Lv, B.-D.; Gong, L.-Z., "An Asymmetric Catalytic Darzens Reaction between Diazoacetamides and Aldehydes Generates *cis* -Glycidic Amides with High Enantiomeric Purity" *Angew. Chem. Int. Ed.* **2009**, *48*, 6503–6506.
- 17) He, L.; Liu, W.-J.; Ren, L.; Lei, T.; Gong, L.-Z., "Storable and Air-Stable Zirconium Complex-Catalyzed Highly Enantioselective Darzens Reaction of Diazoacetamide with Aldehydes" *Adv. Synth. Catal.* **2010**, *352*, 1123–1127.
- 18) Kobayashi, S.; Ueno, M.; Saito, S.; Mizuki, Y.; Ishitani, H.; Yamashita, Y., "Air-stable, storable, and highly efficient chiral zirconium catalysts for enantioselective Mannich-type, aza Diels–Alder, aldol, and hetero Diels–Alder reactions" *Proc. Natl. Acad. Sci.* **2004**, *101*, 5476–5481.
- 19) Liu, G.; Zhang, D.; Li, J.; Xu, G.; Sun, J., "A highly enantioselective Darzens reaction between diazoacetamides and aldehydes catalyzed by a (+)-pinanediol-Ti(O*i*Pr)<sub>4</sub> system" *Org. Biomol. Chem.* **2013**, *11*, 900–904.
- 20) Chai, G. L.; Han, J. W.; Wong, H. N., "Hydroxytetraphenylenes as Chiral Ligands: Application to Asymmetric Darzens Reaction of Diazoacetamide with Aldehydes." *Synthesis* **2016**, *49*, 181–87.
- 21) Antilla, J. C.; Wulff, W. D., "Catalytic Asymmetric Aziridination with a Chiral VAPOL–Boron Lewis Acid." *J. Am. Chem. Soc.* **1999**, *121*, 5099–5100.
- 22) Antilla, J. C.; Wulff, W. D., "Catalytic Asymmetric Aziridination with Arylborate Catalysts Derived from VAPOL and VANOL Ligands." *Angew. Chem., Int. Ed.* **2000**, *39*, 4518–21.
- 23) Desai, A.; Wulff, W. D., "Controlled Diastereo- and Enantioselection in a Catalytic Asymmetric Aziridination." *J. Am. Chem. Soc.* **2010**, *132*, 13100–13103.
- 24) Hashimoto, T.; Uchiyama, N.; Maruoka, K., "Trans-Selective Asymmetric Aziridination of Diazoacetamides and N-Boc Imines Catalyzed by Axially Chiral Dicarboxylic Acid." *J. Am. Chem. Soc.* **2008**, *130*, 14380–14381.

- 25) Vetticatt, M. J.; Desai, A.; Wulff, W. D., "How the binding of substrates to a chiral polyborate counterion governs diastereoselection in an aziridination reaction: H-bonds in equipoise" *J. Am. Chem. Soc.* **2010**, *132*, 13104–13107.
- 26) Gupta, A. K.; Mukherjee, M.; Hu, G.; Wulff, W. D., "BOROX Catalysis: Self-Assembled Amino-BOROX and Imino-BOROX Chiral Brønsted Acids in a Five Component Catalyst Assembly/Catalytic Asymmetric Aziridination." *J. Org. Chem.* **2012**, *77*, 7932–7944.
- 27) Vetticatt, M. J.; Desai, A.; Wulff, W. D., "Isotope effects and mechanism of the asymmetric BOROX Brønsted acid catalyzed aziridination reaction" *The J. Am. Chem. Soc.* **2013**, *78*, 5142–5152.
- 28) Llewellyn, D. B.; Adamson, D.; Arndtsen, B. A., "A Novel Example of Chiral Counteranion Induced Enantioselective Metal Catalysis: The Importance of Ion-Pairing in Copper-Catalyzed Olefin Aziridination and Cyclopropanation" *Org. Lett.* **2000**, *2*, 4165–4168.
- 29) Chen, D.; Sundararaju, B.; Krause, R.; Klankermayer, J.; Dixneuf, P.; Leitner, W., "Asymmetric Induction by Chiral Borate Anions in Enantioselective Hydrogenation Using a Racemic Rh-Binap Catalyst." *ChemCatChem* **2010**, *2*, 55–57.
- 30) Periasamy, M.; Venkatraman, L.; Sivakumar, S.; Sampathkumar, N.; Ramanathan, C. R., "A New, Convenient Method of Resolution of Racemic 1, 1'-Bi-2-naphthol Using Boric Acid and (R)-(+)- $\alpha$ -Methylbenzylamine" *J. Org. Chem.* **1999**, *64*, 7643–7645.
- 31) Carter, C.; Fletcher, S.; Nelson, A., "Towards Phase-Transfer Catalysts with a Chiral Anion: Inducing Asymmetry in the Reactions of Cations." *Tetrahedron, Asymmetry*, **2003**, *14*, 1995–2004.
- 32) Yin, X.; Zheng, L.; Mohammadlou, A.; Cagnon, B.; Wulff, W. D., "The Resolution of Vaulted Biaryl Ligands via meso-Borate Esters of Quinine and Quinidin" *Manuscript under revision*.
- 33) Herschlag, D.; Pinney, M. M., "Hydrogen Bonds: Simple after All?" *Biochemistry*, **2018**, *57*, 3338–3352.
- 34) Yong, G.; Ding, Z.; Wulff, W. D., "Vaulted Biaryls in Catalysis: A Structure-Activity Relationship Guided Tour of the Immanent Domain of the VANOL Ligand." *Chem. Eur. J.* **2013**, *19*, 15565–15571.
- 35) Hansch, C.; Leo, A.; Taft, R. W., "A survey of Hammett substituent constants and resonance and field parameters" *Chem. Rev.* **1991**, *91*, 165–195.
- 36) Hekmanek, S., "<sup>11</sup>B NMR spectra of boranes, main-group heteroboranes, and substituted derivatives. Factors influencing chemical shifts of skeletal atoms" *Chem. Rev.* **1992**, *92*, 325–362.

- 37) Zhang, Y.; Desai, A.; Lu, Z.; Hu, G.; Ding, Z.; Wulff, W. D., "Catalytic Asymmetric Aziridination with Borate Catalysts Derived from VANOL and VAPOL Ligands: Scope and Mechanistic Studies." *Chem. Eur. J.* **2008**, *14*, 3785–3803.
- 38) Gupta, A.; Mukherjee, M.; Wulff, W. D., "Multicomponent Catalytic Asymmetric Aziridination of Aldehydes." *Org. Lett.* **2011**, *13*, 5866–69.
- 39) Zhang, Y.; Lu, Z.; Desai, A.; Wulff, W. D., "Mapping the Active Site in a Chemzyme: Diversity in the N-Substituent in the Catalytic Asymmetric Aziridination of Imines." *Org. Lett.* **2008**, *10*, 5429–5432.
- 40) Mukherjee, M.; Gupta, A.; Lu, Z.; Zhang, Y.; Wulff, W. D., "Seeking Passe-Partout in the Catalytic Asymmetric Aziridination of Imines: Evolving Toward Substrate Generality for a Single Chemzyme" *J. Org. Chem.* **2010**, *75*, 5643–5660.
- 41) Williams, A. L.; Johnston, J. N., "The Brønsted Acid-Catalyzed Direct Aza-Darzens Synthesis of N-Alkyl cis-Aziridines" *J. Am. Chem. Soc.* **2004**, *126*, 1612–1613.

## **Chapter 2**

**Chameleon catalyst: Aluminum-VANOL Aluminum-VAPOL Catalysts as**

**Efficient Catalysts in the Epoxidation of Aldehydes and Aziridination of**

**Imines,**

**Total Synthesis of (–)-Tedanalactam**



## 2.1. Introduction: A brief history of aluminum catalysts in catalytic asymmetric synthesis

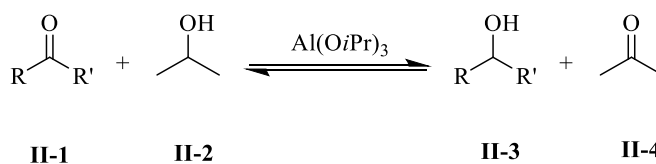
Aluminum biaryl complexes have been used in numerous asymmetric catalytic reactions because of the ease of preparation of these complexes and also the remarkable Lewis acidity that the aluminum possesses. Usually, these complexes have been applied in the activation of carbonyls such as aldehydes and ketones in asymmetric transformations.

### 2.1.1. Aluminum catalyzed asymmetric catalytic reduction of ketone

#### 2.1.1.1. Meerwein–Ponndorf–Verley reduction

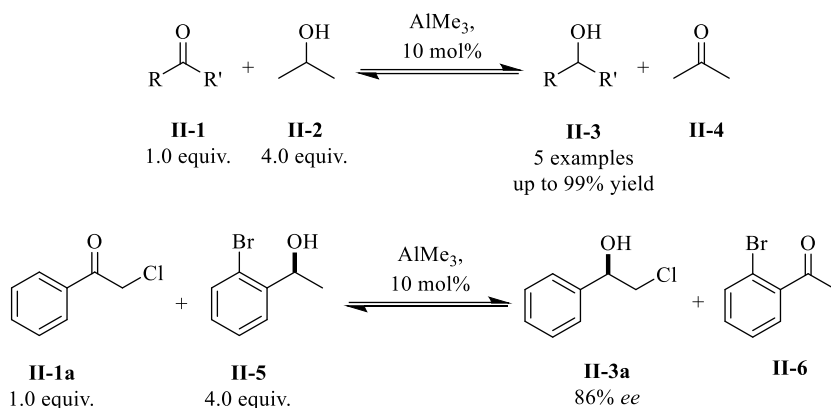
The Meerwein-Ponndorf-Verley (MPV) reduction of aldehyde and ketones using *i*PrOH as the reducing agent in the presence of  $\text{Al}(\text{O}i\text{Pr})_3$  has been an important reaction in organic synthesis (scheme II-1). This reaction was reported over 90 years ago by Meerwein, Schmidt, Ponndorf, and Verley. The catalytic version of the classic MSPV reduction had been difficult to achieve; presumably, due to the aggregation of  $\text{Al}(\text{O}i\text{Pr})_3$ .<sup>1</sup>

**Scheme II-1.** MPV Reduction



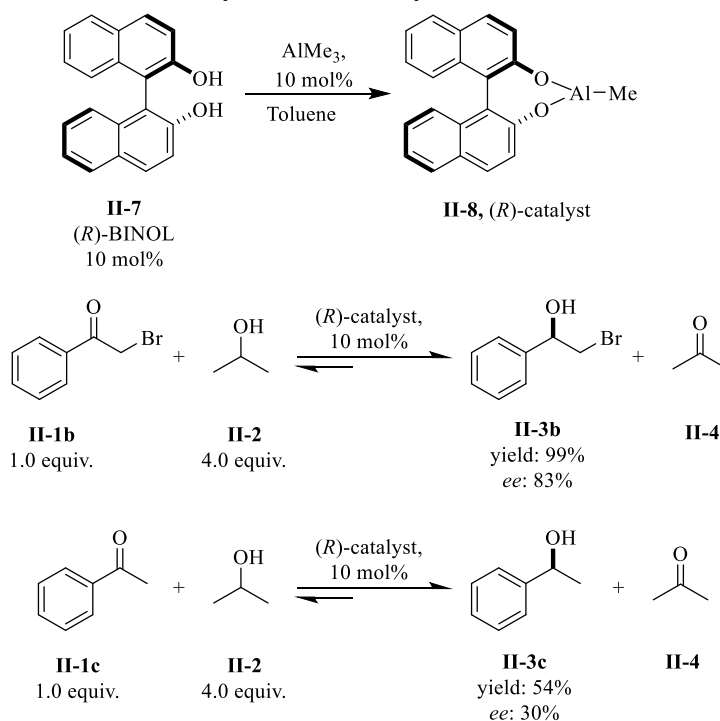
In 2001, Nguyen reported a successful catalytic MPV reduction using alkylaluminum as the precatalyst.<sup>2</sup> The active aluminum alkoxide catalyst for this reaction was assembled *in situ* from trimethylaluminum in the presence of a super stoichiometric amount of *i*PrOH and found that generated in this manner the  $\text{Al}(\text{O}i\text{Pr})_3$  was much less prone to aggregate (scheme II-2). The new protocol enabled Nguyen to develop a chemoselective methodology in the reduction of ketone **II-1a** to alcohol **II-3a**. In this report, stereoselective reduction of ketone **II-1a** with chiral hydride sources **II-5** were also investigated and chiral alcohol **II-3a** with 80-60% *ee* was obtained.

### Scheme II-2. Catalytic MPV reduction



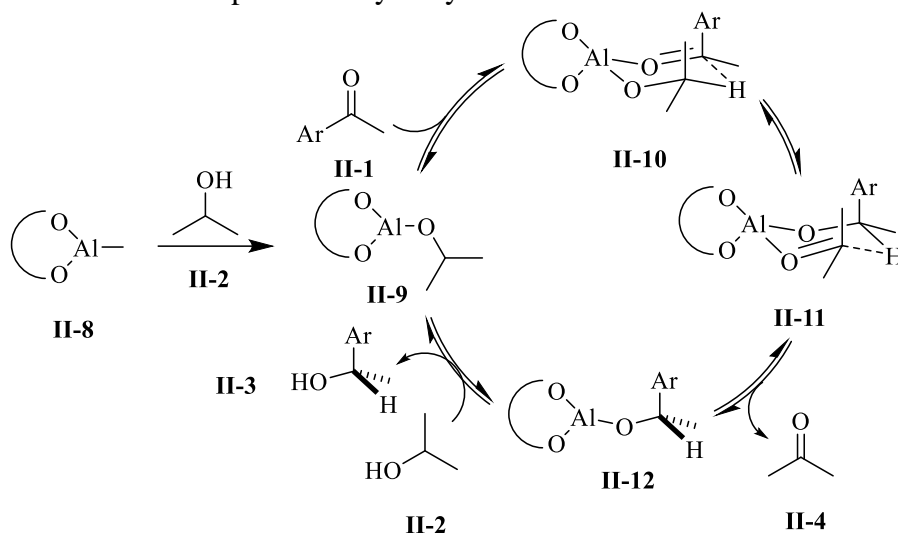
Later in 2002, the same group reported the asymmetric catalytic MPV reduction catalyzed by BINOL-aluminum complex (scheme II-3).<sup>3</sup> The active catalyst **II-8** which was synthesized *in situ*, by mixing 1.0 equiv (S)-BINOL **II-7** and 1.0 equiv  $\text{AlMe}_3$ , catalyzed the asymmetric reduction of ketone **II-1b** and yielded the 2° alcohol **II-3b** in 99% yield and 83% *ee*. Poor *ee* was obtained by using acetophenone **II-1c** as the substrate. The enhanced *ee* of substrate **II-1b** over acetophenone **II-1c** was presumably because of the coordination of  $\alpha$ -bromo substituent to the aluminum center.

### Scheme II-3. Asymmetric catalytic MPV reduction



The suggested mechanism for this MPV reduction is depicted in scheme 4.<sup>4,5</sup> It was proposed that the association of active catalyst **II-9**, which is formed *in situ* via the reaction of aluminum complex **II-8** with *i*PrOH **II-2**, with ketone **II-1** generates complex **II-10**. This coordination complex keeps the hydride donor **II-2** and hydride acceptor **II-1** in close proximity. The hydride transfer from alcohol to ketone proceeds via a six-membered transition state and produces enantioenriched alcohol **II-3** with acetone as the volatile side product.

**Scheme II-4.** Proposed catalytic cycle



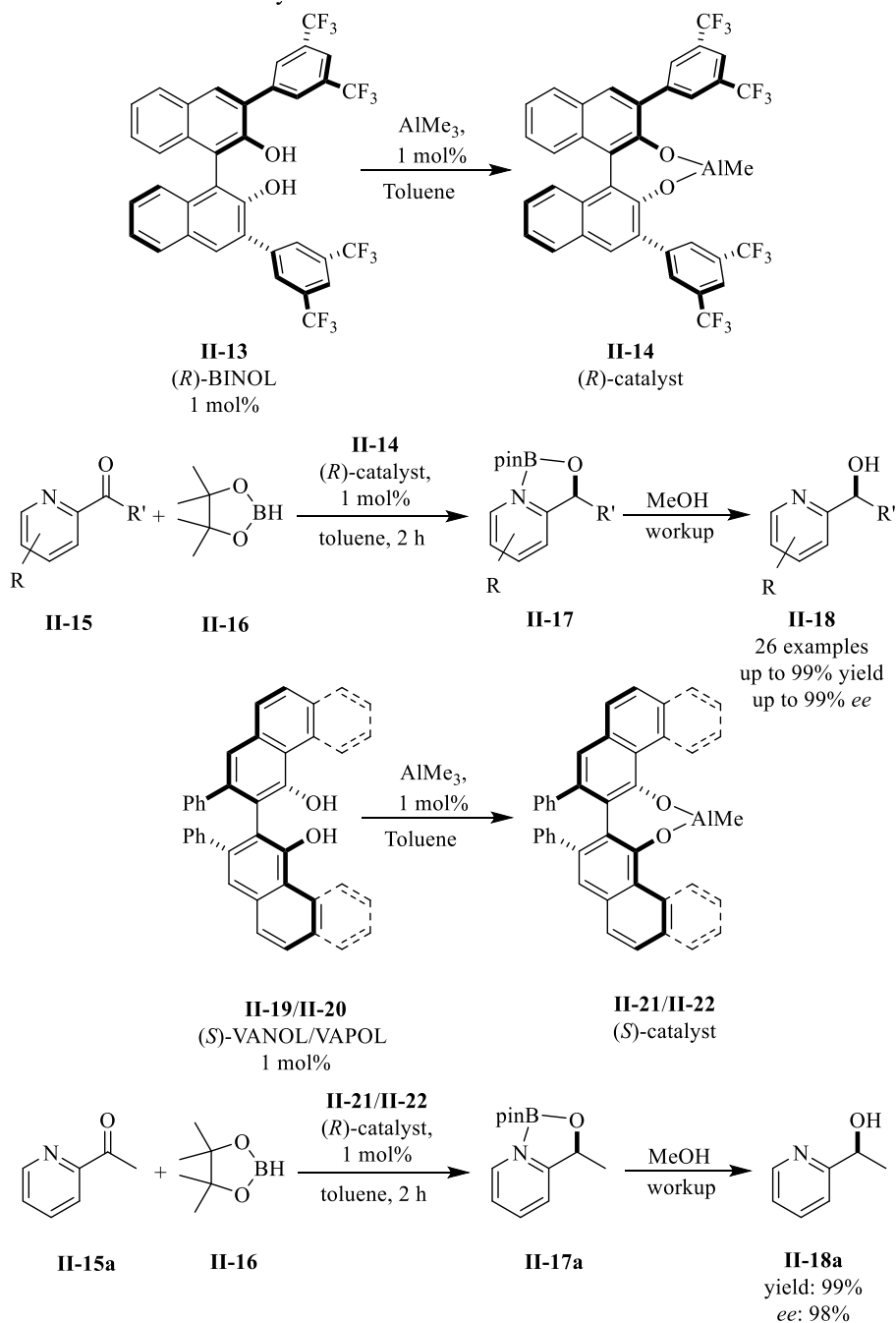
#### 2.1.1.2. Asymmetric hydroboration of ketone

In 2019, Rueping reported the asymmetric catalytic hydroboration of ketones catalyzed by aluminum BINOL complexes **II-14** (scheme II-5).<sup>6</sup> Catalysts prepared from VANOL **II-19** and VAPOL **II-20** ligands were also equally effective in this reaction. Complex **II-14** performed excellently in the reduction of hetroaryl ketones **II-15** and yielded the desired alcohol **II-18** in high yield and *ee*.

The active catalyst prepared from BINOL **II-13** and AlMe<sub>3</sub> is proposed to be a dimeric aluminum complex **II-23** based on crystal structure which undergoes a transformation in the presence of substrate **II-15** and produces complex **II-24** (scheme II-6). In presence of HBPIn **II-16**, BINOL

aluminum hydride complex **II-28** is produced via  $\sigma$  bond metathesis of B-H and Al-O (transition state **II-25**).

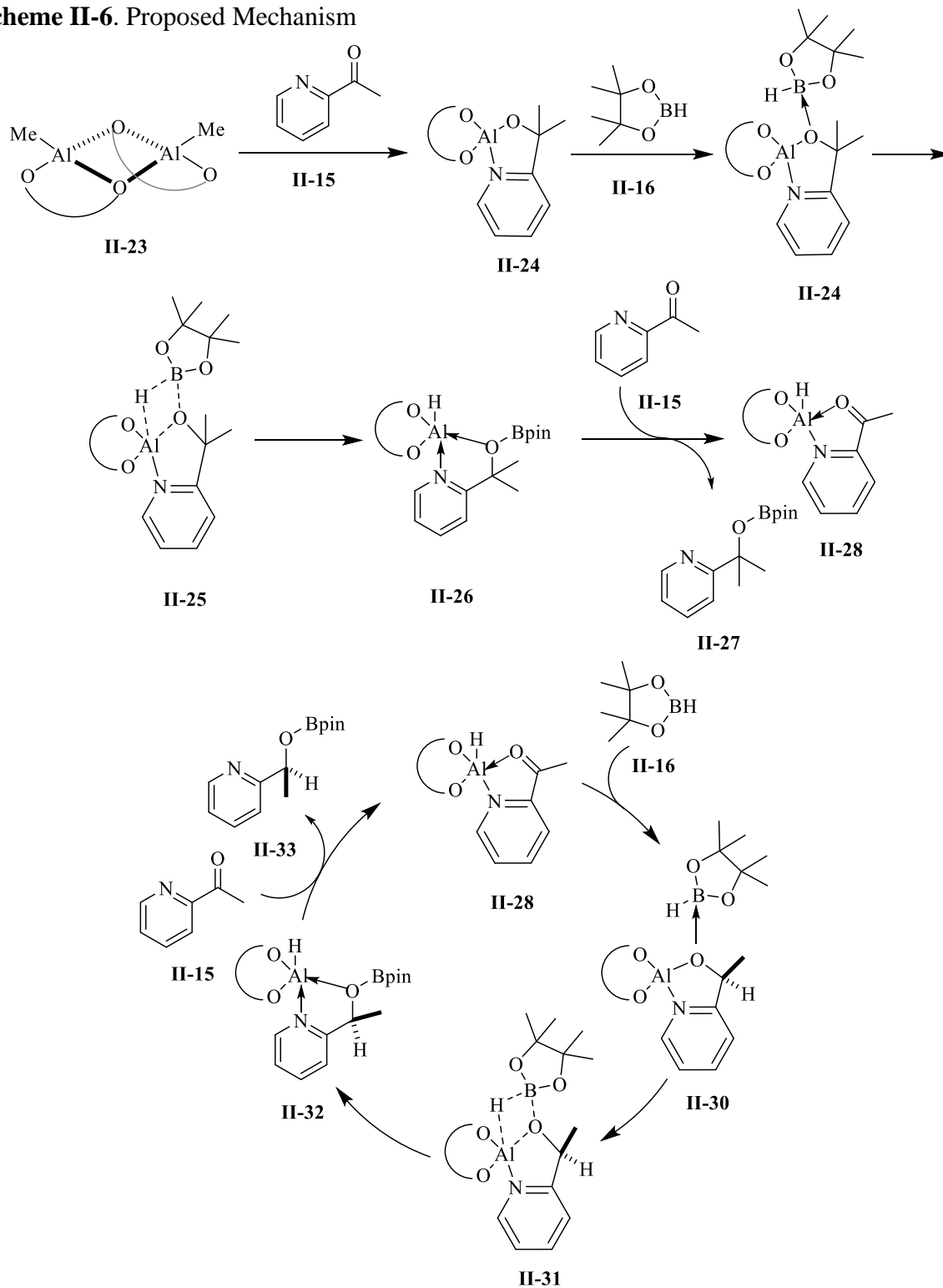
**Scheme II-5.** Ketone hydroboration



The produced aluminum hydride complex **II-28** acts as the active catalyst and participates in the reduction of ketone **II-15** to alcohol **II-18** (scheme II-5) which is depicted in scheme 6. This report

was the first successful and detailed mechanistic study of hydroboration of hetroaryl ketone **II-15** catalyzed by BINOL aluminum complex **II-14**.

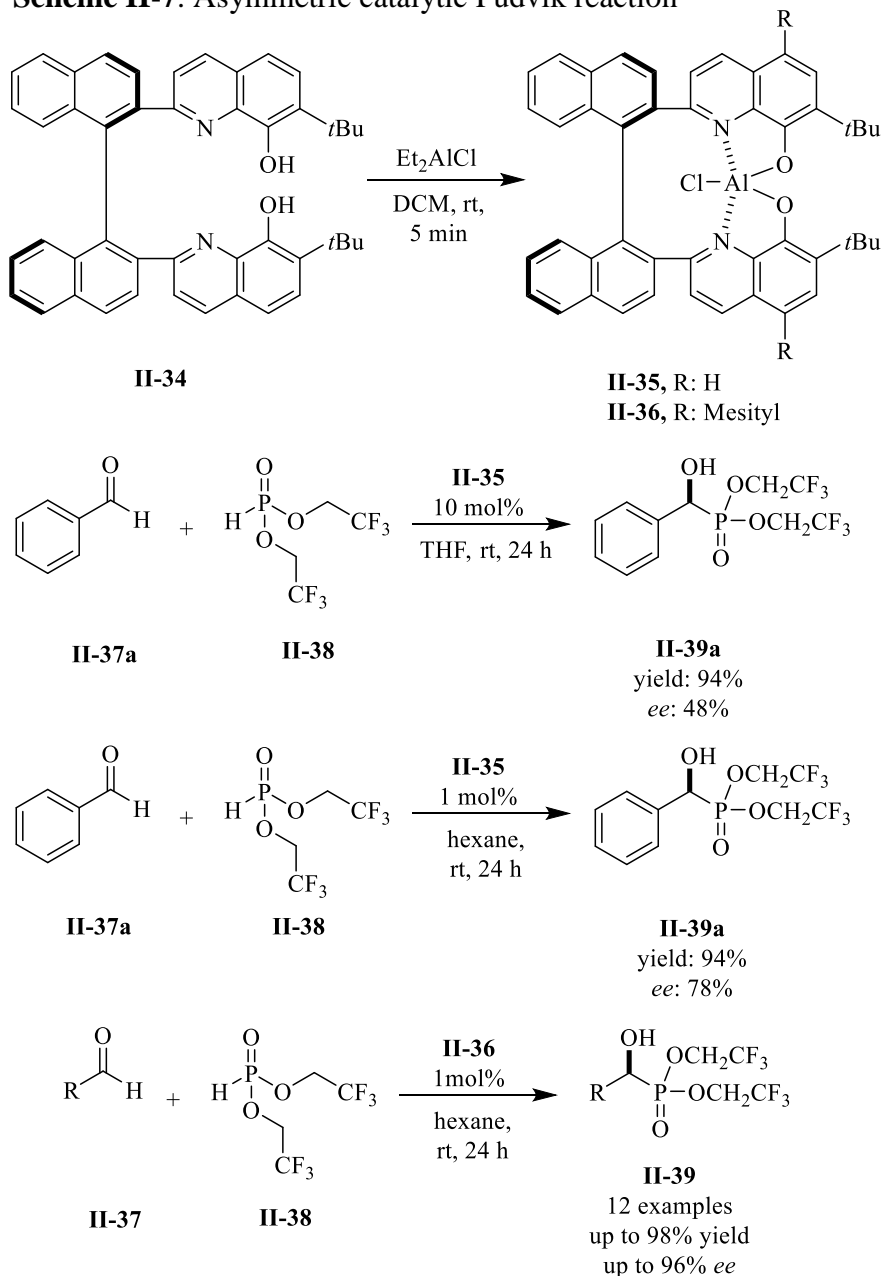
**Scheme II-6.** Proposed Mechanism



### 2.1.2. Asymmetric catalytic Pudovik reaction

The Pudovik reaction has received a great deal of attention recently because of its power to generate bioactive phosphono derivatives of  $\alpha$ -hydroxy carboxylic acids.<sup>7</sup>

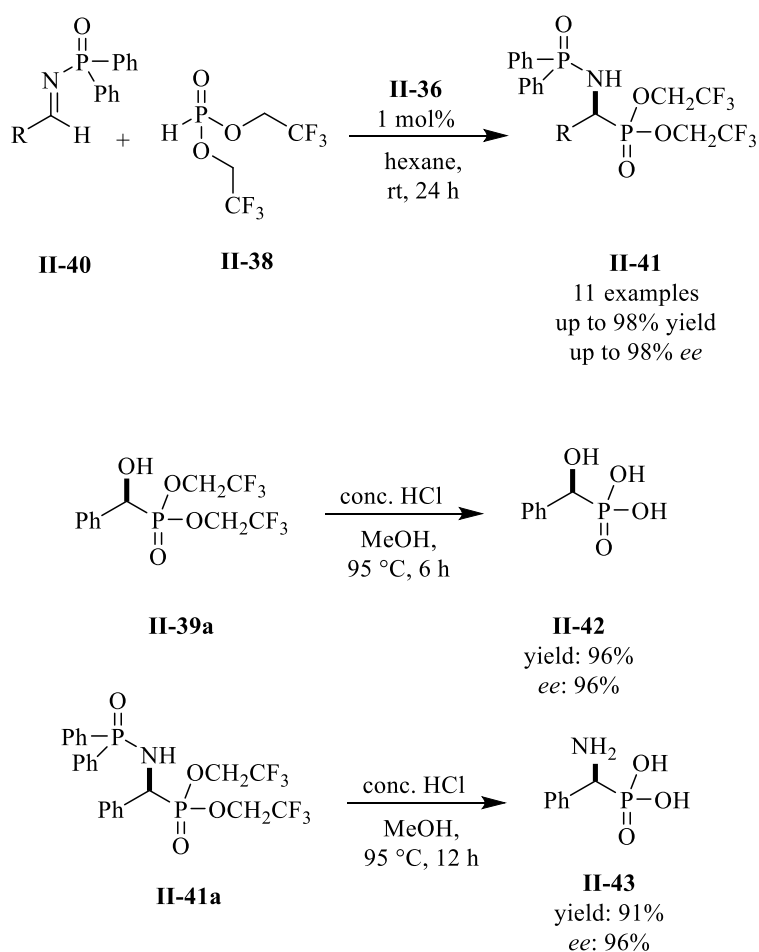
**Scheme II-7.** Asymmetric catalytic Pudovik reaction



In 2011, Yamamoto reported a highly efficient Pudovik reaction catalyzed by chiral tethered bis(8-quinolinato)(TBOx) aluminum complex **II-35** or **II-36** (scheme II-7).<sup>8</sup> Interestingly, by decreasing

catalyst loading from 5 mol% to 1 mol% and also changing the solvent from THF to hexanes a 30% increase in *ee* was observed. Supposedly, a low concentration of the catalyst difavors catalyst aggregation. Further optimization, yielded the desired product in excellent yield and *ee*.

**Scheme II-8.** Asymmetric catalytic Pudvik reaction



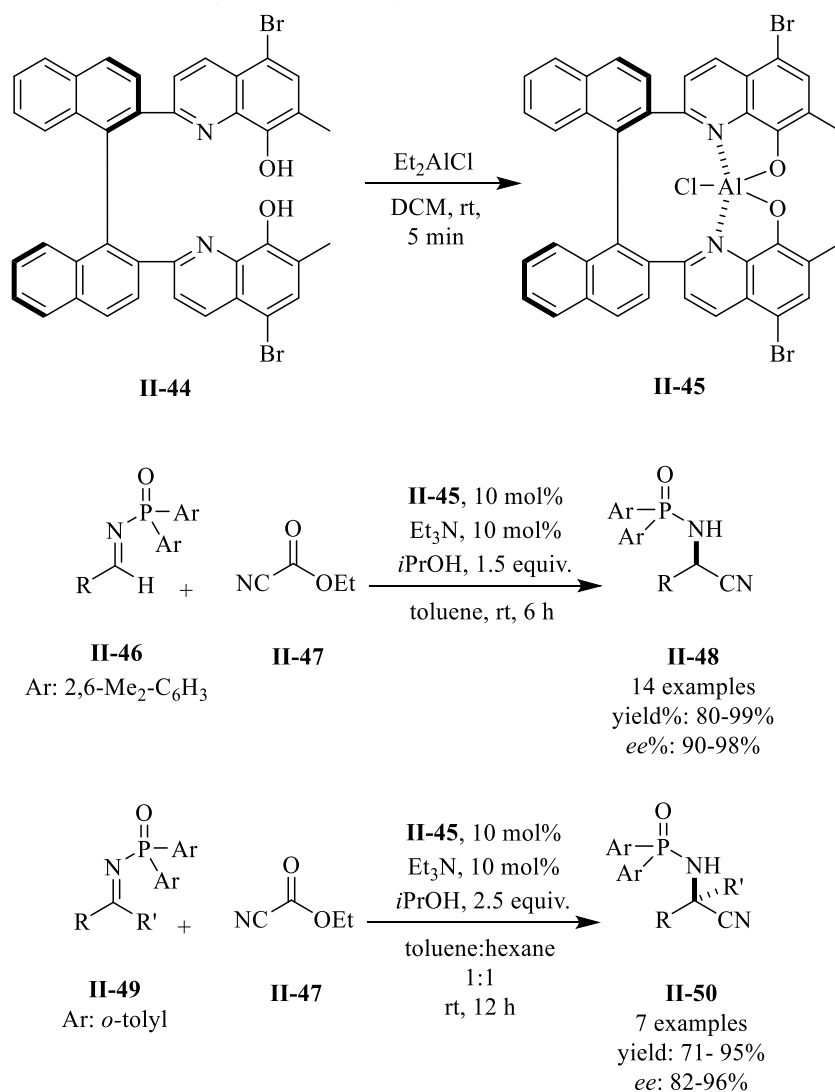
Moreover, the aluminum complex **II-36** was also evaluated in the synthesis of optically active  $\alpha$ -aminophosphonate **II-41**.<sup>8</sup> Synthesis of the enantioenriched  $\alpha$ -aminophosphonate has attracted lots of attention because of their antifungal and antibacterial activity and also being used as a protein inhibitor. It was observed that diphenylphosphinoyl group was the optimum protecting group and under the optimum reaction condition  $\alpha$ -aminophosphonates **II-41** was produced with high yield and excellent enantioselectivity. It was also shown that the  $\alpha$ -hydroxy **II-39a** and  $\alpha$ -

aminophosphonate **II-41a** underwent smooth deprotection and yielded  $\alpha$ -hydroxy **II-42** and  $\alpha$ -aminophosphonic acids **II-43** with maintained enantiomeric excess (scheme II-8).

### 2.1.3. Asymmetric catalytic Strecker reaction of aldimines and ketimines

Aluminum complex **II-45** was used in the asymmetric catalytic Strecker reaction of aldimines and ketimines (scheme II-9).<sup>9</sup>

**Scheme II-9.** Asymmetric catalytic Strecker reaction



The aforementioned reaction has been an important one in asymmetric catalysis since the synthesis of  $\alpha$ -amino acid derivatives would be possible via the hydrolysis of the product of this reaction. The reaction was performed in the presence of a catalytic amount of Et<sub>3</sub>N or DMAP in order to

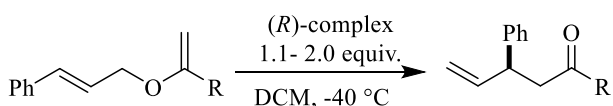


activate the cyanide source. In addition, the super stoichiometric amount of *i*PrOH had a beneficial impact on the outcome of the reaction; presumably, suppressing product inhibition. Catalyst **II-45** was highly effective in hydrocyanation of aldimines **II-46** and ketimines **II-49** and yielded the desired products in high yields and enantioselectivities.

#### 2.1.4. Claisen rearrangement

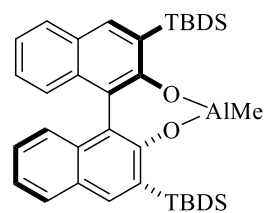
In 1995, Yamamoto was reported the first successful asymmetric Claisen rearrangement mediated by BINOL aluminum complex **II-53**.<sup>10</sup> It was observed that the vinyl allyl ethers with trimethylsilyl **II-51a** and trimethylgermyl **II-51b** substituents yielded enantioenriched acylsilanes **II-52a** and acylgermanes **II-52b** with good yield and good enantioselectivity.

**Scheme II-10.** Asymmetric Claisen reaction



**II-51a**, R: SiMe<sub>2</sub>Ph  
**II-51b**, R: GeMe<sub>3</sub>

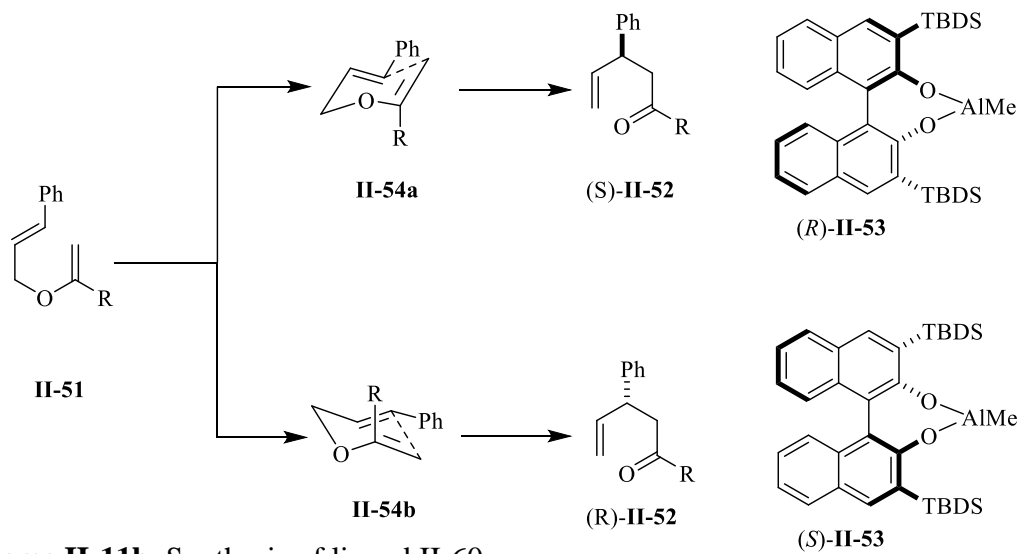
**II-52a**, R: SiMe<sub>2</sub>Ph  
 yield: 76%, *ee*: 90%  
**II-52b**, R: GeMe<sub>3</sub>  
 yield: 68%, *ee*: 93%



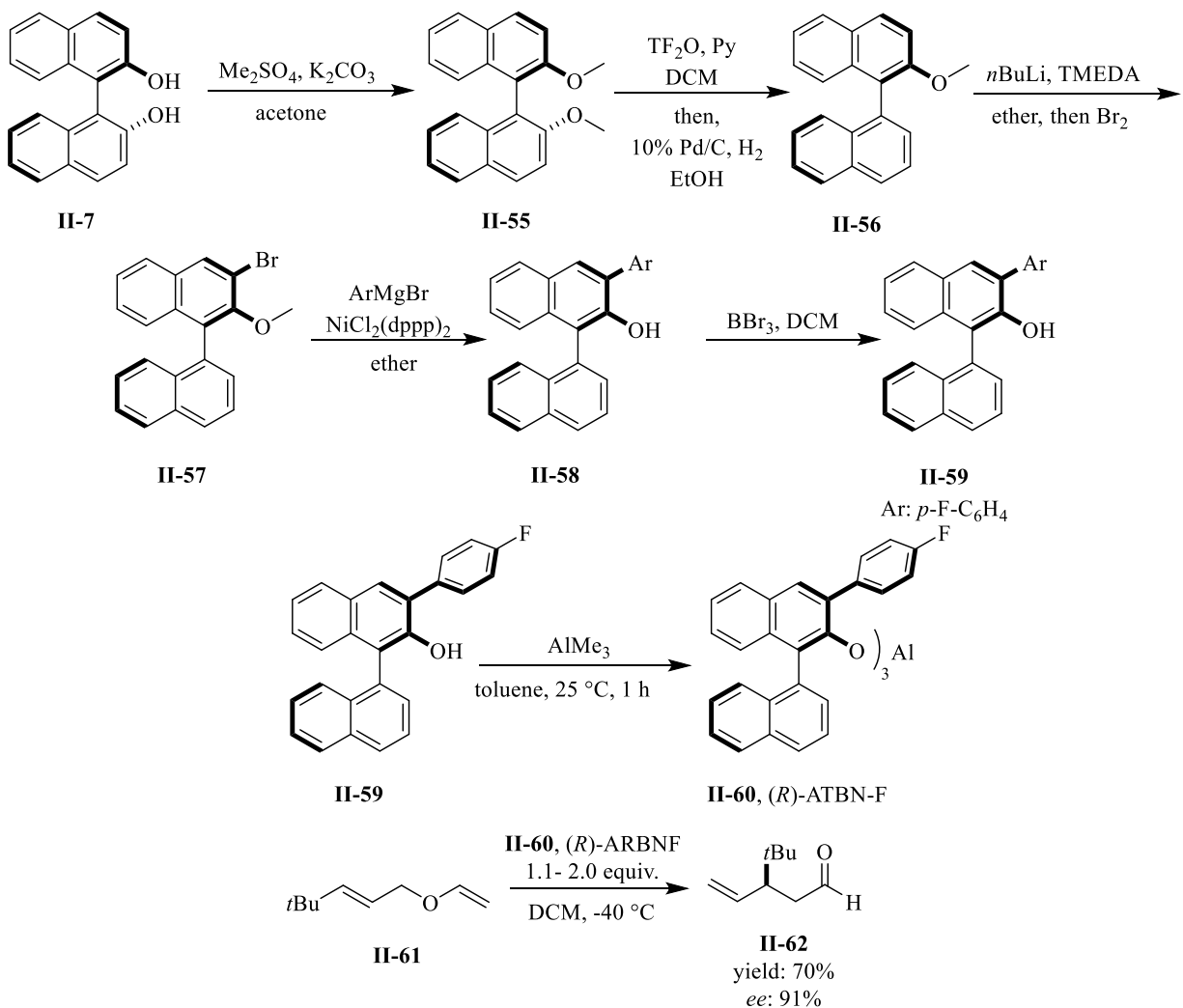
**II-53**  
 (R)-catalyst

The same allyl vinyl ether presumably undergo cyclization via two enantiomeric six-membered chair-like transition states (**II-54a**, **II-54b**) as illustrated in scheme 11a which can produce the two enantiomers of the product **II-52** (scheme II-11a). A second aluminum catalyst was published in 1995 by Yamamoto for the asymmetric Claisen rearrangement and tolerated a broad scope of the substrates that did not require the presence of silyl or germlyl substituents (scheme II-11b).<sup>11</sup> This method still had the drawback of resulting stoichiometric amount of catalyst. This reaction was mediated by chiral aluminum complex **II-60** which was assembled *in situ* by treating 3.0 equiv of ligand **II-59** and 1.0 equiv of AlMe<sub>3</sub>. Starting from commercially available (*R*)-BINOL, ligand **II-59** was synthesized in 6 steps with an overall 38% yield as depicted in scheme II-11.

**Scheme II-11a. Asymmetric Claisen reaction**



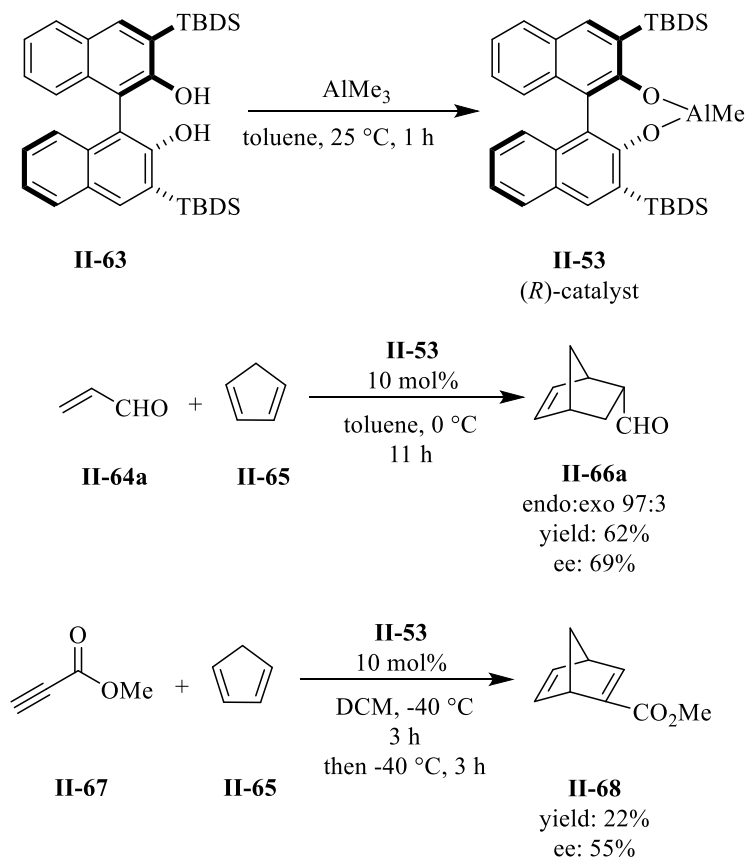
**Scheme II-11b. Synthesis of ligand II-60**



### 2.1.5. Diels-Alder reaction

Undoubtedly, the Diels-Alder reaction has been one of the most important reactions in organic chemistry. After over a century since its discovery, attempts are still ongoing in order to develop practical methods in the asymmetric assembly of enantiopure Diels-Alder adduct. The first asymmetric catalytic Diels-Alder reaction catalyzed by a chiral aluminum complex was reported by Yamamoto in 1992 (scheme II-12).<sup>12</sup> In this report, the active catalyst was synthesized *in situ* by treating  $\text{AlMe}_3$  with BINOL ligand **II-63**. In the presence of 10 mol% of catalyst **II-53** the desired cyclo-adduct product, **II-66** was produced in good yield and diastereoselectivity; however, in moderate *ee*. Further attempts in the optimization of the reaction resulted in a slight improvement of the enantioselectivity.

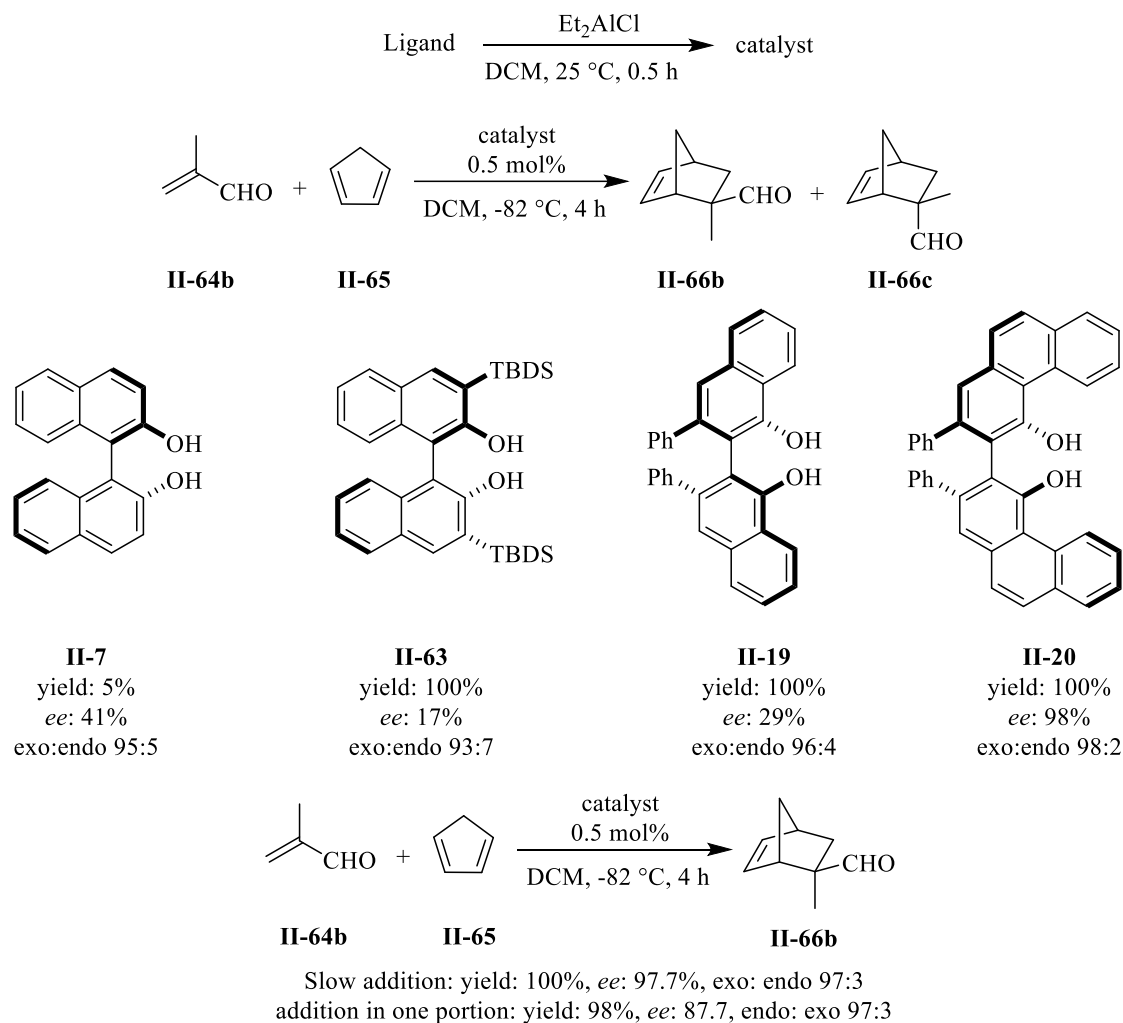
**Scheme II-12.** Asymmetric catalytic Diels-Alder reaction



Catalyst **II-53** was also used in the synthesis of the cycloadduct from diene **II-65** and dienophile **II-67** which was the first example of using an acetylenic dienophile in the asymmetric Diels-Alder reaction catalyzed by a chiral catalyst.

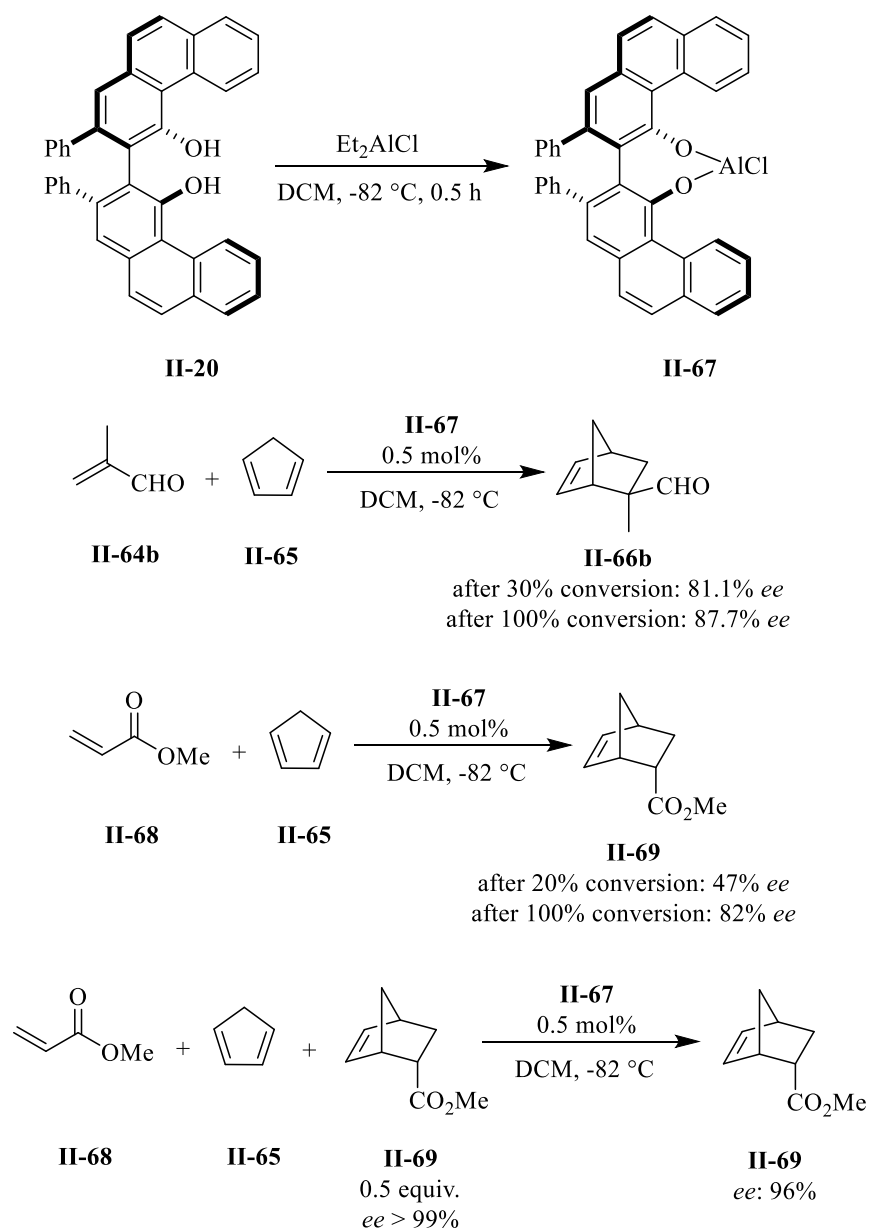
The VANOL **II-19** and VAPOL **II-20** ligands were also evaluated in aluminum catalyst for the asymmetric Diels-Alder reaction in our group in 1993 (scheme II-13).<sup>13a, 13b</sup> Initial attempts revealed that the BINOL ligands **II-7** and **II-63** and the VANOL ligand **II-19** were less selective than VAPOL **II-20** as the chiral ligand in generating a chiral catalyst with Et<sub>2</sub>AlCl. After further optimization, the best conditions was found to involve the slow addition of dienophile **II-64b**. The reaction was started with 10% of the dienophile **II-64b** added at the beginning of the reaction and rest added over 3 hours with a syringe pump to give **II-66b** 100% yield, 97.7% *ee* with an *exo/endo* ratio of 97:3. Addition of the dienophile **II-64b** in one portion produced the desired product in lower asymmetric induction (97.7% *ee* vs. 87.7% *ee*). Interestingly, it was observed that the *ee* of the reaction was increasing with the percent conversion. The asymmetric induction of this reaction at an early stage (30% conversion) was 81.1% but after 100% conversion, it was 87.7%. Further studies were conducted in order to understand this amplification in *ee*. Since the reaction of methacrolein **II-64b** with diene was too fast to follow over time, methyl acrylate **II-68** was studied instead (scheme II-14). After 20% conversion, 47% *ee* was obtained which was increased to 82% *ee* at the end of the reaction. Finally, the reaction was conducted in the presence of 0.5 equiv. optically pure product **II-69** and the desired product was produced **II-69** in 96% *ee*, significantly higher than observed 82% *ee* for this reaction. After this observation, the next question was whether the bulkiness or the chirality of compound **II-69** was responsible for this positive cooperation between catalysts **II-67** and product **II-69**.

**Scheme II-13.** Asymmetric catalytic Diels-Alder reaction



Bulky aldehydes and esters were used as additives in this reaction and a significant increase in *ee* was observed (scheme II-15). Aldehydes proved to be more effective than esters since the coordination of an aldehyde to the catalyst would be expected to be better than an ester because of steric reasons. It was interesting to observe that bulky dicarbonyls such as **II-76** performed excellent in this reaction and yielded enantiopure cycloadduct **II-69** in 80% yield and 92% *ee* at 0 °C, while the same reaction with no additive produced cycloadduct **II-69** with only 37% *ee*.

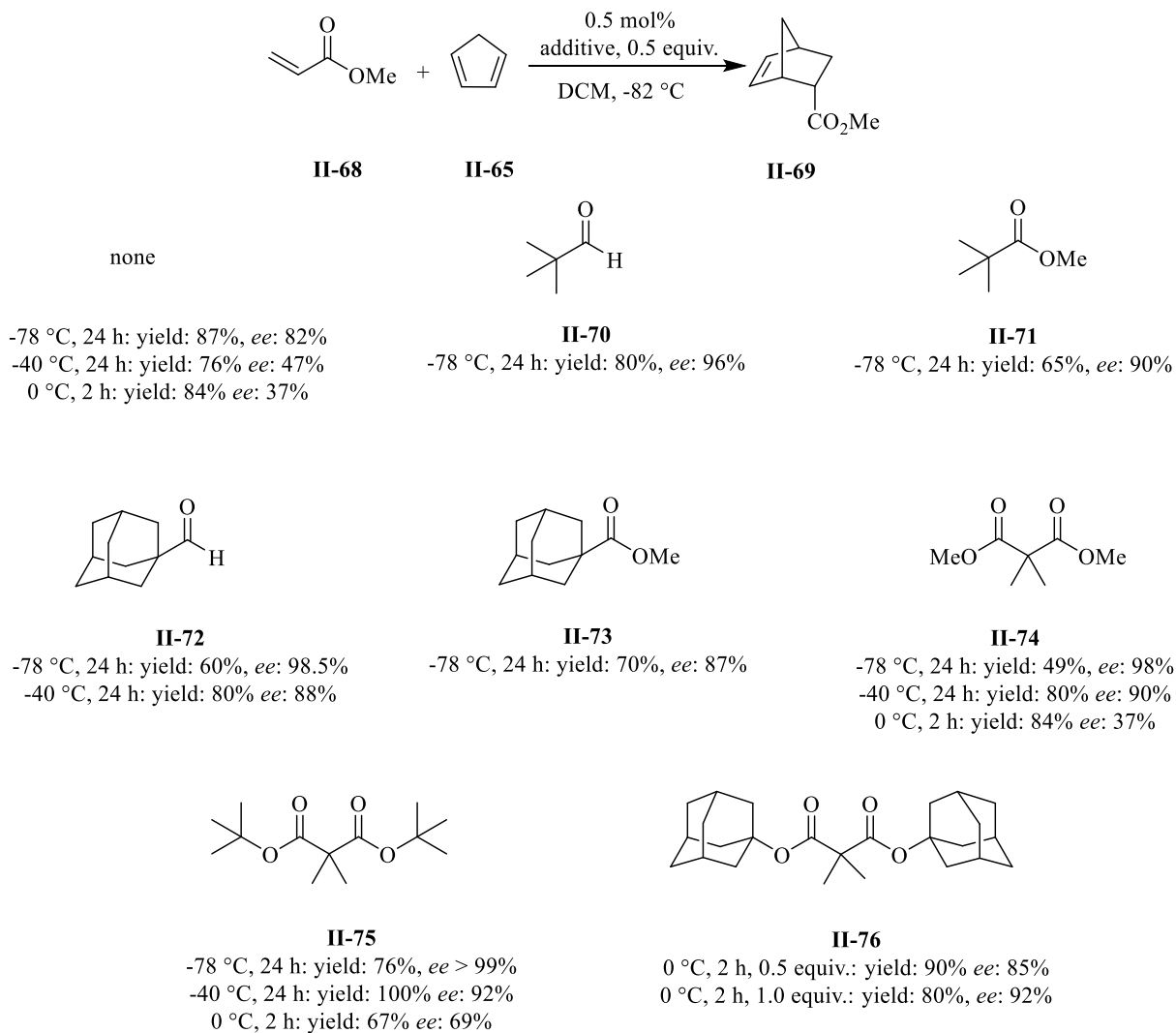
**Scheme II-14.** Asymmetric catalytic Diels-Alder reaction



The positive cooperation between catalyst **II-67** and product **II-69** in the absence of additives would be explained in the proposed mechanism in scheme 16. It is assumed that the complex **II-78** is the major species at the beginning of the reaction. As the reaction proceeds, complex **II-80** becomes the major species which leads to a higher asymmetric induction. In the presence of a bulky dicarbonyl as the additive, the aluminum catalyst adopt an octahedral structure where the

four oxygens of the VAPOL ligand and dicarbonyl occupy the equatorial positions in a meridinal arrangement and the chloride and acrylate occupy the axial ones (structure **II-81**, scheme II-16). Based on a CPK model, facial arrangement around the aluminum atom is not as favorable due to steric hindrance (structure **II-82**, scheme II-16).

#### Scheme II-15. Additives in the Diels-Alder reaction



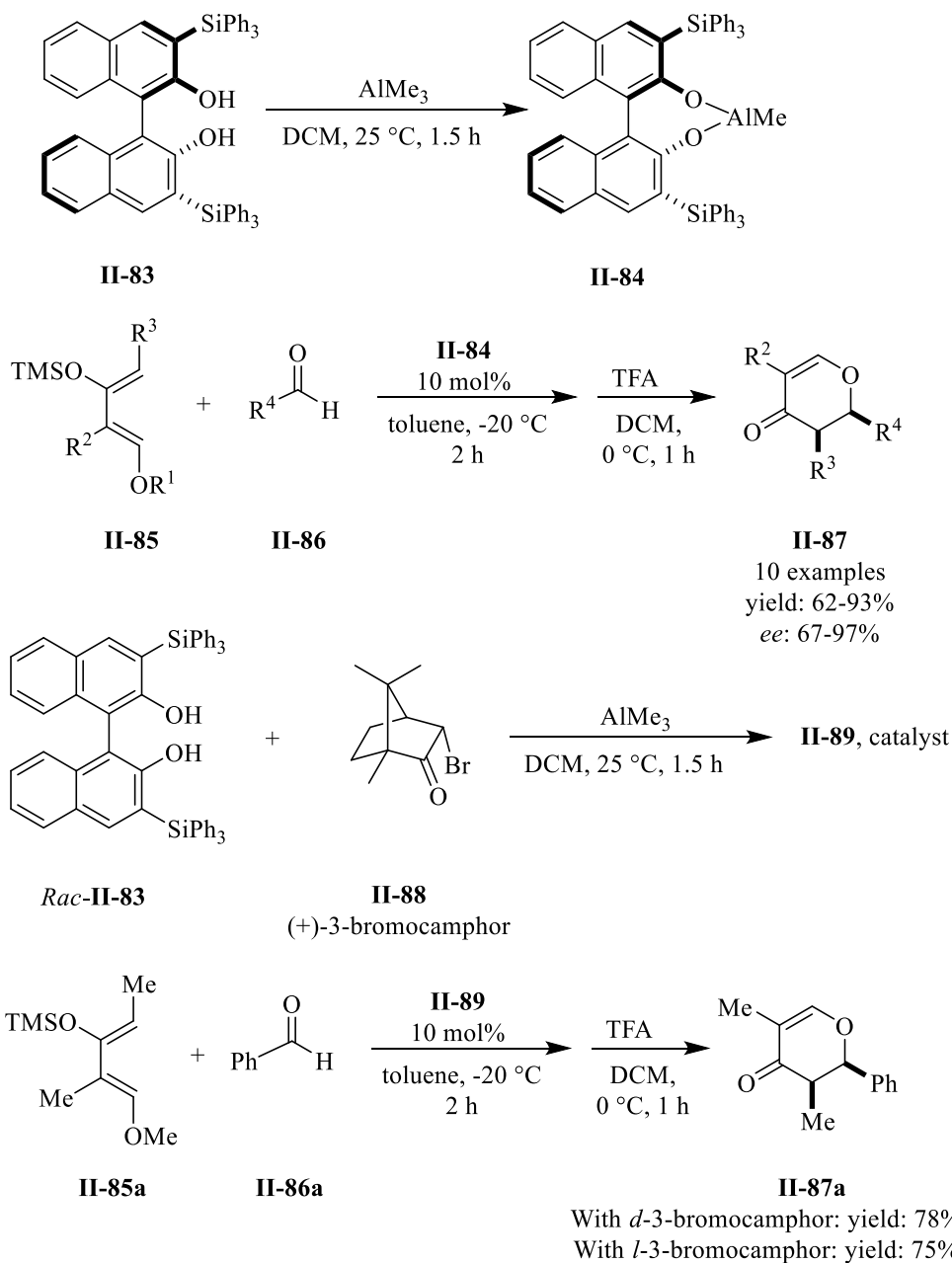
#### 2.1.6. Hetero atom Diels-Alder reaction

Heteroatom Diels-Alder have also been investigated with chiral aluminum catalyst. Yamamoto utilized the ligand **II-83** in the first asymmetric catalytic heteroatom Diels-Alder reaction (scheme II-17).<sup>14</sup> This ligand was prepared from (*R*)-3,3'-dibromo-BINOL in two steps. Reacting 1.1 equiv





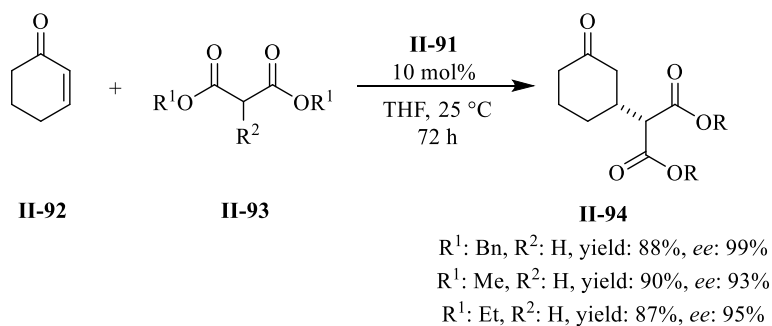
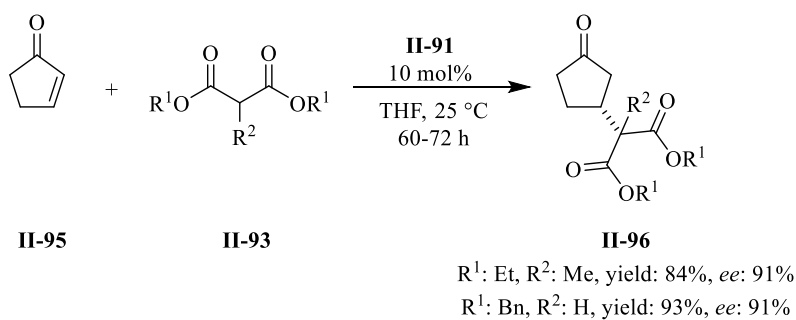
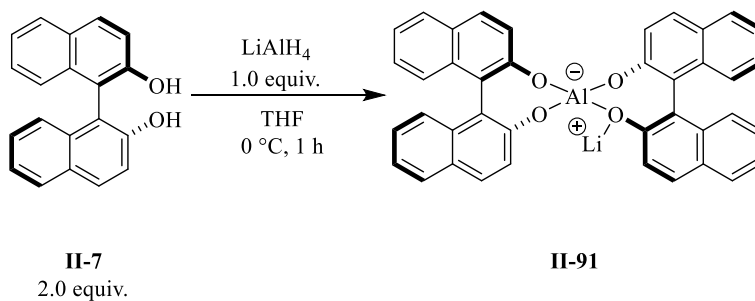
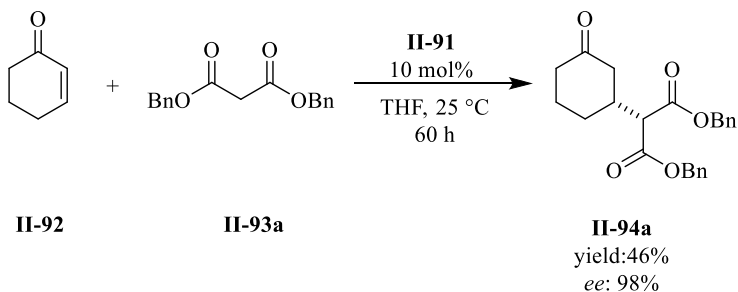
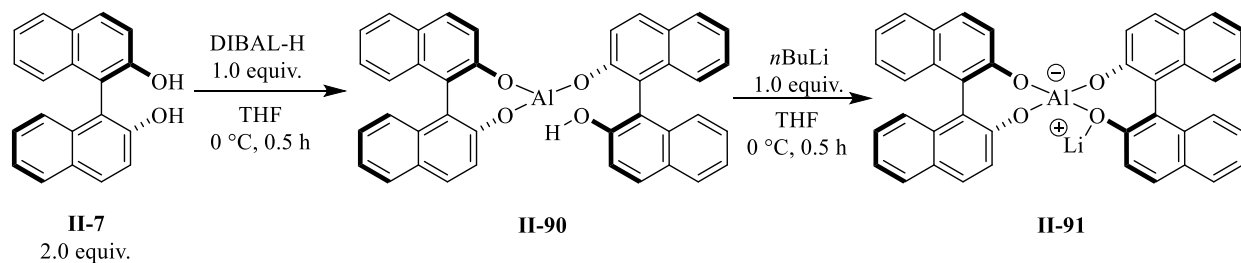
**Scheme II-17.** Asymmetric catalytic heteroatom Diels-Alder reaction



### 2.1.7. Catalytic asymmetric Michael addition reactions

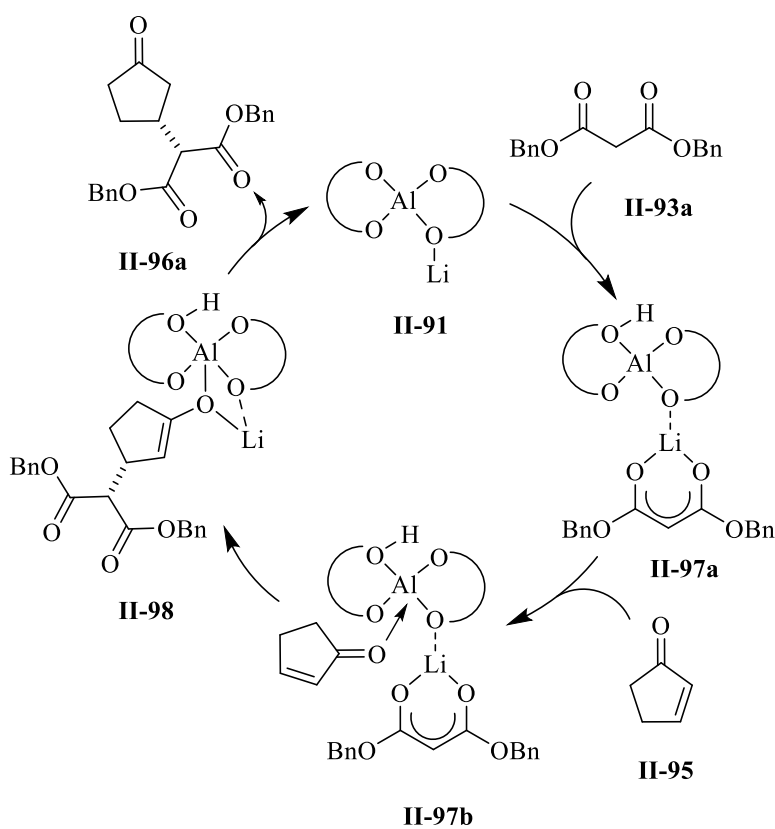
In 1996 Shibasaki reported the asymmetric catalytic Michael addition of malonates to enones catalyzed by the heterobimetallic aluminum, lithium and BINOL complex (ALB) **II-91** (scheme II-18).<sup>16</sup>

**Scheme II-18.** Catalytic asymmetric Michael addition reactions



The catalyst **II-91** was prepared by reacting 1.0 equiv of diisobutyl-aluminum hydride with 2.0 equiv of BINOL **II-7** at 0 °C for half-hour followed by reacting the resulting solution with 1.0 equiv. of *n*-BuLi for another half hour. The catalyst was highly effective in the asymmetric Michael addition of dibenzyl malonate **II-93a** with cyclohexanone **II-92** and yielded the desired Michael adduct **II-94a** in 46% yield and 98% *ee*. It was shown that the active catalyst could also be prepared by reacting 1.0 equiv LiAlH<sub>4</sub> and 2.0 equiv BINOL **II-7**. This catalyst performed well in the Michael addition to cyclopentenone produced the desired product **II-96** in high yield and excellent *ee*. The crystal structure of active catalyst **II-91** in presence of cyclohexenone **II-92** in THF was obtained. The structure revealed a spiro-aluminate BINOL complex and where the lithium in **II-91** was coordinated to one of the oxygens of the BINOL ligand and the oxygen of cyclohexenone.

**Scheme II-19.** Proposed mechanism



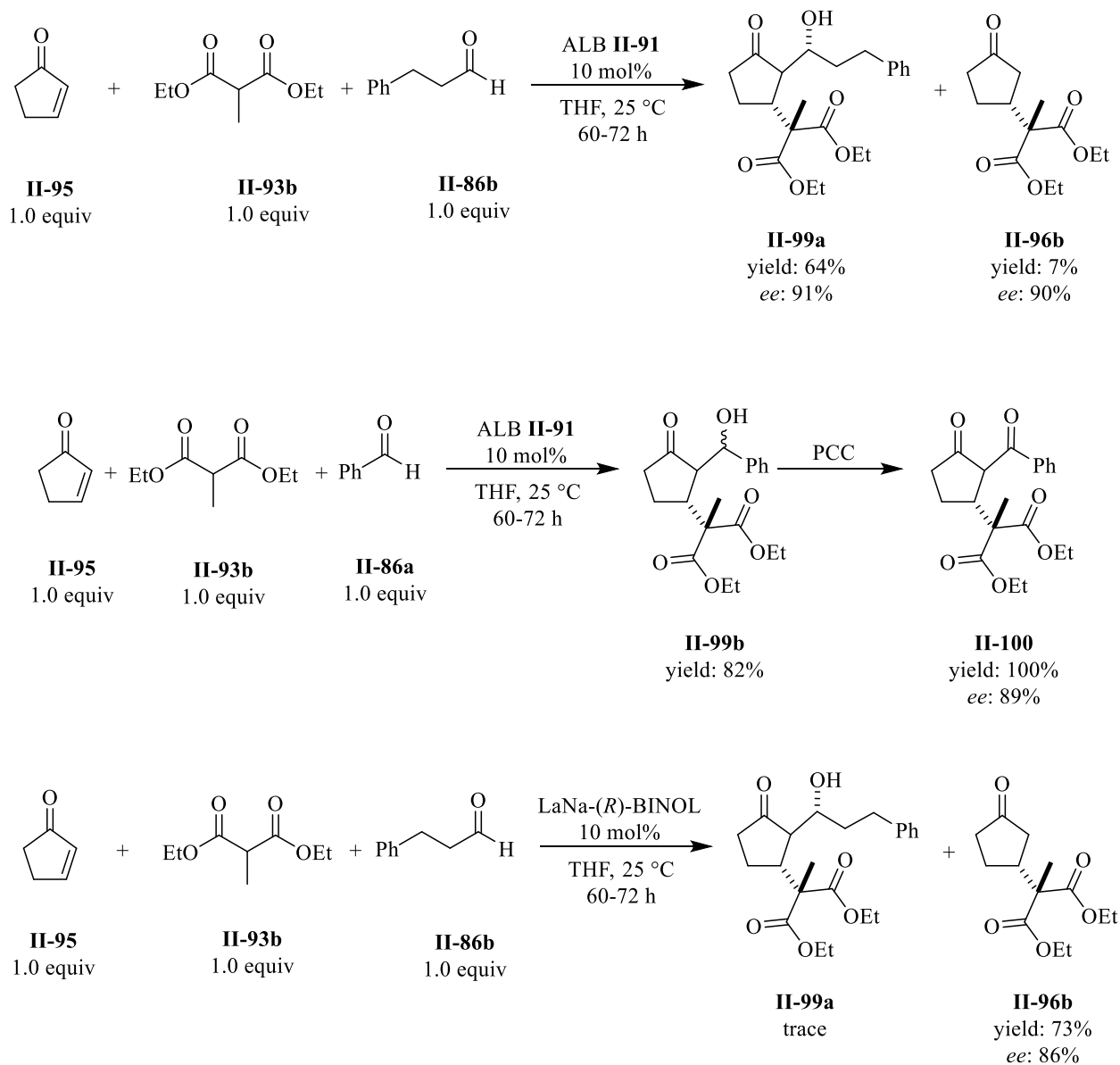
Since the electronegativity value of lithium (1.0) is smaller than the aluminum (1.5), treating ALB catalyst **II-91** with malonate **II-93** should result in the generation of lithium enolate aluminum complex **II-97a**. Then the cyclohexenone will be activated via coordination to the aluminum center and subsequent nucleophilic attack of the lithium enolate to the activated cyclopentenone (intermediate **II-97**) followed by intramolecular proton transfer (intermediate **II-98**) to give the desired product **II-96a** (scheme II-19).

The mechanism depicted in scheme 19 suggested the formation of aluminum enolate intermediate **II-98**; therefore, the possibility of trapping this enolate with other electrophiles such as aldehydes was evaluated (scheme II-20). Conducting the tandem Michael-aldol reaction with dihydrocinnamyl aldehyde **II-86b** (1.0 equiv) as the electrophile in a multi-component manner with **II-95** and **II-93b** catalyzed by ALB catalyst **II-91**, produced compound **II-99a** as a single isomer in good yield and excellent enantioselectivity. However, the same reaction with benzaldehyde **II-86a** yielded a mixture of diastereomers with a 82% combined yield. The *ee* of compound **II-99b** was measured after oxidation to the diketone **II-100** which was found to be 89%. Interestingly, when the LaNa-BINOL catalyst in which the aluminum center in **II-91** was replaced with the lanthanum, was used in place of ALB catalyst **II-91**, the exclusive formation of Michael adduct **II-96b** in 73% yield and 86% *ee* was observed. This result suggested a fast intramolecular proton transfer in the LaNa-BINOL system which obviated the trapping of the lanthanum enolate by an aldehyde.

The reaction between malonate **II-93b** and ALB catalyst **II-91** triggers the reaction and produces the lithium enolate aluminum complex (scheme II-21). The reaction of the lithium enolate with cyclopentenone is activated further via coordination of the cyclopentenone to the aluminum center (scheme II-21, intermediate **II-101**) which gives the aluminum enolate **II-102**. Subsequent reaction

of this enolate with aldehyde **II-86b** followed by protonation of the resulting alkoxide (scheme II-21, intermediate **II-103**) completes the catalytic cycle and generates the desired product **II-99a**.

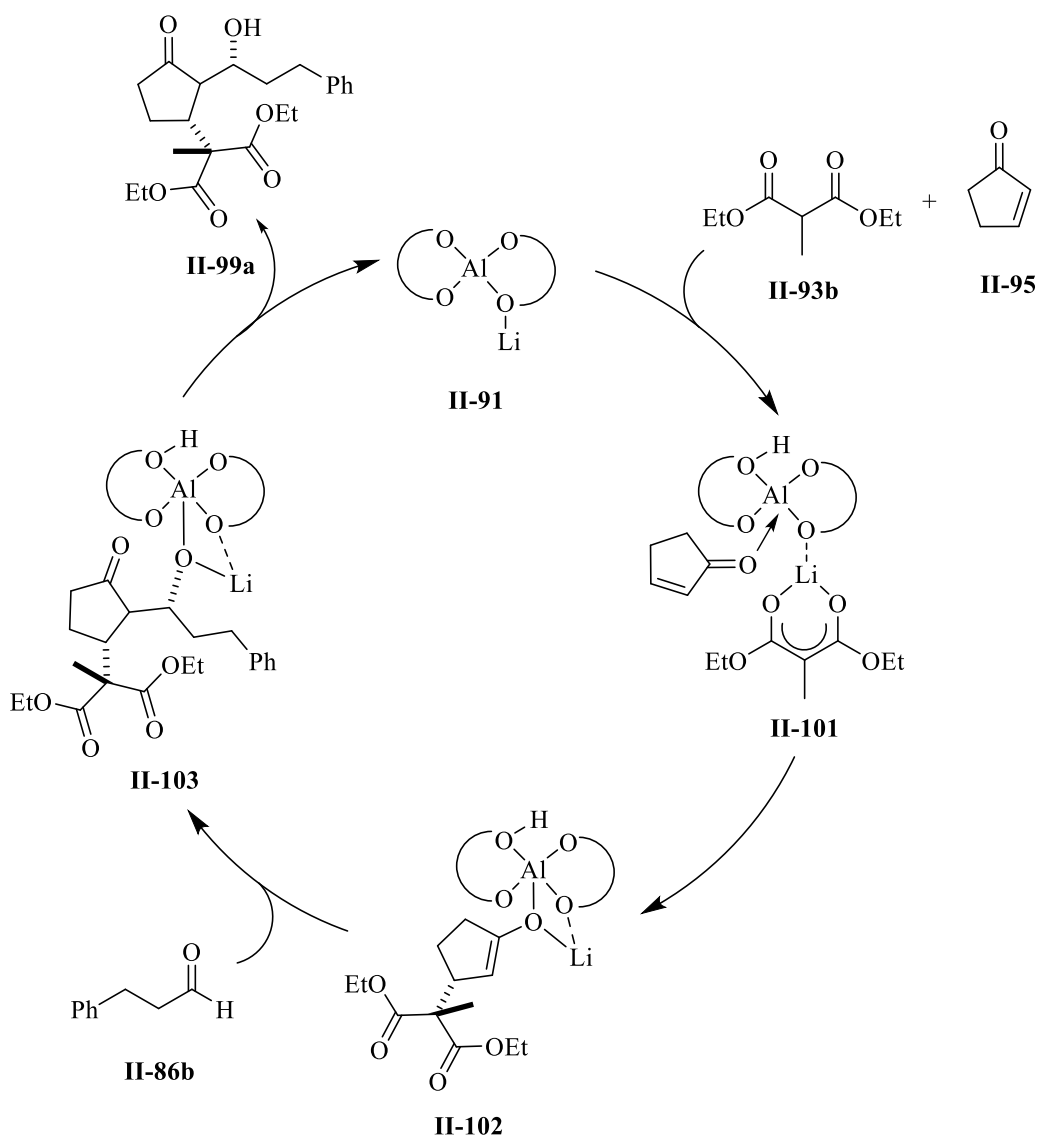
**Scheme II-20.** Asymmetric tandem Michael addition enolate reaction



Later in 1997, Feringa utilized the heterobimetallic ALB catalyst **II-91** developed by Shibasaki, in asymmetric conjugate addition of nitroesters **II-105** to enones **II-104**.<sup>17</sup> Under the optimum reaction conditions, product **II-106** was produced in good yield and moderate enantioselectivity. A strong temperature dependence was observed for this reaction (7% *ee* at 25 °C vs 74% *ee* at -30

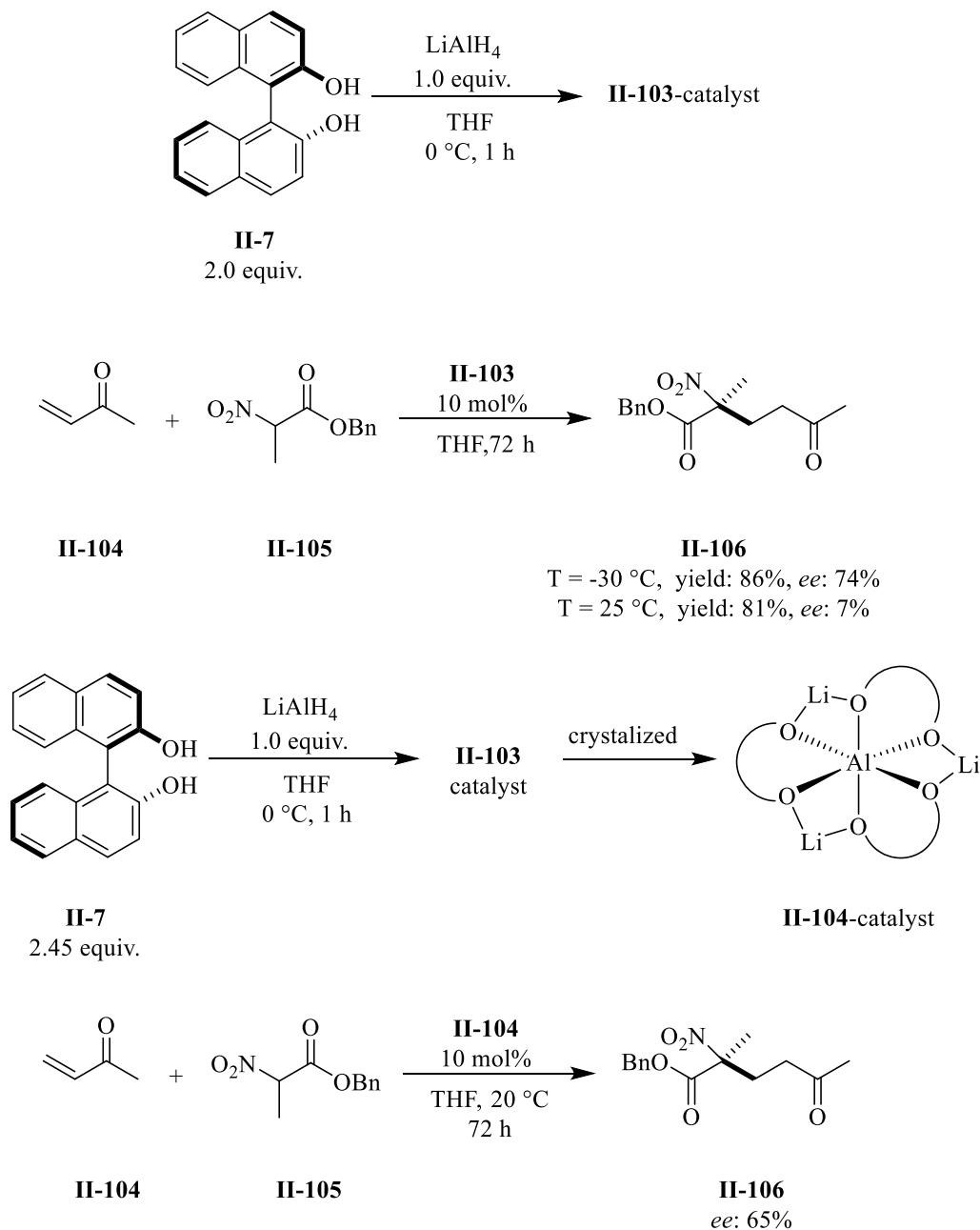
°C) presumably due to competing reactions catalyzed by different chiral aluminum species in the reaction. After further optimization, it was found that the active catalyst was the one that was prepared by mixing 2.45 equiv of BINOL ligand **II-7** and 1.0 equiv of  $\text{LiAlH}_4$ . By growing crystals, from this solution they were able to identify the hexa-coordinated octahedral  $\text{Li}_3\text{AlBINOL}_3$  species **II-164** (scheme II-22). An aluminum NMR study reveals that this solution contains three different aluminum species.

**Scheme II-21.** Proposed mechanism



Crystal of complex **II-104** efficiently catalyzed the conjugated addition of nitroester **II-105** to methyl vinyl ketone **II-104** to yield the product **II-106** in 65% *ee*. Based on this observation, either the complex **II-104** was participating in the catalytic process or it was the precursor for the active catalyst.

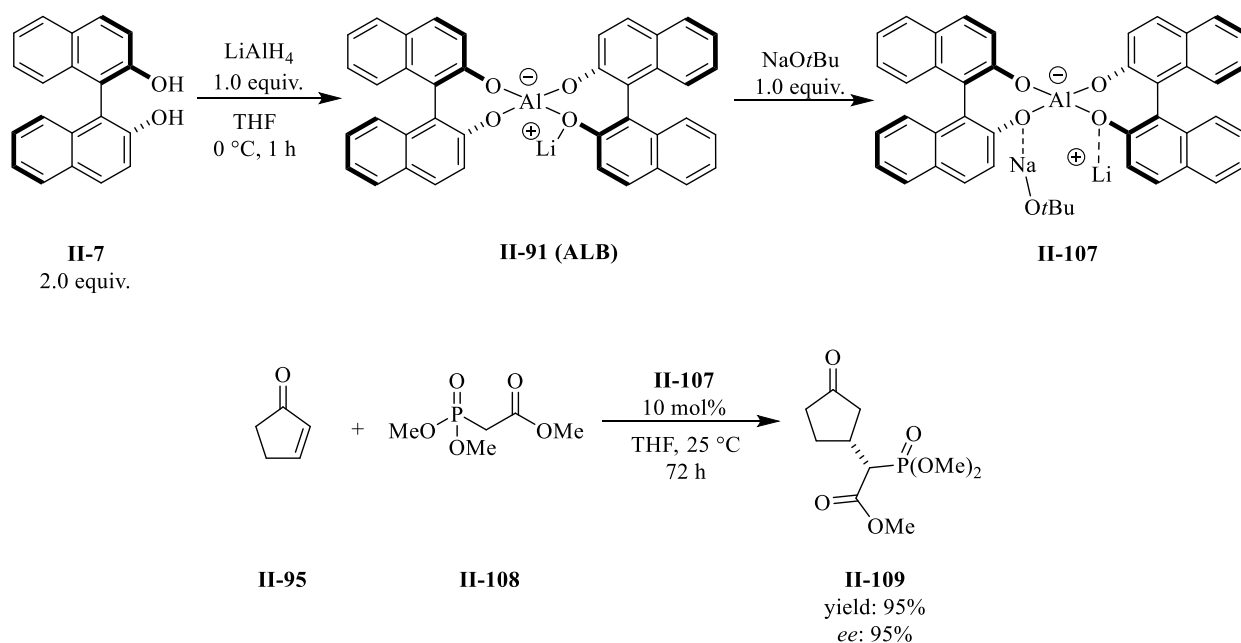
**Scheme II-22.** Conjugate addition of nitroso to enone



### 2.1.8. Asymmetric Michael addition of Horner-Wadsworth-Emmons reagents and enones

The most interesting feature of heterobimetallic chiral ALB complex **II-91** was revealed in the reaction of a HWE reagent with an enone.<sup>18</sup> Unlike the standard HWE reaction in which the phosphonate compound **II-108** reacts with enone and yields predominantly E-alkenes, in the presence of ALB-NaOtBu catalyst **II-107** and under optimum reaction conditions, causes this reaction to give the 1,4-adduct **II-109** in good yield and enantioselectivity (scheme II-23).

**Scheme II-23.** Asymmetric Michael addition of Horner-Wadsworth-Emmons reagents and enones

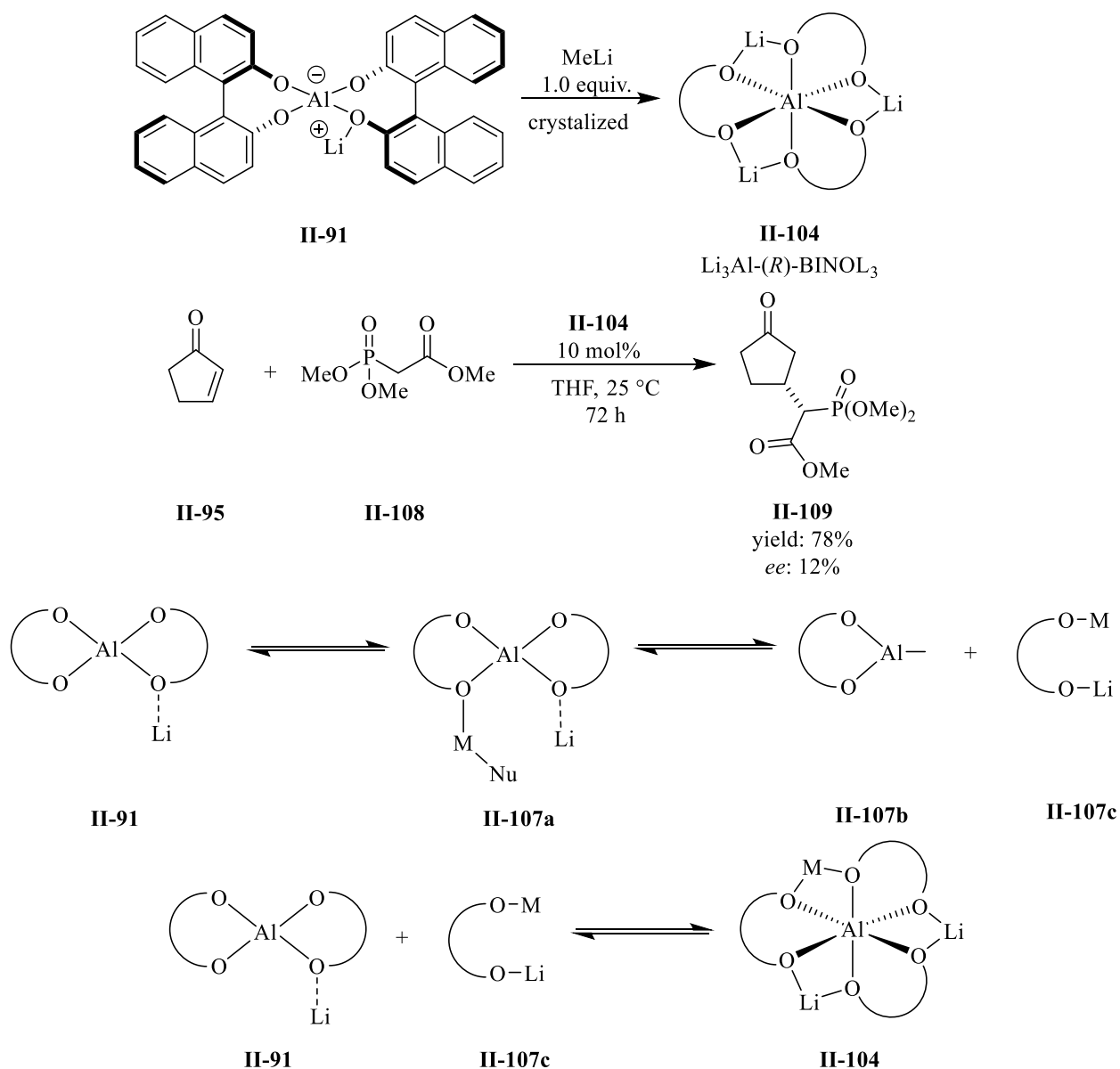


The reaction of ALB catalyst **II-91** with methyl lithium as the base produced a crystalline complex and the structure of this complex was found by Shibasaki to be a hexacoordinated octahedral complex **II-104** with X-ray structural analysis (the same structure which was reported by Feringa, scheme II-22).<sup>17</sup> The stable crystal aluminum species **II-104** was used as the catalyst in the conjugated addition of HWE reagent **II-108** with enone **II-95** and the desired Michael adduct **II-109** was afforded in 78% yield but only 12% *ee*, clearly showing that the crystalline aluminum complex **II-104** is not the active catalyst in this reaction. The author proposed the mechanism in



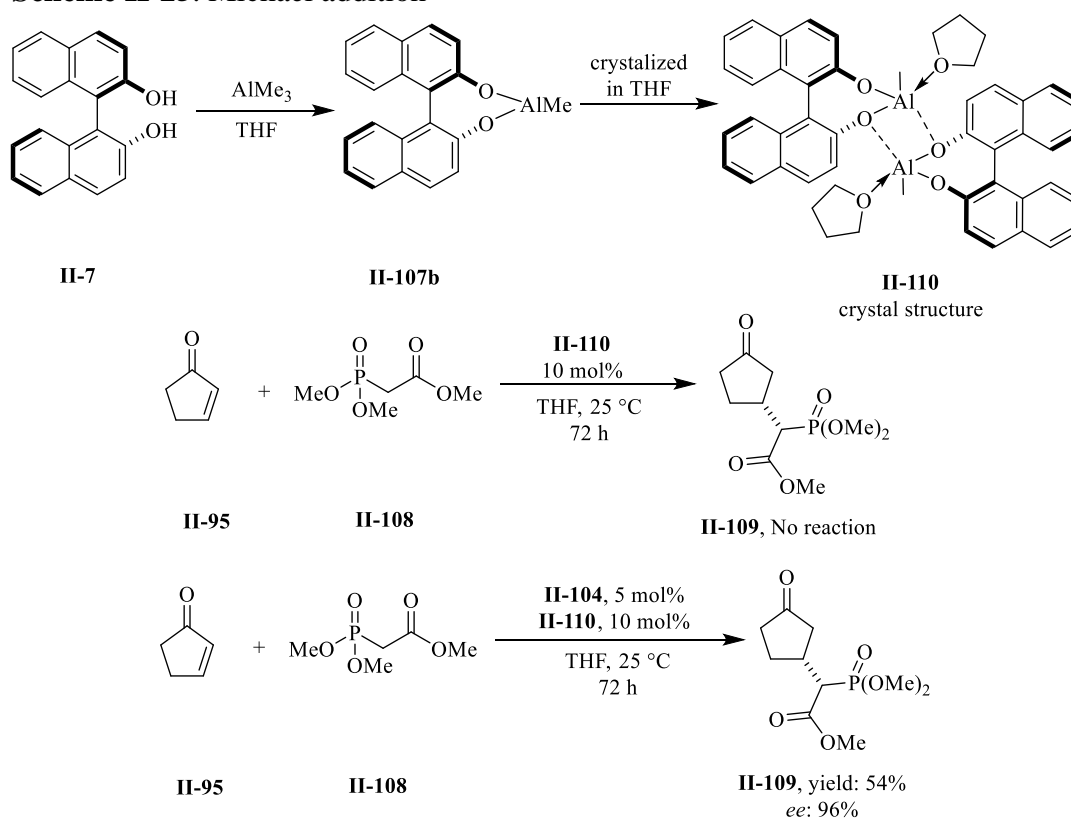
scheme 24 for the formation of this complex. ALB catalyst **II-91** would react with lithium enolate and produces complex **II-107** which undergoes subsequent disproportionation and generates a three coordinated aluminum complex **II-107b** and BINOL bis-alkoxide **II-107c**. Hexacoordinate aluminum complex **II-104** would be produced via the reaction of bis-alkoxide BINOL species **II-107c** with ALB complex **II-91**.

**Scheme II-24.** Proposed mechanism



Next, it was assumed by Shibasaki that the aluminum complex **II-108** might be the active catalyst; therefore, this complex was prepared by treatment of  $\text{AlMe}_3$  (1.0 equiv.) with BINOL **II-7** (1.0 equiv.). The structure of this catalyst was determined to be a dimeric pentacoordinate THF aluminum species **II-110**. The use of this catalyst turned out not to promote the Michael addition reaction at all. Interestingly, it was found that a 2:1 mixture of aluminum complex **II-110** and **II-104** was able to catalyze the reaction between cyclohexanone and phosphonate **II-108** and yielded the desired product in 54% yield and 96% *ee*. Since the aluminum complex **II-91** and **II-107c** did not promote the Michael addition reaction and also the use of aluminum complex **II-104** produced the adduct **II-109** in low enantioinduction, it was suggested that the aluminum species **II-107** which was generated *in situ* by treatment of ALB catalyst **II-91** with a metal alkoxide might be the actual active catalyst in this reaction.

**Scheme II-25.** Michael addition

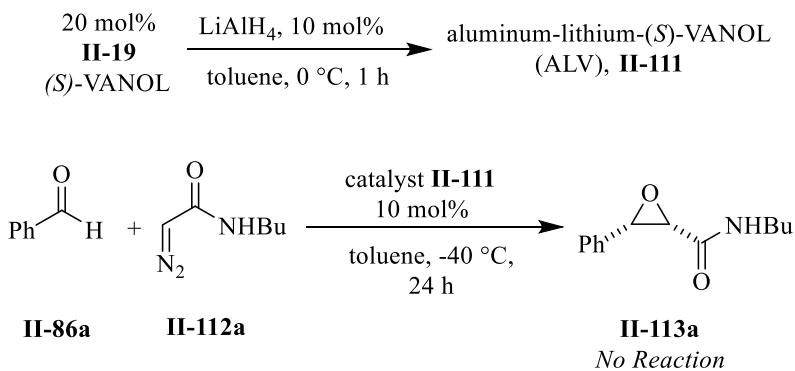


## 2.2. Evaluating the Aluminum VANOL/VAPOL complexes as efficient catalysts in asymmetric catalytic epoxidation of aldehydes.

### 2.2.1. Optimization of epoxidation reaction

Inspired by our recent discovery of asymmetric catalytic epoxidations of aldehydes with diazoacetamide catalyzed by VANOL meso-borate catalyst, one of the subject of this thesis will be to evaluate Al-VANOL and Al-VAPOL catalysts in this epoxidation reaction.<sup>19</sup> Reacting 1.0 equiv of  $\text{LiAlH}_4$  with 2.0 equiv of (*R*)-VANOL **II-19** produced heterobimetallic aluminum-lithium-VANOL complex (ALV) **II-111**. The BINOL version of this catalyst has been reported by Shibasaki to be effective in a number of asymmetric catalytic reactions.<sup>16,18</sup> Unfortunately, no product was observed after conducting the epoxidation of benzaldehyde with diazo acetamide **II-112a** the presence of 10 mol% ALV catalyst **II-111** (scheme II-26).

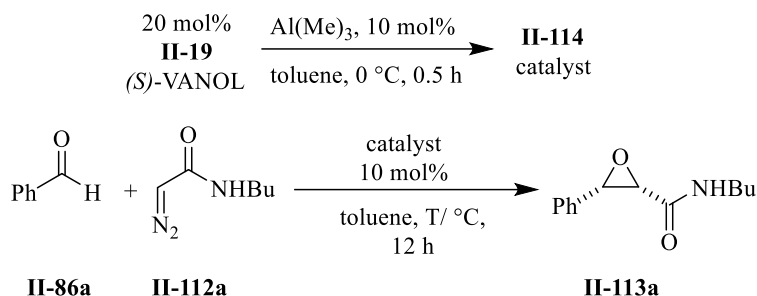
**Scheme II-26.** Epoxidation reaction



Surprisingly, when the epoxidation reaction was performed with the aluminum catalyst **II-114** which was prepared from  $\text{AlMe}_3$  (1.0 equiv.) and VANOL **II-19** (2.0 equiv.), a 19% yield (NMR) was obtained of the desired epoxide **II-113a** at  $-40\text{ }^\circ\text{C}$  (table II-1, entry 1). Further optimization of the temperature revealed the optimum temperature for this reaction to be  $0\text{ }^\circ\text{C}$  which gave the epoxide in 80% yield and 72% *ee* (table II-1, entry 3). Higher temperatures are detrimental to the yield of the reaction presumably due to a competing Roskamp reaction although a study of this

was not pursued (entry 4). Interestingly, the enantiomeric excess of the epoxide was not affected by altering the temperature of the reaction.

**Table II-1.** Temperature optimization in aluminum catalyzed epoxidation reaction

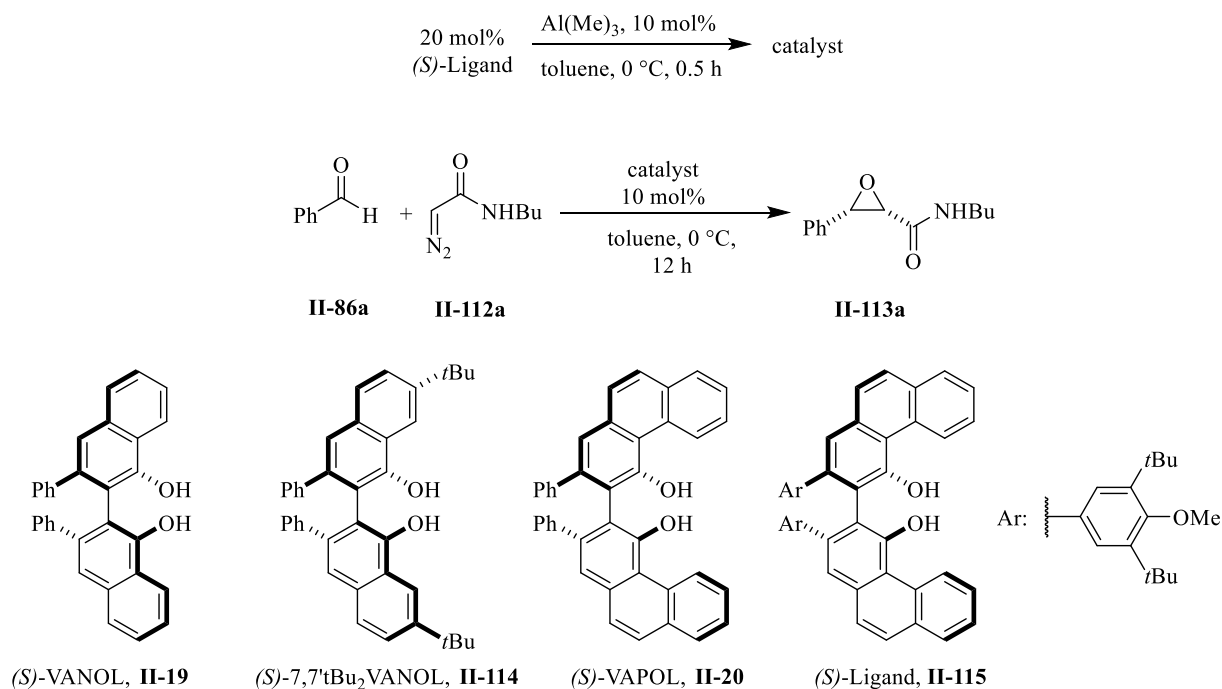


entry	T/°C	isolated yield%	ee%
1	-40 °C	19 <sup>1</sup>	<i>not determined</i>
2	-20 °C	57	72
3	0 °C	80	72
4	25 °C	62	72

Unless otherwise specified, all of the reactions were done in toluene at 0 °C for 12 h with 0.5 mmol of diazo compound **II-112** and 0.6 mmol of aldehyde. 1. NMR yield

Next, we turned our attention to the optimization of the solvent system. CH<sub>2</sub>Cl<sub>2</sub> was as effective as toluene and produced epoxide **II-113a** with comparable results (table II-2, entry 2). However, solvents containing heteroatoms such as THF and acetonitrile delivered the epoxide in poor yields (entry 3 and 4). These solvents are presumably coordinating to the catalyst and preventing the coordination of aldehyde, and thus stopping the reaction. BINOL did not perform well in this reaction and gave the epoxide in 60% yield and only 4% *ee* (entry 5). The catalyst generated from 7,7'-*t*Bu<sub>2</sub>VANOL produced epoxide **II-113a** in higher *ee* compared with VANOL but in moderate yield (entry 1 vs 6). We were delighted to observe excellent yield and excellent *ee* while conducting the reaction with the catalyst derived from the VAPOL ligand **II-20** (entry 7). Ligand **II-115** also performed excellently and afforded the epoxide in 88% yield and 99% *ee* (entry 8).

**Table II-2.** Solvent and ligand optimization in aluminum VANOL/VAPOL catalyzed epoxidation reaction



entry	Ligand	Solvent	isolated yield%	ee%
1	<i>(S)</i> -VANOL, <b>II-19</b>	toluene	80	72
2	<i>(S)</i> -VANOL, <b>II-19</b>	DCM	80	72
3	<i>(S)</i> -VANOL, <b>II-19</b>	THF	46	84
4	<i>(S)</i> -VANOL, <b>II-19</b>	MeCN	6 <sup>1</sup>	<i>N.D.</i>
5	<i>(S)</i> -BINOL, <b>II-7</b>	toluene	60	4
6	<i>(S)</i> -7,7' <i>t</i> Bu <sub>2</sub> VANOL, <b>II-114</b>	toluene	46	84
7	<i>(S)</i> -VAPOL, <b>II-20</b>	toluene	81	98
8	<i>(S)</i> -Ligand, <b>II-115</b>	toluene	88	99

Unless otherwise specified, all of the reactions were done in toluene at 0 °C for 12 h with 0.5 mmol of diazo compound **II-112** and 0.6 mmol of aldehyde.  
1. NMR yield

Decreasing the catalyst loading to 5 mol% produced similar results (table II-3, entry 1 vs 2). With 2.5 mol% catalyst loading, the reaction worked fine albeit with a slight deterioration in *ee* and yield (entry 3). However, conducting the reaction with 1 mol% catalyst loading resulted in only 30% NMR yield (entry 4).

**Table II-3.** Study of catalyst loading and diazo compound

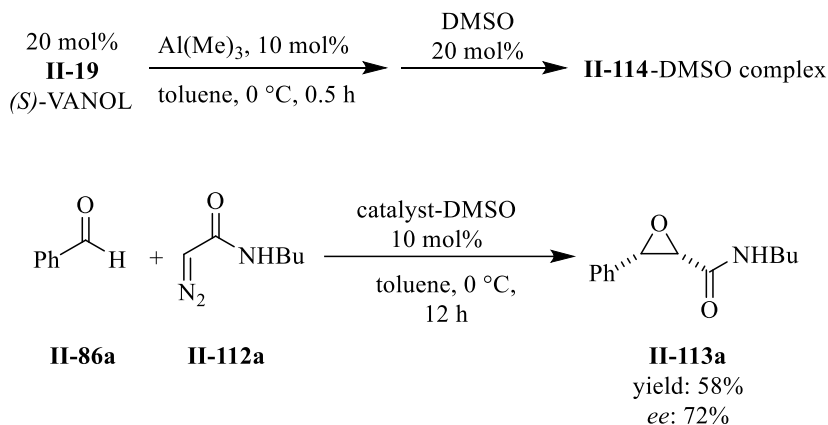
$  \begin{array}{c}  2X \text{ mol\%} \\  \text{II-20} \\  (S)\text{-VAPOL}  \end{array}  \xrightarrow[\text{toluene, } 0^\circ\text{C, } 0.5 \text{ h}]{\text{Al(Me)}_3, X \text{ mol\%}}  \begin{array}{c}  \text{II-116} \\  \text{catalyst}  \end{array}  $				
$  \begin{array}{c}  \text{Ph}-\text{CHO} + \text{CH}_2=\text{N}_2-\text{C(=O)R} \\  \text{II-86a} \quad \quad \text{II-112}  \end{array}  \xrightarrow[\text{toluene, } 0^\circ\text{C, } 12 \text{ h}]{\text{catalyst } X \text{ mol\%}}  \begin{array}{c}  \text{Ph}-\text{CH}(\text{O})-\text{CH}_2-\text{C(=O)R} \\  \text{II-113}  \end{array}  $				
entry	R	cat. loading%	Isolated yield%	ee%
1	II-112a, NHBu	10	81	98
2	II-112a, NHBu	5	86	97
3	II-112a, NHBu	2.5	61	95
4 <sup>1</sup>	II-112a, NHBu	1	30 <sup>2</sup>	<i>not determined</i>
6 <sup>3</sup>	II-112b, NHBn	5	84	99
7 <sup>3</sup>	II-112c, NHPH	5	59	99
8 <sup>3</sup>	II-112d, OEt	5	<i>not determined</i>	<i>not determined</i>

Unless otherwise specified, all of the reactions were done in toluene at 0 °C for 12 h with 0.5 mmol of diazo compound **II-112** and 0.6 mmol of aldehyde. 1. The reaction was quenched after 21 h. 2. NMR yield. 3. The reaction was quenched after 3 h

Different diazo compounds were also evaluated during the course of epoxidation and it turned out that the N-benzyl diazo acetamide **II-112b** is the optimum reagent (entry 6). The reaction with N-phenyl diazo acetamide **II-112c** produced epoxide with high enantioinduction but with lower yield presumably because of its poor solubility in toluene (table II-3, entry 7). In contrast, no product was detected when the reaction was carried out with ethyl diazo acetate **II-112d** instead the alkylated VAPOL ligand was observed in the crude mixture of the reaction.

Previously, we have demonstrated that DMSO had a profound effect on the epoxidation of aldehydes with diazo acetamides. The effect of DMSO was also examined in epoxidation reaction catalyzed by aluminum catalyst (scheme II-27). The reaction was conducted in the presence of 10 mol% DMSO, interestingly, no change in the *ee* of the epoxide was observed although a slight decrease in yield was observed (scheme II-27, vs table 2 entry 1).

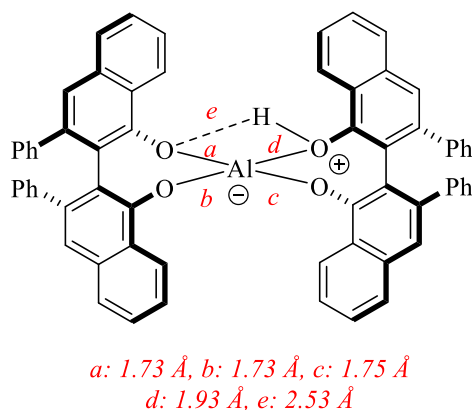
**Scheme II-27.** Epoxidation reaction catalyzed by aluminum-VANOL-DMSO complex



The exact structure of the active catalyst is not known yet. However, we assume that the active catalyst is formed from two molecules of VANOL ligand and one molecule of aluminum. The VANOL-aluminum catalyst with the structure **II-114** was investigated computationally and the optimized structure revealed a tetrahedral aluminum species (scheme II-28). Three oxygens of two VANOL ligands are bound to the aluminum with 1.73, 1.73, and 1.75 Å. The fourth oxygen

bearing a hydrogen is coordinated to the aluminum with a 1.93 Å bond length. This structure also demonstrates a weak intramolecular hydrogen bond with a distance of 2.53 Å.

**Scheme II-28.** Structure of **II-114**, aluminum-VANOL catalyst



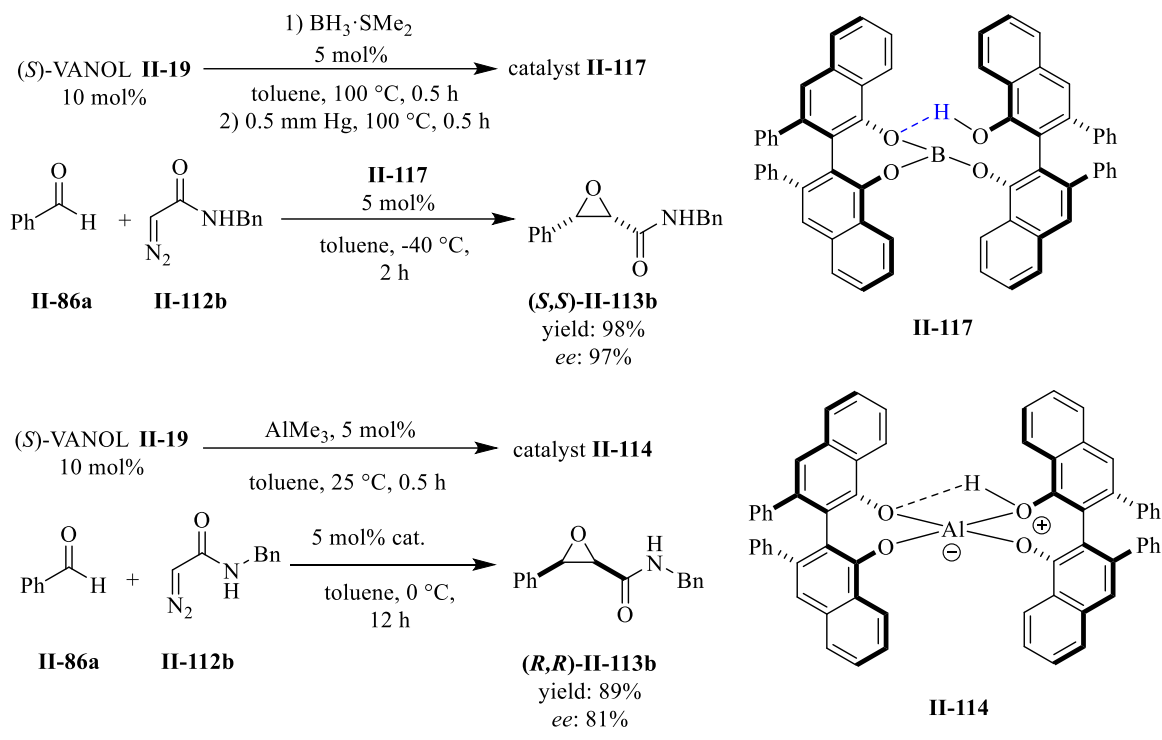
The most interesting feature of aluminum VANOL catalyst **II-114** is the reversal in enantioselectivity compared with boron VANOL catalyst **II-117** (scheme II-29). Specifically, benzaldehyde **II-86a** undergoes epoxidation in presence of boron-(*S*)-VANOL catalyst **II-117** to give the (2*S*, 3*S*)-*N*-benzyl-3-phenyloxirane-2-carboxamide **II-113b**; whereas, the same reaction catalyzed with aluminum-(*S*)-VANOL catalyst **II-114** produces (2*R*, 3*R*)-*N*-benzyl-3-phenyloxirane-2-carboxamide **II-113b**. The nature of the reversal of enantioselectivity is not known at this time.

### 2.2.2. Epoxidation of aromatic aldehydes catalyzed by aluminum-VAPOL catalyst.

To evaluate the substrate scope of the epoxidation reaction catalyzed by aluminum-VAPOL catalyst **II-114**, first we centered our attention on aromatic substrates. The reaction of benzaldehyde **II-86a** with *N*-butyl diazo acetamide **II-112a** yielded the epoxide **II-113a** in 80% yield and 72% *ee*. Increasing the catalyst loading to 10 mol% did not improve the *ee* of the reaction any further and similar results were obtained. To our delight, conducting the epoxidation reaction with *N*-benzyl diazo acetamide **II-112b** in place of *N*-butyl diazo acetamide **II-112a**, improved

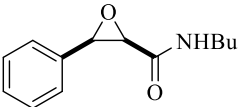
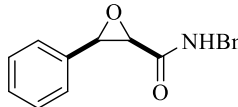
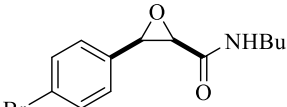
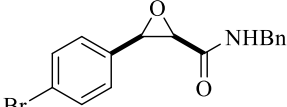
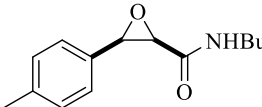
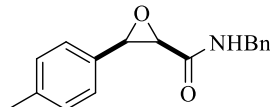
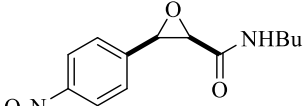
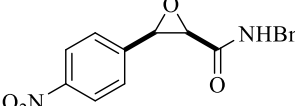
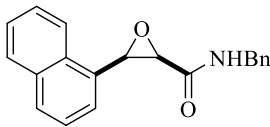
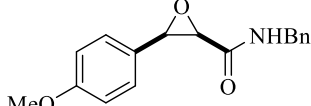


**Scheme II-29.** Enantioinduction reversal in epoxidation reaction catalyzed with boron and aluminum catalysts



the *ee* of the reaction to 81%. VAPOL **II-20** proved to be more efficient in this reaction than the VANOL **II-19** and produced epoxide **II-113b** in excellent yield and *ee* (84% yield, 99% *ee*). The reaction of 4-bromo-benzaldehyde with N-butyl diazo acetamide **II-112a** gave epoxide **II-118a** in 77% yield and 85% *ee*. The same reaction with N-benzyl diazoacetamide **II-112b** improved the *ee* to 99% *ee*. The same effect was observed in the epoxidation of para-tolualdehyde with N-butyl and N-benzyl diazo acetamides. N-butyl diazo acetamide **II-112a** gave the epoxide **II-119a** in 66% yield and 93% *ee*; whereas, the same reaction with N-benzyl diazo acetamide **II-112b** afforded the epoxide **II-119b** in 73% yield and 99% *ee*. Moderate *ee* was obtained in the epoxidation of 4-nitrobenzaldehyde with 5 mol% catalyst loading for both diazo acetamide **II-112a** and **II-112b**. We were pleased to observe a significant increase in *ee* with 10 mol% catalyst loading for this substrate from diazo acetamide **II-112b**.

**Table II-4.** Scope of aromatic substrates

$  \begin{array}{c}  2X \text{ mol\%} \\  (S)\text{-Ligand}  \end{array}  \xrightarrow[\text{toluene, 25 } ^\circ\text{C, 0.5 h}]{\begin{array}{c} 1) \text{ AlMe}_3, X \text{ mol\%} \\ (S)\text{-catalyst} \end{array}}  $		
$  \begin{array}{c}  \text{R}'\text{-CHO} + \text{II-112} \\  \text{N}_2 \\  \text{H}  \end{array}  \xrightarrow[\text{toluene, 0 } ^\circ\text{C, 12 h}]{X \text{ mol\% } (S)\text{-cat.}}  $		
 <p><b>II-113a</b>  <i>(S)</i>-VANOL, 5 mol% Cat.  yield: 80%, ee: 72%  <i>(S)</i>-VANOL, 10 mol% Cat.  yield: 81%, ee: 72%  <i>(S)</i>-VAPOL, 5 mol% Cat.  yield: 86%, ee: 97%  <i>(S)</i>-VAPOL, 10 mol% Cat.  yield: 81%, ee: 98%</p>	 <p><b>II-113b</b>  <i>(S)</i>-VANOL, 10 mol% Cat.  yield: 89%, ee: 81%  <i>(S)</i>-VAPOL, 5 mol% Cat.  yield: 97%, ee: 99%  <i>(R)</i>-VAPOL, 5 mol% Cat.<sup>1</sup>  yield: 72%, ee: -99%  <i>(S)</i>-VAPOL, 10 mol% Cat.  yield: 84%, ee: 99%</p>	 <p><b>II-118a</b>  <i>(S)</i>-VAPOL, 5 mol% Cat.  yield: 77%, ee: 85%</p>
 <p><b>II-118b</b>  <i>(S)</i>-VAPOL, 5 mol% Cat.  yield: 90%, ee: 99%  <i>(R)</i>-VAPOL, 5 mol% Cat.<sup>1</sup>  yield: 79%, ee: -98%</p>	 <p><b>II-119a</b>  <i>(S)</i>-VAPOL, 5 mol% Cat.  yield: 66%, ee: 93%</p>	 <p><b>II-119b</b>  <i>(S)</i>-VAPOL, 5 mol% Cat.  yield: 76%, ee: 99%  <i>(R)</i>-VAPOL, 10 mol% Cat.<sup>1</sup>  yield: 73%, ee: -99%</p>
 <p><b>II-120a</b>  <i>(S)</i>-VAPOL, 5 mol% Cat.  yield: 36%, ee: 71%</p>	 <p><b>II-120b</b>  <i>(S)</i>-VAPOL, 5 mol% Cat.  yield: 55%, ee: 62%  <i>(R)</i>-VAPOL, 10 mol% Cat.<sup>1</sup>  yield: 70%, ee: -93%</p>	 <p><b>II-121b</b>  <i>(S)</i>-VAPOL, 5 mol% Cat.  yield: 93%, ee: 99%  <i>(R)</i>-VAPOL, 10 mol% Cat.<sup>1</sup>  yield: 74%, ee: -99%</p>
	 <p><b>II-122b</b>  <i>(S)</i>-VAPOL, 10 mol% Cat.  yield: 10% (NMR), ee: not determined</p>	

1. enantiomer of the epoxide was obtained

1-Naphthaldehyde as the substrate also performed well under the optimum reaction conditions and produced epoxide **II-121b** in excellent yield and enantioselectivity. Unfortunately, the epoxidation of 4-methoxybenzaldehyde resulted in a very sluggish reaction and the desired product **II-122b** was observed in only 10% NMR yield.

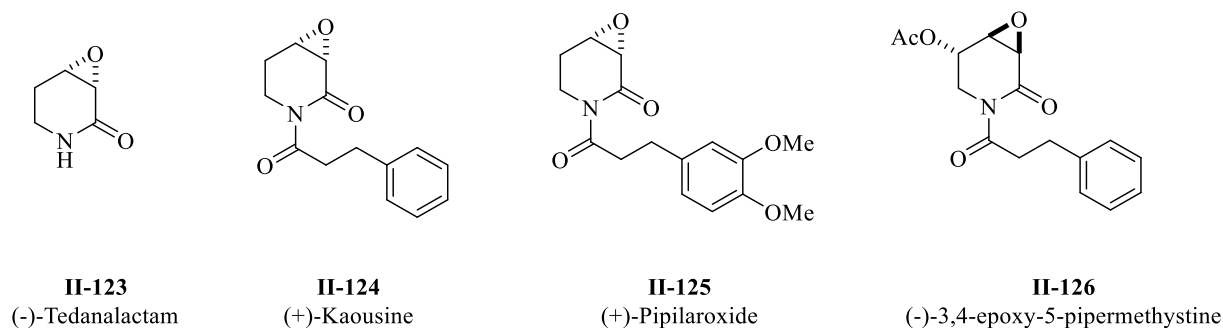
### 2.2.3. Epoxidation of aliphatic aldehydes and the total synthesis of (–)-tedanalactam

#### 2.2.3.1. Introduction: A summary of all previous synthesis of (–)-tedanalactam

One of our goals in the epoxidation project was to apply this methodology to the synthesis piperidine alkaloids from the kava shrub (piper methysticum G). This shrub is the main ingredient of traditional beverages of the south pacific islanders. Due to its relaxing anti-anxiety effect, it has become popular as a dietary supplement in Europe and thus an important agricultural product. Recent studies are raising concerns about its possible damage to the liver. Lactones are the main components of this shrub; however, recently there has been interest in piperidine alkaloids from this plant including the four compounds which are shown in scheme II-30.<sup>20,21</sup>

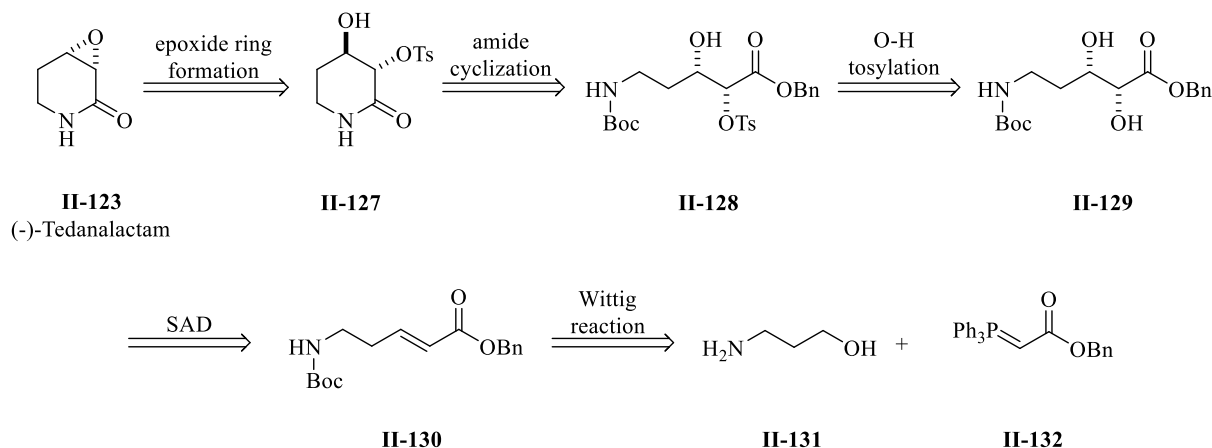
The (–)-tedanalactam **II-123** and its derivatives have been the subject of total synthesis four times in literature. The first total synthesis of this compound was reported in 2009 by Tilve.<sup>22</sup> Retrosynthesis analysis for the Tilve synthesis is depicted in scheme II-31. It was envisioned that

**Scheme II-30.** Piperidine alkaloides in kava shrub



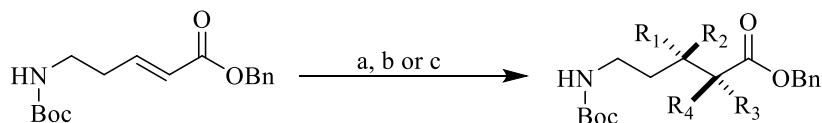
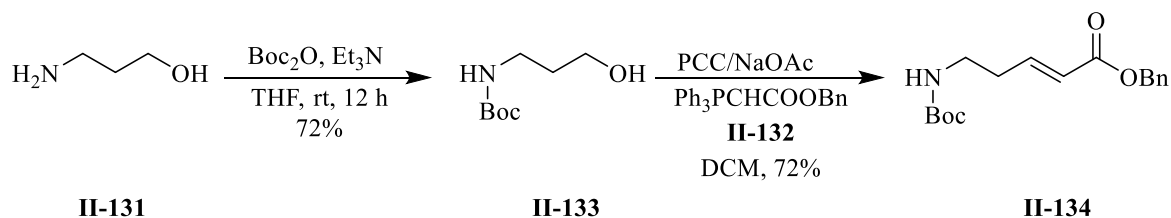
the (–)-Tedanalactam **II-123** could be synthesized from compound **II-131** via sequential Wittig reaction, asymmetric Sharpless dihydroxylation, lactonization, and oxirane ring formation.

**Scheme II-31.** Retrosynthesis analysis of (–)-tedanalactam **II-123** by Tilve <sup>22</sup>



The Tilve synthesis of (–)-tedanalactam **II-123** commenced with N-Boc protection of 3-amino-1-propanol **II-131** followed by subsequent PCC oxidation produced the desired aldehyde. Reacting the resulting aldehyde with phosphorane **II-132** afforded the *E*-alkene **II-134** in 52% overall 3 steps. The *racemic* diol **II-135** and both enantiomers of diol **II-135** were synthesized via the Upjohn dihydroxylation procedure or the asymmetric Sharpless dihydroxylation (scheme II-32). Selective tosylation of diol **II-135a** gave compound **II-136** which was converted to the desired lactam **II-127** via amine deprotection and subsequent cyclization. Finally, both *racemic* and enantiopure tedanalactam were produced by treating lactam **II-127** with liquid ammonia which resulted in epoxide ring formation in 51% yield overall 3 steps. This report presented an efficient synthesis of (–)-tedanalactam **II-123** in 7 steps with 26% overall yield starting from commercially available 3-amino-1-propanol.

**Scheme II-32.** Total synthesis of (-)-tedanalactam<sup>22</sup>

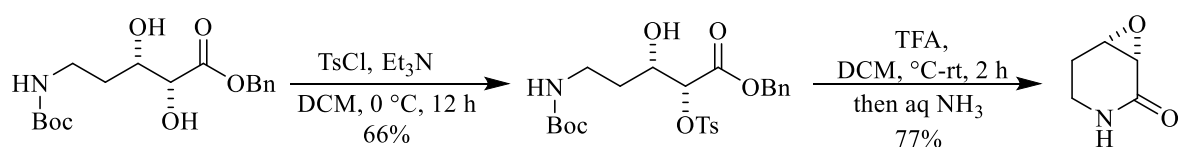


**II-134**

**II-135a:**  $R_1 = R_3 = \text{OH}, R_2 = R_4 = \text{H},$

**II-135b:**  $R_1 = R_3 = \text{H}, R_2 = R_4 = \text{OH},$

Reaction condition	yield	ratio a:b
a) $\text{OsO}_4/\text{NMO}/\text{no catalyst}$	83%	1:1
b) AD-mix a: $(\text{DHQ})_2\text{-PHAL}$	77%	95.5:4.5
c) AD-mix b: $(\text{DHQD})_2\text{-PHAL}$	71%	3:97



**II-135a**

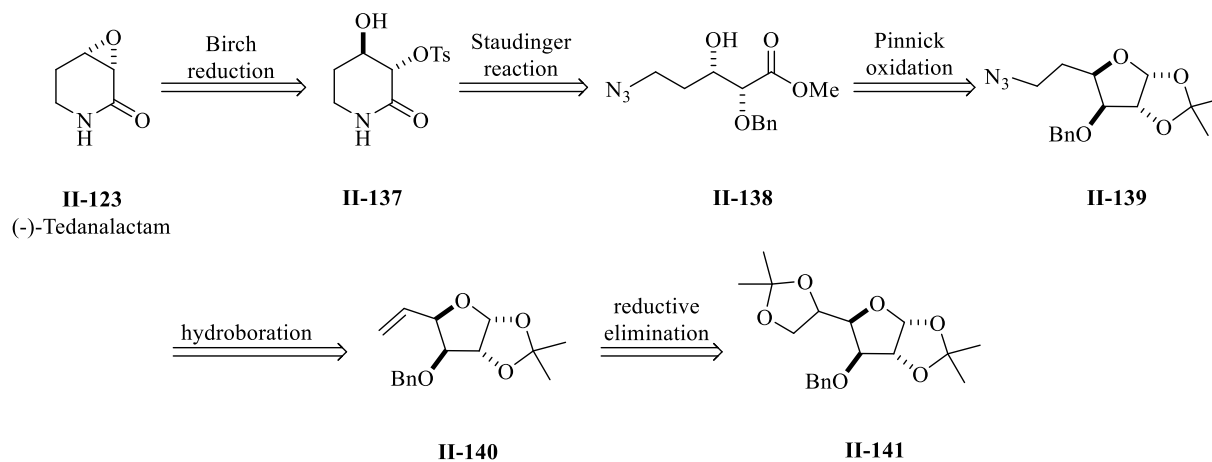
**II-136**

**II-123**

(-)-Tedanalactam

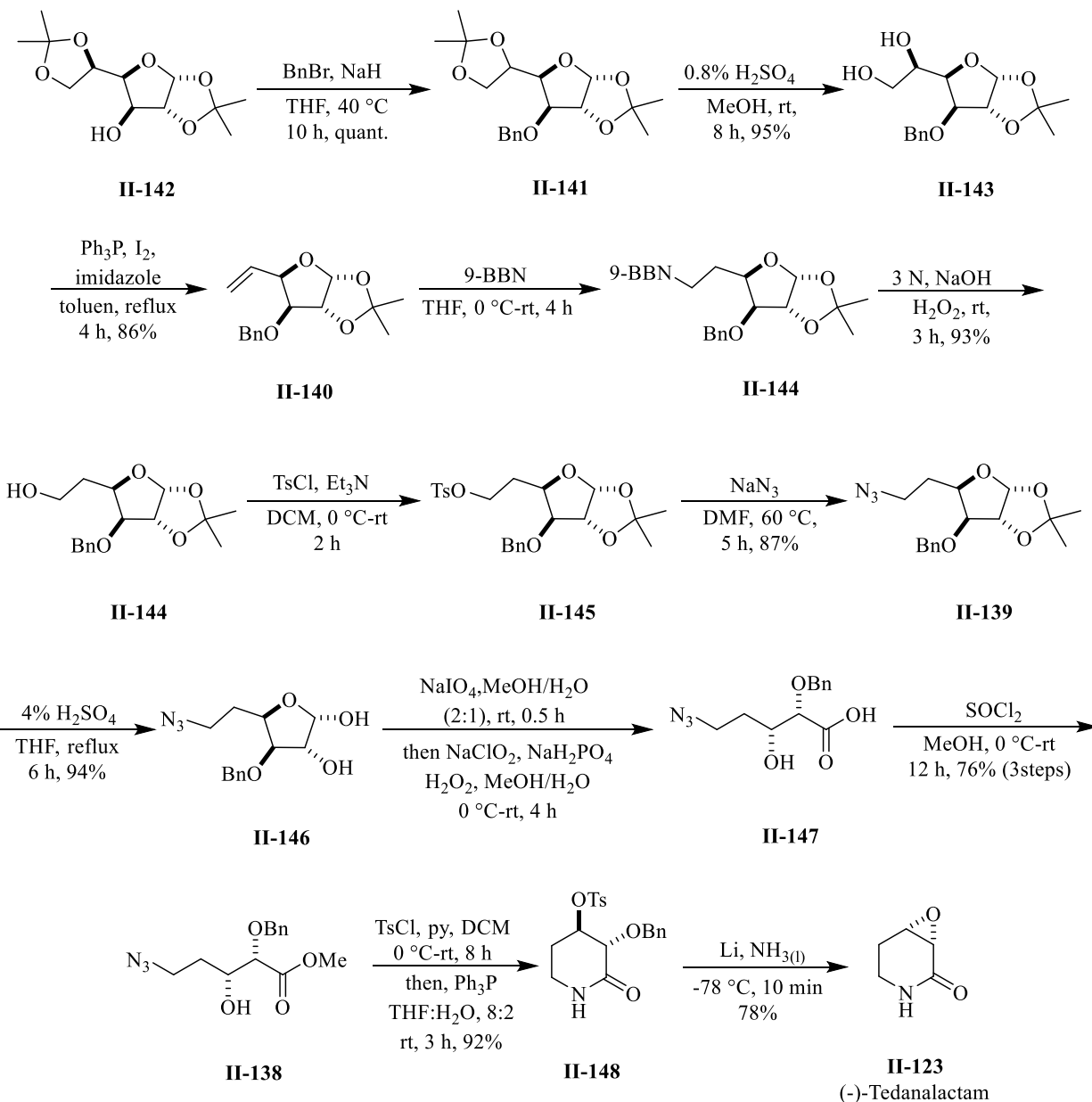
In 2015, Nagarapu reported the total synthesis of (-)-tedanalactam **II-123** in 13 steps starting with acetone-D-glucose **II-141**.<sup>23</sup> As illustrated in the retrosynthetic analysis in scheme II-33, (-)-tedanalactam **II-123** was proposed to be accessible from compound **II-138** via Birch reduction and a Staudinger reaction. Starting with acetone-D-glucose **II-141**, the synthesis of compound **II-138** would be possible via reductive deoxygenation of a diol, hydroboration and Kraus-Pinnick oxidation.

**Scheme II-33.** Retrosynthesis of (-)-tedanalactam by Nagarapu<sup>23</sup>



The benzylation of acetonide-D-glucose **II-142** initiated the total synthesis of (-)-tedanalactam **II-123** and gave compound **II-141** in quantitative yield (scheme II-34). Selective deprotection of one of the acetonide followed by reduction of the resulting diol produced alkene **II-140** in 82% yield overall two steps. Alkene **II-140** underwent hydroboration and oxidation which generated the primary alcohol **II-144** in 93% yield. The alcohol **II-144** was converted to the azide **II-139** via tosylation and azidation in 87% yield for the 2 steps. Acetonide deprotection, oxidative cleavage of the diol and Kraus-Pinnick oxidation afforded carboxylic acid **II-147** which was taken to the next step without further purification. Carboxylic acid **II-147** was converted to methyl ester **II-138** in 71% yield overall for 4 steps. Tosylation followed by Staudinger reduction gave a primary amine which underwent spontaneous cyclization and afforded lactam **II-148**. The yield for these two steps was determined to be 92%. Finally, the synthesis of (-)-tedanalactam **II-123** was accomplished by deprotection of benzyl alcohol **II-148** followed by the epoxide ring formation in 78% yield. In this report, enantiopure (-)-tedanalactam **II-123** was synthesized in 13 steps with 28.5% overall yield.

**Scheme II-34.** Total synthesis of (-)-tedanalactam by Nagarapu<sup>23</sup>



Sartillo-Piscil reported a short and efficient synthesis of (-)-tedanalactam **II-123** and piplaroxide **II-155** in 2016 (scheme II-36).<sup>24</sup> Lactam **II-123** was unraveled to chiral (*S*)-(-)-4-methoxy- $\alpha$ -methylbenzylamine **II-149**. Ring closing metathesis and allylamine oxidation to glycidicin in presence of NaOCl<sub>2</sub> were the key reactions in this synthesis.<sup>25</sup> In spite of the efficiency of this





intermediate (+/-)-**II-157** was synthesized in 77% yield. The total synthesis was carried out by partial reduction of nitrile **II-157** to aldehyde **II-158** followed by reductive amination with amine **II-149** to give the 2° amine **II-159** in 67% yield. N-allylation, acidification and subsequent RCM catalyzed by 2<sup>nd</sup> generation Hoveyda-Grubbs catalyst afforded a 1:1 diastereomeric mixture of compound **II-161** which were separated by column chromatography. Each diastereomer of **II-161** was subjected to the C-H oxidation and substrate-controlled epoxidation of the double bond mediated by NaClO<sub>2</sub>. This substrate-controlled strategy performed well and the product **II-162** was isolated as a single diastereomer. TBS deprotection with TBAF produced compound **II-163** and the structure and absolute stereochemistry of this intermediate was determined unequivocally via x-ray structural analysis. Finally, the total synthesis 3 $\alpha$ , 4 $\alpha$ -epoxy-5 $\beta$ -pipermethystine **II-165** was accomplished via a number of transformation including *O*-acylation of hydroxyl group, CAN mediated deprotection of compound **II-164** and *N*-acylation in 34% yield overall in three steps.

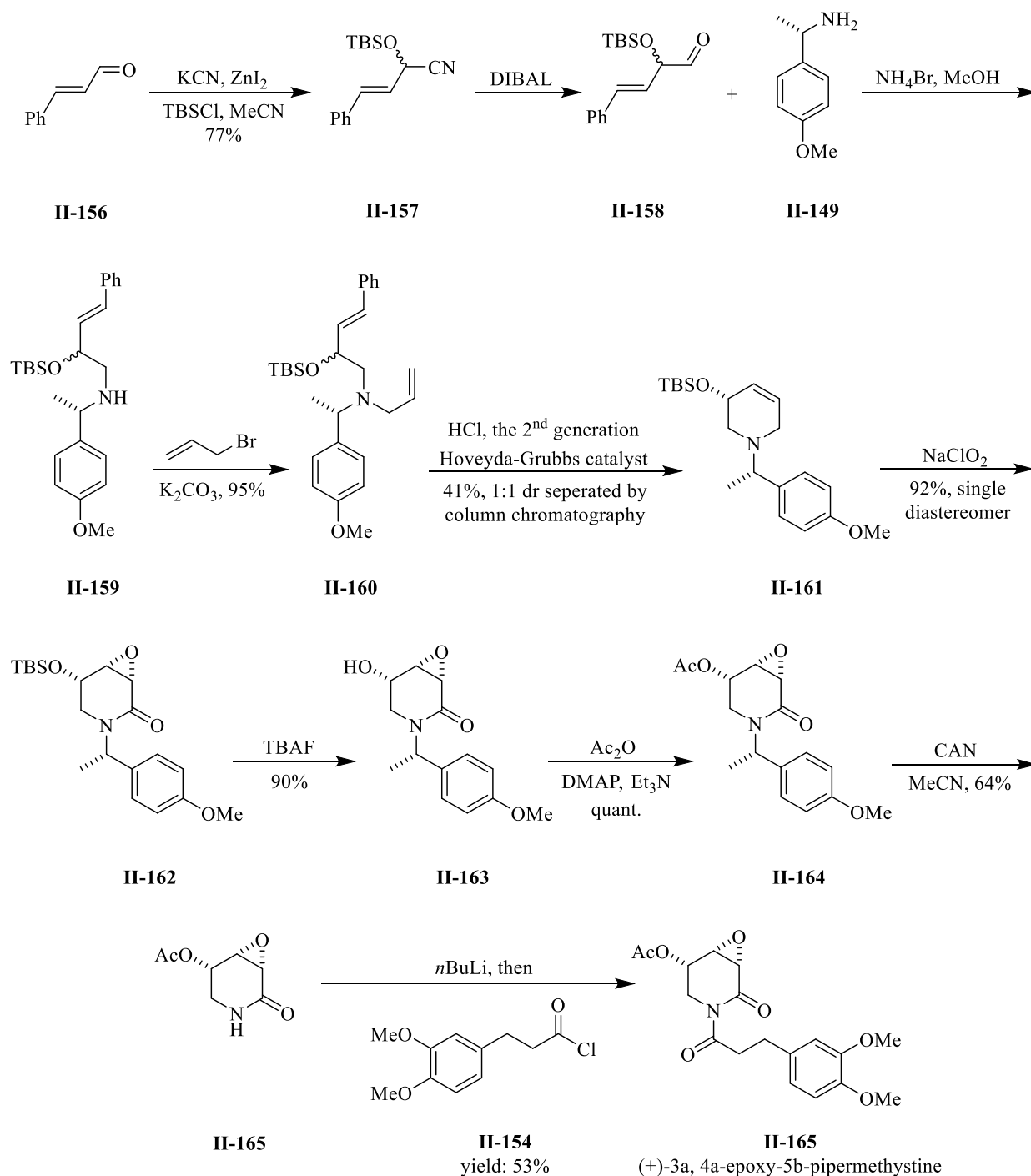
#### 2.2.3.2. Aluminum catalyzed epoxidation of aliphatic aldehydes

Our interest in the total synthesis of (-)-tedanalactam **II-123** led us to evaluate the epoxidation of aliphatic aldehyde **II-167** bearing leaving group in carbon 3. It was envisioned that the asymmetric catalytic epoxidation of aldehyde **II-167**, followed by amide cyclization and deprotection would produce (-)-tedanalactam **II-123** in 3 steps.

Previously, we have been reported the boron-VANOL-DMSO **II-117**-DMSO catalyst as an extremely active catalyst in the epoxidation of aldehydes with diazo acetamide.<sup>19</sup> For example, this catalyst catalyzed the reaction of butanal **II-166** with *N*-benzyl diazo acetamide **II-112b** and gave the epoxide **II-170** in 99% yield and 99% *ee* (table II-5, entry 1). However, after conducting the epoxidation with 3-bromo-propanal **II-167** under the standard reaction conditions, no desired epoxide **II-171** was detected in the NMR spectrum of the crude reaction mixture. Careful analysis

of the crude NMR spectrum suggested that the alkylation of VANOL was the major side product. Presumably, the aldehyde **II-167** reacted with VANOL ligand first due to its higher reactivity.

**Scheme II-36.** Total synthesis of natural product II-165 presented by Sartillo-Piscil



**Table II-5.** Epoxidation of aldehyde II-166 to II-69

<div style="display: flex; align-items: center; justify-content: space-around;"> <div style="text-align: center;"> <math>\text{R-CH}_2\text{-CH}_2\text{-CHO}</math>  <b>II-166</b>, R: Me  <b>II-167</b>, R: Br  <b>II-168</b>, R: OTBS  <b>II-169</b>, R: OTBDPS         </div> <div style="text-align: center;"> <math>\text{N}_2\text{C(=O)NHR'}</math>  <b>II-112b</b>, R': Bn  <b>II-112e</b>, R': PMB         </div> <div style="text-align: center;"> <math>\text{R-CH}_2\text{-CH}_2\text{-CH(CHO)-CH}_2\text{-C(=O)NHR'}</math>  <b>II-170</b>, R: Me, R': Bn  <b>II-171</b>, R: Br, R': Bn  <b>II-172</b>, R: OTBS, R': Bn,  <b>II-173</b>, R: OTBS, R': PMB  <b>II-174</b>, R: OTBDPS, R': PMB         </div> </div> <p style="text-align: center;">             1) <math>\text{BH}_3\cdot\text{SMe}_2</math> (X mol%), 2) 0.5 mm Hg, 100 °C, 0.5 h              DMSO (2X mol%), (S)-VANOL (2X mol%)              Toluene, 100 °C, 0.5 h              Toluene, T/ °C, time/ h           </p>										
entry	R	R'	Cat. (X mol%)	DMSO (X mol%)	T/°C	t/h	Conv. <sup>1</sup>	Epoxide (NMR yield) <sup>1</sup>	ee	β-ketoamide
1	CH <sub>3</sub>	Bn	5	20	-40	12	99	99	99	0
2	Br	Bn	5	20	-40	12	65	<1 <sup>1</sup>	N.D.	N.D.
3	OTBS	Bn	5	0	-40	12	15	<12 <sup>1</sup>	N.D.	N.D.
4	OTBS	Bn	5	20	-40	12	10	<5 <sup>1</sup>	N.D.	N.D.
5	OTBS	PMB	5	0	-40	12	9	<5 <sup>1</sup>	N.D.	N.D.
6	OTBS	PMB	10	20	0	12	16	11 <sup>1</sup>	N.D.	N.D.
7	OTBS	PMB	10	20	-40	12	9	<5 <sup>1</sup>	N. D.	N. D.
8	OTBS	PMB	20	40	-40	12	72	51	65	17
9	OTBS	PMB	20	40	0	12	99	47	66	34
10	OTBS	PMB	20	0	0	12	99	70	56	28
11 <sup>2</sup>	OTBS	PMB	10	0	0	12	21	19	N. D.	-
12	OTBDS	PMB	10	20	0	12	87	44	50	24
13	OTBDS	PMB	20	0	0	12	99	65	52	34

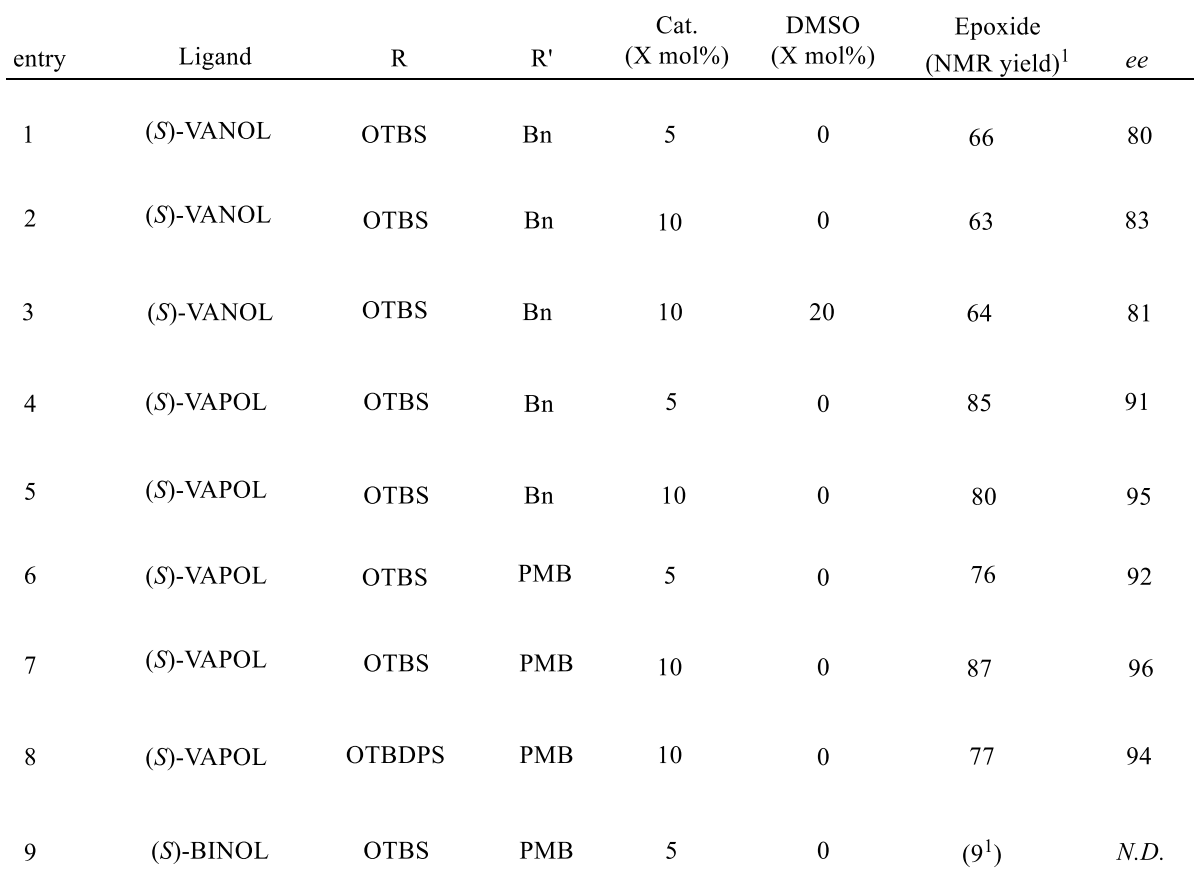
Unless otherwise specified, all of the reactions were done in toluene at 0 °C for 12 h with 0.5 mmol of diazo compound **II-112** and 0.6 mmol of aldehyde. 1. Conversions and yields in parenthesis are determined by NMR using Ph<sub>3</sub>CH as internal standard, 2. The reaction was done with VAPOL as ligand

In order to overcome this obstacle, 3-*tert*-butyl-dimethylsilyloxypropanal **II-168** was used in place of aldehyde **II-167**. Conducting the epoxidation reaction with aldehyde **II-168** and *N*-benzyl diazoacetamide **II-112b** produced the desired epoxide **II-172** in 12% NMR yield (entry 3).

The same catalyst in the presence of 10 mol% DMSO did not performed well and only trace amounts of epoxide **II-172** was detected (entry 4). Changing the protecting group on the diazoacetamide from *N*-benzyl to *N*-paramethoxybenzyl (PMB) **II-112e** did not improve the yield of the reaction (entries 5 vs 3). Poor results were also obtained when the catalyst loading was increased to 10 mol% (entry 6). Interestingly, by increasing the catalyst loading to 20 mol%, 99% conversion was observed but the epoxide **II-173** was produced in moderate yield (51%) and moderate *ee* (65%) and also a 17% yield of  $\beta$ -ketoamide was observed as a side product (entry 8). Increasing the temperature to 0 °C gave the epoxide in slightly lower yield (47%) with similar *ee* (66%) (entry 9). We were surprised to observe a higher yield for this reaction by leaving out the DMSO; however, a 10% decrease in the *ee* was observed (entry 10). The catalyst prepared from the VAPOL ligand produced only 19% yield (NMR) of the desired epoxide **II-173** (entry 11). Less unsatisfactory results were obtained by using TBDPS as the protecting group in place of TBS (entry 12 and 13).

Disappointed by the VANOL-boron catalyst **II-117** in epoxidation of substrate **II-168**, we turned our attention toward the aluminum-VANOL/VAPOL **II-114/II-116** catalysts (table II-6). To our delight, the aluminum catalyst **II-114** prepared from the (*S*)-VANOL ligand, catalyzed the epoxidation of aldehyde **II-168** with *N*-benzyl diazoacetamide **II-112b** and afforded the epoxide **II-172** in 66% yield and 80% *ee* (entry 1). The reaction gave a slight increase in *ee* when the catalyst loading was increased from 5 to 10 mol% (entry 2). Next, the effect of a catalytic amount of DMSO in this reaction was assessed. The catalyst **II-114** was prepared under standard

**Table II-6.** Epoxidation of aldehyde II-171 catalyzed by chiral aluminum complexes

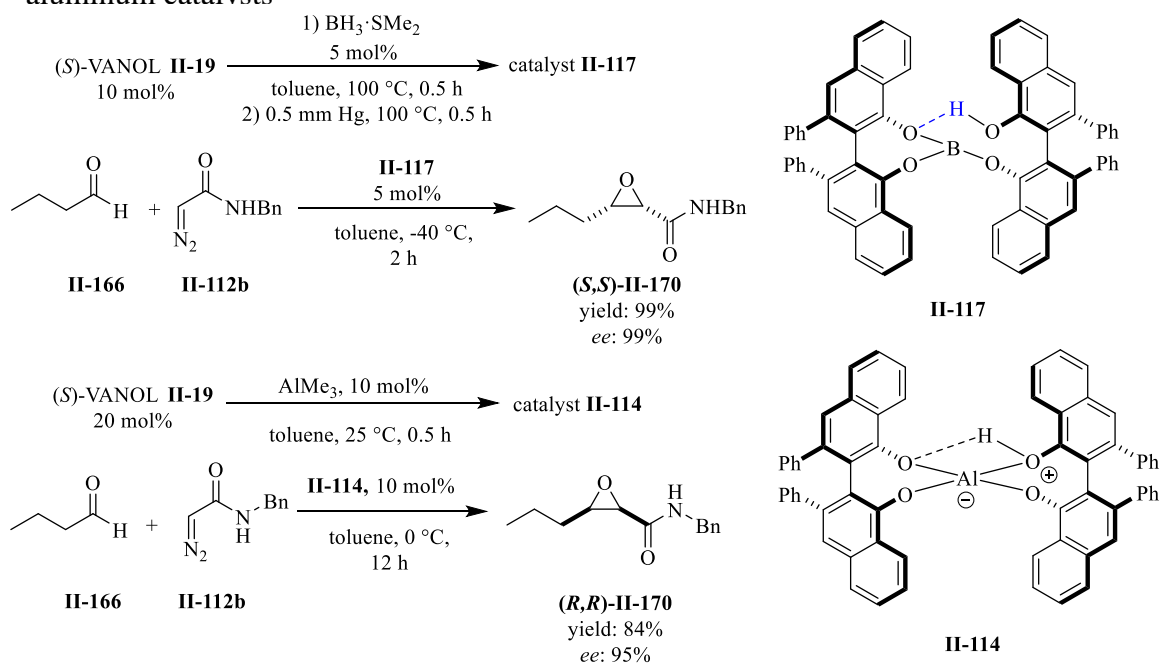


126

aluminum catalyst (entry 3). We were thrilled to observe excellent yield and *ee* by an aluminum catalyst prepared from (*S*)-VAPOL (entry 4). The use of diazo acetamide **II-112e** gave the epoxide **II-173** in similar fashion with the VAPOL catalyst (entry 6). The *ee* was increased to 96% in the latter case by increasing the catalyst loading to 10 mol% (entry 5). Similar results were obtained with *N*-para-methoxybenzyl diazo acetamide **II-112e** and and aldehyde with TBDPS **II-169** as the protecting group (entry 7 and 8). Very poor yield was obtained with the aluminum catalyst derived from (*S*)-BINOL ligand (entry 9).

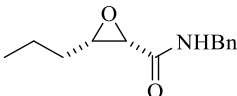
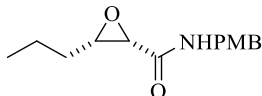
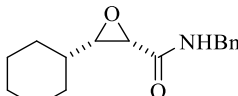
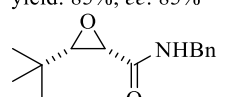
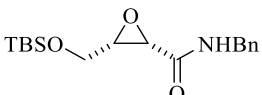



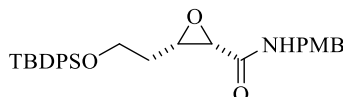
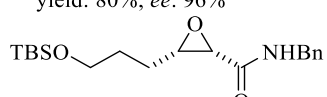
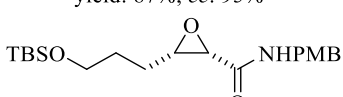
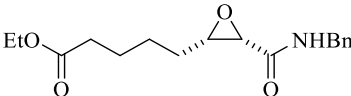
It is also worth to mention that the reversal in enantioinduction was also investigated with aliphatic aldehyde catalyzed by both aluminum VANOL catalyst **II-114** and boron VANOL catalyst **II-117**. Interestingly, aldehyde **II-166** undergoes epoxidation in presence of boron-(*S*)-VANOL catalyst **II-117** to give the (2*S*, 3*S*)-*N*-benzyl-3-propyloxirane-2-carboxamide **II-170**; whereas, the same reaction catalyzed with aluminum-(*S*)-VANOL catalyst **II-114** produces (2*R*,3*R*)-*N*-benzyl-3-propyloxirane-2-carboxamide **II-170** (scheme II-37).

**Scheme II-37.** Enantioinduction reversal in epoxidation reaction catalyzed with boron and aluminum catalysts



A range of aliphatic aldehydes were examined with the optimized epoxidation conditions given in table 6. Subjecting *n*-butanal to the standard epoxidation condition, yielded the desired product **II-170** in 62% yield and 89% *ee* with the VAPOL aluminum catalyst (table II-7). For this substrate it was found that the VANOL aluminum catalyst produced slightly higher *ee* than the VAPOL aluminum catalyst. Similar results were obtained by reacting *n*-butanal with *N*-*para*-methoxybenzyl diazo acetamide **II-112e** to give the epoxide **II-175**. With 10 mol% aluminum-VAPOL catalyst loading, cyclohexanecarboxaldehyde underwent smooth epoxidation to give **II-176** in 81% yield and 94% *ee* with 10 mol% catalyst loading. The same reaction with 5 mol% catalyst loading produced the epoxide **II-176** in 68% yield and 88% *ee*. Trimethylacetaldehyde performed poorly in the presence of 5 mol% of the VAPOL aluminum catalyst and produced the epoxide **II-177** in 15% yield. To our delight, 99% *ee* was obtained with 10 mol% catalyst loading. 2-*tert*-butyldimethylsilyloxyethanal gave epoxide **II-178** with moderate *ee* under optimum reaction conditions (56%). Unfortunately, the *ee* of this reaction could not be improved with either and increase to 10 mol% catalysts or the use of diazo acetamide **II-112e** to give epoxide **II-129**. The epoxidation of 4-*tert*-butyldimethylsilyloxybutanal with *N*-benzyl diazo acetamide and *N*-*para*-methoxybenzyl diazo acetamide produced epoxides **II-180** and **II-181** with moderate *ee* with 5 mol% of the aluminum-VAPOL catalyst. However, excellent enantioinduction was obtained by performing the reaction in the presence of 10 mol% catalyst. An ester moiety in the aldehyde was also tolerated under the optimum reaction conditions and produced epoxide **II-182** in 74% yield and 96% *ee*. Conducting the same reaction with boron-VANOL **II-117** catalyst afforded epoxide in 80% and 91% *ee* (see table II-7, foot note 2). The yield and *ee* were slightly improved when the reaction was performed in presence of the catalytic amount of DMSO (see table II-7, foot note 3).

**Table II-7.** Substrate scope of aliphatic aldehyde

$  \begin{array}{c}  \text{2X mol\%} \\  \text{(R)-Ligand}  \end{array}  \xrightarrow[\text{toluene, 25 } ^\circ\text{C, 0.5 h}]{\text{1) AlMe}_3, \text{X mol\%}}  \text{(R)-catalyst}  $		
$  \text{R}'\text{-CHO} + \text{N}_2\text{C(=O)NHR} \xrightarrow[\text{toluene, 0 } ^\circ\text{C, 12 h}]{\text{X mol\% (R)-cat.}} \text{R}'\text{-CH(O)-CH}_2\text{-C(=O)NHR}  $		
 <p><b>II-170</b>  <i>(R)</i>-VANOL, 5 mol% Cat.  yield: 74%, ee: 92%  <i>(S)</i>-VANOL, 10 mol% Cat.<sup>1</sup>  yield: 84%, ee: -95%  <i>(S)</i>-VAPOL, 5 mol% Cat.<sup>1</sup>  yield: 62%, ee: -89%  <i>(R)</i>-VAPOL, 5 mol% Cat.  yield: 85%, ee: 85%</p>	 <p><b>II-175</b>  <i>(S)</i>-VAPOL, 5 mol% Cat.<sup>1</sup>  yield: 50%, ee: -86%  <i>(R)</i>-VAPOL, 10 mol% Cat.  yield: 79%, ee: 94%</p>	 <p><b>II-176</b>  <i>(R)</i>-VAPOL, 5 mol% Cat.  yield: 69%, ee: 85%  <i>(S)</i>-VAPOL, 5 mol% Cat.<sup>1</sup>  yield: 68%, ee: -88%  <i>(R)</i>-VAPOL, 10 mol% Cat.  yield: 81%, ee: 94%</p>
 <p><b>II-177</b>  <i>(S)</i>-VAPOL, 5 mol% Cat.<sup>1</sup>  yield: 15% (NMR), ee: <i>N.D.</i>  <i>(R)</i>-VAPOL, 10 mol% Cat.  yield: 50%, ee: 99%</p>	 <p><b>II-178</b>  <i>(S)</i>-VAPOL, 5 mol% Cat.<sup>1</sup>  yield: 78%, ee: -56%  <i>(R)</i>-VAPOL, 10 mol% Cat.  yield: 73%, ee: 58%</p>	 <p><b>II-179</b>  <i>(S)</i>-VAPOL, 5 mol% Cat.<sup>1</sup>  yield: 73%, ee: -50%  <i>(R)</i>-VAPOL, 10 mol% Cat.  yield: 86%, ee: 54%</p>
 <p><b>II-172</b>  <i>(S)</i>-VANOL, 5 mol% Cat.<sup>1</sup>  yield: 66%, ee: -80%  <i>(S)</i>-VAPOL, 5 mol% Cat.<sup>1</sup>  yield: 85%, ee: -91%  <i>(R)</i>-VAPOL, 10 mol% Cat.  yield: 80%, ee: 96%</p>	 <p><b>II-173</b>  <i>(S)</i>-VANOL, 5 mol% Cat.<sup>1</sup>  yield: 63%, ee: -83%  <i>(S)</i>-VAPOL, 5 mol% Cat.<sup>1</sup>  yield: 76%, ee: -92%  <i>(R)</i>-VAPOL, 10 mol% Cat.  yield: 87%, ee: 95%</p>	 <p><b>II-174</b>  <i>(S)</i>-VAPOL, 10 mol% Cat.<sup>1</sup>  yield: 77%, ee: -94%</p>
 <p><b>II-180</b>  <i>(S)</i>-VAPOL, 5 mol% Cat.<sup>1</sup>  yield: 84%, ee: -50%  <i>(R)</i>-VAPOL, 10 mol% Cat.  yield: 88%, ee: 92%</p>	 <p><b>II-181</b>  <i>(S)</i>-VAPOL, 5 mol% Cat.<sup>1</sup>  yield: 67%, ee: -51%  <i>(R)</i>-VAPOL, 10 mol% Cat.  yield: 78%, ee: 88%</p>	 <p><b>II-182</b>  <i>(S)</i>-VAPOL, 5 mol% Cat.<sup>1</sup>  yield: 75%, ee: -76%  <i>(R)</i>-VAPOL, 10 mol% Cat.  yield: 74%, ee: 96%  <i>(R)</i>-VANOL, 10 mol% Cat.<sup>2</sup>  yield: 80%, ee: 91%  <i>(R)</i>-VAPOL, 10 mol% Cat.<sup>3</sup>  yield: 99%, ee: 95%</p>

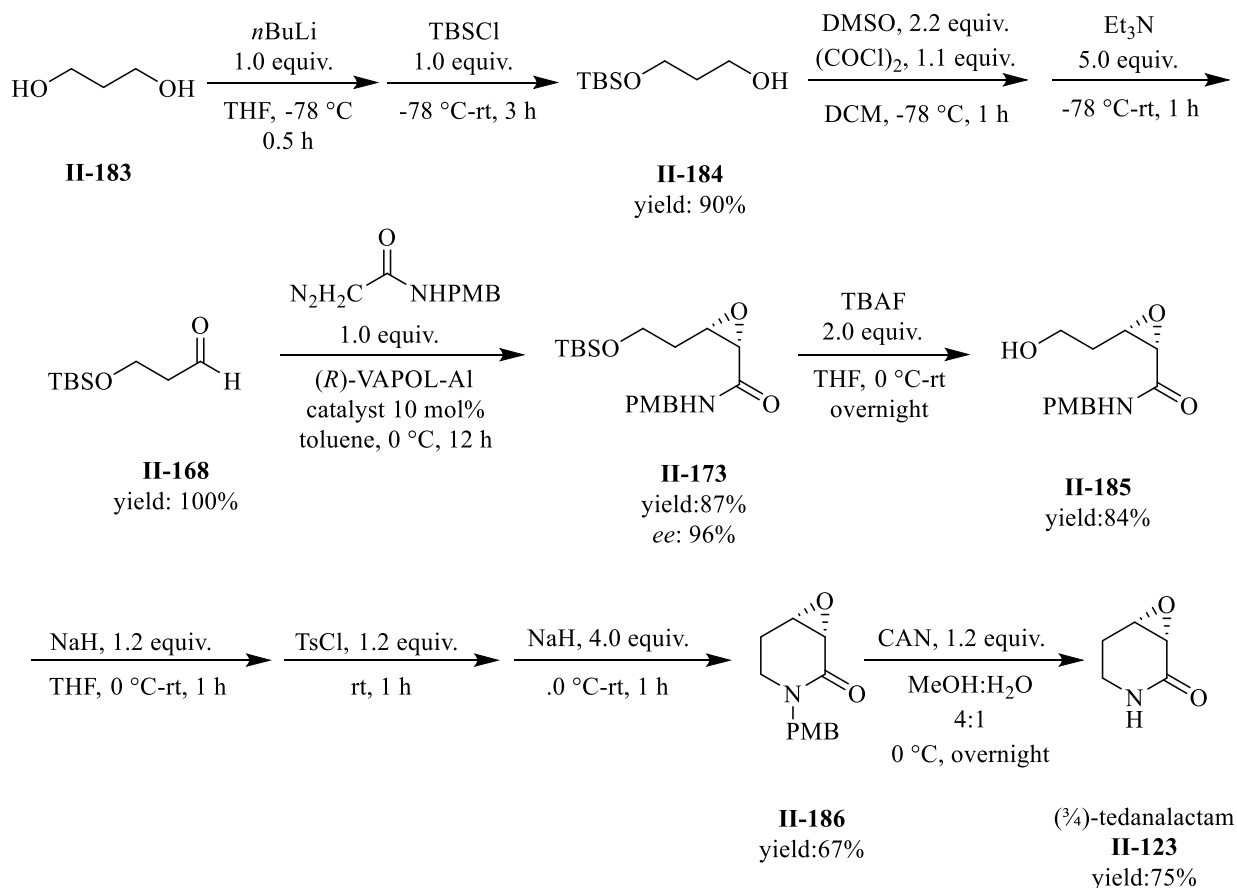
Unless otherwise specified, all of the reactions were done in toluene at 0 °C for 12 h with 0.5 mmol of diazo compound **II-112** and 0.6 mmol of aldehyde. 1. enantiomer of the epoxide was produced. 2. Boron-VANOL catalyst was used. 3. Boron-VANOL-DMSO catalyst was used



### 2.2.3.3. Total synthesis of (–)-tedanalactam

Total synthesis of (–)-tedanalactam **II-123** starts with a two step synthesis of 3-*tert*-butyldimethylsilyloxypropanal **II-168** (scheme II-38). This aldehyde was commercially available but due to its expensiveness and low quality, we decided to prepare it fresh. 3-*tert*-butyldimethylsilyloxypropanol **II-184** was prepared in 90% yield by reacting 1,3-propane diol **II-183** with 1.0 equiv. of *n*-BuLi followed by addition of TBSCl. The mono-protected alcohol **II-184** was subjected to Swern oxidation which yielded the desired aldehyde **II-168** in quantitative yield. The epoxidation of 3-*tert*-butyldimethylsilyloxypropanal **II-168** follows the conditions given in entry 2 of table 6 and the epoxide **II-173** was produced in 87% yield and 96% *ee* in presence of 10 mol% aluminum-VAPOL catalyst loading. Then the epoxide **II-173** was subjected to TBS

**Scheme II-38.** Total synthesis of (–)-tedanalactam



deprotection with TBAF and the hydroxyl epoxide **II-185** was produced in 84% yield. *In situ* tosylation followed by base induced cyclization was gave the PMB-protected (–)-tedanalactam **II-186** in 67% yield overall for the two steps. Finally, the synthesis of (–)-tedanalactam **II-123** was accomplished by PMB-deprotection in 75% yield by oxidation with CAN.

### 2.3. Aluminum VANOL/VAPOL complexes as efficient catalysts in asymmetric catalytic aziridination of imine

The next goal was to determine the ability of aluminum-VANOL/VAPOL catalysts to effect the asymmetric aziridination of imines. To do so, first, the catalyst ALV was prepared by reacting 2.0 equiv of VANOL ligand and 1.0 equiv LiAlH<sub>4</sub>. The aziridine **II-188a** was not detected from imine **II-187a** and diazoacetate **II-112d** by using ALV catalyst (table II-8, entry 1). Interestingly, when the catalyst was prepared from AlMe<sub>3</sub> and VANOL the desired product was isolated in 67% yield and 76% *ee* (entry 2). Decreasing the temperature to 0 °C increased the *ee* to 82%; however, with a slight deterioration of the yield (entry 2 vs 3). To our delight, 7,7'-*t*Bu<sub>2</sub>VANOL **II-114** ligand performed excellently and produced the aziridine **II-188a** in 68% yield and 93% *ee* (entry 4). Conducting the same reaction at lower temperatures revealed no change in *ee* but a slower reaction was observed with a substantial decrease in the yield (entry 5). Surprisingly, VAPOL **II-20** and ligand **II-115** which were the optimum ligands in the epoxidation reaction performed poorly in this aziridination reaction. The catalyst prepared from VAPOL produced the aziridine **II-188a** with moderate yield but with extremely low *ee* (entry 6). No product was detected by using a catalyst derived from AlMe<sub>3</sub> and ligand **II-115** (table II-2 entry 8) (table II-8, entry 7). The catalyst prepared from BINOL proved to be less than desirable in this reaction since the aziridine was isolated with moderate yield and *ee* (entry 8). We were surprised to observe the poor performance of the MEDAM protecting group in imine **II-187b** since it was the optimum protecting group in the

aziridination reaction catalyzed by VANOL-spiroborate catalyst (entry 9 and 10). The reaction of

**Table II-8.** Aziridination reaction catalyzed by spiro-aluminate catalyst II-189

$$2X \text{ mol\% } (S)\text{-Ligand} \xrightarrow[\text{toluene, rt, 0.5 h}]{M, X \text{ mol\%}} \text{catalyst}$$

$$\text{Ph-CH=N-PG} + \text{CH}_2\text{=N}_2\text{-C(=O)OEt} \xrightarrow[\text{Toluene, T/}^\circ\text{C, 12 h}]{X \text{ mol\% cat.}} \text{Ph-CH}_2\text{-CH}_2\text{-N-PG} + \text{CH}_2\text{=N}_2\text{-C(=O)OEt}$$

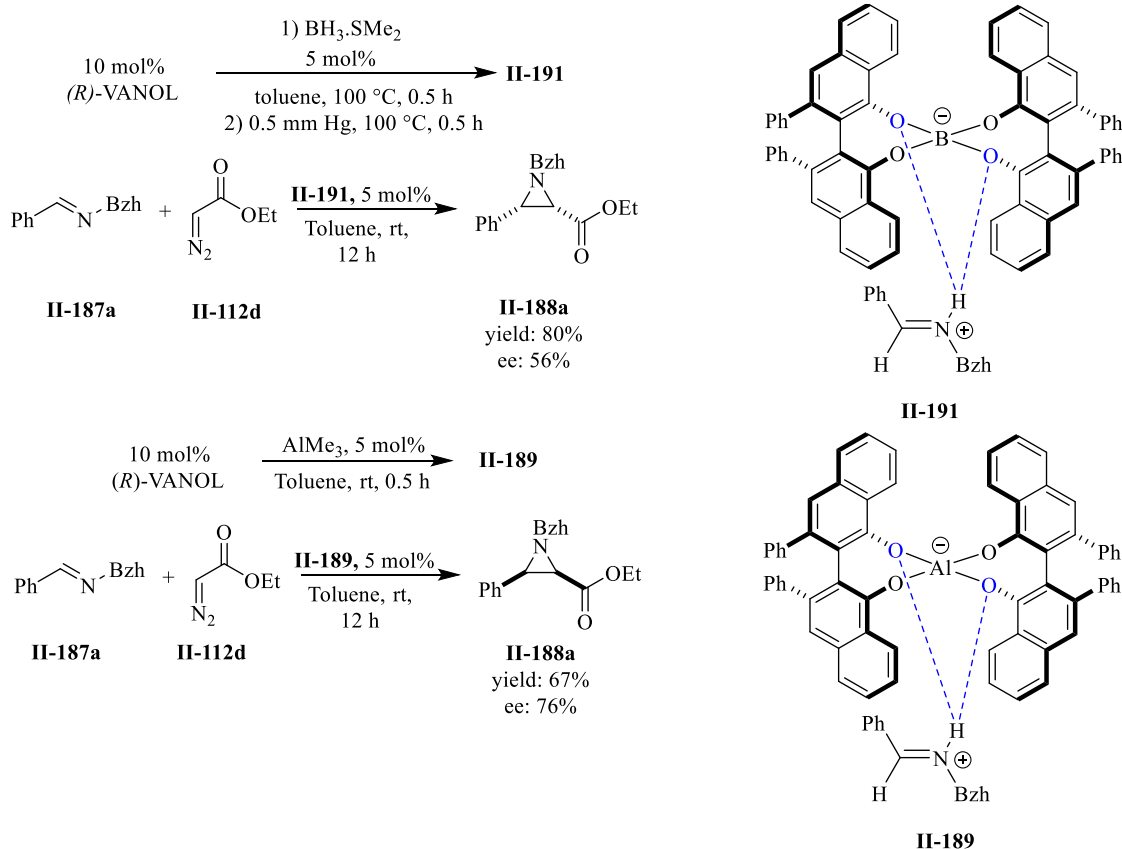
PG: Bzh, **II-187a**      **II-112d**      PG: Bzh, **II-188a**  
 PG: MEDAM, **II-187b**      PG: MEDAM, **II-188b**

entry	Ligand	R	M	Cat. (X mol%)	T/°C	isolated yield%	ee%
1	( <i>S</i> )-VANOL, <b>II-19</b>	Bzh	LiAlH <sub>4</sub>	10	25	-	-
2	( <i>S</i> )-VANOL, <b>II-19</b>	Bzh	AlMe <sub>3</sub>	10	25	67	76
3	( <i>S</i> )-VANOL, <b>II-19</b>	Bzh	AlMe <sub>3</sub>	10	0	58	82
4	( <i>S</i> )-7,7'- <i>t</i> Bu <sub>2</sub> VANOL, <b>II-114</b>	Bzh	AlMe <sub>3</sub>	10	25	68	93
5	( <i>S</i> )-7,7'- <i>t</i> Bu <sub>2</sub> VANOL, <b>II-114</b>	Bzh	AlMe <sub>3</sub>	10	0	25	92
6	( <i>S</i> )-VAPOL, <b>II-20</b>	Bzh	AlMe <sub>3</sub>	10	25	56	-3
7	( <i>S</i> )-Ligand, <b>II-115</b> <sup>2</sup>	Bzh	AlMe <sub>3</sub>	10	25	6 <sup>1</sup>	<i>N.D.</i>
8	( <i>S</i> )-BINOL, <b>II-7</b>	Bzh	AlMe <sub>3</sub>	10	25	43	47
9	( <i>S</i> )-VANOL, <b>II-19</b>	MEDAM	AlMe <sub>3</sub>	10	25	31 <sup>1</sup>	<i>N.D.</i>
10	( <i>S</i> )-7,7'- <i>t</i> Bu <sub>2</sub> VANOL, <b>II-114</b>	MEDAM	AlMe <sub>3</sub>	10	25	20 <sup>1</sup>	<i>N.D.</i>
11	( <i>S</i> )-VANOL, <b>II-19</b>	Bzh	AlMe <sub>3</sub>	5	25	49	77
12	( <i>S</i> )-VANOL, <b>II-19</b>	Bzh	AlMe <sub>3</sub>	2.5	25	4 <sup>1</sup>	<i>N.D.</i>

Unless otherwise specified, all of the reactions were done in toluene at 0 °C for 12 h with 0.5 mmol of diazo compound **II-112** and 0.6 mmol of aldehyde. 1. Yield determined from the NMR spectrum of the crude reaction mixture with Ph<sub>3</sub>CH as the internal standard. 2. For structure of this ligand see table 2.

imine **II-187a** catalyzed by the VANOL derived catalyst gave essentially the same *ee* with either 5 mol% or 10 mol% catalyst but the yield dropped with only 5 mol% catalyst (entry 2 vs 11). However, in the presence of 2.5 mol% catalyst, only a 4% yield of the aziridine was detected in the NMR spectrum of the crude reaction mixture (entry 12).

**Scheme II-39.** Enantioinduction reversal in aziridination reaction catalyzed with boron and aluminum catalysts



We were surprised to observe the reversal in enantioinduction in the aziridination reaction of imine **II-187a** with diazoacetate **II-112d** catalyzed by both spiroaluminate-VANOL catalyst **II-189** and spiroborate-VANOL catalyst **II-191**. Specifically, benzhydryl imine **II-187a** undergoes aziridination in presence of spiroborate-*(R)*-VANOL catalyst **II-191** to give the ethyl (2*S*,3*S*)-1-benzhydryl-3-phenylaziridine-2-carboxylate **II-188a**; whereas, the same reaction catalyzed with

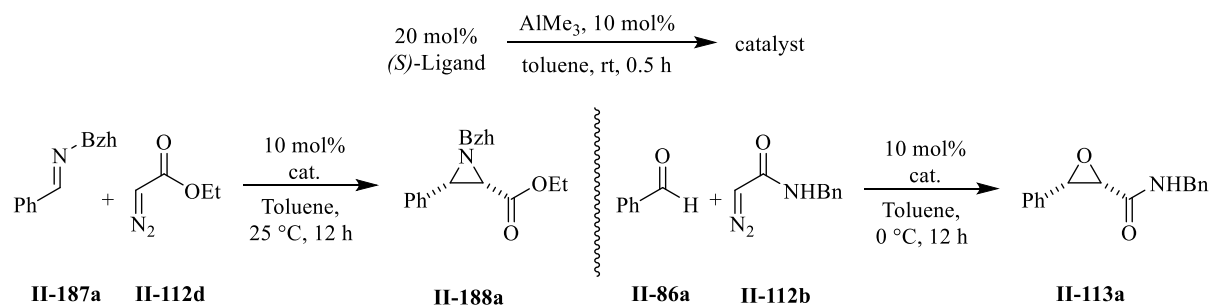
spiroaluminate-(*R*)-VANOL catalyst **II-189** produces ethyl (2*R*,3*R*)-1-benzhydryl-3-phenylaziridine-2-carboxylate **II-188a** (scheme 40).

## 2.4. Aluminum VANOL/VAPOL complexes as chameleon catalysts

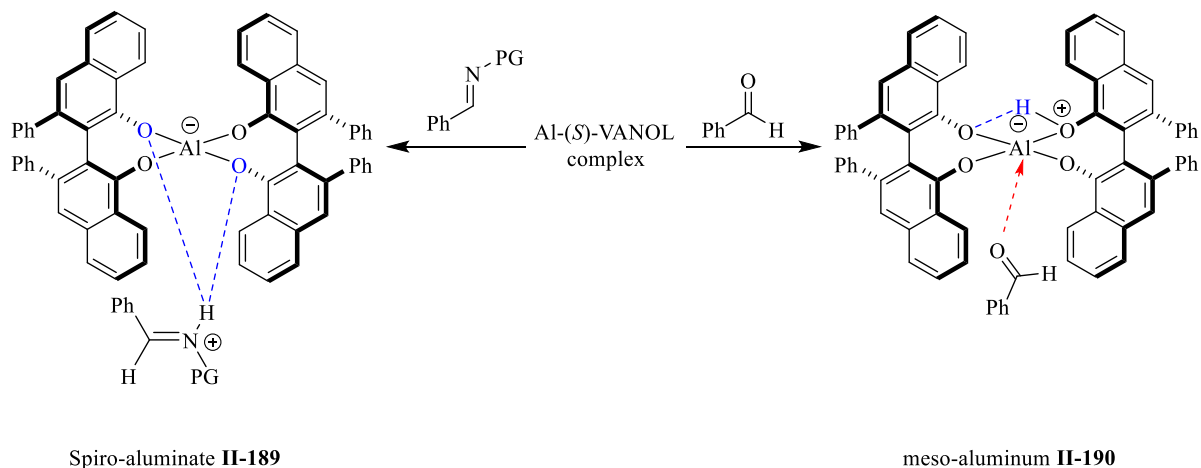
What is the mechanism for the epoxidation and aziridination reactions mediated by aluminum catalyst? To answer this question we looked closely into the results from both reactions.

It is interesting to note that the VAPOL catalyst gives the highest induction for the epoxidation

**Scheme II-40.** Aluminum-VANOL catalyst possess chameleon behavior



entry	Ligand	yield%	ee%	entry	Ligand	yield%	ee%
3	( <i>S</i> )-VANOL	67	76	3	( <i>S</i> )-VANOL	80	72
4	( <i>S</i> )-7,7'- <i>t</i> Bu <sub>2</sub> VAPOL	68	93	4	( <i>S</i> )-7,7'- <i>t</i> Bu <sub>2</sub> VAPOL	46	84
6	( <i>S</i> )-VAPOL	56	-3	6	( <i>S</i> )-VAPOL	81	99



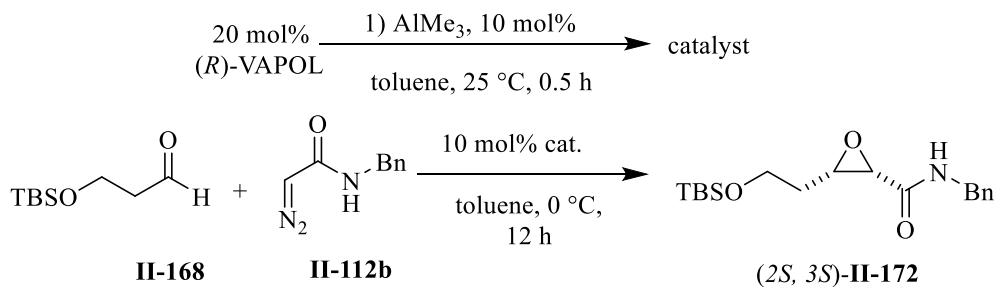
reaction but the lowest for the aziridination reaction, suggesting very different mechanisms for each reaction (scheme II-40).

We believe these aluminum catalysts are acting as a Lewis acid catalyst in the reaction of aldehydes and a Brønsted acid catalyst in the reaction of imines. In other words, meso-aluminum **II-190** complex is the active catalyst in the epoxidation reaction (scheme II-40, structure **II-190**) and the aziridination reaction is catalyzed by spiro-aluminate catalyst (scheme II-40, structure **II-189**). However, there is no direct experimental evidence to show the dual nature of the aluminum VANOL/VAPOL complexes; therefore, more mechanistic studies need to be carried out to define the differences in the mechanisms of the epoxidation and aziridination reactions.

## 2.5. Conclusion

In summary, we have discovered and developed new aluminum VANOL and aluminum VAPOL complexes as efficient catalysts in the epoxidation of aldehydes with diazo acetamides. The total synthesis of (–)-tedanalactam was also accomplished in only 5 steps with excellent enantioinduction in 37% overall yield. A short and highly efficient synthesis of this natural product was presented which indicates the strength of this methodology. Aluminum VANOL complex were also found to be highly efficient in the aziridination reaction. Initial results suggest that the aluminum VANOL/VAPOL complexes are catalyzing the epoxidation and aziridination reactions via two different mechanisms; however, more experiments are required to show the chameleon behavior of these complexes. Enantioinduction reversal was also observed for both aziridination and epoxidation reactions catalyzed by (*R*)-aluminum catalyst compared with (*R*)-boron catalyst which presented a distinct feature between these two catalysts.

## 2.6. Experimental



*General procedure for preparation of catalyst stock solution:* A flame dried 25 mL round bottom flask filled with nitrogen was charged with **(R)-VAPOL** (0.149 mmol, 82.0 mg) and toluene (3 mL). The resulting mixture was stirred at room temperature for 5 minutes until the ligand was fully dissolved then  $\text{AlMe}_3$  (0.075 mmol, 38  $\mu\text{L}$ , 2M solution in toluene) was added and the reaction mixture was stirred at room temperature for 30 minutes.

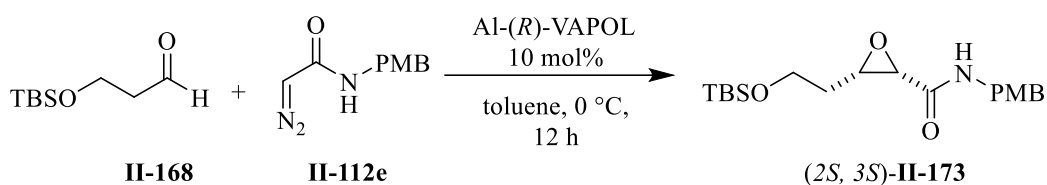
*General procedure for the epoxidation reaction catalyzed with aluminum-VAPOL catalyst:*

**(2S,3S)-3-(2-((tert-butyldimethylsilyl)oxy)ethyl)-N-benzyl-oxirane-2-carboxamide** **II-172:**

Another flame dried round bottom flask filled with nitrogen was charged with  $N$ -benzyl diazomalonamide (0.49 mmol, 88 mg) **II-168**, toluene (3 mL) and aldehyde 3-tert-butyldimethylsilyloxypropanal (0.591 mmol, 127  $\mu\text{L}$ ) **2a**. The obtained cloudy mixture and the catalyst stock solution were cooled down to 0 °C and stirred at 0 °C for 10 min. Then 2 mL of catalyst stock solution was transferred to the round bottom flask containing the starting materials using syringe and the obtained mixture was stirred at 0 °C for 12 h. Then the reaction was quenched by adding 1 mL of methanol followed by transferring the crude mixture of reaction to a 50 mL round bottom flask and evaporating the solvent under reduced pressure. The crude epoxide was purified via column chromatography (20 x 250 mm, 3:1 to 1:1 hexane: ethyl acetate as eluent) and epoxide **II-172** was obtained as a yellowish oil in 80% (0.399 mmol, 142 mg) isolated yield. The enantiomeric excess of epoxide **II-172** was determined to be 96% with chiral HPLC (PIRKLE

COVALENT (*R,R*) WHELK-O 1 column, 94:6 hexane/2-propanol at 228 nm, flow-rate: 1 mL/min): retention times:  $R_t$  = 18.9 min (major enantiomer, ent-**II-172**) and  $R_t$  = 21.6 min (minor enantiomer, **II-172**).

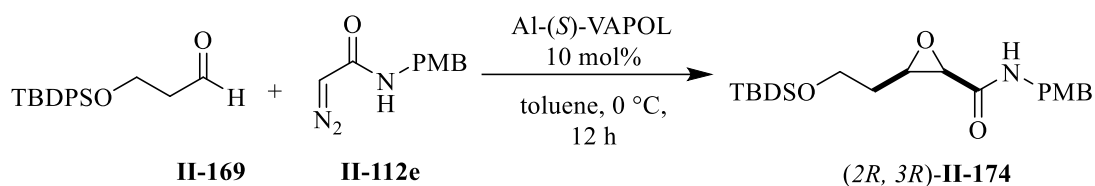
Spectral data for epoxide **II-172**:  $^1\text{H}$  NMR (500 MHz, Chloroform-*d*)  $\delta$  0.05 (s, 6H), 0.89 (s, 9H), 1.64 (ddt,  $J$  = 14.2, 7.4, 5.8 Hz, 1H), 1.81 (dtd,  $J$  = 14.3, 6.5, 4.9 Hz, 1H), 3.36 (dt,  $J$  = 7.5, 4.8 Hz, 1H), 3.57 (d,  $J$  = 4.8 Hz, 1H), 3.76 (t,  $J$  = 6.2 Hz, 2H), 4.39 – 4.52 (m, 2H), 6.49 (t,  $J$  = 6.1 Hz, 1H), 7.21 – 7.32 (m, 3H), 7.28 – 7.37 (m, 2H).  $^{13}\text{C}$  NMR (126 MHz, Chloroform-*d*)  $\delta$  -5.44, -5.41, 18.25, 25.86, 31.09, 42.99, 54.99, 56.31, 59.89, 127.73, 127.90, 128.78, 137.55, 167.22. IR: 3305brs, 2928w, 1660s, 1096s, 881s, 775s, 729m, 698s. HRMS (ESI-TOF)  $m/z$  336.2039,  $[(M+H)^+]$ ; calcd for  $\text{C}_{18}\text{H}_{30}\text{NO}_3\text{Si}$ : 336.1994].



(2*S*,3*S*)-3-(2-((*tert*-butyldimethylsilyl)oxy)ethyl)-*N*-(4-methoxybenzyl)oxirane-2-carboxamide **II-173**: Epoxide **II-173** was synthesized from aldehyde **II-168** (0.591 mmol, 127  $\mu\text{L}$ ) and diazo compound **II-112e** (0.499 mmol, 103 mg) catalyzed by aluminum-(*R*)-VAPOL catalyst prepared with the general procedure with a 12 h reaction time. The crude product was purified via column chromatography (20 x 250 mm, 3:1 to 1:1 hexane: ethyl acetate as eluent) and epoxide **II-173** was obtained as a yellowish oil in 87% (0.435 mmol, 159 mg) isolated yield. The enantiomeric excess of epoxide **II-173** was determined to be 95% with chiral HPLC (PIRKLE COVALENT (*R,R*) WHELK-O 1 column, 90:10 hexane/2-propanol at 228 nm, flow-rate: 1 mL/min): retention times:  $R_t$  = 19.24 min (major enantiomer, ent-**II-173**) and  $R_t$  = 25.98 min (minor enantiomer, **II-173**).



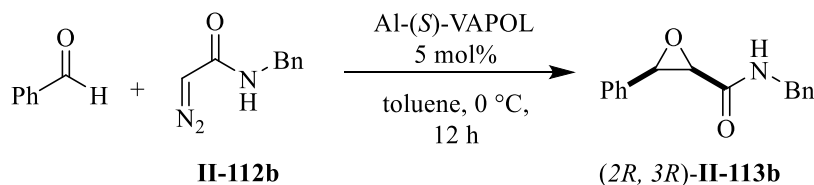
Spectral data for epoxide **II-173**:  $^1\text{H}$  NMR (500 MHz, Chloroform-*d*)  $\delta$  0.03 (m, 6H), 0.88 (s, 9H), 1.61 (ddt,  $J$  = 14.2, 7.5, 5.8 Hz, 1H), 1.71 – 1.84 (m, 1H), 3.34 (dt,  $J$  = 7.5, 4.8 Hz, 1H), 3.55 (d,  $J$  = 4.8 Hz, 1H), 3.71 – 3.81 (m, 5H), 4.38 (d,  $J$  = 5.9 Hz, 2H), 6.40 (t,  $J$  = 6.2 Hz, 1H), 6.82 – 6.89 (m, 2H), 7.15 – 7.23 (m, 2H).  $^{13}\text{C}$  NMR (126 MHz, Chloroform-*d*)  $\delta$  -5.45, -5.42, 18.24, 25.85, 31.06, 42.43, 54.97, 55.27, 56.27, 59.89, 114.11, 129.25, 129.26, 129.64, 167.08. HRMS (ESI-TOF)  $m/z$  366.2136, [(M+H) $^+$ ]; calcd for  $\text{C}_{19}\text{H}_{32}\text{NO}_4\text{Si}$ : 366.2100]. IR: 3310 brs, 2950w, 1654s, 1512s, 1247s, 1094s, 830s, 778s.  $[\alpha]^{20}_{\text{D}}$  (*c* 1.0,  $\text{CHCl}_3$ ): 0.0481.



(2*R*,3*R*)-3-(2-((*tert*-butyldiphenylsilyl)oxy)ethyl)-*N*-(4-methoxybenzyl)oxirane-2-carboxamide **II-174**: Epoxide **II-174** was synthesized from aldehyde **II-169** (0.599 mmol, 188 mg) and diazo compound **II-112e** (0.499 mmol, 103 mg) catalyzed by aluminum-(*S*)-VAPOL catalyst prepared with the general procedure with a 12 h reaction time. The crude product was purified via column chromatography (20 x 250 mm, 3:1 to 1:1 hexane: ethyl acetate as eluent) and epoxide **II-174** was obtained as a yellowish oil in 77% (0.385 mmol, 188) isolated yield. The enantiomeric excess of epoxide **II-174** was determined to be 94% with chiral HPLC (PIRKLE COVALENT (*R,R*) WHELK-O 1 column, 93:7 hexane/2-propanol at 228 nm, flow-rate: 1 mL/min): retention times:  $R_t$  = 33.7 min (minor enantiomer, ent-**II-174**) and  $R_t$  = 48.8 min (major enantiomer, **II-174**).

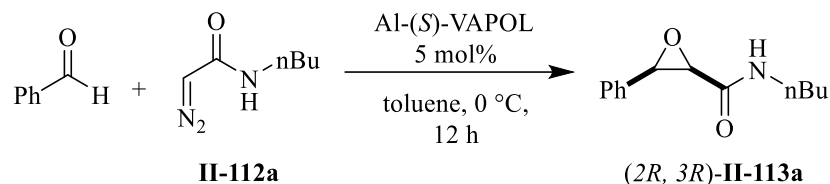
Spectral data for epoxide **II-174**:  $^1\text{H}$  NMR (500 MHz, Chloroform-*d*)  $\delta$  1.07 (s, 9H), 1.07, 1.56 – 1.67 (m, 1H), 1.89 (dddd,  $J$  = 14.3, 7.1, 5.9, 4.5 Hz, 1H), 3.40 – 3.54 (m, 1H), 3.57 (d,  $J$  = 4.8 Hz, 1H), 3.78 (s, 3H), 3.77 – 3.87 (m, 2H), 4.37 (d,  $J$  = 5.9 Hz, 2H), 6.37 (t,  $J$  = 5.9 Hz, 1H), 6.81 – 6.90 (m, 2H), 7.14 – 7.21 (m, 2H), 7.36 – 7.43 (m, 4H), 7.40 – 7.48 (m, 2H), 7.63 – 7.70 (m, 4H).

$^{13}\text{C}$  NMR (126 MHz, Chloroform-*d*)  $\delta$  15.31, 19.18, 26.80, 30.88, 42.42, 54.98, 55.27, 56.30, 60.85, 114.12, 127.73, 127.74, 129.24, 129.74, 129.75, 133.40, 133.43, 135.53, 159.12, 167.07. HRMS (ESI-TOF)  $m/z$  490.243, [(M+H<sup>+</sup>); calcd for C<sub>29</sub>H<sub>36</sub>NO<sub>4</sub>Si: 490.2413]. [ $\alpha$ ]<sub>D</sub><sup>20</sup> (c 1.0, CHCl<sub>3</sub>): -0.0403.



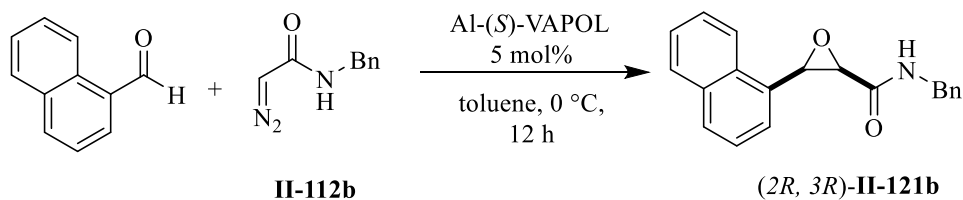
**(2R,3R)-3-phenyl-N-benzyl-oxirane-2-carboxamide II-113b**: Epoxide **II-113b** was synthesized from benzaldehyde (0.59 mmol, 62  $\mu\text{L}$ ) and diazo compound **II-112b** (0.49 mmol, 88 mg) catalyzed by aluminum-(*S*)-VAPOL catalyst prepared with the general procedure with a 12 h as the reaction time. The crude product was purified via column chromatography (20 x 250 mm, 3:1 to 1:1 hexane: ethyl acetate as eluent) and epoxide **II-113b** was obtained as a white solid in 97% (0.485 mmol, 123 mg) isolated yield. The enantiomeric excess of epoxide **II-113b** was determined to be 99% with chiral HPLC (PIRKLE COVALENT (*R,R*) WHELK-O 1 column, 90:10 hexane/2-propanol at 228 nm, flow-rate: 1 mL/min): retention times:  $R_t$  = 31.4 min (minor enantiomer, ent-**II-113b**) and  $R_t$  = 43.24 min (major enantiomer, **II-113b**).

Spectral data for epoxide **II-113b**:  $^1\text{H}$  NMR (500 MHz, Chloroform-*d*)  $\delta$  7.40 – 7.27 (m, 5H), 7.24 – 7.13 (m, 3H), 6.75 – 6.69 (m, 2H), 6.19 (s, 1H), 4.38 – 4.27 (m, 2H), 4.07 (dd,  $J$  = 14.9, 4.9 Hz, 1H), 3.85 (d,  $J$  = 4.8 Hz, 1H).  $^{13}\text{C}$  NMR (126 MHz, Chloroform-*d*)  $\delta$  42.70, 56.36, 58.29, 126.56, 127.31, 127.42, 128.52, 128.55, 133.04, 137.00, 166.13. These spectral data are in good agreement with literature values.<sup>19</sup>



**(2R,3R)-3-phenyl-N-(n-butyl)oxirane-2-carboxamide II-113a:** Epoxide **II-113a** was synthesized from benzaldehyde (0.59 mmol, 62  $\mu\text{L}$ ) and diazo compound **II-112a** (0.50 mmol, 74 mg) catalyzed by aluminum-(*S*)-VAPOL catalyst prepared with the general procedure with a 12 h reaction time. The crude product was purified via column chromatography (20 x 250 mm, 3:1 to 1:1 hexane: ethyl acetate as eluent) and epoxide **II-113a** was obtained as a white solid in 86% (0.43 mmol, 94 mg) isolated yield. The enantiomeric excess of epoxide **II-113a** was determined to be 97% with chiral HPLC (PIRKLE COVALENT (*R,R*) WHELK-O 1 column, 93:7 hexane/2-propanol at 228 nm, flow-rate: 1 mL/min): retention times:  $R_t = 24.63$  min (minor enantiomer, ent-**II-113a**) and  $R_t = 31.46$  min (major enantiomer, **II-113a**).

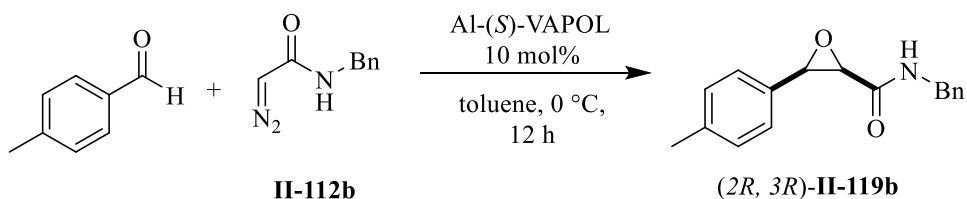
Spectral data for epoxide **II-113a**:  $^1\text{H}$  NMR (500 MHz, Chloroform-*d*)  $\delta$  0.65 (t,  $J = 7.5$  Hz, 3H), 0.80- 1.00 (m, 4H), 2.75-2.83 (m, 1H), 2.98-3.07 (m, 1H), 3.70 (d,  $J = 5.0$  Hz, 1H), 4.24 (d,  $J = 5.5$  Hz, 1H), 5.85 (brs, 1H), 7.20-7.32 (m, 5H);  $^{13}\text{C}$  NMR (126 MHz, Chloroform-*d*)  $\delta$  13.46, 19.51, 31.06, 38.10, 56.17, 57.96, 126.38, 128.20, 128.27, 133.07, 165.86. These spectral data are in good agreement with literature values.<sup>19</sup>



**(2R, 3R)-3-(naphthalene-1-yl)-N-benzyl-oxirane-2-carboxamide II-121b:** Epoxide **II-121b** was synthesized from 1-naphthalenecarboxaldehyde (0.60 mmol, 82  $\mu\text{L}$ ) and diazo compound **II-112b** (0.50 mmol, 88 mg) catalyzed by aluminum-(*S*)-VAPOL catalyst prepared with the general

procedure with a 12 h reaction time. The crude product was purified via column chromatography (20 x 250 mm, 3:1 to 1:1 hexane: ethyl acetate as eluent) and epoxide **II-121b** was obtained as a white solid in 93% isolated yield (0.465 mmol, 141 mg). The enantiomeric excess of epoxide **II-121b** was determined to be 99% with chiral HPLC (PIRKLE COVALENT (*R,R*) WHELK-O 1 column, 85:15 hexane/2-propanol at 228 nm, flow-rate: 1 mL/min): retention times:  $R_t$  = 22.25 min (minor enantiomer, ent-**II-121b**) and  $R_t$  = 64.47 min (major enantiomer, **II-121b**). mp: 92-93 °C.

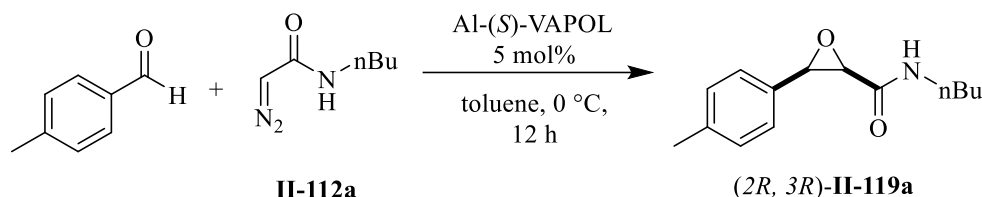
$^1\text{H}$  NMR (500 MHz, Chloroform-*d*)  $\delta$  3.94 (dd,  $J$  = 15.0, 4.9 Hz, 1H), 4.10 (d,  $J$  = 4.7 Hz, 1H), 4.22 (dd,  $J$  = 15.0, 7.1 Hz, 1H), 4.72 (d,  $J$  = 4.7 Hz, 1H), 6.06 (d,  $J$  = 6.1 Hz, 1H), 6.43 – 6.49 (m, 2H), 6.98 – 7.05 (m, 2H), 7.07 – 7.14 (m, 1H), 7.33 (dd,  $J$  = 8.2, 7.0 Hz, 1H), 7.48 (dt,  $J$  = 7.1, 1.2 Hz, 1H), 7.56 (dddd,  $J$  = 19.5, 8.1, 6.8, 1.4 Hz, 2H), 7.83 (dd,  $J$  = 8.3, 1.2 Hz, 1H), 7.87 – 7.93 (m, 1H), 8.10 – 8.16 (m, 1H).  $^{13}\text{C}$  NMR (126 MHz, Chloroform-*d*)  $\delta$  42.54, 56.28, 57.63, 123.63, 124.54, 124.99, 126.46, 126.94, 127.05, 127.10, 128.33, 128.54, 129.03, 129.29, 131.06, 133.31, 136.93, 166.30. IR: 3334brs, 1651s, 1528s, 772m, 742s, 762s, 606s. HRMS (ESI-TOF)  $m/z$  304.1404, [(M+H<sup>+</sup>); calcd for C<sub>20</sub>H<sub>18</sub>NO<sub>2</sub>: 304.1337].  $[\alpha]_D^{20}$  (*c* 1.0, CHCl<sub>3</sub>): 1.2002.



(2*R*, 3*R*)-3-(4-methyl-phenyl)-*N*-benzyl-oxirane-2-carboxamide **II-119b**: Epoxide **II-119b** was synthesized from aldehyde *para*-tolylaldehyde (0.60 mmol, 71  $\mu\text{L}$ ) and diazo compound **II-112b** (0.50 mmol, 88 mg) catalyzed by aluminum-(*S*)-VAPOL catalyst prepared with the general procedure with a 12 h reaction time. The crude product was purified via column chromatography (20 x 250 mm, 3:1 to 1:1 hexane: ethyl acetate as eluent) and epoxide **II-119b** was obtained as a

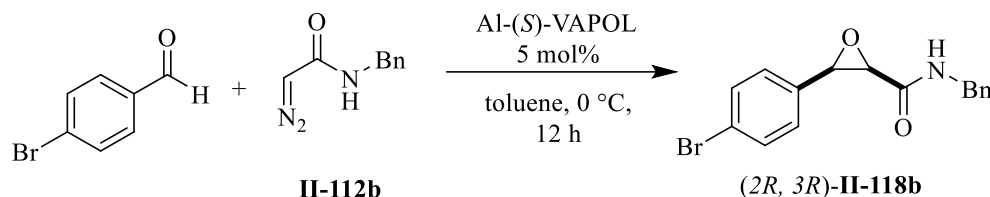
white solid in 76% isolated yield (0.379 mmol 102 mg). The enantiomeric excess of epoxide **II-119b** was determined to be 99% with chiral HPLC (PIRKLE COVALENT (*R,R*) WHELK-O 1 column, 90:10 hexane/2-propanol at 228 nm, flow-rate: 1 mL/min): retention times:  $R_t$  = 30.45 min (minor enantiomer, ent-**II-119b**) and  $R_t$  = 45.1 min (major enantiomer, **II-119b**). mp: 76-77 °C.

$^1\text{H}$  NMR (500 MHz, Chloroform-*d*)  $\delta$  2.36 (s, 3H), 3.82 (d,  $J$  = 4.7 Hz, 1H), 4.04 (dd,  $J$  = 14.9, 4.9 Hz, 1H), 4.28 – 4.40 (m, 2H), 6.18 (t,  $J$  = 6.1 Hz, 1H), 6.68 – 6.74 (m, 2H), 7.09 (d,  $J$  = 7.9 Hz, 2H), 7.11 – 7.19 (m, 2H), 7.15 – 7.23 (m, 3H), 7.24 – 7.34 (m, 0H).  $^{13}\text{C}$  NMR (126 MHz, Chloroform-*d*)  $\delta$  21.32, 42.67, 56.39, 58.26, 126.45, 127.22, 127.44, 128.37, 129.18, 130.01, 137.08, 138.23, 166.28. IR: 3290brs, 1659s, 1532s, 696s. HRMS (ESI-TOF)  $m/z$  268.1374,  $[(\text{M}+\text{H})^+]$ ; calcd for  $\text{C}_{17}\text{H}_{18}\text{NO}_2$ : 268.1337]  $[\alpha]^{20}_{\text{D}}$  (*c* 1.0,  $\text{CHCl}_3$ ): 0.273.



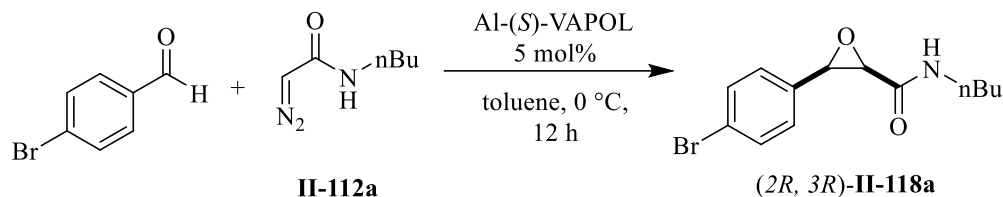
(2*R*, 3*R*)-3-(4-methyl-phenyl)-*N*-(*n*-butyl)-oxirane-2-carboxamide **II-119a**: Epoxide **II-119a** was synthesized from *para*-tolylaldehyde (0.60 mmol, 71  $\mu\text{L}$ ) and diazo compound **II-112a** (0.50 mmol, 74 mg) catalyzed by aluminum-(*S*)-VAPOL catalyst prepared with the general procedure with a 12 h reaction time. The crude product was purified via column chromatography (20 x 250 mm, 3:1 to 1:1 hexane: ethyl acetate as eluent) and epoxide **II-119a** was obtained as a white solid in 66% isolated yield (0.330 mmol, 79.3 mg). The enantiomeric excess of epoxide **II-119a** was determined to be 93% with chiral HPLC (PIRKLE COVALENT (*R,R*) WHELK-O 1 column, 93:7 hexane/2-propanol at 228 nm, flow-rate: 1 mL/min): retention times:  $R_t$  = 25.13 min (minor enantiomer, ent-**II-119a**) and  $R_t$  = 37.54 min (major enantiomer, **II-119a**).

$^1\text{H}$  NMR (500 MHz, Chloroform-*d*)  $\delta$  0.65 (t,  $J$  = 7.0 Hz, 3H), 0.80- 0.88 (m, 2H), 0.91-0.99 (m, 2H), 2.25 (s, 3H), 2.74-2.82 (m, 1H), 3.01-3.10 (m, 1H), 3.67 (d,  $J$  = 4.5 Hz, 1H), 4.20 (d,  $J$  = 4.5 Hz, 1H), 5.84 (brs, 1H), 7.06 (d,  $J$  = 7.5 Hz, 2H), 7.16 (d,  $J$  = 8.0 Hz, 2H);  $^{13}\text{C}$  NMR (126 MHz, Chloroform-*d*)  $\delta$  13.50, 19.54, 21.03, 31.16, 38.13, 56.21, 57.95, 126.31, 128.86, 130.08, 138.05, 166.0. These spectral data are in good agreement with literature values.<sup>19</sup>



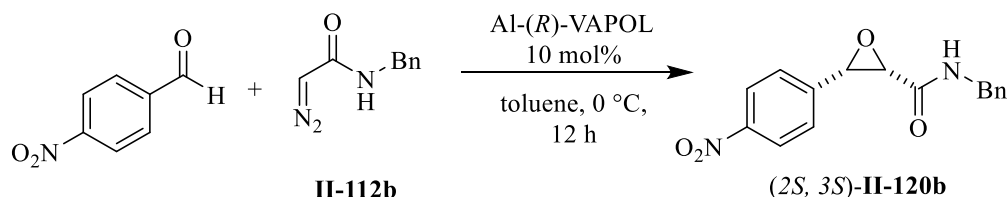
**(2R, 3R)-3-(4-bromo-phenyl)-N-benzyl-oxirane-2-carboxamide II-118b**: Epoxide **II-118b** was synthesized from *para*-bromobenzaldehyde (0.591 mmol, 111 mg) and diazo compound **II-112b** (0.50 mmol, 88 mg) catalyzed by aluminum-(*S*)-VAPOL catalyst prepared with the general procedure with a 12 h reaction time. The crude product was purified via column chromatography (20 x 250 mm, 3:1 to 1:1 hexane: ethyl acetate as eluent) and epoxide **II-118b** was obtained as a white solid in 90% isolated yield (0.395 mmol, 131 mg). The enantiomeric excess of epoxide **II-118b** was determined to be 99% with chiral HPLC (PIRKLE COVALENT (*R,R*) WHELK-O 1 column, 85:15 hexane/2-propanol at 228 nm, flow-rate: 1 mL/min): retention times:  $R_t$  = 21.26 min (minor enantiomer, ent-**II-118b**) and  $R_t$  = 29.18 min (major enantiomer, **II-118b**).

$^1\text{H}$  NMR (500 MHz, Chloroform-*d*)  $\delta$  3.85 (d,  $J$  = 4.8 Hz, 1H), 4.00 (dd,  $J$  = 14.8, 4.6 Hz, 1H), 4.28 (d,  $J$  = 4.8 Hz, 1H), 4.44 (dd,  $J$  = 14.7, 7.5 Hz, 1H), 6.15 (t,  $J$  = 5.9 Hz, 1H), 6.70 – 6.76 (m, 2H), 7.16 – 7.29 (m, 5H), 7.36 – 7.43 (m, 2H).  $^{13}\text{C}$  NMR (126 MHz, Chloroform-*d*)  $\delta$  42.72, 56.25, 57.65, 122.69, 127.46, 127.51, 128.22, 128.58, 131.69, 132.00, 136.94, 165.65. These spectral data are in good agreement with literature values.<sup>19</sup>



**(2R, 3R)-3-(4-bromo-phenyl)-N-(n-butyl)-oxirane-2-carboxamide II-118a:** Epoxide **II-118a** was synthesized from *para*-bromobenzaldehyde (0.590 mmol, 111 mg) and diazo compound **II-112a** (0.50 mmol, 74 mg) catalyzed by aluminum-(*S*)-VAPOL catalyst prepared with the general procedure with a 12 h reaction time. The crude product was purified via column chromatography (20 x 250 mm, 3:1 to 1:1 hexane: ethyl acetate as eluent) and epoxide **II-118a** was obtained as a white solid in 77% isolated yield (0.385 mmol, 115 mg). The enantiomeric excess of epoxide **II-118a** was determined to be 85% with chiral HPLC (PIRKLE COVALENT (*R,R*) WHELK-O 1 column, 90:10 hexane/2-propanol at 228 nm, flow-rate: 1 mL/min): retention times:  $R_t$  = 18.05 min (minor enantiomer, ent-**II-118a**) and  $R_t$  = 26.19 min (major enantiomer, **II-118a**).

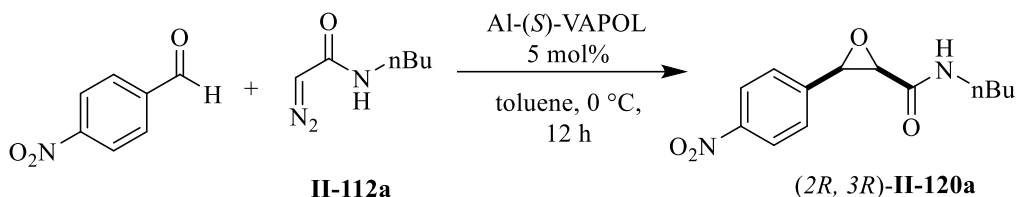
$^1\text{H}$  NMR (500 MHz, Chloroform-*d*)  $\delta$  0.70 (t,  $J$  = 7.5 Hz, 3H), 0.86- 0.95 (m, 2H), 0.99-1.06 (m, 2H), 2.77-2.85 (m, 1H), 3.02-3.12 (m, 1H), 3.71 (d,  $J$  = 4.5 Hz, 1H), 4.19 (d,  $J$  = 4.0 Hz, 1H), 5.87 (brs, 1H), 7.17 (d,  $J$  = 7.5 Hz, 2H), 7.40 (d,  $J$  = 7.5 Hz, 2H).  $^{13}\text{C}$  NMR (126 MHz, Chloroform-*d*)  $\delta$  13.51, 19.57, 31.20, 38.19, 56.14, 57.34, 122.41, 128.14, 131.37, 132.14, 165.48. These spectral data are in good agreement with literature values.<sup>19</sup>



**(2S,3S)-3-(4-nitro-phenyl)-N-benzyl-oxirane-2-carboxamide II-120b:** Epoxide **II-120b** was synthesized from *para*-nitrobenzaldehyde (0.590 mmol, 111 mg) and diazo compound **II-112b** (0.50 mmol, 74 mg) catalyzed by aluminum-(*R*)-VAPOL catalyst prepared with the general

procedure with a 12 h reaction time. The crude product was purified via column chromatography (20 x 250 mm, 3:1 to 1:1 hexane: ethyl acetate as eluent) and epoxide **II-120b** was obtained as a white solid in 70% isolated yield (0.350 mmol, 105 mg). The enantiomeric excess of epoxide **II-120b** was determined to be 93% with chiral HPLC (PIRKLE COVALENT (*R,R*) WHELK-O 1 column, 85:15 hexane/2-propanol at 228 nm, flow-rate: 1 mL/min): retention times:  $R_t = 39.79$  min (major enantiomer, ent-**II-120b**) and  $R_t = 48.53$  min (minor enantiomer, **II-120b**). mp: 116-117 °C.

$^1\text{H}$  NMR (500 MHz, Chloroform-*d*)  $\delta$  3.89 – 3.99 (m, 2H), 4.38 (d,  $J = 4.9$  Hz, 1H), 4.44 (dd,  $J = 14.5, 7.9$  Hz, 1H), 6.17 (s, 1H), 6.77 – 6.83 (m, 2H), 7.13 (ddt,  $J = 8.3, 6.5, 1.4$  Hz, 2H), 7.15 – 7.23 (m, 1H), 7.40 – 7.47 (m, 2H), 7.99 – 8.06 (m, 2H).  $^{13}\text{C}$  NMR (126 MHz, Chloroform-*d*)  $\delta$  42.70, 56.27, 57.26, 123.59, 127.39, 127.69, 127.75, 128.51, 139.79. IR: 3314brs, 1665s, 1512s, 1342s, 743m, 668s. HRMS (ESI-TOF)  $m/z$  299.1056, [( $\text{M}+\text{H}^+$ ); calcd for  $\text{C}_{16}\text{H}_{15}\text{N}_2\text{O}_4$ : 299.1031]  $[\alpha]^{20}_{\text{D}}$  ( $c$  1.0,  $\text{CHCl}_3$ ): 0.9559.

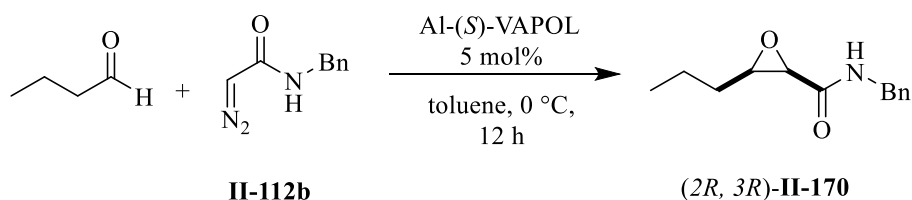


(2*R*, 3*R*)-3-(4-nitro-phenyl)-*N*-benzyl-oxirane-2-carboxamide **II-120a**: Epoxide **II-120a** was synthesized from *para*-nitrobenzaldehyde (0.590 mmol, 111 mg) and diazo compound **II-112a** (0.50 mmol, 74 mg) catalyzed by aluminum-(*S*)-VAPOL catalyst prepared with the general procedure with a 12 h reaction time. The crude product was purified via column chromatography (20 x 250 mm, 3:1 to 1:1 hexane: ethyl acetate as eluent) and epoxide **II-120a** was obtained as a white solid in 36% isolated yield (0.18 mmol, 48 mg). The enantiomeric excess of epoxide **II-120a** was determined to be 71% with chiral HPLC (PIRKLE COVALENT (*R,R*) WHELK-O 1 column,



90:10 hexane/2-propanol at 228 nm, flow-rate: 1 mL/min): retention times:  $R_t$  = 50.34 min (minor enantiomer, ent-**II-120a**) and  $R_t$  = 57.11 min (major enantiomer, **II-120a**).

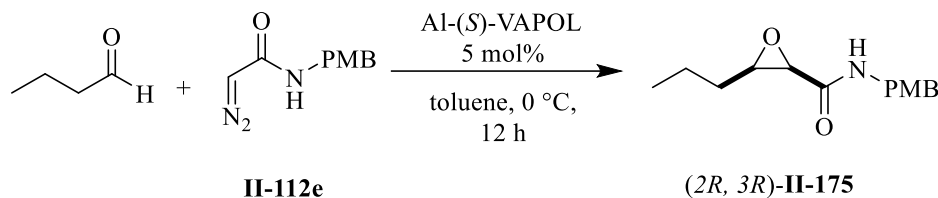
$^1\text{H}$  NMR (500 MHz, Chloroform-*d*)  $\delta$  0.65 (t,  $J$  = 7.5 Hz, 3H), 0.84- 0.94 (m, 2H), 0.98-1.06 (m, 2H), 2.82-2.90 (m, 1H), 2.98-3.07 (m, 1H), 3.80 (d,  $J$  = 5.0 Hz, 1H), 4.32 (d,  $J$  = 4.5 Hz, 1H), 5.97 (brs, 1H), 7.51 (d,  $J$  = 9.0 Hz, 2H), 8.15 (d,  $J$  = 8.5 Hz, 2H).  $^{13}\text{C}$  NMR (126 MHz, Chloroform-*d*)  $\delta$  13.36, 19.57, 31.22, 38.28, 56.45, 57.09, 123.42, 127.52, 140.27, 147.78, 164.91. These spectral data are in good agreement with literature values.<sup>19</sup>



(2*R*,3*R*)-3-propyl-*N*-benzyl-oxirane-2-carboxamide **II-170**: Epoxide **II-170** was synthesized from butanal (0.60 mmol, 55  $\mu\text{L}$ ) and diazo compound **II-112b** (0.50 mmol, 88 mg) catalyzed by aluminum-(*S*)-VAPOL catalyst prepared with the general procedure with a 12 h reaction time. The crude product was purified via column chromatography (20 x 250 mm, 5:1 to 1:1 hexane: ethyl acetate as eluent) and epoxide **II-170** was obtained as a white solid in 62% isolated yield (0.31 mmol, 68 mg). The enantiomeric excess of epoxide **II-170** was determined to be 89% with chiral HPLC (PIRKLE COVALENT (*R,R*) WHELK-O 1 column, 90:10 hexane/2-propanol at 228 nm, flow-rate: 1 mL/min): retention times:  $R_t$  = 18.26 min (minor enantiomer, ent-**II-170**) and  $R_t$  = 22.08 min (major enantiomer, **II-170**).

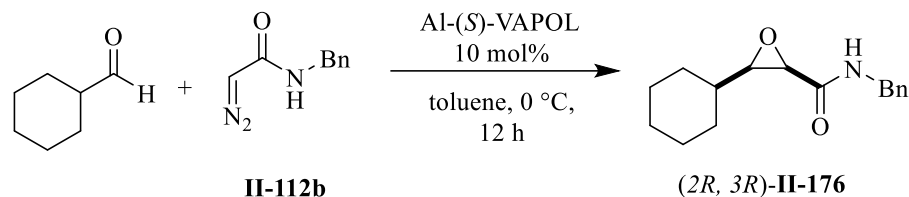
$^1\text{H}$  NMR (500 MHz, Chloroform-*d*)  $\delta$  0.82 (t,  $J$  = 7.0 Hz, 3H), 1.38 (m, 4H), 3.06 (d,  $J$  = 4.5 Hz, 1H), 3.43 (d,  $J$  = 4.5 Hz, 1H), 4.31 (dd,  $J$  = 14.5, 5.5 Hz, 1H), 4.43 (dd,  $J$  = 14.5, 6.0 Hz, 1H), 6.52 (brs, 1H), 7.17-7.25 (m, 5H).  $^{13}\text{C}$  NMR (126 MHz, Chloroform-*d*)  $\delta$  13.66, 19.20, 29.45, 42.74,

55.02, 58.31, 127.49, 127.74, 128.44, 137.62, 167.19. These spectral data are in good agreement with literature values.<sup>19</sup>



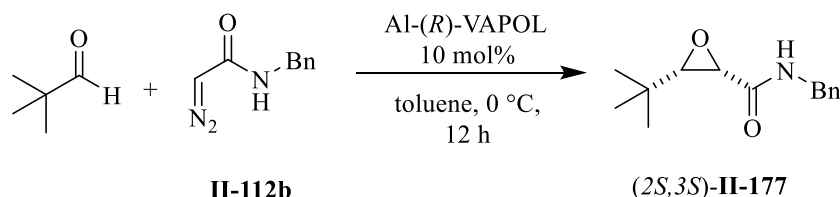
(2R, 3R)-3-propyl-N-(4-methoxybenzyl)-oxirane-2-carboxamide **II-175**: Epoxide **II-175** was synthesized from butanal (0.60 mmol, 55  $\mu$ L) and diazo compound **II-112e** (0.495 mmol, 103 mg) catalyzed by aluminum-(S)-VAPOL catalyst prepared under explained general procedure with a 12 h as the reaction time. The crude product was purified via column chromatography (20 x 250 mm, 3:1 to 1:1 hexane: ethyl acetate as eluent) and epoxide **II-175** was obtained as a white solid in 50% isolated yield (0.25 mmol, 63 mg). The enantiomeric excess of epoxide **II-175** was determined to be 86% with chiral HPLC (PIRKLE COVALENT (R,R) WHELK-O 1 column, 90:10 hexane/2-propanol at 228 nm, flow-rate: 1 mL/min): retention times:  $R_t$  = 16.42 min (minor enantiomer, ent-**II-175**) and  $R_t$  = 19.3 min (major enantiomer, **II-175**). mp: 62-64  $^{\circ}$ C

$^1\text{H}$  NMR (500 MHz, Chloroform-*d*)  $\delta$  0.90 (ddd,  $J$  = 7.2, 5.4, 2.1 Hz, 3H), 1.39 – 1.53 (m, 4H), 3.16 (pd,  $J$  = 4.9, 4.0, 1.8 Hz, 1H), 3.51 (d,  $J$  = 4.8 Hz, 1H), 3.79 (s, 3H), 4.33 (dd,  $J$  = 14.5, 5.7 Hz, 1H), 4.45 (dd,  $J$  = 14.4, 6.2 Hz, 1H), 6.41 (s, 1H), 6.81 – 6.88 (m, 2H), 7.15 – 7.22 (m, 2H).  $^{13}\text{C}$  NMR (126 MHz, Chloroform-*d*)  $\delta$  13.83, 19.37, 29.61, 42.37, 55.19, 55.28, 58.50, 114.08, 129.26, 129.79, 159.11, 167.19. IR: 3270brs, 2963w, 1645s, 1511s, 1241s, 1031m, 605s, 569m. HRMS (ESI-TOF)  $m/z$  250.1465, [(M+H) $^+$ ]; calcd for  $\text{C}_{14}\text{H}_{20}\text{NO}_3$ : 250.1443] [ $\alpha$ ] $^{20}_{\text{D}}$  (*c* 1.0,  $\text{CHCl}_3$ ): 0.1538.



**(2R, 3R)-3-cyclohexyl-N-benzyl-oxirane-2-carboxamide II-176:** Epoxide **II-176** was synthesized from cyclohexanecarboxaldehyde (0.60 mmol, 73  $\mu$ L) and diazo compound **II-112b** (0.50 mmol, 88 mg) catalyzed by aluminum-(S)-VAPOL catalyst prepared with the general procedure with a 12 h reaction time. The crude product was purified via column chromatography (20 x 250 mm, 3:1 to 1:1 hexane: ethyl acetate as eluent) and epoxide **II-176** was obtained as a white solid in 68% isolated yield (0.34 mmol, 89 mg). The enantiomeric excess of epoxide **II-176** was determined to be 88% with chiral HPLC (PIRKLE COVALENT (*R,R*) WHELK-O 1 column, 90:10 hexane/2-propanol at 228 nm, flow-rate: 1 mL/min): retention times:  $R_t$  = 16.42 min (minor enantiomer, ent-**II-176**) and  $R_t$  = 19.29 min (major enantiomer, **II-176**).

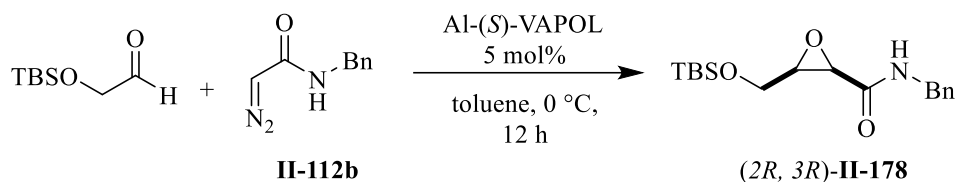
$^1\text{H}$  NMR (500 MHz, Chloroform-*d*)  $\delta$  0.85-1.10 (m, 6H), 1.52-1.61 (m, 4H), 1.75 (d,  $J$  = 11.0 Hz, 1H), 2.79 (s, 1H), 3.45 (d,  $J$  = 3.5 Hz, 1H), 4.22 (dd,  $J$  = 14.5, 5.0 Hz, 1H), 4.55 (dd,  $J$  = 14.5, 7.0 Hz, 1H), 6.51 (brs, 1H), 7.18-7.25 (m, 5H).  $^{13}\text{C}$  NMR (126 MHz, Chloroform-*d*)  $\delta$  25.06, 25.85, 28.22, 30.30, 36.50, 42.70, 55.08, 62.60, 127.51, 127.79, 128.60, 137.80, 167.26 (one  $\text{sp}^3$  carbon not located). These spectral data were in agreement with literature values.<sup>19</sup>



**(2S, 3S)-3-cyclohexyl-N-benzyl-oxirane-2-carboxamide II-177:** Epoxide **II-177** was synthesized from 2,2-dimethylpropanal (0.60 mmol, 65  $\mu$ L) and diazo compound **II-112b** (0.50 mmol, 88 mg) catalyzed by aluminum-(R)-VAPOL catalyst prepared under explained general procedure with a

12 h as the reaction time. The crude product was purified via column chromatography (20 x 250 mm, 3:1 to 1:1 hexane: ethyl acetate as eluent) and epoxide **II-177** was obtained as a white solid in 50% isolated yield (0.250 mmol, 58.3 mg). The enantiomeric excess of epoxide **II-177** was determined to be 99% with chiral HPLC (Daicel Chirapack OD-H column, 94:6 hexane/2-propanol at 228 nm, flow-rate: 1 mL/min): retention times:  $R_t$  = 7.14 min (major enantiomer, ent-**II-177**) and  $R_t$  = 13.32 min (minor enantiomer, **II-177**).

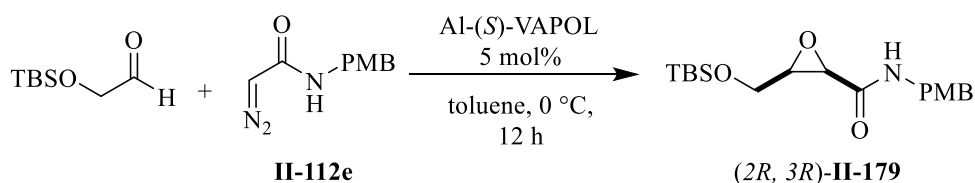
$^1\text{H}$  NMR (500 MHz, Chloroform- $d$ )  $\delta$  0.89 (s, 9H), 1.47 (d,  $J$  = 5.0 Hz, 1H), 1.37 (d,  $J$  = 5.0 Hz, 1H), 4.20 (dd,  $J$  = 14.0, 5.0 Hz, 1H), 4.48 (dd,  $J$  = 14.0, 6.0 Hz, 1H), 6.45 (brs, 1H), 7.20-7.30 (m, 5H).  $^{13}\text{C}$  NMR (126 MHz, Chloroform- $d$ )  $\delta$  26.46, 31.78, 43.35, 55.93, 67.25, 127.73, 128.24, 128.71, 136.90, 167.27. These spectral data were in agreement with literature values.<sup>19</sup>



*(2R,3R)-3-(2-((tert-butyldimethylsilyl)oxy)methyl)-N-benzyl-oxirane-2-carboxamide* **II-178**:

Epoxide **II-178** was synthesized from 2-((tert-butyldimethylsilyl)oxy)acetaldehyde (0.590 mmol, 115  $\mu\text{L}$ ) and diazo compound **II-112b** (0.50 mmol, 88 mg) catalyzed by aluminum-(*S*)-VAPOL catalyst prepared with the general procedure with a 12 h reaction time. The crude product was purified via column chromatography (20 x 250 mm, 3:1 to 1:1 hexane: ethyl acetate as eluent) and epoxide **II-178** was obtained as a yellowish oil in 78% isolated yield (0.390 mmol, 125 mg). The enantiomeric excess of epoxide **II-178** was determined to be 56% with chiral HPLC (PIRKLE COVALENT (*R,R*) WHELK-O 1 column, 90:10 hexane/2-propanol at 228 nm, flow-rate: 1 mL/min): retention times:  $R_t$  = 20.67 min (minor enantiomer, ent-**II-178**) and  $R_t$  = 22.98 min (major enantiomer, **II-178**).

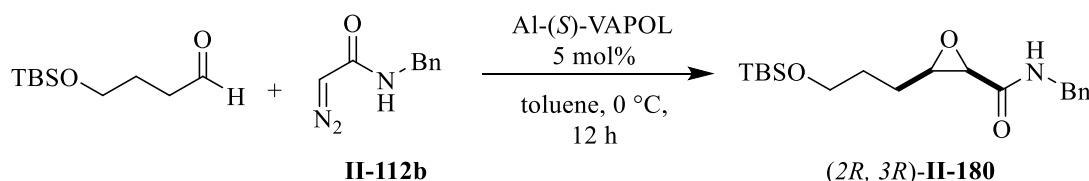
$^1\text{H}$  NMR (500 MHz, Chloroform-*d*)  $\delta$  -0.02 (s, 6H), 0.86 (s, 9H), 3.32 – 3.39 (m, 1H), 3.43 – 3.51 (m, 1H), 3.59 (d,  $J$  = 4.8 Hz, 1H), 3.88 (dd,  $J$  = 12.1, 3.2 Hz, 1H), 4.36 (dd,  $J$  = 14.6, 5.6 Hz, 1H), 4.53 (dd,  $J$  = 14.5, 6.5 Hz, 1H), 6.48 (d,  $J$  = 6.3 Hz, 1H), 7.23 – 7.33 (m, 3H), 7.30 – 7.37 (m, 2H).  $^{13}\text{C}$  NMR (126 MHz, Chloroform-*d*)  $\delta$  -5.38, -5.36, 18.28, 25.80, 43.01, 54.06, 58.77, 61.24, 127.83, 127.96, 128.85, 137.42, 166.47. IR: 3299brs, 2930w, 1658s, 1512s, 1248s, 1092s, 1034m, 834s, 776m. HRMS (ESI-TOF)  $m/z$  322.1872, [(M+H) $^+$ ]; calcd for C<sub>17</sub>H<sub>28</sub>NO<sub>3</sub>Si: 322.1838]. [ $\alpha$ ] $^{20}_{\text{D}}$  (*c* 1.0, CHCl<sub>3</sub>): 0.0252.



**(2R,3R)-3-(2-((tert-butyldimethylsilyl)oxy)methyl)-N-(4-methoxy-phenyl)-oxirane-2-carboxamide II-179:** Epoxide **II-179** was synthesized from 2-((tert-butyldimethylsilyl)oxy)acetaldehyde (0.590 mmol, 115  $\mu\text{L}$ ) and diazo compound **II-112e** (0.490 mmol, 103 mg) catalyzed by aluminum-(*S*)-VAPOL catalyst prepared under explained general procedure with a 12 h as the reaction time. The crude product was purified via column chromatography (20 x 250 mm, 3:1 to 1:1 hexane: ethyl acetate as eluent) and epoxide **II-179** was obtained as a yellowish oil in 73% isolated yield (0.365 mmol, 128 mg). The enantiomeric excess of epoxide **II-179** was determined to be 50% with chiral HPLC (PIRKLE COVALENT (*R,R*) WHELK-O 1 column, 90:10 hexane/2-propanol at 228 nm, flow-rate: 1 mL/min): retention times:  $R_t$  = 19.69 min (minor enantiomer, ent-**II-179**) and  $R_t$  = 23.44 min (major enantiomer, **II-179**).

$^1\text{H}$  NMR (500 MHz, Chloroform-*d*)  $\delta$  0.03 (s, 6H), 0.86 (s, 9H), 3.30 – 3.37 (m, 1H), 3.40 – 3.50 (m, 1H), 3.56 (d,  $J$  = 4.8 Hz, 1H), 3.79 (s, 2H), 3.86 (dd,  $J$  = 12.1, 3.1 Hz, 1H), 4.28 (dd,  $J$  = 14.4, 5.5 Hz, 1H), 4.46 (dd,  $J$  = 14.4, 6.5 Hz, 1H), 6.44 (t,  $J$  = 6.0 Hz, 1H), 6.81 – 6.88 (m, 2H), 7.13 –

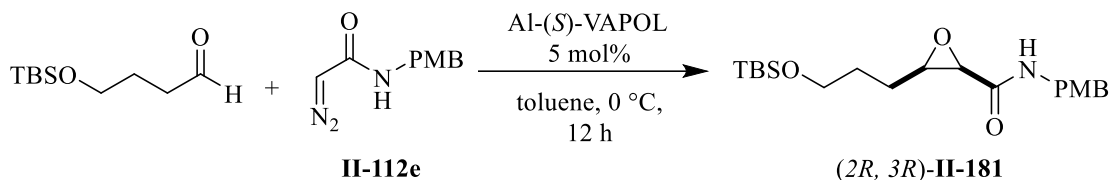
7.23 (m, 2H).  $^{13}\text{C}$  NMR (126 MHz, Chloroform-*d*)  $\delta$  -5.38, -5.37, 18.28, 25.80, 42.44, 54.03, 55.27, 58.74, 61.22, 114.18, 129.33, 129.57, 159.19, 166.35. IR: 3299brs, 2928w, 1661s, 1092s, 834s, 777m, 731w, 697m. HRMS (ESI-TOF)  $m/z$  352.1964, [(M+H<sup>+</sup>); calcd for C<sub>18</sub>H<sub>30</sub>NO<sub>4</sub>Si: 352.1944].  $[\alpha]_D^{20}$  (*c* 1.0, CHCl<sub>3</sub>): 0.1218.



*(2R,3R)*-3-(2-((*tert*-butyldimethylsilyl)oxy)propyl)-*N*-benzyl-oxirane-2-carboxamide **II-180**:

Epoxide **II-180** was synthesized from 4-((*tert*-butyldimethylsilyl)oxy)butanal (0.590 mmol, 135  $\mu\text{L}$ ) and diazo compound **II-112b** (0.50 mmol, 88 mg) catalyzed by aluminum-(*S*)-VAPOL catalyst prepared with the general procedure with a 12 h reaction time. The crude product was purified via column chromatography (20 x 250 mm, 3:1 to 1:1 hexane: ethyl acetate as eluent) and epoxide **II-180** was obtained as a yellowish oil in 84% isolated yield (0.420 mmol, 159 mg). The enantiomeric excess of epoxide **II-180** was determined to be 50% with chiral HPLC (PIRKLE COVALENT (*R,R*) WHELK-O 1 column, 90:10 hexane/2-propanol at 228 nm, flow-rate: 1 mL/min): retention times:  $R_t$  = 12.98 min (minor enantiomer, ent-**II-180**) and  $R_t$  = 15.55 min (major enantiomer, **II-180**).

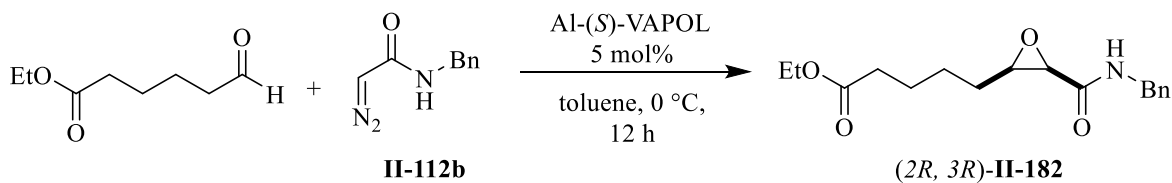
$^1\text{H}$  NMR (500 MHz, Chloroform-*d*)  $\delta$  0.01 (s, 6H), 0.88 (s, 9H), 1.52 – 1.65 (m, 2H), 1.66 (tdd,  $J$  = 10.3, 6.0, 2.0 Hz, 2H), 3.21 (td,  $J$  = 6.3, 4.8 Hz, 1H), 3.52 – 3.66 (m, 3H), 4.45 (qd,  $J$  = 14.7, 6.0 Hz, 2H), 6.48 (t,  $J$  = 6.2 Hz, 1H), 7.23 – 7.37 (m, 5H).  $^{13}\text{C}$  NMR (126 MHz, Chloroform-*d*)  $\delta$  -5.34, 18.00, 18.28, 24.42, 25.91, 29.18, 42.96, 55.34, 58.55, 62.26, 127.72, 127.90, 128.76, 137.59, 167.28. IR: 3301brs, 2928w, 1660s, 1095s, 833s, 774s, 698w. HRMS (ESI-TOF)  $m/z$  350.2239, [(M+H<sup>+</sup>); calcd for C<sub>19</sub>H<sub>32</sub>NO<sub>3</sub>Si: 350.2151].



*(2R,3R)*-3-(2-((*tert*-butyldimethylsilyl)oxy)propyl)-*N*-(4-methoxy-benzyl)-oxirane-2-carboxamide

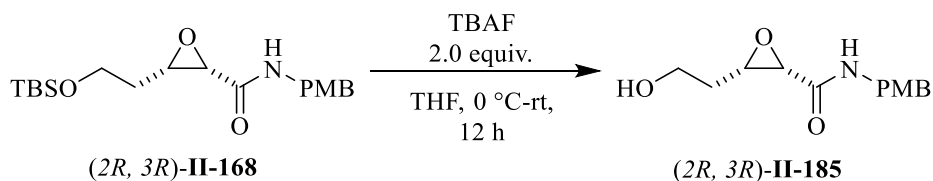
**II-181**: Epoxide **II-181** was synthesized from 4-((*tert*-butyldimethylsilyl)oxy)butanal (0.599 mmol, 135  $\mu$ L) and diazo compound **II-112e** (0.499 mmol, 103 mg) catalyzed by aluminum-(*S*)-VAPOL catalyst prepared with the general procedure with a 12 h reaction time. The crude product was purified via column chromatography (20 x 250 mm, 3:1 to 1:1 hexane: ethyl acetate as eluent) and epoxide **II-181** was obtained as a yellowish oil in 67% isolated yield (0.335 mmol, 127 mg). The enantiomeric excess of epoxide **II-181** was determined to be 51% with chiral HPLC (PIRKLE COVALENT (*R,R*) WHELK-O 1 column, 90:10 hexane/2-propanol at 228 nm, flow-rate: 1 mL/min): retention times:  $R_t$  = 30.97 min (minor enantiomer, ent-**II-181**) and  $R_t$  = 41.86 min (major enantiomer, **II-181**).

$^1\text{H}$  NMR (500 MHz, Chloroform-*d*)  $\delta$  0.01 (s, 6H), 0.87 (s, 9H), 1.50 – 1.62 (m, 2H), 1.59 – 1.70 (m, 2H), 3.20 (td,  $J$  = 6.3, 4.7 Hz, 1H), 3.53 (d,  $J$  = 4.8 Hz, 1H), 3.54 – 3.64 (m, 2H), 3.79 (s, 3H), 4.32 – 4.44 (m, 2H), 6.40 (t,  $J$  = 5.9 Hz, 1H), 6.81 – 6.88 (m, 2H), 7.15 – 7.22 (m, 2H).  $^{13}\text{C}$  NMR (126 MHz, Chloroform-*d*)  $\delta$  -5.36, 18.27, 24.40, 25.90, 29.19, 42.40, 55.26, 55.33, 58.51, 62.27, 114.09, 129.25, 129.71, 159.12, 167.11. IR: 3309brs, 2928w, 1662s, 1512s, 1247s, 1095s, 1035w, 833s, 774s, 731w. HRMS (ESI-TOF)  $m/z$  380.2338, [( $\text{M}+\text{H}^+$ ); calcd for  $\text{C}_{20}\text{H}_{34}\text{NO}_4\text{Si}$ : 380.2257]  $[\alpha]_D^{20}$  ( $c$  1.0,  $\text{CHCl}_3$ ): 0.054.



*Ethyl 5-((2S,3S)-3-(benzylcarbamoyl)oxiran-2-yl)pentanoate II-182*: Epoxide **II-182** was synthesized from ethyl 6-oxohexanoate (0.60 mmol, 95 mg) and diazo compound **II-112b** (0.50 mmol, 88 mg) catalyzed by 5 mol% aluminum-(*S*)-VAPOL catalyst prepared with the general procedure with a 12 h reaction time. The crude product was purified via column chromatography (20 x 250 mm, 3:1 to 1:1 hexane: ethyl acetate as eluent) and epoxide **II-182** was obtained as a yellowish oil in 75% isolated yield (0.370 mmol, 113 mg). The enantiomeric excess of epoxide **II-182** was determined to be 76% with chiral HPLC (PIRKLE COVALENT (*R,R*) WHELK-O 1 column, 85:15 hexane/2-propanol at 228 nm, flow-rate: 1 mL/min): retention times:  $R_t = 33.45$  min (minor enantiomer, ent-**II-182**) and  $R_t = 39.6$  min (major enantiomer, **II-182**).

$^1\text{H}$  NMR (500 MHz, Chloroform-*d*)  $\delta$  1.25 (t,  $J = 7.2$  Hz, 4H), 1.49 (qdt,  $J = 9.9, 7.5, 3.6$  Hz, 3H), 1.55 – 1.65 (m, 2H), 2.25 (t,  $J = 7.4$  Hz, 2H), 3.12 – 3.20 (m, 1H), 3.54 (d,  $J = 4.7$  Hz, 1H), 4.12 (q,  $J = 7.1$  Hz, 2H), 4.41 (dd,  $J = 14.6, 5.8$  Hz, 1H), 4.51 (dd,  $J = 14.6, 6.3$  Hz, 1H), 6.48 (t,  $J = 5.8$  Hz, 1H), 7.25 – 7.37 (m, 5H).  $^{13}\text{C}$  NMR (126 MHz, Chloroform-*d*)  $\delta$  14.25, 24.52, 25.53, 27.39, 33.94, 42.95, 55.21, 58.34, 60.31, 127.74, 127.93, 128.78, 137.64, 167.15, 173.31. IR: 3325brs, 2930w, 1729s, 1662s, 1572s, 1162s, 699s. HRMS (ESI-TOF)  $m/z$  306.1732, [(M+H) $^+$ ]; calcd for  $\text{C}_{17}\text{H}_{24}\text{NO}_4$ : 306.1705]  $[\alpha]_D^{20}$  (c 1.0,  $\text{CHCl}_3$ ): 0.1193.

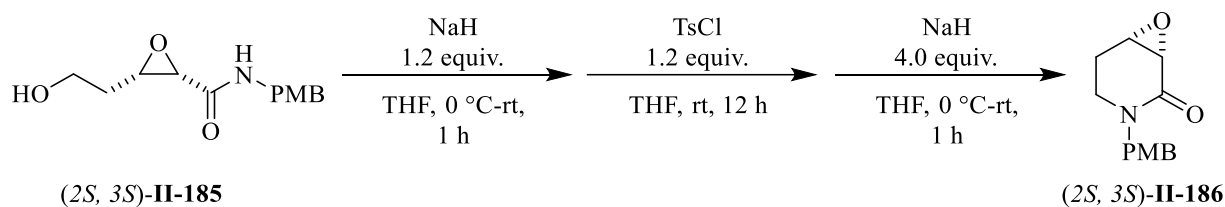


*(2R,3R)-3-(2-hydroxyethyl)-N-(4-methoxybenzyl)oxirane-2-carboxamide II-185*: To a solution of epoxide **II-168** (0.490 mmol, 183 mg) in 5 mL THF in a 25 mL round bottom flask at 0 °C was added tetrabutylammonium fluoride (1 mmol, 1M solution in THF, 1 mL) and the resulting solution was stirred at room temperature for 12 h. After removing the solvent under reduced



pressure the resulting crude mixture was purified via column chromatography (20 x 250 mm, 1:1 hexane: ethyl acetate, pure ethyl acetate and 19:1 ethyl acetate: methanol) and compound **II-185** was obtained as a white solid in 84% yield (0.420 mmol, 106 mg). mp: 75-76 °C.

<sup>1</sup>H NMR (500 MHz, Chloroform-*d*) δ 1.70 – 1.82 (m, 2H), 3.34 (td, *J* = 6.4, 4.8 Hz, 1H), 3.57 (d, *J* = 4.8 Hz, 1H), 3.80 (s, 3H), 3.75 – 3.87 (m, 2H), 4.32 – 4.45 (m, 2H), 6.44 (s, 1H), 6.83 – 6.90 (m, 2H), 7.14 – 7.25 (m, 2H). <sup>13</sup>C NMR (126 MHz, Chloroform-*d*) δ 30.76, 42.52, 54.77, 55.30, 56.47, 59.71, 114.14, 129.32, 129.51, 159.18, 167.16. IR: 3259brs, 1646s, 1511s, 1249s, 1031s, 806s, 572m. HRMS (ESI-TOF) *m/z* 274.1138, [(M+Na<sup>+</sup>); calcd for C<sub>13</sub>H<sub>17</sub>NO<sub>4</sub>Na: 273.0977], [α]<sub>D</sub><sup>20</sup> (c 1.0, CHCl<sub>3</sub>): 0.0161.

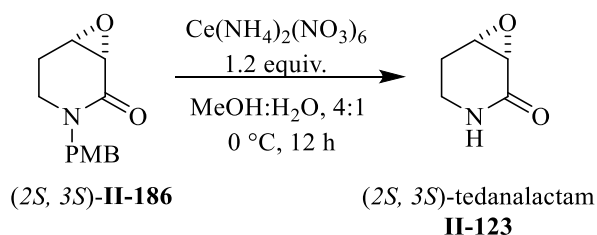


(1*S*,6*S*)-3-(4-methoxybenzyl)-7-oxa-3-azabicyclo[4.1.0]heptan-2-one **II-186**. A flamed dried 25 mL round bottom flask was charged with compound **II-185** (0.499 mmol, 126 mg), and 5 mL THF. Then the resulting solution was cooled down to 0 °C, followed by addition of NaH (0.5 mmol, 60% dispersed in mineral oil, 20 mg). The reaction was warmed up to room temperature and stirred for an additional 1 h. Next, the reaction vessel was cooled down to 0 °C and freshly purified 4-toluenesulfonyl chloride (0.590 mmol, 115 mg) was slowly added. The resulting solution was warmed up to room temperature and stirred for another hour. After cooling down the temperature of the reaction to 0 °C, NaH (2.0 mmol, 60% dispersed in mineral oil, 80 mg) was added slowly followed by gradual warming up to room temperature and stirring at ambient temperature for 1 h. Then, the reaction was quenched with careful addition of saturated aq NH<sub>4</sub>Cl. The aqueous layer was separated and extracted three times with ethyl acetate. The combined organic layer was

washed with brine, dried over Na<sub>2</sub>SO<sub>4</sub> and purified via column chromatography (20 x 250 mm, 2:1 to 0:1 hexane: ethyl acetate). Compound **II-186** was obtained as pure white solid in 67% yield (0.33 mmol, 78 mg). The structure of this compound was confirmed unequivocally with x-ray structural analysis (CCDC number: 1972358). mp: 67-68 °C. mp of crystal: 68-69 °C.

<sup>1</sup>H NMR (500 MHz, Chloroform-*d*) δ 1.90 (ddd, *J* = 14.4, 12.7, 6.1 Hz, 1H), 2.23 (dq, *J* = 14.6, 2.7, 2.2 Hz, 1H), 2.86 – 2.95 (m, 1H), 3.28 (td, *J* = 12.6, 4.3 Hz, 1H), 3.53 (d, *J* = 4.1 Hz, 1H), 3.58 (t, *J* = 3.4 Hz, 1H), 3.78 (d, *J* = 2.0 Hz, 3H), 4.38 (d, *J* = 14.6 Hz, 1H), 4.59 (d, *J* = 14.5 Hz, 1H), 6.81 – 6.87 (m, 2H), 7.11 – 7.18 (m, 2H). <sup>13</sup>C NMR (126 MHz, Chloroform-*d*) δ 24.10, 39.84, 49.79, 50.98, 53.04, 55.26, 114.02, 128.54, 129.26, 159.06, 166.66. IR: 1641s, 1512m, 1246s, 811m, 588m. HRMS (ESI-TOF) *m/z* 234.1153, [(M+H)<sup>+</sup>]; calcd for C<sub>13</sub>H<sub>16</sub>NO<sub>3</sub>: 234.1130], [α]<sup>20</sup><sub>D</sub> (*c* 1.0, CHCl<sub>3</sub>): 0.3521.

The crystal of compound **II-186** was grown under following condition: 20 mg of compound **II-186** was dissolved in 5 mL of anhydrous diethylether in a 20 mL vial. Then the vial was covered with a aluminum foil which had holes in it. Slow evaporation of diethyl ether, induced the subsequent crystal growth.



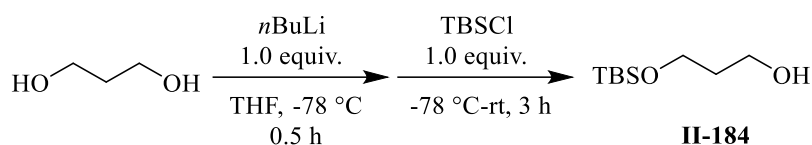
(–)-tedanalactam **II-123**: To the stirring solution of compound **II-186** (0.490 mmol, 117 mg) in 12.5 mL methanol: water (4:1) at 0 °C was added Ce(NH<sub>4</sub>)<sub>2</sub>(NO<sub>3</sub>)<sub>6</sub> (0.590 mmol, 329 mg) and the resulting mixture was stirred at 0 °C for 12 hour. The reaction was quenched with the addition of saturated NH<sub>4</sub>Cl. The aqueous layer was separated and extracted three times with ethyl acetate. The combined organic layer was washed with brine, dried over Na<sub>2</sub>SO<sub>4</sub> and purified via column

chromatography (20 x 250 mm, 2:1 to 0:1 hexane: ethyl acetate then 19:1 ethyl acetate: methanol).

Compound **II-123** was obtained as a yellow oil in 75% yield (0.375 mmol, 42.1 mg).

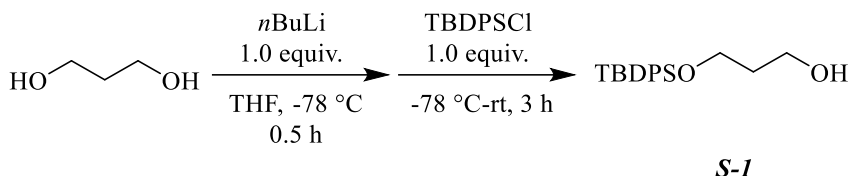
$^1\text{H}$  NMR (500 MHz, Chloroform-*d*)  $\delta$  1.95 – 2.07 (m, 1H), 2.28 (dddd,  $J$  = 14.6, 4.3, 2.8, 1.2 Hz, 1H), 3.03 (dt,  $J$  = 12.3, 6.1, 1.4 Hz, 1H), 3.27 – 3.46 (m, 2H), 3.58 – 3.63 (m, 1H), 6.66 (s, 1H).

$^{13}\text{C}$  NMR (126 MHz, Chloroform-*d*)  $\delta$  23.51, 35.27, 50.66, 53.14, 169.14. HRMS (ESI-TOF)  $m/z$  114.0584,  $[(\text{M}+\text{H}^+)]$ ; calcd for  $\text{C}_5\text{H}_7\text{NO}_2$ : 114.0555],  $[\alpha]^{20}_{\text{D}}$  (0.1 M, MeOH): -7.1. Literature value:  $[\alpha]^{20}_{\text{D}}$  (0.1 M, MeOH): -7.9 These data matched with literature values.<sup>20,21</sup>



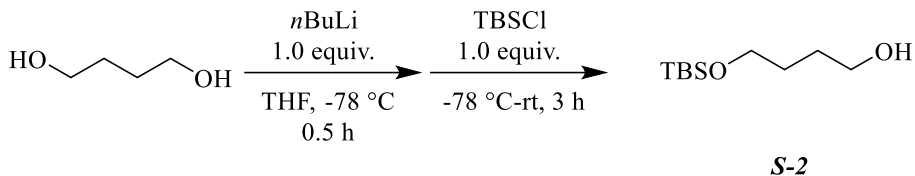
*General procedure 2: mono-protection of diol:*<sup>27</sup>

*3-((tert-butyldimethylsilyl)oxy)propan-1-ol II-184:* To a stirring solution of 1,3-propan-diol (42 mmol, 3.0 mL) in 80 mL of THF at -78 °C was added *n*-BuLi (42 mmol, 2.5 M in hexane, 17 mL) and the resulting solution was stirred at the same temperature for 30 minutes. Then a solution of *t*BuMe<sub>2</sub>SiCl (42.1 mmol, 6.33 g) in 10 mL THF was added to the stirring solution at -78 °C followed by warming up the reaction vessel to room temperature and stirring it at ambient temperature for 3 h. The reaction was quenched by slow addition of saturated NH<sub>4</sub>Cl. Then the aqueous layer was separated, extracted three times with diethyl ether. The combined organic layer was washed with brine and dried over Na<sub>2</sub>SO<sub>4</sub>. After removing the solvent under reduced pressure, the crude mixture was purified via column chromatography (20 x 250 mm, 5:1 to 2:1 hexane: ethyl acetate) and the desired product was obtained as a colorless oil in 90% isolated yield (38 mmol, 7.2 g).  $^1\text{H}$  NMR (500 MHz, Chloroform-*d*)  $\delta$  -0.02 (s, 6H), 0.86 (s, 9H), 1.73 (p,  $J$  = 5.7 Hz, 2H), 3.73 (m, 2H) 3.75 (dt,  $J$  = 5.2 Hz, 2H).  $^{13}\text{C}$  NMR (126 MHz, Chloroform-*d*)  $\delta$  -5.51, 18.17, 25.86, 34.13, 62.47, 62.97. These data are in agreement with literature values.<sup>27</sup>



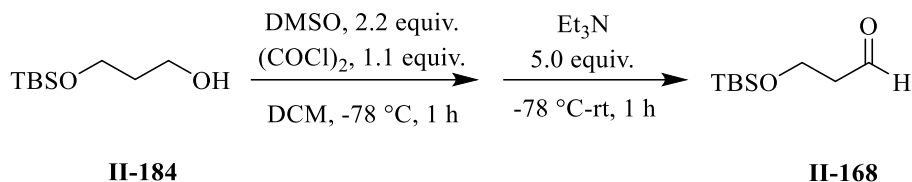
**3-((tert-butyldiphenylsilyl)oxy)propan-1-ol S1:** Compound **S1** was synthesized from 1,3-propanediol (42 mmol, 3.1 mL) and *t*BuPh<sub>2</sub>SiCl (42.01 mmol, 11.54 g) with the general procedure 2. The resulting alcohol **S1** was purified via column chromatography (20 x 250 mm, 5:1 to 2:1 hexane: ethyl acetate) and a white solid was afforded as the pure product in 87% yield (36.54 mmol, 11.49 g).

<sup>1</sup>H NMR (500 MHz, Chloroform-*d*) δ 1.07 (s, 9H), 1.83 (p, *J* = 5.7 Hz, 2H), 2.42 (s, 1H), 3.86 (t, *J* = 5.6 Hz, 4H), 7.37 – 7.45 (m, 4H), 7.42 – 7.49 (m, 2H), 7.67 – 7.75 (m, 4H). <sup>13</sup>C NMR (126 MHz, Chloroform-*d*) δ 19.09, 26.83, 34.20, 62.06, 63.37, 127.77, 129.80, 133.20, 135.55. These data are in agreement with literature values.<sup>28</sup>



**4-((tert-butyldimethylsilyl)oxy)butan-1-ol S2:** Compound **S2** was synthesized from 1,3-butanediol (34 mmol, 3.0 mL) and *t*BuMe<sub>2</sub>SiCl (34 mmol, 5.1 g) with the general procedure 2. The resulting alcohol **S2** was purified via column chromatography (20 x 250 mm, 5:1 to 2:1 hexane: ethyl acetate) and a colorless oil was afforded as the pure product in 76% yield (25.8 mmol, 5.28 g).

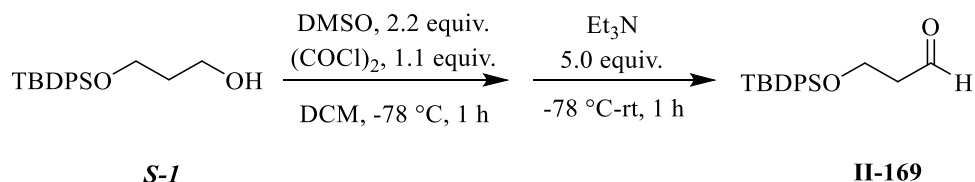
<sup>1</sup>H NMR (500 MHz, Chloroform-*d*) δ 0.06 (s, 6H), 0.89 (s, 9H), 1.57 – 1.70 (m, 4H), 3.60 – 3.69 (m, 4H). <sup>13</sup>C NMR (126 MHz, Chloroform-*d*) δ -5.42, 18.28, 25.88, 29.88, 30.24, 62.74, 63.34. These data are in agreement with literature values.<sup>29</sup>



*General procedure 3: Swern oxidation:*

*3-((tert-butyldimethylsilyl)oxy)propanal II-168:* In a flamed dried 500 mL round bottom flask under N<sub>2</sub>, DMSO (33 mmol, 2.3 mL) and CH<sub>2</sub>Cl<sub>2</sub> (100 mL) were added. Then the reaction vessel was cooled down to -78 °C and a solution of oxalyl chloride (16.5 mmol, 1.01 mL) in 10 mL CH<sub>2</sub>Cl<sub>2</sub> was slowly added. After 10 minutes, alcohol **II-184** (15 mmol, 2.8 g) as a solution in 7.5 mL of CH<sub>2</sub>Cl<sub>2</sub> was added slowly and the reaction mixture was stirred at -78 °C for 1 h. The reaction mixture was warmed up to room temperature after the addition of Et<sub>3</sub>N (75 mmol, 10 mL) and it was quenched by the addition of saturated NH<sub>4</sub>Cl. The organic layer was separated and washed with saturated CuSO<sub>4</sub> solution and brine. The resulting solution was dried over Na<sub>2</sub>SO<sub>4</sub> and the solvent was removed under reduced pressure. Simple distillation (b.p. 65 °C, 1 mmHg) afforded pure aldehyde **II-168** as a colorless oil in quantitative yield (15 mmol, 2.8 g).

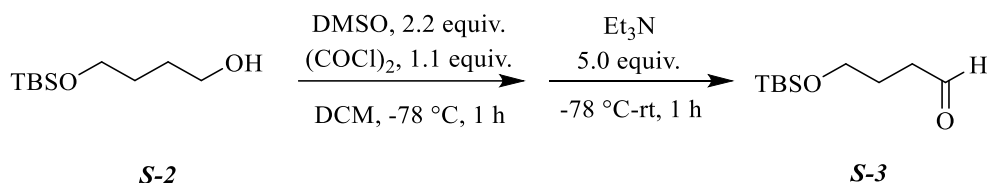
<sup>1</sup>H NMR (500 MHz, Chloroform-*d*) δ 0.06 (s, 6H), 0.86 (t, *J* = 1.2 Hz, 9H), 2.57 (tdd, *J* = 6.0, 2.2, 0.9 Hz, 2H), 3.97 (td, *J* = 6.0, 0.9 Hz, 2H), 9.78 (td, *J* = 2.0, 0.8 Hz, 1H). <sup>13</sup>C NMR (126 MHz, Chloroform-*d*) δ -5.47, 18.19, 25.78, 46.53, 57.37, 202.01. These data are in good agreement with literature values.<sup>30</sup>



*3-((tert-butyldiphenylsilyl)oxy)propanal II-169:* Aldehyde **II-169** was prepared from alcohol **S1** (9.5 mmol, 3.1 g) with the general procedure 3 and purified via column chromatography (20 x 250

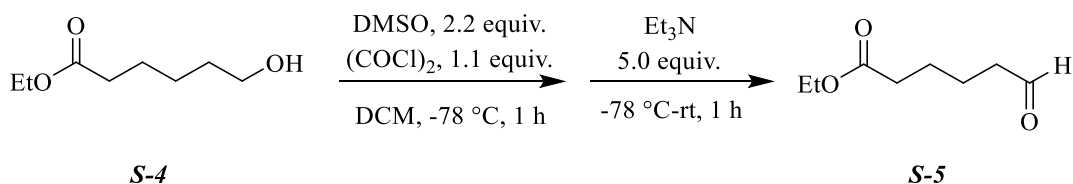
mm, 19:1 to 9:1 hexane: ethyl acetate) which afforded a white solid as the pure product in 78% yield (7.41 mmol, 2.32 g).

$^1\text{H}$  NMR (500 MHz, Chloroform-*d*)  $\delta$  1.04 (s, 9H), 2.61 (td,  $J = 6.0, 2.2$  Hz, 2H), 4.03 (t,  $J = 6.0$  Hz, 2H), 7.36 – 7.44 (m, 4H), 7.41 – 7.49 (m, 2H), 7.63 – 7.70 (m, 4H), 9.83 (t,  $J = 2.2$  Hz, 1H).  $^{13}\text{C}$  NMR (126 MHz, Chloroform-*d*)  $\delta$  19.13, 26.74, 46.37, 58.27, 127.76, 129.81, 133.21, 135.53, 201.95. These data are in agreement with literature values.<sup>31</sup>



*4-((tert-butyldimethylsilyl)oxy)butanal S-3*: Aldehyde **S-3** was prepared from alcohol **S-2** (14.7 mmol, 3.01 g) with the general procedure 3 and purified via column chromatography (20 x 250 mm, 19:1 to 9:1 hexane: ethyl acetate) which afforded a colorless oil as the pure product in quantitative yield (14.7 mmol, 2.97 g).

$^1\text{H}$  NMR (500 MHz, Chloroform-*d*)  $\delta$  0.03 (s, 6H), 0.89 (s, 9H), 1.86 (tt,  $J = 7.0, 6.0$  Hz, 2H), 2.51 (td,  $J = 7.1, 1.7$  Hz, 2H), 3.65 (t,  $J = 6.0$  Hz, 2H), 9.79 (t,  $J = 1.7$  Hz, 1H). These data are in agreement with the literature values.<sup>29</sup>



*ethyl 6-oxohexanoate S-5*: Aldehyde **S-5** was prepared from ethyl 6-hydroxyhexanoate **S-4** (18 mmol, 3.0 mL) with the general procedure 3 and purified via simple distillation which afforded the pure product as a colorless oil in 80% yield (14.72 mmol, 2.328 g).

$^1\text{H}$  NMR (500 MHz, Chloroform-*d*)  $\delta$  1.21 (t,  $J = 7.1$  Hz, 3H), 1.57 – 1.69 (m, 4H), 2.24 – 2.33 (m, 2H), 2.39 – 2.47 (m, 2H), 4.08 (q,  $J = 7.2$  Hz, 2H), 9.73 (t,  $J = 1.6$  Hz, 1H).  $^{13}\text{C}$  NMR (126 MHz, Chloroform-*d*)  $\delta$  14.19, 21.44, 24.32, 33.92, 43.46, 60.29, 173.18, 202.06. These data are in agreement with literature value.<sup>32</sup>

## REFERENCES



## REFERENCES

- 1) Nishide, K.; Node, M., “Recent Development of Asymmetric Syntheses Based on the Meerwein-Ponndorf-Verley Reduction.” *Chirality* **2002**, *14*, 759–67.
- 2) Campbell, E. J.; Zhou, H.; Nguyen, S. T., “Catalytic Meerwein–Pondorf–Verley Reduction by Simple Aluminum Complexes.” *Org. Lett.* **2001**, *3*, 2391–2393.
- 3) Campbell, E. J.; Zhou, H.; Nguyen, S. T., “The Asymmetric Meerwein--Schmidt--Ponndorf--Verley Reduction of Prochiral Ketones with iPrOH Catalyzed by Al Catalysts.” *Angew. Chem. Int. Ed.* **2002**, *41*, 1020–1022.
- 4) Cohen, R.; Graves, C. R.; Nguyen, S. T.; Martin, J. M. L.; Ratner, M. A., “The Mechanism of Aluminum-Catalyzed Meerwein–Schmidt–Ponndorf–Verley Reduction of Carbonyls to Alcohols.” *J. Am. Chem. Soc.* **2004**, *126*, 14796–14803.
- 5) Graves, C. R.; Zhou, H.; Stern, C. L.; Nguyen, S. T., “A Mechanistic Investigation of the Asymmetric Meerwein–Schmidt–Ponndorf–Verley Reduction Catalyzed by BINOL/AlMe<sub>3</sub> Structure, Kinetics, and Enantioselectivity.” *J. Org. Chem.* **2007**, *72*, 9121–9133.
- 6) Lebedev, Y.; Polishchuk, I.; Maity, B.; Guerreiro, M. D. V.; Cavallo, L.; Rueping, M., “Asymmetric Hydroboration of Heteroaryl Ketones by Aluminum Catalysis.” *J. Am. Chem. Soc.* **2019**, *141*, 19415–19423.
- 7) Arai, T.; Bougauchi, M.; Sasai, H.; Shibasaki, M., “Catalytic Asymmetric Synthesis of  $\alpha$ -Hydroxy Phosphonates Using the Al–Li–BINOL Complex.” *J. Org. Chem.* **1996**, *61*, 2926–2927.
- 8) Abell, J. P.; Yamamoto, H., “Catalytic Enantioselective Pudovik Reaction of Aldehydes and Aldimines with Tethered bis(8-Quinolinato) (TBOx) Aluminum Complex.” *J. Am. Chem. Soc.* **2008**, *130*, 10521–10523.
- 9) Abell, J. P.; Yamamoto, H., “Dual-Activation Asymmetric Strecker Reaction of Aldimines and Ketimines Catalyzed by a Tethered bis(8-Quinolinolato) Aluminum Complex.” *J. Am. Chem. Soc.* **2009**, *131*, 15118–15119.
- 10) Maruoka, K.; Banno, H.; Yamamoto, H., “Asymmetric Claisen Rearrangement Catalyzed by Chiral Organoaluminum Reagent.” *J. Am. Chem. Soc.* **1990**, *112*, 7791–7793.
- 11) Maruoka, K.; Saito, S.; Yamamoto, H., “Molecular Design of a Chiral Lewis Acid for the Asymmetric Claisen Rearrangement.” *J. Am. Chem. Soc.* **1995**, *117*, 1165–1166.

- 12) Maruoka, K.; Concepcion, A. B.; Yamamoto, H., "Asymmetric Diels-Alder Reaction of Cyclopentadiene and Methyl Acrylate Catalyzed by Chiral Organoaluminum Reagents." *Bull. Chem. Soc. Jpn.* **1992**, *65*, 3501–3503.
- 13) Heller, D. P.; Goldberg, D. R.; Wulff, W.D., "Positive Cooperativity of Product Mimics in the Asymmetric Autoinduction of Diels–Alder Reactions Catalyzed by a VAPOL–Aluminum Catalyst." *J. Am. Chem. Soc.* **1997**, *119*, 10551–10552.
- 14) Maruoka, K.; Itoh, T.; Shirasaka, T.; Yamamoto, H., "Asymmetric Hetero-Diels-Alder Reaction Catalyzed by a Chiral Organoaluminum Reagent." *J. Am. Chem. Soc.* **1988**, *110*, 310–312.
- 15) Maruoka, K.; Yamamoto, H., "Generation of Chiral Organoaluminum Reagent by Discrimination of the Racemates with Chiral Ketone." *J. Am. Chem. Soc.* **1989**, *111*, 789–90.
- 16) Arai, T.; Sasai, H.; Aoe, K.; Okamura, K.; Date, T.; Shibasaki, M., "A New Multifunctional Heterobimetallic Asymmetric Catalyst for Michael Additions and Tandem Michael- Aldol Reactions." *Angew. Chem. Int. Ed.* **1996**, *35*, 104–106.
- 17) Keller, E.; Veldman, N.; Spek, A. L.; Feringa, B. L., "Catalytic Enantioselective Michael Addition Reactions of  $\alpha$ -Nitroesters to  $\alpha,\beta$ -Unsaturated Ketones." *Tetrahedron: Asymmetry* **1997**, *8*, 3403-3413.
- 18) Arai, T.; Sasai, H.; Yamaguchi, K.; Shibasaki, M., "Regioselective Catalytic Asymmetric Reaction of Horner–Wadsworth–Emmons Reagents with Enones: The Odyssey of Chiral Aluminum Catalysts." *J. Am. Chem. Soc.* **1998**, *120*, 441–442.
- 19) Gupta, A. K.; Yin, X.; Mukherjee, M.; Desai, A.; Mohammadlou, A.; Jurewicz, K.; Wulff, W. D., "Catalytic Asymmetric Epoxidation of Aldehydes with Two VANOL-Derived Chiral Borate Catalysts." *Angew. Chem. Int. Ed.* **2019**, *58*, 3361–3367.
- 20) Cronan, J. M.; Cardellina, J. H., "A Novel  $\delta$ -Lactam from the Sponge *Tedania Ignis*." *Nat.l Prod. Lett.* **1994**, *5*, 85–88.
- 21) Lago, J. H. G.; Kato, M. J., "3 $\alpha$ ,4 $\alpha$ -Epoxy-2-Piperidone, a New Minor Derivative from Leaves of *Piper Crassinervium* Kunth (Piperaceae)." *Nat. Prod. Res.* **2007**, *21*, 910–914.
- 22) Majik, M. S.; Parameswaran, P. S.; Tilve, S. G., "Total Synthesis of (–)- and (+)-Tedanalactam." *J. Org. Chem.* **2009**, *74*, 6378–6381.
- 23) Konda, S.; Kurva, B.; Nagarapu, L.; Dattatray, A. M., "A Stereoselective Approach for the Total Synthesis of (–)-Tadanalactam from Acetonide-D-Glucose." *Tetrahedron Lett.* **2015**, *56*, 834–836.

- 24) Romero-Ibañez, J.; Xochicale-Santana, L.; Quintero, L.; Fuentes, L.; Sartillo-Piscil, F., "Synthesis of the Enantiomers of Tedanalactam and the First Total Synthesis and Configurational Assignment of (+)-Piplaroxide." *J. Nat. Prod.* **2016**, 79, 1174–1178.
- 25) Fuentes, L.; Osorio, U.; Quintero, L.; Höpfl, H.; Vázquez-Cabrera, N.; Sartillo-Piscil, F., "Direct Chemical Method for Preparing 2,3-Epoxyamides Using Sodium Chlorite." *J. Org. Chem.* **2012**, 77, 5515–5524.
- 26) Osorio-Nieto, U.; Vázquez-Amaya, L. Y.; Höpfl, H.; Quintero, L.; Sartillo-Piscil, F., "The Direct and Highly Diastereoselective Synthesis of 3,4-Epoxy-2-Piperidones. Application to the Total Synthesis and Absolute Configurational Assignment of 3 $\alpha$ ,4 $\alpha$ -Epoxy-5 $\beta$ -Pipermethystine." *Org. Biomol. Chem.* **2017**, 16, 77–88.
- 27) Han, J.; Liu, L.; Chang, Y.; Yue, G.; Guo, J.; Zhou, L.; Li, C.; Yang, Z., "Asymmetric Total Synthesis of Caribenol A via an Intramolecular Diels-Alder Reaction." *J. Org. Chem.* **2013**, 78, 5492–5504.
- 28) Barry, C. S.; Bushby, N.; Harding, J. R.; Willis, C. L., "Stereoselective Synthesis of the Tetrahydropyran Core of Polycarveroside A." *Org. Lett.* **2005**, 7, 2683–2686.
- 29) Trost, Barry M., and Mark J. Bartlett. 2012. "Transition-Metal-Catalyzed Synthesis of Aspergillide B: An Alkyne Addition Strategy." *Org. Lett.* 14, 1322–1325.
- 30) Liu, X.; Deaton, T. M.; Haeffner, F.; Morken, J. P., "A Boron Alkylidene-Alkene Cycloaddition Reaction: Application to the Synthesis of Aphanamal." *Angew. Chem. Int. Ed.* **2017**, 56, 11485–11489.
- 31) Wullschleger, C. W.; Gertsch, J.; Altmann, K., "Synthesis and Biological Activity of 7,8,9-Trideoxy- and 7 R DesTHP-Peloruside A." *Chem. Eur. J.* **2013**, 19, 13105–13111.
- 32) Sanford, A. B.; Thane, T. A.; McGinnis, T. M.; Chen, P.; Hong, X.; and Jarvo, E. R., "Nickel-Catalyzed Alkyl-Alkyl Cross-Electrophile Coupling Reaction of 1,3-Dimesylates for the Synthesis of Alkylcyclopropanes." *J. Am. Chem. Soc.* **2020**, 142, 5017–5023.

## **Chapter 3**

**Rational Design of VANOL/VAPOL Imidodiphosphorimidate Catalysts**

**And**

**Their Application in Asymmetric Halonium-Ion Induced Spiroketalization**

**And**

**Asymmetric Intramolecular Schmidt Reaction**

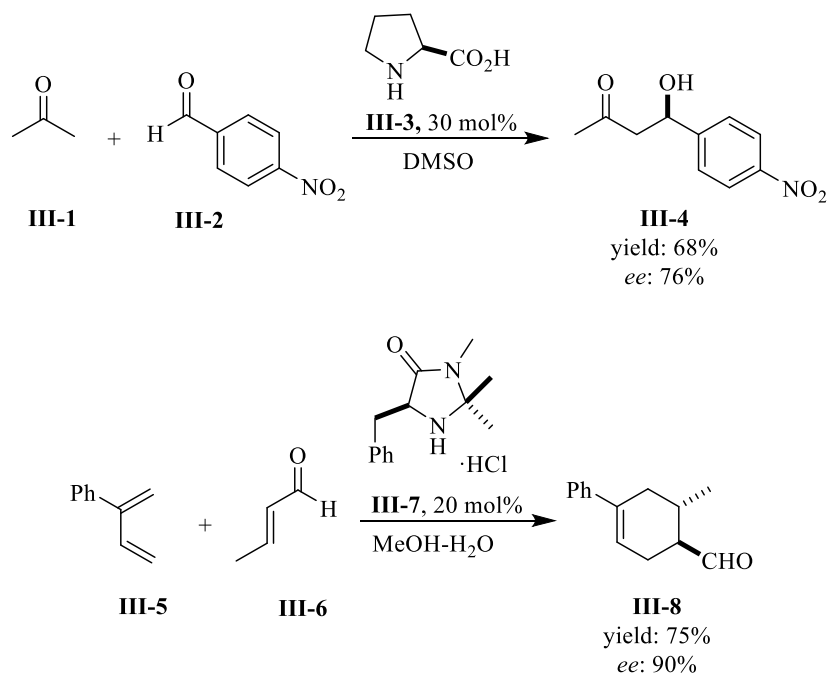
### 3.1. Introduction

Brønsted acid catalysis has been an important field in organic synthesis. Among all of the chiral Brønsted acid catalysts that have been developed chiral phosphoric acid catalysts have received a great deal of attention these days.<sup>1</sup> These catalysts and their derivatives have been used as efficient organocatalysts in numerous organic transformations including asymmetric catalysis,<sup>2</sup> photo redox catalysis<sup>3,4</sup> and polymer chemistry<sup>5</sup>. Attempts are still ongoing in this field to design active chiral biaryl phosphoric acid catalysts with a well-defined chiral environment around the active site.

#### 3.1.1. The discovery of chiral biaryl phosphoric acid catalyst

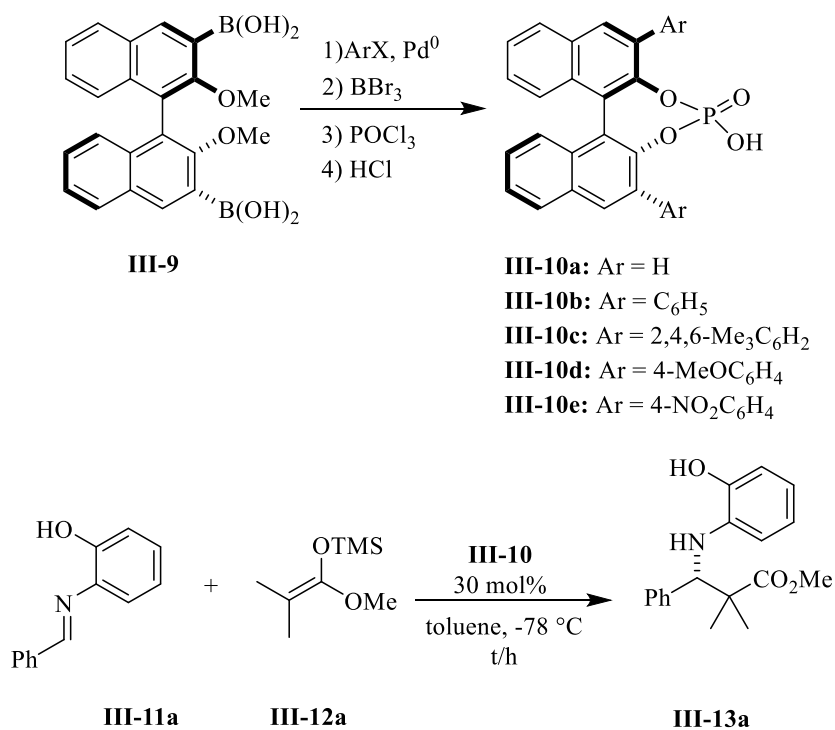
The concept of organocatalysts in forging C-C bond formation was first introduced by List, Barbas and Macmillan in 2000.<sup>6,7</sup> List and Barbas reported the use of Proline as an efficient catalyst in the direct asymmetric aldol reaction. Macmillan reported the use of catalyst **III-7** in catalyzing asymmetric Diels-Alder reactions (scheme III-1).

**Scheme III-1.** Proline catalyzed asymmetric C-C formation



Despite the advancement in Proline-catalyzed organic transformations, Brønsted acid catalysis remained ill-developed until 2003 when Akiyama reported the use of BINOL phosphoric acid catalysts in the Mannich reaction (table III-1).<sup>8,9</sup>

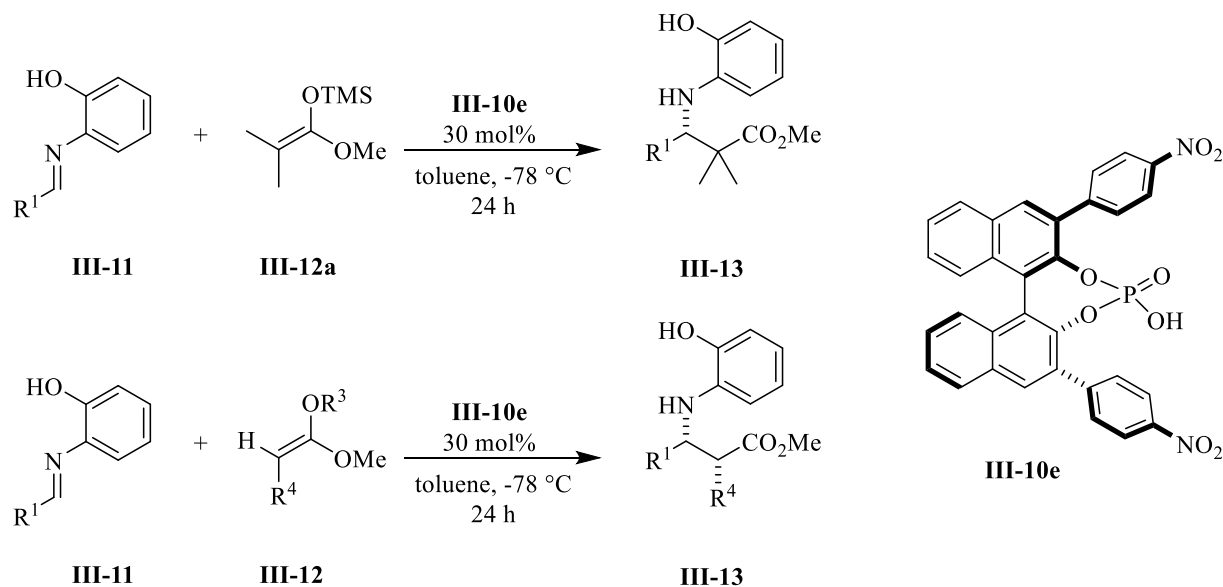
**Table III-1.** Catalyst optimization in a Mannich-type reaction



entry	Ar	time/h	yield%	ee%
1	H	22	57	0
2	C <sub>6</sub> H <sub>5</sub>	20	100	27
3	2,4,6-Me <sub>3</sub> C <sub>6</sub> H <sub>2</sub>	27	100	60
4	4-MeOC <sub>6</sub> H <sub>4</sub>	46	99	52
5	4-NO <sub>2</sub> C <sub>6</sub> H <sub>4</sub>	4	96	87

BINOL catalyst **III-10a** was prepared from the reaction of BINOL with phosphorous oxychloride and the use of this catalyst in the Mannich reaction of aldimine **III-11a** and ketene silyl acetal **III-12a** which delivered product **III-13a** with no enantioinduction (table III-1, entry 1). To improve the enantioselectivity, a library of BINOL phosphoric acid catalysts bearing various substituents in 3,3'-positions were synthesized and examined in this reaction. After screening these catalysts, it was found that the one with *para*-nitro-phenyl as the substituent in the 3,3'-positions, **III-10e** was the optimum catalyst (Table III-1, entry 5). Further optimization and substrate scope screening yielded the Mannich adduct **III-13** in excellent yield and enantioselectivity.<sup>9</sup> Mono-substituted ketene silyl acetals also performed well and produced the desired adduct with high *syn* selectivity (scheme III-2).<sup>9</sup>

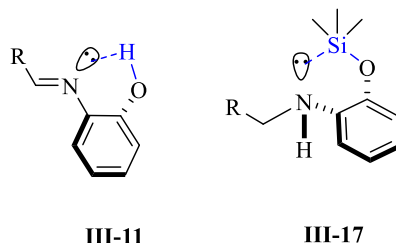
**Scheme III-2.** Asymmetric catalytic Mannich-type reaction



One of the interesting features of this report was its strategy to overcome product inhibition. A prevalent obstacle in Mannich reaction is the higher affinity of the product toward the catalyst due to its higher basicity than the starting materials. This problem was resolved by placing a hydroxy group in *ortho* position of the aryl substituent on the nitrogen. As a result, the lone pair on the

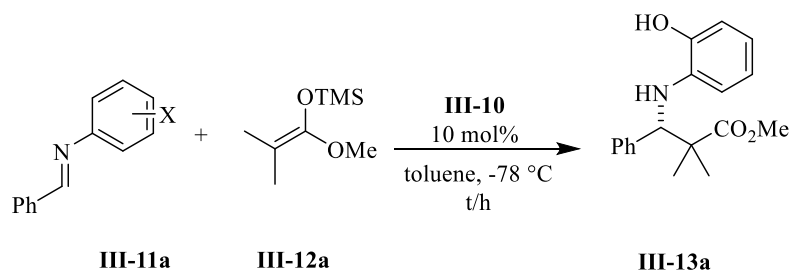
amine **III-17** will form a Lewis base-Lewis acid adduct with the silyloxy group which led to a decrease in its basicity; however, imine **III-11** forms a weaker hydrogen bond with the hydroxy group due to the higher electronegativity of imine over amine and also the limitation which was posed by the geometry of the imine (scheme III-3).

**Scheme III-3.** Basicity of imine vs amine

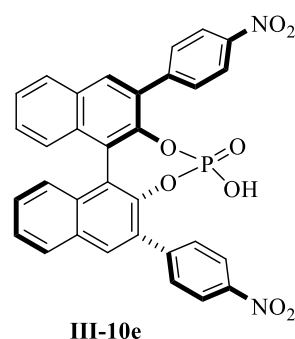


The presence of the *ortho*-hydroxy substituent was also crucial in achieving high induction in asymmetric Mannich reaction. Conducting the same reaction with the *para*-hydroxy phenyl group as the nitrogen substituent yielded the desired adduct **III-13a** in only 20% *ee* and with a substantial decrease in yield (Table III-2, entry 2).

**Table III-2.** The effect of hydroxy group on reactivity in Mannich reaction



entry	X	time/h	yield%	<i>ee</i> %
1	2-OH	13	98	89
2	4-OH	33	28	20
3	2-OCH <sub>3</sub>	46	56	3
4	H	43	76	39

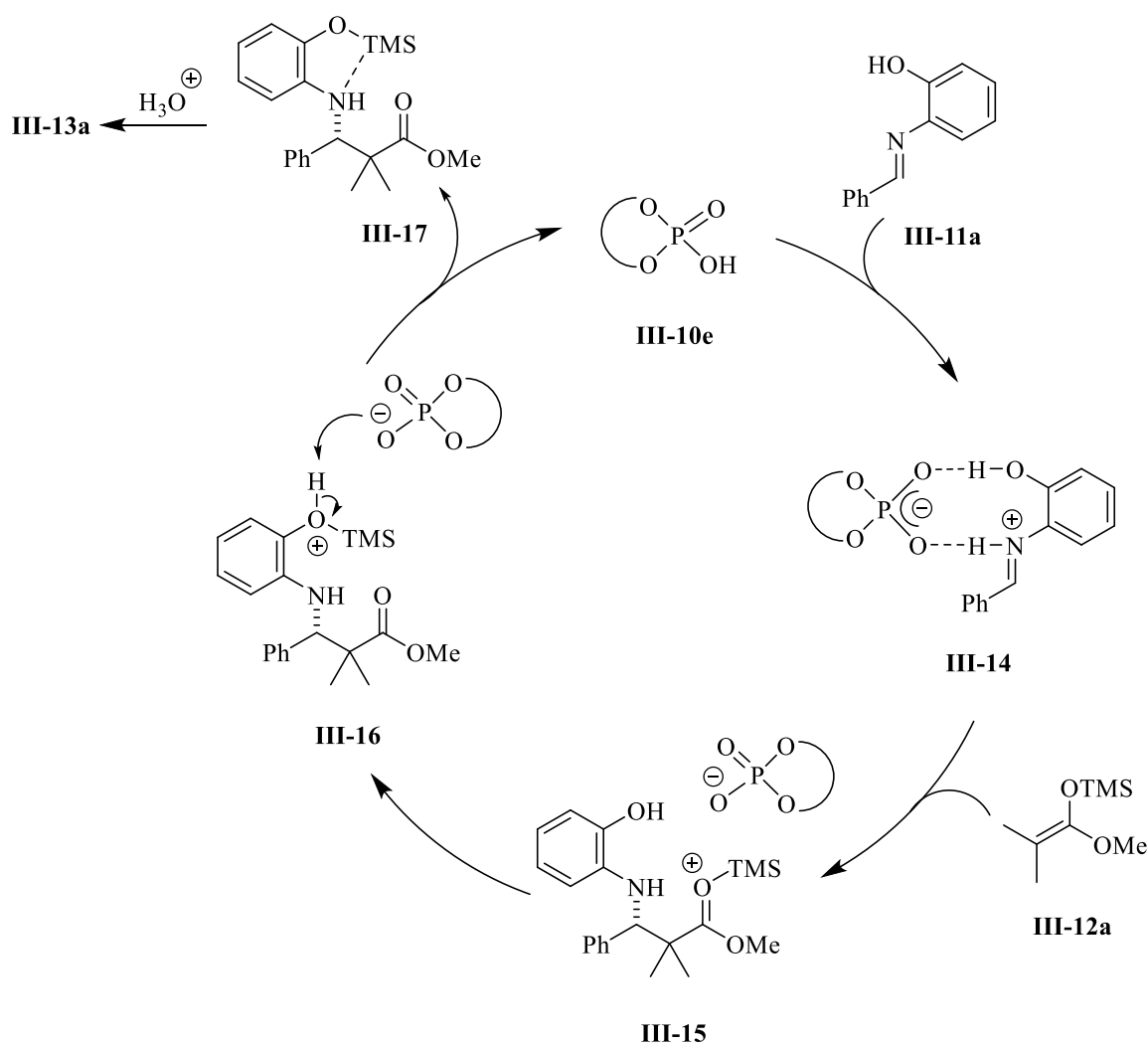




Also, performing the reaction with imine **III-11a** bearing methoxy group as the substituent in the *ortho* position produced amine **III-13a** in only 3% *ee* which indicated the importance of placing hydroxyl group in *ortho* position (table III-2, entry 3).<sup>10</sup>

After an extensive computational study, Akiyama was able to propose the mechanism for this asymmetric catalytic Mannich reaction (scheme III-4).

**Scheme III-4.** Proposed mechanism



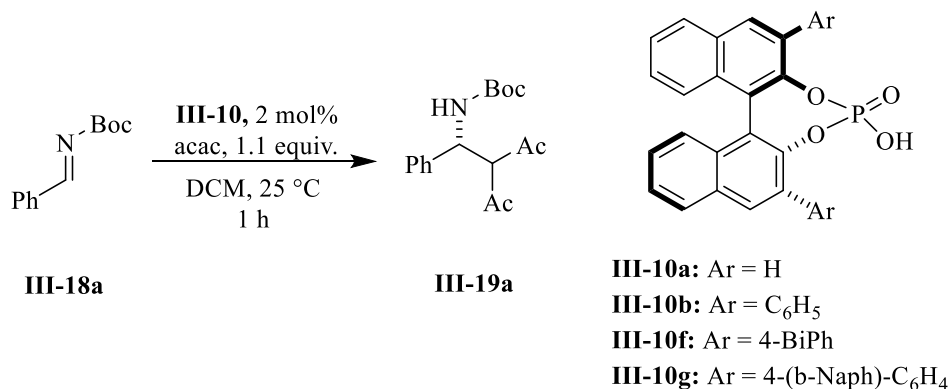
The mechanism of this reaction was triggered via the deprotonation of the catalyst which formed the ion-pair **III-14**. It is proposed that the second hydrogen bond between the catalyst and the

hydroxy moiety of the imine is responsible for achieving high induction presumably by rigidifying the structure in the enantiodetermining step. The mechanistic cycle continues via the reaction of the activated imine **III-14** with the silyl ketene acetal **III-12a** which produces the intermediate **III-15**. An intramolecular silyl transfer to the hydroxy moiety followed by its deprotonation regenerates the catalyst **III-10e** and yields intermediate **III-17**. Eventually, the hydrolysis of intermediate **III-17** affords the desired product **III-13a**.

Chiral phosphoric acid catalysts have also been used in other asymmetric organic transformations such as hydrophosphonylation of imines and inverse electron demand heteroatom Diels-Alder reactants by the same group.<sup>11,12</sup>

Later in 2004, Terada also reported the asymmetric Mannich reaction of *N*-Boc-protected imines

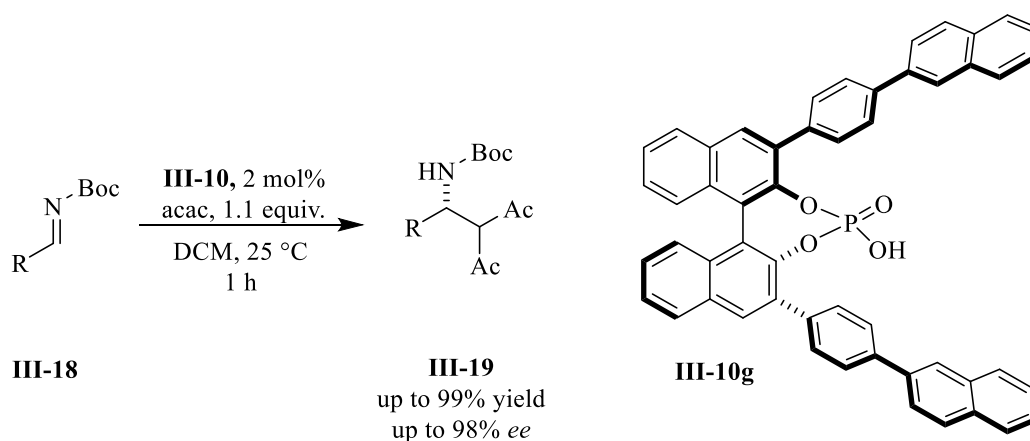
**Table III-3.** Catalyst optimization in the Mannich-type reaction of *N*-Boc-imine **III-18a**



entry	Ar	yield%	ee%
1	H	92	12
2	C <sub>6</sub> H <sub>5</sub>	95	56
3	4-Ph-C <sub>6</sub> H <sub>4</sub>	88	90
4	4-(b-Naph)-C <sub>6</sub> H <sub>4</sub>	99	95

and acetyl acetone.<sup>13</sup> When the BINOL phosphoric acid **III-10a** was used as the catalyst, the product **III-19a** was produced in excellent yield but in only 12% *ee*. Further optimization revealed that 4-(naphthalen-1-yl) phenyl was the optimum substituent and the product **III-19a** was produced in excellent yield and excellent *ee* (table 3). A wide substrate scope was possible and the enantioenriched products **III-19** were afforded in excellent yield an asymmetric induction (scheme III-5).

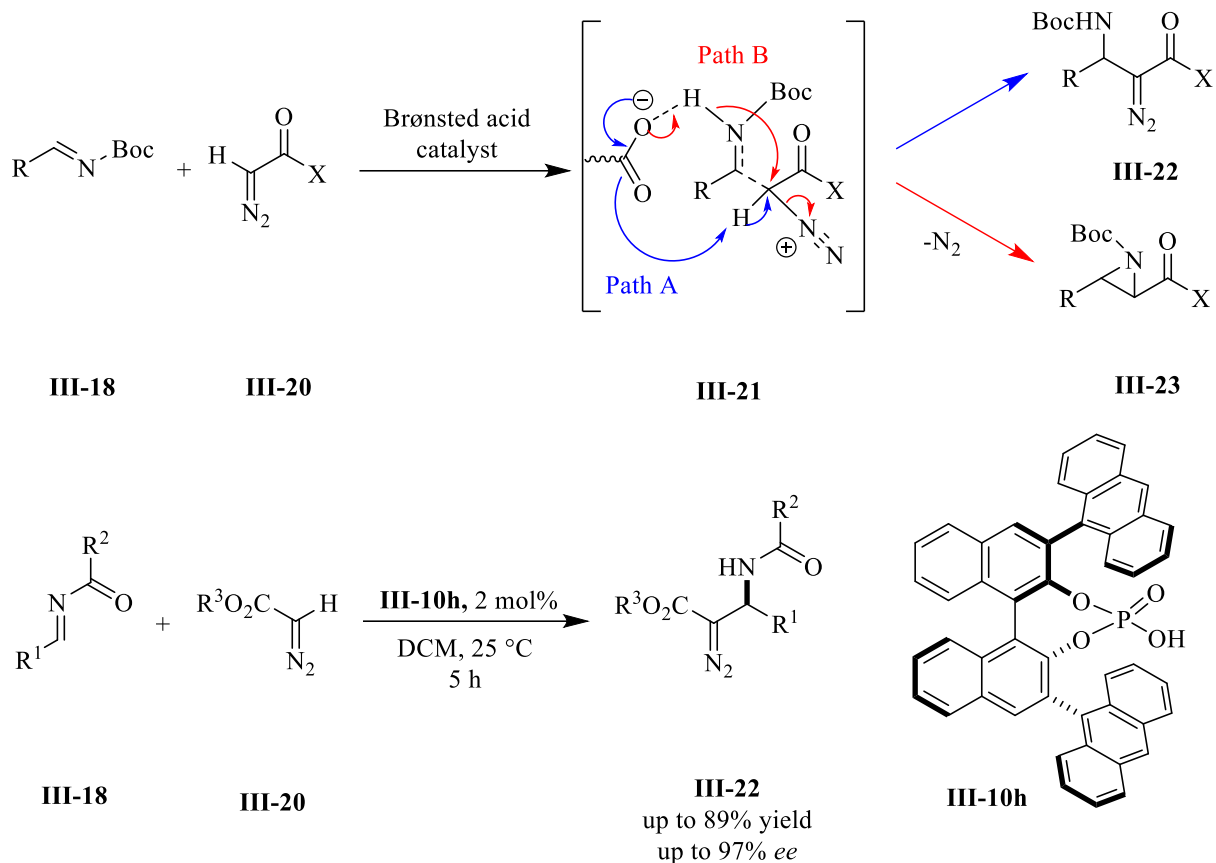
**Scheme III-5.** Catalyst optimization in Mannich-type reaction of N-Boc-imine **III-18**



In 2005 the BINOL phosphoric acid catalysts **III-10** were also investigated in the direct alkylation of  $\alpha$ -diazo ester **III-20** by the same group.<sup>14</sup> One of the common methods in the synthesis of chiral aziridines is the reaction of diazo compounds **III-20** with imines **III-18** in presence of Lewis acid or Brønsted acid catalysts which is well documented in our lab and others.<sup>15,16,17,18</sup> It was assumed that the same reaction catalyzed by chiral phosphoric acid catalyst **III-10** would produce  $\alpha$ -alkylated diazo compound **III-22** since the phosphate anion is basic enough to deprotonate transition state **III-21** (path A, scheme III-6). It was also thought that the aziridination reaction (path B) would be slower than deprotonation (path A) because of the energy demand associated with the formation of the aziridine ring. With these assumptions, the direct alkylation reaction of diazo compound **III-20** was conducted in presence of catalyst **III-10h** and the alkylated product

**III-22** was obtained in 59% yield and 90% *ee* as the sole product of this reaction. A wide substrate scope of substituents was tolerated and the desired alkylated products **III-22** were obtained in good yield and excellent enantioselectivity.

**Scheme III-6.** Direct alkylation of diazo compound



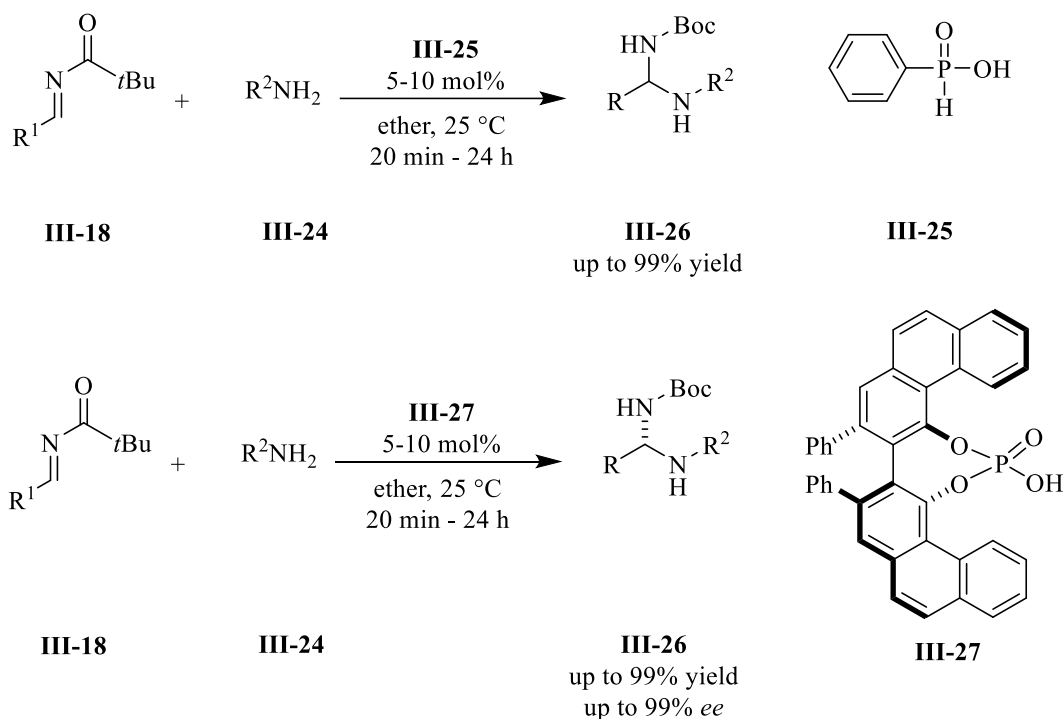
Same group also used BINOL phosphoric acid-based catalysts were used in other reactions such as aza-Friedel-Crafts reaction, Friedel-Crafts reaction, aza-ene-type reaction/cyclization cascade and etc.<sup>19,20</sup>

### 3.1.2. VAPOL and VANOL phosphoric acid catalysts

VAPOL phosphoric acid **III-27** was synthesized in 2007 by Jon Antilla for the first time and was used in the asymmetric amidation of imines.<sup>21,22</sup> In this report, the synthesis of racemic aminal **III-26** was investigated with the non-chiral organocatalyst **III-25** (scheme III-7). A wide range of

amides and carbamates were tolerated and hemiaminals **III-26** were produced in moderate to excellent yield. Next, the viability of the asymmetric catalytic amidation of imines was explored and it turned out that the VAPOL phosphoric acid **III-27** was the superior catalyst over the BINOL phosphoric acid. Catalyst **III-27** catalyzed the asymmetric amidation reaction with good yields and enantioselectivity.

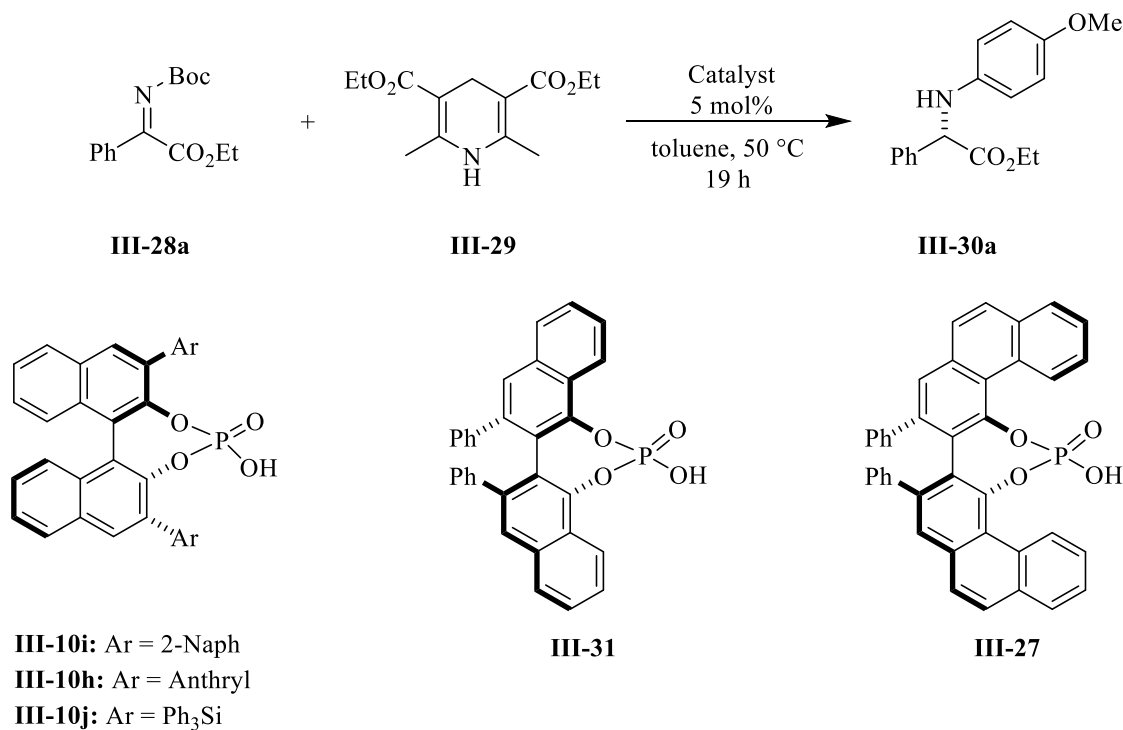
**Scheme III-7.** Direct alkylation of diazo compound



In another report in 2007, Antilla reported the use of VANOL hydrogen phosphate **III-31** and VAPOL hydrogen phosphate **III-27** in the asymmetric reduction of imines **III-28** with Hantzsch ester **III-29** (scheme III-8).<sup>23</sup> Initial screening of biaryl phosphoric acid catalysts proved the effectiveness of VAPOL phosphoric acid **III-27** over the VANOL **III-31** and the BINOL derivatives phosphoric acid **III-10**. Imine **III-28a** underwent asymmetric reduction and produced amine **III-30a** with excellent yield and excellent enantioselectivity in presence of VAPOL phosphoric acid catalyst **III-27** (table III-4, entry 5). However, the same reaction catalyzed with

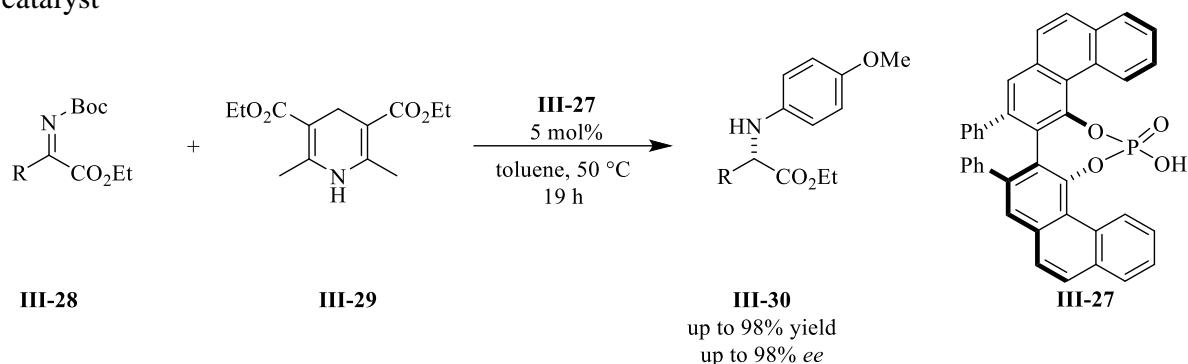
VANOL phosphoric acid **III-31** produced the amine **III-30a** in <5% yield and only 17% *ee* (table III-4, entry 4). Catalyst **III-27** was an efficient catalyst in catalyzing the reduction of a wide range of substrates in good yield and excellent induction (scheme III-8).

**Table III-4.** Catalyst optimization in the asymmetric reduction of imine



entry	catalyst	yield%	<i>ee</i> %
1	<b>III-10i</b>	29	27
2	<b>III-10h</b>	77	80
3	<b>III-10j</b>	6	1
4	<b>III-31</b>	<5	17
5	<b>III-27</b>	99	96

**Scheme III-8.** Asymmetric reduction of imine **III-28** catalyzed by chiral phosphoric acid catalyst



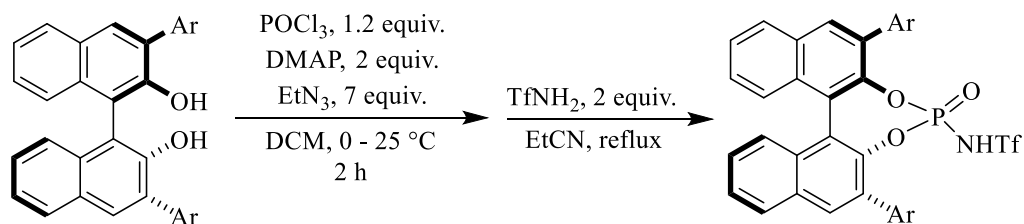
The VAPOL phosphoric acid catalyst has been also utilized in desymmetrization of *meso*-aziridines by Antilla's research group.<sup>24</sup>

### 3.1.3. Discovery and development of *N*-Triflyl-BINOL phosphoramidate

After landmark discovery of the effectiveness of chiral BINOL phosphoric acid in asymmetric catalysis by Akiyama and Terada, these catalysts have become widely accepted by organic chemists and utilized in numerous asymmetric transformations. However, the main drawback of these chiral phosphoric acid catalysts was its weak acidity; therefore, it was mainly used in the activation of more basic substrates such as imines and aziridines. In 2006, Yamamoto reported a breakthrough in Brønsted acid catalysis.<sup>26</sup> His hypothesis was to increase the acidity by incorporating strong electron-withdrawing groups such as *N*-triflyl group into the chiral phosphoric acid.<sup>25</sup> *N*-triflyl phosphoryl BINOL derivatives were prepared via phosphorylation and amidation of optically active BINOL derivatives. This catalyst was investigated in Diels-Alder reactions between ethyl vinyl ketone **III-35** and diene **III-36**. Optically active BINOL phosphoric acid **III-10b** did not show any reactivity presumably due to its lower acidity (table III-5, entry 1). Interestingly, *N*-triflyl phosphoryl BINOL catalyst **III-34b**, catalyzed the reaction of ethyl vinyl ketone **III-35** with diene **III-36** and the Diels-Alder **III-37** adduct was produced in 95% yield and 92% *ee* (table III-5, entry 3). The silylated catalyst **III-38b** was also evaluated in the Diels-Alder

reaction; however, no cycloadduct product was observed with 5 mol% catalyst loading (scheme III-9).

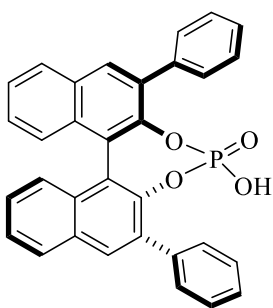
**Table III-5.** N-triflyl BINOL phosphoramidate catalyzed Diels-Alder reaction



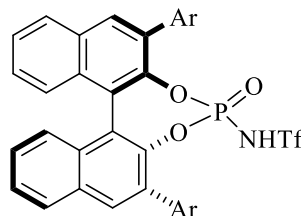
**III-32**, Ar = C<sub>6</sub>H<sub>5</sub>

**III-33**, Ar = 1,3,5-(*i*-Pr)<sub>3</sub>C<sub>6</sub>H<sub>2</sub>

**III-34**

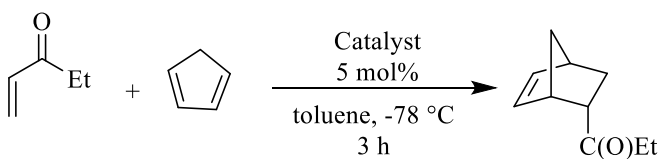


**III-10b**



**III-34a**: Ar = C<sub>6</sub>H<sub>5</sub>

**III-34b**: Ar = 1,3,5-(*i*-Pr)<sub>3</sub>C<sub>6</sub>H<sub>2</sub>



**III-35**

**III-36**

**III-37**

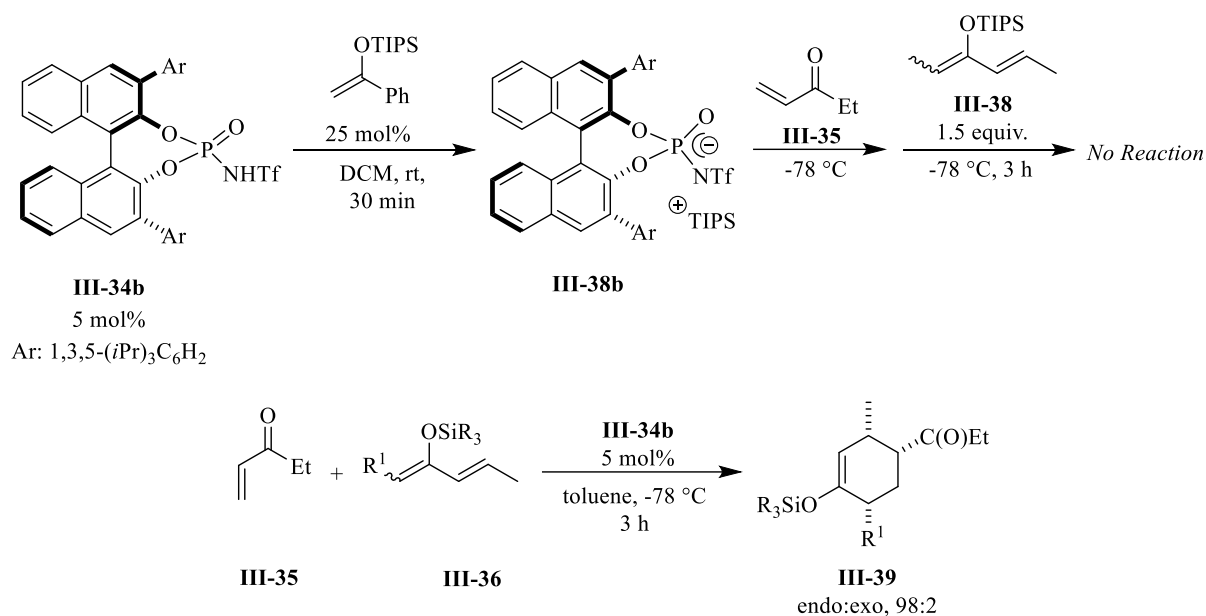
endo:exo, 98:2

entry	catalyst	yield%	ee%
1	<b>III-10b</b>	0	<i>N.D.</i>
2	<b>III-34a</b>	<10	<i>N.D.</i>
3	<b>III-34b</b>	95	92



A good range of substrates were tolerated under the standard reaction condition and the desired cycloadducts **III-39** were obtained in good yield and enantio-induction (scheme III-9). Catalyst **III-34** turned out to be an effective catalyst in asymmetric 1,3-dipolar cycloaddition of nitrones with ethyl vinyl ether reported by Yamamoto in 2008 (not shown).<sup>27</sup> Rueping also reported the use of catalyst **III-34** in asymmetric Nazarov cyclization (not shown).<sup>28</sup>

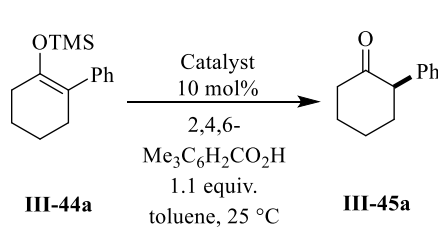
**Scheme III-9.** N-triflyl BINOL phosphoramidate catalyzed Diels-Alder reaction



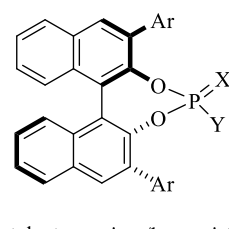
It is known that in the periodic table, acidity increases by moving from top to bottom in a group. A good example is the pK<sub>a</sub> of PhOH (18.0), PhSH (10.3), and PhSeH (7.1) in DMSO and the reason is the ability of the conjugated base to stabilize the negative charge. Inspired by this fact, Yamamoto designed the BINOL Brønsted acid catalysts **III-40** to **III-43** bearing thio and seleno groups in place of oxygen (table III-6).<sup>29</sup> BINOL phosphoramidate catalysts were prepared from optically active BINOL via thio- and seleno-phosphorylation followed by amidation. The x-ray structural analysis of catalyst **III-42b** revealed a phosphorous-sulfur double bond; therefore, the acidic proton should be located on NTf group. Next, the enantioselective protonation of prochiral silyl enol ether **III-44a** was explored in the presence of a stoichiometric amount of 2,4,6-

trimethylbenzoic acid as the proton source. Interestingly, catalysts **III-40** and **III-41** did not promote the reaction at all; presumably, due to their lower acidity. However, catalysts **III-34a**, **III-42a**, and **III-43** yielded the desired product in quantitative yield. It is also interesting to note that the catalyst **III-42a** and **III-43** bearing thio and seleno groups afforded the product **III-45a** in higher enantioselectivity and also faster reaction than the catalyst **III-34a**. After further optimization, it turned out that the catalyst **III-42b** is the optimum catalyst and under the optimum reaction conditions it catalyzed the asymmetric protonation of a wide range silyl enol ether **III-44** bearing an aromatic component in  $\alpha$ -position. Moderate enantioselectivity was obtained with silyl enol ether **III-44** bearing an aliphatic component in the  $\alpha$ -position.

**Table III-6.** N-triflyl BINOL phosphoramidate catalyzed enantioselective protonation of silyl enol ether



**III-44a**



**III-40:** X=O, Y=OH, Ar = 2,4,6-(*i*Pr)<sub>3</sub>C<sub>6</sub>H<sub>2</sub>

**III-41:** X=O, Y=SH, Ar = 2,4,6-(*i*Pr)<sub>3</sub>C<sub>6</sub>H<sub>2</sub>

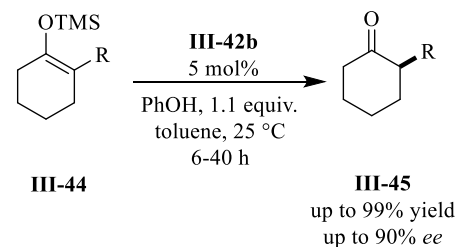
**III-34a:** X=O, Y=NHTf, Ar = 2,4,6-(*i*Pr)<sub>3</sub>C<sub>6</sub>H<sub>2</sub>

**III-42a:** X=S, Y=NHTf, Ar = 2,4,6-(*i*Pr)<sub>3</sub>C<sub>6</sub>H<sub>2</sub>

**III-42b:** X=S, Y=NHTf, Ar = 4-*i*Bu-2,6-(*i*Pr)<sub>2</sub>C<sub>6</sub>H<sub>2</sub>

**III-43:** X=Se, Y=NHTf, Ar = 2,4,6-(*i*Pr)<sub>3</sub>C<sub>6</sub>H<sub>2</sub>

entry	catalyst	time/h	yield%	ee%
1	<b>III-40</b>	96	<i>N.R.</i>	<i>N.D.</i>
2	<b>III-41</b>	96	<i>N.R.</i>	<i>N.D.</i>
3	<b>III-34a</b>	4.5	98	54
4	<b>III-42a</b>	4.5	97	78
5	<b>III-43</b>	3.5	97	72



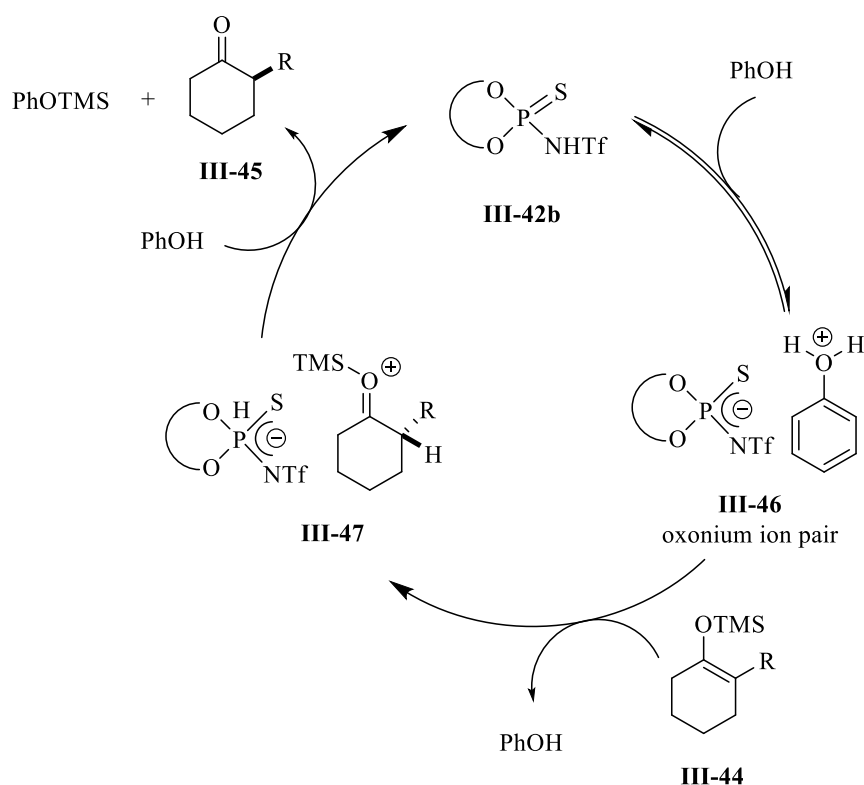
**III-44**

**III-45**  
up to 99% yield  
up to 90% ee

It is also worth noting that the asymmetric catalytic protonation of silyl enol ether **III-44** did not get promoted in the absence of an achiral proton donor even in the presence of the stoichiometric

amount of catalyst **III-42b**. Based on this observation, a two-step sequence was proposed for the mechanism of this reaction. First, the intermediate chiral oxonium ion pair **III-46** is generated via the protonation of the achiral proton donor with chiral Brønsted acid catalyst **III-42b**. Next, the rapid proton exchange between chiral intermediate **III-46** and silyl enol ether **III-44** followed by a subsequent desilylation of resulting chiral ion pair intermediate **III-47** yields the enantio-enriched ketone **III-45** and regenerates the catalyst **III-42b**.

**Scheme III-10.** Proposed mechanism for enantioselective protonation of silyl enol ether



Yamamoto also reported the use of catalyst **III-42** in other asymmetric transformations including Mukaiyama aldol reaction, Hosomi-Sakurai reaction, and others (not shown).<sup>30,31</sup>

### 3.1.4. Synthesis of *N*-Triflyl-VANOL/VAPOL phosphoramidate

Our group reported the gram-scale synthesis of *N*-triflyl-VANOL/VAPOL phosphoramidates in 2010.<sup>32</sup> An efficient synthesis of catalyst **III-53b** derived from ligand **III-52b** was also introduced

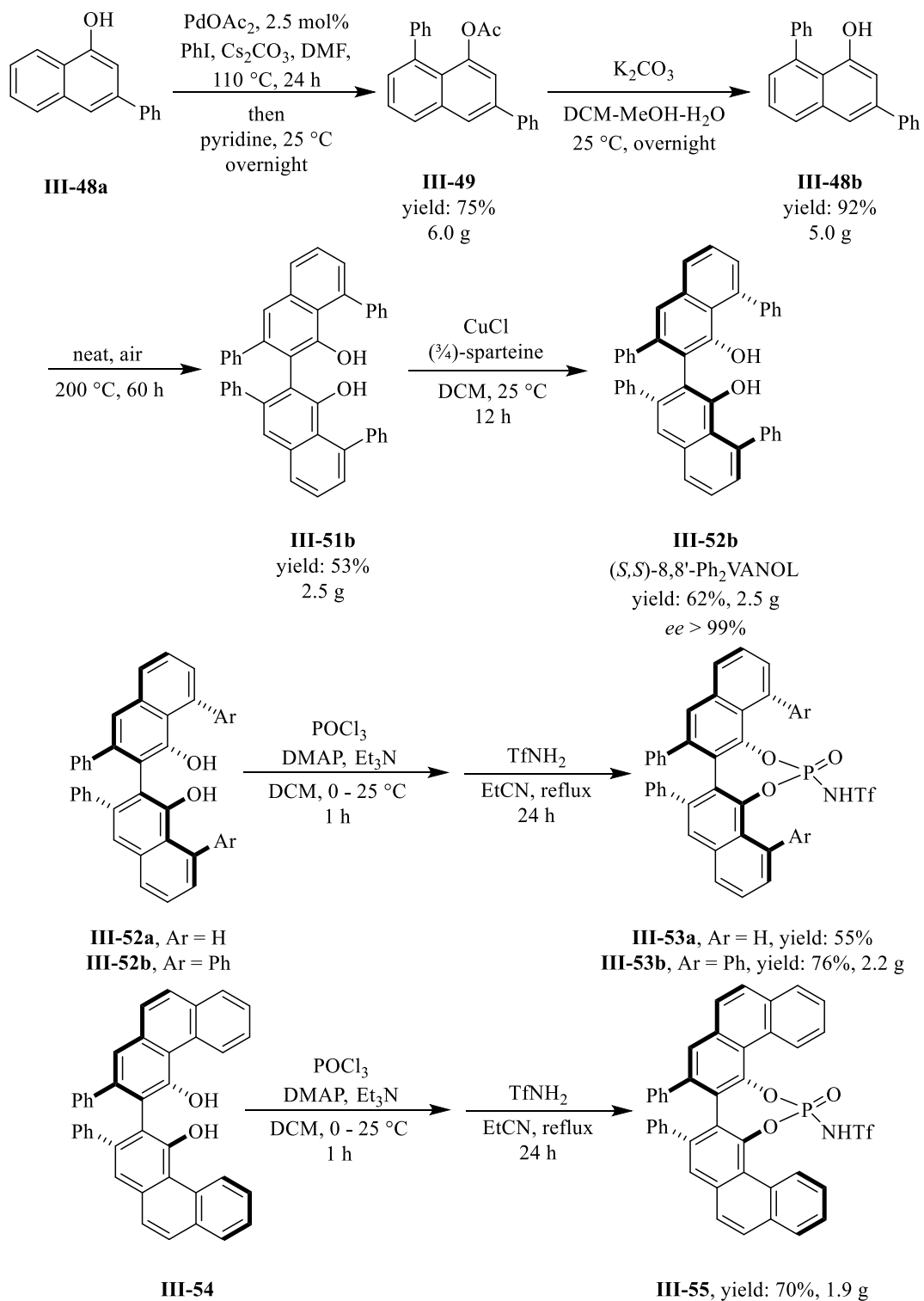
(scheme III-11). Ligand **III-52b** was synthesized from VANOL monomer **III-48a** via transition metal-catalyzed C-H activation and aryl coupling followed by dimerization and deracemization. However, neither *N*-triflyl-VAPOL nor *N*-triflyl-VANOL phosphoramides have ever been utilized in any asymmetric transformations.

### 3.1.5. Rational design and synthesis of imidodiphosphoric acid catalysts

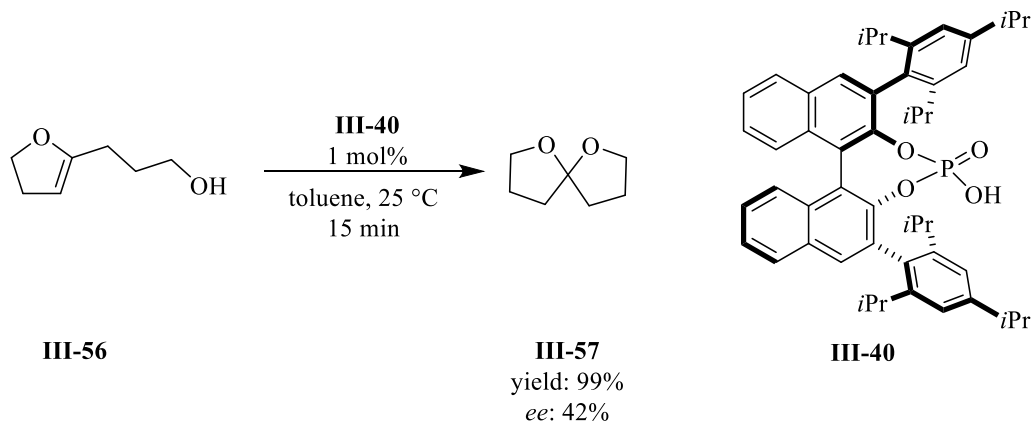
List group was interested in spiroacetalization of substrate **III-56** catalyzed by Brønsted acid catalysts. An extensive study of chiral phosphoric acids and phosphoramides revealed the inefficiency of these catalysts in catalyzing this asymmetric acetalization. The best induction was obtained with catalyst **III-40** which was found to be 41% *ee*.<sup>33</sup> Therefore, it was concluded that the lack of well-defined asymmetric space around the active site was responsible for the low induction.

The active site of these chiral phosphoric acid catalyst is bifunctional and consists of both Brønsted acid (OH) and Lewis base (O) sites (scheme III-13, structure A). The success of this catalyst is partly because of its ability to be bifunctional since both of these active sites can stabilize the transition state of a specific asymmetric transformation. Introducing substituents in 3,3'-positions of BINOL ligand creates chiral space around the active site of the chiral phosphoric acid; however, these substituents are pointing away from the active site (structure B). *N*-triflyl BINOL phosphoramide bearing substituents on sulfur creates a better chiral environment around the active site by bringing further steric demand close to it (structure C); however, the free rotation around the N-S bond enables the catalyst (structure C) to adopt two distinct isomers, *O,O*-*syn* and *O,O*-*anti* (structure D) which provides flexibility to the relative position of the Brønsted acid and Lewis base components of the catalyst and leads to a reduced selectivity.

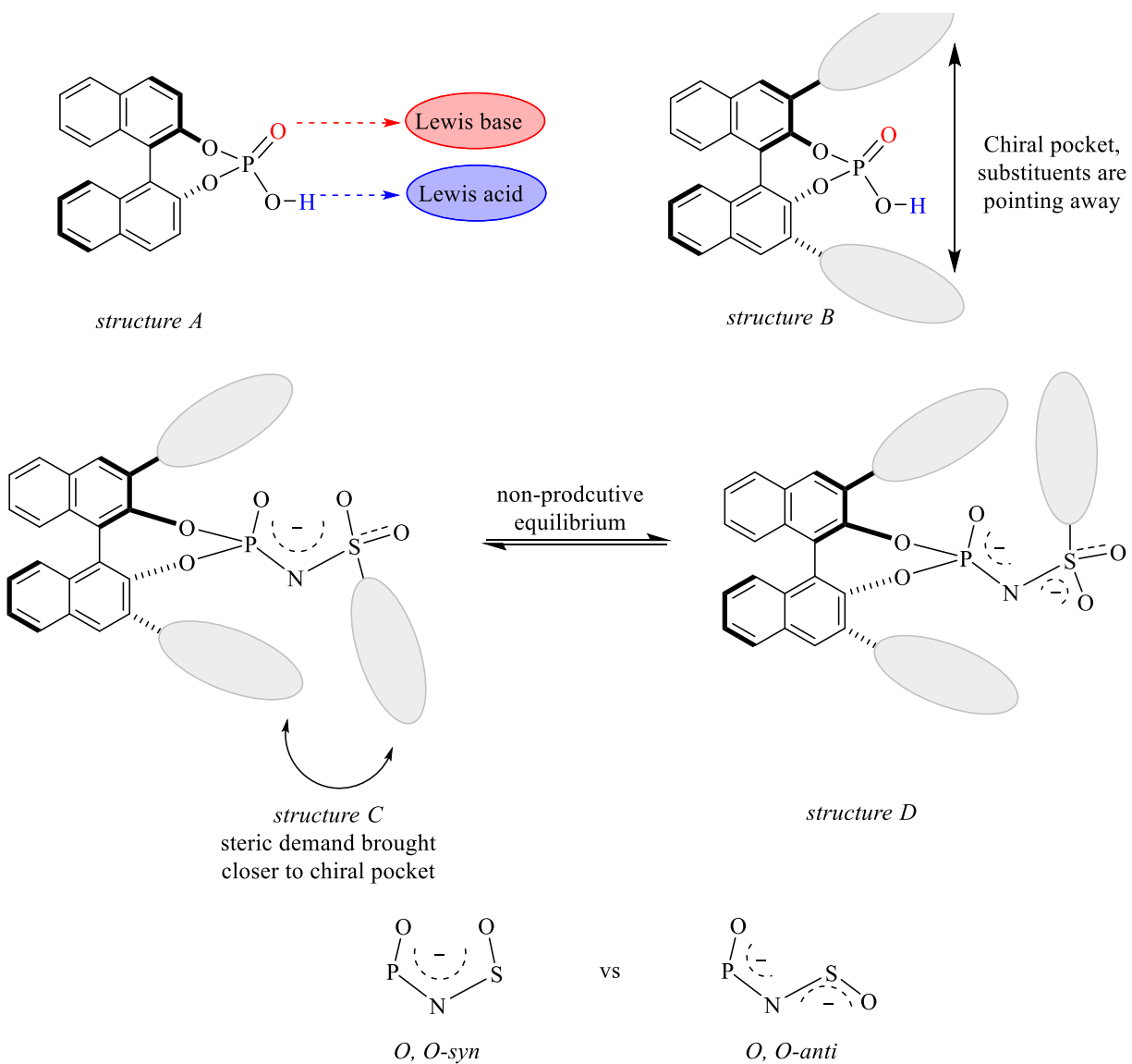
**Scheme III-11.** Synthesis of VANOL/VAPOL phosphoramidate



**Scheme III-12.** BINOL phosphoric acid catalyzed asymmetric spiroketalization

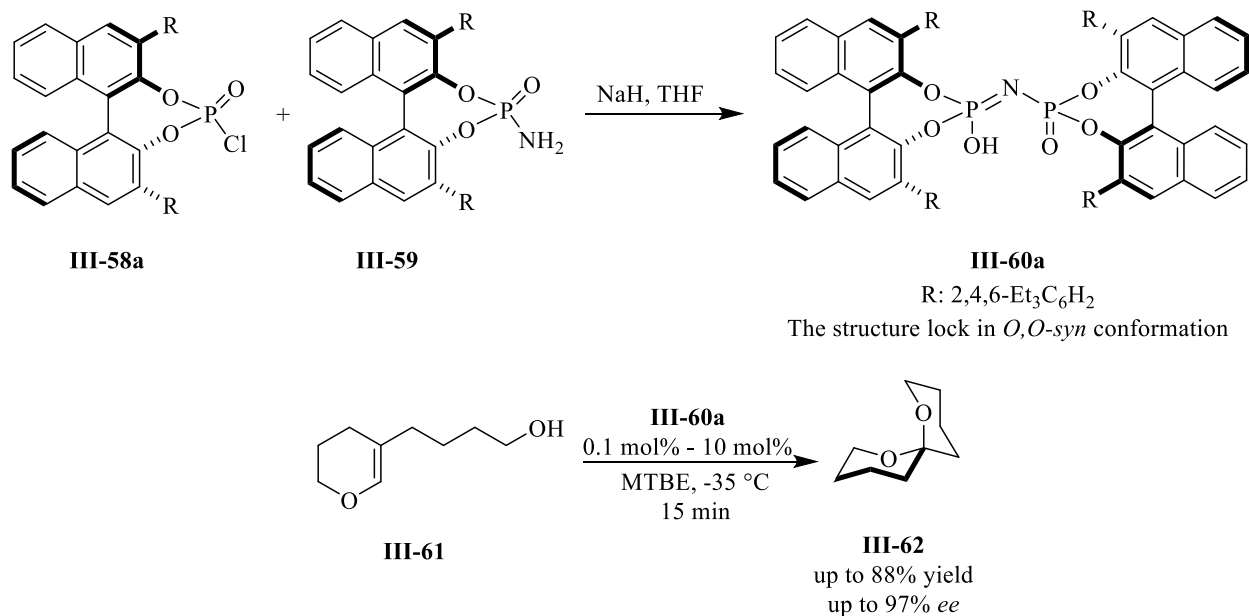


**Scheme III-13.** Dual functionality of BINOL phosphoric acid



These considerations led the List research group to design a new class of highly efficient BINOL Brønsted acid catalysts of the type **III-60** (scheme III-14).<sup>33</sup> These imidodiphosphoric acid catalysts were synthesized via reacting equimolar amounts of phosphoramidate **III-59** and phosphoryl chloride **III-58** in the presence of a strong base such as NaH. The structure of this catalyst was unequivocally determined to be a dimeric species via x-ray structural analysis.<sup>33</sup> The crystal structure also revealed that the catalyst exists exclusively as the *O,O*-*syn* isomer presumably because of steric hindrance imposed by BINOL subunits in 3,3'-positions. It was assumed that the rigidity of the chiral microenvironment around the active site caused by the unique structure of this catalyst might improve the performance of the catalyst. To test this hypothesis, the newly designed confined Brønsted acid catalyst **III-60a** was investigated in the asymmetric spiroacetalization reaction and it turned out under the optimum reaction conditions, spiroacetal **III-62** was afforded in excellent yield and enantioselectivity.

**Scheme III-14.** Confined BINOL Brønsted acid catalyzed asymmetric spiroketalization

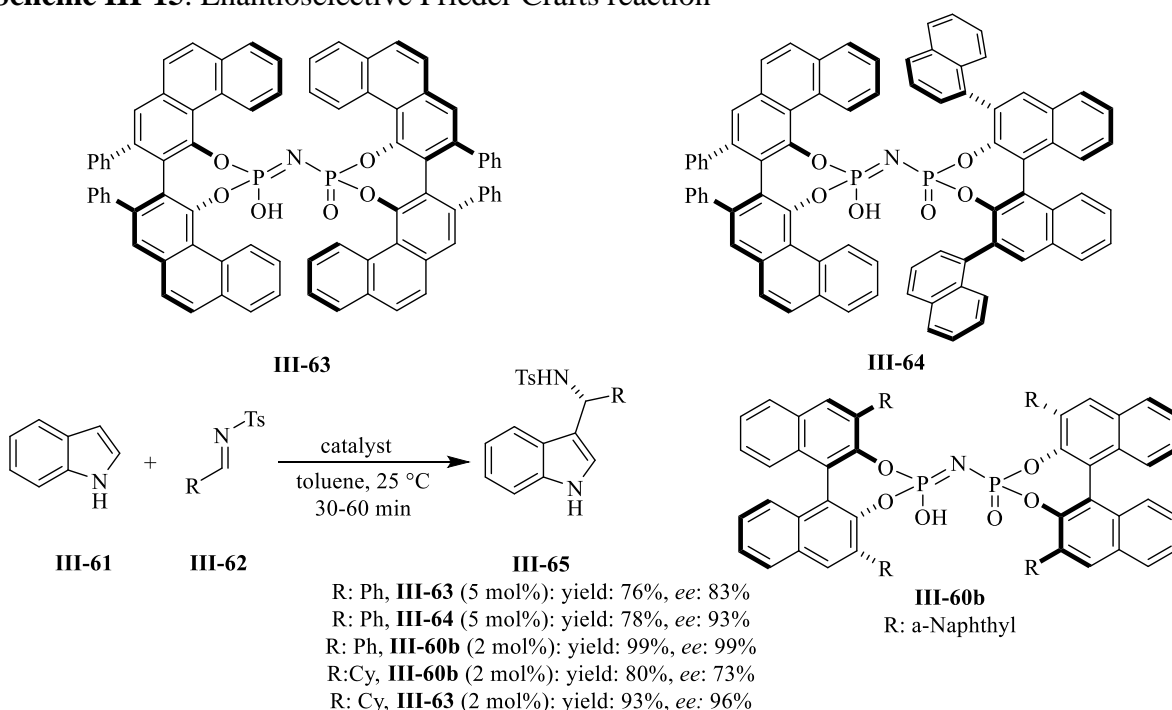


The utility of BINOL imidodiphosphoric acid catalyst was explored in numerous asymmetric transformations including enantioselective sulfoxidation, asymmetric acetalization, resolution of chiral diols, asymmetric carbonyl-ene reaction and asymmetric vinylogous Prins cyclizations (not shown).<sup>34,35,36,37,38</sup>

### 3.1.6. Synthesis and catalytic investigation of VAPOL imidodiphosphoric acid catalyst

The synthesis and the use of VAPOL imidodiphosphoric acid **III-63** along with the hybrid imidodiphosphoric acid **III-64** catalysts first appeared in a report by Jiang in 2013 (scheme III-15).<sup>39</sup> These catalysts were used in the enantioselective Friedel-Crafts reaction and gave the desired product **III-65** in good yield and moderate to good enantioselectivity. However, further catalyst screening revealed that the imidodiphosphoric acid **III-60b** was superior and produced the desired Friedel-Crafts product **III-65** from aromatic substrates in excellent yield and perfect enantioinduction. Further substrate screening revealed that the VAPOL **III-63** was more effective in catalyzing Friedel-Crafts reaction of aliphatic substrates (scheme III-15).

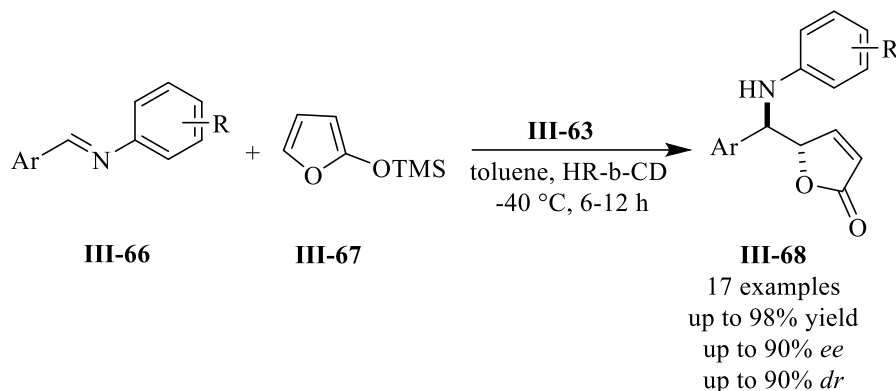
**Scheme III-15.** Enantioselective Friedel-Crafts reaction





Later in 2018, successful use of the VAPOL imidodiphosphoric acid catalyst **III-63** was reported by the same group in asymmetric vinylogous Mannich reaction of aldimine **III-66** with 2-(trimethylsilyloxy)furan **III-67**.<sup>40</sup> Under the optimized reaction conditions, a number of butenolides **III-68** were synthesized in excellent yield and *ee* along with high diastereoselectivity.

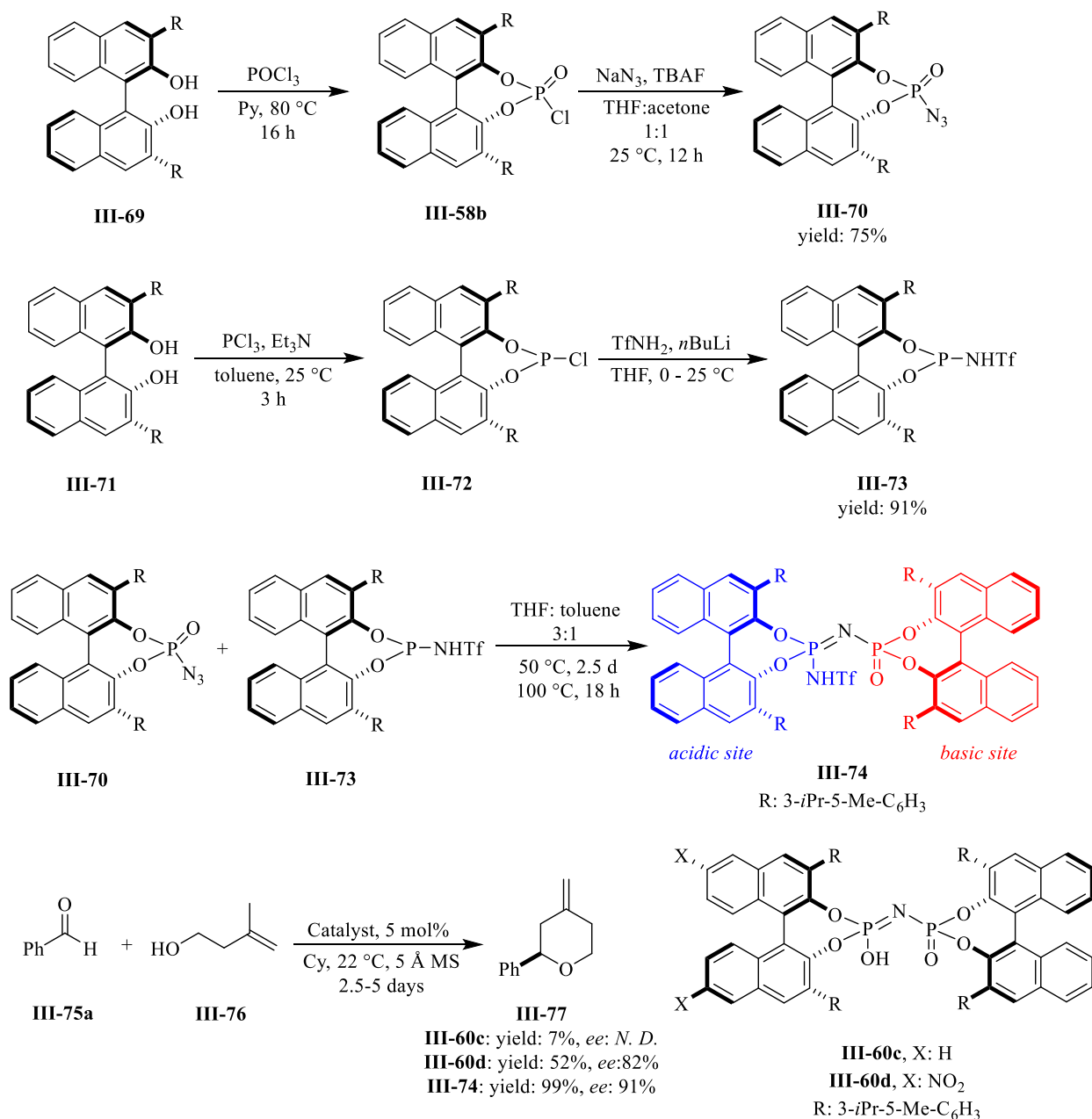
**Scheme III-16.** Asymmetric vinylogous Mannich reaction



### 3.1.7. Further attempts to improve the acidity of confined Brønsted acid catalyst

The Prins reaction was an interest of the List research group; however, their previously developed imidodiphosphoric acid **II-60c** catalyst was not able to promote the reaction at all, presumably due to its insufficient acidity.<sup>41</sup> Introduction of nitro groups in 6,6'-positions of BINOL ligand increased the acidity of the catalyst to the point where, the catalyst **III-60d** promoted the Prins reaction with promising results (52% yield and 82% *ee* vs. 13% yield). Inspired by Yamamoto's strategy in increasing the acidity of the phosphoric acid catalyst, an oxo group of the imidodiphosphoric acid catalyst was replaced with the strong electron withdrawing NSO<sub>2</sub>CF<sub>3</sub>. Such a change not only increased the acidity of the catalyst **III-74** but it did also allow the modulation of the Brønsted acid and Lewis acid compartment of the bifunctional catalyst.<sup>41</sup> The aforementioned catalyst was synthesized as depicted in scheme III-17 in a multigram manner. Catalyst **III-74** converted substrate **III-75** to the functionalized enantioenriched tetrahydropyran **III-77** in good yield and good enantioselectivity (91% *ee* vs 82% *ee*, scheme III-17).

### Scheme III-17. Asymmetric Prins cyclization



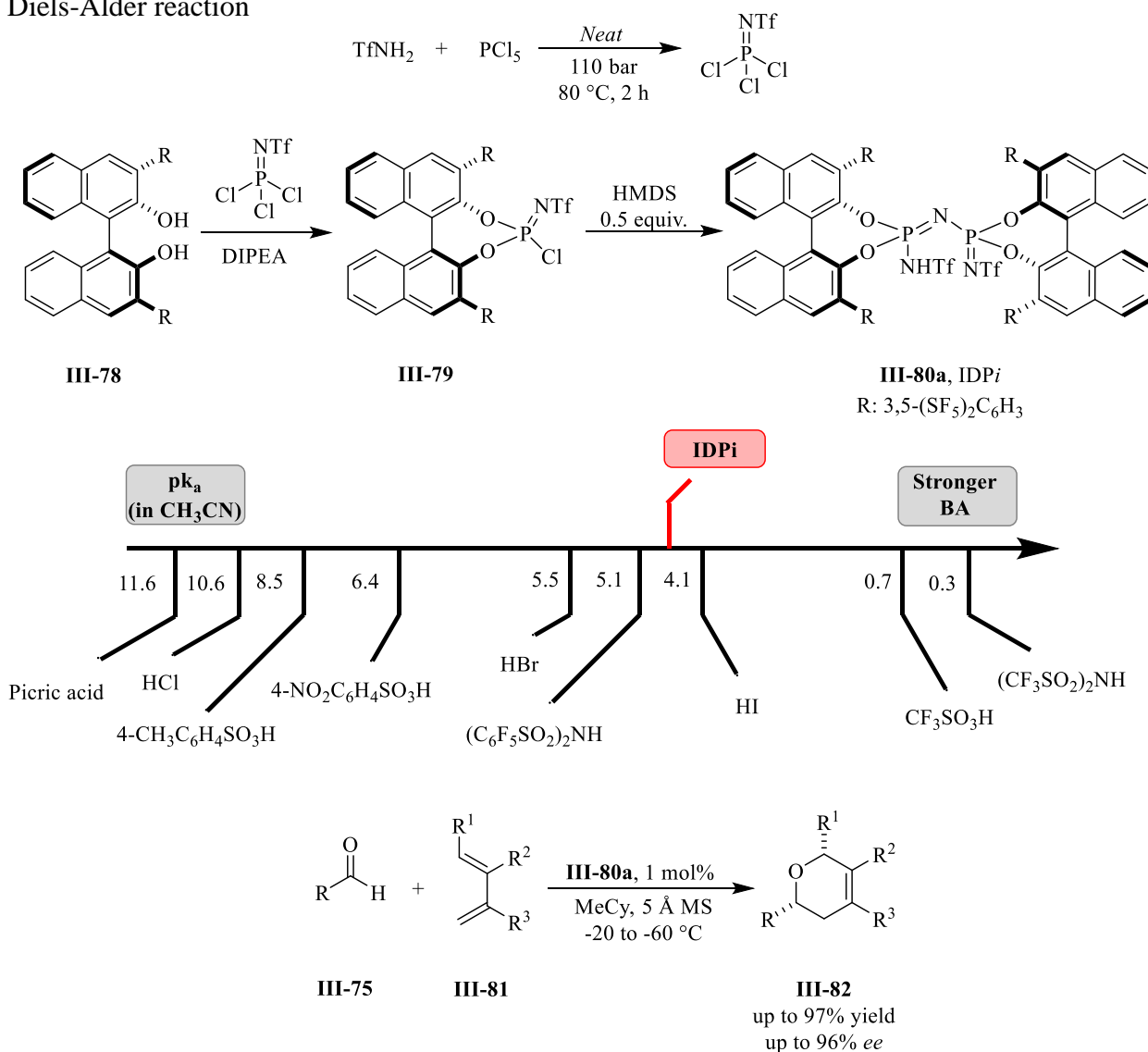
### 3.1.8. Extremely active imidodiphosphorimide (IDP<sub>i</sub>) organocatalysts; a breakthrough in

#### Brønsted acid catalysis

The synthesis of ((trifluoromethyl)sulfonyl)phosphorimidoyl trichloride (TfNPCl<sub>3</sub>) enabled List to access the synthesis of extremely active Brønsted acid catalyst (scheme III-18).<sup>42</sup> The oxo (O) and hydroxy (OH) groups in imidodiphosphoric acid were replaced with NTf as the strong

electron-withdrawing group. Introduction of these groups makes the catalyst **III-80a** possess a  $pK_a$  of 4.6 in MeCN which is comparable with the acidity of HI in MeCN (4.1). The exceptional acidity of the IDPi catalyst **III-80a** enabled List to report a general method for the HDA (heteroatom Diels-Alder) reaction with the unactivated diene (3,4-dimethylbutadiene).<sup>43</sup> This was a landmark report in asymmetric HDA reaction since the previous examples involved the reaction of aldehydes with activated dienes such as Danishefsky diene.

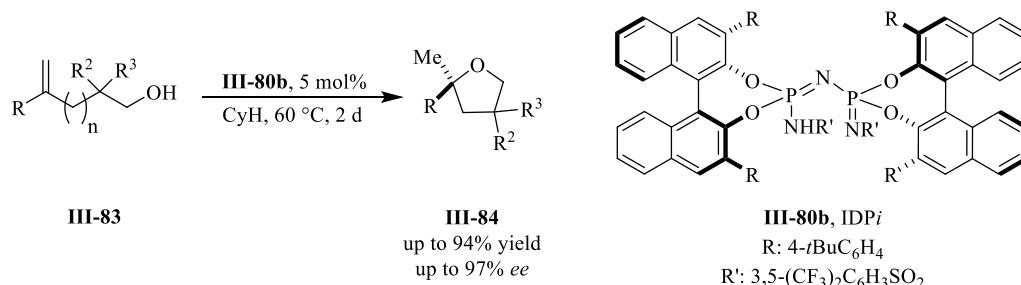
**Scheme III-18.** Synthesis and catalytic utility of imidodiphosphorimidate IDPi in hetero-atom Diels-Alder reaction



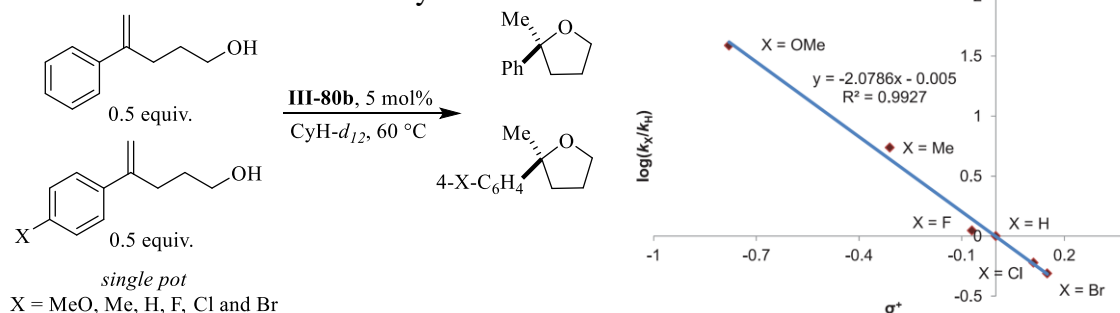
Aromatic aldehydes along with the aliphatic ones underwent [4+2]-cycloaddition reaction and cycloadduct **III-82** was produced in excellent induction.

In 2018, for the first time in the history of asymmetric catalysis, the enantioselective protonation of an alkene was reported and was made possible by an IDPi catalyst (scheme III-19a).<sup>44</sup> The strong acidity as well as the confined and well defined chiral pocket empowered the IDPi catalyst **III-80b** to catalyze the proto-cyclization of substrate **III-83** which led to the production of enantioenriched functionalized tetrahydrofurans **III-84**. Next, in order to get more information about the mechanism of this reaction a Hammett study was conducted which looked into the correlation between  $\text{Log}(k_x/k_H)$  and  $\sigma^+$ .

**Scheme III-19a.** Enantioselective olefin protonation



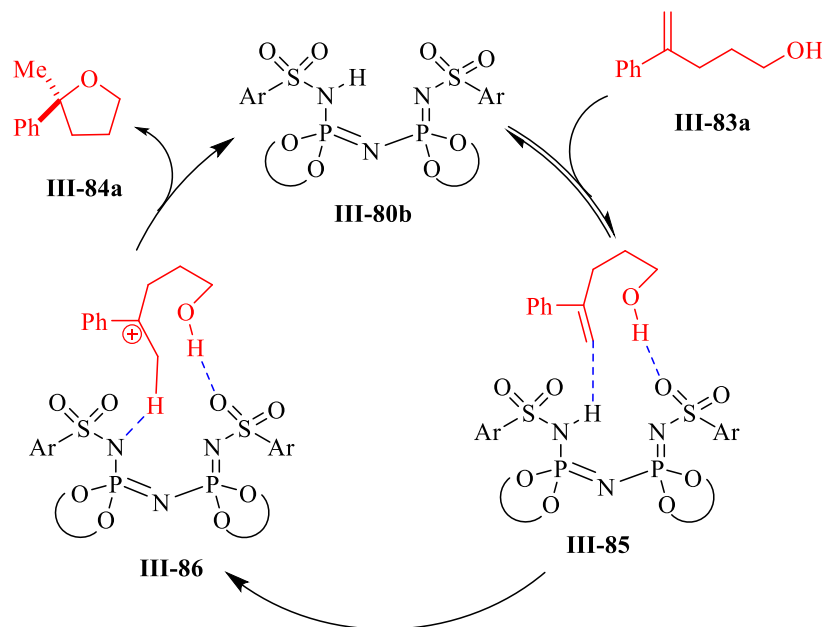
**Scheme III-19b.** Hammett study



These results were consistent with the asynchronous concerted mechanism; therefore, it was proposed that the mechanism of the reaction proceeds via the association of catalysts **III-80b** and substrate **III-83a**. The succeeding protonation of the alkene produces the carbocationic

intermediate **III-86** followed by nucleophilic attack of the hydroxy group and subsequent deprotonation to afford product **III-84b** which closes the catalytic cycle (scheme III-20).

**Scheme III-20.** Proposed mechanism for enantioselective protonation of olefin



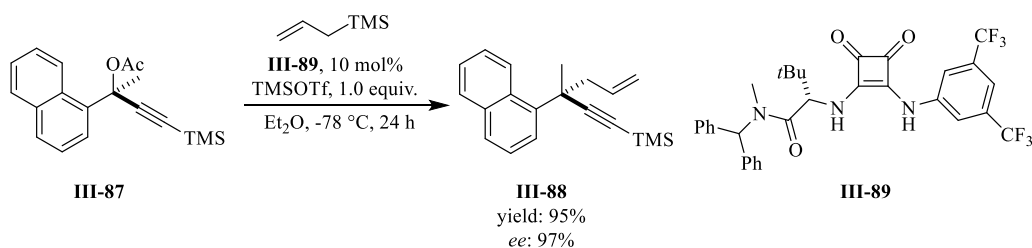
To expand the utility of the extremely active IDPi catalyst **III-80**, its ability in controlling the stereochemistry in non-classical carbocations was investigated (scheme III-21c). Performing a stereoselective reaction on a classical carbocation is quite challenging presumably since one of the competing reactions is elimination. Very recently, Jacobsen reported an elegant approach to induce stereoselectivity in  $S_N1$  reaction (scheme III-21b).<sup>45</sup> The challenge becomes even harder in performing stereoselective reactions with non-classical carbocations due to its unique structure that it can adopt (scheme III-21a). However, in 2019, these obstacles were alleviated and the first stereoselective reaction on this particular unusual carbocation was reported by Benjamin List in 2019 (scheme III-21c).<sup>46</sup> The reaction of *rac*-norbornane **III-90** bearing a trichloroacetimidate in the exo position with IDPi catalyst **III-80c** produced the non-classical carbocation which was trapped with trimethoxybenzene as the nucleophile and produced the desired product **III-91** in

84% yield and a 97:3 enantiomeric ratio. In contrast, the endo norbornane **III-92** reacted slower; therefore, the reaction was conducted under slightly harsher conditions (room temperature and ethyl acetate as the solvent).

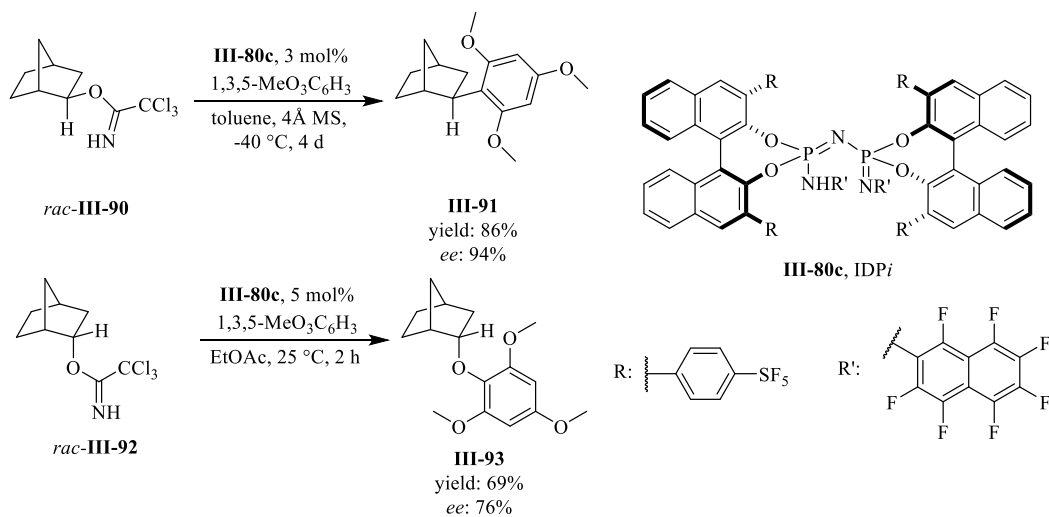
### Scheme III-21a. Classical carbocation vs. non-classical carbocation



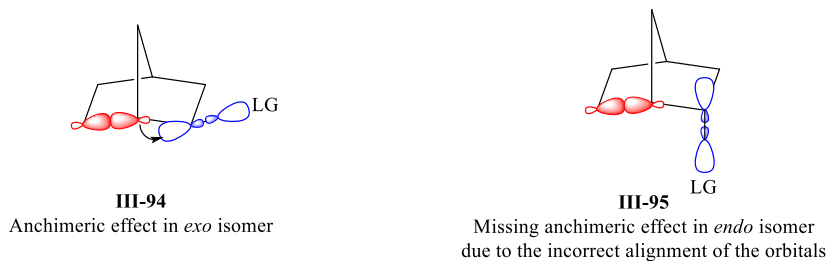
### Scheme III-21b. Enantioselective S<sub>N</sub>1 reaction reported by Jacobsen



### Scheme III-21c. Stereoselective reaction onto non-classical carbocation

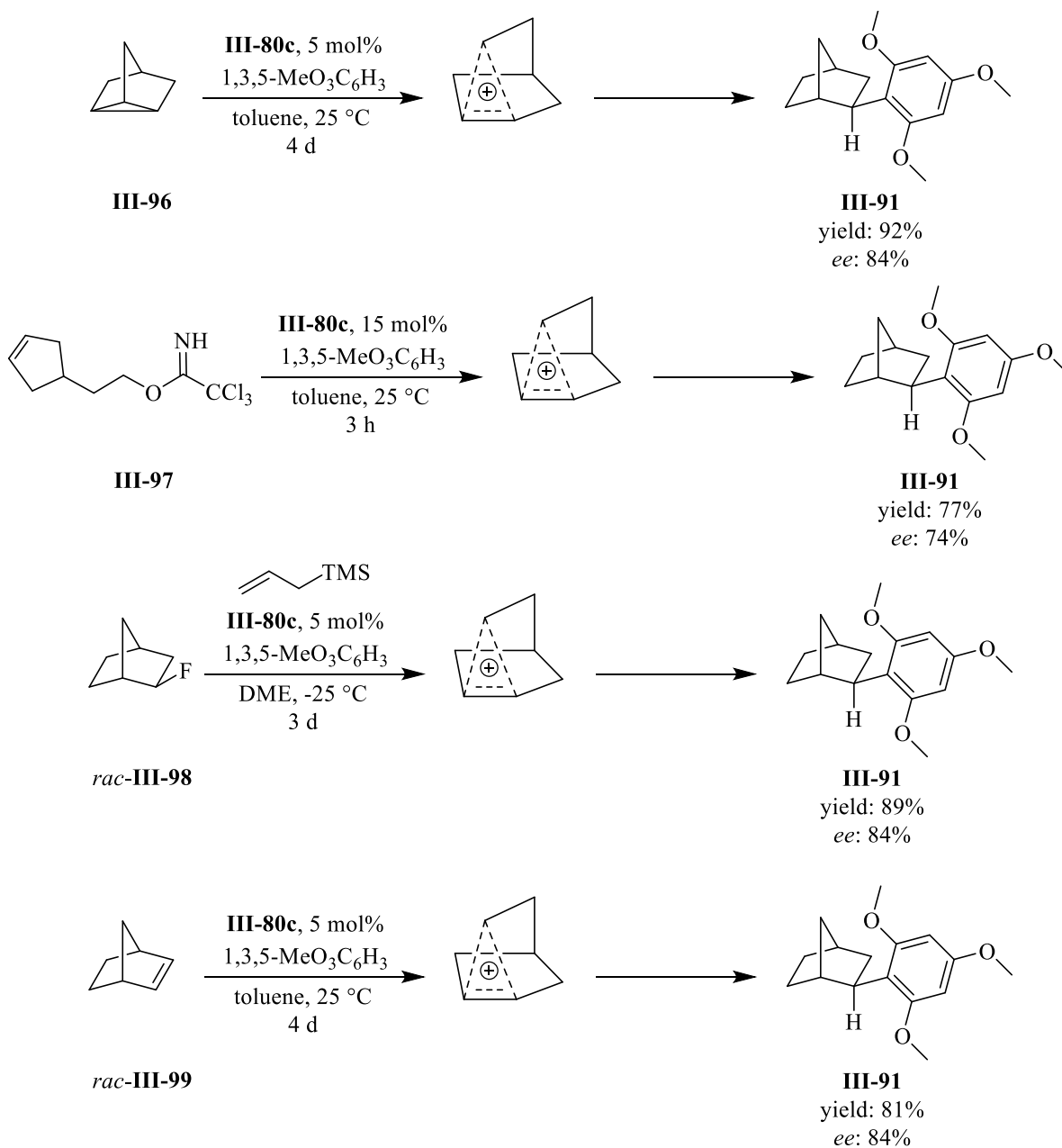


### Scheme III-21d. Anchimeric effect in exo vs. endo isomer



After 2 h, the desired product **III-93** was afforded in good yield and 88:12 enantiomeric ratio. The exo isomer **III-90** was converted to product **III-91** in 2 minutes in 70% yield and 88:15 enantiomeric ratio under exactly the same conditions. This difference in the reactivity profile of endo and exo isomers was explained by Winstein.<sup>47</sup>

**Scheme III-22.** Generation of non-classical carbocation with various substrates



In this report by List, it was shown that the exo isomer is 350 times more reactive than the endo isomer in a polar aprotic solvent and the reason is because of anchimeric assistance of C<sub>1</sub>-C<sub>6</sub>  $\sigma$ -bond in exo isomer (structure **III-94**, scheme III-21d). However, due to the wrong alignment of C<sub>1</sub>-C<sub>6</sub>  $\sigma$  bond and  $\sigma^*$  of the leaving group, the endo isomer is not enjoying the aforementioned anchimeric effect which leads to a slower reaction (structure **III-95**, scheme 21d). The reaction of hydrocarbon **III-96** with IDPi catalyst also afforded the non-classical carbocation via C-C  $\sigma$ -bond activation which was trapped with 1,3,5-trimethoxybenzene and yielded product **III-91** in good yield and good enantiomeric excess (scheme III-22). The reactivity of hydrocarbon **III-96** toward the IDPi catalyst **III-80c** is presumably due to the ring strain. The non-classical carbocation was also produced via cation- $\pi$  cyclization, C-F bond activation, and olefin protonation and the subsequent reaction of this intermediate with appropriate nucleophile afforded the desired product **III-91** in excellent results (scheme III-22).

The extraordinary acidity of the IDPi catalysts and also the tunability of its chiral pocket enabled List research group to successfully conduct numerous organic transformations in an asymmetric manner such as asymmetric Diels-Alder reactions and asymmetric Nazarov cyclizations.<sup>48,49</sup>

### **3.2. Extremely active imidodiphosphorimidate catalysts for asymmetric halonium-ion induced spiroketalization**

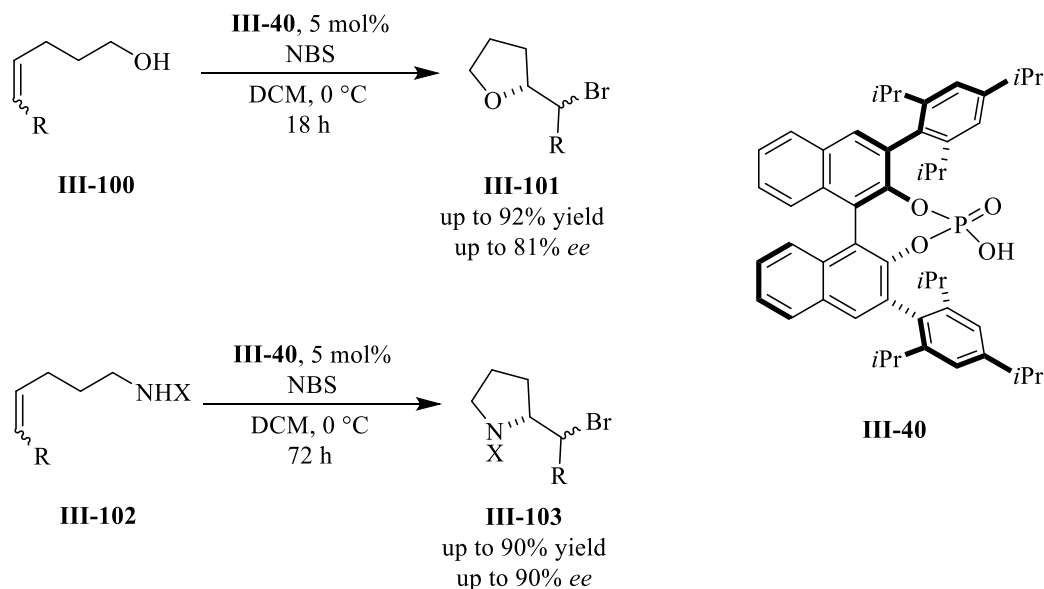
#### **3.2.1. Brønsted acid catalyzed halofunctionalization of alkenes**

Asymmetric halo functionalization of alkenes is a valuable tool in the construction of enantioenriched alkyl halides.<sup>50</sup> This field has received a great deal of attention recently and attempts to develop a practical method for asymmetric halofunctionalization are still ongoing.<sup>51</sup> One of the earliest examples of halofunctionalization catalyzed by chiral phosphoric acid was presented by Shi in 2011 (scheme III-23).<sup>52</sup> In this report, catalyst **III-40** mediated the reaction



between NBS and  $\gamma$ -hydroxy alkenes **III-100** to afford the desired products **III-101** in excellent yield and good enantioselectivity. The same reaction was conducted with  $\gamma$ -amino alkene **III-102** which produced halofunctionalized pyrrolidines **III-103** in up to 90% *ee*. It is interesting to note that the reaction was stereospecific and the cyclization occurred via 5-exo-trig ring closing mechanism.

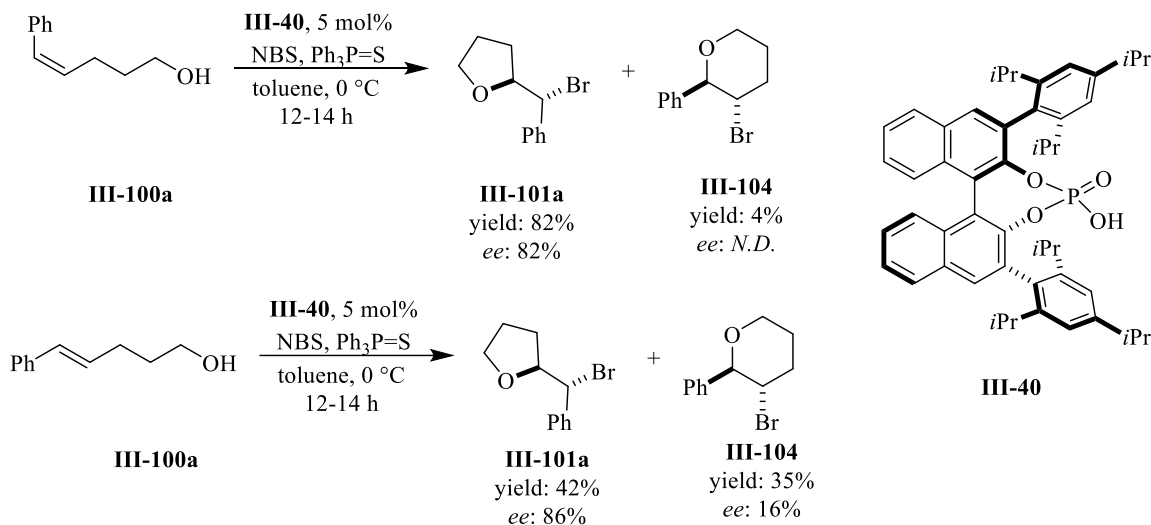
**Scheme III-23.** Enantioselective bromocyclization catalyzed by BINOL phosphoric acid catalyst



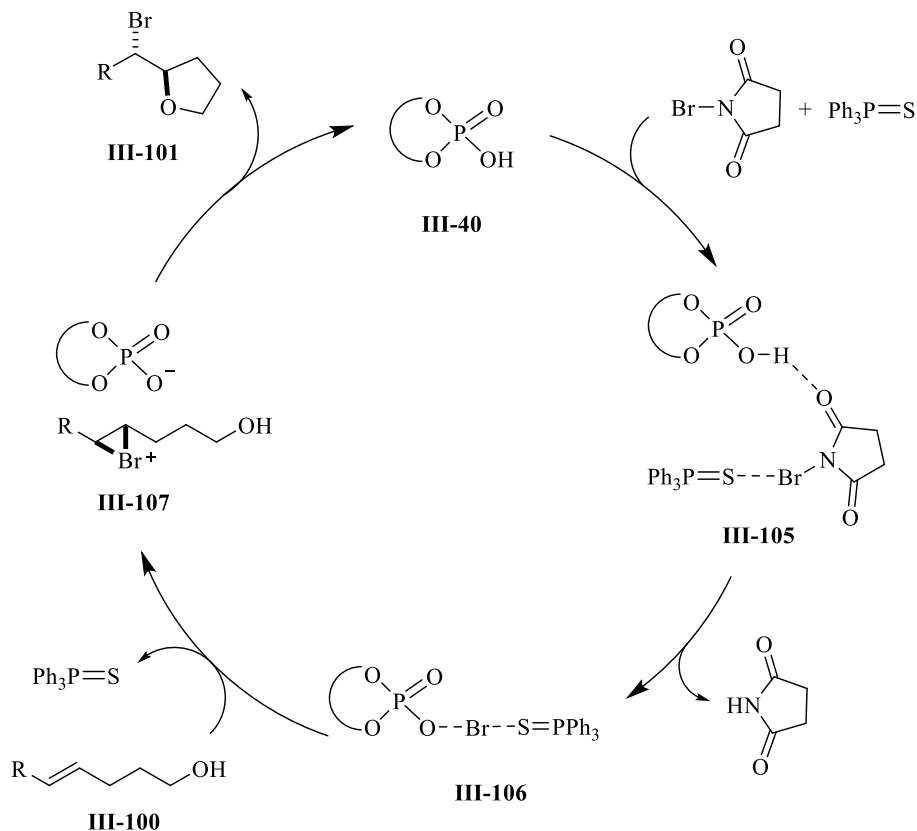
Same year, Scott Denmark reported the successful use of a cooperative Lewis base/Brønsted acid catalytic system in the bromoethrification of substrate **III-100a** (scheme III-24a).<sup>53</sup> It was assumed that an achiral Lewis base would activate the NBS as the halonium source and concomitant replacement of succinimide with the conjugated base of the chiral Brønsted acid **III-40**. Therefore, a complete bromium ion transfer to the chiral Brønsted acid catalyst **III-40** was proposed which led to the enantioselective bromoethrification (scheme III-24b). The catalyst design was rewarded and Z-alkene **III-100a** was converted to the enantioenriched alkylated tetrahydrofuran **III-101a** in good yield and enantioselectivity. Interestingly, conducting the same reaction with E-alkene **III-100a** yielded a mixture of isomers **III-101a** and **III-104**. The combined yield was 77% with *e.r.*

of 93:7 for the isomer **III-101a** and 58:42 for the isomer **III-104**. VAPOL phosphoric acid was also used in this reaction but poor induction and selectivity were obtained.

**Scheme 24a.** Enantioselective bromocyclization catalyzed by BINOL phosphoric acid catalyst

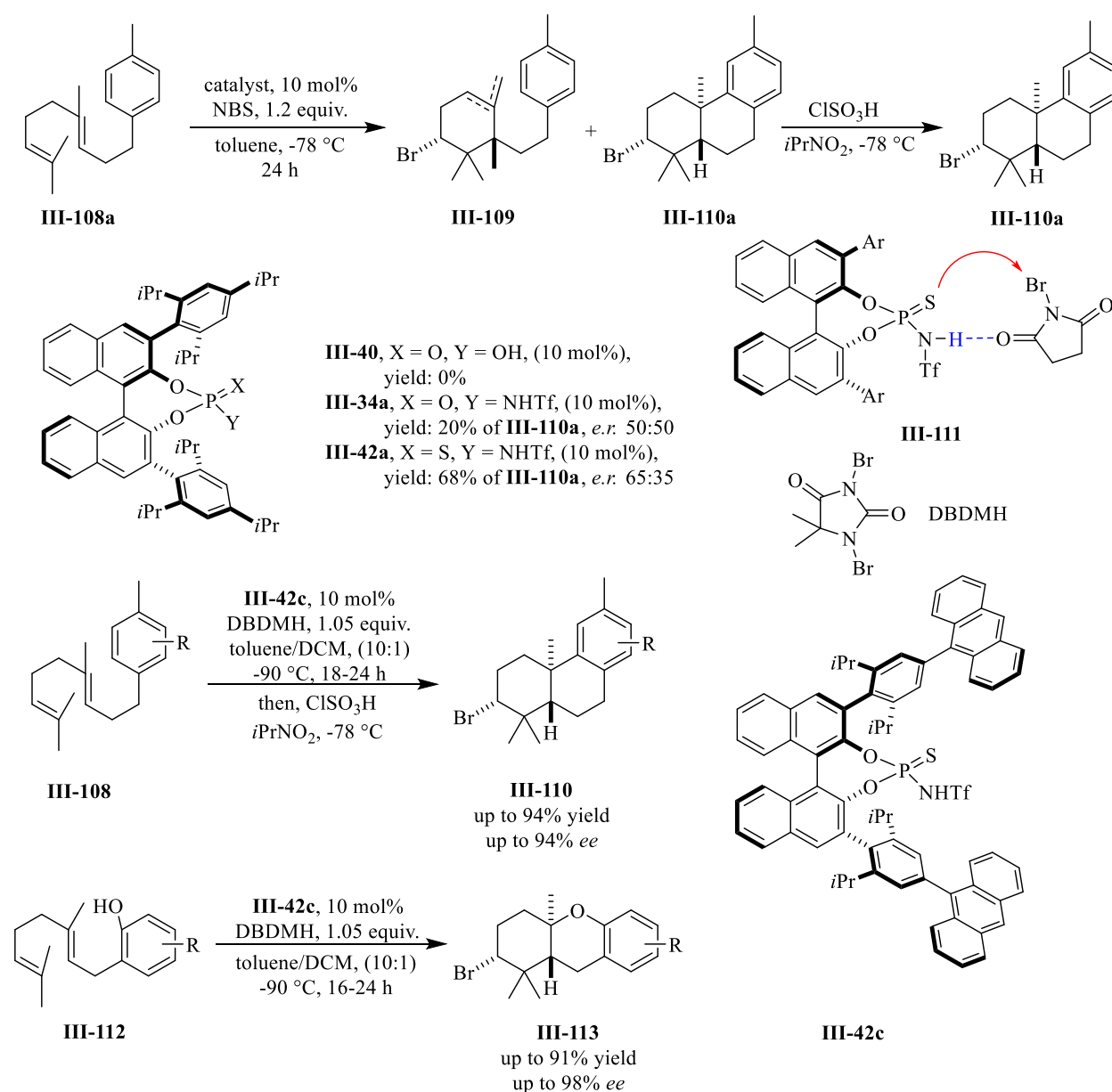


**Scheme 24b.** Proposed mechanism for the bromocyclization with **III-40**



In 2017, Yamamoto reported a successful asymmetric bromonium ion-induced polyene cyclization catalyzed by chiral biaryl Brønsted acid catalyst **III-42** (scheme III-24c).<sup>54</sup> Initially, the reaction was conducted with BINOL phosphoric acid catalyst **III-40** and N-bromosuccinimide (NBS) as the bromonium source; however, no product was observed. Performing the same reaction with *N*-triflyl BINOL phosphoramidate catalyst **III-34a** led to a 20% conversion but with 50:50 enantiomeric ratio. It should be noted that the bromocyclization in presence of catalyst **III-34a**

**Scheme III-24c. Enantioselective polyene cyclization**

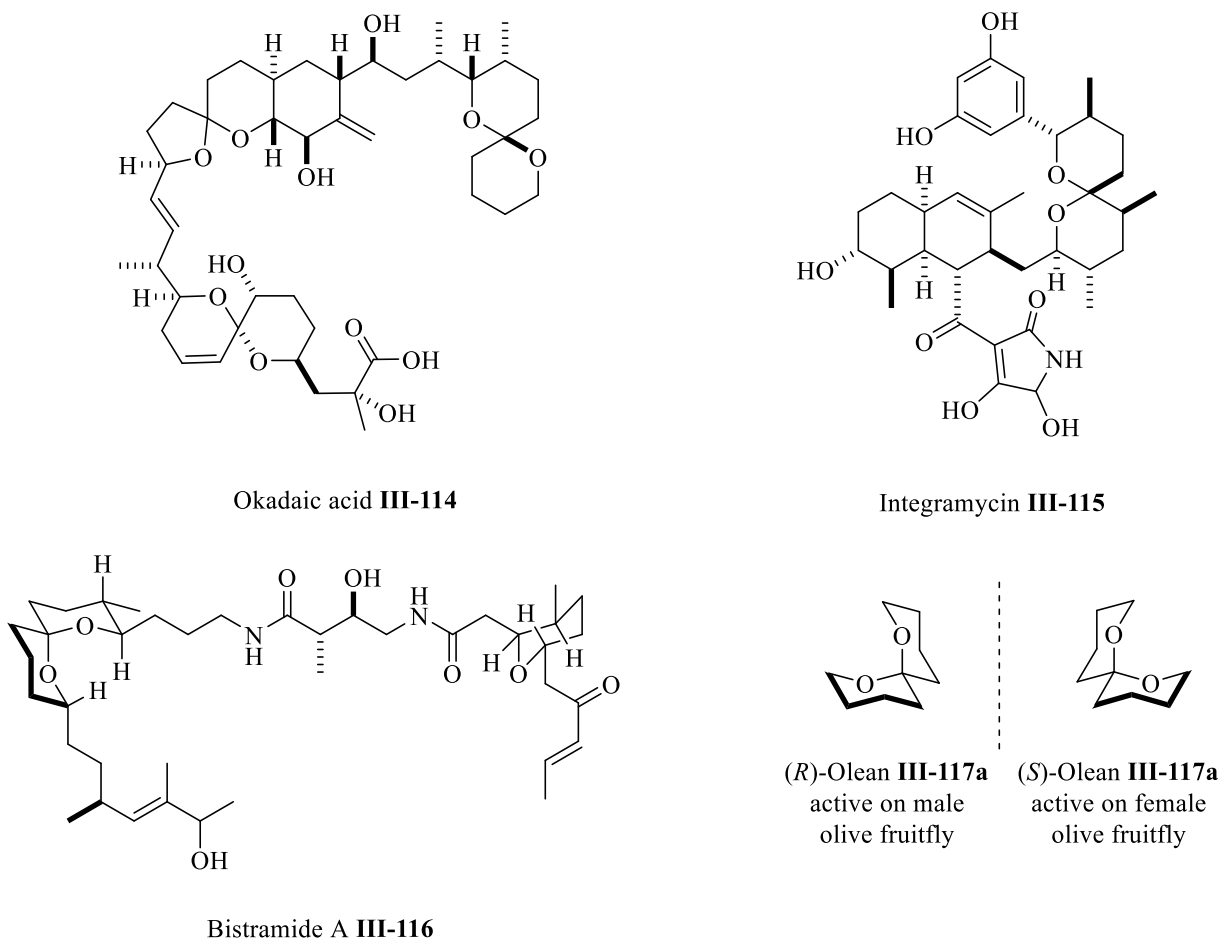


produced partial cyclized product **III-109** along with the fully cyclized one. Therefore, in order to induce full cyclization, the crude reaction mixture was reacted with chlorosulfonic acid. Interestingly, *N*-triflyl BINOL thiophosphoramidate **III-42a** gave the desired product **III-110a** in good yield (68%) and a 65:35 enantiomeric ratio. The efficiency of the thiophosphoramidate catalyst **III-42a** over the phosphoramidate catalysts **III-34a** led Yamamoto to assume that the Lewis basicity of the sulfur component of the catalyst also plays a pivotal role as well as Brønsted acid component of the catalyst. Based on this observation, complex **III-111** was proposed in order to demonstrate the dual activation of NBS with catalyst **III-42** during the course of the reaction. Further optimization revealed catalyst **III-42c** as the optimum catalyst and DBDMH (1,3-dibromo-5,5-dimethylhydantoin) as the optimum bromonium source which converted a wide range of homogerylbenzenes **III-108** to the desired products **III-110** in good yield and enantioselectivity. Bromocyclization of geranylphenols **III-112** were also investigated under the optimum reaction conditions and the brominated cyclized products **III-113** were furnished in good to excellent yield and also enantioinduction.

### 3.2.2. Chemical synthesis of spiroketals

Spiroketals are important motifs in organic chemistry and a wide range of natural products such as okadaic acid **III-114**, integramycin **III-115**, and Bistramide **III-116** bear spiroketals as the core part of their structure.<sup>55</sup> In addition, (*R*)-Olean **III-17** is the simplest 6,6-spiroketal and is the female-produced sex pheromone while the other enantiomer (*S*)-Olean **III-17** is the male-produced sex pheromone (scheme III-25). Due to the prevalence of the spiroketals in nature and also their application in pharma, these motifs are the subject of numerous studies in asymmetric catalysis and attempts are still ongoing to develop a practical method in the synthesis of enantioenriched functionalized spiraketals.

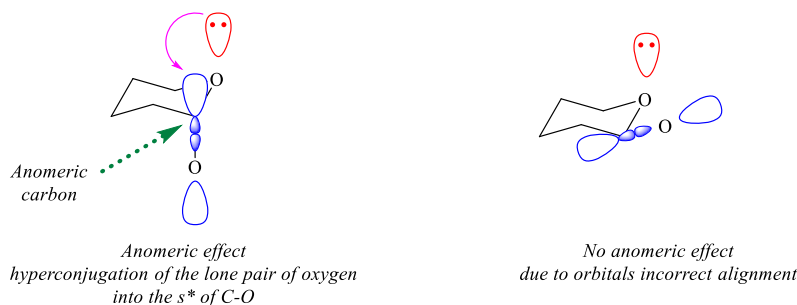
**Scheme III-25.** Natural products containing spiroketals component



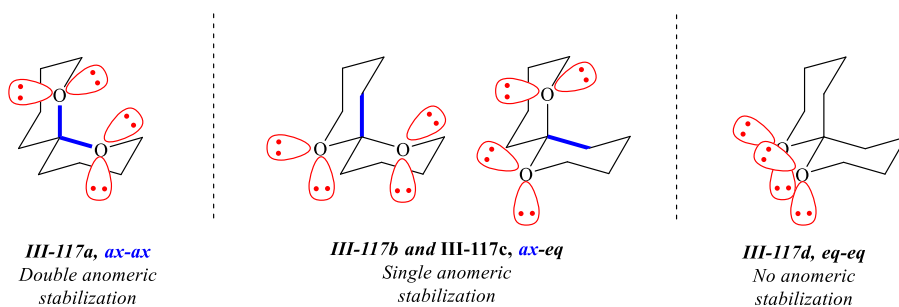
Most of the natural products and also bioactive molecules most often contain 6,6- 5,5- and 6,5- spiroketals. Four isomers would be possible for 6,6-spiroketals and in all of them two C-O single bonds are coming together in the junction of two rings. In the first isomer **III-117a**, two C-O bonds are occupying axial positions, in the second and third isomers **III-117b** and **III-117c**, one of the C-O bonds occupies axial position while the other one is located in equatorial position. In the last isomer **III-117d** both of the C-O bonds are placed in equatorial positions (scheme III-26b). Further studies on the stability of these isomers revealed that the first isomer is the most stable isomer while the fourth one is the least stable.<sup>56</sup> This stability trend could be explained via the anomeric effect which is the result of the occupation of the axial position by an electronegative atom (oxygen

in this case) in pyranose despite its unfriendly 1,3-diaxial interaction (scheme III-26a). The widely accepted explanation for the anomeric effect is the delocalization (hyperconjugation) of the lone pair of the pyran's oxygen into the  $\sigma^*$  of the C-O in the axial position which brings 1.4-2.4 kcal/mol stability to this system.<sup>56</sup> However, no anomeric stabilization is observed when the substituent on the anomeric carbon is in an equatorial orientation due to the incorrect alignment of the oxygen's lone pair and  $\sigma^*$  of the C-O bond. The spiroketal **III-117a** is extraordinary stable because of this fact that this isomer is enjoying dual anomeric effect (*ax-ax*); however, isomers **III-117b** and **III-117c** are stabilized via only one anomeric effect (*ax-eq*) and isomer **III-117d** does not have any anomeric stabilization which makes it the least stable among the four isomers (*eq-eq*).

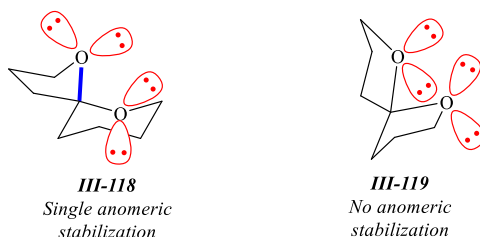
**Scheme III-26a.** Anomeric effect in spiroketal



**Scheme III-26b.** Anomeric effect in [6,6]-spiroketal



**Scheme III-26c.** Anomeric effect in [6,5] and [5,5]-spiroketals

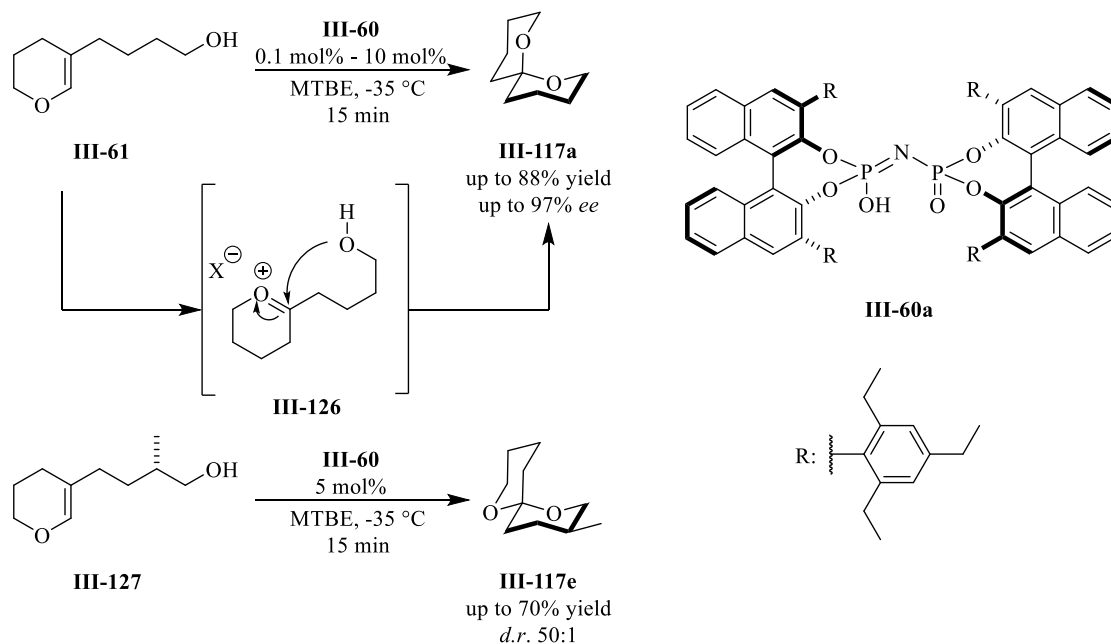




To do so, substrate **III-124** was prepared in a two-directional homologation in two steps starting with compound **III-121** followed by alcohol deprotection. A single diastereomer was obtained after thermodynamically induced spiroketalization of substrate **III-124** and subsequent epimerization of methyl groups in the  $\alpha$ -positions of the carbonyls.

List research group in 2012 reported a different and novel approach to the synthesis of enantioenriched spiroketals (scheme III-28).<sup>33</sup> In this strategy, dihydropyrans bearing a pendant alcohol underwent diastereo and enantioselective spiroketalization in presence of imidodiphosphoric acid catalyst **III-60a** and gave the desired product **III-117a** in excellent yield and asymmetric induction. Further investigation revealed that the same catalyst is capable of overriding the thermodynamic preference in the formation of spiroketal; therefore, several substrates such as **III-127** bearing a chiral center underwent kinetically controlled spiroketalization and non-thermodynamically stable spiroketals were produced in good to excellent diastereoselectivity.

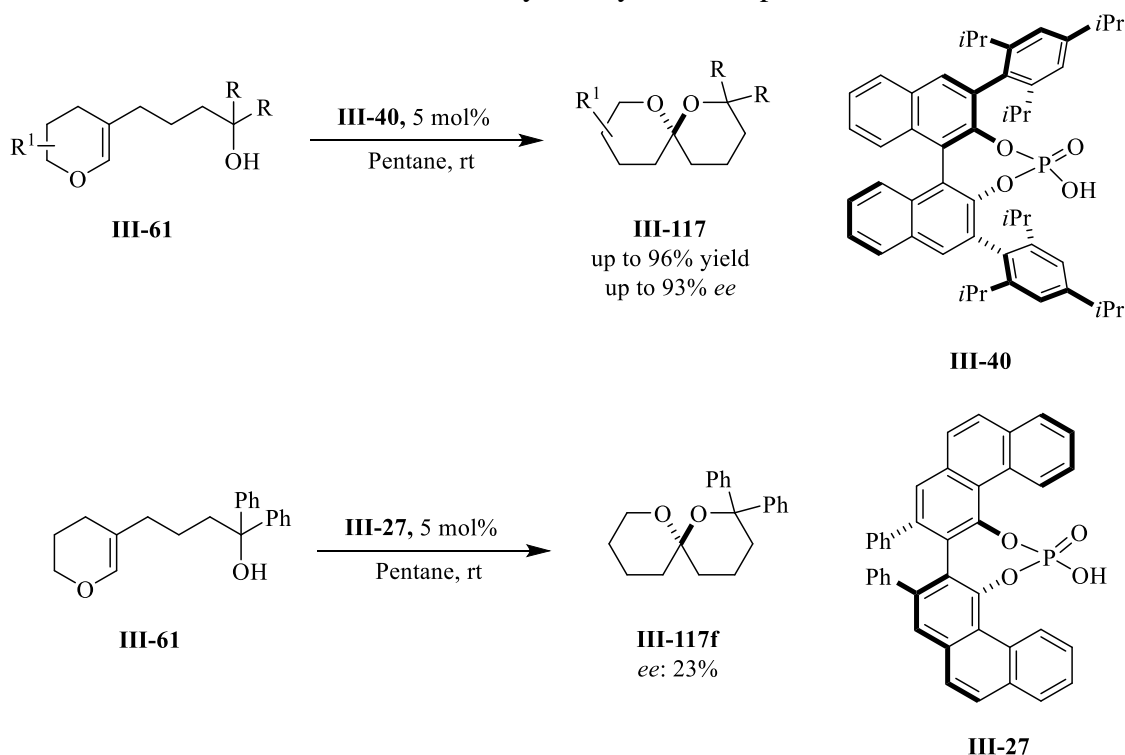
**Scheme III-28.** Confined BINOL Brønsted acid catalyzed asymmetric spiroketalization





Same approach was used by Nagorny in 2012 to access enantioselective spiroketalization catalyzed by chiral phosphoric acid **III-40**.<sup>58</sup> VAPOL phosphoric acid was also investigated in this reaction; however, unsatisfactory results were obtained.

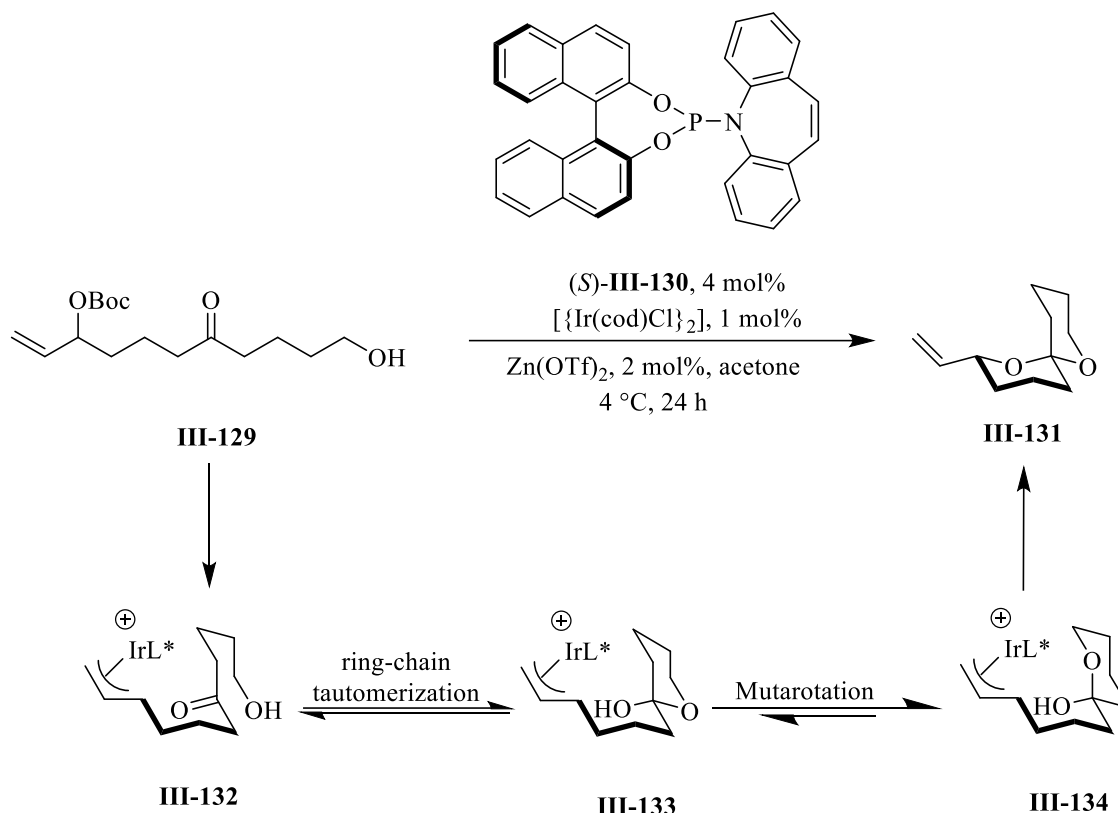
**Scheme III-29.** BINOL Brønsted acid catalyzed asymmetric spiroketalization



Despite the excellence of Brønsted acid-catalyzed spiroketalizations presented by List and Nagorny, these methodologies suffer from a limited substrate scope especially for accessing functionalized spiroketals. In 2017, Carreira overcame this limitation by reporting a highly efficient vinyl-substituted spiroketal formation catalyzed by chiral Ir-(P,olefin)complex (scheme III-30).<sup>59</sup> It was assumed that the substrate **III-129** bearing Boc-protected allylic alcohol forms  $\pi$ -allyl complex **III-132** in presence of an *in situ* generated chiral iridium catalyst. The face selectivity is determined in this step by the influence of the chirality of the phosphorimidite ligand **III-130**. Ring-chain tautomerization furnished  $\pi$ -allyl iridium complex hemiacetal **III-133** which

was transformed into the vinyl substituted spiroketal **III-131** via mutarotation and subsequent nucleophilic attack of the hydroxy group of hemiacetal **III-134**.

**Scheme III-30.** Vinyl substituted spiroketal synthesis catalyzed by Ir-(P,olefin) complex

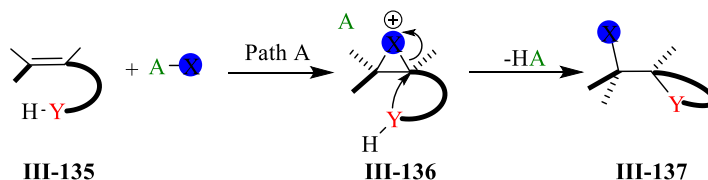


### 3.2.3. Mechanistically inspired halonium ion-induced spiroketalization

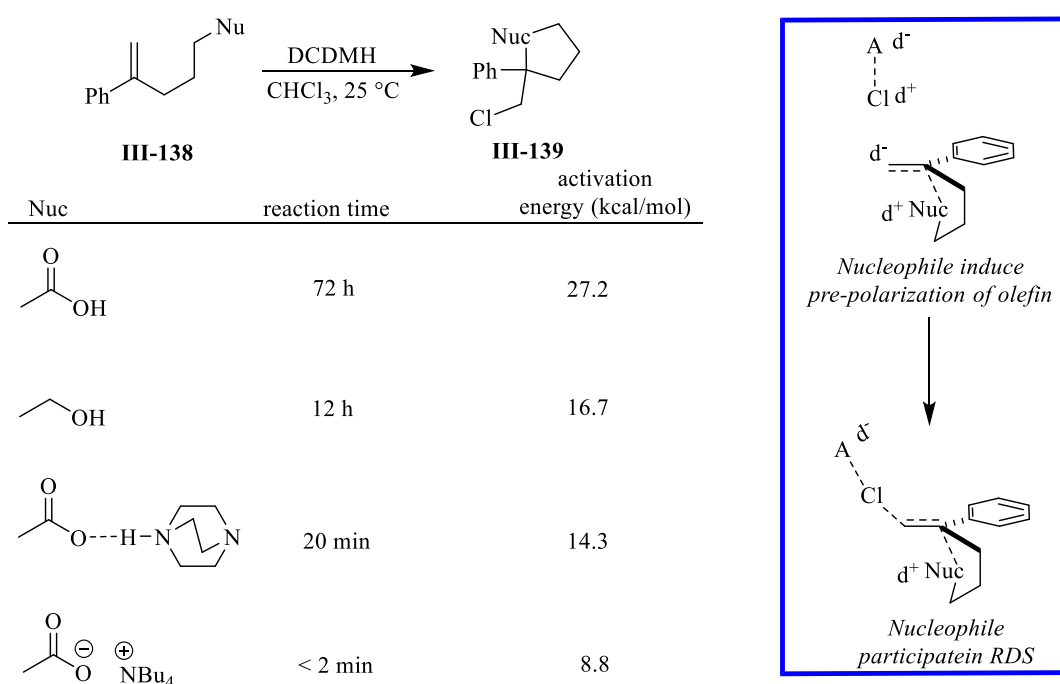
The halofunctionalization of olefins is a valuable method in organic synthesis which enables chemists to access a wide range of enantioenriched intermediates that are used in the synthesis of natural products as well as bioactive compounds.<sup>60</sup> In terms of mechanism, the addition of halide (X) to the alkene is believed to be triggered by the formation of three-membered cationic intermediate **III-136**, a so-called halonium ion via electrophilic attack of the halide (X), followed by trapping the cationic adduct with an appropriate nucleophile (Nu) (scheme III-31a). In the classical mechanism for halofunctionalization, the rate of the reaction is dependent on the nature

of the alkene and the role of the nucleophile is neglected. However, this notion was challenged by the landmark report from Borhan's lab in 2016.<sup>61,62</sup>

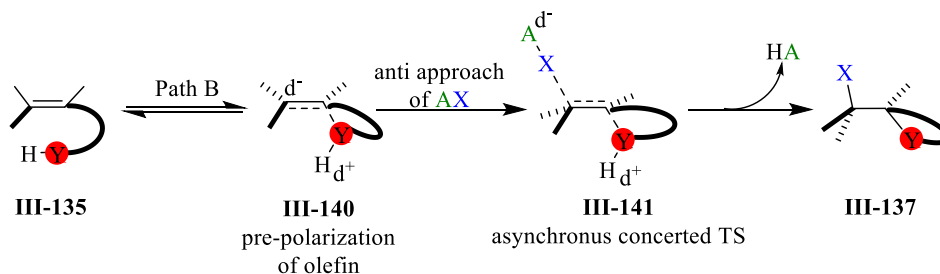
**Scheme III-31a.** Commonly depicted electrophilic addition of halide to olefin



**Scheme III-31b.** The effect of nucleophile in the halofunctionalization of olefin



**Scheme III-31c.** Nucleophile-assisted alkene activation (NAAA)

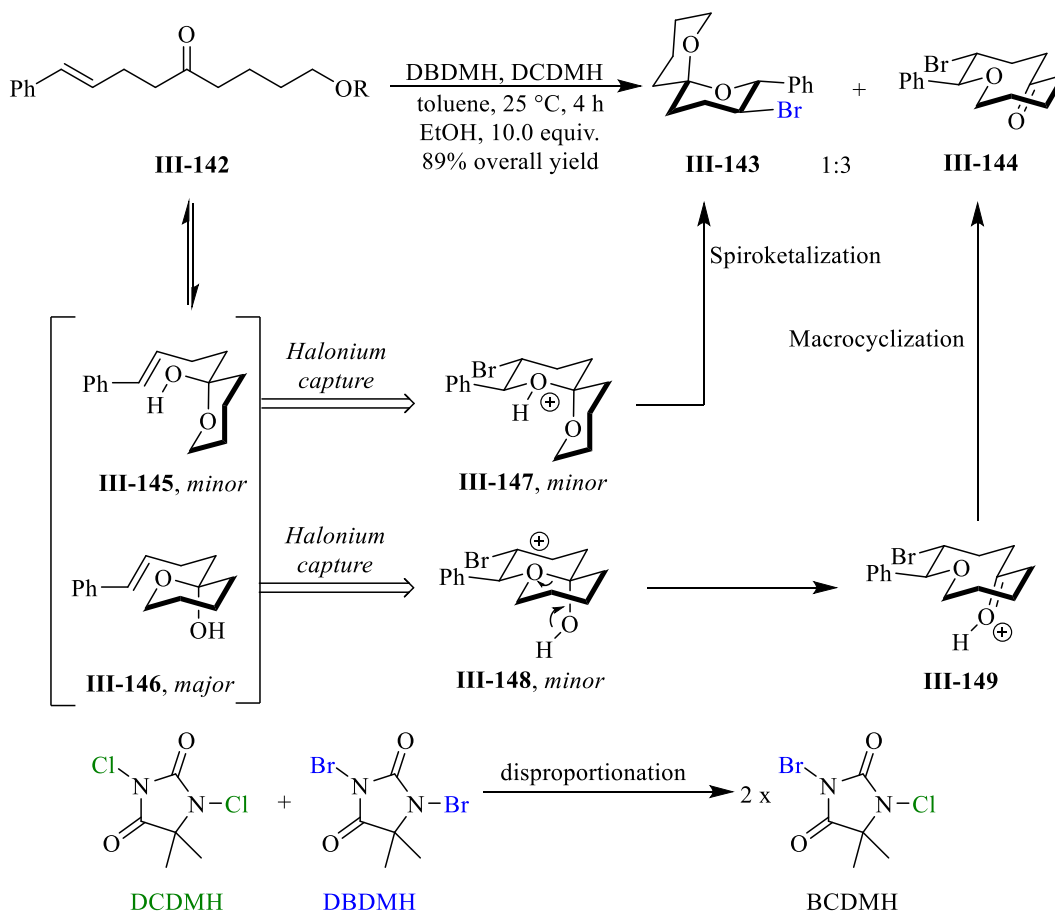


This challenge was brought by performing a detailed mechanistic study of the chloro-etherification reaction, which demonstrated a strong correlation between the rate of the reaction and the nature of the nucleophile (scheme III-31b). Thus, in order to explain this observation, it was suggested that the substrate **III-138** is pre-organize before participation in the reaction. The aforesaid pre-organization occurs via the interaction between the non-bonding orbital of the nucleophile and the  $\pi^*$  of alkene which pre-activates the alkene and sets it up for further transformation. As a result, an asynchronous concerted mechanism was proposed for the halofunctionalization of olefin (path B, scheme III-31c). The term nucleophile-assisted alkene activation (NAAA) was used to designate to this phenomena by Borhan to accentuate the importance of the nucleophile in the halofunctionalization of olefins (scheme III-31c). Usually, olefins alone are inept substrates in the halofunctionalization reaction in the absence of NAAA effects. Also, no experimental evidence was obtained for the presence of three-membered ring cationic adduct **III-136** in the halofunctionalization of the alkene.

The halofunctionalization of the alkene **III-142** tethered with a ketone moiety as the nucleophile was investigated in the context of NAAA.<sup>63</sup> It was assumed that the halofunctionalization of substrate **III-142** would produce an oxocarbenium intermediate (not shown) which could also be intercepted by the pendant alcohol and produce the spiroketal **III-143**. Initial screening of the bromonium sources proved the incompetence of NBS and DBDMH in delivering the spiroketal **III-143**. Further optimization revealed 3-bromo-1-chloro-5,5-dimethylhydantoin (BCDMH) as the optimum halonium source which was generated *in situ* by reacting an equimolar of DCDMH and DBDMH. Surprisingly, the desired spiroketal **III-143** was isolated as the minor product along with the macrocycle **III-144** as the major product after conducting the reaction of substrate **III-142** with BCDMH as the halonium source (scheme III-

32). This product distribution indicated an existing equilibrium between substrate **III-142** and its hemiacetal forms **III-145** and **III-146**. The interception of the hydroxy group in bromo functionalization in hemiacetal **III-145** produced the desired spiroketal **III-143** while the interception of the oxygen moiety embedded in the six-membered ring, **III-146**, yielded the macrocycle **III-144**.

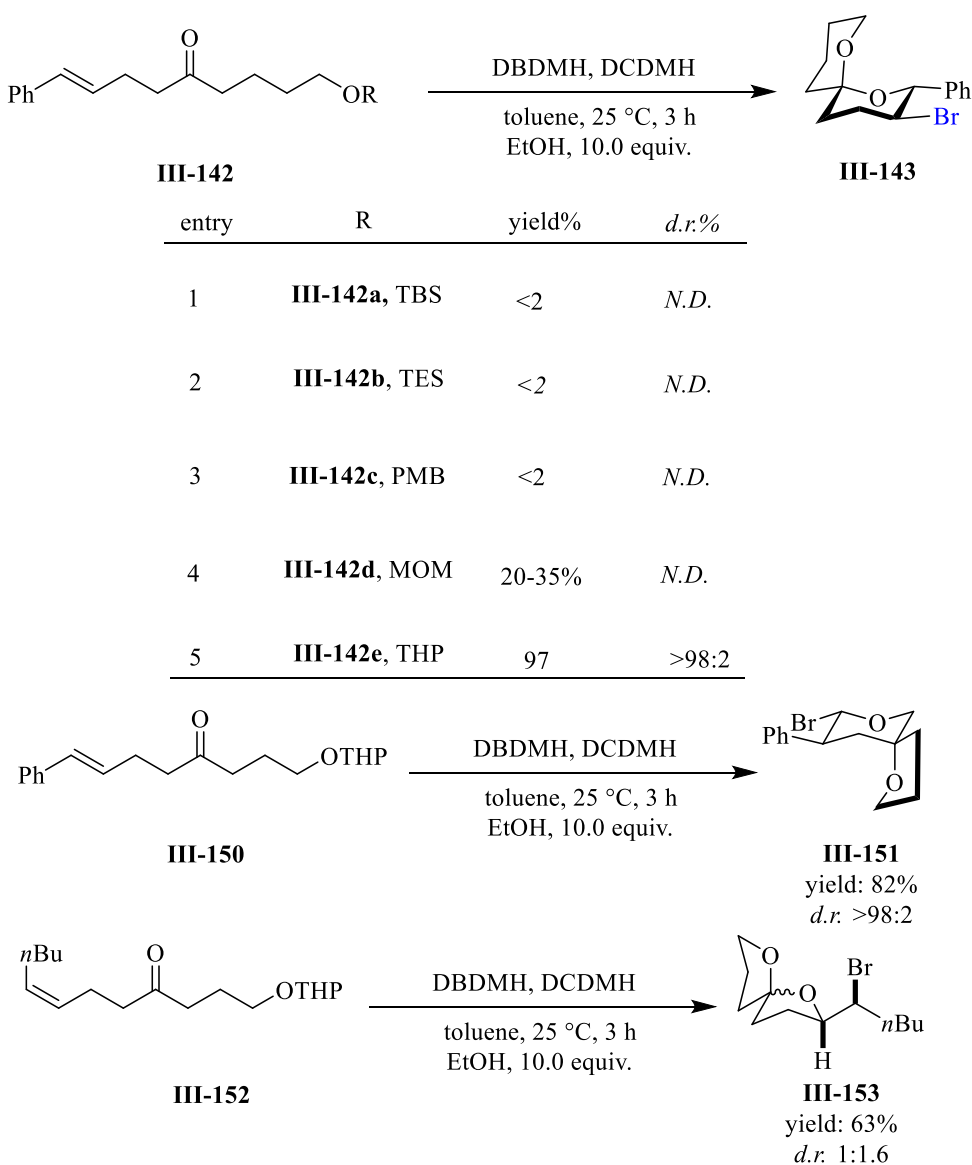
**Scheme III-32.** Bromo Spiroketalization with unprotected pendant alcohol



The protection of the pendant hydroxy moiety to suppress the macrocyclization of substrate **III-142** was considered and different protecting groups such as TBS, TES, and PMB were evaluated; however, only trace amounts of the desired spiroketal was observed (scheme III-33). Interestingly, the MOM protecting group gave spiroketal **III-143** in 20-35% yield. Finally using THP as the protecting group gave the desired spiroketal **III-143** in excellent yield and diastereoselectivity.

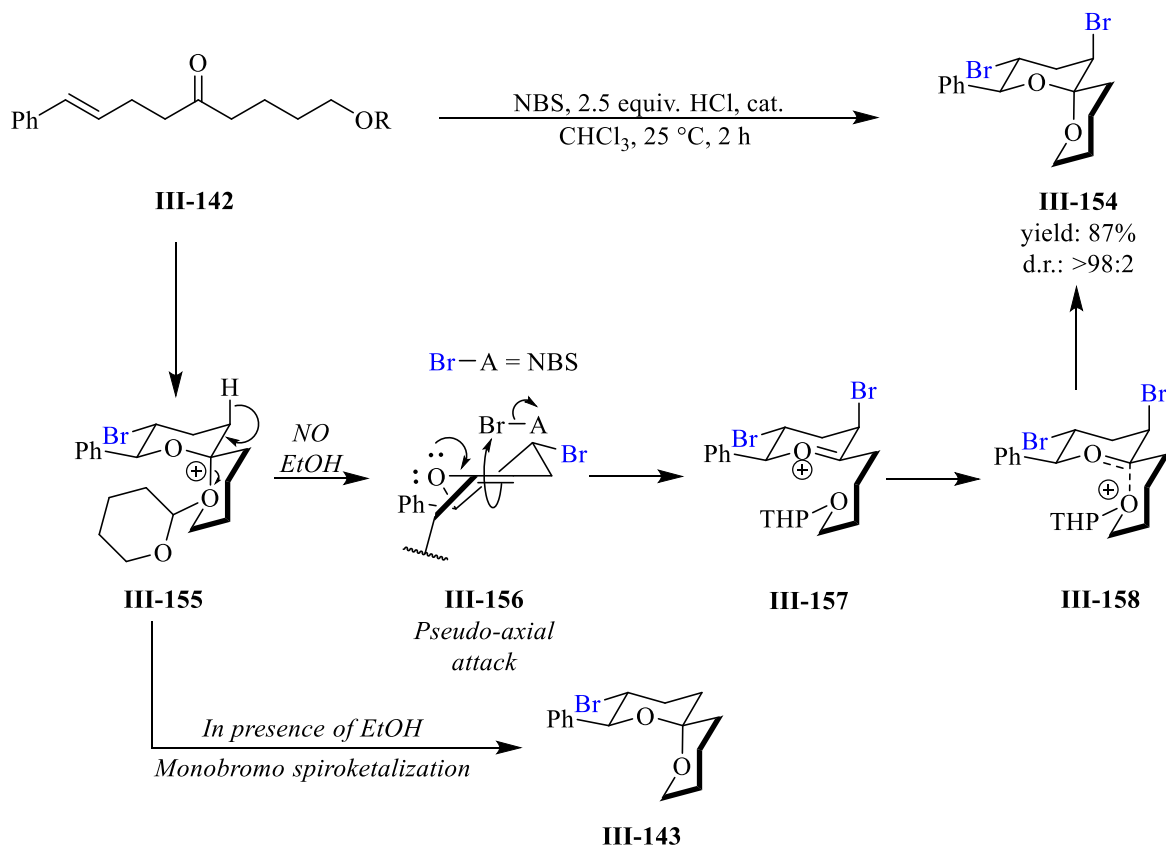
The [6,5]-spiroketal **III-151** was also obtained in good yield and excellent diastereoselectivity; however, the [5,5]-spiroketal **III-153** was produced in only a 2:1 diastereomeric ratio. The drastic decrease of the diastereomeric ratio in the [5,5]-spiroketal **III-153** is thought to be because of its inability to be stabilized via an anomeric effect. It should be noted that the presence of ethanol is critical to achieving high yield during the course of the reaction since it facilitates the THP removal.

**Scheme III-33.** Stereoselective halonium ion induced spiroketalization



Surprisingly, by leaving out the ethanol and in the presence of catalytic amount of HCl, the dibrominated spiroketal **III-154** was observed as the sole product in excellent yield and exceptional diastereoselectivity (scheme III-34). The structure of compound **III-154** was also confirmed unequivocally with x-ray structural analysis. It was assumed that in the absence of ethanol, intermediate **III-155** undergoes  $\alpha$ -deprotonation and produces dihydropyran **III-156**. The reaction of the dihydropyran **III-156** with another equivalent of NBS yields the dibrominated oxonium **III-157** which eventually affords the desired product **III-154**. The exceptional diastereoselectivity originates from trapping the second bromonium ion via pseudo-axial approach (structure **III-56**, scheme III-34).

**Scheme III-34.** Dibromo Spiroketalization in the absence of EtOH



### 3.2.4. Asymmetric catalytic halonium ion-induced spiroketalization

Inspired by the early studies of Denmark and Yamamoto in halofunctionalization of olefin, in collaboration with Borhan's lab, it was hypothesized that the use of VANOL/VAPOL derived Brønsted acid catalysts might catalyze the asymmetric bromonium ion initiated spiroketalization. Three goals were followed in this project including 1) synthesis and development of a library of VANOL/VAPOL Brønsted acid catalysts, 2) design an efficient VANOL/VAPOL Brønsted acid catalyst for the bromonium ion-induced spiroketalization and 3) demonstrate the efficiency of VANOL/VAPOL derived Brønsted acid catalysts over the BINOL derived Brønsted acid catalysts.

**Table III-7.** BINOL, VANOL and VAPOL Brønsted acid catalyst catalyzed asymmetric spiroketalization

entry	catalyst	Yield%	ee%
1	( <i>R</i> )-III-159	60	<5
2	( <i>S</i> )-III-160	32	7
3	( <i>R</i> )-III-161	70	11
4	( <i>R</i> )-III-162a	93	16
5	( <i>S</i> )-III-162b	80	42

(*R*)-III-159

(*S*)-III-160

(*R*)-III-161, X = S, Y = NHTf  
(*R*)-III-162a, X = NTf, Y = NHTf

(*S*)-III-162b

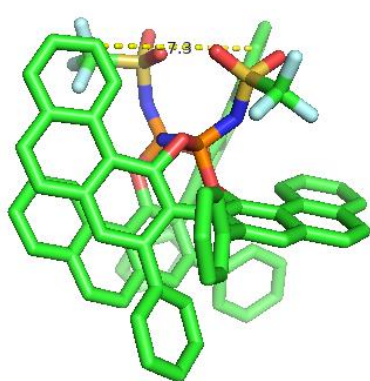
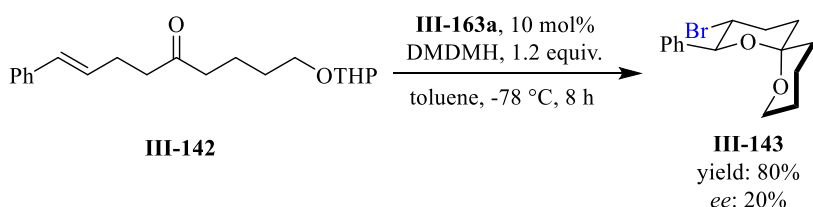
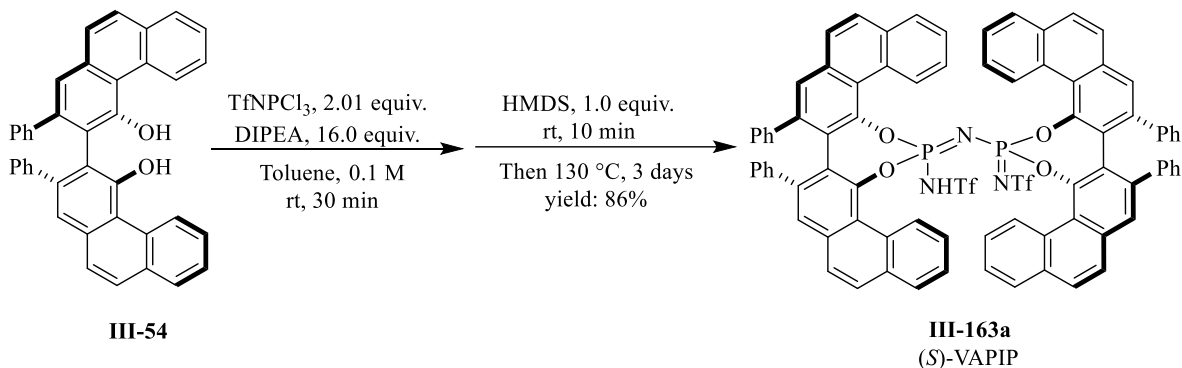


The spiroketalization was conducted with BINOL derived *N*-triflyl phosphoramidimide **III-159** catalysts and DBDMH as the bromonium source. The desired spiroketal **III-143** was obtained in good yield; however, with only 5% *ee* (table III-7, entry 1). The (*S*)-VAPOL catalyst **III-160** gave the spiroketal **III-143** with unsatisfactory results. The 7,7'-*t*Bu<sub>2</sub>VANOL derived Brønsted acid catalysts **III-161** and **III-162a** proved to be more efficient than the VAPOL **III-160** and BINOL **III-159** catalysts. Spiroketal **III-143** was produced in good yield and slightly improved *ee* with 7,7'-*t*Bu<sub>2</sub>VANOL *N*-triflylthiophosphoramidate **III-161** as the catalyst. Interestingly, the introduction of *N*-triflyl amide onto the catalyst improve the yield to 93% yield and the *ee* to 16%. We were delighted to observe a substantial increase in the enantiomeric induction of the spiroketal by utilizing *N*-triflylphosphoramidimide **III-162b** derived from the 7,7'-(2-Naph)<sub>2</sub>VANOL ligand. However, further screening of *N*-triflylphosphoramidimide derived from VANOL derivatives did not improve the asymmetric induction of the spiroketalization.

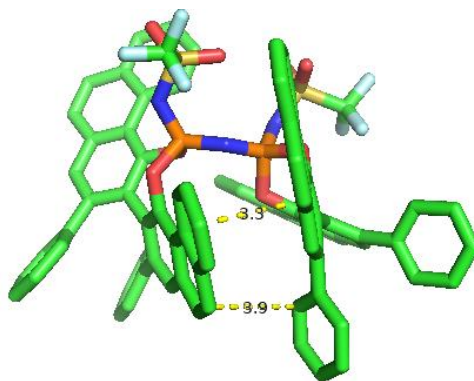
Next, we turned our attention toward VAPOL/VANOL imidodiphosphorimide catalysts and investigate their performance in the spiroketalization reaction inspired by List IDP*i* catalyst. First VAPOL imidodiphosphorimide (VAPIP) catalyst **III-163a** was prepared in excellent yield by reacting (*S*)-VAPOL **III-54** with *N*-triflylphosphorimidoyl trichloride and 0.5 equiv of HMDS (scheme III-35a). Performing the spiroketalization with VAPIP catalyst **III-163a** gave the desired product **III-143** in good yield but with moderate induction. Structure analysis of VAPIP catalyst **III-163a** by x-ray revealed that two phenanthrene components of each VAPOL ligand swing over the active site and create a C<sub>2</sub> symmetric chiral environment with a distance of 3.3 Å. In addition, there is a  $\pi$ - $\pi$  stacking between two the phenanthryl components of each VAPOL ligand with a distance of 3.3 Å. Also a C-H- $\pi$  interaction is observed between the phenanthryl of one ligand and the phenyl moiety in the backbone of the other one with a distance of 3.9 Å. However, since the

asymmetric environment around the active site was not well established, the spiroketal **III-143** was produced with low induction.

**Scheme III-35a.** Asymmetric catalytic spiroketalization catalyzed by VAPIP catalyst **III-163**



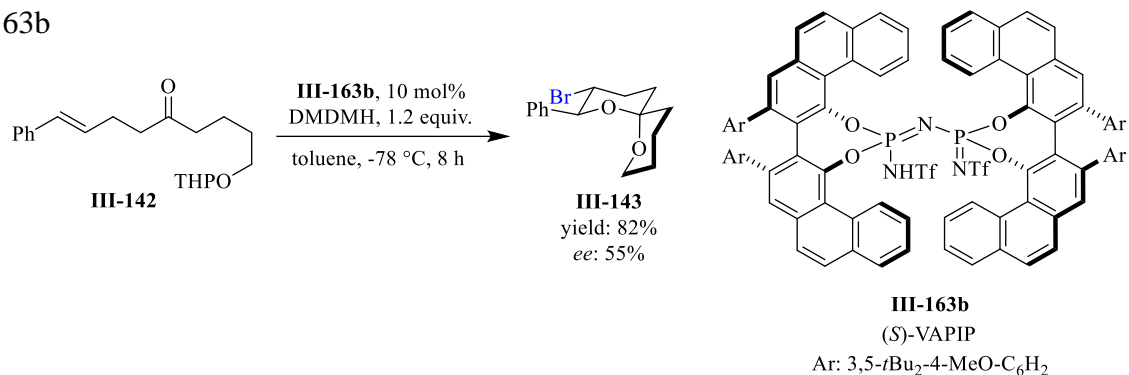
The length of chiral pocket



p-p and C-H-p interaction in VAPIP catalyst

Next, the reaction was conducted with VAPIP catalyst **III-163 b**. It was supposed that introducing bulky groups in the backbone of the VAPOL ligand **III-54** might improve the chiral pocket by changing the dihedral angle between the phenanthryl groups of the ligand. Our hypothesis was rewarded as the spiroketal **III-143** was produced in 55% enantiomeric excess. Attempts to grow the crystal of the catalyst **III-163b** were unsuccessful (scheme III-35b).

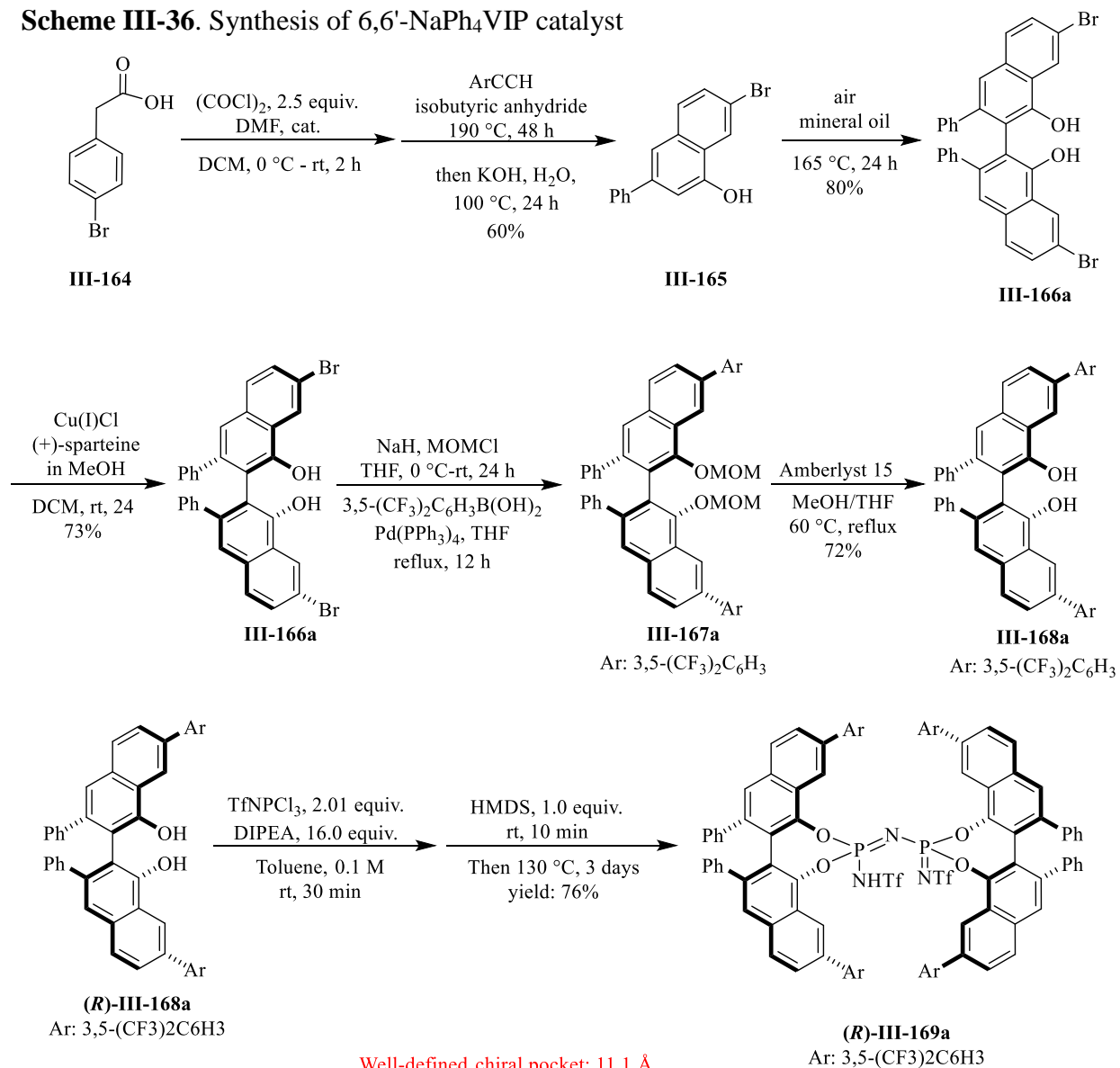
**Scheme III-35b.** Asymmetric catalytic spiroketalization catalyzed by VAPIP catalyst **III-163b**



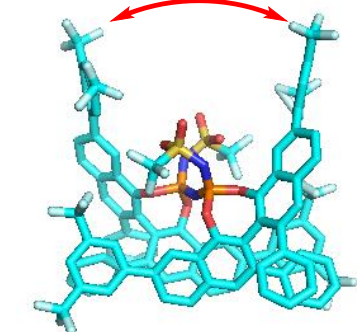
We turned our attention toward the VANOL ligand and its derivatives since the derivatization of the VAPOL ligand is a tedious task. The next hypothesis was to place substituents in the 7,7'-position of the VANOL ligand in order to produce a more well defined chiral microenvironment around the active site. The 7,7'-dibromoVANOL ligand **III-166a** was synthesized from 4-bromophenyl acetic acid **III-164**. Converting the carboxylic acid to acyl chloride followed by a subsequent cycloaddition-electrocyclization reaction (CAEC) to yield 7-bromo-3-phenylnaphthalen-1-ol **III-165** in 60% yield. Oxidative coupling and deracemization mediated by copper-sparteine afforded enantiopure 7,7'-Br<sub>2</sub>-VANOL ligand **III-166a** in 73% yield and 99% *ee*. MOM protection, Suzuki coupling with 3,5-(CF<sub>3</sub>)<sub>2</sub>C<sub>6</sub>H<sub>3</sub>B(OH)<sub>2</sub> and deprotection of the MOM group gave (*R*)-7,7'-(3,5-(CF<sub>3</sub>)<sub>2</sub>C<sub>6</sub>H<sub>3</sub>)<sub>2</sub>VANOL **III-168a** in 76% yield overall three steps (scheme III-36).<sup>64</sup>

Ligand **III-168a** underwent a smooth transformation into VIP catalyst **III-169a** in excellent yield. To our delight, catalyst **III-169a** performed well in the spiroketal formation reaction and gave the product **III-143** in 70% yield and 55% *ee* (scheme III-37). The structure analysis of this catalyst revealed a better defined chiral pocket with the asymmetric occupation of the space around the active site by the aryl substituents with a distance of 11.1 Å. Similar results were obtained with VIP catalyst **III-169b** (scheme III-37).

**Scheme III-36.** Synthesis of 6,6'-NaPh<sub>4</sub>VIP catalyst

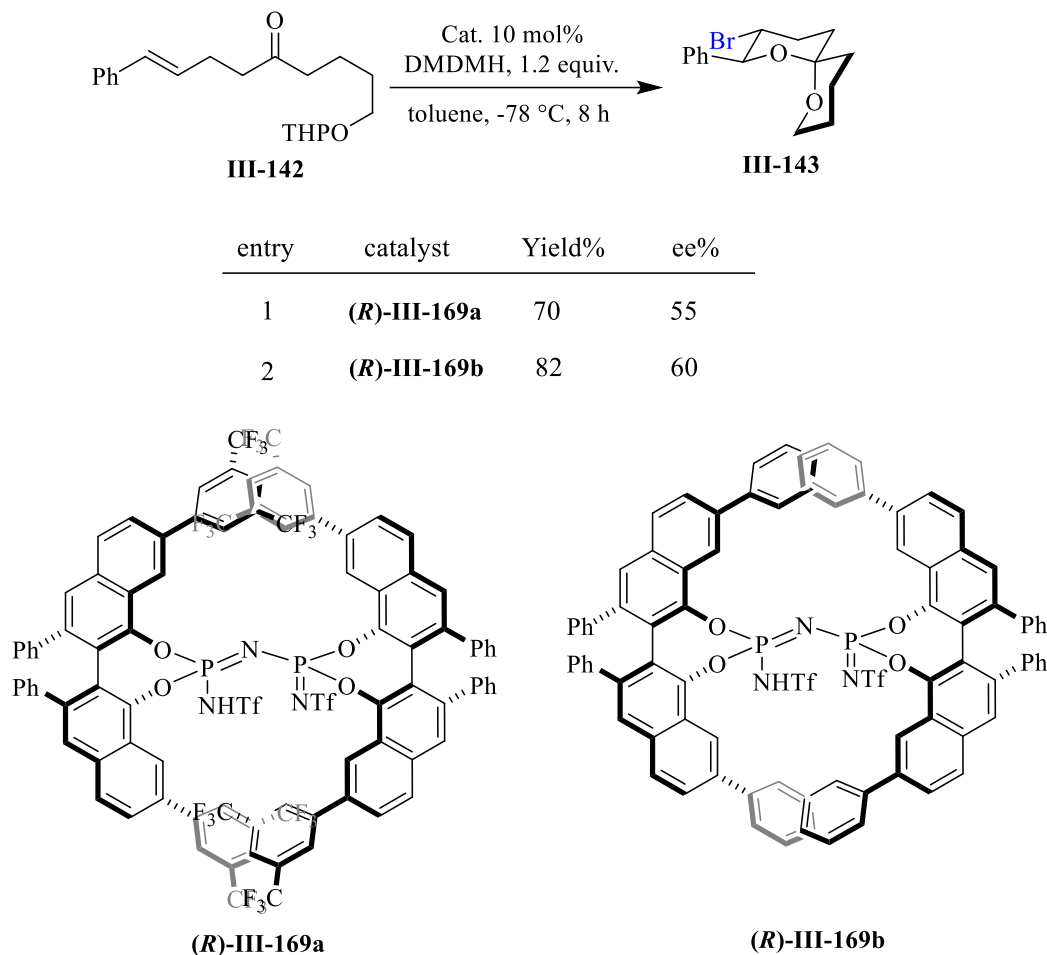


Well-defined chiral pocket: 11.1 Å



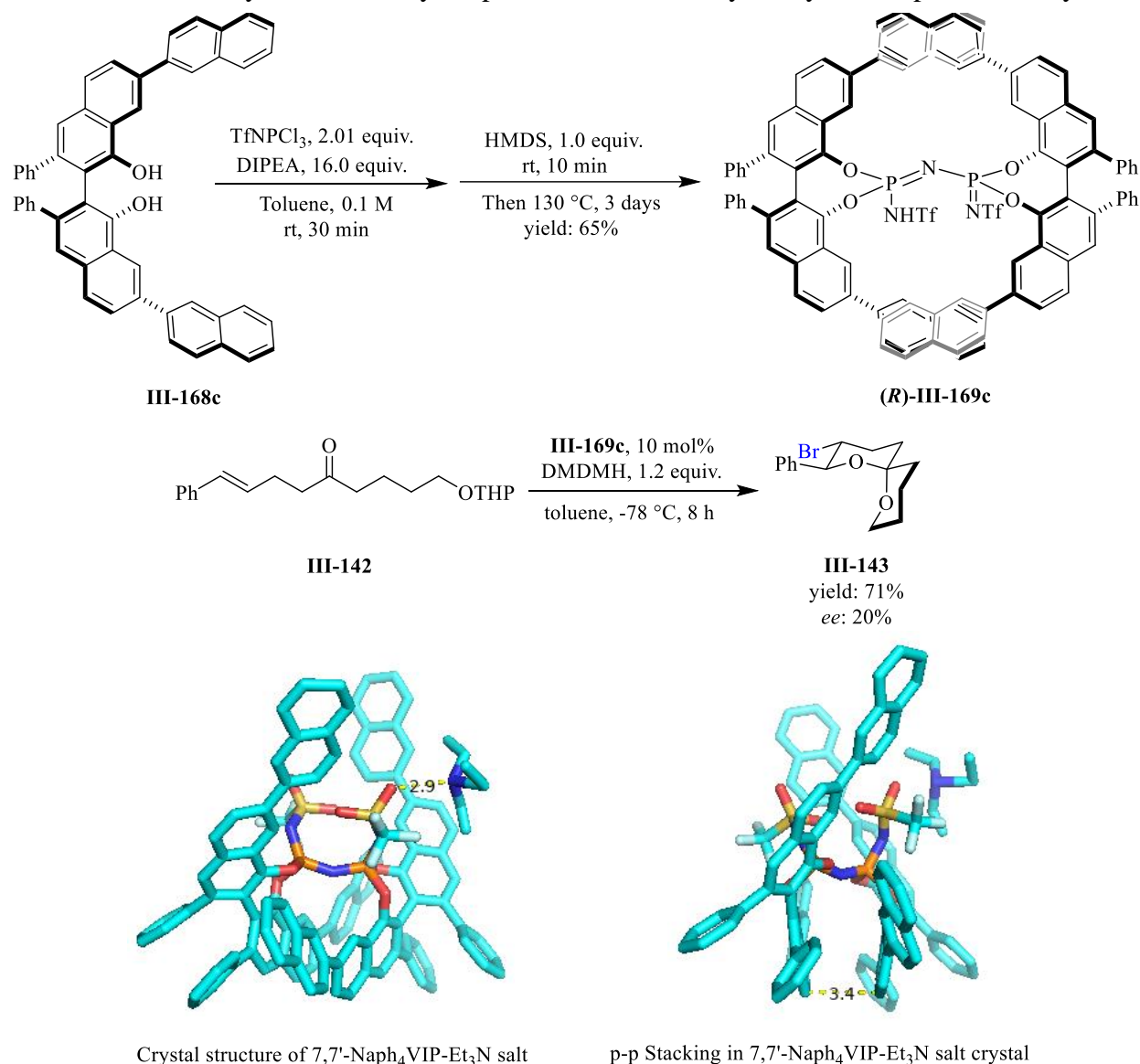
Crystal structure of ((CF<sub>3</sub>)<sub>2</sub>C<sub>6</sub>H<sub>3</sub>)<sub>4</sub>VIP

**Scheme III-37.** Asymmetric catalytic spiroketalization catalyzed by 7,7'-Ar<sub>4</sub>VIP catalyst



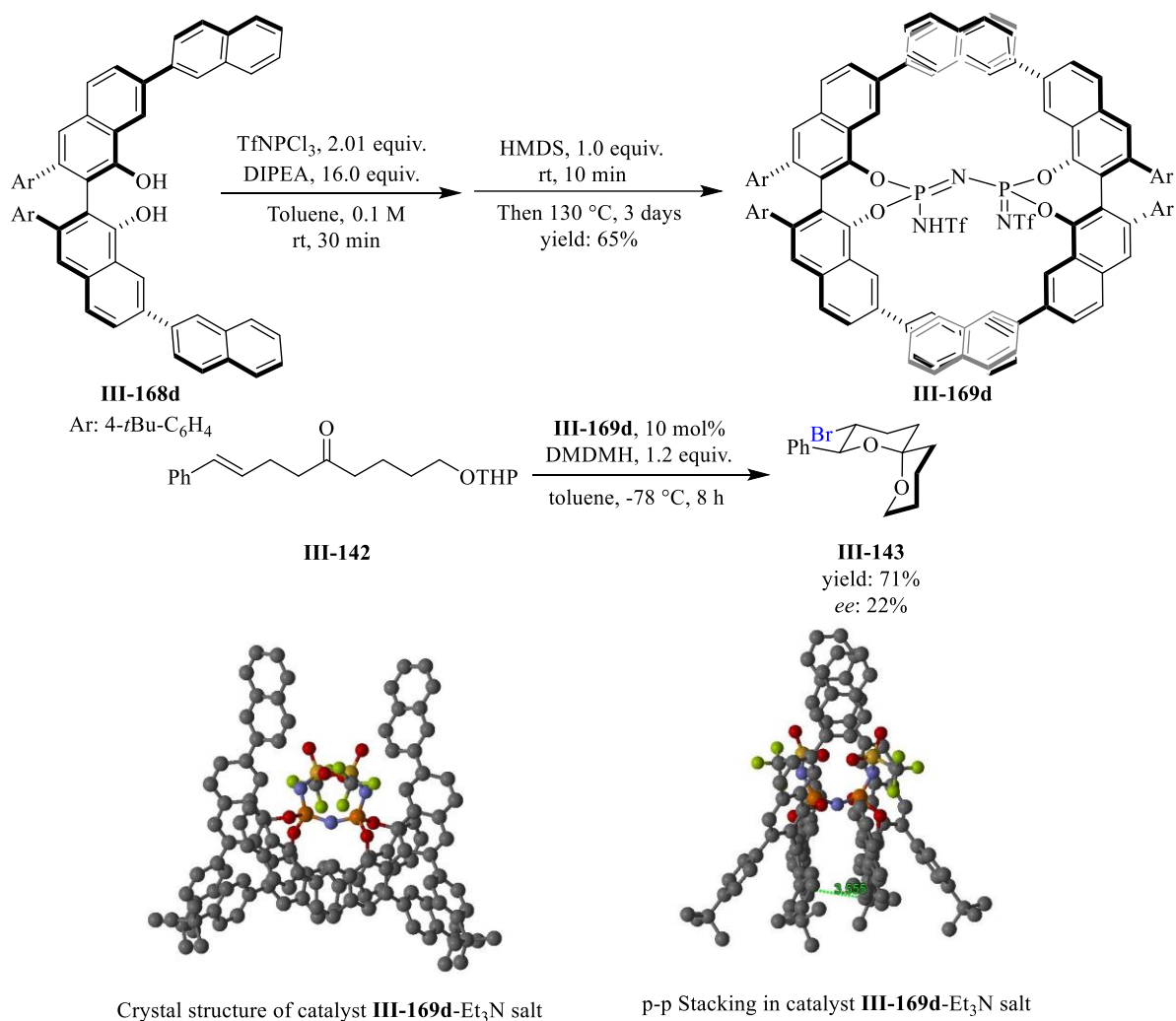
We were surprised to observe VIP catalyst **III-169c** derived from 7,7'-(2-Naph<sub>2</sub>)VANOL ligand **III-168c** catalyzed the spiroketalization reaction with a substantial decrease in the induction compared to catalysts **III-169a** and **III-169b** (scheme III-38 vs scheme III-37). The crystal structure analysis of VIP **III-169c** triethylammonium salt showed protonated amine species hydrogen bonded to the catalyst located outside of the chiral pocket and also a  $\pi$ - $\pi$  stacking of the aryl units below the active site with a distance of 3.4 Å; however, the reason for the resulting low asymmetric induction was not clear at this point.

**Scheme III-38.** Asymmetric catalytic spiroketalization catalyzed by 7,7'-Naph<sub>4</sub>VIP catalyst



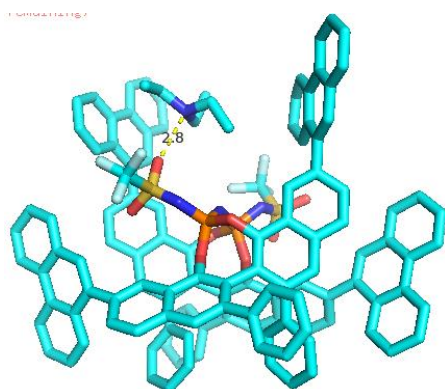
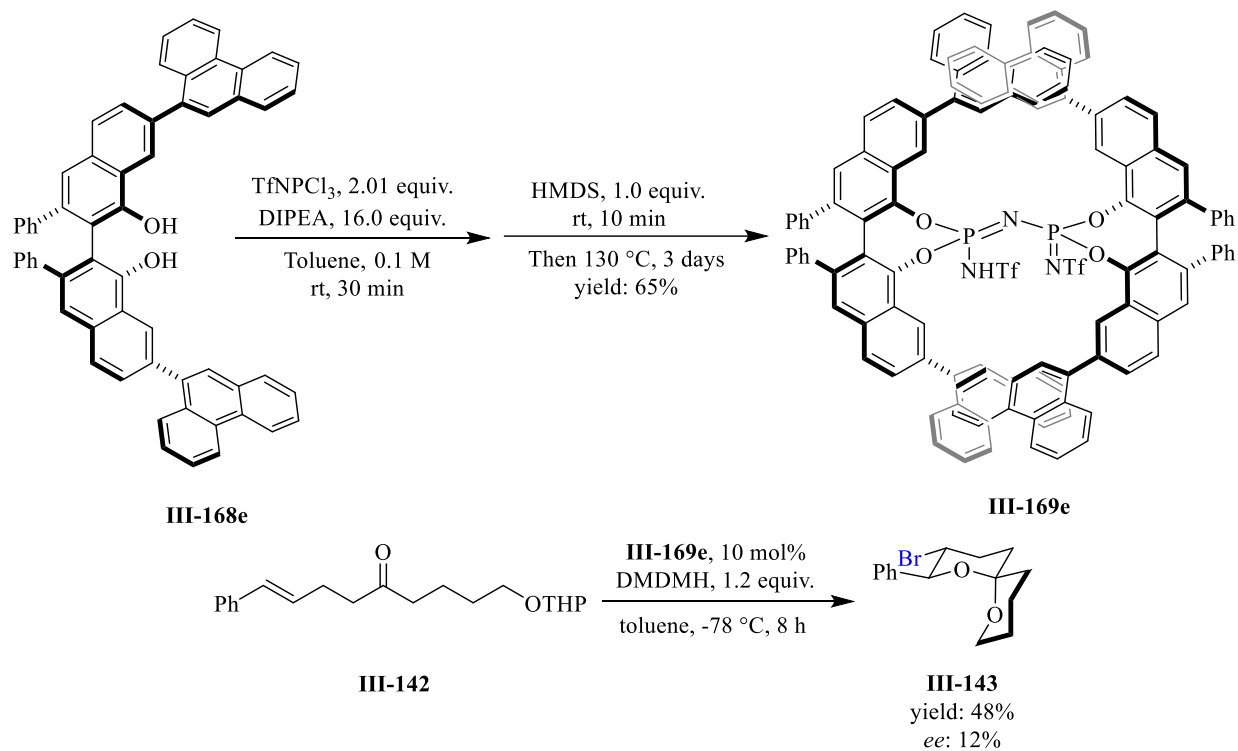
Our next strategy was to introduce *tert*-butyl groups at the *para*-position of a phenyl group in the 3,3'-positions of VANOL **III-168d** in order to alter the dihedral angle between the naphthalene groups (scheme III-39). It was thought that a change in the dihedral angle in the ligand **III-168d** might change the chiral pocket in catalyst **III-169d**. However, no significant differences in the structure of VIP catalyst **III-169d** was observed compared to VIP catalysts **III-169c**. As a result, performing the spiroketalization reaction with catalyst **III-169d** produced similar result.

**Scheme III-39.** Asymmetric catalytic spiroketalization catalyzed by catalyst III-165j

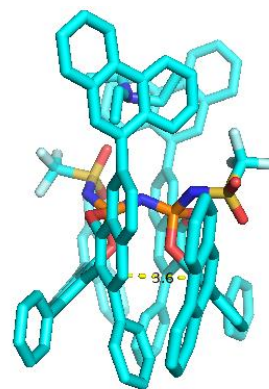


The synthesis and catalytic properties of the VIP catalyst **III-169e** derived from ligand **III-168e** bearing two 9-phenanthryl groups in the 7,7'-positions was also investigated in the spiroketal formation. Replacing naphthyl groups in the 7,7'-positions with phenanthryl groups resulted in the formation of product **III-143** even in lower induction (scheme 40 vs scheme 39, 20% *ee* vs 12% *ee*).

**Scheme III-39.** Asymmetric catalytic spiroketalization catalyzed by catalyst **III-165j**



Crystal structure of catalyst **III-169e-Et<sub>3</sub>N** salt



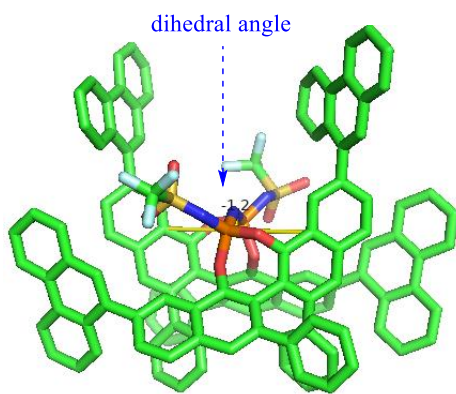
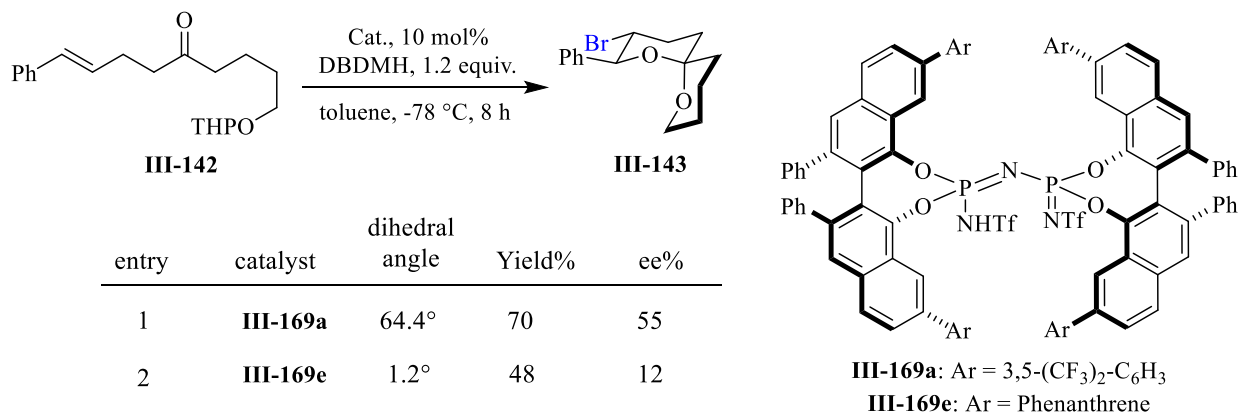
p-p Stacking in catalyst **III-169e-Et<sub>3</sub>N** salt

Despite the disappointment in these results, it was interestingly to observed a decreasing trend in the asymmetric induction with the increase in size of aromatic substituents in 7,7'-positions. A phenyl group as the substituent yielded the desired product **III-143** in highest induction (60% *ee*, scheme III-37) while the phenanthryl group as the substituent yield the spiroketal **III-143** with

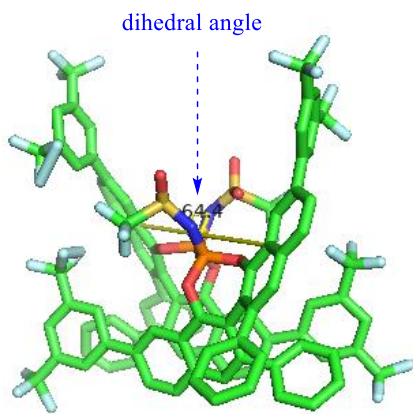
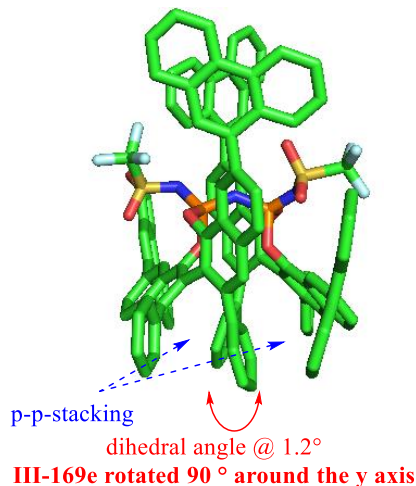


lowest induction (12% *ee*, scheme III-40). To explore the nature of this trend, the crystal structure of catalysts **III-169a** and **III-169e** were compared (scheme III-41).

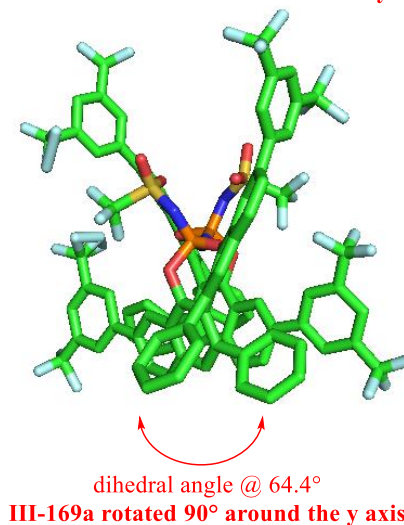
**Scheme III-41.** Dihedral angle effect in spiroketalization



Crystal structure of catalyst **III-169e**



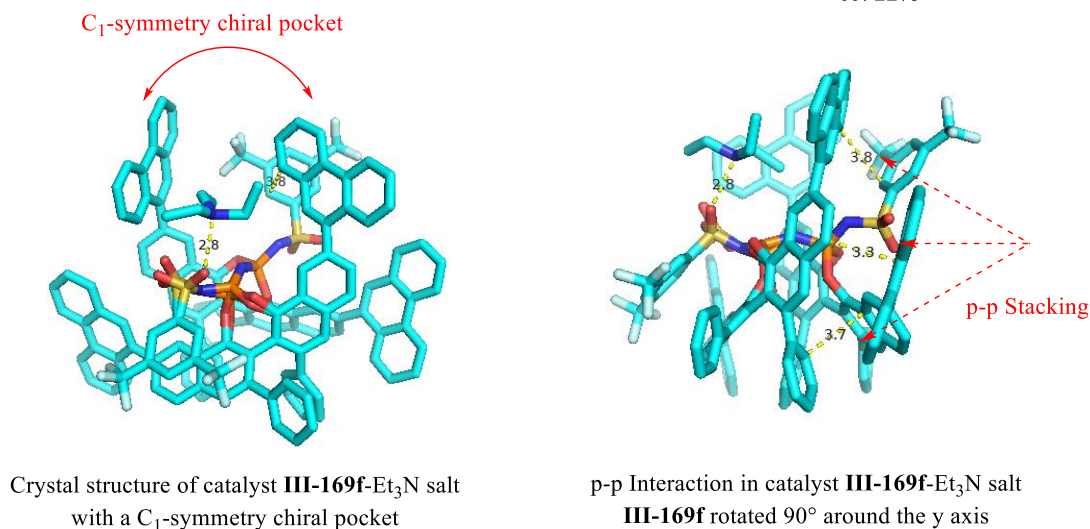
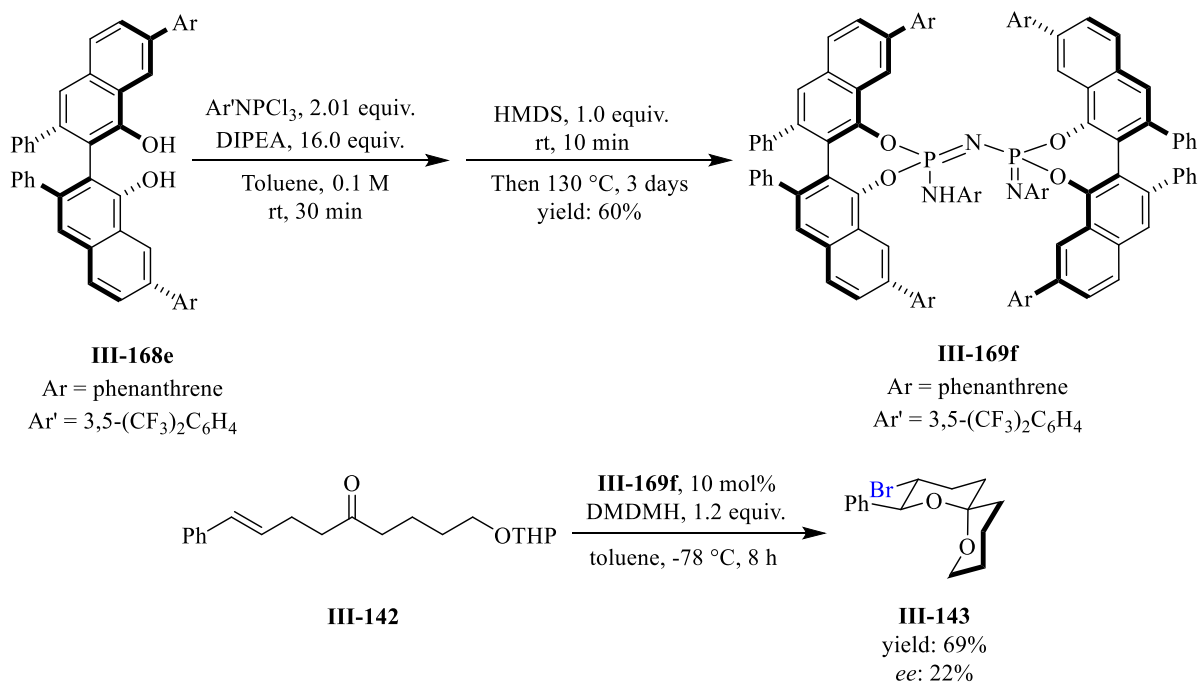
Crystal structure of catalyst **III-169a**



After evaluating the structure of catalyst **III-169a** it was found that this catalyst possesses a large dihedral angle ( $\sim 64.4^\circ$ ) between two VANOL ligands of the catalyst which enables the substitution in the 7,7'-positions to produce a  $C_2$ -asymmetric environment around the active site. However, increasing the size of the aromatic substituents (phenanthrene) has caused the catalyst **III-169e** to be squeezed and coerced to adopt a less than  $<1^\circ$  dihedral angle due to the existing  $\pi$ - $\pi$ -stacking in the bottom part of the catalyst. As a result, the phenanthrene substituents are obliged to adopt a face-to-face orientation and deterioration of the chiral space around the active site. Therefore, catalyst **III-169e** produced spiroketal **III-143** with only 12% asymmetric induction (scheme III-41).

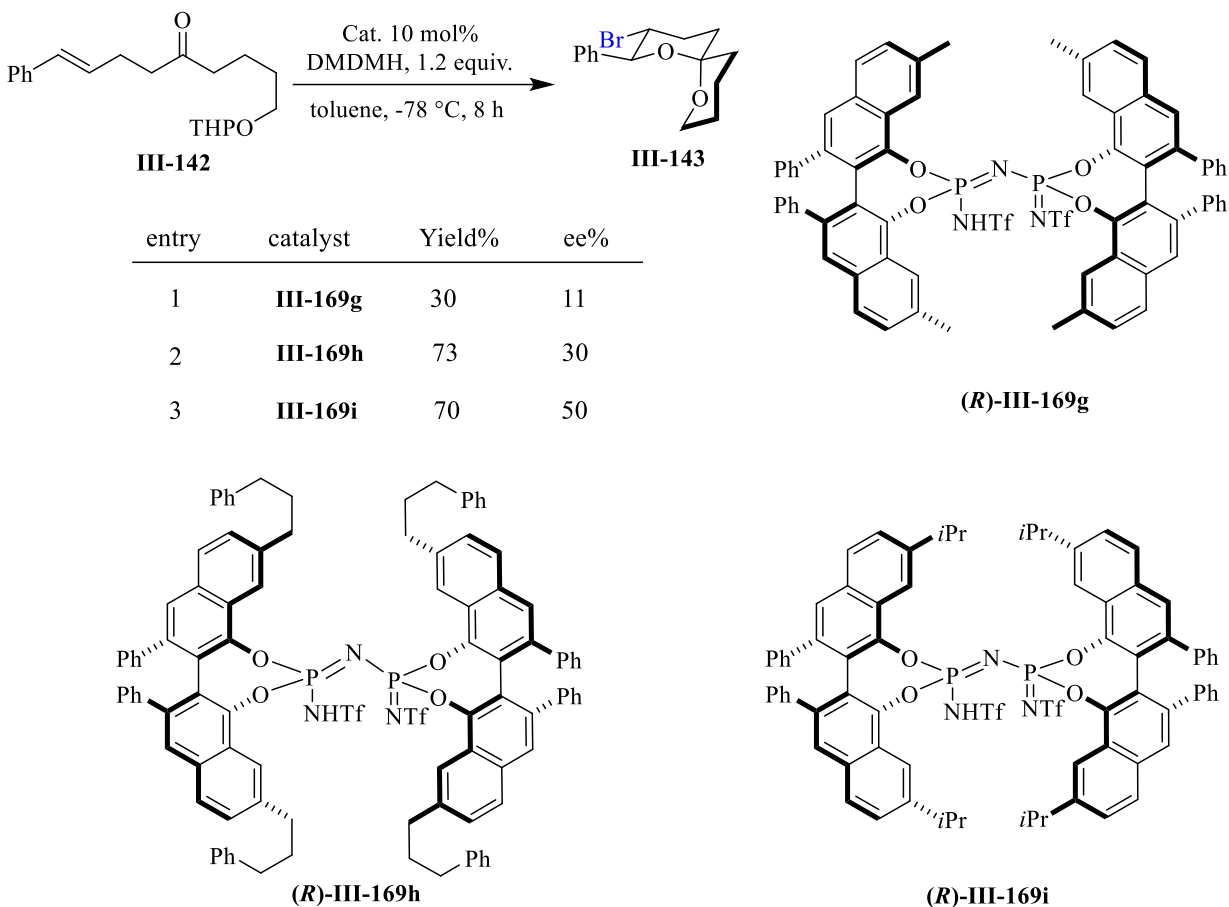
Interestingly, replacing the  $CF_3$  group on the nitrogen in the VIP catalyst **III-169e** with a 3,5- $(CF_3)_2C_6H_3$  group gave catalyst **III-169f** which catalyze the spiroketalization to give desired spiroketal **III-143** in higher induction (22% *ee* vs 12% *ee*, scheme III-42). To understand the observed increase in enantiomeric excess, the crystal structure of catalyst **III-169f**- $Et_3N$  salt was investigated. This divulged that the  $\pi$ - $\pi$ -interaction with a distance of 3.8 Å between 3,5- $(CF_3)_2C_6H_3$  substituent and phenanthryl subunit enabled the catalyst to adopt a  $C_1$  symmetry around the active site. Presumably the reduced symmetry surrounded the active site in VIP catalyst **III-169f** is responsible for the observed increase in enantioselectivity.

**Scheme III-42.** Asymmetric catalytic spiroketalization catalyzed by catalyst III-169f



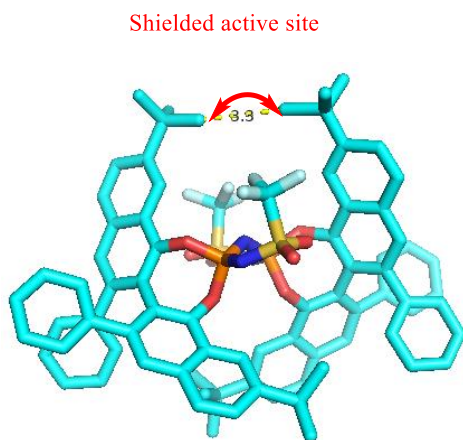
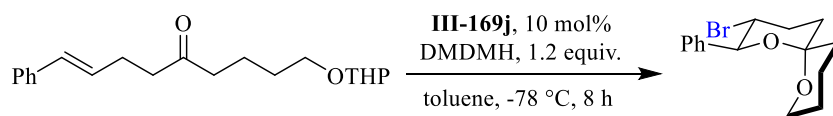
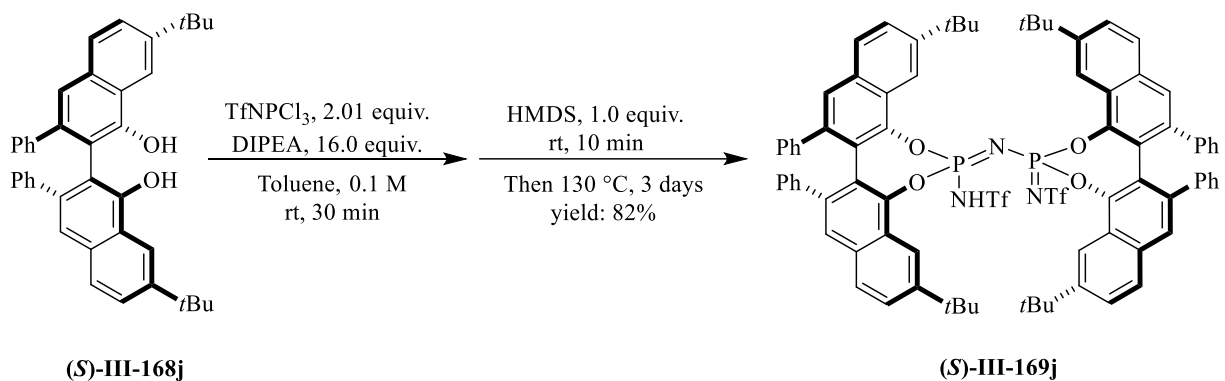
Our next strategy was to design a VIP catalyst bearing aliphatic substituents in the 7,7'-positions. VIP catalyst **III-169g** derived from the VANOL ligand bearing methyl substituents in the 7,7'-positions produced the desired spiroketal **III-143** in low yield and also low induction (scheme III-43).

**Scheme III-43.** Asymmetric catalytic spiroketalization catalyzed by 7,7'-R<sub>4</sub>VIP catalyst

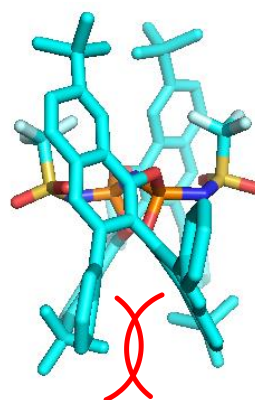


Catalyst **III-169h** bearing 3-phenylpropyl substituents in the 7,7' positions produced better yield; however, with only 30% *ee*. To our delight, VIP catalyst **III-169i** derived from the 7,7'-*i*Pr<sub>2</sub>VANOL ligand produced the desired product in 70% yield and 50% *ee* (scheme III-43). It was interesting to observe that the *ee* of the spiroketalization reaction was increased with the bulkiness of the substituents in the 7,7' positions. Therefore, the VIP catalyst **III-169j** was prepared from 7,7'-*t*Bu<sub>2</sub>VANOL **III-168j** ligand and was investigated in the spiroketalization reaction (scheme 44). Surprisingly, moderate yield and asymmetric induction were obtained after conducting the reaction with 10 mol% of the VIP catalyst **III-169j**.

**Scheme III-44.** Asymmetric catalytic spiroketalization catalyzed by 7,7'-*t*Bu<sub>4</sub>VIP catalyst



Crystal structure of 7,7'-*t*Bu<sub>4</sub>VIP  
with shielded active site

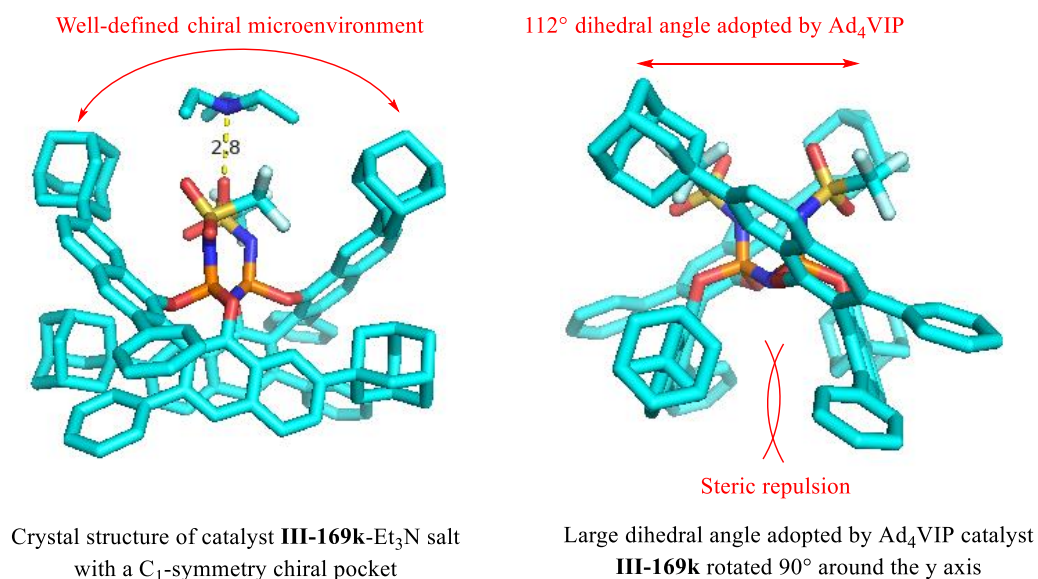
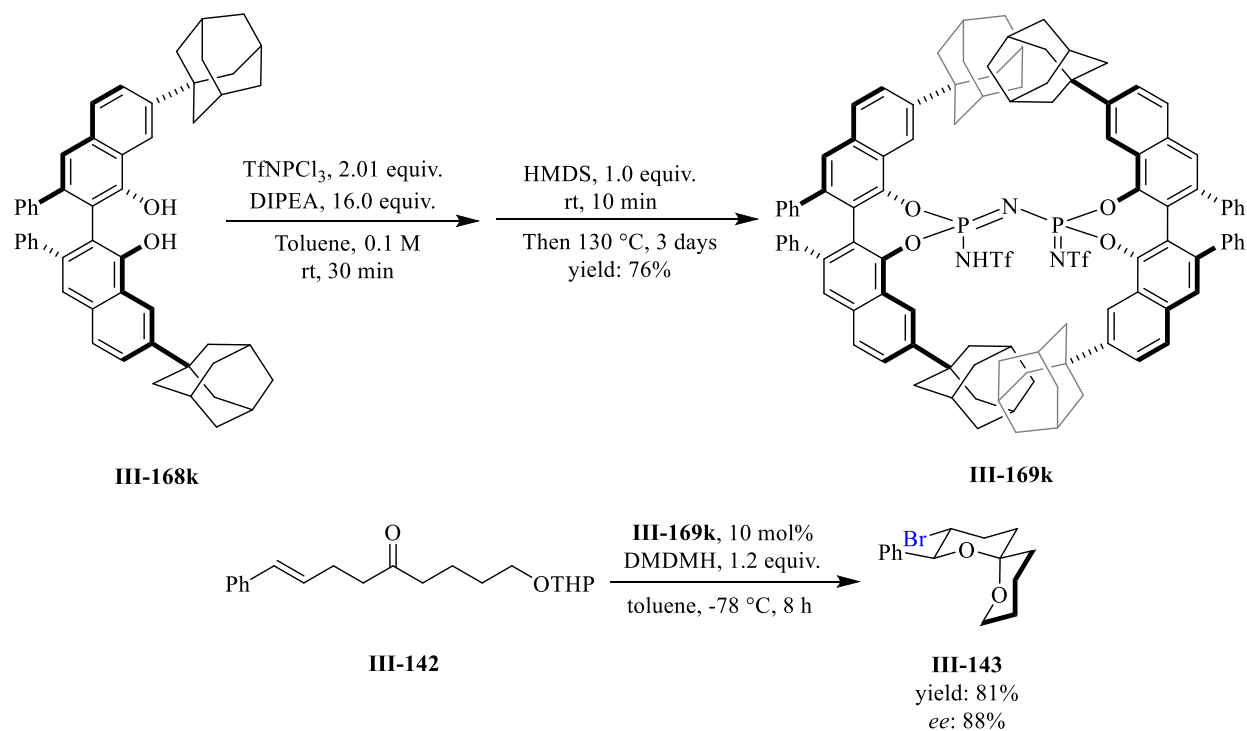


Repulsion between *t*Bu and naphthyl units  
**III-169j** rotated  $90^\circ$  around the *y* axis

To understand the poor performance of the VIP catalysts **III-169j**, it was subject to the structural analysis with x-ray crystallography. Interestingly, it was observed that the bulky *t*-butyl groups have caused two of the naphthalene units to swing up over the active site and shielded it with a distance of 3.3 Å. Presumably, this shielding was accounted for the inferior performance of the catalyst **III-169j** compared with catalyst **III-169i** (50% *ee*, scheme 43 vs 34% *ee*, scheme III-44).

Based on the results obtained from the crystal structure analysis of VIP catalyst derivatives, it was concluded that adamantane could be the optimum substituent in the 7,7'-positions of the VANOL ligand for the following reasons. The rigidity and also bulkiness of the adamantane along with its inability to form  $\pi$ - $\pi$  stacking should provide a well-defined chiral pocket. To test our

**Scheme III-45.** Asymmetric catalytic spiroketalization catalyzed by catalyst **III-169k**

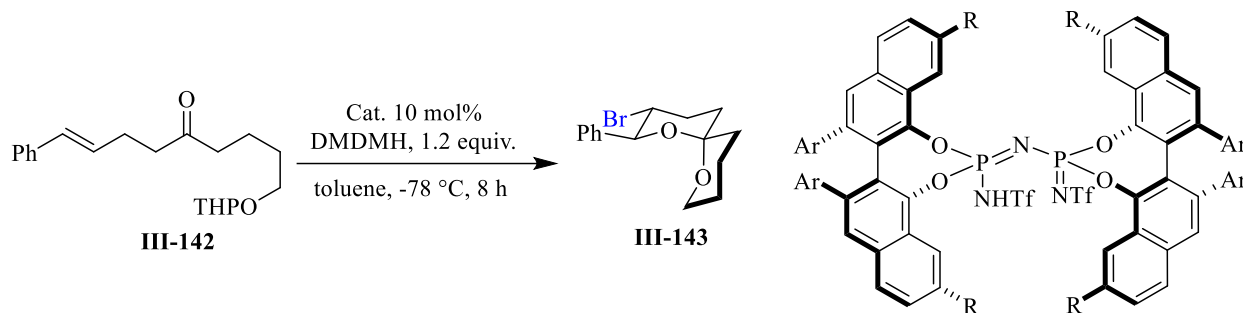


speculation, VIP catalyst **III-169k** was synthesized from 7,7'-Ad<sub>2</sub>VANOL ligand **III-168k** in excellent yield (scheme III-45). Analyzing the structure of VIP catalyst **III-169k** triethylammonium salt disclosed a large dihedral angle between two VANOL ligands possessed by this catalyst (112°). The observed large angle in VIP catalyst **III-169k** originates from the steric repulsion of adamantyl component of one VANOL ligand with the phenyl component of the other VANOL ligand below the active site which creates a well-established C<sub>2</sub> asymmetric chiral environment around the active site. Our rational design of the catalyst was rewarded and the spiroketal was produced in excellent yield and induction (scheme III-45).

The fact that a number of the imidodiphosphorimidate catalysts could form crystals suitable for x-ray diffraction was very important in this work. The solid state structure of these catalysts revealed changes in conformat as a consequence of introduction of different substituents in various positions in the catalysis. Assuming that the solid-state structures were also relevant in solution, changes in the conformations could be anticipated with certain changes in the substituents. Scheme 46 indicates the correlation between the dihedral angle between two VANOL ligands of the VIP catalysts with the asymmetric induction of the product in the spiroketalization reaction (scheme III-46).

Now, we are set to accomplish the screening substrate scope for the asymmetric catalytic halonium ion-induced spiroketalization reaction.

**Scheme III-46.** Asymmetric catalytic spiroketalization catalyzed by 7,7'-R<sub>4</sub>VIP catalyst



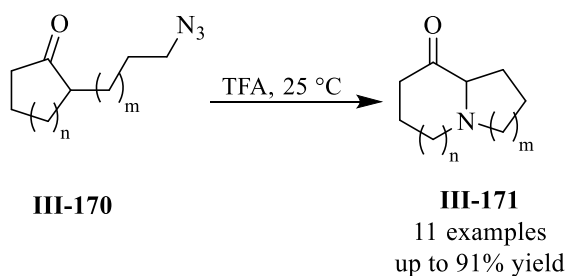
entry	catalyst	R	Ar	Dihedral Angle	Yield%	ee%
1	III-169a	3,5-(CF <sub>3</sub> ) <sub>2</sub> C <sub>6</sub> H <sub>3</sub>	Ph	64°	70	55
2	III-169c	2-Naphthyl	Ph	67°	71	20
3	III-169d	2-Naphthyl	4- <i>t</i> Bu-C <sub>6</sub> H <sub>4</sub>	59°	71	22
4	III-169e	9-Phenanthryl	Ph	1°	47	12
5	III-169j	<i>t</i> Bu	Ph	7°	57	34
6	III-169k	Ad	Ph	112°	81	88

### 3.3. Asymmetric catalytic intramolecular Schmidt reaction

#### 3.3.1. Introduction

The Schmidt reaction has been a valuable methodology in organic synthesis since its discovery by Karl Schmidt in 1924 and has twice been the subject of an *Organic Reactions* Reviews.<sup>65,66</sup> In 1991, Aubé reported the intramolecular Schmidt reaction of an alkyl azide which involved the insertion of a tethered azide into a ketone to give a lactam (scheme III-47).<sup>67</sup>

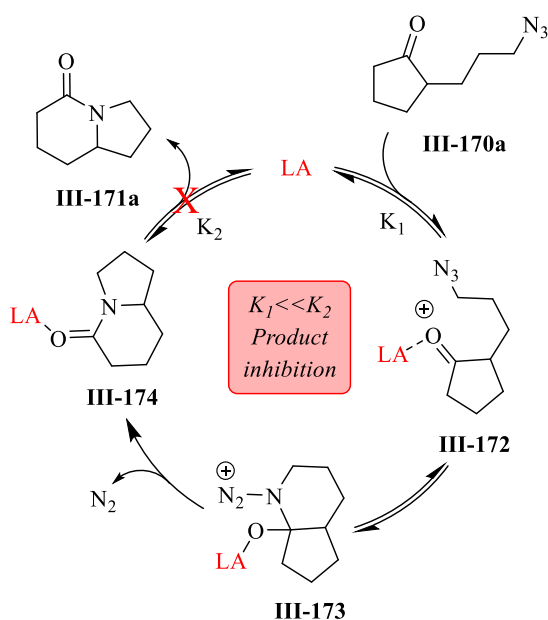
**Scheme III-47.** Intramolecular Schmidt reaction





However, the main challenge in the Schmidt reaction is to overcome the need for super stoichiometric amount of Lewis acid or Brønsted acid promoter to achieve high conversion. The reason for the necessity of the excess amount of promoter relies in the mechanism of Schmidt reaction as shown in scheme 48. First, the ketone **III-170a** is activated via the coordination of the promoter (Lewis acid in this case). Next, the activated ketone **III-172** is intercepted by the tethered azide which produces azidohydrin intermediate **III-173**. Finally, antiperiplanar bond migration followed by subsequent nitrogen gas extrusion affords lactam-Lewis acid complex **III-174**. The resulting lactam is more basic than the ketone which causes the product inhibition; therefore, an excess amount of Lewis acid should be used to achieve high conversion in this reaction. Developing an efficient asymmetric catalytic method for this reaction has also been a difficult task to achieve because of this reason (scheme III-48). Asymmetric versions of this reactions that turnover have involved chiral auxiliaries.

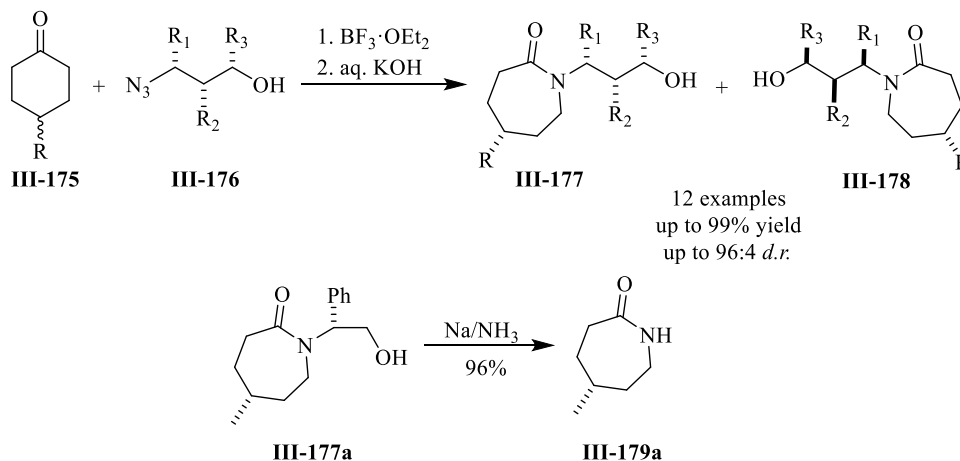
**Scheme III-48.** Product inhibition in the Schmidt reaction



The first asymmetric Schmidt reaction with the use of chiral auxiliaries was reported by Aubé in 2003.<sup>68</sup> In this report, chiral  $\beta$ -hydroxy azides (not shown) and  $\gamma$ -hydroxyalkyl azides **III-176** was

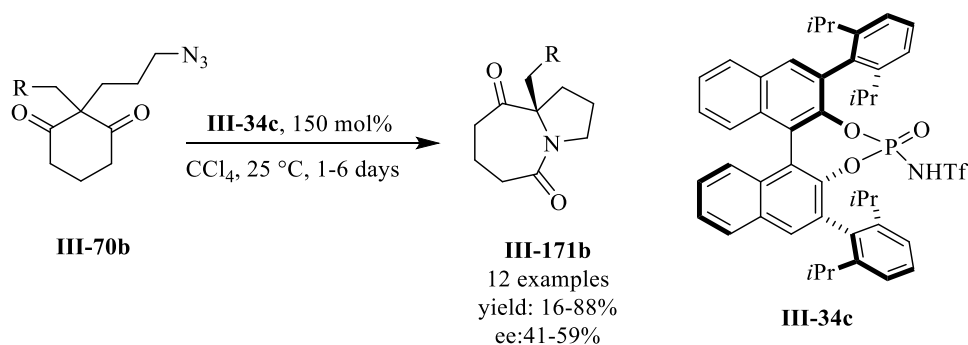
utilized in the desymmetrization of cyclohexanones **III-175** mediated by the super stoichiometric amount of triFluoroborate etherate as the Lewis acid. Lactam **III-174** was produced in good to excellent yields and diastereomeric ratios. In addition, the chiral auxiliaries were removed via reductive cleavage, and enantioenriched 2° lactam **III-179a** was produced in good yield (96%).

**Scheme III-49.** Asymmetric intramolecular Schmidt reaction with chiral auxiliaries



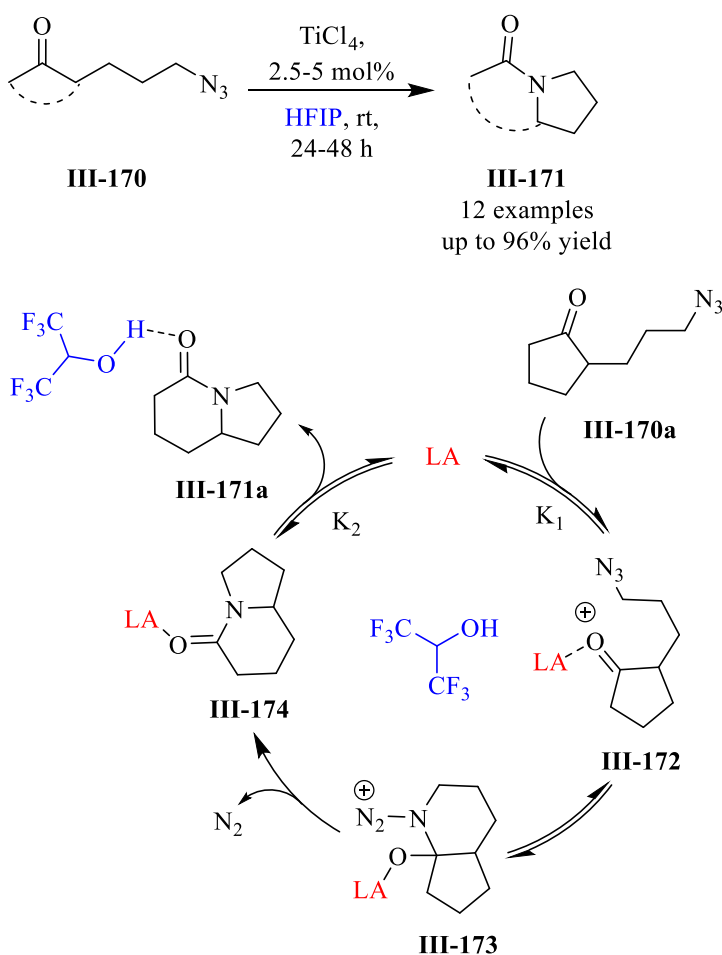
To date, there is only one report about an asymmetric Schmidt reaction which involves the use of a super stoichiometric amount of a chiral Brønsted acid catalyst (150%). Tu and Zhang in 2011 described the desymmetrization of diketones **III-170b** to give pyrroloazepine skeletons **III-171b**.<sup>69</sup> After screening several BINOL phosphoramidate catalysts, the best was catalyst **III-34c** which gave 39-58% *ee* and 18-88% yield over a range of 12 examples.

**Scheme III-50.** Asymmetric Schmidt reaction mediated by chiral Brønsted acid



In 2013, Aubé reported the first catalytic version of the intramolecular Schmidt reaction with a non-chiral Lewis acid.<sup>70</sup> It was found that strong hydrogen-bond-donating solvent such as hexafluor-2-propanol enabled the use of a substoichiometric amount of Lewis acid such as  $\text{TiCl}_4$  as the catalyst in this reaction (scheme III-51). Since lactam **III-171a** is a better hydrogen bond acceptor than the ketone **III-170a**, it was assumed that the interaction of HFIP with lactam **III-171a** would be stronger than the same interaction with ketone; therefore, HFIP replaces the Lewis acid catalyst by forming a stronger hydrogen bond with the lactam **III-171a** which leads to the liberation of the catalyst and subsequent closing of the catalytic cycle (proposed mechanism in scheme III-51).

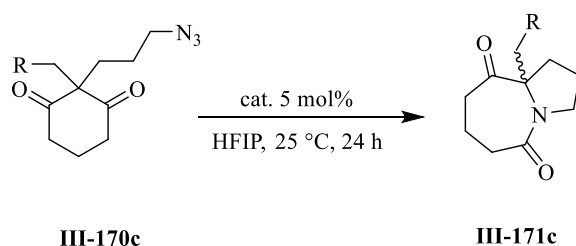
**Scheme III-51.** Overcoming product inhibition in Schmidt reaction



### 3.3.2. VIP catalyst catalyzed intramolecular Schmidt reaction

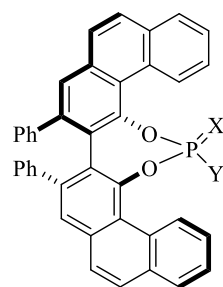
Inspired by Aubé's report after catalytic Schmidt reaction, it was theorized that the Brønsted acid catalysts might catalyze the asymmetric Schmidt reaction in the presence of a polar protic solvent such as HFIP. To test our hypothesis, a library of VANOL/VAPOL Brønsted acid catalysts was investigated in the desymmetrization of diketone **III-170c**. First, the reaction was conducted in the presence of 5 mol%  $\text{TiCl}_4$  as the Lewis acid catalyst, and the desired product was produced in 94% yield (table III-8, entry 1). As a control experiment, in the absence of a catalyst, no product was obtained (entry 2). VAPOL phosphoric acid as the catalyst **III-27** was investigated; however, no product was observed and the alkyl azide **III-170c** was recovered in quantitative yield (entry 3). VAPOL phosphoramidate **III-53a** and VAPOL thiophosphoramidate **III-160** catalysts turned out not to catalyze the reaction at all (entry 4 and 5). Interestingly, desired product **III-170c** was observed with VAPOL *N*-triflylphosphoramidate catalyst **III-180** albeit with only 2% NMR yield.

**Table III-8.** Asymmetric catalytic Schmidt reaction



entry	catalyst	Yield%	ee%
1	$\text{TiCl}_4$	94	<i>N.D.</i>
2	<i>No catalyst</i>	<i>N.D.</i> <sup>1</sup>	<i>N.D.</i> <sup>2</sup>
3	( <i>R</i> )- <b>III-27</b>	<i>N.D.</i>	<i>N.D.</i>
4	( <i>S</i> )- <b>III-53a</b>	<i>N.D.</i>	<i>N.D.</i>
5	( <i>R</i> )- <b>III-160</b>	<i>N.D.</i>	<i>N.D.</i>
6	( <i>R</i> )- <b>III-179</b>	2 <sup>3</sup>	<i>N.D.</i>

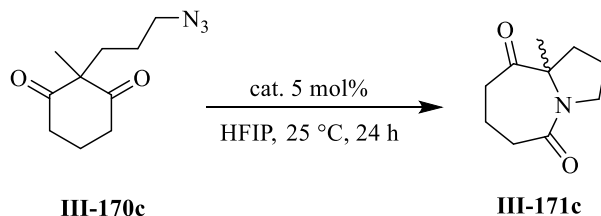
Unless otherwise specified, all of the reaction was conducted with 0.5 mmol compound **III-169c** 2 ml HFIP and 5 mol% catalyst. 1. *N.D.*: Not Detected. 2. *N.D.*: Not Determined. 3. NMR yield



**III-27**, X: O, Y: OH  
**III-53a**, X: O, Y: NHTf  
**III-160**, X: S, Y: NHTf  
**III-180**, X: NTf, Y: NTf

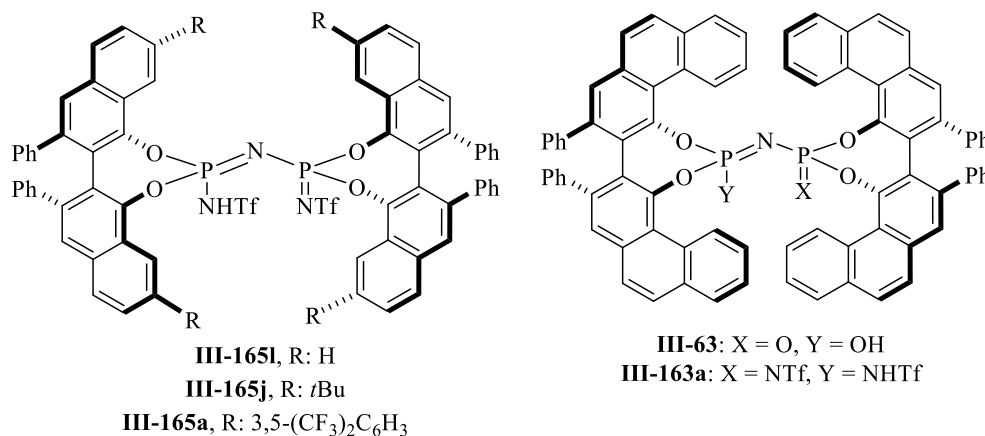
We were delighted to observe VIP catalyst **III-165i** catalyzed the intramolecular Schmidt reaction in moderate yield (table III-9 entry 1). Increasing the catalyst loading to 10 mol% gave the desired product in 71% yield (entry 2). Further increase in catalyst loading to 20 mol% increased the yield of the reaction to 89% (entry 3).

**Table III-9.** Imidophosphoramidate catalyst catalyzed Schmidt reaction



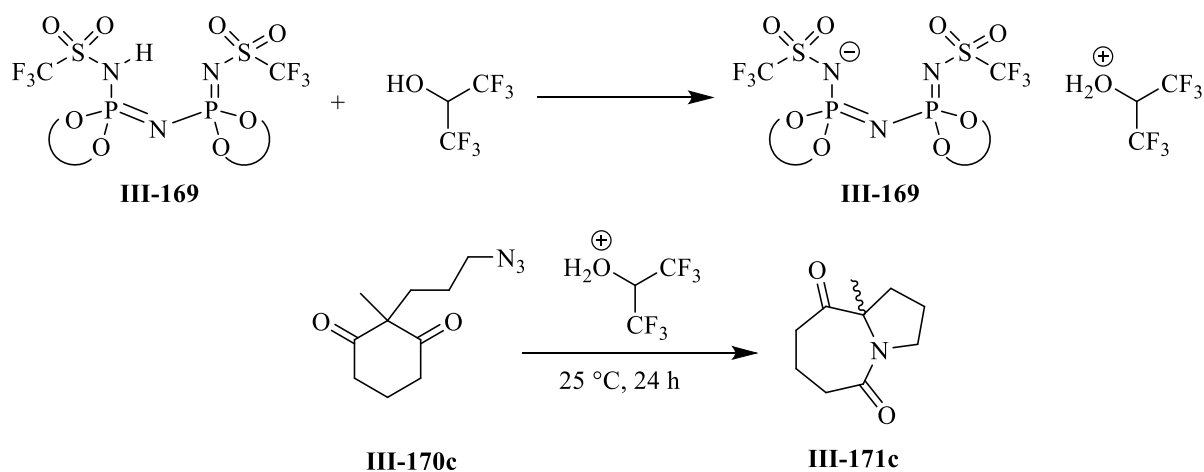
entry	catalyst	catalyst loading%	solvent	Yield%	ee%
1	<b>III-165i</b>	5	HFIP	54	<i>racemic</i>
2	<b>III-165i</b>	10	HFIP	71	<i>racemic</i>
3	<b>III-165i</b>	20	HFIP	89	<i>racemic</i>
4 <sup>1</sup>	<b>III-165i</b>	5	DCM	<i>N.D.</i>	<i>N.D.</i>
5	<b>III-165j</b>	10	HFIP	<i>N.D.</i>	<i>N.D.</i>
6	<b>III-165j</b>	100	DCM	<i>N.D.</i>	<i>N.D.</i>
7	<b>III-160a</b>	10	HFIP	32	<i>racemic</i>
8	<b>III-63</b>	10	HFIP	<i>N.D.</i>	<i>N.D.</i>
9 <sup>2</sup>	<b>III-163a</b>	10	HFIP/DCM	56	<i>racemic</i>

Unless otherwise specified, all of the reaction was conducted with 0.5 mmol compound **III-169c** and 2 mL of HFIP, 1. 1.0 equiv. of HFIP was used, 2. 4:1 ratio of HFIP and DCM was used in order to help the solubility of the catalyst **III-163a**



However, all of three reactions resulted in *racemic* products. No product was observed after performing the reaction with a stoichiometric amount (1.0 equiv) of  $(\text{CF}_3)_2\text{CHOH}$  with  $\text{CH}_2\text{Cl}_2$  as solvent which indicated the important role of  $(\text{CF}_3)_2\text{CHOH}$  as the solvent (entry 4). Conducting the reaction with VIP catalyst **III-165j** resulted in the quantitative recovery of the alkyl azide **III-170c** after 24 hours (entry 5). The reaction did not proceed even in the presence of a stoichiometric amount of catalyst **III-165j** and the reason could be because of the shielded active site adopted by this catalyst (table III-9, entry 6). The Schmidt reaction was also performed in the presence of VIP catalyst **III-165a**; however, the product was isolated in 32% yield with no asymmetric induction (entry 7). The use of 10 mol% VAPIP catalyst **III-163a** produced similar results (entry 9). VAPOL imidodiphosphoric acid was also utilized as the catalyst; however, no product was observed and the starting material was fully recovered (entry 8). A feasible explanation for the formation of *racemic* product with imidodiphosphoramidate catalysts **III-165** is the extreme acidity of these catalysts which might protonate  $(\text{CF}_3)_2\text{CHOH}$ . Therefore, protonated  $(\text{CF}_3)_2\text{CHOH}$  could be the actual catalyst which catalyzes the intramolecular Schmidt reaction in non-asymmetric fashion.

**Scheme III-52.** Protonated HFIP is the actual catalyst in Schmidt

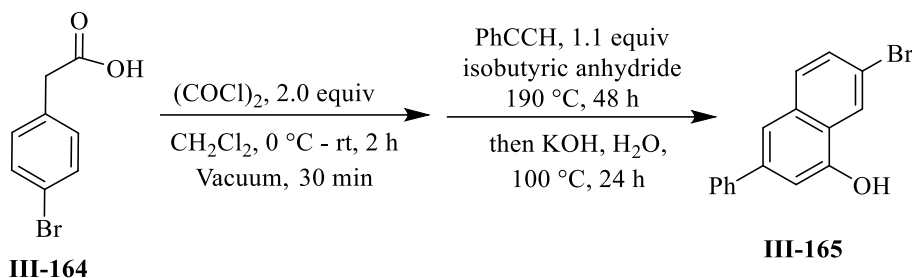


### 3.4. Summary

In summary, we have developed a library of VANOL/VAPOL Brønsted acid catalysts and investigated their utility in asymmetric halonium ion-induced spiroketalizations and intramolecular Schmidt reactions. Rational design of VANOL imidophosphoramidate (VIP) catalysts enabled us to develop an efficient VIP catalyst bearing adamantyl substituents in the 7,7'-positions. The inability of adamantyl to form  $\pi$ - $\pi$  stacking interactions, the bulkiness, and also the rigidity of its structure allowed the VIP catalyst to establish a well-defined  $C_2$  symmetry chiral microenvironment around the active site. The aforementioned catalyst catalyzed the halonium ion-induced spiroketalization and yielded the desired product in excellent asymmetric induction. Despite the success in spiroketal formation catalyzed by VIP catalysts, however, the same catalysts performed poorly in intramolecular Schmidt reaction and the desired product was obtained with no asymmetric induction in *racemic* form. The reason may be due to the fact that HFIP is used as the solvent to suppress the product inhibition, however, the extreme acidity of VIP catalysts protonated the HFIP. Therefore, the protonated HFIP may act as the actual catalyst and catalyze the Schmidt reaction in a non-asymmetric fashion. As a result, the challenge of discovering an efficient catalyst for Schmidt reaction remains unconquered and waiting for brilliant minds to crack this hard nut.

### 3.5. Experimental

#### General procedure for the synthesis of 7-substituted-3-phenyl-1-naphthols (procedure I):

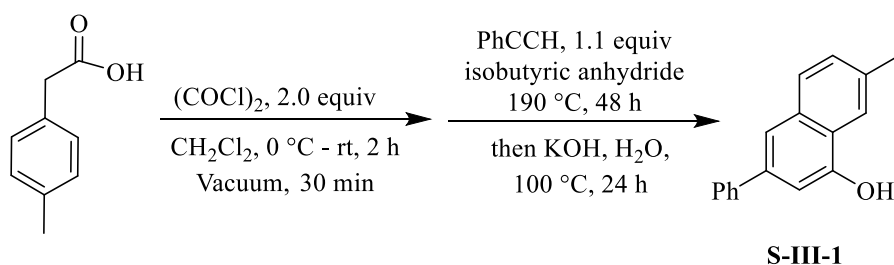


**Synthesis of 7-bromo-3-phenyl-1-naphthol III-165:** A flamed dried 500 mL round bottom flask connected to a bubbler and then into a beaker filled with saturated solution of NaOH was added 4-bromo-phenylacetic acid (90 mmol, 19 g) and 90 mL CH<sub>2</sub>Cl<sub>2</sub> (1 M) and the resulting solution was cooled down to 0 °C followed by careful addition of (COCl)<sub>2</sub> (180 mmol, 15.4 mL) in a period of 30 min. After stirring the mixture for 1 h at 0 °C, the cold bath was removed and the reaction was allowed to warm up to the room temperature and stirred at room temperature for another hour. The volatiles were removed under reduced pressure and the resulting yellowish liquid was used in the next step without further purification. To the resulting acyl chloride in 500 mL round bottom flask fitted with two condensers stacked on top of each with a gentle flow of nitrogen across the top of the condenser was added phenyl acetylene (120 mmol, 13.2 mL) and isobutyric anhydride (181 mmol, 30.1 mL) (it should be noted that the use of two condensers is crucial in this reaction in order to achieve full conversion). The resulting mixture was stirred at 190 °C for 48 h with a continuous flow of nitrogen across the top of the condenser. Next the reaction was cooled down to 60 °C followed by the slow addition of a solution of KOH (536 mmol, 30.1 g) in 150 mL H<sub>2</sub>O. The resulting two layered mixture was stirred at 100 °C for 24 h. Next the mixture was cooled down to room temperature followed by the addition of 200 mL of ethyl acetate and stirred for 10 min. The aqueous layer was extracted with ethyl acetate (3 X 100) and the combined organic layer



was washed with brine, dried over Na<sub>2</sub>SO<sub>4</sub> and filtered over Celite bed. The resulting black solution was concentrated under reduced pressure and purified via column chromatography (50 X 300 mm, CH<sub>2</sub>Cl<sub>2</sub>: Hexane 1:3 to 1:0) which gave the desired product **III-165** as an off-white solid in 60% yield (54 mmol, 16 g).

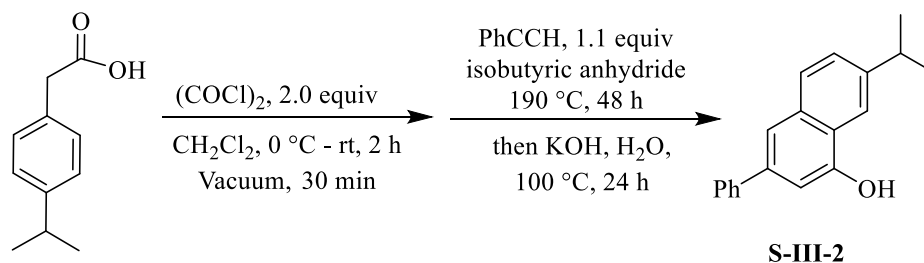
Spectral data for **III-165**: <sup>1</sup>H NMR (500 MHz, Chloroform-*d*) δ 5.37 (s, 1H), 7.09 (d, *J* = 1.6 Hz, 1H), 7.35 – 7.43 (m, 1H), 7.44 – 7.51 (m, 2H), 7.55 – 7.65 (m, 2H), 7.62 – 7.69 (m, 2H), 7.72 (d, *J* = 8.7 Hz, 1H), 8.37 (d, *J* = 2.0 Hz, 1H). <sup>13</sup>C NMR (126 MHz, Chloroform-*d*) δ 104.50, 113.82, 114.53, 119.53, 119.88, 122.49, 122.93, 124.15, 124.84, 125.55, 128.58, 134.62, 135.72, 146.10. These spectral data are in agreement with literature value.<sup>71</sup>



**Synthesis of 7-methyl-3-phenyl-1-naphthol S-III-1:** Compound **S-III-1** was prepared from 4-methyl-phenylacetic acid (69 mmol, 10 g), phenylacetylene (75.9 mmol, 8.33 mL) and (*i*PrCO)<sub>2</sub>O (138 mmol, 23.1 mL) according to the procedure I and the crude product was purified via column chromatography on silica gel (50 mm X 300 mm, hexane: CH<sub>2</sub>Cl<sub>2</sub>, 3:1, 2:1 and 1:1 as the eluent). The desired compound **S-III-1** was obtained as a white solid in 32% isolated yield (26.2 mmol, 6.14 g).

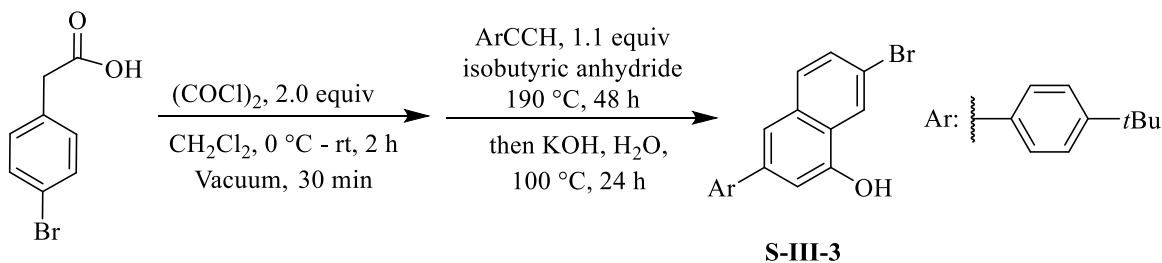
Spectral data for **S-III-1**: <sup>1</sup>H NMR (500 MHz, Chloroform-*d*) δ 2.55 (d, *J* = 0.8 Hz, 3H), 5.27 – 5.32 (m, 1H), 7.07 (d, *J* = 1.6 Hz, 1H), 7.33 – 7.40 (m, 2H), 7.43 – 7.55 (m, 2H), 7.62 (t, *J* = 1.1 Hz, 1H), 7.64 – 7.71 (m, 2H), 7.77 (d, *J* = 8.3 Hz, 1H), 7.94 (dq, *J* = 1.8, 0.9 Hz, 1H). <sup>13</sup>C NMR (126 MHz, Chloroform-*d*) δ 21.93, 108.42, 118.59, 120.31, 123.57, 127.21, 127.29, 127.92,

128.78, 129.13, 133.19, 135.15, 137.87, 140.97, 151.16. These spectral data are in agreement with the literature value.<sup>71</sup>



**Synthesis of 7-iso-propyl-3-phenyl-1-naphthol S-III-2:** Compound **S-III-2** was prepared from 4-methylphenylacetic acid (28.1 mmol, 5.01 g), phenylacetylene (31 mmol, 3.4 mL) and (*i*PrCO)<sub>2</sub>O (56.2 mmol, 9.41 mL) according to the procedure I and the crude product was purified via column chromatography on silica gel (50 mm X 300 mm, hexane: CH<sub>2</sub>Cl<sub>2</sub>, 3:1, 2:1 and 1:1 as the eluent). The desired compound **S-III-2** was obtained as a white solid in 52% isolated yield (14.6 mmol, 3.83 g).

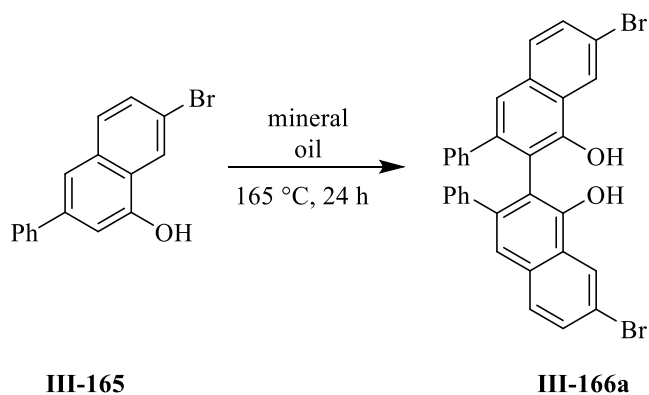
Spectral data for **S-III-2**: <sup>1</sup>H NMR (500 MHz, Chloroform-*d*) δ 1.38 (d, *J* = 6.9 Hz, 6H), 3.13 (hept, *J* = 6.9 Hz, 1H), 5.43 (s, 1H), 7.07 (d, *J* = 1.6 Hz, 1H), 7.34 – 7.42 (m, 1H), 7.43 – 7.51 (m, 3H), 7.63 – 7.71 (m, 3H), 7.83 (d, *J* = 8.5 Hz, 1H), 8.01 (dd, *J* = 1.8, 0.9 Hz, 1H). <sup>13</sup>C NMR (126 MHz, Chloroform-*d*) δ 24.01, 34.51, 108.43, 117.64, 118.59, 123.60, 126.78, 127.25, 127.31, 128.11, 128.81, 133.62, 138.00, 141.01, 146.12, 151.43. These data are in agreement with the literature values.<sup>71</sup>



**Synthesis of 7-bromo-3-(4-(*tert*-butyl)phenyl)-1-naphthol S-III-3:** Compound **S-III-3** was prepared from 4-bromophenylacetic acid (60.1 mmol, 12.9 g), 4-*tert*butyl-phenylacetylene (80.1 mmol, 14.4 mL) and (*i*PrCO)<sub>2</sub>O (158 mmol, 19.9 mL) according to the procedure I and the crude product was purified via column chromatography on silica gel (50 mm X 300 mm, hexane: CH<sub>2</sub>Cl<sub>2</sub>, 3:1, 2:1 and 1:1 as the eluent). The desired compound **S-III-3** was obtained as a white solid in 36% isolated yield (21.6 mmol, 7.67 g), mp 162-164 °C.

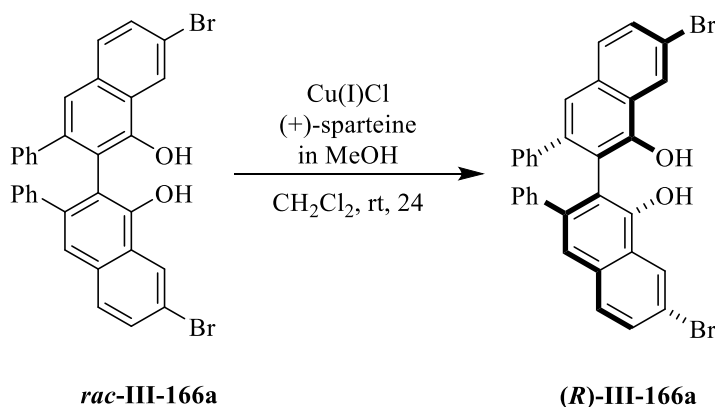
Spectral data for **S-III-3**: <sup>1</sup>H NMR (500 MHz, Chloroform-*d*) δ 1.39 (s, 9H), 5.35 (s, 1H), 7.09 (d, *J* = 1.5 Hz, 1H), 7.47 – 7.53 (m, 2H), 7.54 – 7.64 (m, 4H), 7.71 (d, *J* = 8.7 Hz, 1H), 8.36 (d, *J* = 1.9 Hz, 1H). <sup>13</sup>C NMR (126 MHz, Chloroform-*d*) δ 31.35, 34.61, 109.20, 118.29, 119.10, 124.26, 124.54, 125.87, 126.85, 129.56, 130.21, 133.36, 137.51, 139.20, 150.79, 150.81. IR: 3554s 2858w 1586m 1236m 1167m 1086m 826s 548m cm<sup>-1</sup>. HRMS (ESI-TOF) *m/z* 353.0579, [(M-H)<sup>-</sup>]; calcd for C<sub>20</sub>H<sub>18</sub><sup>79</sup>BrO: 353.0541].

**General procedure for the synthesis of enantiopure 7,7'-disubstituted-VANOL ligand (procedure II):**



**Oxidative phenol-coupling of compound III-165:** To a 500 mL three neck round bottom flask which was equipped with a stir bar and cooling condenser was added compound **III-165** (47.2 mmol, 14.1 g) and 55 mL of mineral oil. Then the reaction was subjected to the air flow via a syringe located one inch above the mixture. The reaction was stirred at 165 °C for 24 h with a

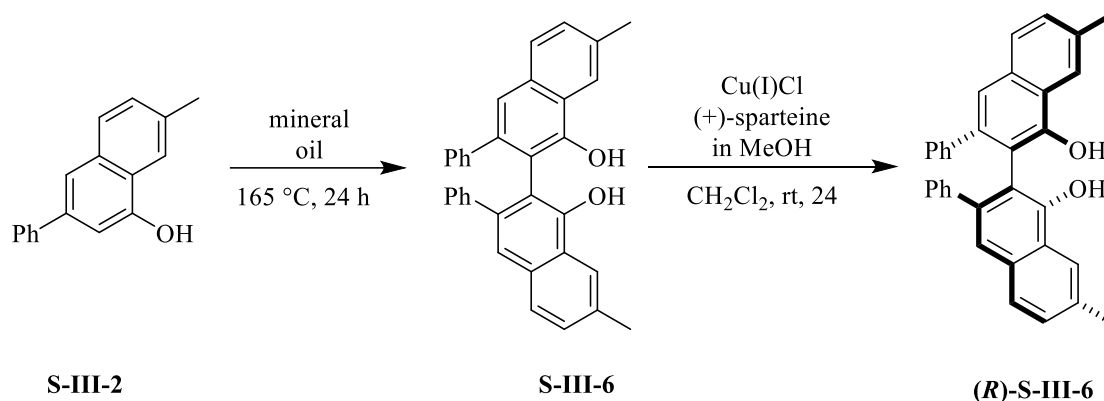
continuous air flow over the reaction. Then the oil bath was removed and the reaction was allowed to cool down to the room temperature followed by the addition of 50 mL CH<sub>2</sub>Cl<sub>2</sub> and 100 mL hexane. The resulting suspension stirred it at room temperature until all of the large chunks were broken up and then cooled down to -20 °C overnight. The resulting solid were collected via filtration and washed with hexane and CH<sub>2</sub>Cl<sub>2</sub> which yielded the desired product **III-166a** in 80% isolated yield (37.8 mmol, 11.3 g).



**De-racemization of compound III-166a:** A 500 mL round bottom flask was charged with (+)-sparteine (35 mmol, 8.2 g), CuCl (17.0 mmol, 1.68 g), 270 mL of MeOH and sonicated under air for 60 min. The flask containing the resulting dark green solution was sealed with septum and purged with argon for 60 min. Concurrently, to a 2 L round bottom flask was added *rac*-7,7'-Br<sub>2</sub>VANOL **III-166a** (10.0 mmol, 5.96 g) and 1020 mL of CH<sub>2</sub>Cl<sub>2</sub> which was also sealed and purged for 60 min with argon gas. The dark green solution of (+)-sparteine-copper complex in the 500 mL round bottom flask was transferred to the 2 L round bottom flask containing *rac*-7,7'-Br<sub>2</sub>VANOL ligand **III-166a** via cannula under argon and the resulting dark green solution was sonicated at room temperature for 15 min. Then the reaction container was wrapped with aluminum foil and stirred at room temperature overnight. The reaction was quenched by the slow addition of 125 mL NaHCO<sub>3</sub> (sat. aq. solution), 400 mL of H<sub>2</sub>O and the crude mixture was

concentrated under reduced pressure. The resulting suspension was extracted with CH<sub>2</sub>Cl<sub>2</sub> (3 X 300 mL) and the combined organic layer was washed with brine, dried over Na<sub>2</sub>SO<sub>4</sub> and filtered through filter paper. Next, the solvent was removed under reduced pressure and the resulting crude mixture was purified via column chromatography on silica gel (30 mm X 250 mm, hexane: CH<sub>2</sub>Cl<sub>2</sub>, 2:1 to 1:1 and 1:2) which afforded pure (*R*)-7,7'-Br<sub>2</sub>VANOL **III-166a** as an off-white foamy solid in 73 % isolated yield (7.3 mmol, 4.3 g). The *ee* was determined to be 99% by HPLC analysis (Pirkle D-Phenylglycine column, 98:2, hexane: *i*PrOH at 254 nm, flow rate 1 mL/min). Retention time: *R*<sub>t</sub> = 26.67 min for (*R*)-isomer (major enantiomer), *R*<sub>t</sub> = 30.92 min for (*S*)-isomer, (minor enantiomer).

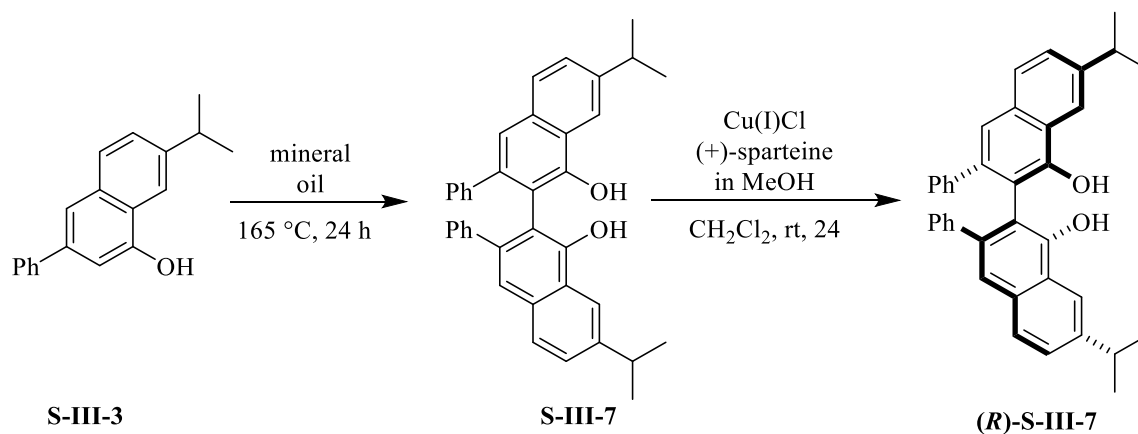
Spectral data for compound (***R***)-**III-166a**: <sup>1</sup>H NMR (500 MHz, Chloroform-*d*) 6.57 – 6.63 (m, 4H), 6.95 (t, *J* = 7.7 Hz, 4H), 7.03 – 7.10 (m, 2H), 7.21 (d, *J* = 0.9 Hz, 2H), 7.55 – 7.64 (m, 4H), 8.54 – 8.58 (m, 2H). <sup>13</sup>C NMR (126 MHz, Chloroform-*d*) δ 115.32, 119.40, 121.42, 124.60, 125.40, 126.67, 127.37, 128.92, 129.30, 130.48, 132.80, 140.05, 141.45, 149.92. These spectral data are in agreement with the literature value.<sup>71</sup>



**Synthesis of (*R*)-7,7'-Me<sub>2</sub>VANOL S-III-6:** Compound *rac*-**S-III-6** was prepared from compound **S-III-2** (2.51 mmol, 1.17 g) and 25 mL mineral oil via oxidative coupling followed by the deracemization of *rac*-**S-III-6** with CuCl (4.2 mmol, 0.42 g) and (+)-sparteine (8.75 mmol, 2.05

mL) according to the procedure II. The crude product was purified via column chromatography on silica gel (50 mm X 300 mm, hexane: CH<sub>2</sub>Cl<sub>2</sub>, 3:1, 2:1 and 1:1 as the eluent). The desired compound **(R)-S-III-6** was obtained as a white solid in 33% isolated overall yield (0.82 mmol, 0.38 g). The *ee* was determined to be 98% by HPLC analysis (Pirkle D-Phenylglycine column, 99:1, hexane: *i*PrOH at 254 nm, flow rate 1 mL/min). Retention time: *R*<sub>t</sub> = 15.61 min for (*R*)-isomer (major enantiomer), *R*<sub>t</sub> = 17.92 min for (*S*)-isomer, (minor enantiomer).

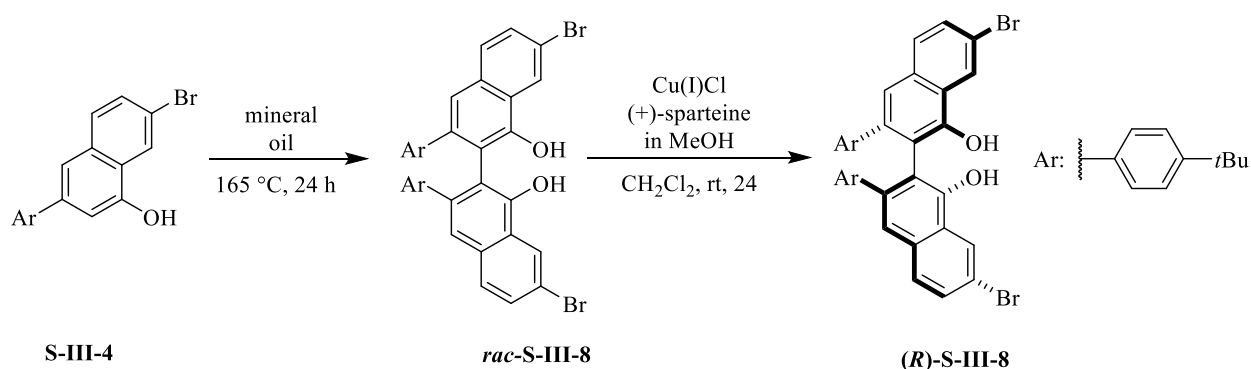
Spectral data for **(R)-S-III-6**: <sup>1</sup>H NMR (500 MHz, Chloroform-*d*) δ 2.60 (d, *J* = 0.9 Hz, 6H), 5.81 (s, 2H), 6.61 – 6.67 (m, 4H), 6.92 – 7.00 (m, 4H), 7.03 – 7.10 (m, 2H), 7.29 (s, 2H), 7.41 (dd, *J* = 8.4, 1.8 Hz, 2H), 7.70 (d, *J* = 8.3 Hz, 2H), 8.13 (dt, *J* = 1.8, 0.9 Hz, 2H). <sup>13</sup>C NMR (126 MHz, Chloroform-*d*) δ 21.97, 112.76, 121.66, 121.79, 122.92, 126.44, 127.39, 127.57, 128.85, 129.70, 132.82, 135.51, 139.66, 140.28, 149.77. These spectral data are in agreement with the literature value.<sup>71</sup>



**Synthesis of (R)-7,7'-*i*Pr<sub>2</sub>VANOL S-III-7:** Compound *rac*-**S-III-7** was prepared from compound **S-III-3** (3.83 mmol, 2.01 g) and 30 mL mineral oil via oxidative coupling followed by the deracemization of *rac*-**S-III-7** with CuCl (6.51 mmol, 0.645 g) and (+)-sparteine (13.4 mmol, 3.08 mL) according to the procedure II. The crude product was purified via column chromatography on silica gel (50 mm X 300 mm, hexane: CH<sub>2</sub>Cl<sub>2</sub>, 3:1, 2:1 and 1:1 as the eluent). The desired

compound **(R)- S-III-7** was obtained as a white solid in 64% isolated yield (2.45 mmol, 1.28 g). The *ee* was determined to be 98% by HPLC analysis (Pirkle D-Phenylglycine column, 99:1, hexane: *i*PrOH at 254 nm, flow rate 1 mL/min). Retention time:  $R_t$  = 18.58 min for (*R*)-isomer (major enantiomer),  $R_t$  = 25.18 min for (*S*)-isomer, (minor enantiomer).

Spectral data for **(R)-S-III-7**:  $^1\text{H}$  NMR (500 MHz, Chloroform-*d*)  $\delta$  1.43 (d,  $J$  = 6.9 Hz, 12H), 3.19 (h,  $J$  = 7.0 Hz, 2H), 5.85 (s, 2H), 6.61 – 6.68 (m, 4H), 6.98 (t,  $J$  = 7.7 Hz, 4H), 7.04 – 7.12 (m, 2H), 7.31 (s, 2H), 7.51 (dd,  $J$  = 8.5, 1.8 Hz, 2H), 7.75 (d,  $J$  = 8.4 Hz, 2H), 8.17 – 8.21 (m, 2H).  $^{13}\text{C}$  NMR (126 MHz, Chloroform-*d*)  $\delta$  23.99, 24.06, 34.54, 112.72, 119.06, 121.81, 122.93, 126.42, 127.30, 127.43, 127.74, 128.89, 133.23, 139.83, 140.35, 146.37, 150.03. These data are in good agreement with the literature value.<sup>71</sup>

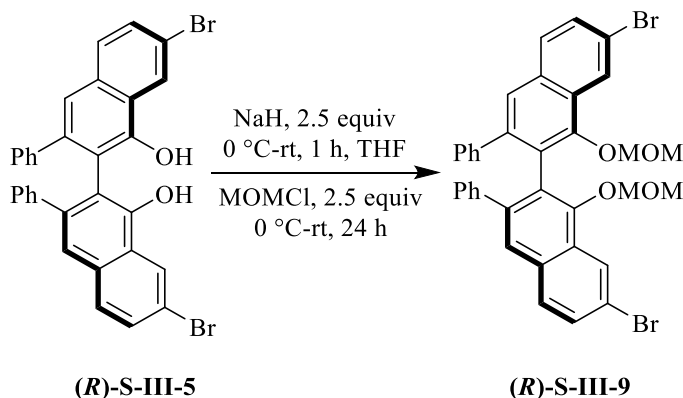


**Synthesis of (R)-S-III-8:** Compound **rac-S-III-8** was prepared from compound **S-III-4** (7 mmol, 5 g) and 50 mL mineral oil via oxidative coupling followed by the deracemization with CuCl (11.9 mmol, 1.18 g) and (+)-sparteine (24.5 mmol, 5.63 mL) according to the procedure II. The crude product was purified via column chromatography on silica gel (50 mm X 300 mm, hexane:  $\text{CH}_2\text{Cl}_2$ , 3:1, 2:1 and 1:1 as the eluent). The desired compound **(R)- S-III-8** was obtained as a white solid in 57% isolated yield (3.99 mmol, 2.83 g). The *ee* was determined to be 99% by HPLC analysis (Pirkle D-Phenylglycine column, 97:3, hexane: *i*PrOH at 254 nm, flow rate 1 mL/min). Retention

time:  $R_t = 16.42$  min for (*R*)-isomer (major enantiomer),  $R_t = 20.34$  min for (*S*)-isomer, (minor enantiomer). mp 73-74 °C.

Spectral data for (*R*)-**S-III-7**:  $^1\text{H}$  NMR (500 MHz, Chloroform-*d*)  $\delta$  1.25 (s, 18H), 5.77 (s, 2H), 6.44 – 6.50 (m, 4H), 6.92 – 6.99 (m, 4H), 7.31 (d,  $J = 0.8$  Hz, 2H), 7.56 – 7.72 (m, 4H), 8.52 (dd,  $J = 1.8, 0.9$  Hz, 2H).  $^{13}\text{C}$  NMR (126 MHz, Chloroform-*d*)  $\delta$  31.27, 34.36, 113.59, 119.64, 121.68, 123.92, 124.47, 125.31, 128.24, 129.35, 130.91, 133.03, 136.62, 140.87, 149.28, 149.70. IR: 3491brs, 2965m, 1097m, 873s, 829s, 560s, 541s. HRMS (ESI+TOF)  $m/z$  707.1158, [(*M*+*H*<sup>+</sup>); calcd for  $\text{C}_{40}\text{H}_{37}^{79}\text{Br}^{79}\text{BrO}_2$ : 707.1144].  $[\alpha]_{\text{D}}^{20} = 1.2181$  (c 1.0,  $\text{CHCl}_3$ ) on >99% *ee*(*R*)-**S-III-7** (HPLC).

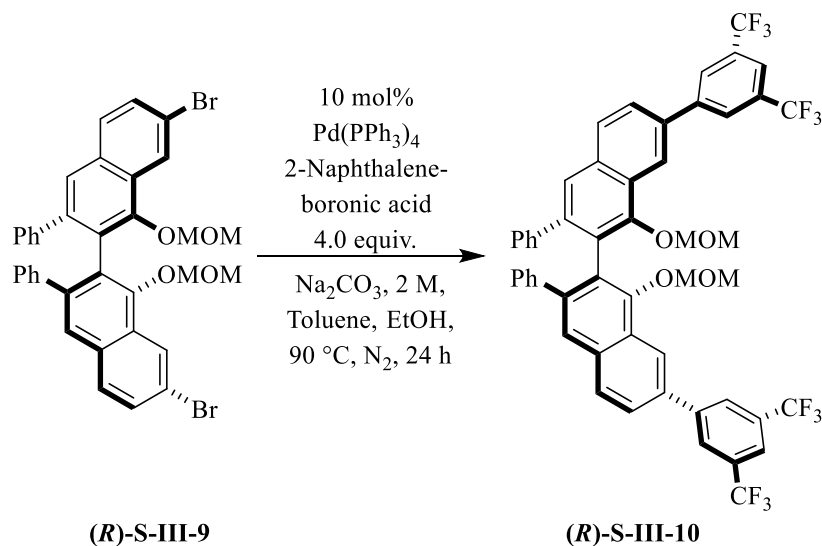
**General procedure for MOM-protection, Suzuki coupling and MOM-deprotection-illustrated for the synthesis of (*R*)-7,7'-(( $\text{CF}_3$ )<sub>2</sub> $\text{C}_6\text{H}_3$ )<sub>2</sub>VANOL ligand **S-III-9** (Procedure III):**



**MOM-protection:** A flame-dried 50 mL round bottom flask was charged with (*R*)-7,7'-Br<sub>2</sub>VANOL ligand **S-III-5** (1.6 mmol, 0.95 g) and 12 mL of dried THF. The mixture was stirred at 0 °C for 10 min followed by the slow addition of NaH (4 mmol, 0.1 g, 60% dispersed in mineral oil). After keeping the reaction for 30 min at 0 °C, the ice bath was removed and the mixture was warmed up to room temperature and stirred for another 30 min. The reaction container was cooled down to 0 °C followed by the addition of  $\text{CH}_3\text{OCH}_2\text{Cl}$  (4 mmol, 0.2 mL) and stirred at room

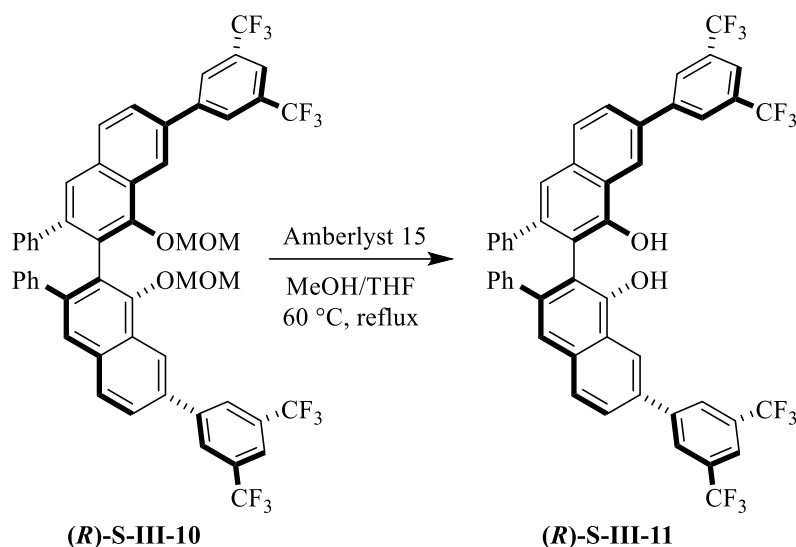


temperature for 24 h. The reaction was quenched by slow addition of  $\text{NH}_4\text{Cl}$  (sat. aq solution) and the aqueous layer was extracted with  $\text{CH}_2\text{Cl}_2$  (3 X 10 mL). The combined organic layer was dried over  $\text{Na}_2\text{SO}_4$  and filtered through filter paper. The solvent was removed via reduced pressure and the crude product was used in the next step without further purification. The conversion was determined to be 99% as judged by TLC.



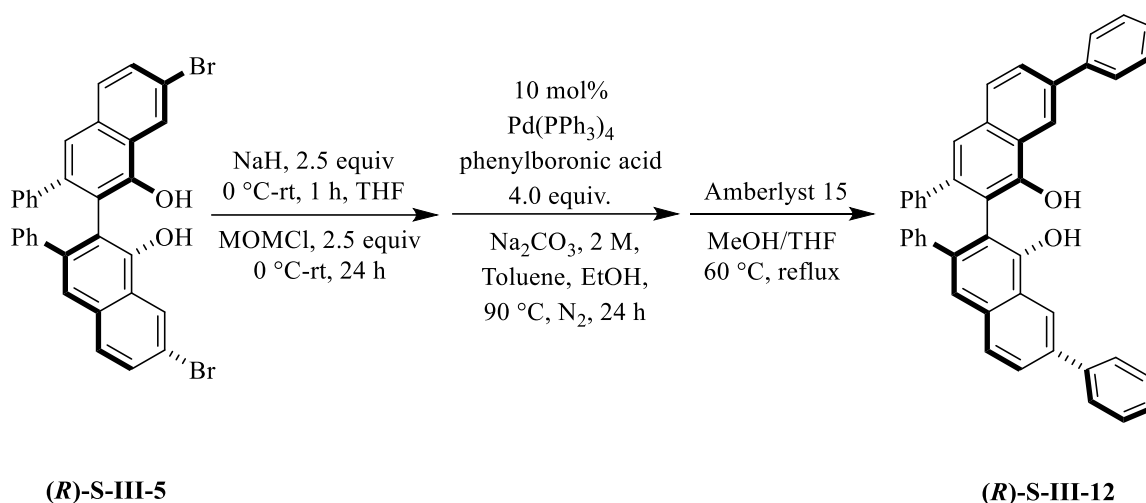
**Suzuki coupling:** A mixture of 2 M  $\text{Na}_2\text{CO}_3$  aq (20 mL) solution, toluene (30 mL) and ethanol (20 mL) was purged with nitrogen gas for 10 min prior to use. The solid from the previous step was added to a 250 mL round bottom flask attached to a condenser. Tetrakis(triphenylphosphine)palladium (0.16 mmol, 0.19 g), 20 mL toluene and 10 mL aq  $\text{Na}_2\text{CO}_3$  (2 M) was added to the reaction container. To this mixture was also added 3,5-bis(trifluoromethyl)phenylboronic acid (6.4 mmol, 1.7 g) as well as 10 mL ethanol and the resulting bilayer solution was refluxed at  $90^\circ\text{C}$  overnight with a continuous flow of the nitrogen over the top of the condenser. The reaction was cooled down to the room temperature followed by the addition of 40 mL of EtOAc. The organic layer was separated, washed with brine, dried over  $\text{Na}_2\text{SO}_4$  and filtered through filter paper. The crude product was concentrated to dryness and

passed through a pad of silica gel using pure  $\text{CH}_2\text{Cl}_2$  as the eluent and used in the next step without further purification.



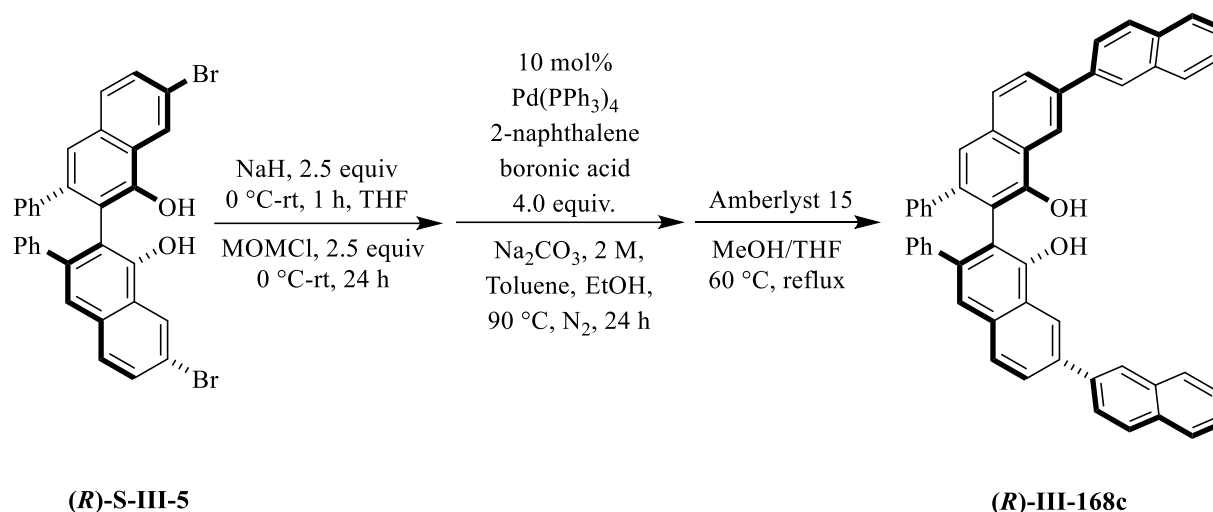
**MOM deprotection:** To a 250 mL round bottom flask attached to a condenser was added the crude product from the previous step, Amberlyst 15 (0.83 g) and 60 mL MeOH:THF (1:1). The solution was stirred at 65 °C overnight with a continuous flow of nitrogen across the top of the condenser. Next, the oil bath was removed and the reaction was filtered through filter paper, concentrated to dryness under reduced pressure and purified via column chromatography (30 mm X 250 mm, hexane: $\text{CH}_2\text{Cl}_2$  3:1, 2:1, 1:1 and 1:2) which afforded the desired ligand as a yellow solid in 72% yield overall three steps (1.15 mmol, 0.993 g).

Spectral data for **(R)-S-III-11**:  $^1\text{H}$  NMR (500 MHz, Chloroform-*d*)  $\delta$  5.98 (s, 2H), 6.63 – 6.69 (m, 4H), 6.99 (t,  $J$  = 7.7 Hz, 4H), 7.10 (td,  $J$  = 7.2, 1.3 Hz, 2H), 7.36 (s, 2H), 7.82 (dd,  $J$  = 8.5, 1.9 Hz, 2H), 7.89 – 7.95 (m, 4H), 8.21 (d,  $J$  = 1.6 Hz, 4H), 8.58 (d,  $J$  = 1.8 Hz, 2H).  $^{13}\text{C}$  NMR (126 MHz, Chloroform-*d*)  $\delta$  113.45, 121.01, 121.60, 121.87, 122.31 (q,  $J$  = 275 Hz), 126.46, 126.97, 127.41 (q,  $J$  = 3.5 Hz), 127.57, 128.79, 129.01, 131.82, 132.09 (q,  $J$  = 35 Hz), 134.26, 135.31, 139.65, 141.69, 143.07, 150.71. These data are in agreement with literature value.<sup>71</sup>



**Synthesis of (R)-S-III-12:** Compound **(R)-S-III-12** was prepared from compound **(R)-S-III-5** (0.84 mmol, 0.51 g), NaH (2.1 mmol, 84 mg),  $\text{CH}_3\text{OCH}_2\text{Cl}$  (2.1 mmol, 0.11 mL), phenylboronic acid (3.34 mmol, 0.412 g), tetrakis(triphenylphosphine)palladium (0.084 mmol, 0.097g) and Amberlyst 15 (0.42 g) according to the general procedure III and the crude product was purified via column chromatography on silica gel (50 mm X 300 mm, hexane:  $\text{CH}_2\text{Cl}_2$ , 3:1, 2:1 and 1:1 as the eluent). The desired compound **(R)-S-III-12** was obtained as a white solid in 61% isolated yield (0.51 mmol, 0.31 g) overall for 3 steps.

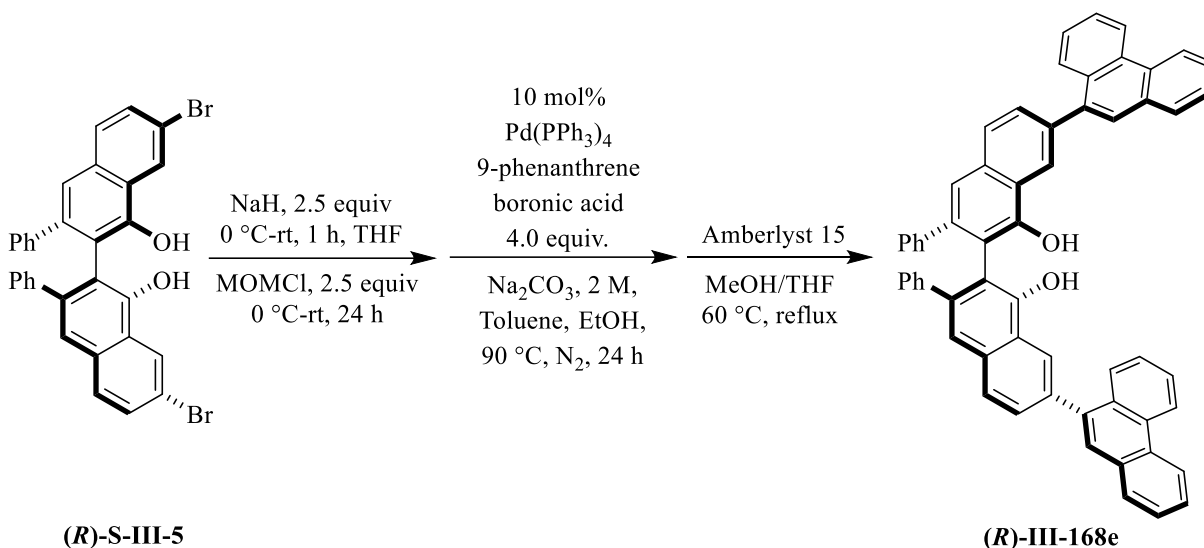
Spectral data for **(R)-S-III-12**:  $^1\text{H}$  NMR (500 MHz, Chloroform-*d*)  $\delta$  6.54 – 6.60 (m, 4H), 6.84 (td,  $J = 7.6, 1.5$  Hz, 4H), 6.94 (td,  $J = 7.2, 1.3$  Hz, 2H), 7.14 (s, 2H), 7.23 – 7.30 (m, 2H), 7.38 (td,  $J = 8.3, 7.9, 1.6$  Hz, 4H), 7.65 – 7.74 (m, 8H), 8.55 (d,  $J = 1.4$  Hz, 2H).  $^{13}\text{C}$  NMR (126 MHz, Chloroform-*d*)  $\delta$  115.55, 120.83, 120.89, 123.95, 126.19, 126.24, 127.15, 127.21, 128.11, 128.77, 129.01, 133.38, 137.48, 140.68, 141.00, 141.28, 151.24. One  $\text{sp}^2$  carbon is not located. These data are in agreement with the literature value.<sup>71</sup>



**Synthesis of (R)-III-168c:** Compound **(R)-III-168c** was prepared from compound **(R)-S-III-5** (0.99 mmol, 0.61 g), NaH (2.5 mmol, 0.11 g), CH<sub>3</sub>OCH<sub>2</sub>Cl (2.5 mmol, 0.13 mL), 2-naphthaleneboronic acid (3.99 mmol, 0.691 g), tetrakis(triphenylphosphine)palladium (0.101 mmol, 0.116 g) and Amberlyst 15 (0.5 g) according to the general procedure III and the crude product was purified via column chromatography on silica gel (50 mm X 300 mm, hexane: CH<sub>2</sub>Cl<sub>2</sub>, 3:1, 2:1 and 1:1 as the eluent). The desired compound **(R)- III-168c** was obtained as a white solid in 75% isolated yield (0.75 mmol, 0.52 g) overall for 3 steps.

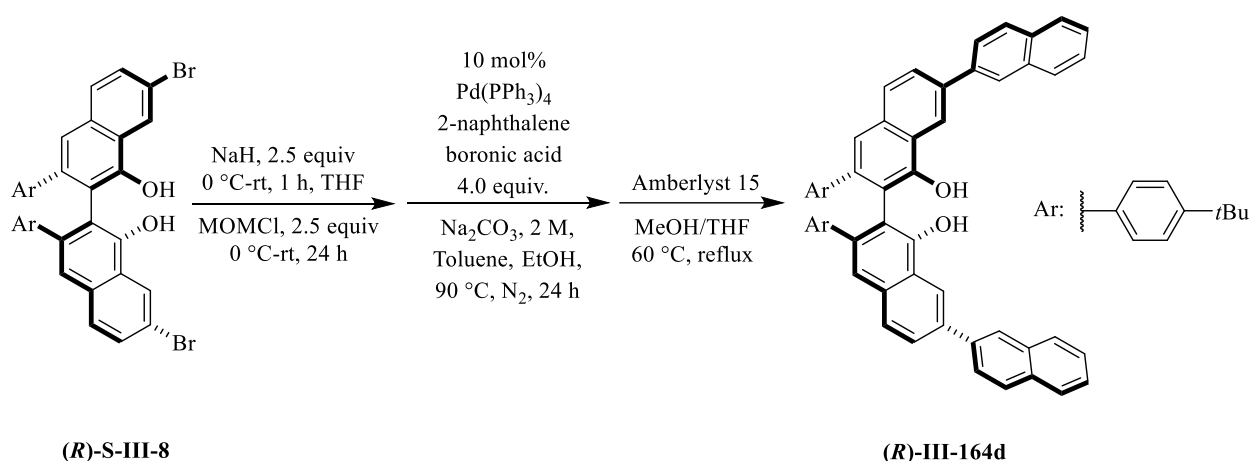
Spectral data for **(R)-III-168c**: <sup>1</sup>H NMR (500 MHz, Chloroform-*d*) δ 6.54 – 6.61 (m, 4H), 6.83 (t, *J* = 7.6 Hz, 4H), 6.89 – 6.96 (m, 2H), 7.14 (s, 2H), 7.32 – 7.42 (m, 4H), 7.70 – 7.78 (m, 4H), 7.76 – 7.89 (m, 8H), 8.13 (d, *J* = 1.6 Hz, 2H), 8.66 – 8.70 (m, 2H). <sup>13</sup>C NMR (126 MHz, Chloroform-*d*) δ 115.81, 120.82, 121.17, 124.09, 125.57, 125.76, 125.88, 126.24, 126.27, 127.14, 127.54, 128.12, 128.21, 128.40, 129.03, 132.48, 133.41, 133.63, 137.18, 138.31, 140.72, 141.45, 151.39.

These data are in agreement with the literature value.<sup>71</sup>



**Synthesis of (R)-III-168e:** Compound **(R)-III-168e** was prepared from compound **(R)-S-III-5** (2.75 mmol, 1.64 g), NaH (6.9 mmol, 0.28 g),  $\text{CH}_3\text{OCH}_2\text{Cl}$  (6.9 mmol, 0.36 mL), 9-phenanthreneboronic acid (11.0 mmol, 1.91 g), tetrakis(triphenylphosphine)palladium (0.275 mmol, 0.319 g) and Amberlyst 15 (1.375 g) according to the general procedure III and the crude product was purified via column chromatography on silica gel (50 mm X 300mm, hexane: DCM, 3:1, 2:1 and 1:1 as the eluent). The desired compound **(R)-III-168e** was obtained as a white solid in 61% isolated yield (1.675 mmol, 1.325 g) overall for 3 steps. mp: 247-248  $^{\circ}\text{C}$ .

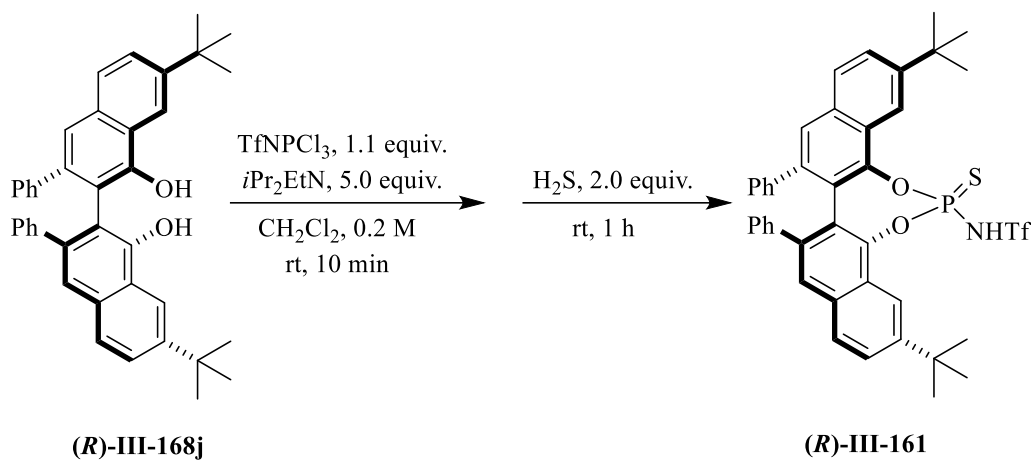
Spectral data for **(R)-III-168e**:  $^1\text{H}$  NMR (500 MHz, Chloroform-*d*)  $\delta$  5.99 (s, 2H), 6.73 – 6.80 (m, 4H), 7.08 (t,  $J = 7.6$  Hz, 4H), 7.13 – 7.21 (m, 2H), 7.47 (s, 2H), 7.60 (ddd,  $J = 8.1, 6.8, 1.2$  Hz, 2H), 7.66 (ddd,  $J = 8.0, 7.0, 1.2$  Hz, 2H), 7.71 (dddd,  $J = 8.3, 7.0, 3.4, 1.4$  Hz, 4H), 7.79 (dd,  $J = 8.3, 1.7$  Hz, 2H), 7.90 (s, 2H), 7.90 – 8.00 (m, 4H), 8.06 (dd,  $J = 8.2, 1.2$  Hz, 2H), 8.57 – 8.61 (m, 2H), 8.77 (d,  $J = 8.2$  Hz, 2H), 8.83 (dd,  $J = 8.5, 1.2$  Hz, 2H).  $^{13}\text{C}$  NMR (126 MHz, Chloroform-*d*)  $\delta$  113.21, 121.97, 122.59, 123.01, 123.03, 123.63, 126.56, 126.64, 126.71, 126.73, 126.93, 126.99, 127.46, 127.59, 128.12, 128.76, 128.98, 130.08, 130.14, 130.71, 131.16, 131.62, 133.81, 138.36, 138.65, 140.21, 140.94, 150.57.  $[\alpha]_D^{20} = -0.6822$  (c 1.0,  $\text{CHCl}_3$ ).



**Synthesis of (R)-III-164d:** Compound **(R)-III-164d** was prepared from compound **(R)-S-III-8** (0.75 mmol, 0.61 g), NaH (1.875 mmol, 0.7520 g), CH<sub>3</sub>OCH<sub>2</sub>Cl (1.87 mmol, 0.101 mL), 2-naphthaleneboronic acid (3.0 mmol, 0.52 g), tetrakis(triphenylphosphine)palladium (0.075 mmol, 0.087 g) and Amberlyst 15 (0.375 g) according to the general procedure III and the crude product was purified via column chromatography on silica gel (50 mm X 300mm, hexane: CH<sub>2</sub>Cl<sub>2</sub>, 3:1, 2:1 and 1:1 as the eluent). The desired compound **(R)-III-164d** was obtained as a white solid in 68% isolated yield (0.51 mmol, 0.38 g) overall for 3 steps. mp 186-187.

Spectral data for **(R)-III-164d**: <sup>1</sup>H NMR (500 MHz, Chloroform-*d*)  $\delta$  1.28 (s, 18H), 6.00 (s, 2H), 6.54 – 6.61 (m, 4H), 6.96 – 7.03 (m, 4H), 7.44 (s, 2H), 7.49 – 7.59 (m, 4H), 7.89 – 7.94 (m, 2H), 7.91 – 8.02 (m, 8H), 8.02 (dd, *J* = 8.5, 1.8 Hz, 2H), 8.28 (d, *J* = 1.3 Hz, 2H), 8.74 (dd, *J* = 1.8, 0.9 Hz, 2H). <sup>13</sup>C NMR (126 MHz, Chloroform-*d*)  $\delta$  31.32, 34.3, 113.29, 121.09, 121.66, 123.25, 124.46, 125.73, 126.05, 126.15, 126.37, 127.21, 127.69, 128.30, 128.38, 128.40, 128.59, 132.72, 133.77, 133.84, 137.15, 138.10, 138.34, 140.65, 149.43, 150.47. IR: 3510brs, 2958m, 829w, 805s, 743s, 522m. HRMS (ESI+TOF) *m/z* 803.3871, [(M+H<sup>+</sup>); calcd for C<sub>60</sub>H<sub>51</sub>O<sub>2</sub>: 803.3889]. [ $\alpha$ ]<sub>D</sub><sup>20</sup> = -0.6932 (c 1.0, CHCl<sub>3</sub>).

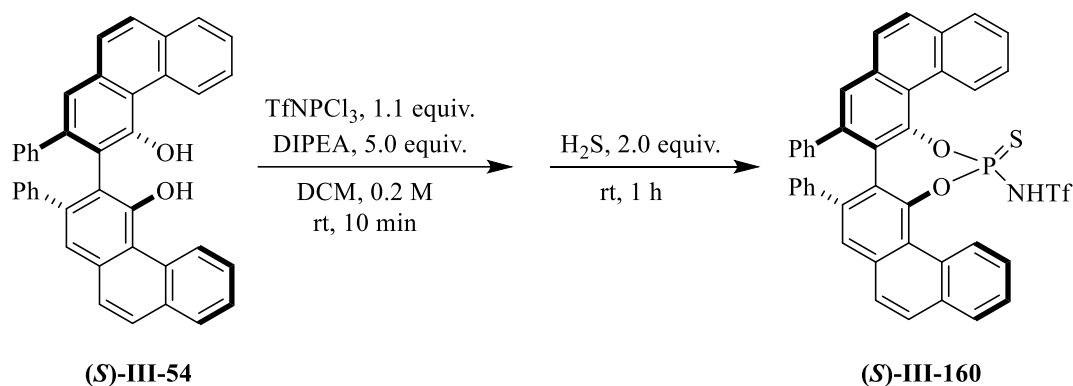
**General procedure for the synthesis of N-triflylthiophosphoramides -illustrated for the synthesis of 7,7'-*t*Bu<sub>2</sub>VANOL N-triflylthiophosphoramides (procedure IV):**



**Synthesis of 7,7'-*t*Bu<sub>2</sub>VANOL N-triflylthiophosphoramides (R)-III-161:** A flame-dried 25 mL round bottom flask under nitrogen was charged with 7,7'-*t*Bu<sub>2</sub>VANOL (**(R)-III-168j**), (1.0 mmol, 0.55 g), 5 mL CH<sub>2</sub>Cl<sub>2</sub> (0.2 M), TfNPCl<sub>3</sub><sup>72</sup> (1.1 mmol, 0.32 g) and *i*Pr<sub>2</sub>EtN (5.0 mmol, 0.87 mL). The mixture was stirred at room temperature for 10 min followed by the addition of H<sub>2</sub>S (2.0 mmol, 2.5 mL, 0.8 M in THF). Once the starting material was fully consumed as judged by TLC, the crude mixture was filtered through a Celite pad, concentrated to dryness under reduced pressure and purified via column chromatography on silica gel (30 mm X 250 mm, pure EtOAc as the eluent) which afforded the desired product as a salt. Compound (**(R)-III-161**) was obtained as the free acid in 99% isolated yield (1.0 mmol, 0.76 g) after acidification with 3.0 M HCl and drying under reduced pressure. mp 182-183 °C.

Spectral data for (**(R)-III-161**): <sup>1</sup>H NMR (500 MHz, Chloroform-*d*) δ 1.53 (m, 18H), 6.46 (td, *J* = 8.5, 1.3 Hz, 4H), 6.94 (td, *J* = 7.6, 4.5 Hz, 4H), 7.11 (qt, *J* = 7.3, 1.3 Hz, 2H), 7.53 (t, *J* = 1.8 Hz, 2H), 7.75 (ddd, *J* = 18.9, 8.7, 1.9 Hz, 2H), 7.81 (dd, *J* = 11.8, 8.6 Hz, 2H), 8.33 – 8.40 (m, 2H). <sup>13</sup>C NMR (126 MHz, Chloroform-*d*) δ 31.13, 35.51, 116.67, 118.24, 126.57 (apparent d), 126.82, 127.34 (d), 127.33 (d), 127.46, 127.78 (overlapping), 128.86, 128.88, 132.54, 139.29, 139.67,

150.03, 151.24.  $^{31}\text{P}$  NMR (202 MHz, Chloroform-*d*)  $\delta$  57.46 (d,  $J = 4.9$  Hz).  $^{19}\text{F}$  NMR (470 MHz, Chloroform-*d*)  $\delta$  -75.50 (d,  $J = 2.8$  Hz). IR: 2959w, 1201s, 901m, 884s, 765m, 696s, 608s  $\text{cm}^{-1}$ . HRMS (ESI+TOF)  $m/z$  760.2134,  $[(\text{M}+\text{H})^+]$ ; calcd for  $\text{C}_{41}\text{H}_{38}\text{F}_3\text{NO}_4\text{PS}_2$ : 760.1932].  $[\alpha]^{20}_{\text{D}} = 1.5100$  ( $c$  1.0,  $\text{CHCl}_3$ ).



**Synthesis of VAPOL *N*-triflylthiophosphoramides (*S*)-III-160:** Compound (*S*)-III-160 was prepared from compound (*S*)-III-54 (1.0 mmol, 0.54 g), 5 mL  $\text{CH}_2\text{Cl}_2$  (0.2 M),  $\text{TfNPCl}_3$ <sup>72</sup> (1.1 mmol, 0.32 g) and DIPEA (5.0 mmol, 0.87 mL) according to the general procedure IV and the crude product was purified via column chromatography on silica gel (30 mm X 250 mm, pure EtOAc as the eluent). The desired compound (*S*)-III-160 was obtained as a white solid in 27% isolated yield (0.27 mmol, 0.21 g). mp 176-177 °C.

Spectral data for (*S*)-III-160:  $^1\text{H}$  NMR (500 MHz, Chloroform-*d*)  $\delta$  6.48 – 6.55 (m, 2H), 6.53 – 6.60 (m, 2H), 6.97 (td,  $J = 7.7, 5.7$  Hz, 4H), 7.07 – 7.17 (m, 2H), 7.66 (d,  $J = 1.3$  Hz, 2H), 7.69 – 7.79 (m, 5H), 7.79 – 7.93 (m, 3H), 8.01 (ddd,  $J = 22.3, 7.7, 1.7$  Hz, 2H), 9.61 (dd,  $J = 8.9, 2.3$  Hz, 2H).  $^{13}\text{C}$  NMR (126 MHz, Chloroform-*d*)  $\delta$  122.29, 122.31, 126.57, 126.94, 127.07, 127.44 (t) 127.74, 127.78, 128.15, 128.50, 128.70, 128.83, 128.93, 129.28, 129.36, 129.49, 129.70, 133.34 (d), 139.06 (d).  $^{31}\text{P}$  NMR (202 MHz, Chloroform-*d*)  $\delta$  52.40 – 52.55 (m).  $^{19}\text{F}$  NMR (470 MHz, Chloroform-*d*)  $\delta$  -76.50 (d,  $J = 2.8$  Hz). IR: 1200s, 891s, 811w, 747m, 696s, 605s  $\text{cm}^{-1}$ . HRMS

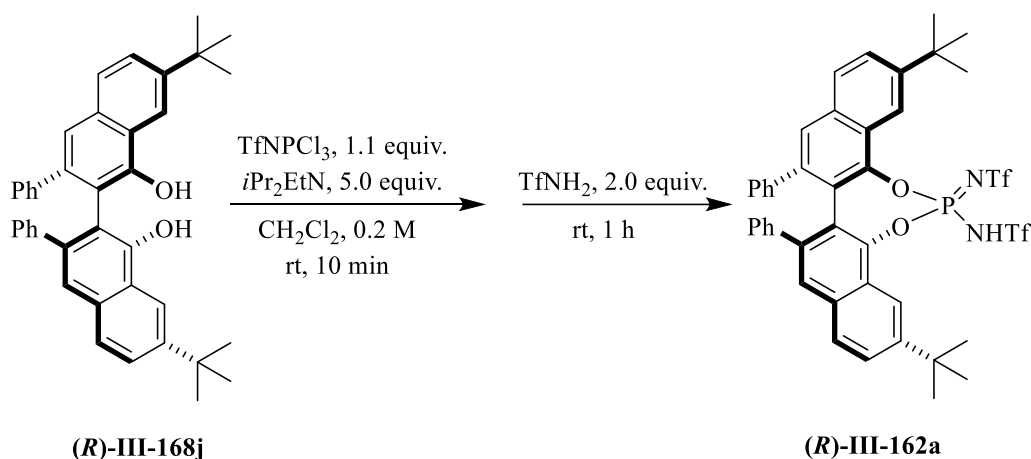


(ESI+TOF)  $m/z$  748.1008,  $[(M+H)^+]$ ; calcd for  $C_{41}H_{26}F_3NO_4PS_2$ : 748.0993].  $[\alpha]^{20}_D = 4.0444$  ( $c$  1.0,  $CHCl_3$ ).

**General procedure for the synthesis of  $N,N'$ -bis(triflyl)phosphoramidimides-illustrated for the synthesis of 7,7'- $t$ Bu<sub>2</sub>VANOL  $N,N'$ -bis(triflyl)phosphoramidimides (procedure V):**

**Synthesis of ((trifluoromethyl)sulfonyl)phosphorimidoyl trichloride:**

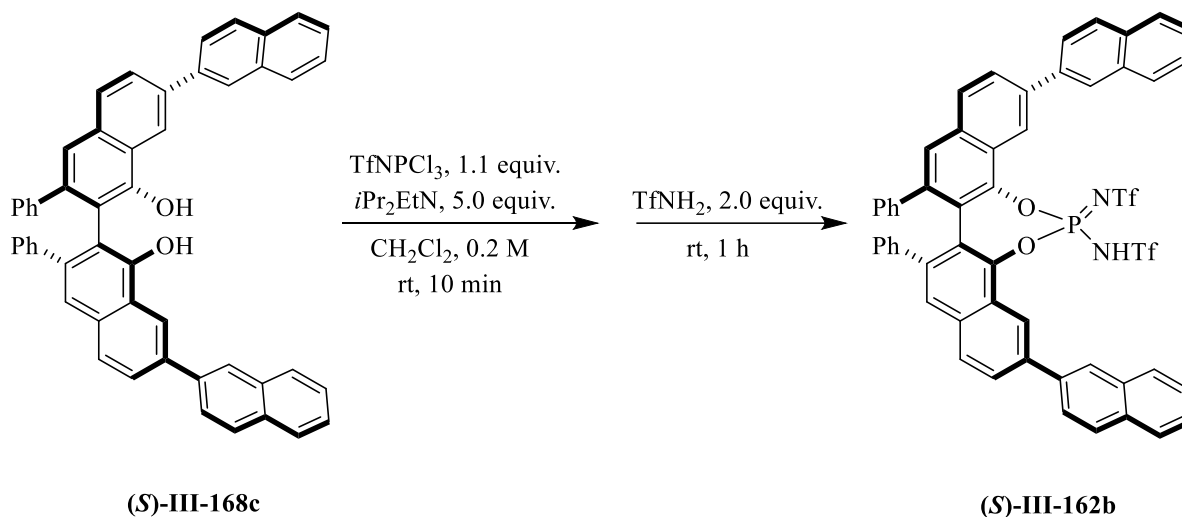
((trifluoromethyl)sulfonyl)phosphorimidoyl trichloride was synthesized via the procedure that is developed in Benjamin List's research group and the spectral data were in good agreement with the literature values.<sup>72</sup>



**Synthesis of 7,7'- $t$ Bu<sub>2</sub>VANOL  $N,N'$ -bis(triflyl)phosphoramidimides ( $R$ )-III-162a:** A flame-dried 25 mL round bottom flask under nitrogen was charged with 7,7'- $t$ Bu<sub>2</sub>VANOL ( $R$ )-III-168j, (1.0 mmol, 0.55 g), 5 mL  $CH_2Cl_2$  (0.2 M),  $TfNPCl_3$  (1.1 mmol, 0.32 g)<sup>72</sup> and  $iPr_2EtN$  (5.0 mmol, 0.87 mL). The mixture was stirred at room temperature for 10 min followed by the addition of  $TfNH_2$  (2.7 mmol, 0.41 g). Once the starting material was fully consumed as judged by TLC, the crude mixture was filtered through a Celite pad, concentrated to dryness under reduced pressure and purified via column chromatography on silica gel (30 mm X 250 mm, pure EtOAc as the eluent) which afforded the desired product as a salt. Compound ( $R$ )-III-162a was obtained as the

free acid in 98% isolated yield (0.98 mmol, 0.86 g) after acidification with 3.0 M HCl and drying under reduced pressure. mp 184-185 °C.

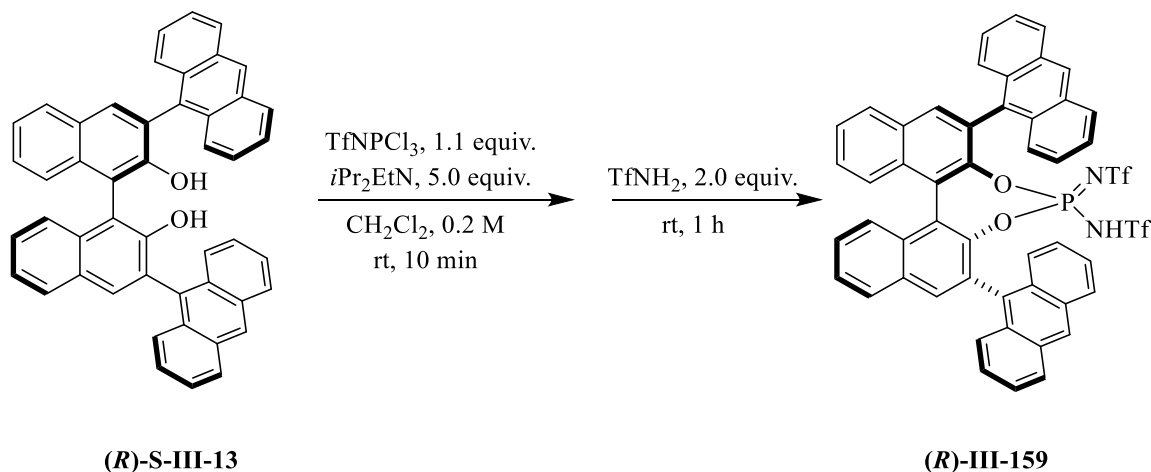
Spectral data for (**R**)-**III-162a**:  $^1\text{H}$  NMR (500 MHz, Chloroform-*d*)  $\delta$  1.52 (s, 18H), 6.48 (dt,  $J = 8.1, 1.0$  Hz, 4H), 6.96 (t,  $J = 7.6$  Hz, 4H), 7.09 – 7.16 (m, 2H), 7.56 (d,  $J = 1.4$  Hz, 2H), 7.77 (dd,  $J = 8.7, 1.8$  Hz, 2H), 7.83 (d,  $J = 8.7$  Hz, 2H), 8.25 – 8.30 (m, 2H).  $^{13}\text{C}$  NMR (126 MHz, Chloroform-*d*)  $\delta$  30.98, 35.35, 116.45, 122.19 (d), 124.75 (d), 126.73, 127.31, 127.69, 127.78, 128.10 (d), 129.01, 132.68, 139.37 (d), 139.43, 143.76 (d), 150.99.  $^{31}\text{P}$  NMR (202 MHz, Chloroform-*d*)  $\delta$  -1.41.  $^{19}\text{F}$  NMR (470 MHz, Chloroform-*d*)  $\delta$  -78.21 (d,  $J = 8.2$  Hz). IR: 2959w, 1200s, 910w, 882s, 765m, 696s, 607s, 586w. HRMS (ESI+TOF)  $m/z$  875.1804, [(M+H) $^+$ ]; calcd for  $\text{C}_{42}\text{H}_{38}\text{F}_6\text{N}_2\text{O}_6\text{PS}_2$ : 875.1813].  $[\alpha]_D^{20} = 0.7799$  ( $c$  1.0,  $\text{CHCl}_3$ ).



**Synthesis of 7,7'-Naphthyl<sub>2</sub>VANOL *N,N'*-bis(triflyl)phosphoramidimidates (S)-III-162b:**

Compound (**S**)-**III-162b** was prepared from compound (**S**)-**III-168c** (0.599 mmol, 0.415 g), 5 mL  $\text{CH}_2\text{Cl}_2$  (1.2 M),  $\text{TfNPCl}_3$  (0.66 mmol, 0.19 g)<sup>72</sup> and  $i\text{Pr}_2\text{EtN}$  (3.0 mmol, 0.52 mL) according to the general procedure V and the crude product was purified via column chromatography on silica gel (30 mm X 250 mm, pure EtOAc as the eluent). The desired compound (**S**)-**III-162b** was obtained as a solid in 66% isolated yield (0.4 mmol, 0.4 g). mp 205-206 °C.

Spectral data for **(S)-III-162b**:  $^1\text{H}$  NMR (500 MHz, Chloroform-*d*)  $\delta$  6.52 – 6.58 (m, 4H), 7.01 (t,  $J$  = 7.6 Hz, 4H), 7.13 – 7.21 (m, 2H), 7.48 – 7.58 (m, 4H), 7.65 (d,  $J$  = 1.4 Hz, 2H), 7.90 (dd,  $J$  = 7.7, 1.5 Hz, 2H), 7.95 – 8.08 (m, 8H), 8.17 (s, 2H), 8.31 (d,  $J$  = 1.6 Hz, 2H), 8.66 – 8.70 (m, 2H).  $^{13}\text{C}$  NMR (126 MHz, Chloroform-*d*)  $\delta$  119.20, 119.83, 122.19, 122.61, 124.68, 124.94, 125.68, 125.72, 125.73, 126.00, 126.08, 126.32, 126.37, 126.41, 126.56, 126.78, 127.07, 127.22, 127.47, 127.61, 127.74, 127.87, 128.23, 128.46, 128.58, 128.71, 128.90, 128.98, 129.06, 132.50, 132.56, 133.09, 133.40, 133.51, 134.01, 137.21, 137.90, 138.59, 138.63, 139.10, 139.33, 139.85, 140.59, 143.31, 144.77.  $^{31}\text{P}$  NMR (202 MHz, Chloroform-*d*)  $\delta$  -11.40.  $^{19}\text{F}$  NMR (470 MHz, Chloroform-*d*)  $\delta$  -77.63. IR: 2950w, 1190s, 1072m, 808m, 694m, 606s, 577m  $\text{cm}^{-1}$ . HRMS (ESI+TOF)  $m/z$  1015.1487,  $[(\text{M}+\text{H})^+]$ ; calcd for  $\text{C}_{54}\text{H}_{34}\text{F}_6\text{N}_2\text{O}_6\text{PS}_2$ : 1015.1500].  $[\alpha]_{\text{D}}^{20} = 2.9505$  ( $c$  1.0,  $\text{CHCl}_3$ ).

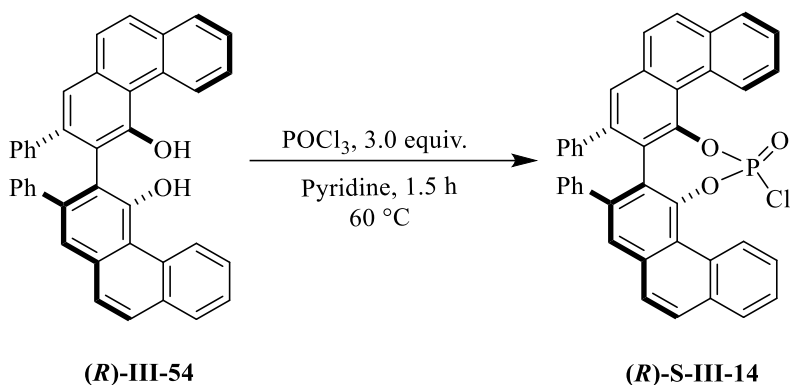


**Synthesis of 3,3'-Anthryl<sub>2</sub>BINOL *N,N'*-bis(triflyl)phosphoramidimidates (*R*)-III-159:**

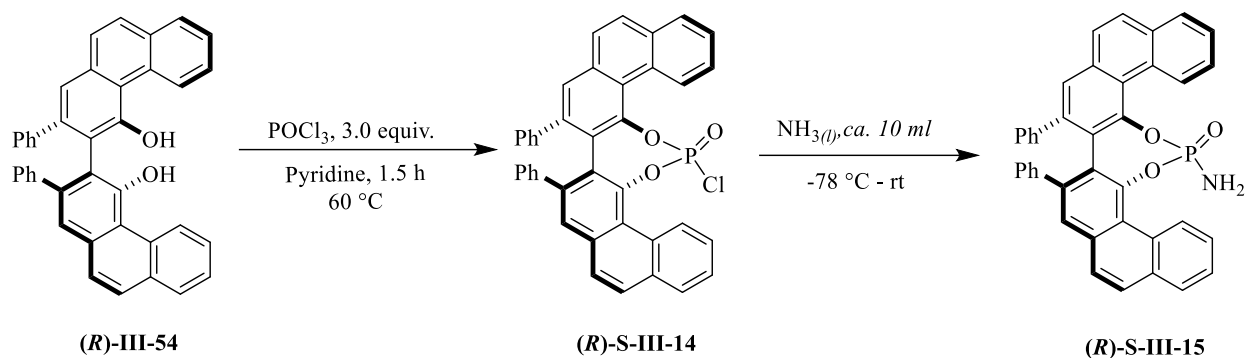
Compound **(R)-III-159** was prepared from compound **(R)-S-III-13** (0.51 mmol, 0.32 g), 5 mL  $\text{CH}_2\text{Cl}_2$  (1.0 M),  $\text{TfNPCl}_3$  (0.55 mmol, 0.16 g)<sup>72</sup> and  $i\text{Pr}_2\text{EtN}$  (2.5 mmol, 0.74 mL) according to the general procedure V and the crude product was purified via column chromatography on silica gel (30 mm X 250 mm, pure EtOAc as the eluent). The desired compound **(S)-III-159** was obtained as a solid in 40% isolated yield (0.2 mmol, 0.2 g). mp 215-217 °C.

Spectral data for **(S)-III-159**:  $^1\text{H}$  NMR (500 MHz, Chloroform-*d*)  $\delta$  7.21 – 7.39 (m, 6H), 7.36 – 7.43 (m, 2H), 7.57 (ddd,  $J$  = 8.4, 6.9, 1.3 Hz, 2H), 7.61 – 7.75 (m, 8H), 7.83 (d,  $J$  = 8.5 Hz, 2H), 7.88 (d,  $J$  = 8.5 Hz, 2H), 8.09 (d,  $J$  = 8.2 Hz, 2H), 8.20 (s, 2H), 8.24 (s, 2H).  $^{13}\text{C}$  NMR (126 MHz, Chloroform-*d*)  $\delta$  15.15, 65.93, 119.84, 122.09, 122.11, 124.89, 124.94, 125.57, 125.88, 126.01, 126.44, 127.08, 127.34, 127.59, 127.80, 128.12, 128.37, 128.74, 130.21, 130.25, 130.54, 130.57, 130.71, 130.93, 131.20, 131.75, 132.56, 132.57, 134.61, 145.88, 145.97.  $^{31}\text{P}$  NMR (202 MHz, Chloroform-*d*)  $\delta$  2.54.  $^{19}\text{F}$  NMR (470 MHz, Chloroform-*d*)  $\delta$  -79.52. IR: 1193s, 1097s, 965m, 728s, 607s, 574m. HRMS (ESI+TOF)  $m/z$  963.1197,  $[(\text{M}+\text{H})^+]$ ; calcd for  $\text{C}_{50}\text{H}_{30}\text{F}_6\text{N}_2\text{O}_6\text{PS}_2$ : 963.1187.  $[\alpha]_D^{20}$  = 0.0144 ( $c$  1.0,  $\text{CHCl}_3$ ).

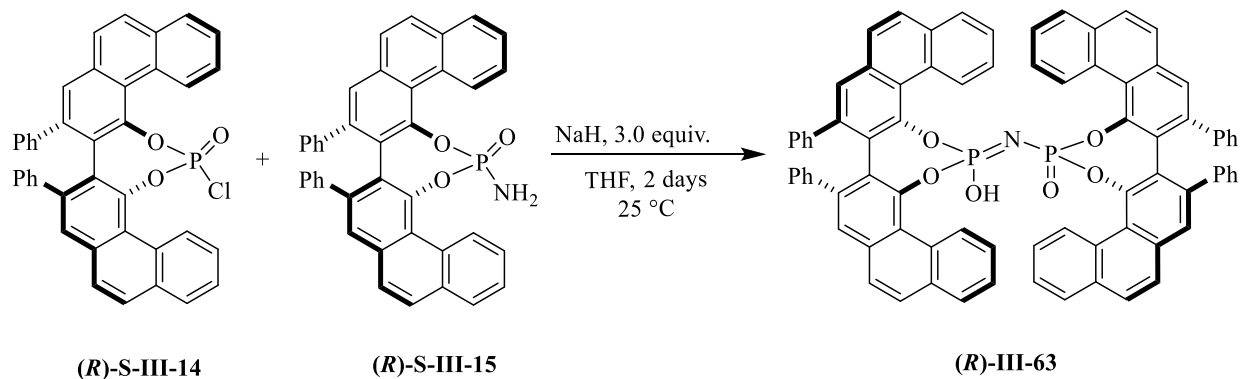
#### Synthesis of VAPOL imidodiphosphoric acid catalyst:



A 25 mL round bottom flask was charged with *(S)*-VAPOL **(R)-III-54** (1.0 mmol, 0.54 g), 3 mL pyridine and  $\text{POCl}_3$  (3.0 mmol, 0.28 mL) under nitrogen gas. The resulting solution was stirred at 65 °C for 1.5 h. Then the solvent was removed under reduced pressure and the crude mixture was passed through a short pad of silica gel with  $\text{CH}_2\text{Cl}_2$  as the eluent which gave the desired product **(R)-S-III-14** in 99% conversion (judged by the TLC). This material was used directly in the preparation of **III-63**.



A 25 mL round bottom flask was charged with (*S*)-VAPOL (***R***)-III-54 (1.0 mmol, 0.54 g), 3 mL pyridine and POCl<sub>3</sub> (3.0 mmol, 0.28 mL) under nitrogen gas. The resulting solution was stirred at 65 °C for 1.5 h then cooled down to -78 °C followed by the condensing of 10 mL of anhydrous ammonia by purging it into the flask. The mixture was warmed up to the room temperature then concentrated under reduced pressure and passed through a short pad of silica gel using pure CH<sub>2</sub>Cl<sub>2</sub> as the eluent which afforded compound (***R***)-S-III-14 as a white solid. The conversion was determined to 99% by TLC. This material was not characterized but taken directly onto the preparation of III-63.

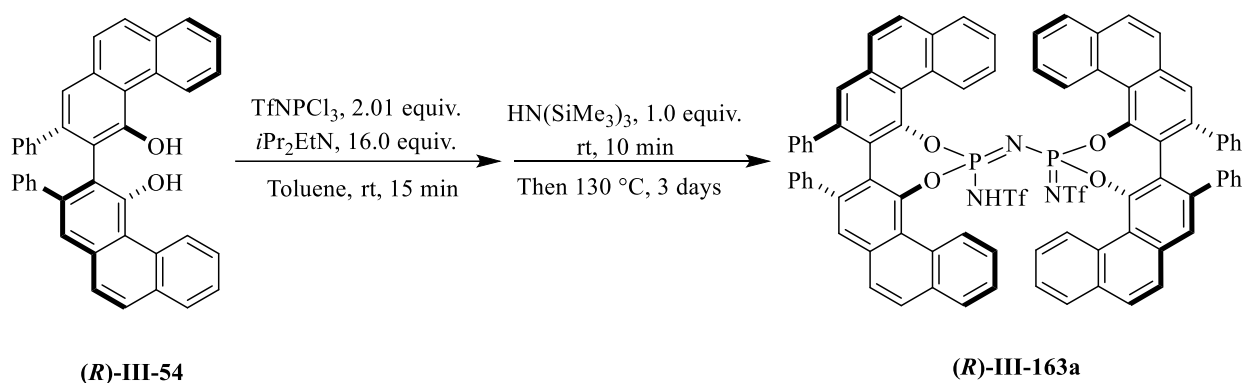


To a solution of compounds (***R***)-S-III-14 and (***R***)-S-III-15 in THF at room temperature was added NaH (3.0 mmol, 0.12 g) and the resulting mixture was stirred at room temperature for 48 h. The reaction was quenched by careful addition of 10% HCl aqueous solution. The organic layer was separated, dried over Na<sub>2</sub>SO<sub>4</sub> and concentrated under reduce pressure. The crude product was

purified via column chromatography (25 mm X 250 mm, hexane:EtOAc, 3:1 to 1:1) which gave compound **(R)-III-63** as a white solid. Acidification of the resulting solution in CH<sub>2</sub>Cl<sub>2</sub> with 3N aqueous HCl for 4 h afforded compound **(R)-III-63** as the free acid in 40% isolated yield (0.44 mmol, 0.43 g).

Spectral data for **(R)-III-63**: <sup>1</sup>H NMR (500 MHz, Chloroform-*d*) δ 6.33 (d, *J* = 7.6 Hz, 4H), 6.38 – 6.43 (m, 4H), 6.86 (t, *J* = 7.6 Hz, 4H), 7.00 (t, *J* = 7.6 Hz, 4H), 7.00 – 7.10 (m, 4H), 7.14 – 7.21 (m, 2H), 7.23 (s, 2H), 7.37 (s, 8H), 7.54 (s, 2H), 7.62 – 7.72 (m, 4H), 7.77 (s, 2H), 7.87 (d, *J* = 8.8 Hz, 2H), 7.97 (dd, *J* = 8.0, 1.4 Hz, 2H), 9.32 (s, 2H), 10.03 (s, 2H). <sup>13</sup>C NMR (126 MHz, DMSO-*d*<sub>6</sub>) δ 121.26, 122.10, 125.74, 125.79, 125.97, 126.03, 126.08, 126.73, 126.81, 126.93, 127.20, 127.64, 127.71, 127.74, 128.14, 128.49, 128.79, 128.85, 129.29, 129.78, 129.82, 130.01, 132.30, 132.37, 133.05, 133.60, 134.10, 140.09, 140.28, 140.99, 149.72, 149.73, 149.76. One sp<sup>2</sup> carbon peak is not located (due to the low solubility of this compound in chloroform-*d*, <sup>13</sup>C-NMR was taken in DMSO). <sup>31</sup>P NMR (202 MHz, Chloroform-*d*) δ -0.84. These data matched with the literature value.<sup>39</sup>

**General procedure for the synthesis of imidodiphosphorimide catalysts-illustrated for the synthesis of VAPOL imidodiphosphorimide (procedure VI):**

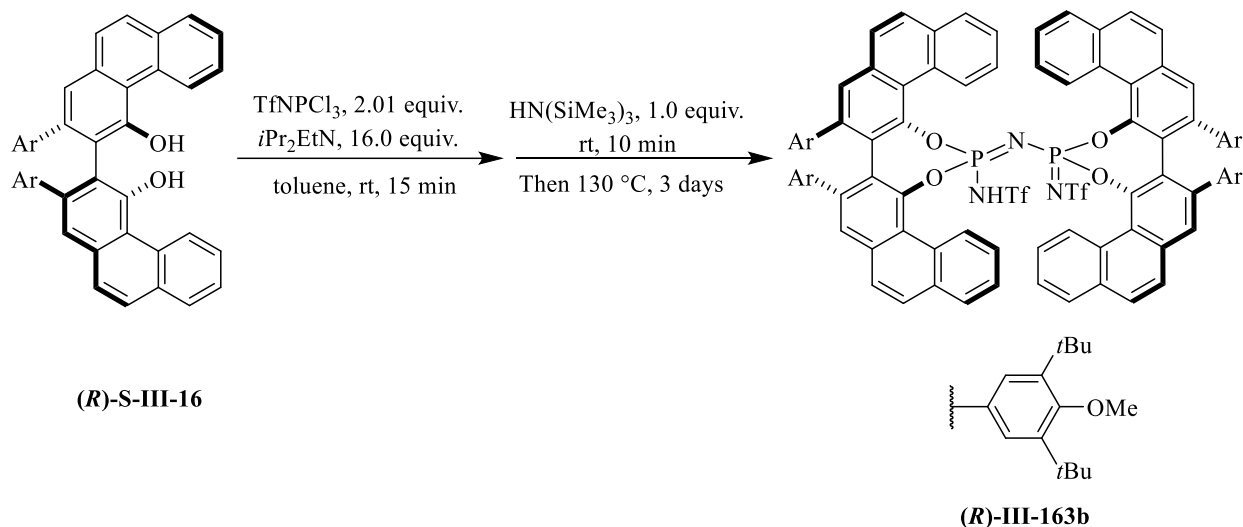


**Synthesis of VAPOL imidodiphosphorimide (VAPIP) (R)-III-163a:** The catalyst was prepared in 25 mL pear-shaped flask in which its 14/20 joint was replaced with a high vacuum threaded T-

shaped Teflon valve. To this flask which was flame-dried and cooled under a continuous flow of the nitrogen from its side arm was added (*S*)-VAPOL (0.93 mmol, 0.51 g), 4 mL freshly distilled anhydrous toluene (0.11 M), *i*Pr<sub>2</sub>EtN (7.44 mmol, 1.23 mL) and TfNPCl<sub>3</sub> (0.93 mmol, 0.27 g).<sup>72</sup> The mixture was stirred at room temperature for 15 min followed by the addition of anhydrous HN(SiMe<sub>3</sub>)<sub>3</sub> (0.44 mmol, 0.093 mL) and stirring at room temperature for 10 min. Then the Teflon valve was closed and the reaction was placed in an oil bath and stirred for three days at 130 °C. After cooling the reaction to the room temperature, the mixture was transferred to a 50 mL round bottom flask and concentrated to dryness under reduced pressure. The resulting mixture was dissolved in CH<sub>2</sub>Cl<sub>2</sub> followed by the addition of 3N aqueous HCl and stirring at room temperature for 1 h. The organic layer was separated and the aqueous layer was extracted with CH<sub>2</sub>Cl<sub>2</sub> (3 X 10 mL). The combined organic layer was dried over Na<sub>2</sub>SO<sub>4</sub> and filtered through filter paper. The solvent was removed under reduced pressure and the resulting product was purified via column chromatography (30 mm X 250 mm, hexane: EtOAc, 3:1, 2:1, 1:1 and 1:2 as the eluent). The resulting off-white solid was dissolved in CH<sub>2</sub>Cl<sub>2</sub> and acidified with 6N aqueous HCl for 1 h at room temperature. The organic layer was separated and concentrated to dryness under reduced pressure to afford the desired product as a white solid in 86% isolated yield (0.39 mmol, 0.57 g). mp: 278-279 °C. CCDC number: 1818678

Spectral data for **III-163a**: <sup>1</sup>H NMR (500 MHz, Chloroform-*d*) δ 6.20 (d, *J* = 7.2 Hz, 4H), 6.35 – 6.41 (m, 4H), 6.83 (t, *J* = 7.7 Hz, 4H), 6.95 – 7.04 (m, 6H), 7.13 – 7.22 (m, 10H), 7.30 (d, *J* = 8.7 Hz, 2H), 7.51 (s, 2H), 7.65 – 7.78 (m, 6H), 7.83 (d, *J* = 8.9 Hz, 2H), 7.99 (dd, *J* = 8.1, 1.5 Hz, 2H), 8.11 (ddd, *J* = 8.5, 6.9, 1.5 Hz, 2H), 9.72 (d, *J* = 8.6 Hz, 2H), 9.80 (d, *J* = 8.7 Hz, 2H). <sup>13</sup>C NMR (126 MHz, Chloroform-*d*) δ 121.08, 121.54, 125.18, 125.90, 126.04, 126.52, 126.55, 126.85, 127.02, 127.09, 127.22, 127.50, 127.75, 127.80, 127.92, 127.95, 128.45, 128.51, 128.59, 128.76,

128.80, 128.89, 129.02, 129.16, 129.96, 132.28, 133.09, 133.42, 134.34, 138.99, 139.29, 139.62, 141.17, 145.73, 146.37.  $^{31}\text{P}$  NMR (202 MHz, Chloroform-*d*)  $\delta$  -11.96.  $^{19}\text{F}$  NMR (470 MHz, Chloroform-*d*)  $\delta$  -79.14. IR: 3049w, 1189s, 1019s, 910m, 746m, 696s, 609s, 568m. HRMS (ESI+TOF)  $m/z$  1444.2448,  $[(\text{M}+\text{H})^+]$ ; calcd for  $\text{C}_{82}\text{H}_{50}\text{F}_6\text{N}_3\text{O}_8\text{P}_2\text{S}_2$ : 1444.2418].  $[\alpha]_D^{20} = -1.8988$  (*c* 1.0,  $\text{CHCl}_3$ ).

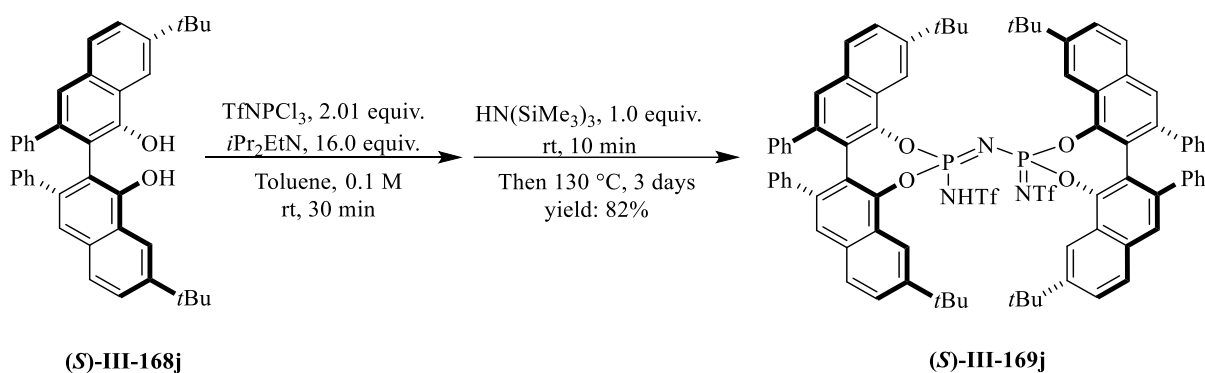


**Synthesis of imidodiphosphorimidate (R)-III-163b:** Compound **(R)-III-163b** was prepared from compound **(R)-S-III-16** (0.51 mmol, 0.32 g), 5 mL toluene (1.0 M),  $\text{TfNPCl}_3$  (0.55 mmol, 0.16 g),<sup>72</sup>  $i\text{Pr}_2\text{EtN}$  (2.5 mmol, 0.74 mL) and  $\text{HN}(\text{SiMe}_3)_3$  (0.18 mmol, 39  $\mu\text{L}$ ) according to the general procedure VI and the crude product was purified via column chromatography on silica gel (30 mm X 250 mm, hexane: EtOAc, 3:1, 2:1, 1:1 and 1:2 as the eluent). The desired compound **(R)-III-163b** was obtained as a solid in 84% isolated yield (0.21 mmol, 0.42 g). mp: 266-267 °C.

Spectral data for **(R)-III-163b**:  $^1\text{H}$  NMR (500 MHz, Chloroform-*d*)  $\delta$  0.96 (s, 36H), 1.09 – 1.19 (m, 36H), 3.52 (s, 6H), 3.74 (s, 6H), 6.56 (s, 4H), 6.62 (s, 4H), 6.94 (t,  $J = 7.4$  Hz, 2H), 7.07 (dd,  $J = 8.0, 1.4$  Hz, 2H), 7.19 (d,  $J = 8.7$  Hz, 2H), 7.24 (s, 2H), 7.34 (d,  $J = 8.7$  Hz, 2H), 7.55 (ddd,  $J = 8.5, 6.8, 1.5$  Hz, 2H), 7.65 (s, 2H), 7.66 – 7.73 (m, 2H), 7.75 (d,  $J = 8.9$  Hz, 2H), 7.83 (d,  $J = 8.9$  Hz, 2H), 7.96 (dd,  $J = 8.1, 1.4$  Hz, 2H), 8.02 (ddd,  $J = 8.6, 6.9, 1.5$  Hz, 2H), 9.48 (d,  $J = 8.5$  Hz,



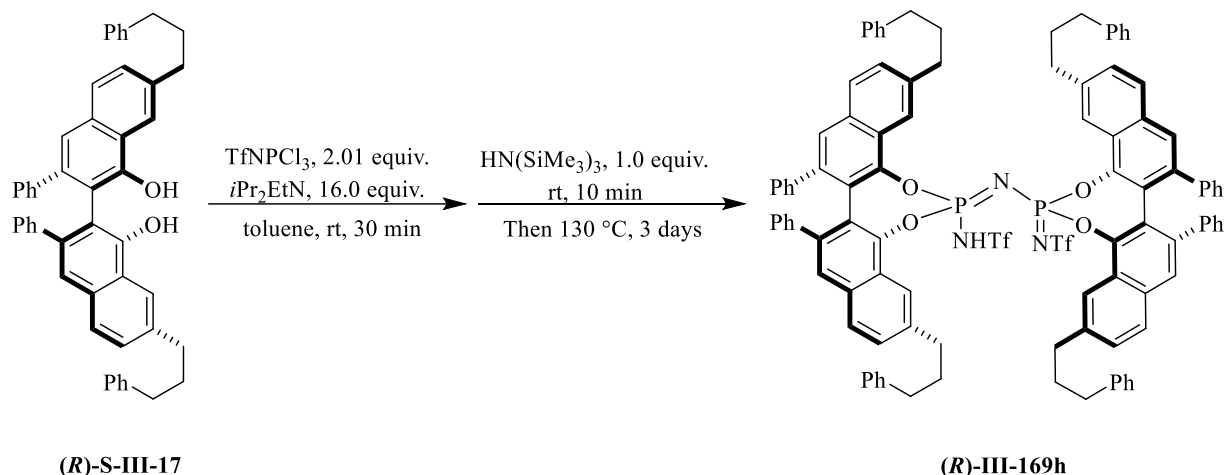
2H), 9.65 (d,  $J = 8.7$  Hz, 2H).  $^{13}\text{C}$  NMR (126 MHz, Chloroform- $d$ )  $\delta$  31.68, 35.19, 63.90, 64.25, 120.89, 121.69, 125.45, 125.98, 126.37, 126.50, 126.67, 126.93, 127.38, 127.49, 127.75, 128.00, 128.10, 128.33, 128.42, 128.65, 128.86, 132.12, 132.92, 132.97, 133.26, 133.53, 134.73, 139.06, 141.05, 142.64, 158.82.  $^{31}\text{P}$  NMR (202 MHz, Chloroform- $d$ )  $\delta$  -12.09.  $^{19}\text{F}$  NMR (470 MHz, Chloroform- $d$ )  $\delta$  -78.92. IR: 2958w, 1198s, 1129m, 1113m, 1014s, 964w, 876s, 808m, 743m, 598s, 568m, 525w  $\text{cm}^{-1}$ . HRMS (ESI+TOF)  $m/z$  2012.7883,  $[(\text{M}+\text{H}^+)]$ ; calcd for  $\text{C}_{118}\text{H}_{121}\text{F}_6\text{N}_3\text{O}_{12}\text{P}_2\text{S}_2$ : 2012.7849].  $[\alpha]_D^{20} = -0.9474$  ( $c$  1.0,  $\text{CHCl}_3$ ).



**Synthesis of imidodiphosphorimidate (S)-III-169j:** Compound (S)-III-169j was prepared from compound (S)-III-168j (0.55 mmol, 0.31 g), 5.5 mL toluene (0.1 M), TfNPCI<sub>3</sub> (0.58 mmol, 0.17 g),<sup>72</sup> *i*Pr<sub>2</sub>EtN (4.4 mmol, 0.77 mL) and HN(SiMe<sub>3</sub>)<sub>3</sub> (0.27 mmol, 57  $\mu\text{L}$ ) according to the general procedure VI and the crude product was purified via column chromatography on silica gel (30 mm X 250 mm, hexane: EtOAc, 3:1, 2:1, 1:1 and 1:2 as the eluent). The desired compound (S)-III-169j was obtained as a solid in 82% isolated yield (0.225 mmol, 0.331 g). mp: 250-251 °C.

Spectral data for (S)-III-169j:  $^1\text{H}$  NMR (500 MHz, Chloroform- $d$ )  $\delta$  1.26 (s, 9H), 1.60 (s, 9H), 4.26 (brs, 1H), 6.05 (d,  $J = 7.5$  Hz, 2H), 6.20 (d,  $J = 7.6$  Hz, 2H), 6.77 (t,  $J = 7.5$  Hz, 2H), 6.89 (t,  $J = 7.6$  Hz, 2H), 6.92 – 7.01 (m, 2H), 7.10 (dd,  $J = 8.1, 3.7$  Hz, 2H), 7.28 (dd,  $J = 8.6, 1.9$  Hz, 1H), 7.40 (s, 1H), 7.72 – 7.81 (m, 2H), 8.16 (d,  $J = 2.0$  Hz, 1H), 8.43 (d,  $J = 1.8$  Hz, 1H).  $^{13}\text{C}$  NMR (126 MHz, Chloroform- $d$ )  $\delta$  30.92, 31.02, 35.00, 35.34, 116.49, 116.99, 121.31, 122.03, 124.42,

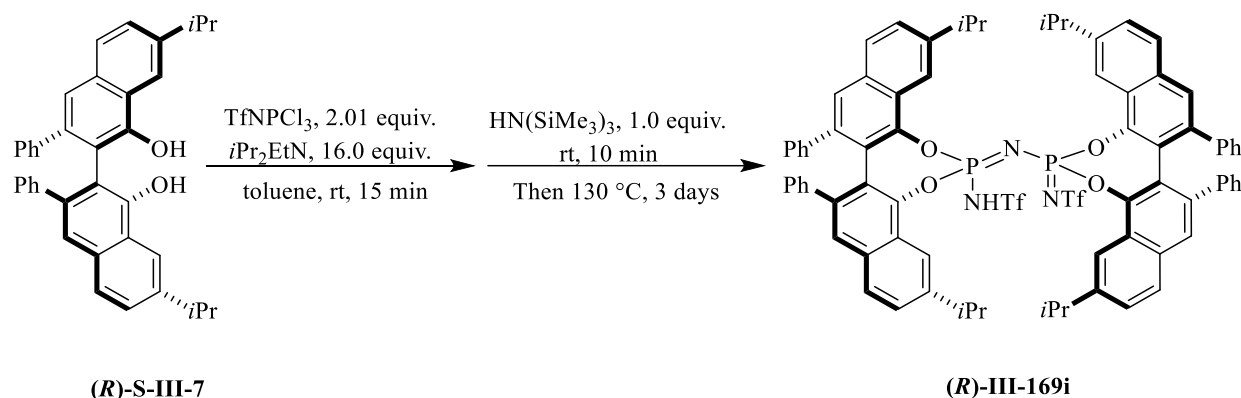
125.01, 126.19, 126.21, 126.44, 126.93, 127.01, 127.15, 127.20, 127.50, 127.58, 128.58, 129.46, 131.92, 132.39, 138.47, 138.81, 139.07, 139.69, 143.65, 144.35, 149.11, 150.48.  $^{31}\text{P}$  NMR (202 MHz, Chloroform-*d*)  $\delta$  -13.14.  $^{19}\text{F}$  NMR (470 MHz, Chloroform-*d*)  $\delta$  -77.94. IR: 2957w, 1200s, 1108s, 1067m, 942m, 764m, 695s, 633w, 599s, 524m, 507s  $\text{cm}^{-1}$ . HRMS (ESI+TOF)  $m/z$  1468.4316,  $[(\text{M}+\text{H})^+]$ ; calcd for  $\text{C}_{82}\text{H}_{74}\text{F}_6\text{N}_3\text{O}_8\text{P}_2\text{S}_2$ : 1468.4297].  $[\alpha]_{\text{D}}^{20} = 0.7386$  ( $c$  1.0,  $\text{CHCl}_3$ ).



**Synthesis of imidodiphosphorimidate (R)-III-169h:** Compound **(R)-III-169h** was prepared from compound **(R)-S-III-17** (0.74 mmol, 0.50 g), 7.4 mL toluene (0.1 M),  $\text{TfNPCl}_3$  (0.74 mmol, 0.21 g),<sup>72</sup>  $i\text{Pr}_2\text{EtN}$  (5.92 mmol, 1.03 mL) and  $\text{HN}(\text{SiMe}_3)_3$  (0.37 mmol, 78  $\mu\text{L}$ ) according to the general procedure VI and the crude product was purified via column chromatography on silica gel (30 mm X 250 mm, hexane: EtOAc, 3:1, 2:1, 1:1 and 1:2 as the eluent). The desired compound **(R)-III-169h** was obtained as a solid in 32% isolated yield (0.12 mmol, 0.20 g). mp: 107-108  $^\circ\text{C}$ .

Spectral data for **(R)-III-169h**:  $^1\text{H}$  NMR (500 MHz, Chloroform-*d*)  $\delta$  1.70 (h,  $J = 7.7, 7.3$  Hz, 4H), 2.07 – 2.20 (m, 2H), 2.26 (ddt,  $J = 19.9, 15.0, 7.7$  Hz, 8H), 2.40 (dt,  $J = 14.4, 7.5$  Hz, 2H), 2.79 – 2.87 (m, 2H), 2.85 – 2.96 (m, 2H), 3.04 (dd,  $J = 9.1, 6.4$  Hz, 4H), 3.95 (brs, 1H), 6.34 (td,  $J = 8.4, 1.3$  Hz, 4H), 6.48 (dd,  $J = 20.6, 7.3$  Hz, 0H), 6.76 (dd,  $J = 8.4, 1.6$  Hz, 1H), 6.82 (t,  $J = 7.6$  Hz, 2H), 6.85 – 6.97 (m, 4H), 7.01 (tt,  $J = 7.4, 1.3$  Hz, 1H), 7.01 – 7.11 (m, 1H), 7.09 – 7.19 (m, 4H),

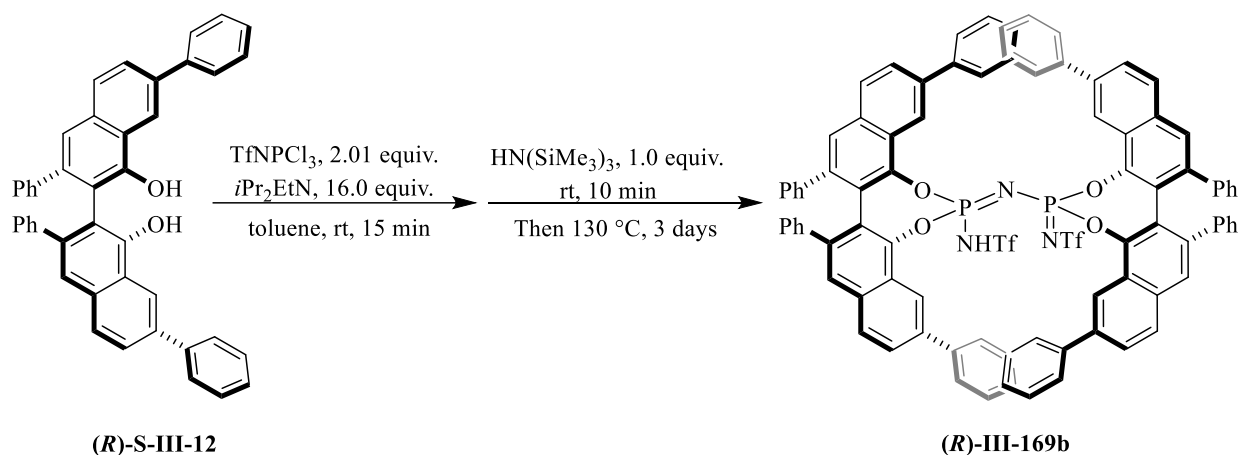
7.17 – 7.27 (m, 2H), 7.28 – 7.37 (m, 4H), 7.46 – 7.60 (m, 3H), 7.84 (d,  $J = 8.5$  Hz, 1H), 8.35 (s, 1H).  $^{13}\text{C}$  NMR (126 MHz, Chloroform- $d$ )  $\delta$  32.27, 33.06, 35.23, 35.72, 35.77, 36.12, 119.11, 120.46, 121.87, 122.56, 124.46, 125.36, 125.63, 125.74, 126.35, 126.63, 127.12, 127.17, 127.61, 127.84, 127.99, 128.18, 128.22, 128.35, 128.56, 128.68, 128.76, 129.12, 129.64, 131.95, 133.02, 138.17, 139.19, 139.29, 139.58, 141.01, 141.87, 142.33, 142.50, 143.16, 144.10.  $^{31}\text{P}$  NMR (202 MHz, Chloroform- $d$ )  $\delta$  -10.65.  $^{19}\text{F}$  NMR (470 MHz, Chloroform- $d$ )  $\delta$  -78.05. IR: 2930w, 1191m, 1067m, 945m, 695s, 602m  $\text{cm}^{-1}$ . HRMS (ESI+TOF)  $m/z$  1716.4926,  $[(\text{M}+\text{H})^+]$ ; calcd for  $\text{C}_{102}\text{H}_{82}\text{F}_6\text{N}_3\text{O}_8\text{P}_2\text{S}_2$ : 1716.4923].  $[\alpha]_{\text{D}}^{20} = -3.0923$  ( $c$  1.0,  $\text{CHCl}_3$ ).



**Synthesis of imidodiphosphorimidate (R)-III-169i:** Compound (R)-III-169i was prepared from compound (R)-S-III-7 (1.54 mmol, 0.803 g), 15 mL toluene (0.1 M), TfNPCl<sub>3</sub> (1.54 mmol, 0.438 g),<sup>72</sup> *i*Pr<sub>2</sub>EtN (12.3 mmol, 2.11 mL) and HN(SiMe<sub>3</sub>)<sub>3</sub> (0.751 mmol, 158  $\mu\text{L}$ ) according to the general procedure VI and the crude product was purified via column chromatography on silica gel (30 mm X 250 mm, hexane: EtOAc, 3:1, 2:1, 1:1 and 1:2 as the eluent). The desired compound (R)-III-169i was obtained as a white solid in 79% isolated yield (0.59 mmol, 0.84 g). mp: 215-216 °C

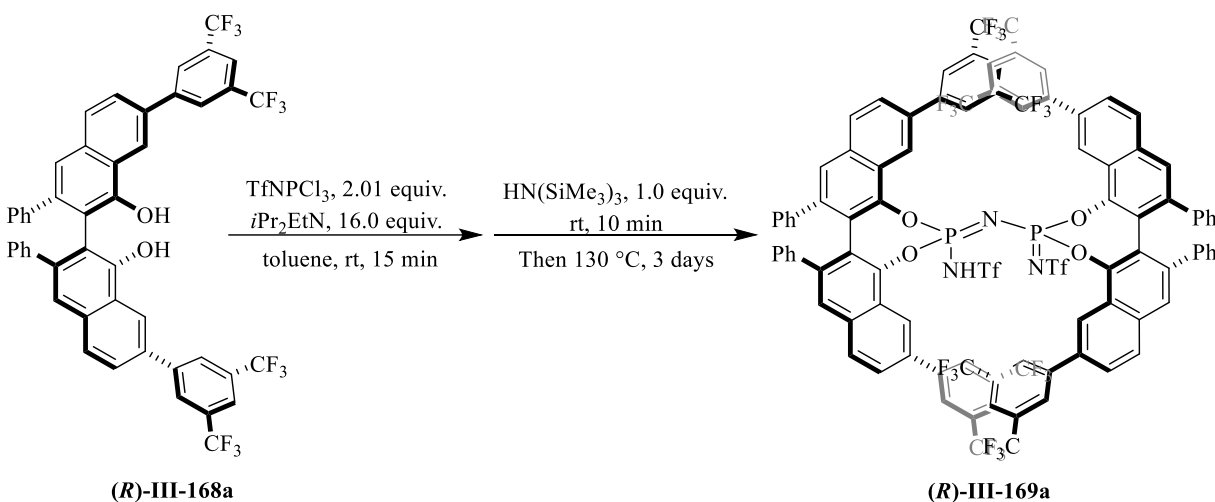
Spectral data for (R)-III-169i:  $^1\text{H}$  NMR (500 MHz, Chloroform- $d$ )  $\delta$  0.84 – 1.02 (m, 6H), 1.14 (d,  $J = 6.8$  Hz, 6H), 1.54 (dd,  $J = 6.9, 6.0$  Hz, 12H), 2.70 (hept,  $J = 7.0$  Hz, 2H), 3.31 (hept,  $J = 6.9$

Hz, 2H), 6.22 – 6.31 (m, 8H), 6.81 (t,  $J = 7.6$  Hz, 4H), 6.85 (brs, 1H), 6.91 – 7.03 (m, 8H), 7.08 (s, 2H), 7.14 (tt,  $J = 7.4, 1.2$  Hz, 2H), 7.21 (d,  $J = 8.4$  Hz, 2H), 7.49 (s, 2H), 7.61 (dd,  $J = 8.5, 1.7$  Hz, 2H), 7.77 – 7.85 (m, 4H), 8.32 (d,  $J = 1.5$  Hz, 2H).  $^{13}\text{C}$  NMR (126 MHz, Chloroform- $d$ )  $\delta$  22.47, 23.77, 23.82, 33.39, 34.74, 117.00, 118.03, 121.57, 122.27, 124.48, 125.33, 126.29, 126.56, 126.84, 127.07, 127.41, 127.58, 127.86, 127.93, 128.00, 128.03, 128.65, 129.20, 132.09, 133.03, 138.20, 139.04, 139.10, 139.61, 143.15, 144.07, 146.95, 148.76.  $^{31}\text{P}$  NMR (202 MHz, Chloroform- $d$ )  $\delta$  -11.97.  $^{19}\text{F}$  NMR (470 MHz, Chloroform- $d$ )  $\delta$  -77.92. IR: 2963w, 1198s, 1081s, 944s, 885m, 767m, 717m, 694s, 635w, 601s, 508w  $\text{cm}^{-1}$ . HRMS (ESI+TOF)  $m/z$  1412.3713,  $[(\text{M}+\text{H})^+]$ ; calcd for  $\text{C}_{78}\text{H}_{66}\text{F}_6\text{N}_3\text{O}_8\text{P}_2\text{S}_2$ : 1412.3671].  $[\alpha]_D^{20} = -1.2053$  ( $c$  1.0,  $\text{CHCl}_3$ ).



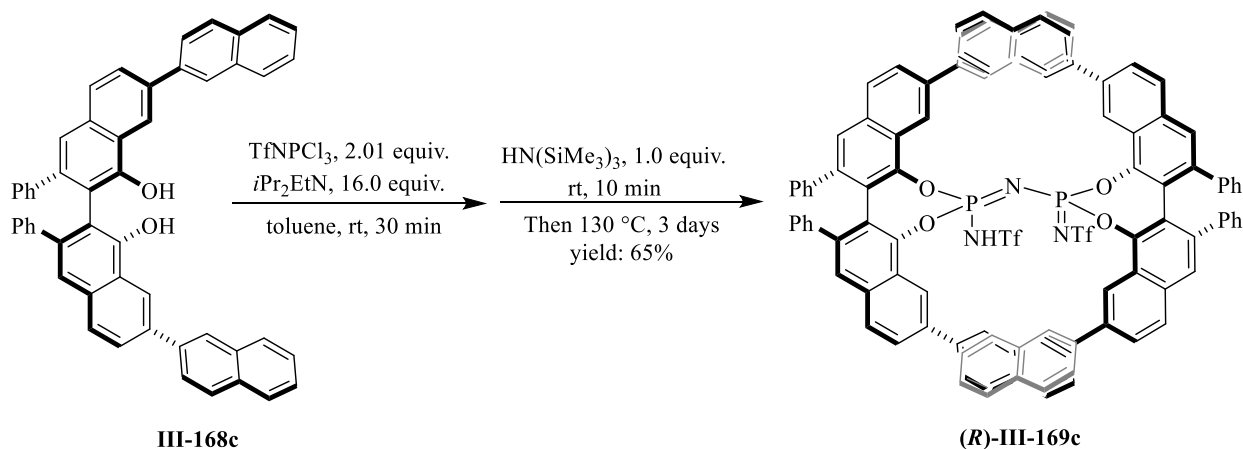
**Synthesis of imidodiphosphorimidate (R)-III-169b:** Compound **(R)-III-169b** was prepared from compound **(R)-S-III-12** (0.45 mmol, 0.26 g), 5 mL toluene (0.1 M), TfNPCI<sub>3</sub> (0.46 mmol, 0.13 g),<sup>72</sup> *i*Pr<sub>2</sub>EtN (3.6 mmol, 0.63 mL) and HN(SiMe<sub>3</sub>)<sub>3</sub> (0.23 mmol, 48  $\mu\text{L}$ ) according to the general procedure VI and the crude product was purified via column chromatography on silica gel (30 mm X 250 mm, hexane: EtOAc, 3:1, 2:1, 1:1 and 1:2 as the eluent). The desired compound **(R)-III-169b** was obtained as a white solid in 49% isolated yield (0.11 mmol, 0.17 g). mp: 320-325  $^\circ\text{C}$  (decomposed).

Spectral data for **(R)-III-169b**:  $^1\text{H}$  NMR (500 MHz, Chloroform-*d*)  $\delta$  5.14 (brs, 1H), 5.89 – 5.94 (m, 4H), 6.18 – 6.24 (m, 4H), 6.45 (s, 4H), 6.76 (t,  $J = 7.6$  Hz, 4H), 6.89 – 7.03 (m, 12H), 7.05 – 7.13 (m, 2H), 7.30 (d,  $J = 8.5$  Hz, 2H), 7.45 (s, 2H), 7.48 – 7.56 (m, 2H), 7.59 – 7.69 (m, 8H), 7.95 (d,  $J = 8.6$  Hz, 2H), 8.04 (ddd,  $J = 17.3, 8.5, 1.6$  Hz, 6H), 8.26 – 8.31 (m, 2H), 8.90 (d,  $J = 1.6$  Hz, 2H).  $^{13}\text{C}$  NMR (126 MHz, Chloroform-*d*)  $\delta$  118.69, 119.06, 122.10, 122.44, 124.45, 125.52, 126.39, 126.45, 126.96, 127.07, 127.29, 127.59, 127.68, 127.84, 128.09, 128.50, 128.69, 128.75, 129.10, 129.25, 132.40, 133.34, 138.66, 138.88, 139.02, 139.26, 139.79, 139.98, 140.54, 140.89, 144.50, 143.92.  $^{31}\text{P}$  NMR (202 MHz, Chloroform-*d*)  $\delta$  -13.05.  $^{19}\text{F}$  NMR (470 MHz, Chloroform-*d*)  $\delta$  -77.71. IR: 1198s, 1073s, 757s, 694s, 602s, 579m, 524w. HRMS (ESI+TOF)  $m/z$  1548.3085,  $[(\text{M}+\text{H}^+)]$ ; calcd for  $\text{C}_{90}\text{H}_{58}\text{F}_6\text{N}_3\text{O}_8\text{P}_2\text{S}_2$ : 1548.3044].  $[\alpha]_D^{20} = 2.5801$  ( $c$  1.0,  $\text{CHCl}_3$ ).



**Synthesis of imidodiphosphorimidate (R)-III-169a:** Compound **(R)-III-169a** was prepared from compound **(R)-III-168a** (1 mmol, 0.9 g), 10 mL toluene (0.1 M),  $\text{TfNPCl}_3$  (1.01 mmol, 0.297 g),<sup>72</sup>  $i\text{Pr}_2\text{EtN}$  (8.41 mmol, 1.46 mL) and  $\text{HN}(\text{SiMe}_3)_3$  (0.522 mmol, 112  $\mu\text{L}$ ) according to the general procedure VI and the crude product was purified via column chromatography on silica gel (30 mm X 250 mm, hexane: EtOAc, 3:1, 2:1, 1:1 and 1:2 as the eluent). The desired compound **(R)-III-169a** was obtained as a white solid in 76% isolated yield (0.397 mmol, 0.831g). mp: 229-230 °C.

Spectral data for **(R)-III-169a**:  $^1\text{H}$  NMR (500 MHz, Chloroform-*d*)  $\delta$  6.02 (d,  $J = 7.5$  Hz, 4H), 6.15 – 6.21 (m, 4H), 6.53 – 6.60 (m, 4H), 6.65 6.76 (t,  $J = 7.5$  Hz, 4H), 7.01 (dt,  $J = 20.0, 7.4$  Hz, 4H), 7.13 (s, 2H), 7.16 (brs, 1H), 7.19 (dt,  $J = 13.6, 6.8$  Hz, 2H), 7.50 – 7.59 (m, 4H), 7.65 (s, 2H), 7.92 (dd,  $J = 8.6, 1.8$  Hz, 2H), 7.95 – 8.05 (m, 8H), 8.28 (d,  $J = 1.8$  Hz, 2H), 8.39 (d,  $J = 1.6$  Hz, 4H), 8.73 (s, 2H).  $^{13}\text{C}$  NMR (126 MHz, Chloroform-*d*)  $\delta$  119.63, 120.54, 121.54, 121.86, 122.34, 122.55, 122.74, 124.03, 124.51, 125.30, 125.50, 126.20, 126.73, 126.81, 127.00, 127.33, 127.59, 127.70, 127.79, 127.82, 128.01, 128.44, 128.65, 129.12, 132.12, 132.36, 132.38, 132.62, 132.92, 133.91, 134.89, 137.81, 137.85, 138.90, 139.85, 140.38, 141.43, 142.96, 143.51, 144.89.  $^{31}\text{P}$  NMR (202 MHz, Chloroform-*d*)  $\delta$  -9.16.  $^{19}\text{F}$  NMR (470 MHz, Chloroform-*d*)  $\delta$  -78.23, -63.37, -62.93. IR: 1276s, 1172m, 1127s, 1106m, 1064m, 682m  $\text{cm}^{-1}$ . HRMS (ESI+TOF)  $m/z$  2092.2063,  $[(\text{M}+\text{H})^+]$ ; calcd for  $\text{C}_{98}\text{H}_{50}\text{F}_{30}\text{N}_3\text{O}_8\text{P}_2\text{S}_2$ : 2092.2036].  $[\alpha]^{20}_{\text{D}} = -3.2145$  ( $c$  1.0,  $\text{CHCl}_3$ ).

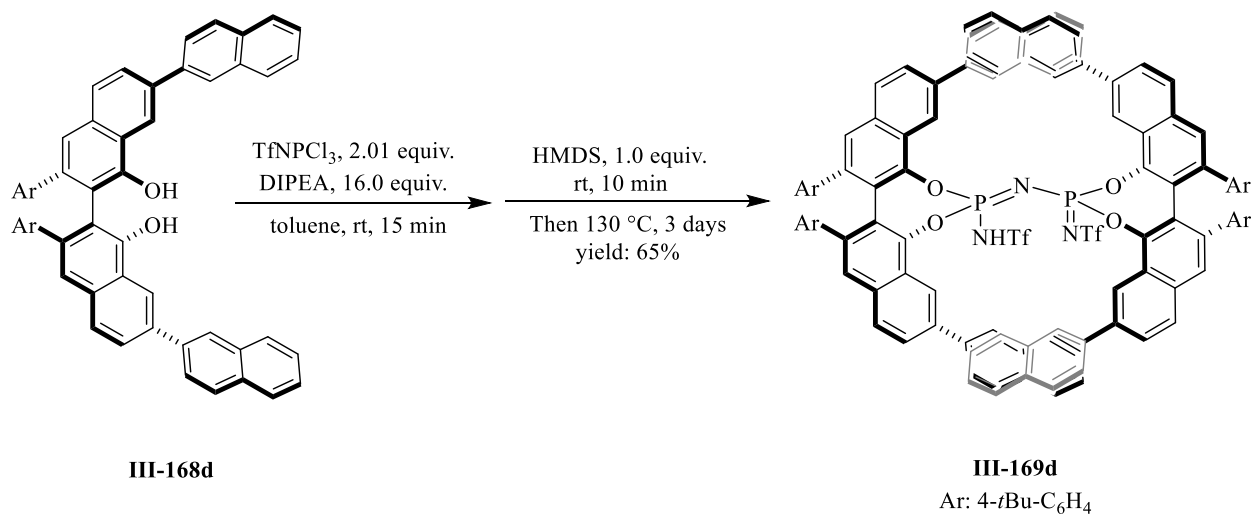


**Synthesis of imidodiphosphorimidate (R)-III-169c:** Compound **(R)-III-169c** was prepared from compound **(R)-III-168c** (0.65 mmol, 0.51 g), 8 mL toluene (0.1 M),  $\text{TfNPCl}_3$  (0.7 mmol, 0.2 g),<sup>72</sup>  $i\text{Pr}_2\text{EtN}$  (5.8 mmol, 1.0 mL) and  $\text{HN}(\text{SiMe}_3)_3$  (0.32 mmol, 76  $\mu\text{L}$ ) according to the general procedure VI and the crude product was purified via column chromatography on silica gel (30 mm X 250 mm, hexane: EtOAc, 3:1, 2:1, 1:1 and 1:2 as the eluent). The desired compound **(R)-III-**

**169c** was obtained as a white solid in 65% isolated yield (0.21 mmol, 0.37 g). mp: 253-255 °C.

CCDC number: 1993813.

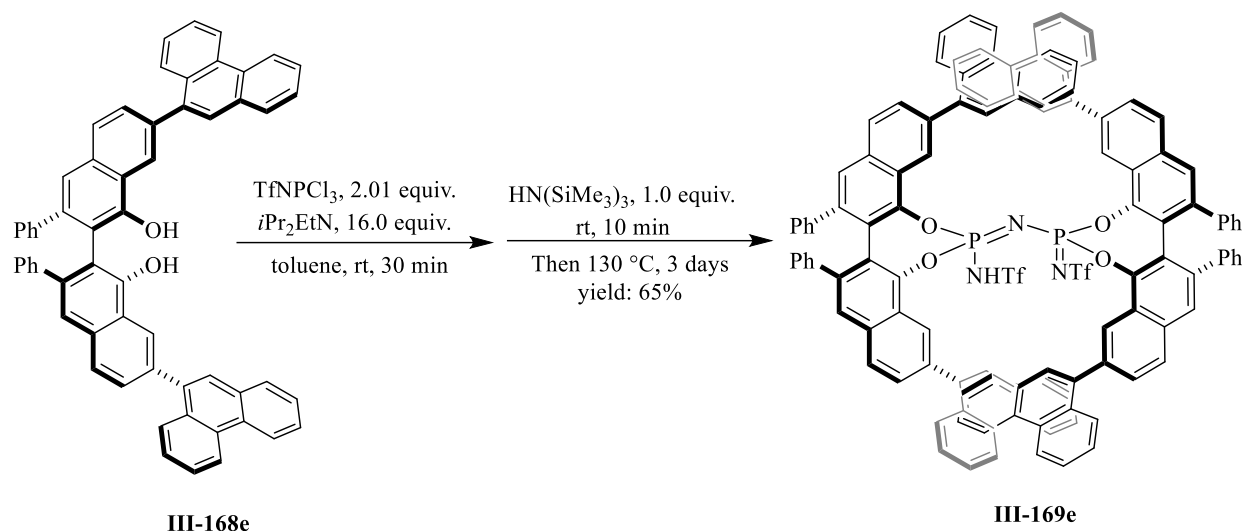
Spectral data for (**R**)-**III-169c**:  $^1\text{H}$  NMR (500 MHz, Chloroform-*d*)  $\delta$  5.26 (s, 4H), 5.95 (s, 4H), 6.17 – 6.23 (m, 4H), 6.26 (brs, 1H), 6.75 (t,  $J = 7.8$  Hz, 4H), 6.87 (tt,  $J = 7.4, 1.2$  Hz, 2H), 6.95 (tt,  $J = 7.3, 1.3$  Hz, 2H), 7.08 (s, 2H), 7.12 – 7.24 (m, 4H), 7.35 – 7.44 (m, 6H), 7.45 (d,  $J = 8.5$  Hz, 2H), 7.51 – 7.67 (m, 8H), 7.80 (dd,  $J = 8.5, 1.9$  Hz, 2H), 7.94 (d,  $J = 8.7$  Hz, 2H), 7.97 – 8.06 (m, 4H), 8.16 (ddd,  $J = 10.5, 8.3, 3.1$  Hz, 6H), 8.29 (dd,  $J = 8.7, 1.8$  Hz, 2H), 8.47 (d,  $J = 1.7$  Hz, 2H), 8.60 (d,  $J = 1.8$  Hz, 2H), 9.17 (d,  $J = 1.7$  Hz, 2H).  $^{13}\text{C}$  NMR (126 MHz, Chloroform-*d*)  $\delta$  119.20, 119.83, 122.19, 122.61, 124.68, 124.94, 125.68, 125.72, 125.74, 126.00, 126.08, 126.32, 126.37, 126.41, 126.56, 126.78, 127.07, 127.22, 127.47, 127.61, 127.74, 127.87, 128.23, 128.46, 128.58, 128.71, 128.90, 128.98, 129.06, 132.50, 132.56, 133.09, 133.40, 133.51, 134.01, 137.21, 137.90, 138.59, 138.63, 139.10, 139.33, 139.85, 140.59, 143.31, 144.77.  $^{31}\text{P}$  NMR (202 MHz, Chloroform-*d*)  $\delta$  -11.40.  $^{19}\text{F}$  NMR (470 MHz, Chloroform-*d*)  $\delta$  -77.63. IR: 1193s, 1072s, 806s, 763m, 694s, 604s, 505m. HRMS (ESI+TOF)  $m/z$  1748.3668,  $[(\text{M}+\text{H})^+]$ ; calcd for  $\text{C}_{106}\text{H}_{66}\text{F}_6\text{N}_3\text{O}_8\text{P}_2\text{S}_2$ : 1748.3671].  $[\alpha]_{\text{D}}^{20} = -4.5498$  ( $c$  1.0,  $\text{CHCl}_3$ ).



**Synthesis of imidodiphosphorimidate (R)-III-169d:** Compound **(R)-III-169d** was prepared from compound **(R)-III-168d** (0.45 mmol, 0.36 g), 5 mL toluene (0.1 M), TfNPCl<sub>3</sub> (0.45 mmol, 0.13 g),<sup>72</sup> DIPEA (3.6 mmol, 0.63 mL) and HMDS (0.22 mmol, 48 µL) according to the general procedure VI and the crude product was purified via column chromatography on silica gel (30 mm X 250 mm, hexane: EtOAc, 3:1, 2:1, 1:1 and 1:2 as the eluent). The desired compound **(R)-III-169d** was obtained as a white solid in 61% isolated yield (0.14 mmol, 0.27 g). mp: 290-291 °C.

Spectral data for **(R)-III-169d**: <sup>1</sup>H NMR (500 MHz, Chloroform-*d*) δ 1.15 (s, 9H), 1.19 (s, 9H) 4.31 (s, 2H), 5.67 (s, 2H), 6.05 – 6.11 (m, 2H), 6.69 – 6.75 (m, 2H), 7.08 (s, 1H), 7.16 – 7.25 (m, 2H), 7.30 – 7.42 (m, 2H), 7.42 – 7.49 (m, 2H), 7.51 – 7.67 (m, 4H), 7.84 (dd, *J* = 8.5, 1.9 Hz, 1H), 7.93 – 8.03 (m, 3H), 8.10 – 8.21 (m, 3H), 8.30 (dd, *J* = 8.6, 1.8 Hz, 1H), 8.42 – 8.46 (m, 1H), 8.59 (d, *J* = 1.8 Hz, 1H), 9.17 (t, *J* = 1.1 Hz, 1H). <sup>13</sup>C NMR (126 MHz, Chloroform-*d*) δ 31.15, 31.21, 34.11, 34.23, 118.80, 119.71, 122.26, 122.71, 123.92, 124.47, 124.65, 124.77, 125.65, 125.72, 125.93, 126.06, 126.29, 126.49, 126.74, 126.83, 127.01, 127.39, 127.43, 127.71, 127.77, 128.01, 128.26, 128.46, 128.69, 128.91, 129.00, 132.47, 132.61, 133.07, 133.44, 133.57, 134.00, 135.71, 136.45, 136.86, 137.96, 139.03, 139.62, 140.52, 148.87, 149.07. <sup>31</sup>P NMR (202 MHz, Chloroform-*d*) δ -11.46. <sup>19</sup>F NMR (470 MHz, Chloroform-*d*) δ -77.62. IR: 2985w, 1465m, 1192s, 1069s, 606s, 557s cm<sup>-1</sup>. HRMS (ESI+TOF) *m/z* 1972.6218, [(M+H)<sup>+</sup>]; calcd for C<sub>122</sub>H<sub>98</sub>F<sub>6</sub>N<sub>3</sub>O<sub>8</sub>P<sub>2</sub>S<sub>2</sub>: 1972.6174]. [α]<sub>D</sub><sup>20</sup> = -4.4873 (*c* 1.0, CHCl<sub>3</sub>).

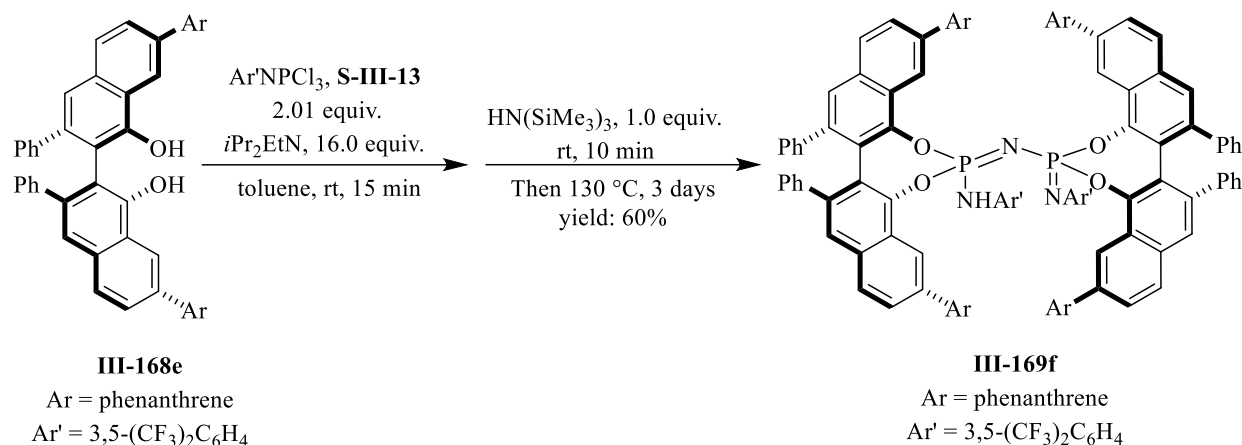




**Synthesis of imidodiphosphorimidate (*R*)-III-169e:** Compound (*R*)-III-169e was prepared from compound (*R*)-III-168e (0.61 mmol, 0.48 g), 6 mL toluene (0.1 M), TfNPCl<sub>3</sub> (0.61 mmol, 0.17 g),<sup>72</sup> *i*PrEtN (4.8 mmol, 0.84 mL) and HN(SiMe<sub>3</sub>)<sub>3</sub> (0.31 mmol, 63 μL) according to the general procedure VI and the crude product was purified via column chromatography on silica gel (30 mm X 250 mm, hexane: EtOAc, 3:1, 2:1, 1:1 and 1:2 as the eluent). The desired compound (*R*)-III-169e was obtained as a solid in 37% isolated yield (0.11 mmol, 0.21 g). mp: 318-320 °C. CCDC number: 1993752

Spectral data for (*R*)-III-169e: <sup>1</sup>H NMR (500 MHz, Chloroform-*d*) δ 5.05 (s, 4H), 6.07 (d, *J* = 7.4 Hz, 4H), 6.32 (d, *J* = 7.6 Hz, 4H), 6.62 (t, *J* = 7.3 Hz, 4H), 6.68-6.93 (m, 6H), 6.96 – 7.07 (m, 4H), 7.09-7.35 (m, 3H), 7.36-8.16 (brs, 32H), 8.40 (s, 2H), 8.63 (s, 2H), 8.76 (dd, *J* = 20.0, 8.5 Hz, 8H) (<sup>1</sup>H-NMR was complicated, most of the proton's peak were broad and overlapped with each other). <sup>13</sup>C NMR (126 MHz, Chloroform-*d*) δ 118.19, 120.78, 120.90, 121.90, 122.06, 122.40, 122.69, 122.87, 126.13, 126.44, 126.66, 126.97, 127.14, 127.36, 127.49, 128.39, 129.00, 129.08, 129.90, 130.09, 130.39, 130.65, 130.95, 131.81, 132.81, 132.89, 138.04, 138.25, 136.16, 139.58, 139.87, 140.02, 144.56, 145.51. <sup>31</sup>P NMR (202 MHz, Chloroform-*d*) δ -3.65. <sup>19</sup>F NMR (470 MHz,

Chloroform-*d*)  $\delta$  -77.88. IR: 1193s, 746m, 724s, 694m, 597m. HRMS (ESI+TOF)  $m/z$  1948.4305, [(M+H<sup>+</sup>); calcd for C<sub>122</sub>H<sub>74</sub>F<sub>6</sub>N<sub>3</sub>O<sub>8</sub>P<sub>2</sub>S<sub>2</sub>: 1948.4298]. [ $\alpha$ ]<sub>D</sub><sup>20</sup> = 0.1803 (*c* 1.0, CHCl<sub>3</sub>).



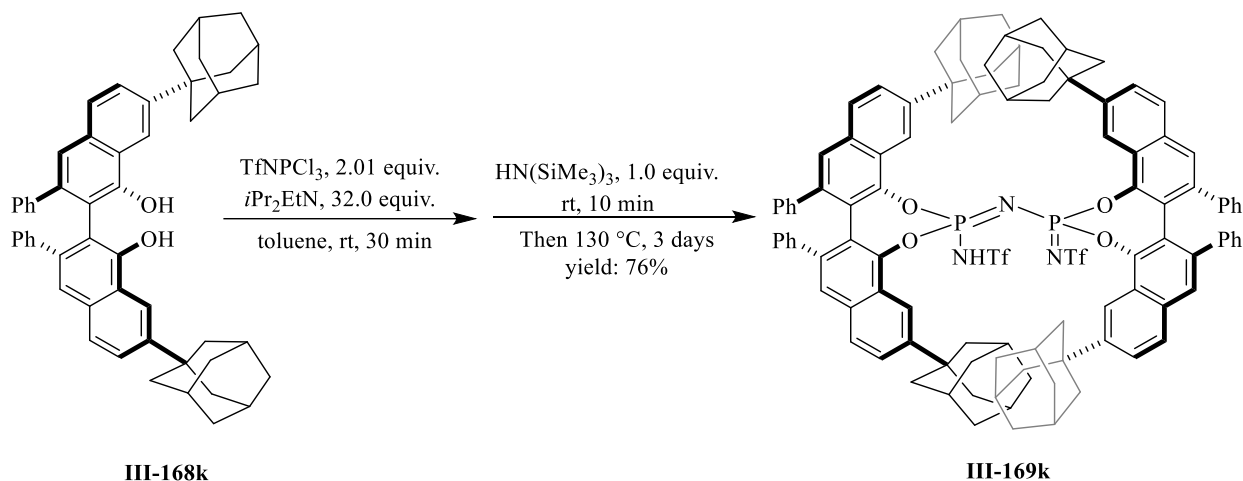
**Synthesis of ((3,5-bis(trifluoromethyl)phenyl)sulfonyl)phosphorimidoyl trichloride S-III-13:**

The phosphorimidoyl trichloride **S-III-13** was prepared *in situ* via the reported procedure published by Benjamin Lits and used without further purification.<sup>44</sup>

**Synthesis of imidodiphosphorimidate (R)-III-169f:** Compound (**R**)-**III-169f** was prepared from compound (**R**)-**III-168e** (0.9 mmol, 0.7 g), 9 mL toluene (0.1 M), 3,5-(CF<sub>3</sub>)<sub>2</sub>C<sub>6</sub>H<sub>4</sub>NPCl<sub>3</sub> (0.91 mmol, 0.33 g) (this compound was synthesized *in situ* by reacting 3,5-(CF<sub>3</sub>)<sub>2</sub>C<sub>6</sub>H<sub>4</sub>NH<sub>2</sub> with PCl<sub>5</sub> at 110 °C under reduced pressure),<sup>44</sup> *i*Pr<sub>2</sub>EtN (7.2 mmol, 1.2 mL) and HN(SiMe<sub>3</sub>)<sub>3</sub> (0.45 mmol, 95  $\mu$ L) according to the general procedure VI and the crude product was purified via column chromatography on silica gel (30 mm X 250 mm, hexane: EtOAc, 3:1, 2:1, 1:1 and 1:2 as the eluent). The desired compound (**R**)-**III-169f** was obtained as a solid in 60% isolated yield (0.27 mmol, 0.60 g). mp: 275-276 °C. CCDC number: 1995199

Spectral data for (**R**)-**III-169f**: <sup>1</sup>H NMR (500 MHz, Chloroform-*d*)  $\delta$  3.67 – 4.39 (m, 4H), 5.75 – 6.44 (m, 9H), 6.44 – 7.13 (m, 16H), 7.13 – 8.33 (m, 42H), 8.37 – 9.10 (m, 8H) (<sup>1</sup>H-NMR was complicated, most of the proton's peak were broad and overlapped with each other). <sup>13</sup>C NMR (126 MHz, Chloroform-*d*)  $\delta$  118.85, 120.98, 121.40, 122.38, 122.79, 122.90, 123.15, 125.07,

125.37, 126.37, 126.46, 126.59, 126.70, 126.82, 126.93, 127.03, 127.12, 127.38, 127.42, 127.59, 127.89, 127.95, 128.19, 128.82, 128.91, 129.07, 130.08, 130.39, 130.54, 130.98, 131.52, 131.60, 131.77, 132.04, 132.87, 132.95, 137.51, 139.08, 139.71, 140.30, 143.66, 145.70.  $^{31}\text{P}$  NMR (202 MHz, Chloroform-*d*)  $\delta$  -5.57.  $^{19}\text{F}$  NMR (470 MHz, Chloroform-*d*)  $\delta$  -63.24, -63.07. IR: 1277s, 1135s, 725s, 694s, 590m  $\text{cm}^{-1}$ . HRMS (ESI+TOF)  $m/z$  2236.4741,  $[(\text{M}+\text{H})^+]$ ; calcd for  $\text{C}_{136}\text{H}_{80}\text{F}_{12}\text{N}_3\text{O}_8\text{P}_2\text{S}_2$ : 2236.4670].  $[\alpha]^{20}_{\text{D}} = -1.2815$  ( $c$  1.0,  $\text{CHCl}_3$ ).



**Synthesis of imidodiphosphorimidate (R)-III-169k:** Compound **(R)-III-169k** was prepared from compound **(R)-III-168k** (1.77 mmol, 1.25 g), 18 mL toluene (0.1 M), TfNPCl<sub>3</sub> (1.77 mmol, 0.503 g),<sup>72</sup> *i*Pr<sub>2</sub>EtN (14.1 mmol, 2.47 mL) and HN(SiMe<sub>3</sub>)<sub>3</sub> (0.881 mmol, 186  $\mu\text{L}$ ) according to the general procedure VI and the crude product was purified via column chromatography on silica gel (30 mm X 250 mm, hexane: EtOAc, 3:1, 2:1, 1:1 and 1:2 as the eluent). The desired compound **(R)-III-169k** was obtained as a white solid in 70% isolated yield (0.612 mmol, 1.09 g). mp: 350-355 °C (decomposed). CCDC number: 1993198

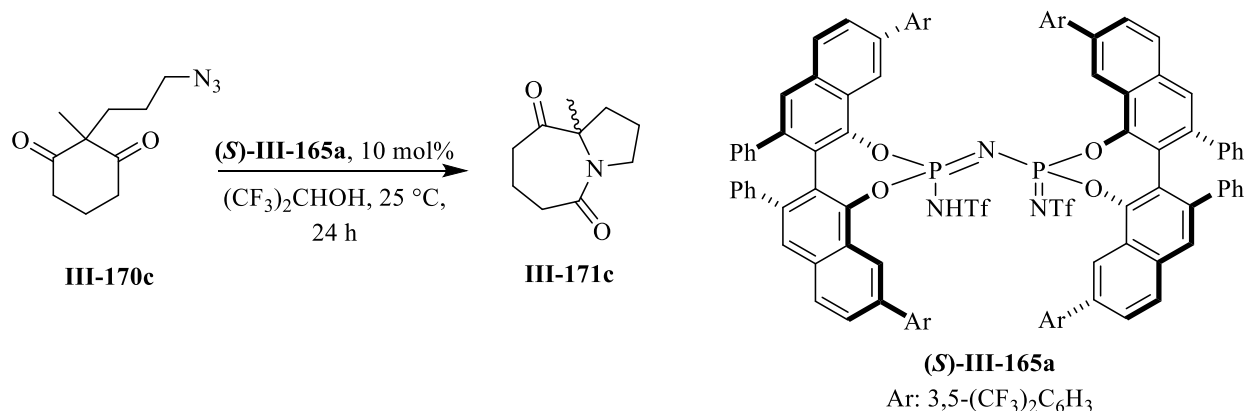
Spectral data for **(R)-III-169k**:  $^1\text{H}$  NMR (500 MHz, Chloroform-*d*)  $\delta$  1.49 (d,  $J = 12.2$  Hz, 6H), 1.63 (d,  $J = 12.4$  Hz, 6H), 1.80 – 2.04 (m, 30H), 2.12 – 2.31 (m, 18H), 4.51 (brs, 1H), 6.24 (dd,  $J = 14.0, 7.6$  Hz, 8H), 6.79 (t,  $J = 7.5$  Hz, 4H), 6.90 (t,  $J = 7.6$  Hz, 4H), 6.97 (t,  $J = 7.4$  Hz, 2H), 7.07

– 7.15 (m, 4H), 7.22 (d,  $J = 8.6$  Hz, 2H), 7.29 (dd,  $J = 8.7, 1.8$  Hz, 2H), 7.44 (s, 2H), 7.64 – 7.88 (m, 4H), 8.10 (d,  $J = 1.8$  Hz, 2H), 8.37 (d,  $J = 1.7$  Hz, 2H).  $^{13}\text{C}$  NMR (126 MHz, Chloroform- $d$ )  $\delta$  15.28, 28.68, 28.97, 36.57, 36.63, 36.84, 36.88, 42.54, 42.71, 116.67, 116.78, 121.24, 122.18, 124.71, 125.05, 126.15, 126.40, 126.50, 126.57, 126.77, 127.24, 127.57, 127.73, 128.55, 129.38, 132.14, 132.61, 138.52, 139.07, 139.20, 139.80, 149.51, 150.67.  $^{31}\text{P}$  NMR (202 MHz, Chloroform- $d$ )  $\delta$  -11.87.  $^{19}\text{F}$  NMR (470 MHz, Chloroform- $d$ )  $\delta$  -78.07. IR: 2899s, 2848m, 1200s, 1071s, 940m, 765s, 694s, 603s, 580m. HRMS (ESI+TOF)  $m/z$  1780.6183,  $[(\text{M}+\text{H})^+]$ ; calcd for  $\text{C}_{106}\text{H}_{98}\text{F}_6\text{N}_3\text{O}_8\text{P}_2\text{S}_2$ : 1780.6174].  $[\alpha]_{\text{D}}^{20} = -0.8541$  ( $c$  1.0,  $\text{CHCl}_3$ ).

### Synthesis of alkyl azide **III-170c**:

Alkyl azide **III-170c** was prepared via the procedure that is developed by Aubé's lab and the spectral data of this azide were in good agreement with the literature value.<sup>70</sup>

### Asymmetric catalytic Schmidt reaction:



To a 10 mL round bottom flask was added VIP catalyst **(S)-III-165a** (0.0490 mmol, 0.105 g), 2 mL  $(\text{CF}_3)_2\text{CHOH}$  and alkyl azide **III-176c** (0.5 mmol, 0.5 mL, 1 M in  $\text{CH}_2\text{Cl}_2$ ). The mixture was stirred at room temperature for 24 h. The solvent was removed under reduced pressure and crude mixture was loaded onto a chromatography column (25 mm X 250 mm, hexane: EtOAc, 1:1 to 0:1 and EtOAc: MeOH, 19:1 as the eluent) which afforded the desired product as a yellow solid in

32% isolated yield (0.16 mmol, 29 mg). The enantiomeric excess of the reaction was determined to be 0% via HPLC analysis (Chiralcel IA column, 97:3 hexane:IPA, 208 nm, flow-rate, 0.5 mL/min): retention times:  $R_t = 15.61$  min and  $R_t = 17.93$  min.

Spectral data for **III-170c**:  $^1\text{H}$  NMR (500 MHz, Chloroform-*d*)  $\delta$  1.41 (s, 3H), 1.81 (ddd,  $J = 11.9$ , 5.3, 3.3 Hz, 1H), 1.86 – 2.05 (m, 4H), 2.06 – 2.20 (m, 1H), 2.23 – 2.47 (m, 3H), 2.88 (td,  $J = 11.3$ , 9.1 Hz, 1H), 3.58 (dt,  $J = 12.4$ , 8.9 Hz, 1H), 3.72 (ddt,  $J = 12.8$ , 6.0, 3.8 Hz, 1H).  $^{13}\text{C}$  NMR (126 MHz, Chloroform-*d*)  $\delta$  20.43, 21.32, 22.70, 33.03, 35.06, 38.50, 46.80, 71.44, 170.50, 212.43.

These spectral data are in agreement with literature values.<sup>69</sup>

### **General method for growing the crystal of VANOL and VAPOL imidodiphosphorimidates**

*Procedure A: Illustrated for  $\text{Ad}_4\text{VIPeEtN}_3$  **III-169k***: To a 4 mL vial was added 20 mg  $\text{Ad}_4\text{VIP-Et}_3\text{N}$  followed by the addition of 1 mL of  $\text{CH}_2\text{Cl}_2$ . Once the catalyst-triethylamine complex was fully dissolved in  $\text{CH}_2\text{Cl}_2$ , 3 mL of hexane was slowly added (the layer between  $\text{CH}_2\text{Cl}_2$  and hexane should not be disturbed). Next, the 4 mL vial was placed into another 20 mL vial, capped and wrapped with parafilm. Finally, the crystal growth was noticed after 24 hours and they were collected after 48 hours.

## REFERENCES

## REFERENCES

- 1) Takahiko, A.; Mori, K., “Stronger Brønsted Acids: Recent Progress.” *Chem. Rev.* **2005**, *115*, 9277.
- 2) Schreyer, L.; Properzi, R.; List, B., “IDPi Catalysis.” *Angew. Chem. Int. Ed.* **2019**, *58*, 12761.
- 3) Proctor, R. S. J.; Davis H. J.; Phipps, R. J., “Catalytic Enantioselective Minisci-Type Addition to Heteroarenes.” *Science* **2018**, *360*, 419–22.
- 4) Shin, N. Y.; Ryss, J. M.; Zhang, X.; Miller, S. J.; Knowles, R. R., “Light-Driven Deracemization Enabled by Excited-State Electron Transfer.” *Science* **2019**, *366*, 364–69.
- 5) Teator, A. J.; Leibfarth, F. A., “Catalyst-Controlled Stereoselective Cationic Polymerization of Vinyl Ethers.” *Science* **2019**, *363*, 1439–43.
- 6) Benjamin, L.; Lerner, R. A.; and Barbas, C. F., “Proline-Catalyzed Direct Asymmetric Aldol Reactions.” *J. Am. Chem. Soc.* **2000**, *122*, 2395–96.
- 7) Ahrendt, K. A. Borths, C. J.; MacMillan, D. W. C. “New Strategies for Organic Catalysis: The First Highly Enantioselective Organocatalytic Diels–Alder Reaction.” *J. Am. Chem. Soc.* **2000**, *122*, 4243–44.
- 8) Huang, Y.; Unni, A. K.; Thadani, A. N.; Rawal, V. H., “Hydrogen Bonding: Single Enantiomers from a Chiral-Alcohol Catalyst.” *Nature* **2003**, *424*, 146.
- 9) Akiyama, T.; Itoh, J.; Yokota, K.; Fuchibe, K., “Enantioselective Mannich-Type Reaction Catalyzed by a Chiral Brønsted Acid.” *Angew. Chem. Int. Ed.* **2004**, *43*, 1566–68.
- 10) Yamanaka, M.; Itoh, J.; Fuchibe, K.; Akiyama, T., “Chiral Brønsted Acid Catalyzed Enantioselective Mannich-Type Reaction.” *J. Am. Chem. Soc.* **2007**, *129*, 6756–64.
- 11) Akiyama, T.; Morita, H.; Itoh, J.; Fuchibe, K., “Chiral Brønsted Acid Catalyzed Enantioselective Hydrophosphonylation of Imines: Asymmetric Synthesis of Alpha-Amino Phosphonates.” *Org. Lett.* **2005**, *7*, 2583–85.
- 12) Akiyama, T.; Morita, H.; Fuchibe, K., “Chiral Brønsted Acid-Catalyzed Inverse Electron-Demand Aza Diels–Alder Reaction.” *J. Am. Chem. Soc.* **2006**, *128*, 13070–71.
- 13) Uraguchi, D.; Terada, M., “Chiral Brønsted Acid-Catalyzed Direct Mannich Reactions via Electrophilic Activation.” *J. Am. Chem. Soc.* **2004**, *126*, 5356–57.
- 14) Uraguchi, D.; Sorimachi, K.; Terada, M., “Organocatalytic Asymmetric Direct Alkylation of Alpha-Diazoester via C–H Bond Cleavage.” *J. Am. Chem. Soc.* **2005**, *127*, 9360–61.

- 15) Antilla, J. C.; Wulff, W. D., "Catalytic Asymmetric Aziridination with Arylborate Catalysts Derived from VAPOL and VANOL Ligands." *Angew. Chem. Int. Ed.* **2000**, *39*, 4518–21.
- 16) Desai, A. A.; Wulff, W. D., "Controlled Diastereo- and Enantioselection in a Catalytic Asymmetric Aziridination." *J. Am. Chem. Soc.* **2010**, *132*, 13100–103.
- 17) Huang, L.; Wulff, W. D., "Catalytic Asymmetric Synthesis of Trisubstituted Aziridines." *J. Am. Chem. Soc.* **2011**, *133*, 8892–95.
- 18) Hashimoto, T.; Nakatsu, H.; Yamamoto, K.; Maruoka, K., "Chiral Brønsted Acid-Catalyzed Asymmetric Trisubstituted Aziridine Synthesis Using  $\alpha$ -Diazoacyl Oxazolidinones." *J. Am. Chem. Soc.* **2011**, *133*, 9730–33.
- 19) Uraguchi, D.; Sorimachi, K.; Terada, M., "Organocatalytic Asymmetric Aza-Friedel-Crafts Alkylation of Furan." *J. Am. Chem. Soc.* **2004**, *126*, 11804–5.
- 20) Terada, M.; Machioka, K.; Sorimachi, K., "Chiral Brønsted Acid-Catalyzed Tandem Aza-Ene Type Reaction/cyclization Cascade for a One-Pot Entry to Enantioenriched Piperidines." *J. Am. Chem. Soc.* **2007**, *129*, 10336–37.
- 21) Rowland, G. B.; Zhang, H.; Rowland, E. B.; Chennamadhavuni, S.; Wang, Y.; Antilla, J. C., "Brønsted Acid-Catalyzed Imine Amidation." *J. Am. Chem. Soc.* **2005**, *127*, 15696–97.
- 22) Liang, Y.; Rowland, E. B.; Rowland, G. B.; Perman, J. A.; Antilla, J. C., "VAPOL Phosphoric Acid Catalysis: The Highly Enantioselective Addition of Imides to Imines." *Chem. Comm.* **2007**, *43*, 4477–79.
- 23) Li, G.; Liang, Y.; Antilla, J. C., "A Vaulted Biaryl Phosphoric Acid-Catalyzed Reduction of  $\alpha$ -Imino Esters: The Highly Enantioselective Preparation of  $\alpha$ -Amino Esters." *J. Am. Chem. Soc.* **2007**, *129*, 5830–31.
- 24) Rowland, E. B.; Rowland, G. B.; Rivera-Otero, E.; Antilla, J. C., "Brønsted Acid-Catalyzed Desymmetrization of Meso-Aziridines." *J. Am. Chem. Soc.* **2007**, *129*, 12084–85.
- 25) Burk, P.; Koppel, I. A.; Koppel, I.; Yagupolskii, L. M.; Taft, R. W., "Superacidity of Neutral Brønsted Acids in Gas Phase." *J. Comput. Chem.* **1996**, *17*, 30–41.
- 26) Nakashima, D.; Yamamoto, H., "Design of Chiral N-Triflyl Phosphoramidate as a Strong Chiral Brønsted Acid and Its Application to Asymmetric Diels–Alder Reaction." *J. Am. Chem. Soc.* **2006**, *128*, 9626–27.
- 27) Jiao, P.; Nakashima, D.; Yamamoto, H., "Enantioselective 1,3-Dipolar Cycloaddition of Nitrones with Ethyl Vinyl Ether: The Difference between Brønsted and Lewis Acid Catalysis." *Angew. Chem. Int. Ed.* **2008**, *47*, 2411–13.



- 28) Rueping, M.; Ieawsuwan, W.; Antonchick, A. P.; Nachtsheim, B. J. "Chiral Brønsted Acids in the Catalytic Asymmetric Nazarov Cyclization—The First Enantioselective Organocatalytic Electrocyclic Reaction." *Angew. Chem. Int. Ed.* **2007**, 46, 2097–2100.
- 29) Cheon, C. H.; Yamamoto, H., "A Brønsted Acid Catalyst for the Enantioselective Protonation Reaction." *J. Am. Chem. Soc.* **2008**, 130, 9246–47.
- 30) Cheol, H. C.; Yamamoto, H., "N-Triflylthiophosphoramidate Catalyzed Enantioselective Mukaiyama Aldol Reaction of Aldehydes with Silyl Enol Ethers of Ketones." *Org. Lett.* **2010**, 12, 2476–79.
- 31) Sai, M.; Yamamoto, H., "Chiral Brønsted Acid as a True Catalyst: Asymmetric Mukaiyama Aldol and Hosomi–Sakurai Allylation Reactions." *J. Am. Chem. Soc.* **2015**, 137, 7091–94.
- 32) Desai, A.; Huang, L.; Wulff, W. D., "Gerald Rowland, and Jon Antilla. 2010. "Gram-Scale Preparation of VAPOL Hydrogenphosphate: A Structurally Distinct Chiral Brønsted Acid." *Synthesis* **2010**, 12, 2106–9.
- 33) Čorić, I.; List, B., "Asymmetric Spiroacetalization Catalysed by Confined Brønsted Acids." *Nature* **2012**, 483, 315–19.
- 34) Liao, S.; Čorić, I.; Wang, Q.; List, B., "Activation of H<sub>2</sub>O<sub>2</sub> by Chiral Confined Brønsted Acids: A Highly Enantioselective Catalytic Sulfoxidation." *J. Am. Chem. Soc.* **2012**, 134, 10765–68.
- 35) Kim, J. H.; Čorić, I.; Vellalath, S.; List, B., "The Catalytic Asymmetric Acetalization." *Angew. Chem. Int. Ed.* **2013**, 52, 4474–77.
- 36) Liu, L.; Leutzsch, M.; Zheng, Y.; Alachraf, W.; Thiel, W.; List, B., "Confined Acid-Catalyzed Asymmetric Carbonyl–Ene Cyclization." *J. Am. Chem. Soc.* **2015**, 137, 13268–71.
- 37) Xie, Y.; Cheng, G.; Lee, S.; Kaib, P. S. J.; Thiel, W.; List, B., "Catalytic Asymmetric Vinylogous Prins Cyclization: A Highly Diastereo- and Enantioselective Entry to Tetrahydrofurans." *J. Am. Chem. Soc.* **2016**, 138, 14538–41.
- 38) Kim, J. H.; Čorić, I.; Palumbo, C.; List, B., "Resolution of Diols via Catalytic Asymmetric Acetalization." *J. Am. Chem. Soc.* **2015**, 137, 1778–81.
- 39) Wu, K.; Jiang, Y.; Fan, Y.; Sha, D.; Zhang, S., "Double Axially Chiral Bisphosphorylimides Catalyzed Highly Enantioselective and Efficient Friedel–Crafts Reaction of Indoles with Imines." *Chem. Eur. J.* **2013**, 19, 474–78.
- 40) Zhou, T.; Gao, J.; Liu, G.; Guan, X.; An, D.; Zhang, S.; Zhang, G., "Chiral VAPOL Imidodiphosphoric Acid-Catalyzed Asymmetric Vinylogous Mannich Reaction for the Synthesis of Butenolides." *Synlett* **2018**, 29, 2006–10.

- 41) Liu, L.; Kaib, P. S. J.; Tap, A.; List, B., "A General Catalytic Asymmetric Prins Cyclization." *J. Am. Chem. Soc.* **2016**, *138*, 10822–25.
- 42) Kaib, P. S. J.; Schreyer, L.; Lee, S.; Properzi, R.; List, B., "Extremely Active Organocatalysts Enable a Highly Enantioselective Addition of Allyltrimethylsilane to Aldehydes." *Angew. Chem. Int. Ed.* **2016**, *55*, 13200–203.
- 43) Liu, L.; Kim, H.; Xie, Y.; Farès, C.; Kaib, P. S. J.; Goddard, R.; List, B., "Catalytic Asymmetric [4+2]-Cycloaddition of Dienes with Aldehydes." *J. Am. Chem. Soc.* **2017**, *139*, 13656–59.
- 44) Tsuji, N.; Kennemur, J. L.; Buyck, T.; Lee, S.; Prévost, S.; Kaib, P. S. J.; Bykov, D.; Farès, C.; List, B., "Activation of Olefins via Asymmetric Brønsted Acid Catalysis." *Science* **2018**, *359*, 1501–5.
- 45) Wendlandt, A. E.; Vangal, P.; Jacobsen, E. N., "Quaternary Stereocentres via an Enantioconvergent Catalytic SN1 Reaction." *Nature* **2018**, *556*, 447–51.
- 46) Properzi, R.; Kaib, P. S. J.; Leutzsch, M.; Pupo, G.; Mitra, R.; De, C. K.; Schreiner, P. R.; List, B., "Strong and Confined Acid Catalysts Impart Stereocontrol onto the Non-Classical 2-Norbornyl Cation," *chemrxiv*. **2019**, 10887914.v1
- 47) Winstein, S.; Trifan, D. S., "The structure of the bicyclo[2,2,1]2-heptyl (norbornyl) carbonium ion." *J. Am. Chem. Soc.* **1949**, *71*, 2953–2953.
- 48) Bae, H. Y.; Höfler, Kaib, D.; P. S. J.; Kasaplar, P.; De, C. K.; Döhring, A.; Lee, S.; Kaupmees, K.; Leito, I.; List, B., "Approaching Sub-Ppm-Level Asymmetric Organocatalysis of a Highly Challenging and Scalable Carbon-Carbon Bond Forming Reaction." *Nature Chem.* **2018**, *10*, 888–94.
- 49) Ouyang, J.; Kennemur, J. L.; De, C. K.; Farès, C.; List, B., "Strong and Confined Acids Enable a Catalytic Asymmetric Nazarov Cyclization of Simple Divinyl Ketones." *J. Am. Chem. Soc.* **2019**, *141*, 3414–18.
- 50) Whitehead, D. C.; Yousefi, R.; Jaganathan, A.; Borhan, B., "An Organocatalytic Asymmetric Chlorolactonization." *J. Am. Chem. Soc.* **2010**, *132*, 3298–3300.
- 51) Jaganathan, A.; Staples, R. J.; Borhan, B., "Kinetic Resolution of Unsaturated Amides in a Chlorocyclization Reaction: Concomitant Enantiomer Differentiation and Face Selective Alkene Chlorination by a Single Catalyst." *J. Am. Chem. Soc.* **2013**, *135*, 14806–13.
- 52) Huang, D.; Wang, H.; Xue, F.; Guan, H.; Li, L.; Peng, X.; Shi, Y., "Enantioselective Bromocyclization of Olefins Catalyzed by Chiral Phosphoric Acid." *Org. Lett.* **2011**, *13*, 6350–53.
- 53) Denmark, S. E.; Burk, M. T., "Enantioselective Bromocycloetherification by Lewis Base/Chiral Brønsted Acid Cooperative Catalysis." *Org. Lett.* **2012**, *14*, 256–59.

- 54) Samanta, R. C.; Yamamoto, H.; “Catalytic Asymmetric Bromocyclization of Polyenes.” *J. Am. Chem. Soc.* **2017**, *139*, 1460–63.
- 55) Zhang, F.; Zhang, S.; Tu, Y.; “Recent Progress in the Isolation, Bioactivity, Biosynthesis, and Total Synthesis of Natural Spiroketal.” *Nat. Prod. Rep.* **2018**, *35*, 75–104.
- 56) Aho, J. E.; Pihko, P. M.; Rissa, T. K., “Nonanomeric Spiroketal in Natural Products: Structures, Sources, and Synthetic Strategies.” *Chem. Rev.* **2005**, *105*, 4406–40.
- 57) Totah, N. I.; Schreiber, S. L., “Thermodynamic Spiroketalization as an Efficient Method of Stereochemical Communication.” *J. Org. Chem.* **1991**, *56*, 6255–56.
- 58) Sun, Z.; Winschel, G. A.; Borovika, A.; Nagorny, P., “Chiral Phosphoric Acid-Catalyzed Enantioselective and Diastereoselective Spiroketalizations.” *J. Am. Chem. Soc.* **2012**, *134*, 8074–77.
- 59) Hamilton, J. Y.; Rössler, S. L.; Carreira, E. M., “Enantio- and Diastereoselective Spiroketalization Catalyzed by Chiral Iridium Complex.” *J. Am. Chem. Soc.* **2017**, *139*, 8082–85.
- 60) Soltanzadeh, B.; Jaganathan, A.; Staples, R. J.; Borhan, B., “Highly Stereoselective Intermolecular Haloetherification and Haloesterification of Allyl Amides.” *Angew. Chem. Int. Ed.* **2015**, *54*, 9517–22.
- 61) Ashtekar, K. D.; Salehi Marzijarani, N.; Jaganathan, A.; Holmes, D.; Jackson, J. E.; Borhan, B., “A New Tool to Guide Halofunctionalization Reactions: The Halenium Affinity (HalA) Scale.” *J. Am. Chem. Soc.* **2014**, *136*, 13355–62.
- 62) Ashtekar, K. D.; Vetticatt, M.; Yousefi, R.; Jackson, J. E.; Borhan, B., “Nucleophile-Assisted Alkene Activation: Olefins Alone Are Often Incompetent.” *J. Am. Chem. Soc.* **2016**, *138*, 8114–19.
- 63) Kumar, D. A.; Gholami, H.; Kiiskilä, L.; Toma, E.; Rahn, C.; Staples, R. J.; Borhan, B., “Development of a Mechanistically Inspired Halenium Atom Induced Diastereoselective Spiroketalization: Modulation of Nucleophile Assisted Alkene Activation.” *Unpublished results*.
- 64) Guan, Y.; Ding, Z.; Wulff, W. D., “Vaulted Biaryls in Catalysis: A Structure-Activity Relationship Guided Tour of the Immanent Domain of the VANOL Ligand.” *Chem. Eur. J.* **2013**, *19*, 15565–71.
- 65) Wolff, H., “The Schmidt Reaction” *Org. React.* **1946**, *3*, 307.
- 66) Wroblewski, A.; Coombs, T. C.; Huh, C. W.; Li, S.; Aubé, J., “The Schmidt Reaction.” *Org. React.* **2012**, *78*, 1-320.

- 67) Aube, J.; Milligan, G. L., "Intramolecular Schmidt Reaction of Alkyl Azides." *J. Am. Chem. Soc.* **1991**, *113*, 8965–66.
- 68) Sahasrabudhe, K.; Gracias, V.; Furness, K.; Smith, B. T.; Katz, C. E.; Reddy, D. S.; Aubé, J., "Asymmetric Schmidt Reaction of Hydroxyalkyl Azides with Ketones." *J. Am. Chem. Soc.* **2003**, *125*, 7914–22.
- 69) Yang, M.; Zhao, Y.; Zhang, S.; Tu, Y.; Zhang, F., "Chiral Brønsted Acid-Promoted Enantioselective Desymmetrization in an Intramolecular Schmidt Reaction of Symmetric Azido 1,3-Hexanediones: Asymmetric Synthesis of Azaquaternary Pyrroloazepine Skeletons." *Chem. Eur. J.* **2011**, *6*, 1344–47.
- 70) Motiwala, H. F.; Fehl, C.; Li, S.; Hirt, E.; Porubsky, P.; Aubé, J., "Overcoming Product Inhibition in Catalysis of the Intramolecular Schmidt Reaction." *J. Am. Chem. Soc.* **2013**, *135*, 9000–9009.
- 71) Yong, G.; Ding, Z.; Wulff, W. D., "Vaulted Biaryls in Catalysis: A Structure-Activity Relationship Guided Tour of the Immanent Domain of the VANOL Ligand." *Chem. Eur. J.* **2013**, *19*, 15565–15571.
- 72) Lee, S.; Kaib, P.; List, B., "N-Triflylphosphorimidoyl Trichloride: A Versatile Reagent for the Synthesis of Strong Chiral Brønsted Acids." *Synlett.* **2017**, *28*, 1478-1480.